Springer Series in Biomaterials Science and Engineering 17

Andy H. Choi
Besim Ben-Nissan *Editors*

Innovative Bioceramics in Translational Medicine I

Fundamental Research

Springer

Springer Series in Biomaterials Science and Engineering

Volume 17

The Springer Series in Biomaterials Science and Engineering addresses the manufacture, structure and properties, and applications of materials that are in contact with biological systems, temporarily or permanently. It deals with many aspects of modern biomaterials, from basic science to clinical applications, as well as host responses. It covers the whole spectrum of biomaterials–polymers, metals, glasses and ceramics, and composites/hybrids–and includes both biological materials (collagen, polysaccharides, biological apatites, etc.) and synthetic materials. The materials can be in different forms: single crystals, polycrystalline materials, particles, fibers/wires, coatings, non-porous materials, porous scaffolds, etc. New and developing areas of biomaterials, such as nano-biomaterials and diagnostic and therapeutic nanodevices, are also focuses in this series. Advanced analytical techniques that are applicable in R&D and theoretical methods and analyses for biomaterials are also important topics. Frontiers in nanomedicine, regenerative medicine and other rapidly advancing areas calling for great explorations are highly relevant.

The Springer Series in Biomaterials Science and Engineering aims to provide critical reviews of important subjects in the field, publish new discoveries and significant progresses that have been made in both biomaterials development and the advancement of principles, theories and designs, and report cutting-edge research and relevant technologies. The individual volumes in the series are thematic. The goal of each volume is to give readers a comprehensive overview of an area where new knowledge has been gained and insights made. Significant topics in the area are dealt with in good depth and future directions are predicted on the basis of current developments. As a collection, the series provides authoritative works to a wide audience in academia, the research community, and industry.

This book series is indexed by the EI Compendex and Scopus databases.

If you are interested in publishing your book in the series, please contact Dr. Mengchu Huang (Email: mengchu.huang@springer.com).

More information about this series at https://link.springer.com/bookseries/10955

Andy H. Choi · Besim Ben-Nissan
Editors

Innovative Bioceramics in Translational Medicine I

Fundamental Research

Springer

Editors
Andy H. Choi
Faculty of Science
University of Technology Sydney
Ultimo, NSW, Australia

Besim Ben-Nissan
Faculty of Science
University of Technology Sydney
Ultimo, NSW, Australia

ISSN 2195-0644 ISSN 2195-0652 (electronic)
Springer Series in Biomaterials Science and Engineering
ISBN 978-981-16-7434-1 ISBN 978-981-16-7435-8 (eBook)
https://doi.org/10.1007/978-981-16-7435-8

This Springer imprint is published by the registered company Springer Nature Singapore Pte Ltd.
The registered company address is: 152 Beach Road, #21-01/04 Gateway East, Singapore 189721, Singapore

Preface

In order to meet the demands of modern-day medical needs, it is of paramount importance that biomaterials and bioceramics transcend their current limitations of simply augmenting or replacing bodily components to a more innovative role where they can interact with cells and tissues. Although the presence of material requirements is common during the design and development of medical devices, relevant clinical prerequisites should also be incorporated so that appropriate prosthetics and implantable components are produced. This resulted in the creation of a highly interdisciplinary field known as translational medicine.

The definition of translational medicine generally agreed upon in the scientific community is that it is the constructive translation of new and innovative technique and information through advancements in basic research performed by interdisciplinary research teams into novel methodologies for preventing, diagnosing, and treating diseases for the benefit of patients and the public at large. Translational medicine has three main pillars: benchside (in the laboratory), bedside (clinical trials), and the community.

Bioceramics employed in medicine and surgery plays a crucial role in expanding the performance and function of medical devices. The science and technology of bioceramics is truly interdisciplinary, and consequently improved or innovative bioceramics can only be achieved through advancements in physical and biological sciences, engineering, and medicine. There have been increasing demands on medical devices that they not only extend life but also improve its quality. Of even greater importance are the exciting and potential opportunities associated with the production of patient-matched ceramic components containing complex shapes with three-dimensional (3D) printing technology.

Gaining a deeper understanding into the correlations between material properties and biological performance will be useful in the design of innovative bioceramics and in addressing issues of implant failure and related infection. The challenge remains in providing safe and efficacious bioceramics with the required properties and an acceptable biocompatibility level. As the field of innovative biomaterials finds increasing applications in cellular and tissue engineering, it will continue to be used in new ways as part of the most innovative therapeutic strategies.

Divided into 2 volumes, the books comprise 23 chapters written by top-notch international surgeons and experts in the fields of orthopedics, maxillofacial surgery, orthodontics, spinal surgery, and biomaterials. It is envisaged that each chapter will provide an in-depth examination of the latest research and clinical advances in hard tissue reconstruction and regenerations and in the treatment of bone diseases such as osteoporosis.

The first volume, ***Fundamental Research***, covers the basic principles and techniques used in the manufacture of bioceramics and biocomposites for various biomedical applications including drug delivery, implantable bionics and the development of the cardiac pacemaker, and bone tissue engineering. Furthermore, self-healing materials have been attracting increasing interest in both engineering and medical applications during the past two decades. Self-healing hydrogels are particularly interesting because of their ability to repair structural damages and recover their original functions, specifically in tissue engineering.

The current emphasis of tissue engineering has changed by seizing the advantage of combining the utilization of living cells with 3D scaffolds to transport vital cells and other biological materials such as stem cells and peptides to the damaged site of the patient with the intention of promoting tissue healing and regeneration. Clinical applications of bioactive composite scaffolds containing bioceramics and biodegradable polymers have attracted much attention during the past three decades. These composite grafts can also provide antibacterial properties when combined with therapeutic metal ions such as silver and copper. Similarly, functionalizing metallic surfaces and bioceramics with antimicrobial peptides would enable the creation of scaffolds and implants that can provide a mechanism against bacterial infection, while at the same time, stimulate bone formation.

The second volume, ***Surgical Applications***, covers the translation of innovative techniques and novel applications of bioceramics and bioceramics-based composite from the laboratory to a clinical environment in areas such as wound management following orthopedic surgical incisions and the application of bioresorbable bone fixation devices and ceramic-polymer biocomposite bone grafts for the repair of damaged tissues in dentistry and orthopedics. The advancement in personalized surgery and the manufacture of patient-specific 3D-printed bioceramic scaffolds for bone regeneration in craniomaxillofacial and spinal surgery are also thoroughly examined in this volume. Furthermore, the incorporation of biogenic materials such as bone morphogenetic proteins as well as regenerative pharmacologic agents like dipyridamole will allow for the development of a new generation of smart bioceramics-based scaffolds that promotes osteoconductivity and more importantly osteoinductivity.

It has been a well-established fact that bone undergoes a continuous process of remodeling or regeneration in which the activities of osteoclasts and osteoblasts are combined. Osteoporosis arises if this relationship became unbalanced and the quantity of bone resorbed exceeds the amount of new bone formed resulting in a reduction in bone strength and an increase in fracture risk. Reducing the fracture risk thus became the primary focus in the treatment of osteoporosis. Monoclonal antibodies have been applied in recent years in the treatment of osteoporosis. In this

volume, we also intended to give our readers a fundamental insight into the basic properties, the technology used in their development, and their clinical application in the treatment of osteoporosis.

Finally, I would like to express my deepest gratitude to all my contributing authors from Australia, France, India, Italy, Japan, Portugal, South Korea, Tanzania, Turkey, the United Kingdom, the United States, and Vietnam for their time and valuable contributions to this informative book during the challenging time of the COVID-19 pandemic. I would also like to thank my great family for their support throughout this endeavor. Also, I would like to give very special thanks to my mentor and co-editor Prof. Besim Ben-Nissan for his friendship, support, and advice for over two decades. Finally, I would like to acknowledge the people at Springer Publishing, especially Mano Priya Saravanan, Ramesh Premnath, and Dharaneeswaran Sundaramurthy, and Prof. Min Wang for their help and for making these two books possible.

Sydney, Australia Andy H. Choi

Contents

Editors and Contributors

About the Editors

Dr. Andy H. Choi is an early career researcher who received his Ph.D. from the University of Technology Sydney (UTS) in Australia in 2004 on the use of computer modelling and simulation known as finite element analysis (FEA) to examine the biomechanical behavior of implants installed into a human mandible. After completing his Ph.D., he expanded his research focus from FEA to sol-gel synthesis of multifunctional calcium phosphate nano coatings and nano composite coatings for dental and biomedical applications.

In late 2010, Dr. Choi was successfully awarded the internationally competitive Endeavour Australia Cheung Kong Research Fellowship Award and undertook post-doctoral training at the Faculty of Dentistry of the University of Hong Kong focusing on the application of FEA in dentistry and the development of calcium phosphate nano-bioceramics.

He is currently serving as an associate editor for the Journal of the Australian Ceramic Society and as an editor for a number of dentistry-related journals. In addition, he is also serving as an editorial board member for several dentistry, nanotechnology, and orthopedics journals. To date, Dr. Choi has published over 50 publications including 5 books and 30 book chapters on calcium phosphate, nano-biomaterial coatings, sol-gel technology, marine structures, drug delivery, tissue engineering, and finite element analysis in nanomedicine and dentistry.

Prof. Besim Ben-Nissan has higher degrees in Metallurgical Engineering (ITU), Ceramic Engineering (University of New South Wales) and a Ph.D. in Mechanical and Industrial Engineering with Biomedical Engineering (University of New South Wales). Over the last four decades together with a large numbers of PhD students and post-doctoral fellows he has worked on production and analysis of various biomedical materials, implants, calcium phosphate ceramics, advanced ceramics (alumina, zirconia, silicon nitrides), sol-gel developed nanocoatings for enhanced bioactivity, corrosion and abrasion protections, optical and electronic ceramics and thermally insulating new generation composites.

He also has contributed to the areas of mechanical properties of sol-gel developed nanocoatings. In the biomedical field, he has involved with the development of materials for slow drug delivery, natural and marine material conversion, implant technology (bioactive materials including conversion of Australian corals to hydroxyapatite bone grafts), biomimetics (learning from nature and its application to regenerative medicine), bio-composites, investigative research on biomechanics and Finite Element Analysis (mandible, knee, hip joints, hip resurfacing), reliability and implant design (modular ceramic knee prosthesis, femoral head stresses). He was part of a research team which initiated the world's first reliable ceramic knee and hydroxyapatite sol gel derived nanocoatings. Since 1990 he has published over 260 papers in journals, five books and over 50 book chapters. He is one of the editors of the Journal of the Australian Ceramic Society and Editorial Board member of three international biomaterials journals. He was awarded "The Australasian Ceramic Society Award" for his contribution to "Ceramic education and research and development in Australia." He also received "Future Materials Award" for his contribution to the "Advanced nanocoated materials field."

He has collaborated with a number of international groups in Japan, USA, Thailand, Finland, Israel, France, UK, Germany and Turkey and held grants from the Australian Academy of Science and the Japan Society for Promotion of Science for collaborative work in the biomedical field in Europe, USA and Japan respectively. After serving as an academic for over 33 years he has

retired, however still active and contributes to science by research in the biomedical field and supervising higher degree students.

Contributors

Besim Ben-Nissan Faculty of Science, Biomaterials and Translational Medicine Group, School of Life Sciences, University of Technology Sydney (UTS), Ultimo, Australia

Andy H. Choi Faculty of Science, Biomaterials and Translational Medicine Group, School of Life Sciences, University of Technology Sydney (UTS), Ultimo, Australia

Gina Choi Faculty of Science, School of Mathematical and Physical Sciences, University of Technology Sydney (UTS), Ultimo, Australia

David J. Cowdery Biomedical Engineering, School of Aerospace, Mechanical and Mechatronic Engineering, Faculty of Engineering, University of Sydney, Sydney, NSW, Australia

Louise Evans Faculty of Science, School of Mathematical and Physical Sciences, University of Technology Sydney (UTS), Ultimo, Australia

Diana Gomes Biomaterials Research Group, School of Metallurgy and Materials, College of Physical Science and Engineering, University of Birmingham, Birmingham, UK

David Green Biomaterials Research Group, School of Metallurgy and Materials, College of Physical Science and Engineering, University of Birmingham, Birmingham, UK

Lukas Gritsch Laboratoire de Physique de Clermont, UMR CNRS 6533, Université Clermont Auvergne, Aubière, France

Ipek Karacan Faculty of Science, Advanced Tissue Engineering and Stem Cell Biology Group, School of Life Sciences, University of Technology Sydney (UTS), Ultimo, Australia

Il Keun Kwon Department of Dental Materials, School of Dentistry, Kyung Hee University, Seoul, Republic of Korea

Bruce Milthorpe Faculty of Science, Advanced Tissue Engineering and Stem Cell Biology Group, School of Life Sciences, University of Technology Sydney (UTS), Ultimo, Australia

J. Miguel Oliveira 3B's Research Group, I3Bs - Research Institute on Biomaterials, Biodegradables and Biomimetics, University of Minho, Headquarters of the European Institute of Excellence on Tissue Engineering and Regenerative Medicine, AvePark, Parque de Ciência e Tecnologia, Zona Industrial da Gandra, Barco, Guimarães, Portugal;
ICVS/3B's-PT Government Associate Laboratory, Braga/Guimarães, Portugal

Makoto Otsuka Faculty of Pharmacy, Research Institute of Pharmaceutical Sciences, Musashino University, Nishi-tokyo, Japan;
Research Institute of Electronics, Shizuoka University, Hamamatsu, Japan

Yuta Otsuka Faculty of Pharmaceutical Sciences, Tokyo University of Science, Noda, Chiba, Japan

Sandra Pina 3B's Research Group, I3Bs - Research Institute on Biomaterials, Biodegradables and Biomimetics, University of Minho, Headquarters of the European Institute of Excellence on Tissue Engineering and Regenerative Medicine, AvePark, Parque de Ciência e Tecnologia, Zona Industrial da Gandra, Barco, Guimarães, Portugal;
ICVS/3B's-PT Government Associate Laboratory, Braga/Guimarães, Portugal

Rui L. Reis 3B's Research Group, I3Bs - Research Institute on Biomaterials, Biodegradables and Biomimetics, University of Minho, Headquarters of the European Institute of Excellence on Tissue Engineering and Regenerative Medicine, AvePark, Parque de Ciência e Tecnologia, Zona Industrial da Gandra, Barco, Guimarães, Portugal;
ICVS/3B's-PT Government Associate Laboratory, Braga/Guimarães, Portugal

Pietro Riccio Biomaterials Research Group, School of Metallurgy and Materials, College of Physical Science and Engineering, University of Birmingham, Birmingham, UK

Andrew J. Ruys Biomedical Engineering, School of Aerospace, Mechanical and Mechatronic Engineering, Faculty of Engineering, University of Sydney, Sydney, NSW, Australia

Jerran Santos Faculty of Science, Advanced Tissue Engineering and Stem Cell Biology Group, School of Life Sciences, University of Technology Sydney (UTS), Ultimo, Australia

Masaya Shimabukuro Department of Biomaterials, Faculty of Dental Science, Kyushu University, Fukuoka, Japan

Edwin K. L. Soh Biomedical Engineering, School of Aerospace, Mechanical and Mechatronic Engineering, Faculty of Engineering, University of Sydney, Sydney, NSW, Australia

Artemis Stamboulis Biomaterials Research Group, School of Metallurgy and Materials, College of Physical Science and Engineering, University of Birmingham, Birmingham, UK

Mohadeseh Zare Biomaterials Research Group, School of Metallurgy and Materials, College of Physical Science and Engineering, University of Birmingham, Birmingham, UK

Chapter 1
Biomaterials and Bioceramics—Part 1: Traditional, Natural, and Nano

Andy H. Choi

Abstract Even though the utilization of manmade and natural materials in the repair and reconstruction of bodily organs and tissues dates back to pre-historic times, their exploitation during the past number of decades have been fast-tracked significantly in the arenas of scientific research and clinical applications. Recognizing on the nanoscale the importance of implant-tissue interactions has resulted in the widespread development and utilization of nanotechnology in biomedical science and engineering. This notion is reinforced by the belief that functional nanostructured materials are proficient of being altered and included into a variety of biomedical implants and devices. Furthermore, natural nanostructured architecture is displayed by a variety of biological systems such as membranes, viruses, and protein complex. Conversely, highly functional architectural structures with interconnecting open pores can be discovered easily from within the marine environment. The exploitation of ready-made organic and inorganic marine skeletons has created opportunities as they could theoretically present one of the modest solutions to significant issues deterring the future research and development concerning regenerative medicine in dentistry and orthopedics such as providing ample and available supplies of osteopromotive analogues and biomineralization proteins as well as a richness of framework designs and devices. Irrespective of the conditions in which marine organisms are utilized (i.e., in their original form or converted to materials more ideal for human implantations), they are structured and created from materials that possess various characteristics and properties especially their chemical composition and high mechanical strength which affirm their potential applications in dentistry and orthopedics. The first part of the two-part chapter aims to give an overview of the different types of biomaterials and bioceramics as well as their production technique that are currently used in a number of clinical applications in dentistry and orthopedics. A brief insight into the nature, morphology, and application of marine-derived biomaterials are also provided.

A. H. Choi (✉)
Faculty of Science, Biomaterials and Translational Medicine Group, School of Life Sciences, University of Technology Sydney (UTS), Ultimo, Australia
e-mail: Andy.H.Choi@alumni.uts.edu.au

A. H. Choi and B. Ben-Nissan (eds.), *Innovative Bioceramics in Translational Medicine I*,
Springer Series in Biomaterials Science and Engineering 17,
https://doi.org/10.1007/978-981-16-7435-8_1

Keywords Nanobiomaterial · Nanobioceramics · Marine biomaterials · Nanocoatings · Surface modifications · Nanocomposite · Adhesives · Bioimaging

1.1 Introduction

Biocompatibility as well as biofunctionality of any biomaterials and bioceramics are the primary factors governing their rate of success from a clinical perspective, and both of which are directly connected to how the biomaterial or bioceramic interacts with the human tissue at the implant interface. Biomaterials and bioceramics were utilized to carry out singular and biologically inert roles such as implants during the early 1970s. A hundred years ago, assortments of materials such as wood and gold have been used to manufacture artificial devices and they were developed to such a stage where these devices could replace various parts within the human body. In addition, these materials were able to interact with bodily tissues and fluids for extended periods without provoking little or if any adverse reactions.

Biomaterials can be labeled as substances that are not drug related and is appropriate to be incorporated into the human body which could replace or strengthen the function of organs or tissues. The inadequacies with these synthetic materials as tissue replacements were emphasized with the growing understanding that tissues and cells of the human body perform many other crucial metabolic and regulatory functions.

Since then, the requirements of biomaterials and bioceramics have reformed to providing a more positive interaction with the host instead of just preserving the basic function without provoking any undesirable response. This concept has been complemented by the ever-increasing demands on medical devices to prolong the duration of life in addition to improving its quality. When used as body interactive materials, bioceramics possess the potential to aid the human body to heal by promoting the regeneration of tissues and thereby restoring physiological functions. This approach is being investigated in the research and development of new generations of bioceramics with an expanded range of medical applications. Clinically, the most widely used materials at the moment are those chosen from a handful of available and well-examined biocompatible ceramics, metals, polymers, and their combinations as hybrids or composites.

Despite the fact that bioceramics are used extensively as implants in dentistry, maxillofacial surgery, and orthopedic, further developments are progressing to increase their functions and achieving improvements in their reliability as well as performance. Above all, the properties, applications and performance of these bioceramics or biomaterials within the human body are determined by the way they are produced and manufactured.

The manner in which the mechanical stresses are transferred to the surrounding bone tissue without producing forces that could endanger its durability is one of the key criteria that determine how successful an implant or prosthesis is from a clinical perspective [1]. Gaining an in-depth insight into the how stresses acting

on the implant/prosthesis are transferred to the surrounding bone structures and the resultant deformation is of utmost significance in the field of prosthetic replacement where the primary intention is to restore the biofunctionality of a patient by replacing damaged bone structure.

In addition to the issue concerning biofunctionality, surgeons and implantologists have recognized the problems associated with the design and materials selection even at the initial stages of this field that resulted in premature loss of implant function due to corrosion, inadequate biocompatibility, or mechanical failure of the component. It is worthy to mention that when investigating the durability of a biomedical material, toughness is a vital mechanical property that needs to be considered which describes the capacity of a material to absorb energy during deformation until the point of fracture.

In comparison to ceramic materials, the high toughness of metals such as titanium and its alloys (e.g. Ti-6Al-4V) can be considered to originate from their crack-tip plasticity. Even though a certain degree of plasticity can also take place at the tip of a crack in a ceramic material, the energy absorption nevertheless is relatively small. As a result, ceramic materials have low fracture toughness (K_{IC}) values, which is a measurement of toughness. For most ceramics including alumina and zirconia, the fracture toughness values are approximately one-fiftieth of those of ductile materials such as titanium (Table 1.1).

The first part of the two-part chapter aims to give an overview of the different types of biomaterials and bioceramics as well as their production technique that are currently used in a number of clinical applications in dentistry and orthopedics. A brief insight into the nature, morphology, and application of marine-derived biomaterials are also provided.

Table 1.1 Comparison between the physical and mechanical properties of biomaterials and human bone tissues [2–6]

	Density	Facture toughness	Tensile strength	Compressive strength	Young's modulus
Units	g/cm^3	MPa $m^{1/2}$	MPa	MPa	GPa
Metallic					
Ti-6Al-4V	4.43	44–66	900–1172	450–1850	114
Bioceramic					
Alumina (Al_2O_3)	3.98	3–5.4	282–551	4400	420
Bioglass® 45S5	–	0.7–1.1	42	500	35
Hydroxyapatite (3% porosity)	–	3.05–3.15	38–48	350–450	7–13
Zirconia (TZP)	5.74–6.08	6.4–10.9	800–1500	1990	210
Human bone tissues					
Cortical bone	1.7–2.0	2–12	82–114	88–164	3.8–11.7
Cancellous bone	–	–	10–20	–	0.2–0.5

1.2 Bioactive, Bioinert, and Bioresorbable

Human tissues react toward these synthetic materials in several ways once they are implanted into the body. The response on the surfaces of implants depends on the mechanism of tissue interaction at a nanoscale level. As a result, three terminologies have been defined which illustrates the responses of tissues towards a biomaterial (Fig. 1.1).

A material can be categorized as bioactive if it will interact upon being implanted into the human body with the surrounding bone tissues and in some cases, with

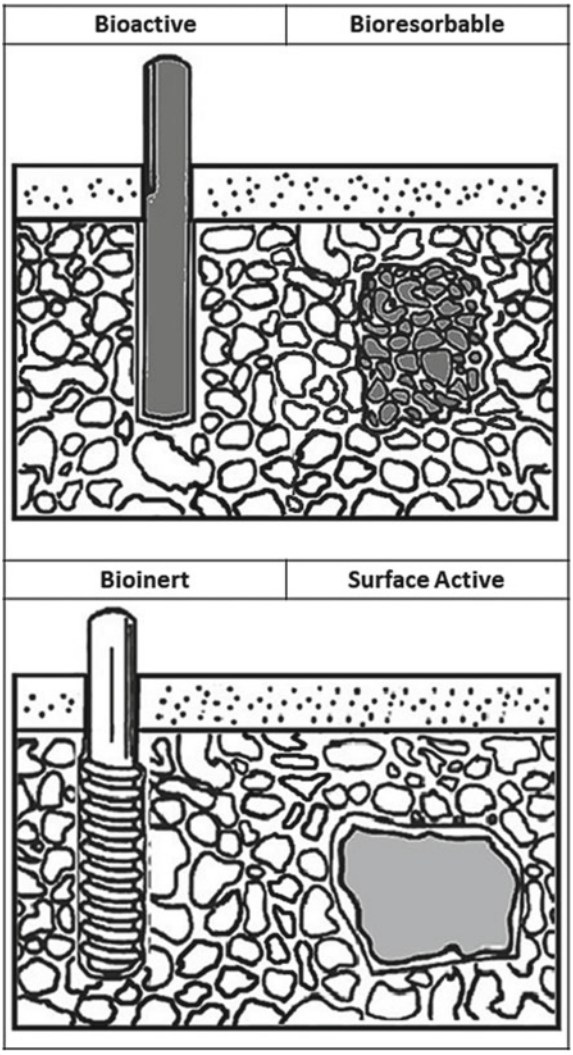

Fig. 1.1 Bioactivity of biomaterials based on tissue responses

soft tissues as well. Similarly, if a material begins to be resorbed or dissolved and replaced gradually by the advancing tissue upon placement within the human body can be referred to as bioresorbable. Human bone tissues and bioceramics such as bioglass are examples of bioresorbable materials. It should also be mentioned that calcium phosphate ceramics are referred to be as both bioactive and bioresorbable.

On the other hand, biomaterials such as titanium, stainless steel, alumina, partially stabilized zirconia, and ultra-high-molecular weight polyethylene are classified as bioinert as they will interact with the surrounding bone tissues minimally after they are inserted into the human body.

1.3 Bioceramics Production Techniques: Traditional to Recent Advancements

As mentioned previously, the method by which biomaterials and bioceramics are manufactured or synthesized will determine their applications and properties in addition to their performance within the human body. Further developments are in progress to expand their applications and attain improvements in their reliability and performance despite the fact that they are utilized extensively for dental implants and as implants in orthopedics and maxillofacial surgery.

The application of ceramics in the areas of orthopedic and maxillofacial implants has conveyed the common reaction that the appropriate use of ceramics can address numerous challenges which exists in surgery since its introduction in the early 1970s. The main intention of generating requirements governing the use of medical grade bioceramics is to distinguish ceramics that are bioinert to a human body for a period of more than a decade. The establishment of such prerequisites is vital given to the fact that these bioceramics are utilized to reconstruct and repair deceased and damaged tissues of the musculo-skeletal system [7].

Bioceramics are used in a number of applications because of their unique physical, thermal, and mechanical properties. However, their strength, density, wear resistance in addition to biocompatibility are more important when they are used in dentistry, orthopedics, or in biomedical applications in general. As a physical property, density is essential. Open porosity is often a crucial measurement and is an important density parameter. The porosity is calculated from the volume of pores present with the material. Open porosity can reduce the strength of a ceramic material and consequently it can have a strong effect on the properties of a ceramic material.

Furthermore, open porosity also allows gases or liquids to permeate into the ceramic. In view of that, it is often essential to determine the density in addition to ascertaining the nature of porosity. According to an investigation by Willmann [8], bioceramics must possess high resistance against corrosion within the human body environment. These issues can be addressed by using high-purity oxide ceramic synthesized from purified raw materials that are free of impurities such as alkaline oxides and silicate.

1.3.1 Hot Pressing and Hot Isostatic Pressing

Hot and cold isostatic pressing as well as wet chemical processing techniques such as co-precipitation and sol–gel are the manufacturing methods most widely used to produce bioceramics along with nanoparticles, nanostructured solid blocks and shapes, and nanocoatings. Pressing in modern ceramic technology involves placing ceramic powders into a mold or cast and compaction is reached through the application of pressure (Fig. 1.2). Hot pressing and hot isostatic pressing are two of the most commonly used approaches in the manufacture of bioceramics.

For the applications of bioceramics in the medical and dental arena, hot isostatic pressing (HIP) can produce ceramics with smaller grain structures and higher densities, both of which are crucial requirements. The process involves pressure and heat applied simultaneously. Pressurized gas such as helium or argon is used to apply pressure from all directions. On the other hand, hot pressing (HP) is a versatile and simple method where pressure is only applied in a uniaxial direction. This technique is capable of producing non-uniform components as well as flat plates or blocks without difficulty.

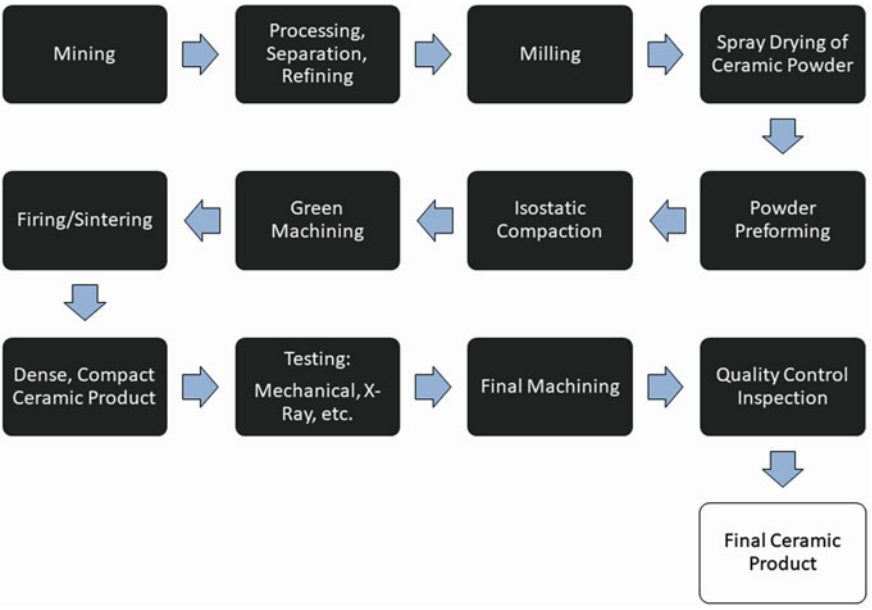

Fig. 1.2 Typical production process of bioceramics

1.3.2 Computer-Assisted Manufacturing

Computer-assisted manufacturing (CAM) together with computer-aided design (CAD) have attracted a great deal of attention over the past thirty years since its introduction in dentistry during the 1970s and early 1980s [9–15]. Using this approach, dental structures and restorations can be manufactured with a great deal of accuracy and relative ease.

In essence, the following stages are involved in the production of a component using CAD/CAM technology [3]:

(1) The relevant data is captured using imaging technologies such as x-ray or CT scan. The captured geometrical data is transformed to digital data using a digitalization tool enabling the data to be processed further using CAD software.
(2) The captured data is used to construct three-dimensional models along with other essential structures such as abutments and crowns utilizing relevant databases and computer design software; and
(3) The production of the designed component using a computer-assisted grinding unit and/or milling machine. Normally, the starting material is a prefabricated block of a certain material and composition such as ceramics (e.g. zirconia and alumina), resin materials, and metals (e.g. titanium and its alloys).

1.3.3 Three-Dimensional (3-D) Printing/Selective Laser Sintering

The manufactures of ceramic components containing complex shapes are made possible in recent times as a direct result of the emergence of three-dimensional (3-D) printing technology and selective laser sintering (SLS). Presently applied for polymers (SLS and stereolithography) and for metals (selective laser melting), 3-D printing has permitted engineers and researchers in the dental, orthopedic, and biomedical arenas to examine the production of new materials such as bioceramics. This approach will be applied in great frequency in the years to come in applications such as bone grafts and in drug delivery to treat post-operative bone infections [16–21].

There are a number of key advantages associated with this production approach including a reduction in the manufacturing cost in addition to the fabrication time. More importantly, it permits the creation of certain shapes that would typically be impossible to manufacture via traditional techniques, which translate to less constraint and limitation placed on the design of the component. This is particularly the case for the production of bone tissue scaffolds where the desired properties such as pore shape and size as well as their interconnectivity are difficult to maintain using conventional production techniques such as freeze-drying [21].

Similar to CAD/CAM technology, 3-D printing can be applied to dentistry and oral and maxillofacial surgery in conjunction with appropriate patient-imaging technology such as CT scans to produce implants and prosthetics with enhancements in dimensional accuracy and surface finish. The result of an animal study has suggested the feasibility of manufacturing site-specific bioceramic scaffolds precisely in clinic to treat alveolar bone defects using 3-D printing technology based on CT scans of individual patients [16]. The result of an in vitro study has also suggested the feasibility of using 3-D printed bioceramic scaffold where they can imitate the important benefits of autogenous bone grafts through the encapsulation of mineralizing bone matrix and homogenously distributed terminally differentiated osteoblasts to treat segmental discontinuity bone defects after surgical implantation [17].

The biggest drawback in spite of the key advantages this manufacturing technique has to offer that needs to be resolved is posed by the materials used. Different to 3-D printed metallic and polymeric components, items manufactured from ceramics using this technology are not "ready-to-use" as post-treatments such as sintering and thermal treatments for debinding at high temperatures are required to increase their strength and to reach acceptable mechanical properties. The use of sintering also poses a problem if 3-D printing is used to produce bioceramics-based components intended for drug-delivery applications as the elevated temperature use during firing process might destroy the bioactivity of the incorporated drug [20].

Physical properties such as high melting temperature poses a challenge for the SLS of ceramic components, hence gaining an in-depth insight into the interactions between the ceramic material and the laser beam could result in the optimization of process control through simple adjustments in parameters such as laser power and exposure time [22, 23]. Furthermore, vital processing and materials issues such as energy consumption and scattering of laser, partial melting and dissolution of ceramics needs to be addressed comprehensively to make this technique cost-effective and efficient for the manufacture of bioceramic components [22, 23]. The SLS of ceramics is complex due to the fact that densification is dependent on the microscale interaction between the ceramic particle/binder and the laser beam. Resolving these issues could also assist in the regulation of residual thermal stress that is causing the formation of cracks in a majority of the manufactured ceramic components at the moment, and occasionally their crumbling.

As described earlier, post-thermal treatments such as sintering that are often needed in the manufacture of ceramic components. The process densifies and strengthens the product by reducing the amount of porosity, which results in volume reduction. More importantly, these dimensional changes are difficult to predict and needs to be taken into consideration when designing and producing implants and prosthetics using SLS technique. In addition, undesired fusion of ceramic particles surrounding the surface of the printed component due to energy diffusion and conduction of the laser beam could also lead to inaccuracy in the dimensions of the final product [22, 24].

On top of the issue of dimensional inaccuracies, concerns centered on the surface finish also need to be considered in the production of components using the SLS technique. However, it can be advantageous in the manufacture of bioceramic scaffolds where rough surface finish is desirable from a biological perspective [23, 25].

The surface of the finished components can also suffer from a phenomenon known as the "staircase effect". This is due to the fact that the component is constructed layer by layer and each layer has to be as thin as possible so that it cannot be distinguished from one another. Poor surface finish could compromise the mechanical properties of the product. Moreover, the addition of an extra step involving polishing or grinding the manufactured component to the production process is needed due to bad surface finish. Consequently, it is possible to reduce the size of the minimal constitutive element of the printed component and ultimately the surface finish by optimizing the shape and size of the starting materials, process parameters such as laser power, and the systems involved in the manufacturing process. A solution to improving the viscosity of the slurry or increasing the absorbance of a laser beam can be found through the advancements in materials science and engineering.

1.3.4 The Sol–Gel Technique

A solution-based synthesis approach known as sol–gel offers a relatively promising and new technique in the manufacture of bioceramic materials such as blocks and thin films. The uniqueness of this methodology lies in its capacity to produce coatings, platelets, powders, monoliths, and fibers of the same composition simply by altering the processing parameters such as viscosity and chemistry of a given solution [3]. In addition, the variety of different compositions that can be synthesized includes mixed oxides, single oxides, as well as non-oxides such as chlorides, nitrides, and borides.

The history of the sol–gel approach and in particular for oxide coatings dates back to the dawn of chemistry. It was first discovered as an application technology in 1846 when the hydrolysis and polycondensation of tetrathylorthosilicate (also referred to as tetraethoxysilane) was observed by Ebelmen [26]. The potential of sol–gel technology was recognized during the production of high-purity glasses since traditional ceramic processing methods were not adequate in the mid-1950s, and as a result, the ideal of utilizing sol–gel technique to manufacture multicomponent and homogeneous glasses was born [27].

Since then, the sol–gel technique has been utilized in a number of high-technology arenas during the late 1980s and 1990s such as in the electronic, laser, and optoelectronic industries [28–30], in the stabilization of radioactive isotopes [31], and in dentistry and orthopedics [32–39].

Compared to conventional ceramic processing techniques, sol–gel syntheses of coatings, spheres, and powders have a number of advantages such as (Fig. 1.3) [40]:

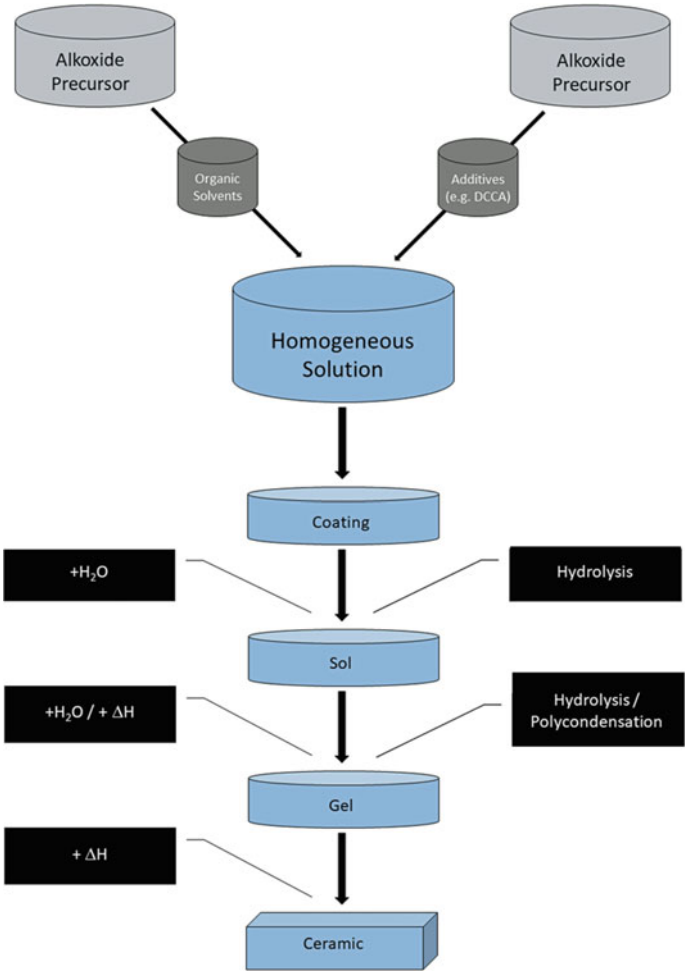

Fig. 1.3 The synthesis of a thin-film ceramic coating via the sol–gel approach

(1) Using simple solutions, coatings, spheres, powders, and fibers can be easily prepared.
(2) Powders possess a high surface-to-volume ratio and therefore a lower sintering temperature will be required to produce ceramics with uniform fine-grained structures and densities near the theoretical values.
(3) The avoidance of grinding translates to the manufacture of a high-purity product.
(4) Increased chemical homogeneity down to atomic scale for aqueous systems where a sol is formed, or molecular scale for alkoxide solutions if liquids have a similar rate of condensation and hydrolysis.

On the other hand, there are several issues concerning the manufacturing of monoliths via this technique [41]:

(1) Removing the volatiles used during the process in an effective manner.
(2) The costs of precursors are relatively high.
(3) During the formation of monolithic solids, there are issues related to the amount of shrinkage and the resultant drying stresses.

1.4 Ceramic Nanobiomaterials, Nanocomposites, and Nanocoatings: Clinical Applications

Throughout the past decade or so, there has been an increase in interests in nanostructured materials for advanced technologies. The current focus in on the manufacture of nanobioceramics and nanocoatings that is applicable in dentistry and orthopedics.

By definition, nanostructured materials refer to a variety of materials that comprises of delicate sizes and structure which falls between 1 and 100 nanometer (nm). A huge development of nanotechnology has been recognized, but nonetheless, such developments have not come as a surprise when it is valued that these nanostructured materials display the capacity to be adapted and integrated into biomedical devices. This is possible since a majority of biological systems such as protein complexes, membranes, and viruses exhibit natural nanostructures.

The microstructure and properties of nanostructured materials are strongly dependent on their processing route as well as their method of synthesis. As a result, it is of vital importance to choose the most appropriate technique in the production of nanomaterials with the preferred property and/or a combination of properties. Future developments are in progress to extend the applications of nanobioceramics and attaining improvements in their reliability and performance even though they are used extensively in dentistry as dental implants, maxillofacial surgery, and orthopedics.

1.4.1 Surface Modifications

A number of tissue responses can occur at the interfaces between hard and soft tissues and the implanted biomaterial (or bioceramic) after surgical implantation. The rate of success of a dental or orthopedic implant is dependent on a number of issues such as the design of the prosthetics, the choice of the material as well as their properties and structures, the way stresses and functional loadings are transmitted from the implant to the surrounding tissues, the surgical technique and procedure used, and the medical and health of the patient.

Regardless of the implant design and materials used, the prevention of inflammatory responses is a critical requirement for any dental and orthopedic implants or prosthetics. In addition, it is also essential for an implant to promote osseointegration and provide sufficient biological fixation.

Problems and concerns related to biological interactions and adhesion to enhance the reliability and longevity of implants and prosthetics over the past thirty years or so have inspired the search for surface modification techniques concerning rapid healing, early osseointegration, and bone-implant adaptability. Applications of surface micro- and macro-texturing as well as utilizing biological and chemical approaches to increase the bioactivity of surfaces of implants has been the primary concern for a large number of research groups within the surgical and biomedical arenas.

Presently, bioinert metals such as titanium and its alloys in addition to cobalt chromium alloys are being used to manufacture dental and orthopedic implants. At present, there are two different techniques normally used to surgically insert orthopedic implants. The first method uses bone cement (primarily poly(methyl methacrylate) or PMMA) for strong adhesion. The second technique utilizes calcium phosphate micro-textured or pre-coated implants to achieve chemical bonding and mechanical interlocking. Concerns centered on the fact that metals do not chemically bond to bone tissue led to the necessity to carry out surface modification prior to surgical implantation. This approach is extensively used on dental and maxillofacial implants in addition to orthopedic prostheses.

Biological fixation is a term used to define the process in which the implant or a prosthetic device is attached firmly to the host tissue through bone-ingrowth with or without the aid of mechanical fixation. Most importantly, the fixation is carried out without the use of any adhesive.

Mechanical interlocking is an added advantage of macro- or micro-texturing. This can be accomplished by fixating wires or beads to the surfaces. Another method is to fabricate porous surfaces in such a manner that they contain suitable surface pores. As a result, the surface areas of these structures are increased and consequently the magnitude of fixation. Similarly, chemical bonding to the surrounding bone tissue under certain conditions can be achieved with implants that has undergone surface modifications. One such approach is to coat the surfaces with bioactive and bioresorbable materials such as calcium phosphate.

The applications and depositions of coatings, irrespective of micro- and/or nanocoatings, on implants and prosthetics is intended to enhance its bioactivity and prevent the release of metal ions and to protect the implant material against biodegradation where possible. Ultimately, this results in a better environment and structure for the growth of new bone tissue [3, 34–39]. In most cases, bioactivity can be improved through the deposition of calcium phosphate coatings in addition to micro- and macro-texturing even though the most vital aspect on bone attachment is the size of the micropores as they are the determining factor related to mechanical attachment and bonding.

Depending on the thickness, both non-metallic and metallic coatings can be categorized as nano-, micro-, and macrocoatings. Scientific representation is typically diversified in relations to the definitions of nanocoatings and thin film coatings. It is debatable as to which term is more suitable as there is no known or widely accepted definition, and consequently, both are used interchangeably.

Thin films with thicknesses less than 1 micron (the range of micron-sized coatings) can be classified as nanocoatings. They may contain isotropic and homogeneous compounds. In general, the thickness of a single-layered coating is below 100 nm. On the other hand, multi-layered coatings can be deposited relatively easily with appropriate biological, physical, mechanical, and chemical properties. Furthermore, multi-layered coatings can be synthesized as nanolaminates containing different compositions or as multi-layered gradient coatings. As previously mentioned, the microstructure and properties of nanocoatings are influenced by issues such as their structure, chemical composition, and thickness in addition to their synthesis and deposition techniques. There are several advantages of using nanocoatings such as purity because of the selection of raw ingredients, variety of deposition methods, the ease of synthesis, capacity to be amalgamated with other compounds or nanoparticles, and their low cost as only small quantities of starting materials are needed for coating process [3, 34–39].

For more than fifty years, titanium and its ternary alloys such as Ti-6Al-4V have been used successfully as implant materials in dentistry, their utilization in orthopedic joint replacement however have been linked to aseptic inflammation. The inflammation was thought to be the result of titanium particles being released into the surrounding micro-environment from the surfaces of implants [41]. The results of a recent study have revealed that particles could be released in a surface type-dependent manner during ultrasonic scaling of titanium implants that may aggravate peri-implantitis [41]. The depositions of bioceramic micro- and/or nanocoatings on these materials are intended to provide safeguard against the release of metal ions, which could bring about a negative host response.

The study by Hench [42] has suggested that an ideal environment for bone growth can be reached and for an implant coated with a biocompatible material to be considered successful from a clinical perspective, the following conditions need to be met:

(a) A reduction in the release of metal ion;
(b) The formation of good mechanical interlocking; and
(c) The availability of a bioactive surface for chemical and biological bonding to take place.

Extensive bone apposition in animal models has been observed after the insertion of implants coated with calcium phosphate. The primary purpose of utilizing calcium phosphate as a bioactive coating is to create a rapid and strong biological attachment to both soft and hard tissue. It was believed that the calcium and phosphate ions released from the coating might stimulate and/or facilitate the growth of new bone tissue on and toward the implant and this in turn support the development of excellent interfacial strength at the implant-tissue interface as a result of these biological interactions.

The solubility of the coating and the rate of bone growth must reach an equilibrium to achieve mechanical integrity under functional loading. Once this integrity is reached, there should be sufficient bonding as well as mechanical properties at

the tissue-implant interface to determine the long-term survivability of an implant or prosthesis [3, 34–39].

Plasma or thermal spraying is by far the most commonly used technique for the deposition of calcium phosphate micron-thick (between 30 to 100 μm) coatings on a commercial scale even though there were serious issues associated with their extensive utilization such as their inadequate bonding strength to the implant surface and the coatings produced is usually non-uniform and contains a mixture of amorphous and crystalline phases resulting in variable solubility. On the other hand, new generation nanocoatings (with thicknesses between 70 and 200 nm) can generate without any difficulty permanent mechanical and chemical bonding once they are deposited onto macro- and micro-textured surfaces. In spite of this, bone mechanical interlocking cannot be generated owing to the thickness of the coating [3, 34–39].

The quality and long-term performance of a calcium phosphate-coated implant are governed by factors such as surface roughness, thickness and crystallinity of the coating, constituent phases, general design of the implant or prosthesis, and the biomechanical functional loading. Synthesized in an acceptable manner, implants nanocoated with calcium phosphate heal faster and display improvements in bone attachment as a consequence of nanostructured grains (Fig. 1.4). Furthermore, the chemistry and surface topography of calcium phosphate crystals within the deposited coating on implants display acceleration in early bone formation and increase in bond strength at the bone-implant interface [3, 34–39].

Histomorphometric and histologic observations showed the formation of new bone around dental implants with nano-sized calcium phosphate particles added to the dual acid-etched surface placed in the human posterior maxilla after two months

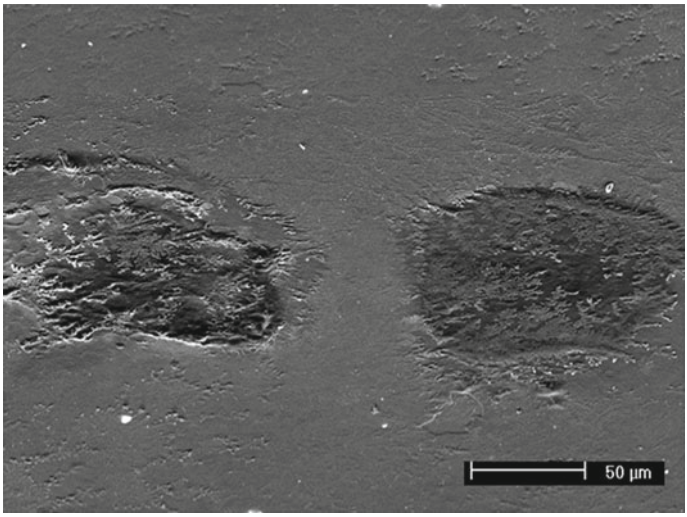

Fig. 1.4 Calcium phosphate nanocoatings after in vitro testing with osteoclasts

of healing, suggesting the nanometric particle deposition of calcium phosphate crystals could be beneficial in reducing the healing period after implantation and thus providing earlier fixation [43]. Further evidence supporting the fact that the osseointegration process is enhanced due to the deposition of nano-calcium phosphate on the surfaces of implants is provided by Jimbo et al. [44]. Gene expression and conventional removal torque evaluation in tissues around nanostructured calcium phosphate-coated implants were compared using real-time reverse transcription with those of uncoated implants inserted into a rabbit model. After three weeks of healing, the tissue quality was found to be improved significantly around the coated implants based on the results from nanoindentation testing. Osteoprogenitor activity after two weeks as well as a significant up-regulation in alkaline phosphatase (ALP) and osteocalcin in the coated implants were observed after four weeks post-implantation. The latter observation suggested progressive mineralization of the bone around the implant. Furthermore, an osteoclast marker adenosine triphosphatase was noticeably higher for the coated implants, suggesting gradual resorption of the calcium phosphate.

The connection between various re-precipitation and dissolution properties of calcium phosphate micro- and nanocoatings with different crystallinities and early bone formation and bonding has also been studied in addition to the effects of surface chemistry and morphology [45]. This hypothesis was supported in a study aimed at gaining an insight into the effects of nanostructured poorly crystalline calcium phosphate nanometer thick coatings on in vitro cellular behavior in which these nanocoatings were found to stimulate the proliferation and attachment of primary dental pulp stem cells and NCTC murine fibroblasts [46]. The outcome of an in vitro investigation of titanium implants coated with calcium phosphate revealed human osteosarcoma HOS TE85 cells attached and proliferated better and expressed alkaline phosphatase (ALP) and osteocalcin to a greater degree on micro-coatings with higher crystallinity when compared to poorly crystallized coatings. Moreover, cell attachment was enhanced on rough coatings but similar results on the ALP and osteocalcin expression level were observed when rough coatings were compared with smooth coatings [47].

1.4.2 Dentistry

The advancement of nanotechnology has revolutionized the field of dentistry and this led to major improvements in materials and their clinical applications. Thorough examinations have been carried out on nanocomposites, nanocoatings, and other nanostructured materials from its improved biological behavior to mechanical properties and cytotoxicity for a number of applications in dentistry and maxillofacial surgery.

A number of special requirements and challenges govern the clinical application of composites posed by the conditions within the oral environment. From the biological perspective, incompatibility can arise from issues such as residual monomers,

polymerization shrinkage, short fibers, but also from nanomaterials and nanoparticles. For instance, an indirect correlation exists between polymerization shrinkage and tissue compatibility. Furthermore, residual monomers may cause a number of adverse biological reactions. Depending on the type of filler material used, they can also play a part in cytotoxicity. In an oral environment, resin-based composites could also be responsible for promoting bacterial growth and this can be the result of a change in volume leading to a marginal gap between restorations and tooth tissue [48].

1.4.2.1 Dental Restorations

The application of composites in dentistry has been widely accepted and utilized as a substitution for metallic restorations. There has been a significant evolution in the composition of resin-based dental composite since its introduction. Resin composites are used for several areas such as pit and fissure sealants and cement for tooth prostheses. To achieve an ideal tooth restoration, a number of issues need to be considered such as restoring the function and aesthetics while at the same time protecting and strengthening the remaining tooth structure. In addition, problems such as leakage should be avoided [49, 50].

Over the past two decades, there has been growing interest in the development of a new composite consists of simply nanoparticles known as nanofill composite. Furthermore, a new category of composite referred to as nanohybrids were developed by combining conventional and nanoscale fillers [51]. Moreover, nanohybrid composites contain a larger range of particle sizes [52]. As mentioned previously, constant improvements and modifications have taken place frequently with resin-based dental composites and the notion behind the development of nanohybrid composites is to provide a solution which is comparable to that of microhybrid composites in terms of strength and superior surface finish (Fig. 1.5) [53, 54]. A number of in vivo and in vitro clinical trials and studies have been carried out to determine the significance and difference between nanofill and nanohybrid composites containing nanoceramic fillers in dental restorations [55–61] and their performance in wear and abrasion resistance as well as surface texture or roughness after activities such as toothbrushing [62].

In addition to reducing the rate of restoration fractures [63], the prevention or inhibition of recurrent dental caries or secondary caries could improve the longevity of composite restorations. One such approach has been the incorporation of amorphous calcium phosphate nanoparticles into a dental resin [64–66]. It has also been suggested that the release of calcium and phosphate ions from the composite can remineralize tooth enamel and dentin lesions in vitro [67, 68].

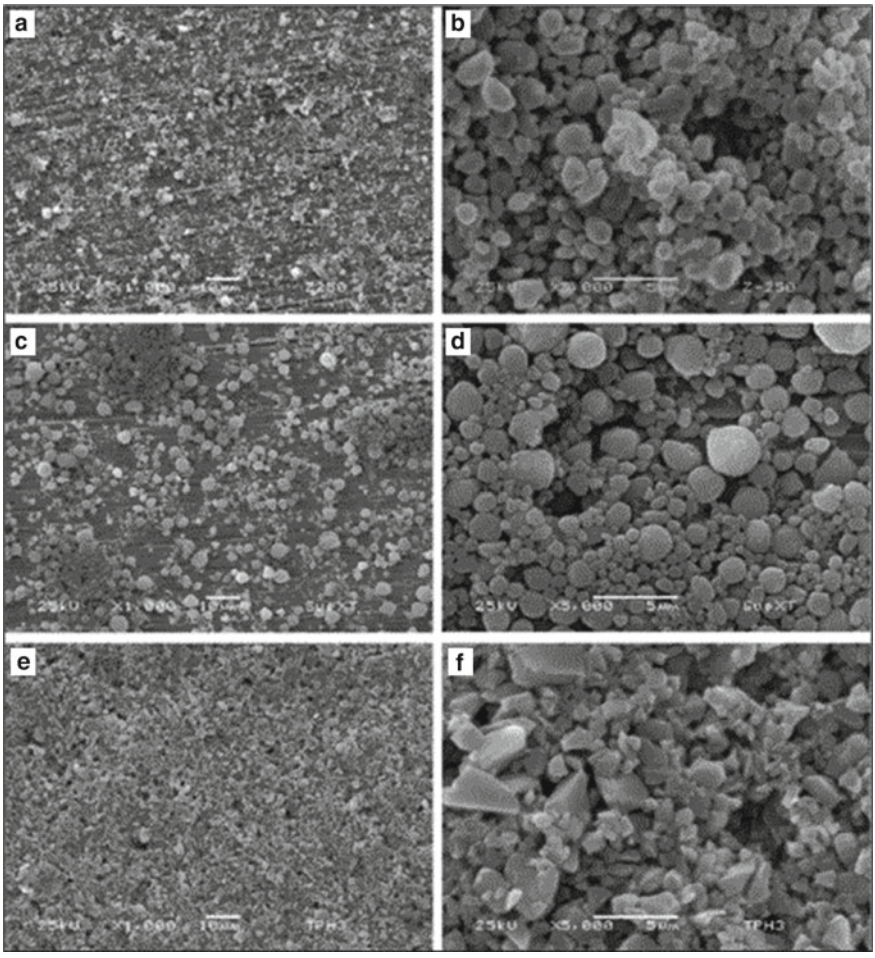

Fig. 1.5 SEM pictures of inorganic fillers. **a** and **b** round-shaped small and medium particles are predominant within microhybrid composite; **c** and **d** nanofilled composites with round-shaped clusters; **e** and **f** irregular-shaped small and medium particles are present within nanohybrid composite. Reprint with permission from [54] (This is an Open Access article: verbatim copying and redistribution of this article are permitted in all media for any purpose, provided this notice is preserved along with the article's original URL (https://meridian.allenpress.com/operative-dentistry/article/34/5/551/107012/Nanohybrid-Resin-Composites-Nanofiller-Loaded))

1.4.2.2 Dentin-Related Issues

During the past decade, a number of professional and consumer products containing bioactive glass have been introduced into the market to treat dentin hypersensitivity [69, 70]. By definition, bioactive glasses are a category of biomaterials that are capable of bonding to both hard and soft living tissues via the creation of a hydroxycarbonate apatite layer on the glass surface [71–73].

Techniques such as sol–gel and spray drying have been used to produce nanoscale bioactive glasses and one approach currently used to manufacture nanoparticles of bioactive glass are based on heating metal–organic precursor compounds through flame spray technology to temperatures above 1000 °C. The formation of molecular nuclei followed by condensation and coalescence is the basic principle behind all gas phase synthesis approaches and the growth of nanoparticles are stimulated by the high temperatures used during the process [74, 75]. Compared to other gas phase techniques, the advantage of the flame spray approach is based on the notion that additional energy is not required for precursors despite the technique is energy intensive. Utilizing the flame spray approach, nanoparticles of bioactive glass between 20 and 50 nm in size were successfully produced and after human dentin were treated with these nanoparticles, it was reported that a noticeable increase in mineral content was observed suggesting rapid remineralization [76].

The regeneration of dental pulp tissue has been a continuing challenge in regenerative dentistry. A three-dimensional nanocomposite scaffold that combines a nanobioceramic such as bioactive glass nanoparticles with a biodegradable and biocompatible polymeric matrix would be an ideal candidate for dental pulp regeneration by uniting the advantages of the two materials where the bioceramic would improve the bioactivity and the polymer would improve the toughness of the resulting nanocomposite [3, 77, 78]. It has been suggested that the incorporation of bioactive glass in a collagen-based nanocomposite could provide an ideal scaffold condition for the regeneration of dentin-pulp complex tissues based on the observations that the nanocomposite is capable of stimulating the differentiation of odontoblastic genes such as dentin sialophosphoprotein and dentin matrix protein I more significantly than just with collagen [79]. Later, the behaviors of human dental pulp stem cells on nanobioactive glass-based nanocomposites with various biopolymer mixtures have been examined and their possible applications in regenerative endodontics investigated [80, 81].

1.4.2.3 Dental Implants

Dental implants can be considered as the nearest equivalent to the replacement of natural tooth and as a result, they are a useful addition in the management of patients who have missing teeth due to developmental anomalies, trauma, or diseases. There are a number of dental implant systems that offer predictable long-term results supported by excellent clinical trials and scientific research. It is of vital importance to establish success criteria for implant systems and for implants to be examined in well-controlled clinical trials [3, 32, 82].

Aluminum oxide, or more commonly known as alumina (Al_2O_3), is the most widely utilized ceramic oxide materials. Medical-grade alumina has very small grain size, a narrow grain-size distribution, and the concentrations of sintering additives are extremely low. Under mechanical loading, such a microstructure is able to prevent static fatigue and slow crack growth. Developed as an alternative to surgical metal alloys, high-purity alumina with a purity of 99.99% has been used in dentistry as

early tooth implants (Tubingen implant) and in orthopedics specifically as femoral head and acetabular components in total hip replacements [2]. Utilizing alumina in articulating surfaces is ideal due to its excellent corrosion and wear resistance, high hardness, and low friction coefficient.

The application of zirconium dioxide or more commonly known as zirconia (ZrO_2) took place after alumina is utilized as a biomaterial and in particular a bioceramic. Even though zirconia is a term that has been widely used in the medical industry, the zirconia product that is used is in fact partially stabilized zirconia or PSZ. Depending on the country of origin, synthesis approach, and on the application, PSZ is a mixture of zirconia with either magnesia, calcia, or yttria [3]. Similar to alumina, PSZ has been widely accepted as a ceramic biomaterial and is frequently used in implant dentistry as whole dental implants and not only as dental implant abutments [82–85].

Both alumina and PSZ have certain possible disadvantages despite the fact that both bioceramics are effective for clinical applications. For instance, alumina is a brittle ceramic with a likelihood of fracture even though it exhibits excellent hardness and wear properties, and this combination of hardness and brittle behavior results in the emergence of certain design restrictions. PSZ, on the other hand, possess only half of the hardness of alumina but its fracture resistance can be enhanced through transformation toughening. This means that the overall toughness and bending strength of PSZ are substantially much higher than alumina. Ideally, the development of a ceramic that combines the best properties of both alumina and zirconia would be perfect.

Presently, the focus of research is centered on one category of PSZ referred to as tetragonal zirconia polycrystal (TZP). The manufacture of TZP is achieved by adding metallic oxides such as yttria or ceria to zirconia. Currently, the main type of zirconia used for medical purposes is yttria-stabilized TZP. This is based on the observation that the mechanical properties can be improved when yttria is used to stabilize zirconia in comparison to other metallic oxide combinations [85]. The amount of yttria in TZP is only approximately two to three mol% [86, 87].

The "transformation toughening" effect is an important feature of yttria-stabilized TZP ceramic. The desirable tetragonal phase comprises of arrays of sub-micrometer-sized grains. As soon as zirconia transforms from tetragonal phase to monoclinic phase, there is a net volumetric expansion in the ceramic grains and this could place the surface of the ceramic into a compressive stress state that assists the material to resist the formation of cracks as well as their propagations. It has been previously reported that the thickness of this residual compressive stress layer is several micrometers [88, 89].

This "metastability" is the reason behind the very high fracture toughness and strength of yttria-stabilized TZP. Furthermore, it is also possible under certain synthesis conditions or more severe environmental conditions of moisture and stresses in which yttria-stabilized TZP is transformed to the monoclinic phase in an aggressive behavior with catastrophic results. Obviously, such a "high metastability" is undesirable for medical implants [86].

In addition to yttria, ceria has also been used as a substitution metallic oxide to stabilize zirconia. In 1998, a new nanocomposite composed of ceria-stabilized

tetragonal zirconia polycrystal and alumina was developed by Nawa et al. [90] known as NANOZR and their potential use as dental implants been investigated in a number of studies [91–95]. According to Nawa et al., NANOZR consists of an intragranular microstructure where alumina nanoparticles were trapped within the zirconia grains and during the sintering process, elongated alumina-like phases are created at the zirconia grains boundaries that were *in-situ* precipitated [90]. Compared to yttria-stabilized zirconia, NANOZR has higher strength as well as fracture toughness [94]. A study by Takano et al. has revealed that the cyclic fatigue strength of NANOZR as specified in ISO 13356 for surgical implants was more than double to that of yttria-stabilized zirconia [94]. Various investigations have also been carried out to study the relationships between surface treatment and roughness on the bioactivity and osseointegration of NANOZR in vitro and in vivo [91–93, 95]. Recently, a study by Komasa et al. proposed the use of an alkali treatment on the surfaces of NANOZR implants could promote the formation of hard tissues surrounding the implant as demonstrated by the amount of new bone around the implant was higher than the untreated samples after implantation into the femur of Sprague–Dawley rats [91].

1.4.3 Delivery Vehicles

The main purpose of a delivery vehicle is to transport bioactive molecules and medically active substances to certain sites within the human body and releasing the encapsulated payload in a controllable manner. For many delivery systems currently used however, the pre-loaded molecules are frequently released upon dispersion of the carrier or drug composites in water. It is particularly problematic and undesirable with this type of premature release specially if the pre-loaded substance (for example an anti-tumor drug) is cytotoxic and could possibly harm healthy tissues and cells before being delivered to the intended site [96].

1.4.3.1 Liposomes

Liposomes are synthetic vehicles that can encapsulate and immobilize efficiently a wide variety of drugs and genes with different structures and sizes. They can also be combined with proteins to treat foreign body wounds, cancer, and diseases [97]. More importantly, the encapsulated biological materials such as peptides are protected from damage and degradation by the liposome. In comparison to microemulsion, a greater loading capacity is offered by liposomes especially for water-soluble additives. Furthermore, the pH, hydrogen ion concentration, and other ionic concentration can be regulated without affecting the core of the liposome.

Stimulations for liposomes are gathered from cells and its close similarity to cell boundaries and delineated sacs. Single and multi-layered spherical bilayer vesicles with thicknesses from 40 nm to 50 μm are typically manufactured by mixing amphipathic lipids in a polar solvent. Highly ordered structures are generated by

lipids through the creation of liquid crystals, which can create three-dimensional bi-continuous cubic organizations. These structures showed promise as sustained delivery systems for proteins and peptides [98].

However, a reduction in the usage of liposomes has been witnessed because of issues such as inadequate storage capacity as well as low encapsulation efficiency [99]. Using crystalline materials, liposome-based structures with a higher degree of organizations and stability can be manufactured quite easily. Moreover, modifying the molecular structure facilitates the regulation and adjustment of drug elution and encapsulation properties.

The utilization of selective liposomes that targets specific cell-surface receptors is a vital approach for mobilizing and guiding liposome-based vehicles to a predetermined location. Unlike vesicles and cells, the availability of biorecognition molecules that permits specific targeting in gene and cancer therapies to take place is lacking in any synthetic delivery systems. The most effective strategy to resolve such issue at the moment is through the utilization of recombinant immunoglobulins. The creation of a composite vehicle based on synthetic polyethylene glycol and liposome can produce a delivery system with enhanced capabilities such as higher targeting abilities. In addition to the deposition of a lipid layer, chitosan coating can also yield certain improvements such as increasing the stability of the delivery system and reducing the chance of leakage of the encapsulated substances.

1.4.3.2 Nano-Hydroxyapatite

Issues such as a relatively short blood circulation time have limited the clinical applications of nanoparticle in drug delivery systems despite their small size that allows them to penetrate small capillaries and be taken up by cells. A number of studies have been carried out to design and develop delivery vehicles with long-circulating-time capability. The most effective approach that can be utilized to overcome such problem and to increase the presence of nanoparticles within blood stream for extended periods is to alter the surfaces of nanoparticles using a variety of polymeric macromolecules or biocompatible non-ionic surfactant [100]. The targeting capability and efficiency of a nanoparticle drug delivery system are often hindered by the rapid recognition of the drug delivery system by the human body. Furthermore, effective and suitable surface modification techniques are also crucial to address possible concerns related to toxicity as well as other technical challenges.

In an effort to govern the ease of delivery and dispersion of a substance to the targeted area using bioceramics, the grain and critical pore size are engineered and altered to fall between several nanometers up to microns. Presently, a variety of nanoceramic-based drug, gene, and protein delivery systems are undergoing clinical evaluation [37, 101]. These nano delivery systems, on the basis of their physical size, also possess the extraordinary characteristic of being able to target and control drug release with extremely high precision.

Novel ideas have been created by nanotechnology for the creation of synthetic bone-like nanomaterials. Due to their extremely high surface area, they provide excellent bioactivity and integration into bone. Bone mineral consists of nanocrystals or nanoplatelets that were described originally as hydroxyapatite and is similar to the mineral dahllite. Until now, it is agreed that bone apatite could be better defined as carbonate hydroxyapatite and the composition of commercial carbonate hydroxyapatite is the same as that of bone mineral apatite. A number of techniques such as sol–gel can be used to synthesize nanopowders and nanoplatelets of bone-like hydroxyapatite. Furthermore, the production of bone-like hydroxyapatite nanoparticles and nanopowders have created new possibilities in the advancement of nanocomposites for dental and orthopedic applications [3, 33–39].

Hydroxyapatite, based on the vast number of published data, is classified as calcium phosphate where it belongs and hence hydroxyapatite will be considered as calcium phosphate from the chemical properties perspective even though it has different reactivities and solubilities within the physiological environment compared to other phosphates. Their specific solubilities as well as their capacity to be degraded and replaced by the newly grown bone tissues ascertains their efficacy as a mean of administrating pharmaceutics and/or therapeutics to successfully treat bone diseases [102, 103]. More importantly, these systems in addition to decreasing toxicity to healthy or non-diseased cells possess the capacity to increase drug efficiency. This translates to significant cost savings for the expensive drug treatment that are being engineered and used at present.

Hard-mineralized materials and their derived structures are ideal as replacements for calcified joint and bone tissues as a result of their biocompatibility and bioresorption capabilities. Biphasic calcium phosphate bone substitutes created from a mixture of β-tri-calcium phosphate (β-TCP) and hydroxyapatite are the most promising material that can be utilized in bone replacement surgery as a drug delivery system in calcified tissues [35]. Using a number of different techniques, investigations are being conducted to improve their biological activity since these minerals by themselves are biologically inert.

A problem that has increasingly become essential and important is the joint release of multiple therapeutic drugs and biological molecules within biomimetic drug delivery systems used in bone reconstruction and repair. For instance, the opinion centered on the procedure currently used in the treatment of osteomyelitis is to attain a collaborative balance between promoting bone repair and regeneration and resorbing antibiotics and drugs. This is based on the notion that there is always a persistent and continuous threat from bacterial infection as a consequence of the highly invasive nature of bone surgery [102]. During the production of biomimetic nanoapatite crystals, this concept was applied as these crystals were engineered to release in an amalgamated fashion via the controlled desorption alendronate and anti-metastatic and/or anti-cancer drugs on its surface [104]. Various surface areas and charges of needle- or plate-shaped crystals are used to determine the release rate of the loaded drugs. The ideas provided by biomimetic materials chemistry has created several key advantages that can be applied in the regeneration of calcified tissues [105, 106].

1.4.3.3 Bioceramics for Radiotherapy and Bioimaging

With ceramic materials, the particulate configuration has found uses in both medical and non-medical arenas. In the treatment of tumors located in organs that are supplied by a single afferent arterial blood supply, particles in the form of microspheres are particularly useful. Microspheres and nanostructurally-altered ceramics have been frequently used in the targeted delivery of radiotherapeutic and chemotherapeutic drugs and agents.

Due to their extraordinary properties such as their encapsulation properties, low density, as well as their large specific surface area as a result of the nanolayer-modified surfaces, a considerable amount of attention has been drawn centered on the synthesis of surface-modified hollow microspheres. These microspheres should therefore be extremely valuable for innovative applications such as the delivery of proteins and drugs. The effectiveness of microparticulate materials in certain applications can be vastly enhanced if they can serve as vehicles for biologically active molecules at the same time. Subsequently, an advantage of porous and surface-modified materials is the increase in surface area available, which greatly affects the loading capability and the rate of release.

Generally, a limited or total loss of organ function is the result of the partial surgical removal or an organ touched by cancer that may or may not be recoverable postoperatively. Consequently, the development of a cancer treatment that only destroys cancerous cells would be desirable such that normal and healthy cells can regenerate after treatment and organ function be preserved. Despite the fact that there are great potentials in the use of radiotherapy, the treatment often results in an insufficient dose delivered to cancer cells particularly if the cells are deep-seated since the irradiation is typically applied from an external source. In addition, severe damage to healthy tissues could also result from the irradiation. Consequently, this led to the development and utilization of microsphere in radiotherapy [107–113].

Yttrium oxide glass microspheres ($17Y_2O_3$-$19Al_2O_3$-$64SiO_2$ (mol%)) synthesized through a conventional melt-quench method were applied clinically in an *in-situ* microsphere-assisted radiation technique. Neutron bombardment will activate the yttrium-89 (^{89}Y) within the glass, which is a non-radioactive isotope, to become the β-emitter ^{90}Y with a half-life of 64.1 h. Once they are injected into a target organ, radioactive glass microspheres with diameters between 20 and 30 μm will become trapped inside the small blood vessels inside the tumor and stopping the supply of nutrients. At the same time, they will also deliver a large and localized dose of short-range highly ionizing β-rays. Only minimal radiation damage will occur among the neighboring healthy tissues since the penetration range of β-rays is relatively short in living tissues (around 2.5 mm). Fundamentally, the radioactive ^{90}Y will resides within the microspheres after their administration due to their high chemical durability. This stability also ensures the radioactivity does not affect any nearby healthy tissues. Within 21 days after its initial preparation, the radioactivity of ^{90}Y will decay to an insignificant level, which means the microspheres will become inactive soon after the cancer treatment. Clinically, these microspheres have been applied in the

treatment of liver cancer in several countries including the USA, China, and Canada [112, 113].

In general, the destruction of cancer cells due to an insufficient supply of oxygen via the blood vessels will take place at a temperature of approximately 43 °C. On the other hand, damage to normal cells will only occur once the temperature reaches around 48 °C. Moreover, the nervous system and blood vessels of tumors are poorly developed, and therefore, they can be heated with relative ease than the surrounding normal tissues. Thermal therapy, also known as thermotherapy or hyperthermia, could provide a solution to treating cancer with very little adverse side effects. Methods such as microwaves, infrared (IR) radiation, ultrasound, and hot water have been utilized to heat tumors. However, such methods cannot deliver effective or local heating for deep-seated tumors. The development of ferromagnetic microspheres (with a diameter between 20 and 30 μm) and nanospheres as thermoseeds have been proven to be valuable during thermal therapy for the effective heating of cancers and particularly for those tumors that are located deep inside the body. The ferromagnetic spheres become trapped within the capillary bed of the tumor once they are injected through the blood vessels during thermal therapy. Heat is produced by the spheres through their hysteresis loss once an alternating magnetic field is applied near the tumor site. This causes the tumors to be heated intensely and locally to a stage where the cancerous cells are destroyed [113, 114].

Adding a florescent or luminescent capability to a drug delivery system used in the treatment of cancer will further enhance their in vivo functionality. Apart from being utilized as a coating material on dental and orthopedic implants and prostheses, a variety of calcium phosphate nanoceramic-based drug delivery vehicles are undergoing clinical evaluation at the moment due to their favorable properties in cancer chemotherapy. In biological imaging, quantum dots (QDs) are the most extensively used inorganic nanoparticles presently for fluorescent imaging [115, 116]. The stability of fluorescent nanoparticles such as quantum dots within biological systems compared to organic dyes makes them appealing as biological probes and a constant interest for applications in targeted delivery of therapeutics as well as in diagnostics [117]. On the other hand, concerns arising from their biocompatibility and their short- and long-term toxicity inside the human body owing to the use of heavy metals such as cadmium during the manufacture of quantum dots needs to be addressed before their widespread applications in areas such as sentinel lymph-node mapping and cancer imaging [116].

It has been postulated and proven by LeGeros [118] that a variety of impurity ions can be replaced within the apatite lattice because of their structure. Additionally, it has also been hypothesized that lanthanide ions such as gadolinium (Gd^{3+}) and europium (Eu^{3+}) are recognized to imitate the functions of calcium ions [119, 120]. Consequently, in an effort to reduce the level of cytotoxicity within a physiological environment and to improve biocompatibility, a number of studies have been carried out to investigate the feasibility of incorporating these rare earth elements as well as conjugating and doping calcium phosphate nanowhiskers and nanoparticles with quantum dots and cyanine dyes (such as indocyanine green) for potential applications in in vivo biological imaging (Fig. 1.6) [117, 119, 121–130].

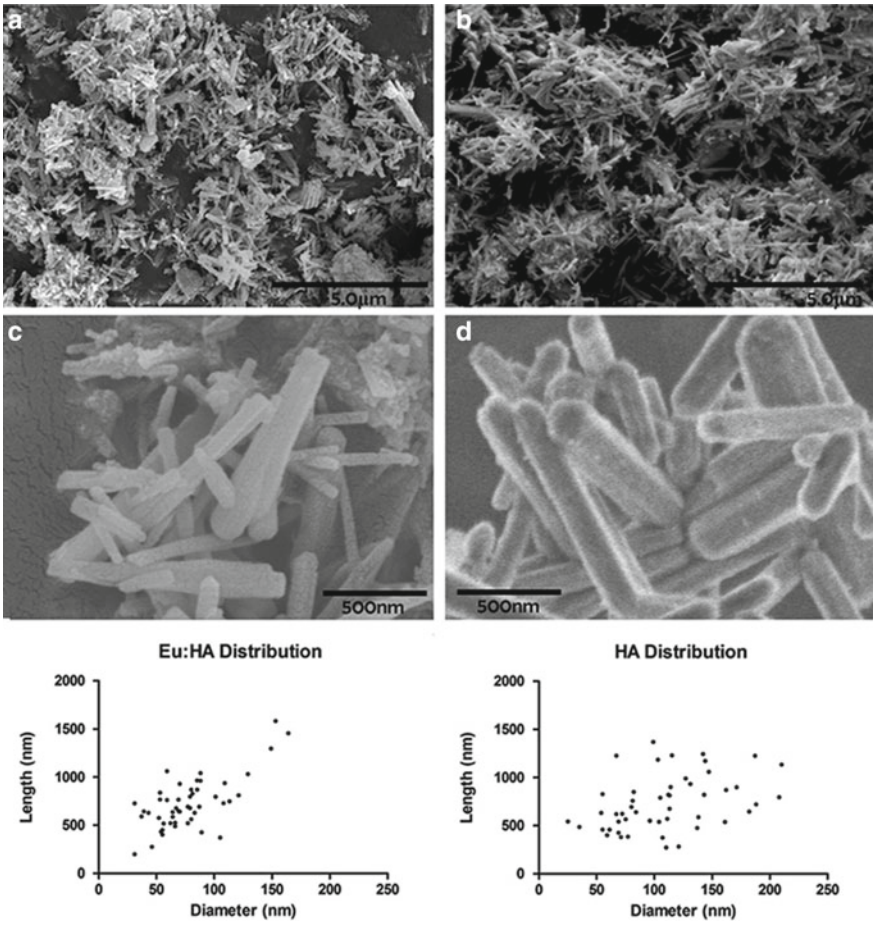

Fig. 1.6 SEM micrographs of **a** and **c** europium: hydroxyapatite nanowhiskers and **b** and **d** undoped hydroxyapatite nanowhiskers. Particle dimension distribution for europium:hydroxyapatite and undoped hydroxyapatite nanowhiskers are also shown with each point represents a single nanowhisker with measurements obtained from SEM images (n = 50). Reprinted with permission from [127]

1.5 Marine-Derived Biomaterials

Desirable properties such as sophistication and complexity are possessed by biomaterials found in nature and we are discovering ways gradually to replicate nature and recreating similar levels of sophistication to a certain degree. For instance, we are only able of recreating microscopic structures with some level of biomimetic detail at the moment using 3-D printing technology. This has been particularly true when it comes to the replication of bioinorganic structures. The use of biological microstructures as templates has emerged as a versatile approach for the recreation of inorganic

structures with identical features. Ordered silica microstructures have been synthesized from bacterial filaments and nanotubes created from tobacco mosaic virus using this approach [131].

Marine organisms are organized and created by materials that comprises of a wide variety of properties and characteristics that might justify the possible application in the biomedical arena. Moreover, the vow to exploit natural marine resources in a sustainable fashion creates an extremely motivating platform for the creation of innovative and novel biomaterials along with both economic and environmental benefits. Hence, different kinds of compounds are increasingly being isolated from marine organisms and transformed into products for various medical applications such as controlled drug delivery devices and in tissue engineering.

The marine environment is distinctively rich in highly functional architectural structures with very fine interconnected pores ranging few hundred microns down to nanometers in size. These marine structures also possess excellent mechanical properties. Above all, several of these marine structures comprises or/composed of inorganic compounds such as calcium phosphates and calcium carbonates containing minerals such as magnesium, strontium, and silicon, which assist in enhancing the properties of hard tissues after implantation. Despite their size, the organic matter within the marine skeletons contains a variety of materials such as protein with very promising possibilities for applications in the medical arena [132–134]. In addition, the high mechanical strength and chemical composition of these marine structures makes them ideal to be utilized in hard tissue replacements in its original form or converted to structures that are more suitable for implantation.

During the last two decades, topics such as soft and hard tissue engineering with more effective designs, discoveries of a new generation of organic molecules, and new pharmaceutical drug delivery systems with enhanced properties have been the primary focus in the field of marine-based structures. The number of studies carried out centered on the applications of biopolymers and proteins produced by marine organisms in the biomedical arena are increasing. Currently, a growing number of materials and compounds such as calcium carbonates and proteins are being identified from marine organisms and applied to the medical field [132, 133].

The earliest marine organisms contain molecules vital for the regulation and guiding bone morphogenesis and particularly the actions accompanying mineral metabolism and deposition. This is based on the discovery and observation that they symbolize the first molecular components known for calcification, morphogenesis, and wound healing. Bone morphogenetic protein, which is the primary cluster of bone growth factors for human bone morphogenesis, has been discovered to be secreted by endodermal cells into the developing skeleton. Off-the-shelf inorganic and organic marine skeletons also possess an ideal environment for the proliferation of added mesenchymal stem cell populations and promoting bone formation, which is acceptable from a clinical perspective.

One of the simplest solutions to critical problems in regenerative medicine as well as supplying frameworks and highly accessible possibilities of osteopromotive analogues, mineralizing proteins, micro- and macrospheres, and nanofibers have

been provided by the design and availability of marine materials. This is demonstrated by the biological efficiency of marine structures such as sponging extracts and nacre seashells to promote bone formation and corals, sponge skeletons, and shells to accommodate self-sustaining musculoskeletal tissues. Converted coral skeletons and coralline apatites are excellent examples in tissue engineering [132, 133], as they have displayed considerable success clinically as templates for tissue reconstruction. These unique three-dimensional marine structures can support the growth and enhancing the differentiation of stem cell progenitors into bone cells. This process is different to standard carbonate frameworks, as they do not induce stem cell differentiation.

Great interests have been shown towards the use of diatoms due to their microscopic size and internal pore network. In addition, they offer means of construction and assembly at the nano and molecular scale, which could potentially benefit the research and development of a new category of drug delivery vehicles [132, 133]. Diatoms are photosynthetic secondary endosymbionts discovered throughout freshwater and marine environments. They have been described as "natural-born" lithographers and responsible for stimulating the production of nanostructured templates for nano-imprint processes where large structural areas with nanometer precision are required [135].

In the quest to identify suitable scaffolding materials, naturally occurring biomatrices such as echinoderm skeletal elements, coral skeletons, marine shell, and sponge skeletons are ideal. These marine materials contain wide-ranging chemical homologies and structural analogies to human extracellular matrices and tissues. Due to their effectiveness, some species of these marine creatures have been utilized to regenerate human bone and cartilage. Yet, the full potential of these marine structures has yet to be harnessed and exploited.

1.5.1 Marine Skeleton

The development of cost effective and efficient ways of manufacturing various calcium phosphate bioceramics from biogenic natural materials has received considerable amounts of research effort in recent years. As mentioned previously, due to their unique composition that is mainly calcium carbonate and architectures, a number of natural land and marine creatures such as land snails, cuttlefish, Mediterranean mussel, echinoderm spines, marine sponges, sea urchins, nacre, sea coral, and seashells were previously reported to be capable of producing calcium phosphate materials for biomedical applications [132, 133, 136–140]. These calcium phosphates include α- and β-tri-calcium phosphate, tetracalcium phosphate, octacalcium phosphate, and hydroxyapatite. Natural skeletons in its entirety have also been employed as templates for transporting biomolecules. Moreover, attempts have been made to use diatom skeletons with an antibody in immunodiagnostics [141].

1.5.2 Marine Sponges

Currently, marine sponges are highly exploited for innovative biological compounds to be potentially used in the treatments of various medical conditions and diseases such as cancer tumors, inflammation, and leukemia. In addition, they are also a source of collagen for the preparation of dermatological and cosmetic products [142, 143]. In total, half of all marine-derived materials are sourced from a wide variety of marine sponges.

Marine sponges share much in common with multicellular tissues. From a morphological and biochemical perspective, resemblances exist between marine sponge and vertebrate extracellular matrix, and this suggest that the basic directions of organization evolved initially by marine sponges. The superior optimized structural design of marine sponges could theoretically provide helpful lessons during the construction of man-made structures using the least number of starting materials but achieving maximum strength [144, 145].

So far, three categories of collagen have been identified from marine sponge. All sponges consist of collagen fibrils secreted in bundles in a similar manner to vertebrates and are 22 nm thin with highly ordered periodic banding. In comparison to vertebrate collagens, the genome organization and amino acid sequence are similar despite the fact that the ultrastructure of collagen is somewhat simple. Likewise, collagen fibrils are intimately associated with proteoglycans that form and shape the design of mammalian tissue at long-range scale. Also discovered in marine sponge collagen fibers are fibronectin, tenascin, and dermatopin polypeptides and cross-react with antibodies raised against vertebrate analogies emphasizing their common origins. Several sponge species contain an analogue of type IV collagen discovered in vertebrate basement membrane collagens [146]. The organization of collagen fibrils is similar to type XIII collagen that causes cells to adhere surfaces [147]. With properties such as cell adherent collagens and fibronectin, there are considerable potential for the future development of collagenous marine sponge as bioactive tissue engineering scaffolds.

The use of collagenous marine sponge skeletons for surgical procedures are especially ideal due to properties such as resistant to high temperature and bacterial attack, highly absorbent, extremely strong, elastic, and soft. Studies have been conducted to investigate the possibility as well as the exact condition required to grow marine sponges commercially and on a large production scale (Fig. 1.7).

Additionally, the intention of cultivating marine sponges is to extract in a larger quantity medically important secondary metabolites than is feasible compared to collection made through conventional bioprospecting. The collagenous composition of the fibers has been found to promote the attachment of all kinds of human cells. Furthermore, the unique layered ultrastructure could provide the answer to their high wettability and adsorption of growth factors onto the collagen fibers, which infuse into attached cells and thus promote their activities. In vivo observation has revealed the formation of tissues to be both well developed and extensive by completely filling

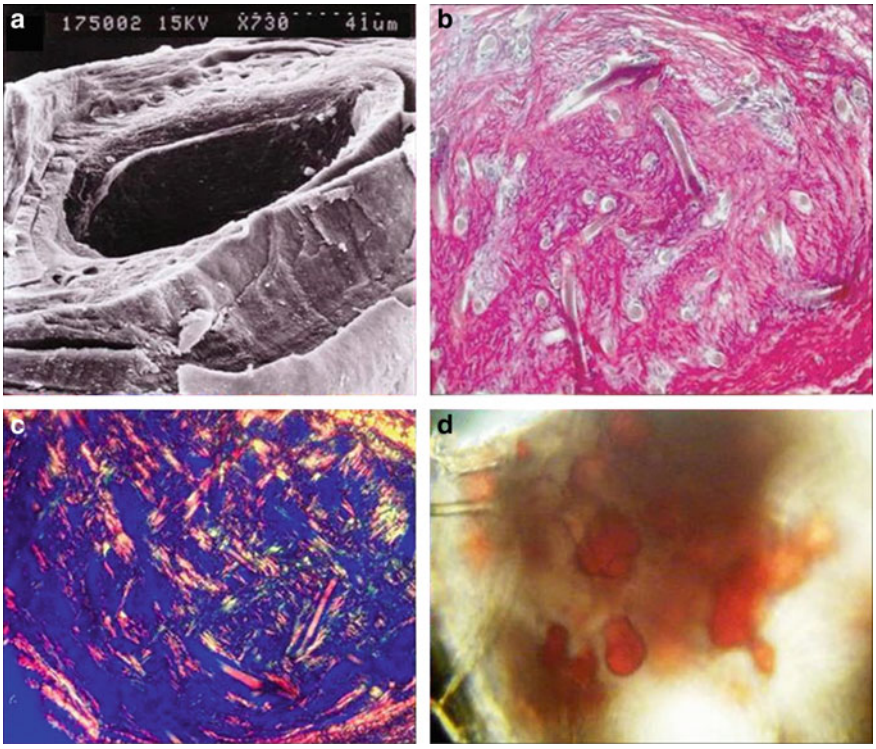

Fig. 1.7 Marine sponge scaffold for tissue engineering of soft and hard human tissues. **a** SEM ultrastructure of marine sponge fiber; **b** histological section through marine sponge filled with foetal cell derived tissue following implantation for 28 days; **c** bi-refringency of developed tissue within marine sponge showing highly ordered organization of collagen fibers; **d** *in-situ* staining of lipid droplets with Oil red-O staining. Reprint with permission from [149]

the entire sponge implant with tissues being the same as neocartilage and immature bone both in terms of structure and quality within four weeks [148].

1.5.3 Marine Shells (Foraminifera)

Foraminifera are single-celled organisms with shells comprising of multi-layered inner chambers frequently added and divided during its growth. Different species with various shapes can exist depending on the environment. These coral sand shells or microspheres to be termed more appropriately possess unique fenestrated structures which have evolved to allow seawater to circulate and collect light for the mutual benefit of symbiotic algal cells that reside inside the shell [133, 134, 149].

Scanning electron microscopy (SEM) imaging and microcomputed tomography (μ-CT) confirmed that these shells were internally permeated by a 3-D network of

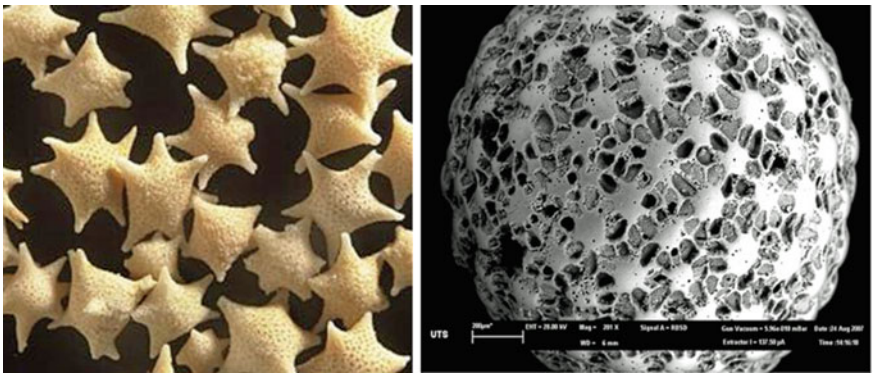

Fig. 1.8 Star Foraminifera structure from Australia (left). (right) SEM image of a Foraminifera (*Baculogypsina sphaerulata*) microsphere and the potential of macrospheres to anchor and transport adherent stem cells fit for transplantation. Modified and reprint with permission from [133] and [149]

microscopic, interconnected channels measuring between 1 and 10 μm in diameter (Fig. 1.8). Moreover, nano- and meso-pores are contained between the micropores surface area. The meso- and micro-interconnected pores within the microstructure can support filtration of Foraminifera in the marine environment.

It is vital that these coral sand shells are converted using the hydrothermal conversion method into more stable and highly crystalline β-TCP and hydroxyapatite [150, 151]. The converted sand shells were further coated with stem cells for orthopedic and maxillofacial applications [152]. Additionally, these foraminifera microspheres were used as bioactive bone grafts and drug delivery devices after conversion to calcium phosphate [153].

1.5.4 Sea Urchins

The spicule of sea urchin, which is similar to teeth and bones, is a composite of inorganic and organic materials that the sea creature synthesizes using the most readily available elements such as calcium, sodium, magnesium, and strontium found in seawater. The spicule is formed inside a cluster of specialized cells and the process commences as the sea urchin lays down a single crystal of calcite, from which the rest of the spicule is created. Starting from the crystalline center, three arms extend at 120° from each other and the three radii are initially amorphous calcium carbonate (between 40 and 100 nm in size) and are transformed gradually to well-organized and oriented calcite (Fig. 1.9). It remains unclear the mechanism behind the conversion, but it has been suggested that the dissolution and ordered precipitation mechanism at known crystallographic orientations of aragonite or calcite might be the cause [154]. The fully developed spicule consisted of a single crystal with an atypical morphology in three-dimensions. It forms a starlike shape and has no facets.

Fig. 1.9 Sea urchin with spicules. Reprint with permission from [133]

A very regular series of pores perforates the skeletal plates of sea urchin. In *Centrostephanus nitidus*, around 75% of the pores are exits for tube feet (pore diameters is approximately 200 μm at the spine bases and up to 600 μm for the tube feet) and 25% are channels connected to the reproductive and alimentary systems. The pore diameters are much larger (between 1000 and 2000 μm) to accommodate a larger quantity of fluids.

In order to produce such unusual morphologies, sea urchin and other marine organisms deposit initially a disordered amorphous mineral phase. This phase is then permitted to transform gradually into a crystal aligned precisely into a lattice with a regular and specific orientation while at the same time retaining their morphology. Simply put, a unique transformation from disordered amorphous to ordered crystalline structures takes place.

The skeleton spines of sea urchin contain large crystals of magnesium-rich calcite that have continuously curved and smooth surfaces and form a three-dimensional fenestrated mineral network. Echinoderm skeletons are constructed from a three-dimensional single crystalline meshwork, which is both intricately shaped and distinctive with a topological structure where every internal channel and pore is in direct contact with each other (periodic minimal surface). It is highly probable that such property aided in tissue development and mass transfer [133].

Spines of the echinoids *Heterocentrotus trigonarius* and *Heterocentrotus mammillatus* can be converted using hydrothermal reaction at 180 °C to bioresorbable magnesium-substituted β-TCP. Most importantly, the conversion retained the three-dimensional interconnected porous morphology of the original spine. Due to the

presence of magnesium in the calcite lattice, it is more preferential for the spines to be converted to magnesium-substituted β-TCP than to form hydroxyapatite. The ion-exchange reaction is thought to be the main conversion mechanism despite the fact that a dissolution-reprecipitation process materializing some calcium phosphate precipitates on the surface of the spine [155]. In vivo studies using a rat model revealed new bone growth up to and encapsulating the magnesium-substituted β-TCP after implanting into femur defects for six weeks. Observations also revealed new bone migrated through the spine pores suggesting good osteoconductivity and bioactivity of the implant [155].

1.5.5 Marine-Derived Bone Adhesive

Utilizing the marine environment to develop an adhesive to repair fracture bone and to fix dental and orthopedic implants in place in a wet and bloody environment is a goal worth achieving. Such an adhesive also needs to provide sufficient mechanical strength to withstand functional loading in addition to being non-toxic and biocompatible [156].

In comparison to synthetic adhesives, ones that are created naturally by marine systems such as marine mussels and sandcastle worms are more durable and provide greater strength. In order to overcome the dynamic ocean environment, marine creatures temporarily or permanently attach to both living and non-living surfaces based on the adhesive strategies developed by the organism [157]. For instance, utilizing an extremely durable and strong natural adhesive, marine mussels affix themselves to a number of surfaces in an aqueous environment. Isolating the proteins responsible for underwater adhesion of marine mussel could provide insights into the conditions and requirements essential for attachment to wet surfaces. Many researchers are focusing on 3,4-dihydroxyphenyl-L-alanine (Dopa), a catecholic amino acid and one of the primary constituents of marine foot proteins due to their adhesive characteristics and strong bidentate interactions with a number of surfaces including metal oxides and minerals [157–161].

Studies over the past three decades on mussel-inspired adhesion have been centering on imitating the remarkable adhesive proteins discovered in the terminal plaque of the mussel byssus and more specifically the mussel foot protein located at the adhesive interface that contains high quantities of Dopa for tissue-specific applications (Fig. 1.10) [159, 162–169]. The number of adhesive-related proteins detected from the marine mussel contributes to its popularity amongst biomimetic researchers but also poses an intricate situation as the biocompatibility and adhesive potential is governed by the type of protein used [156, 170, 171].

The sandcastle worm *Phargmatopoma californica* construct hard shells and tube reefs using sand particles and shells from the sea floor mixed with the secreted proteinaceous cement (Fig. 1.11) [172–174]. According to Stewart et al. [174], the proteinaceous cement creates a solid foam through covalent crosslinking and this foam-like architecture increases the toughness of the cement. The toughness of the

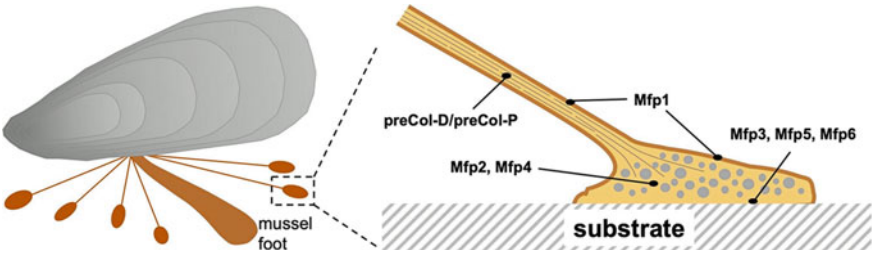

Fig. 1.10 The mussel byssus. Mussels secrete many byssal threads to securely attach to underwater surfaces and withstand the high forces exerted by waves. During formation of a byssal thread, glands along the mussel foot secrete a mixture of byssal collagens and mussel foot proteins (mpfs) that self-assemble and solidify into the thread shaft and the adhesive plaque. The core of the adhesive plaque consists of a porous complex coacervate with mussel foot proteins with low DOPA concentrations (mpf 2, 4). Mussel foot proteins at the adhesive interface (mfp 3, 5, 6) have high DOPA content. Reprint with permission from [162]

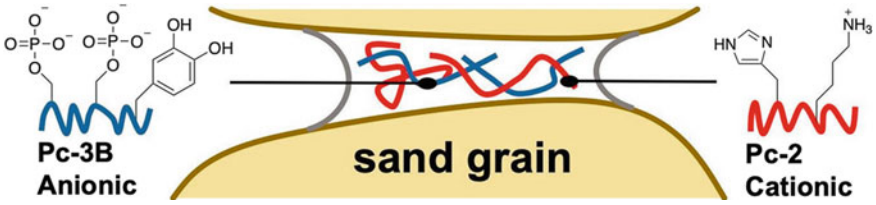

Fig. 1.11 The sandcastle worm connects sand grains to build tubular dwellings. The load bearing bioadhesive that connects sand particles consists of a complex coacervate of highly phosphorylated anionic proteins (Pc-3B) and cationic proteins (Pc-2). Reprint with permission from [162]

cement as well as its ability to strongly adhere to several materials provide vital framework in the development of a biomimetic adhesive for the repair of bone fractures and soft tissues as well as bonding dental implants into fresh extraction sockets [174–179].

1.5.6 Marine Structures in Drug Delivery

Numerous questions are considered during the creation of a drug delivery system for a specific application: (1) The toxicity of the pharmaceutics to be delivered; (2) The chemical and physical properties of the material used to construct the delivery vehicle; (3) The administration routes; (4) The loading efficiency; (5) The rate of degradation; and (6) The practicality for large-scale production.

The basic principle that outlines the description of a drug delivery system remained unchanged despite the advancements in technology has created sophisticated and innovative drug delivery systems. In comparison to conventional drug consumption

such as injection or tablet, slow drug delivery systems allow the delivery and release of a preloaded pharmaceutical agent with duration and dosage control to a local and specific area. This results in a therapeutically relevant amount or concentration of active drug being delivered while at the same time causing minimal systemic side effects to the human body.

It has been shown that there are possible benefits of using alginate, ceramics, polymers, and polysaccharides as materials during the synthesis of drug delivery vehicles [3, 102]. Due to their ease of conversion to calcium phosphate, marine materials such as shells and coral exoskeletons demonstrate better potential as slow drug delivery material. Furthermore, their intricate interconnected pores and their controllable rates of dissolution offer a more persistent drug loading and hence provide a more predictable drug release rate. Both factors are crucial as they will clearly impact the effectiveness of the drug delivery system.

Two significant restrictions concerning the development of marine biopharmaceutics are the issues of consistent supply source and purity. Marine materials such as shells and corals (in natural and synthetic forms) are widely abundant and commercially available and thereby making it an attractive source of materials for clinical and research applications.

Marine materials must first undergo a painstaking process to examine the purity, morphology, and composition from collection to manufacturing before finally applied in the medical arena. Furthermore, the suitability of a marine material for drug loading and its slow dissolution without resulting in any adverse effect to the patient must be determined prior to utilization as a carrier material. Examinations can be performed with increased sensitivity with modern screening techniques to ensure the material is of the highest quality within the limits of detection. It is also a requirement for any organic matter and foreign entities to be removed before the sterilization of calcium carbonate material except in special cases. Submersion in sodium hypochlorite solution can remove any residual organic constituents and this is followed by drying at around 100 °C [102].

Marine-derived calcium carbonate exoskeletons has been known to possess fast rate of degradation, which is not ideal for long-term drug therapy, but perhaps beneficial in applications that requires fast acting and short-term therapy. Converting marine-derived calcium carbonate exoskeletons into hydroxyapatite and/or β-tri calcium phosphate via hydrothermal exchange conversion is more ideal as these compositions are better suited for certain drug delivery situations due to their stability and high crystallinity compared to other calcium phosphates. A ratio of 1.5 between calcium and phosphorus is required for the hydrothermal conversion of calcium carbonate exoskeletons to β-tri calcium phosphate. Depending on the size of the material to be converted, a conversion period of 48 h would complete the transformation while a period of less than 24 h would produce carbonated tri-calcium phosphate [3, 33–39]. More importantly, the original architecture of the marine exoskeletons remains unchanged throughout the chemical conversion to calcium phosphate, and therefore making the adsorption of the designated drug compounds possible [3, 33–39].

The application of Foraminifera as slow drug delivery vehicles has created novel ideas to incorporate a variety of therapeutic drugs such as antibiotics into the microstructure [102]. Foraminifera spheres with drugs can spontaneously degrade and progressively release entrapped biological contents introduced during synthesis. In addition, the porous architecture enables the microspheres to be dissolved within the physiological environment into calcium and phosphate ions along with the absorbed pharmaceutics. The release profile reveals relatively slow and local release of drugs such as gentamicin, bisphosphonate, and simvastatin from the microspheres for extended periods with a loading efficiency of 75% [3, 33–39]. The deposition of an apatite thin film around the β-tri calcium phosphate regulates the release of the loaded simvastatin by approximately 50% and thereby prolonging the release of the loaded drug into the local area and extending the therapeutic efficacy of the drug delivery system [35, 101, 102].

1.6 Concluding Remarks

Generally, the advantages of utilizing advanced ceramic materials in the biomedical and dental arena has been fully comprehended. Expanding our knowledge of biomaterials and bioceramics could prove beneficial during the design of next generational implants and prostheses. An important area in biomedical materials research is to gain an insight into the relationship between the surface properties and the biological responses of materials.

Bioceramics with very fine grain structures and densities close to its theoretical value can only be manufactured through advancements in the production process such as the utilization of hot isostatic pressing. The viability of creating ceramics with higher densities also leads to improvements in mechanical strength as well as preventing the propagation of cracks and ultimately the fracture of the ceramic material. Partially stabilized zirconia and alumina are used currently with great success in dentistry as implants and in maxillofacial surgery. Likewise, the applications of bioactive glasses as body-interactive materials is crucial when it comes to restoring physiological functions, and their use can be further explored by incorporating biogenic materials and certain drugs, which are designed to enhance their capabilities and functionality.

For more than a decade, interest in nanostructured materials in dentistry and medicine has been expanding and it is predicted that implants and materials containing nanomaterials will increase for applications such as tissue engineering and slow drug delivery systems. A major disadvantage suffered by synthetic dental and orthopedic implants and prostheses currently is their inability to adapt to local tissue environment. If synthesized and deposited properly, nanomedical coatings based on bioceramics such as calcium phosphate and bioglass are designed to reduce corrosion and the amount of ion released from the implant or prosthesis, while at the same time altering its surface to promote osseointegration. Surface modification by nanocoating deposition has become a crucial research tool to help us understand

the influence of chemical and structural surface properties on material-biosystem interactions. Surface modifications intended for controlling biological response is expected to create new opportunities for creating new and better medical devices and implants in a more efficient manner and at a faster rate once a deeper understanding is achieved.

The issue of surface interactions will get more complicated in a changing world where implants and medical devices will be surface modified not only by biomaterials but also with biogenic materials such as stem cells and bone morphogenic proteins. New generations of medical implants and devices with these functionalized surfaces will need nanoscale surface properties measuring techniques that can be utilized to describe both inorganic materials and living tissues in addition to the interfacial reactions between implant and bone tissue. These measurements are crucial for future modeling and design of implants and prostheses.

Structures in nature possess desirable properties and we are slowing discovering new techniques of recreating nature to similar levels of sophistication despite only to a limited extent. The utilization of biological microstructures as templates is an inventive method to replicate inorganic structures with identical features. Furthermore, biological microstructures have a distinct significance to synthesize replacements for calcified tissues and this can be accomplished through biomineral-inspired materials chemistry. The idea is to apply consecutive developmental system pathways that nature uses to fabricate skeletons from molecules into macro- and microscopic structures.

Since the last decade, marine structures have been extensively investigated from soft and hard tissue engineering to slow or controlled drug delivery. The new approaches include the application of natural inorganic and organic skeletons, micro- and nano-slow drug delivery systems, devices that incorporates stem cells, proteins, and peptides, and new medical treatment protocols inspired by unique designs. The oceans still contain a vast diversity of structures that are unique for biomedical applications and possibilities to be explored as well as lessons to be learnt by researchers on how they are grown and synthesized by nature. The introduction of the hydrothermal conversion method has enabled scientists to develop drug carries using a wide variety of suitable marine-based exoskeletons and materials with distinctive structures, and it has been proven advantageous to use calcium phosphate as a delivery vehicle derived from marine exoskeletons.

References

1. Skalak R (1983) Biomechanical considerations in osseointegrated prostheses. J Prosthet Dent 49:843–848
2. Ben-Nissan B, Choi AH, Cordingley RC (2008) Alumina ceramics. In: Kokubo T (ed) Bioceramics and their clinical applications. Woodhead Publishing, England, pp 233–242
3. Choi AH, Ben-Nissan B (2018) Anatomy, modeling and biomaterial fabrication for dental and maxillofacial applications. Bentham Science Publishers, United Arab Emirates

4. Clupper DC, Hench LL, Mecholsky JJ (2004) Strength and toughness of tape cast bioactive glass 45S5 following heat treatment. J Eur Ceram Soc 24:2929–2934
5. Clupper DC, Gough JE, Embanga PM et al (2004) Bioactive evaluation of 45S5 bioactive glass fibres and preliminary study of human osteoblast attachment. J Mater Sci Mater Med 15:803–808
6. Thompson ID, Hench LL (1998) Mechanical properties of bioactive glasses, glass-ceramics and composites. Proc Inst Mech Eng H 212:127–136
7. Hench LL (1988) Bioactive ceramics. In: Ducheyne P, Lemons JE (eds) Bioceramics: materials characteristics *vs. in vivo* behavior. Annual of the New York Academy of Science, New York, pp 54–71.
8. Willmann G (1998) Ceramics for total hip replacement—what a surgeon should know. Orthopedics 21:173–177
9. Dartora NR, Maurício Moris IC, Poole SF et al (2021) Mechanical behavior of endocrowns fabricated with different CAD-CAM ceramic systems. J Prosthet Dent 125:117–125
10. Krajangta N, Sarinnaphakorn L, Didron PP et al (2020) Development of silicon nitride ceramic for CAD/CAM restoration. Dent Mater J 39:633–638
11. Papadopoulos K, Pahinis K, Saltidou K et al (2020) Evaluation of the surface characteristics of dental CAD/CAM materials after different surface treatments. Materials 13:981. https://doi.org/10.3390/ma13040981
12. Sinhori BS, Monteiro S Jr, Bernardon JK et al (2018) CAD/CAM ceramic fragments in anterior teeth: a clinical report. J Esther Restor Dent 30:96–100
13. Zarina R, Jaini JL, Raj RS (2017) Evolution of the software and hardware in CAD/CAM systems used in dentistry. Int J Prev Clin Dent Res 4:1–8
14. Strub JR, Rekow ED, Witkowski S (2006) Computer-aided design and fabrication of dental restorations: current systems and future possibilities. J Am Dent Assoc 137:1289–1296
15. Duret F, Blouin JL, Duret B (1988) CAD-CAM in dentistry. J Am Dent Assoc 117:715–720
16. Shao H, Sun M, Zhang F et al (2018) Custom repair of mandibular bone defects with 3D printed bioceramic scaffolds. J Dent Res 97:68–76
17. Adel-Khattab D, Giacomini F, Gildenhaar R et al (2018) Development of a synthetic tissue engineered three-dimensional printed bioceramic-based bone graft with homogenously distributed osteoblasts and mineralizing bone matrix *in vitro*. J Tissue Eng Regen Med 12:44–58
18. Ferrage L, Bertrand G, Lenormand P et al (2017) A review of the additive manufacturing (3DP) of bioceramics: alumina, zirconia (PSZ) and hydroxyapatite. J Aust Ceram Soc 53:11–20
19. Meininger S, Mandal S, Kumar A et al (2016) Strength reliability and *in vitro* degradation of three-dimensional powder printed strontium-substituted magnesium phosphate scaffolds. Acta Biomater 31:401–411
20. Inzana JA, Trombetta RP, Schwarz EM et al (2015) 3D printed bioceramics for dual antibiotic delivery to treat implant-associated bone infection. Eur Cell Mater 30:232–247
21. Chang CH, Lin CY, Liu FH et al (2015) 3D printing bioceramic porous scaffolds with good mechanical property and cell affinity. PLoS One 10:e0143713
22. Lin K, Sheikh R, Romanazzo S et al (2019) 3D printing of bioceramic scaffolds—barriers to the clinical translation: from promise to reality, and future perspective. Materials 12:2660. https://doi.org/10.3390/ma12172660
23. Kolan KCR, Leu MC, Hilmas GE et al (2012) Effect of material, process parameters, and simulated body fluids on mechanical properties of 13–93 bioactive glass porous constructs made by selective laser sintering. J Mech Behav Biomed Mater 13:14–24
24. Hwa LC, Rajoo S, Noor AM et al (2017) Recent advances in 3D printing of porous ceramics: a review. Curr Opin Solid State Mater Sci 21:323–347
25. Kolan KCR, Thomas A, Leu MC et al (2015) *In vitro* assessment of laser sintered bioactive glass scaffolds with different pore geometries. Rapid Prototyp J 21:152–158
26. Ebelmen J (1846) Untersuchungen über die verbindung der borsaure und kieselsaure mit aether. Ann Chim Phys Ser 57:319–355

27. Roy DM, Roy R (1954) An experimental study of the formation and properties of synthetic serpentines and related layer silicates. Am Mineral 39:957–975
28. Floch HG, Belleville PF, Priotton JJ et al (1995) Sol-gel optical coatings for lasers. J Am Ceram Soc Bull 74:60–63
29. Avellaneda CO, Macedo MA, Florentino AO et al (1994) Sol-gel coatings for optoelectronic devices. In: Proceedings SPIE Vol. 2255, optical materials technology for energy efficiency and solar energy conversion XIII, Freiburg, Germany, 9 Sept 1994. https://doi.org/10.1117/12.185396
30. Yoldas BE (1984) Wide-spectrum anti-reflective coatings for fused silica and other glasses. Appl Opt 23:1418
31. Bartlett JR, Woolfrey JL (1990) Preparations of multicomponent ceramic powders by sol-gel processing. In: Zelinski BJJ, Brinker CJ, Clark DE et al (eds) Better ceramic through chemistry, 4th edn. Materials Research Society, Pennsylvania, pp 191–196
32. Choi AH, Conway RC, Cazalbou S et al (2018) Maxillofacial bioceramics in tissue engineering: production techniques, properties, and applications. In: Thomas S, Balakrishnan P, Sreekala MS (eds) Fundamental biomaterials: ceramics. Woodhead publishing series in biomaterials, Cambridge, pp 63–93
33. Choi AH, Ben-Nissan B (2017) Calcium phosphate nanocomposites for biomedical and dental applications: recent developments. In: Thakur VK, Thakur MK, Kessler MR (eds) Handbook of composites from renewable materials. Wiley, New Jersey, pp 423–450
34. Ben-Nissan B, Choi AH (2017) Calcium phosphate nanocoatings: production, physical and biological properties, and biomedical applications. In: Thian ES, Huang J, Aizawa M (eds) Nanobioceramics for healthcare applications. World Scientific Publishing, Singapore, pp 105–149
35. Choi AH, Ben-Nissan B (2015) Calcium phosphate nanocoatings and nanocomposites, part I: recent developments and advancements in tissue engineering and bioimaging. Nanomedicine 10:2249–2261
36. Choi AH, Ben-Nissan B, Matinlinna JP et al (2013) Current perspective: calcium phosphate nanocoatings and nanocomposite coatings in dentistry. J Dent Res 92:853–859
37. Ben-Nissan B, Choi AH (2010) Nanoceramics for medical applications. In: Geckeler N (ed) Advanced nanomaterials. Wiley-VCH Verlag GmbH and Co, Germany, pp 523–553
38. Choi AH, Ben-Nissan B (2007) Sol-gel production of bioactive nanocoatings for medical applications: part II: current research and development. Nanomedicine 2:51–61
39. Ben-Nissan B, Choi AH (2006) Sol-gel production of bioactive nanocoatings for medical applications: part I: an introduction. Nanomedicine 1:311–319
40. Turner CW (1991) Sol-gel process—principles and applications. Ceram Bull 70:1487–1490
41. Eger M, Sterer N, Liron T et al (2017) Scaling of titanium implants entrains inflammation-induced osteolysis. Sci Rep 7:39612. https://doi.org/10.1038/srep39612
42. Hench LL (1991) Bioceramics, from concept to clinic. J Am Ceram Soc 74:1487–1510
43. Orsini G, Piattelli M, Scarano A et al (2007) Randomized, controlled histologic and histomorphometric evaluation of implants with nanometer-scale calcium phosphate added to the dual acid-etched surface in the human posterior maxilla. J Periodontol 78:209–218
44. Jimbo R, Xue Y, Hayashi M et al (2011) Genetic responses to nanostructured calcium-phosphate-coated implants. J Dent Res 90:1422–1427
45. Oh S, Tobin E, Yang Y et al (2005) *In vivo* evaluation of hydroxyapatite coatings of different crystallinities. Int J Oral Maxillofac Implants 20:726–731
46. Surmeneva MA, Surmeneva RA, Nikonova YA et al (2014) Fabrication, ultra-structure characterization and *in vitro* studies of RF magnetron sputter deposited nano-hydroxyapatite thin films for biomedical applications. Appl Surf Sci 317:172–180
47. Kim HW, Kim HE, Salih V et al (2005) Sol-gel-modified titanium with hydroxyapatite thin films and effect on osteoblast-like cell responses. J Biomed Mater Res A 74:294–305
48. Zhang M, Matinlinna JP (2012) E-glass fiber reinforced composites in dental applications. SILICON 4:73–78

49. Luthria A, Srirekha A, Hegde J et al (2012) The reinforcement effect of polyethylene fibre and composite impregnated glass fibre on fracture resistance of endodontically treated teeth: an *in vitro* study. J Conserv Dent 15:372–376
50. Summitt JB, Robbins JW, Hilton JT et al (2006) Fundamentals of operative dentistry: a contemporary approach, 3rd edn. Quintessence Publishing Co. Inc, Illinois
51. Swift E Jr (2005) Nanocomposites. J Esthet Restor Dent 17:3–4
52. Saunders SA (2009) Current practicality of nanotechnology in dentistry. Part 1: focus on nanocomposite restoratives and biomimetics. Clin Cosmet Investig Dent 1:47–61
53. Melander J, Dunn WP, Link MP et al (2011) Comparison of flexural properties and surface roughness of nanohybrid and microhybrid dental composites. Gen Dent 59:342–347
54. de Moraes RR, Gonçalves Lde S, Lancellotti AC et al (2009) Nanohybrid resin composites: nanofiller loaded materials or traditional microhybrid resins? Oper Dent 34:551–557
55. Demirci M, Tuncer S, Sancakli HS et al (2018) Five-year Clinical evaluation of a nanofilled and a nanohybrid composite in class IV cavities. Oper Dent 43:261–271
56. Yazici AR, Antonson SA, Kutuk ZB et al (2017) Thirty-six-month clinical comparison of bulk fill and nanofill composite restorations. Oper Dent 42:478–485
57. de Andrade AK, Duarte RM, Medeiros e Silva FD et al (2011) 30-month randomised clinical trial to evaluate the clinical performance of a nanofill and a nanohybrid composite. J Dent 39:8–15
58. Mahmoud SH, El-Embaby AE, AbdAllah AM et al (2008) Two-year clinical evaluation of ormocer, nanohybrid and nanofill composite restorative systems in posterior teeth. J Adhes Dent 10:315–322
59. Dresch W, Volpato S, Gomes JC et al (2006) Clinical evaluation of a nanofilled composite in posterior teeth: 12-month results. Oper Dent 31:409–417
60. Efes BG, Dörter C, Gömeç Y et al (2006) Two-year clinical evaluation of ormocer and nanofill composite with and without a flowable liner. J Adhes Dent 8:119–126
61. Ernst CP, Brandenbusch M, Meyer G et al (2006) Two-year clinical performance of a nanofiller vs a fine-particle hybrid resin composite. Clin Oral Investig 10:119–125
62. Senawongse P, Pongprueksa P (2007) Surface roughness of nanofill and nanohybrid resin composites after polishing and brushing. J Esthet Restor Dent 19:265–275
63. Taha DG, Abdel-Samad AA, Mahmoud SH (2011) Fracture resistance of maxillary premolars with class II MOD cavities restored with ormocer, nanofilled, and nanoceramic composite restorative systems. Quintessence Int 42:579–587
64. Zhang L, Weir MD, Chow LC et al (2016) Novel rechargeable calcium phosphate dental nanocomposite. Dent Mater 32:285–293
65. Moreau JL, Weir MD, Giuseppetti AA et al (2012) Long-term mechanical durability of dental nanocomposites containing amorphous calcium phosphate nanoparticles. J Biomed Mater Res B Appl Biomater 100:1264–1273
66. Moreau JL, Sun L, Chow LC et al (2011) Mechanical and acid neutralizing properties and bacteria inhibition of amorphous calcium phosphate dental nanocomposite. J Biomed Mater Res B Appl Biomater 98:80–88
67. Weir MD, Ruan J, Zhang N (2017) Effect of calcium phosphate nanocomposite on *in vitro* remineralization of human dentin lesions. Dent Mater 33:1033–1044
68. Weir MD, Chow LC, Xu HH (2012) Remineralization of demineralized enamel via calcium phosphate nanocomposite. J Dent Res 91:979–984
69. Ben-Nissan B, Choi AH, Macha I (2017) Advances in bioglass and glass ceramics for biomedical applications. In: Li Q, Mai YW (eds) Biomaterials for implants and scaffolds. Springer series in biomaterials science and engineering (SSBSE), Germany, pp 133–161
70. Hench LL, Greenspan D (2013) Interactions between bioactive glass and collagen: a review and new perspectives. J Aust Ceram Soc 49:1–40
71. Gross U, Kinne R, Schmitz HJ et al (1988) The response of bone to surface active glass/glass-ceramics. CRC Crit Rev Biocomput 4:2–15
72. Hench LL, Wilson J (1984) Surface active materials. Science 226:630–636

73. Hench LL, Splinter RJ, Allen WC et al (1972) Bonding mechanisms at the interface of ceramic prosthetic materials. J Biomed Mater Res Symp 2:117–141
74. Boccaccini AR, Erol M, Stark WJ et al (2010) Polymer/bioactive glass nanocomposites for biomedical applications: a review. Compos Sci Technol 70:1764–1776
75. Stark WJ, Mädler L, Maciejewski M et al (2003) Flame synthesis of nanocrystalline ceria-zirconia: effect of carrier liquid. Chem Commun 5:588–589
76. Vollenweider M, Brunner TJ, Knecht S et al (2007) Remineralization of human dentin using ultrafine bioactive glass particles. Acta Biomater 3:936–943
77. Keller L, Offner D, Schwinté P et al (2015) Active nanomaterials to meet the challenge of dental pulp regeneration. Materials 8:7461–7471
78. Albuquerque MT, Valera MC, Nakashima M et al (2014) Tissue-engineering-based strategies for regenerative endodontics. J Dent Res 93:1222–1231
79. Bae WJ, Min KS, Kim JJ et al (2012) Odontogenic responses of human dental pulp cells to collagen/nanobioactive glass nanocomposites. Dent Mater 28:1271–1279
80. Moonesi Rad R, Atila D, Akgün EE et al (2019) Evaluation of human dental pulp stem cells behavior on a novel nanobiocomposite scaffold prepared for regenerative endodontics. Mater Sci Eng C Mater Biol Appl 100:928–948
81. Kim GH, Park YD, Lee SY et al (2015) Odontogenic stimulation of human dental pulp cells with bioactive nanocomposite fiber. J Biomater Appl 29:854–866
82. Choi AH, Matinlinna J, Ben-Nissan B (2013) Effects of micromovement on the changes in stress distribution of partially stabilized zirconia (PS-ZrO_2) dental implants and bridge during clenching: a three-dimensional finite element analysis. Acta Odontol Scand 71:72–81
83. Giordano R, Sabeosa CE (2010) Zirconia: material background and clinical application. Compend Contin Educ Dent 31:710–715
84. Depprich R, Zipprich H, Ommerborn M et al (2008) Osseointegration of zirconia implants: an SEM observation of the bone-implant interface. Head Face Med 4:25
85. Manicone PF, Rossi Iommetti P, Raffaelli L (2007) An overview of zirconia ceramics: basic properties and clinical applications. J Dent 35:819–826
86. Clarke IC, Manaka M, Green DD et al (2003) Current status of zirconia used in total hip implants. J Bone Joint Surg Am 85A:73–84
87. Garvie RC, Hannink RH, Pascoe RT (1975) Ceramic steel? Nature 258:703–704
88. Piconi C, Maccauro G (1999) Zirconia as a ceramic biomaterial. Biomaterials 20:1–25
89. Yoshimura M, Noma T, Kawabata K et al (1987) Role of H_2O on the degradation process of Y-TZP. J Mater Sci Lett 6:465
90. Nawa M, Nakamoto S, Sekino T et al (1998) Tough and strong Ce-TZP/alumina nanocomposites doped with titania. Ceramic Int 24:497–506
91. Komasa S, Nishizaki M, Zhang H et al (2019) Osseointegration of alkali-modified NANOZR implants: an *in vivo* study. Int J Mol Sci 20:842
92. Okabe E, Ishihara Y, Kikuchi T et al (2016) Adhesion properties of human oral epithelial-derived cells to zirconia. Clin Implant Dent Relat Res 18:906–916
93. Han JM, Hong G, Matsui H et al (2014) The surface characterization and bioactivity of NANOZR *in vitro*. Dent Mater J 33:210–219
94. Takano T, Tasaka A, Yoshinari M et al (2012) Fatigue strength of Ce-TZP/Al_2O_3 nanocomposite with different surfaces. J Dent Res 91:800–804
95. Yamashita D, Machigashira M, Miyamoto M et al (2009) Effect of surface roughness on initial responses of osteoblast-like cells on two types of zirconia. Dent Mater J 28:461–470
96. Giri S, Trewyn BG, Lin VS (2007) Mesoporous silica nanomaterial-based biotechnological and biomedical delivery systems. Nanomedicine 2:99–111
97. Schroeder A, Turjeman K, Schroeder JE et al (2010) Using liposomes to target infection and inflammation induced by foreign body injuries or medical implants. Expert Opin Drug Deliv 7:1175–1189
98. Rizwan SB, Boyd BJ, Rades T et al (2010) Bicontinuous cubic liquid crystals as sustained delivery systems for peptides and proteins. Expert Opin Drug Deliv 7:1133–1144

99. Soppimath KS, Aminabhavi TM, Kulkarni AR et al (2001) Biodegradable polymeric nanoparticles as drug delivery devices. J Control Release 70:1–20
100. Wu C, Chang J, Zhai W et al (2007) A novel bioactive porous bredigite ($Ca_7MgSi_4O_{16}$) scaffold with biomimetic apatite layer for bone tissue engineering. J Mater Sci Mater Med 18:857–864
101. Choi AH, Ben-Nissan B, Conway RC et al (2014) Advances in calcium phosphate nanocoatings and nanocomposites. In: Ben-Nissan B (ed) Advances in calcium phosphate biomaterials. Springer series in biomaterials science and engineering (SSBSE), Germany, pp 485–509
102. Ben-Nissan B, Macha I, Cazalbou S et al (2016) Calcium phosphate nanocoatings and nanocomposites, part 2: thin films for slow drug delivery and osteomyelitis. Nanomedicine 11:531–544
103. Victor SP, Sharma CP (2012) Calcium phosphates as drug delivery systems. J Biomater Tissue Eng 2:269–279
104. Palazzo B, Iafisco M, Laforgia M et al (2007) Biomimetic hydroxyapatite-drug nanocrystals as potential bone substitutes with antitumor drug delivery properties. Adv Funct Mater 17:2180–2188
105. Mann S (1995) Biomineralization and biomimetic materials chemistry. J Mater Chem 5:935–946
106. Mann S, Ozin GA (1996) Synthesis of inorganic materials with complex form. Nature 382:313–318
107. Arslan B, Padela MT, Madassery S et al (2018) Combination ipsilateral lobar and segmental radioembolization using glass yttrium-90 microspheres for treatment of multifocal hepatic malignancies. J Vasc Interv Radiol 29:1110–1116
108. James T, Hill J, Fahrbach T et al (2017) Differences in radiation activity between glass and resin 90y microspheres in treating unresectable hepatic cancer. Health Phys 112:300–304
109. Mikell JK, Mahvash A, Siman W et al (2016) Selective internal radiation therapy with yttrium-90 glass microspheres: biases and uncertainties in absorbed dose calculations between clinical dosimetry models. Int J Radiat Oncol Biol Phys 96:888–896
110. Gates VL, Marshall KG, Salzig K et al (2014) Outpatient single-session yttrium-90 glass microsphere radioembolization. J Vasc Interv Radiol 25:266–270
111. Kawashita M, Matsui N, Li Z et al (2011) Preparation, structure, and *in vitro* chemical durability of yttrium phosphate microspheres for intra-arterial radiotherapy. J Biomed Mater Res B Appl Biomater 99:45–50
112. Kawashita M, Takayama Y, Kokubo T et al (2006) Enzymatic preparation of hollow yttrium oxide microspheres for in situ radiotherapy of deep-seated cancer. J Am Ceram Soc 89:1347–1351
113. Kawashita M, Shineha R, Kim HM et al (2003) Preparation of ceramic microspheres for in situ radiotherapy of deep-seated cancer. Biomaterials 24:2955–2963
114. Kawashita M, Tanaka M, Kokubo T et al (2005) Preparation of ferrimagnetic magnetite microspheres for in situ hyperthermic treatment of cancer. Biomaterials 26:2231–2238
115. Wang Y, Chen L (2011) Quantum dots, lighting up the research and development of nanomedicine. Nanomedicine 7:385–402
116. Zhang H, Yee D, Wang C (2008) Quantum dots for cancer diagnosis and therapy: biological and clinical perspectives. Nanomedicine 3:83–91
117. Hasna K, Kumar SS, Komath M et al (2013) Synthesis of chemically pure, luminescent Eu^{3+} doped HAp nanoparticles: a promising fluorescent probe for *in vivo* imaging applications. Phys Chem Chem Phys 15:8106–8111
118. LeGeros R (1965) Effect of carbonate ion the lattice parameters of apatite. Nature 24:403–404
119. Chen F, Huang P, Zhu YJ et al (2012) Multifunctional Eu^{3+}/Gd^{3+} dual-doped calcium phosphate vesicle-like nanospheres for sustained drug release and imaging. Biomaterials 33:6447–6455
120. Barta CA, Sachs-Barrable K, Jia J et al (2007) Lanthanide containing compounds for therapeutic care in bone resorption disorders. Dalton Trans 21:5019–5030

121. Sundarabharathi L, Parangusan H, Ponnamma D et al (2018) *In-vitro* biocompatibility, bioactivity and photoluminescence properties of Eu^{3+}/Sr^{2+} dual-doped nano-hydroxyapatite for biomedical applications. J Biomed Mater Res B Appl Biomater 106:2191–2201
122. Xie Y, He W, Li F et al (2016) Luminescence enhanced Eu^{3+}/Gd^{3+} co-doped hydroxyapatite nanocrystals as imaging agents *in vitro* and *in vivo*. ACS Appl Mater Interfaces 8:10212–10219
123. Chen MH, Yoshioka T, Ikoma T et al (2014) Photoluminescence and doping mechanism of theranostic Eu^{3+}/Fe^{3+} dual-doped hydroxyapatite nanoparticles. Sci Technol Adv Mater 15:055005
124. Cheng F, Sun K, Zhao Y et al (2014) Synthesis and characterization of HA/YVO_4: Yb^{3+}, Er^{3+} up-conversion luminescent nano-rods. Ceram Int 40:11329–11334
125. Jadalannagari S, Deshmukh K, Verma AK et al (2014) Lanthanum-doped hydroxyapatite nanoparticles as biocompatible fluorescent probes for cellular internalization and biolabeling. Sci Adv Mater 6:312–319
126. Ashokan A, Gowd GS, Somasundaram VH et al (2013) Multifunctional calcium phosphate nano-contrast agent for combined nuclear, magnetic and near-infrared *in vivo* imaging. Biomaterials 34:7143–7157
127. Wagner DE, Eisenmann KM, Nestor-Kalinoski AL et al (2013) A microwave-assisted solution combustion synthesis to produce europium-doped calcium phosphate nanowhiskers for bioimaging applications. Acta Biomater 9:8422–8432
128. Altinoğlu EI, Russin TJ, Kaiser JM et al (2008) Near-infrared emitting fluorophore-doped calcium phosphate nanoparticles for *in vivo* imaging of human breast cancer. ACS Nano 2:2075–2084
129. Guo Y, Shi D, Lian J et al (2008) Quantum dot conjugated hydroxylapatite nanoparticles for *in vivo* imaging. Nanotechnology 19:175102
130. Mondejar SP, Kovtun A, Epple M (2007) Lanthanide-doped calcium phosphate nanoparticles with high internal crystallinity and with a shell of DNA as fluorescent probes in cell experiments. J Mater Chem 17:4153–4159
131. Mann S (1983) Mineralization in biological systems. Struct Bond 54:125
132. Choi AH, Ben-Nissan B (eds) (2019) Marine-derived biomaterials for tissue engineering applications. Springer series in biomaterials science and engineering, vol 14, Singapore
133. Choi AH, Cazalbou S, Ben-Nissan B (2016) Biomimetics and marine materials in drug delivery and tissue engineering. In: Antoniac I (ed) Handbook of bioceramics and biocomposites. Springer Publishing, Germany, pp 521–544
134. Parker AR, Martini N (2006) Structural color in animals-simple to complex optics. Opt Laser Technol 38:315–322
135. Mock T, Samanta MP, Iverson V et al (2008) Whole-genome expression profiling of the marine diatom *Thalassiosira pseudonana* identifies genes involved in silicon bioprocesses. Proc Natl Acad Sci USA 105:1579–1584
136. Macha IJ, Ozyegin LS, Chou J et al (2013) An alternative synthesis method for di calcium phosphate (monetite) powders from mediterranean mussel (mytilus galloprovincialis) shells. J Aust Ceram Soc 49:122–128
137. Rocha JH, Lemos AF, Agathopoulos S et al (2006) Hydrothermal growth of hydroxyapatite scaffolds from aragonitic cuttlefish bones. J Biomed Mater Res A 77:160–168
138. Martina M, Subramanyam G, Weaver JC et al (2005) Developing microporous bicontinuous materials as scaffolds for tissue engineering. Biomaterials 26:5609–5616
139. Green D, Walsh D, Yang X et al (2004) Stimulation of human bone marrow stromal cells using growth factor-encapsulated calcium carbonate porous microspheres. J Mater Chem 14:2206–2212
140. Roy DM, Linnehan S (1974) Hydroxyapatite formed from coral skeleton carbonate by hydrothermal exchange. Nature 247:220–222
141. Townley HE, Parker AR, White-Cooper H (2008) Exploitation of diatom frustules for nanotechnology: tethering active biomolecules. Adv Funct Mater 18:369–374
142. Nicklas M, Schatton W, Heinemann S et al (2009) Preparation and characterization of marine sponge collagen nanoparticles and employment for the transdermal delivery of 17b-estradiolhemihydrate. Drug Dev Ind Pharm 35:1035–1042

143. Swatschek D, Schatton W, Kellermann J et al (2002) Marine sponge collagen: isolation, characterization and effects on the skin parameters surface pH, moisture and sebum. Eur J Pharm Biopharm 53:107–113
144. Miserez A, Weaver JC, Thurner PJ et al (2008) Effects of laminate architecture on fracture resistance of sponge biosilica: lessons from nature. Adv Funct Mater 18:1241–1248
145. Aizenberg J, Weaver JC, Thanawala MS et al (2005) Skeleton of *Euplectella sp* structural hierarchy from the nanoscale to the macroscale. Science 309:275–278
146. Boute N, Exposito JY, Boury-Esnault N et al (1996) Type IV collagen in sponges, the missing link in basement membrane ubiquity. Biol Cell 88:37–44
147. Exposito JY, Cluzel C, Garrone R et al (2002) Evolution of collagens. Anat Rec 268:302–316
148. Vago R, Plotquin D, Bunin A et al (2002) Hard tissue remodeling using biofabricated coralline biomaterials. J Biochem Biophys Methods 50:253–259
149. Ben-Nissan B, Choi AH, Green DW (2019) Marine derived biomaterials for bone regeneration and tissue engineering: learning from nature. In: Choi AH, Ben-Nissan B (eds) Marine-derived biomaterials for tissue engineering applications. Springer series in biomaterials science and engineering, vol 14. Singapore, pp 51–78
150. Chou J, Valenzuela SM, Santos J et al (2014) Strontium- and magnesium-enriched biomimetic β-TCP macrospheres with potential for bone tissue morphogenesis. J Tissue Eng Regen Med 8:771–778
151. Chou J, Ben-Nissan B, Green DW et al (2011) Targeting and dissolution characteristics of bone forming and antibacterial drugs by harnessing the structure of microspherical shells from coral beach sand. Adv Eng Mater 13:93–99
152. Green DW, Li G, Milthorpe B et al (2012) Adult stem cell coatings for regenerative medicine. Mater Today 15:60–66
153. Chou J, Ito T, Bishop D et al (2013) Controlled release of simvastatin from biomimetic β-TCP drug delivery system. PLoS ONE 8:e54676. https://doi.org/10.1371/journal.pone.0054676
154. Raz S, Hamilton P, Wilt F et al (2003) The transient phase of amorphous calcium carbonate in sea urchin larval spicules: the involvement of proteins and magnesium ions in its formation and stabilization. Adv Funct Mater 13:480–486
155. Ben-Nissan B, Green DW (2013) Marine materials in drug delivery and tissue engineering: from natural role models, to bone regeneration and repair and slow delivery of therapeutic drugs, proteins and genes. In: Kim S-K (ed) Marine biomaterials. Taylor and Francis/CSR Books, Boca Raton, pp 575–602
156. Norton MR, Kay GW, Brown MC et al (2020) Bone glue—the final frontier for fracture repair and implantable device stabilization. Int J Adhes Adhes 102:102647. https://doi.org/10.1016/j.ijadhadh.2020.102647
157. Silverman HG, Roberto FF (2007) Understanding marine mussel adhesion. Mar Biotechnol 9:661–681
158. Waite JH (2017) Mussel adhesion—essential footwork. J Exp Biol 220:517–530
159. Sousa MP, Mano JF (2017) Cell-adhesive bioinspired and catechol-based multilayer free-standing membranes for bone tissue engineering. Biomimetics 2:19
160. Yu J, Wei W, Menyo MS et al (2013) Adhesion of mussel foot protein-3 to TiO_2 surfaces: the effect of pH. Biomacromol 14:1072–1077
161. Wang J, Liu C, Lu X et al (2007) Co-polypeptides of 3,4-dihydroxyphenylalanine and L-lysine to mimic marine adhesive protein. Biomaterials 28:3456–3468
162. Balkenende DWR, Winkler SM, Messersmith PB (2019) Marine-inspired polymers in medical adhesion. Eur Polym J 116:134–143
163. Yin D, Komasa S, Yoshimine S et al (2019) Effect of mussel adhesive protein coating on osteogenesis *in vitro* and osteointegration *in vivo* to alkali-treated titanium with nanonetwork structures. Int J Nanomedicine 14:3831–3843
164. Song WK, Kang JH, Cha JK et al (2018) Biomimetic characteristics of mussel adhesive protein-loaded collagen membrane in guided bone regeneration of rabbit calvarial defects. J Periodontal Implant Sci 48:305–316

165. Choi BH, Cheong H, Ahn JS et al (2015) Engineered mussel bioglue as a functional osteoinductive binder for grafting of bone substitute particles to accelerate *in vivo* bone regeneration. J Mater Chem B 3:546–555
166. Yang HS, Park J, La WG et al (2012) 3,4-dihydroxyphenylalanine-assisted hydroxyapatite nanoparticle coating on polymer scaffolds for efficient osteoconduction. Tissue Eng Part C Methods 18:245–251
167. Hong JM, Kim BJ, Shim JH et al (2012) Enhancement of bone regeneration through facile surface functionalization of solid freeform fabrication-based three-dimensional scaffolds using mussel adhesive proteins. Acta Biomater 8:2578–2586
168. Waite JH, Andersen NH, Jewhurst S et al (2005) Mussel adhesion: finding the tricks worth mimicking. J Adhesion 81:297–317
169. Grande DA, Pitman MI (1988) The use of adhesives in chondrocyte transplantation surgery. Preliminary studies. Bull Hosp Jt Dis Orthop Inst 48:140–148
170. Kord Forooshani P, Lee BP (2017) Recent approaches in designing bioadhesive materials inspired by mussel adhesive protein. J Polym Sci A Polym Chem 55:9–33
171. Lu Q, Danner E, Waite JH et al (2013) Adhesion of mussel foot proteins to different substrate surfaces. J R Soc Interface 10:20120759
172. Sun C, Fantner GE, Adams J et al (2007) The role of calcium and magnesium in the concrete tubes of the sandcastle worm. J Exp Biol 210:1481–1488
173. Zhao H, Sun C, Stewart RJ et al (2005) Cement proteins of the tube-building polychaete Phragmatopoma californica. J Biol Chem 280:42938
174. Stewart RJ, Weaver JC, Morse DE et al (2004) The tube cement of Phragmatopoma californica: a solid foam. J Exp Biol 207:4727–4734
175. British Dental Journal (2020) UK dentistry involved in groundbreaking clinical trial for new orthopaedic material. Br Dent J 229:158. https://doi.org/10.1038/s41415-020-2030-8
176. Costa RR, Soares da Costa D et al (2019) Bioinspired baroplastic glycosaminoglycan sealants for soft tissues. Acta Biomater 87:108–117
177. Kirillova A, Kelly C, von Windheim N et al (2018) Bioinspired mineral-organic bioresorbable bone adhesive. Adv Healthc Mater 7:e1800467. https://doi.org/10.1002/adhm.201800467
178. Mann LK, Papanna R, Moise KJ Jr et al (2012) Fetal membrane patch and biomimetic adhesive coacervates as a sealant for fetoscopic defects. Acta Biomater 8:2160–2165
179. Winslow BD, Shao H, Stewart RJ et al (2010) Biocompatibility of adhesive complex coacervates modeled after the sandcastle glue of Phragmatopoma californica for craniofacial reconstruction. Biomaterials 31:9373–9381

Andy H. Choi is an early career researcher who received his Ph.D. from the University of Technology Sydney (UTS) in Australia in 2004 on the use of computer modelling and simulation known as finite element analysis (FEA) to examine the biomechanical behavior of implants installed into a human mandible. After completing his Ph.D., he expanded his research focus from FEA to sol–gel synthesis of multifunctional calcium phosphate nano coatings and nano composite coatings for dental and biomedical applications.

In late 2010, Dr. Choi was successfully awarded the internationally competitive Endeavour Australia Cheung Kong Research Fellowship Award and undertook post-doctoral training at the Faculty of Dentistry of the University of Hong Kong focusing on the application of FEA in dentistry and the development of calcium phosphate nano-bioceramics.

He is currently serving as an associate editor for the Journal of the Australian Ceramic Society and as an editor for a number

of dentistry-related journals. In addition, he is also serving as an editorial board member for several dentistry, nanotechnology, and orthopedics journals. To date, Dr. Choi has authored over 50 publications including 4 books and 30 book chapters on calcium phosphate, nano-biomaterial coatings, sol–gel technology, marine structures, drug delivery, tissue engineering, and finite element analysis in nanomedicine and dentistry.

Chapter 2
Biomaterials and Bioceramics—Part 2: Nanocomposites in Osseointegration and Hard Tissue Regeneration

Andy H. Choi

Abstract A very effective method of improving the life quality of patients is having the capacity to repair and engineer new functional tissues and in the last forty years, tissue engineering and surface modifications have the potential to accomplish this goal. Many questions concerning the interactions of nanomaterials with both soft and hard tissues have been addressed by a multi-disciplinary team of scientists, engineers, and surgeons. More importantly, the exciting and potential possibilities associated with the use of nanostructured materials and nanocomposites as body interactive materials that assist the body to heal by promoting the regeneration of tissues, hence restoring physiological functions. During the last decade, nanostructured materials has attracted a considerable amount of awareness in areas such as medicine and dentistry, and the emphasis at the moment is on the manufacture of nanocomposites that are applicable to a variety of biomedical applications such as tissue engineering and regeneration. Nanocomposites can be defined as an assortment of two or more materials where at least one of those materials should be on a nanometer-scale. By utilizing the composite approach and secondary substitution phases, it is possible to produce nanocomposites with mechanical properties similar to those of human cortical and cancellous bone. The in vivo cytotoxicity and biocompatibility have been the primary consideration in determining the long-term success of any biomaterials and biocomposites. Presently, the most widely used nanocomposite for biomedical and dental applications is manufactured using several well-characterized and available bioceramics in conjunction with metals and polymers (both natural and synthetic). This approach is currently being explored in the development of next generation nanocomposites with an expanded range of dental and biomedical applications. The last part of the two-part chapter aims to give an overview into the production and types of bio-nanocomposites being examined for applications in implant dentistry as a surface modification approach to improve bone-implant bonding and as tissue engineering scaffolds in the treatment of bone defects.

A. H. Choi (✉)
Faculty of Science, Biomaterials and Translational Medicine Group, School of Life Sciences, University of Technology Sydney (UTS), Ultimo, Australia
e-mail: Andy.H.Choi@alumni.uts.edu.au

A. H. Choi and B. Ben-Nissan (eds.), *Innovative Bioceramics in Translational Medicine I*,
Springer Series in Biomaterials Science and Engineering 17,
https://doi.org/10.1007/978-981-16-7435-8_2

Lastly, brief insights into the application of marine structures in bone grafts and in the treatment of bone disease are also provided.

Keywords Surface modification · Nanocomposites · Tissue engineering scaffold · Bone regeneration · Osteomyelitis · Bioactive glass · Calcium phosphate · Hydroxyapatite · Coral skeleton · Nacre

2.1 Introduction

Nanocomposites can be defined as an assortment of two or more materials where at least one of those materials should be on a nanometer-scale. By utilizing the composite approach and secondary substitution phases, it is possible to produce nanocomposites with mechanical properties such as Young's Modulus and strength similar to those of human cortical and cancellous bone. Nanocomposites can be manufactured by either mixing physically or through the incorporation of a new element into an existing nanosized material. This introduction permits the modification of the nanomaterial's properties and this may in turn offer new function for the material [1–4].

An alternative form of nanocomposite known as the gel system has been developed and ideal for biomedical applications. It is a three-dimensional network immersed in a fluid and the system can entrap nanostructured materials. Matching the specific requirements of biomedical devices is made possible through the gel approach as the properties of nanomaterials can be enhanced and modified. Additionally, acrylamide hydrogel has been used to entrap indicator dyes for the development of intracellular biosensors [5, 6], while carbon nanotube aqueous gel was developed for applications in enzyme-based biosensors [7].

Nanogel, which is a flexible, nanosized hydrophilic polymer gel, is an example of a gel system that can be applied as drug delivery carriers [8, 9]. According to a study by Vinogradov et al., drugs can be loaded spontaneously into the nanogel after they were synthesized and swollen in water [8]. The creation of dense nanoparticles occurs once the gel collapses due to a decrease in the solvent volume.

For applications in dentistry and tissue engineering, the most widely used materials now are those selected from a dozen or so well-characterized and available biocompatible polymers, metals, ceramics, in addition to their combinations as composites and hybrids. The research and development of new nanocomposites and nanolaminates applicable to implant dentistry and regenerative medicine are driven at an astonishing rate by the combined efforts of novel synthesis approach and the advancement into new enabling methodologies such as surface modification, bioinspired (biomimetics), microscale, and nanoscale fabrications. The last part of the two-part chapter aims to give an overview into the production and types of bionanocomposites being examined for applications in implant dentistry as a surface modification approach to improve bone-implant bonding and as tissue engineering scaffolds in the treatment of bone defects. Lastly, brief insights into the application

of marine structures in bone grafts and in the treatment of bone disease are also provided.

2.2 Osseointegration of Implants: Issues and Concerns

One of the primary concerns in biomedical materials research is the relationship between surface properties and the biological responses of materials. Currently, dental and orthopedic implants are produced from metals such as titanium alloy and bioinert cobalt chromium alloys. Their major disadvantage is failure to adapt to the local tissue environment and do not chemically bond to bone unless modified. At present, two different methods are used to insert orthopedic implants surgically. The first uses bone cement (predominately poly(methyl methacrylate) or PMMA) for strong adhesion. The second approach utilizes bioactive ceramic coating to coat porous or micro-textured implants for chemical bonding and mechanical interlocking. This technique is extensively applied to dental and maxillofacial implants in addition to orthopedic prostheses.

From a dental perspective, establishing the success criteria for implant systems are vital and to test implants in well-controlled clinical manner. The most obvious sign of implant failure is mobility and its influence on the surrounding bone tissue. In addition, preventing inflammatory responses and osteolysis is a critical requirement for any implant regardless of the material used in its manufacturing (i.e., ceramic, polymer, of metal). Bone remodeling occurs during the first year of function in response to occlusal forces and to establish normal dimensions of the peri-implant soft tissues.

The stability of the implant at the time of insertion is extremely important and after an implantation, a number of tissue responses can take place at the interface between hard or soft tissues and the implant. Numerous factors can affect the success rate of a dental implant or prosthesis such as the properties and structures of the materials used, the surgical procedure or technique employed, the design of the implant or device, biomechanics and application and impact of the functional loading and finally, the medical condition and health of the patient.

2.2.1 Biological Activities and Cellular Responses

While metals such as titanium and its ternary alloys (for example Ti-6Al-4V) have been applied successfully for more than half a century, its relationship with aseptic inflammation particularly in orthopedic joint replacements believed to be the result of titanium particles releasing from the surfaces of implants and prostheses into the surrounding microenvironment has been a concern [10]. It has been revealed that particles could be released in a surface type-dependent fashion after ultrasonic scaling of titanium implants that may aggravate peri-implantitis [10]. Surface modification

and the utilization of bioceramic coatings (both nanocoatings and nanocomposite coatings) on these materials are intended to offer protection against the release of metal ions which might trigger a negative host response. Ultimately, this provides an improved environment and structure for the growth of new bone [1–4, 11, 12].

Concerns and problems during the past three decades related to biological interactions and adhesion to improve the reliability and longevity of implants and prostheses have driven the assessment of surface modification towards bone-implant adaptability, rapid healing, and early osseointegration. Biological fixation is used to define the way the implant or prostheses is bonded firmly to the host tissue through bone in-growth (with or without the help of mechanical fixation) and not requiring the use of any adhesives. Surface improvements by increasing bioactivity through biological and chemical processes and surface micro- and macro-texturing have been the primary emphasis for researchers in the dental and surgical arena.

Studies based on human trials and animal models have demonstrated that the deposition of a thin hydroxyapatite and other calcium phosphate coatings on surfaces of implants accelerated early bone formation as well as an increase in bond strength between bone and implant [13–21]. It has been shown that the interfacial area or the healing zone between the hydroxyapatite coating and mature bone was found to be rich in mesenchymal stem cells (MSCs) and collagen after 2 weeks post-implantation, which differentiated into osteoblast phenotype and formed osteoid, the non-mineralized bone indicating the commencement of bone regeneration (Fig. 2.1) [14]. Similar observations were made 4 weeks post-implantation where implants coated with nanostructured calcium phosphate inserted into the rabbit femur generated significantly great bone-to-implant contact relative to non-coated titanium implants [15].

Even though many biomaterials have been introduced in dentistry, tissue engineering, and orthopedics, calcium phosphate owing to its similarity to human bone and above all, its dissolution characteristics that enable bone growth and regeneration, holds a special consideration. It should be mentioned that in this chapter the

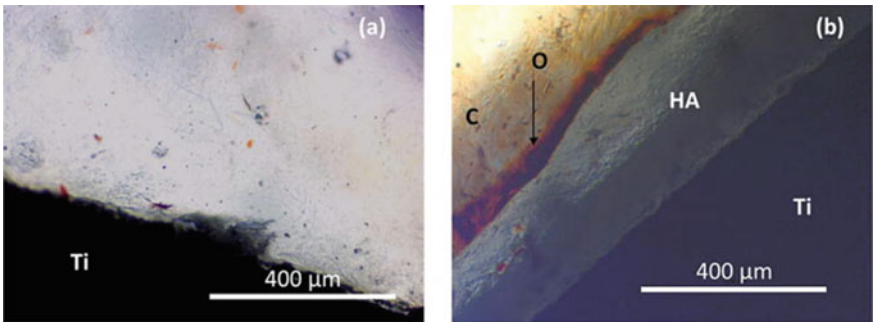

Fig. 2.1 Optical photomicrograph of a longitudinal section of **a** uncoated titanium and **b** hydroxyapatite-coated titanium, implanted in rat femur at 2 weeks showing (O) non-mineralized osteoid, and **c** collagen matrix with Putative Mesenchymal Cells (Goldner's Masson Trichrome stain). Reprinted with permission from [14]

chemical properties would be viewed from the standpoint that hydroxyapatite is calcium phosphate given that most of the information published on hydroxyapatite is categorized under calcium phosphate where hydroxyapatite also belongs, even though hydroxyapatite will have reactivities and properties within the physiological environment different from those of other phosphates.

2.2.2 Surface Modification of Implants and Prostheses

The ability to generate an ideal environment for bone growth has been used to determine if an implant or prosthesis coated with a biocompatible material is successful from a clinical perspective, which involves reducing the amount of metal ions being released, the formation of adequate mechanical interlocking, and the accessibility of a bioactive surface for biological and chemical bonding [1–4, 11, 12].

As explained in the previous section, calcium phosphate has been demonstrated to be an ideal material for dental and orthopedic coatings in a number of studies and extensive bone apposition in animal models when synthesized in a correct manner, and based on these findings [13–21], it can be said that the long-term performance and quality of an implant and/or prosthesis coated with calcium phosphate are determined by various factors such as crystallinity, surface chemistry, constituent phases, surface topography, porosity, and thickness of the coating (Fig. 2.2) [1–4, 11, 12].

Although chemically similar to the mineral component of hard tissues and bones in mammals, porous calcium phosphate has unfavorable mechanical properties and consequently, they cannot be utilized in load-bearing applications. Biological apatites are the inorganic phases of calcified tissues such as bones and teeth and have been idealized as calcium hydroxyapatite. Nevertheless, their lattice parameters are different in addition to their association with other ions such as magnesium and CO_3 and typically calcium-deficient [11, 12]. This created a motivation for the synthesis

Fig. 2.2 Calcium phosphate-coated dental implants

and deposition of both thin and thick coatings on metallic alloys. Utilizing calcium phosphate due to its bioactivity as coatings on metallic alloys such as Ti-6Al-4V allows the union of the two materials' key properties to create a single and functional component [11, 12]. Consequently, it is important to gain an understanding into the mechanisms behind biofixation that takes place when calcium phosphate coating is used. It has been proposed that an increase in the concentration of calcium and phosphate due to the partial dissolution of the apatite into the microenvironment, followed by the formation of carbonate apatite microcrystals and their amalgamation with the organic matrix of bone causing biological growth of bone tissue [22].

2.2.3 Nanocomposite Coatings: Production Techniques

Four general conventional industrial coating techniques were envisioned during the past three decades for the synthesis of bioactive calcium phosphate coatings for clinical applications [11, 12, 23–25]. Currently, coating methods such as sol–gel and thermal or plasma spraying have been used in the deposition of calcium phosphate coating, with plasma spraying being the primary deposition technique utilized for medical applications. Despite its extensive use, there were serious concerns around the coatings deposited by plasma spraying, such as the coatings produced are relatively thick, highly porous and contains amorphous phases. More importantly, the deposited coatings are typically non-uniform and bonds poorly to metal implants. Given the fact that high temperature is used during plasma spraying, it is well-known that hydroxyapatite will undergo dissolution to calcium oxide and β-tri-calcium phosphate, which will cause complications within the physiological environment as these phases have much quicker rates of dissolution.

Another concern is a decrease in mechanical properties of titanium substrates when thick coatings are produced as it is essential to sinter powder ceramics at temperatures of 1000 °C or above. If the temperature is below 882.5 °C or the beta phase transus temperature, commercially pure titanium retains a hexagonal close-packed (HCP) crystal structure (alpha phase). On the other hand, titanium will undergo transformation to a body-centered cubic structure (beta phase) if the temperature is higher than the transus temperature. This transformation will create strains within the titanium substrate that degrades the bond strength of the ceramic coating [26]. The newer sol–gel coating process uses much lower temperatures and thus averting the problems caused by the phase transformation of titanium.

To achieve ideal bioactivity and biocompatibility during the production of implant materials is vital and nanocoatings (particularly those synthesized using the sol–gel approach) can offer an efficient and cost-effective approach in altering the interactions of the implant with the "host" environment. Superior strength, hardness, and bioactivity are known to be displayed by nanocrystalline coatings because of the grain sizes falling in the nanometer range [11, 12, 27]. During the early 1990s, several nanoscale calcium phosphate coatings synthesized using the sol–gel technique were introduced ranging from mixed calcium phosphates to 100% pure hydroxyapatite with a mixture

of amorphous to finely crystalline phases [27]. The thickness of the coating produced also varied based factors such as chemistry, viscosity, and the coating methods used (Fig. 2.3) [27].

The fabrication of new nanocomposites and nanolaminates that are applicable to an extensive range of applications such as surface-modified dental and orthopedic implants/prostheses for improved soft and hard tissue attachment and scaffolding material with increased bioactivity for tissue regeneration and engineering has been ongoing. Since 2000, the development of nanoceramic composite based on calcium phosphate has been the focus for biomedical and dental researchers. Typically, the

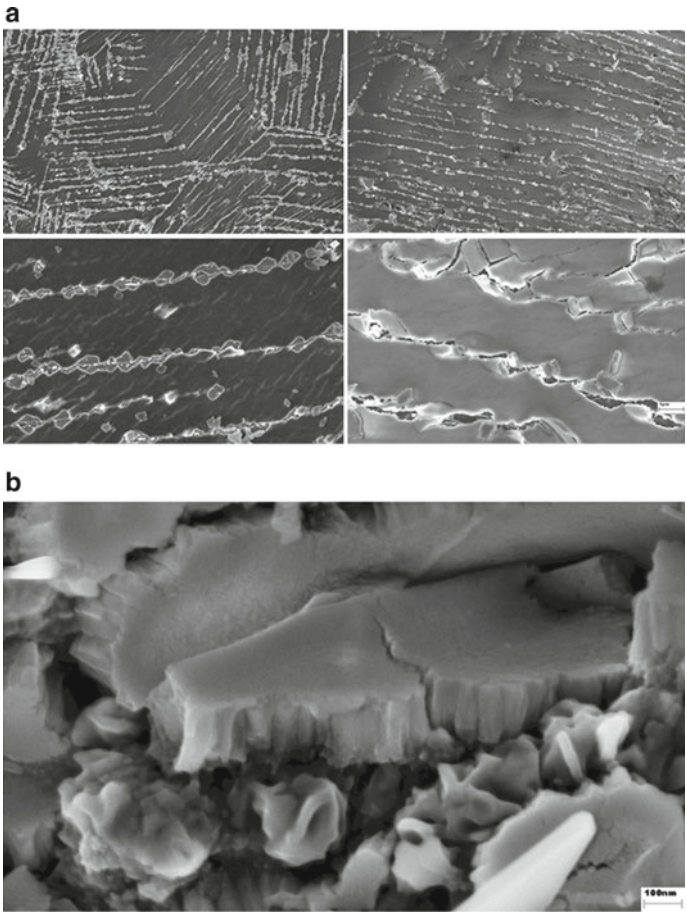

Fig. 2.3 Sol–gel nanocoating of hydroxyapatite on Ti-6Al-4V substrates. The thickness of the coating is approximately 70 nm. **a** Results of the adhesion testing revealed the behavior of the nanocoating under tensile loads, mainly crack arrest and crack branching, which is indicative of excellent fracture toughness behavior. Please note the slip lines of the titanium alloy and the formation of the cracks in these lines. **b** Catastrophic failure of the coating and fracture of the titanium substrate under the coating. Reprinted with permission from [27]

thickness of a single-layered coating is less than 100 nm. Coatings that contain multiple layers with suitable mechanical, biological, physical, and chemical properties can be manufactured with relative ease and can be applied with different compositions as multi-layered gradient coatings or nanolaminates [1]. As such, one form of nanocomposite coating is a multilayered, nanolaminated mixed nanocoatings and this can be manufactured by laminating various nanocoatings together to achieve the desired properties, structures, and thickness [1].

The properties of the calcium phosphate-based nanocomposite coatings and nanolaminates are dependent on the dispersion or secondary phase. Currently, the development of new generations of nanocomposite coatings containing synthetic and natural nanomaterials such as bioglass, collagen, and chitosan are being pursued to promote osseointegration [4]. Polymeric materials have also been applied as the dispersion phase in nanocomposites with calcium phosphate. A study has hypothesized that cellular responses at the bone-titanium implant interface can be induced if a maleic polyelectrolyte such as sodium maleate-vinyl acetate copolymer is added to calcium phosphate. Cells grown on the coated surfaces induced a higher proliferation rate and the incorporation of a sodium maleate copolymer improved surface bio-adhesion than compared to just calcium phosphate [28].

2.2.3.1 Biological Materials

A greater emphasis will be focused on the addition of molecular and nanoscale-based biological materials such as bone morphogenetic proteins, liposomes, and peptides to calcium phosphate coatings in the future in an attempt to reduce the timeframe for implant integration and to improve and promote osseointegration of dental and orthopedic implants and prostheses. Moreover, the current trends are centered on the incorporation of stem cells, growth factors, bone morphogenetic proteins, and several pharmaceuticals into multifunctional nanocoatings.

Chitosan

The bioactivity of chitosan, despite the fact that it is one of the most widely examined material in tissue engineering, will require enhancements for certain tissues and therefore making them not as ideal if used as a stand-alone material [29]. More importantly, the poor mechanical properties of chitosan have restricted their use in load-bearing applications and its combination with reinforcing bioactive materials is designed to reduce these weaknesses. For that reason, it is added to calcium phosphate to overcome these shortcomings [4]. Studies have shown that composite coatings of calcium phosphate and chitosan demonstrated increased osteoconductivity and biodegradation along with sufficient mechanical strength [30, 31].

Collagen

It has been suggested that the unique nanocomposite structure of human bone tissue could be replicated by a composite consists of calcium phosphate and collagen, and this combination can be beneficial as the ductile properties of collagen counterbalance the poor fracture toughness of calcium phosphate [32–38]. In 2010, a study has revealed the osteogenic behavior of rat bone marrow cells could be stimulated in vitro by calcium phosphate-collagen composite coatings even if the coating thickness is less than 100 nm. The composite coating is also able to enhance osteoblast differentiation compared to pure calcium phosphate coatings based on accelerated mineral deposition and a decrease in proliferation [36]. In another animal model study, observations after four weeks post-implantations revealed calcium phosphate-collagen nanocomposite coated titanium rods were virtually surrounded by new bone tissue without encapsulation and had the highest ratio of bone contact when placed under the periosteum of a rat calvarium, while calcium phosphate-coated as well as uncoated specimens were encapsulated with fibrous tissues. Additionally, the nanocomposite-coated rods generated the highest bonding strength to bone [35].

Bone Morphogenetic Proteins

After sintering at a high temperature, commercial calcium phosphate ceramics display a very low specific surface area as well as poor surface reactivity. Despite calcium phosphate is an exceptional osteoconductive material, their osteoinductive properties seem rather weak. It has been proposed that the biological and surface properties of these ceramics can be improved by coating the surfaces with nanocrystalline carbonated apatite and such a layer could encourage biological activity by stimulating the creation of nanopores and increasing the specific surface area [39]. Enhancements in surface reactivity were verified in an adsorption investigation utilizing an osteogenic growth factor, recombinant human bone morphogenetic protein-2 (rhBMP-2). The study also revealed the ceramic is capable of adsorbing more of the protein and releasing it in a prolonged fashion. It was also concluded that the coated ceramic combined with rhBMP-2 could improve bone formation as observed in an in vivo ovine animal model.

Over the last decade, rhBMP-2 has become one of the most extensively investigated protein for applications in oral and maxillofacial surgery such as maxillary sinus floor augmentation, alveolar grafting, and mandibular reconstruction [40–49]. Bone morphogenetic proteins (BMPs) are multi-functional growth factors that belong to the superfamily of transforming growth factor β (TGFβ) [50, 51]. In recent years, their roles in cellular functions in postnatal and adult animals have been comprehensively examined [50, 51]. The actions of BMPs were first realized in 1965 [52], but it was not until the late 1980s after the replication of human BMP-2 and BMP-4 in addition to the sequencing and purification of bovine BMP-3 (osteogenin) that the protein accountable for bone induction were identified [53–55]. Isolated originally from demineralized bone matrix, rhBMP-2 possesses the capacity to stimulate cell

differentiation into chrondroblasts and osteoblasts to begin the process of forming new cartilage and bone tissue [53, 56, 57].

In vivo studies have revealed the application of a calcium phosphate coating (either deposited using conventional coating technique or synthesized biomimetically) can potentially be used to transport growth factors such as BMP in an attempt to enhance peri-implant bone regeneration and their gradual release from the coating has been hypothesized to be the result of cell-mediated degradation [58–62]. Furthermore, BMP can be incorporated and signaling factors be steadily released from the coating during in vivo degradation [60–62]. Also, it was postulated that the combination of calcium phosphate coating and rhBMP-2 could result in significant improvement in bone apposition if the implant is immersed into a protein solution before implantation [60]. In vivo observation confirmed coatings containing rhBMP-2 generated the greatest bone-to-implant contact and bone area fraction occupancy after three weeks of implantation. However, the study also revealed there was not a significant enhancement in bone response if rhBMP-2 was adsorbed directly onto the surfaces of titanium implants but still noticeably higher than uncoated implants.

The deposition of a calcium phosphate layer based on precipitation in a simulated body fluid (SBF) solution has also created new opportunities for the incorporation of BMP-2 to enhance the osseointegration of dental implants. Studies were carried out to gain an understanding into the in vivo osteoinductive capacity of these "self-assembled" or biomimetic coatings containing BMP-2 deposited onto titanium implants [61, 62] and more recently on zirconia [58]. Using a well-established ectopic (subcutaneous) ossification model in rats, the biomimetic coating display the capacity to release BMP-2 at a constant rate in vivo and in a sufficient amount to induce bone formation at an ectopic site. Most of all, their findings also suggested that the coating is able to sustain this osteogenic activity for an extended period as well as carrying out this task with a high degree of efficiency and at a low pharmaceutical level. However, their later study revealed there is no substantial influence on the osteoconductivity during the early phases of osseointegration of implants if calcium phosphate is used as a coating to deliver BMP-2 [61]. The bone-interface coverage and the volume of bone deposited within the peri-implant space were greatest for calcium phosphate coated implants that contains no BMP-2. Uncoated implants along with BMP-2 adsorbed calcium phosphate coated implants produced the lowest quantity of bone deposited and bone-interface coverage.

As previously suggested, the combined efforts of osteoconductive apatite and osteoinductive BMP-2 can create a much greater osteogenic surface environment on titanium surfaces [63]. In order to maintain the rate of release of growth factors, BMP-2 is coupled with negatively charged chondroitin sulfate to create a BMP-2 nanocomplex. Titanium coated with calcium phosphate that contains BMP-2 nanocomplex demonstrated faster cell proliferation once mouse osteoblast cells were seeded on the surfaces in comparison to titanium alone and titanium surfaces only coated with calcium phosphate. The gene expressions of bone-specific markers such as type I collagen and osteocalcin were significantly upregulated by the utilization of BMP-2 nanocomplex. Similar observation was also noticed during the examination of ALP activity.

The release of growth factors such as the ostogenic BMP-2 and the angiogenic vascular endothelial growth factor (VEGF) from bioceramics delivery vehicles such as calcium phosphate has been well documented to influence the magnitude of bone formation in animal models [64–68]. Observations from a recent in vivo study has suggested the use of calcium phosphate for the combined delivery of both BMP-2 and VEGF can result in considerable increase in the formation of new bone as well as enhancements in osteogenic potential [64]. However, the effectiveness of calcium phosphate especially in the form of a coating and their utilization to transport growth factors aimed at improving osseointegration at the bone-implant interface remained unclear. Using biomimetically octacalcium phosphate-coated implants, the efficacy of dual delivery of recombinant human BMP-2 and recombinant human VEGF on osseointegration were assessed [67, 68]. After 2 weeks of post-implantation into frontal skulls of domestic pigs, bone volume density values were improved for biomimetically-coated implants containing the combination of recombinant human BMP-2 and recombinant human VEGF but did not significantly improve bone-implant contact after 4 weeks post-implantation [68]. They also suggested based on the results of their later in vivo study that the dual delivery of growth factors favored bone mineralization as well as expression of vital bone matrix proteins [67].

Peptides

Besides using BMPs to bio-functionalize surfaces of implants, biomimetic peptides such as P-15 and RGD have also been studied for their possible roles in improving the cellular interactions with biomaterials. More importantly, they can be synthetically manufactured, and purification can be carried out relatively easily [69–72]. Within these biomimetic active peptides, only a cell-binding sequence is contained and by imitating cell-binding sites biologically, the RGD (Arg-Gly-Asp) peptide has been hypothesized to promote cell adhesion [73].

Calcium phosphate coatings combined with an RGD-containing peptide deposited on implant surfaces could potentially enhance the attachment and differentiation of osteoblast. As hypothesized, the osteoconductivity of calcium phosphate was strengthened by the availability of peptide. Once implanted into bone, the protein absorption on calcium phosphate surfaces is altered after the peptide pretreatment [71]. The enhancement in osseointegration may be due to the preferential attachment of cells such as osteoprogenitors to calcium phosphate surfaces. It has also been postulated that the immobilization of RGD on anodized titanium via chemical grafting could enhance the osseointegration of implants [74].

On the contrary, observations from another study revealed there is only weak evidence supporting titanium implants coated with RGD peptides could possibly enhance peri-implant bone formation in the alveolar process despite in vitro studies hypothesizing the use of RGD results in improvements in cell attachment [75]. Similarly, in vivo observations were also noticed as an increase in bone density was not recorded outside the bone-implant interface even though a significant bone stimulating effect can be generated by cyclic RGD at the interface [76]. Furthermore,

the potential benefits concerning the use of RGD peptides to functionalize implants coated with calcium phosphate and their effect on osseointegration was questioned [77]. Their results demonstrated the presence of RGD in calcium phosphate disks implanted into rat tibiae significantly inhibited bone formation in addition to the amount of new bone in direct contact with the implant perimeter after 5 days post-implantation [77]. These marginal healing responses has been hypothesized to be due to the uncontrolled signaling responses at the implant-tissue interface by unregulated or sub-optimal integrin binding [78]. In addition, observations from another study proposed structural changes in peptides adsorbed onto titanium as a response to its surface characteristics or low peptide adsorption reduces the likelihood of osteoblast adhesion to be promoted [79].

As a result of the contradictory clinical results produced by the RGD peptides, the search for an alternative peptide sequence that can be applied as an implant coating is a goal worth pursuing. In comparison to RGD-containing peptides, studies have demonstrated that a biomimetic bone matrix known as P-15 was more potent when competing with collagen for cell binding [69, 70, 80]. This biomimetic matrix is a synthetic, 15-amino-acid residue peptide that is identical to the ^{766}GTPGPQGIAGQRGVV^{780} sequence of the type I collagen α1(I) chain [80]. In 2010, a study was carried out to examine the hypothesis that faster osseointegration process can be achieved if surfaces of dental implants were coated with calcium phosphate and P-15 peptides. After 14 and 30 days of post-implantation into the forehead region of 12 adult pigs, a significant higher percentage of bone-to-implant contact was recorded on implants containing high concentration of P-15 as revealed by the results of histomorphometric analysis. An increase in peri-implant bone density at 30 days was detected on implants containing both high and low concentrations of P-15 peptide [70]. Using a canine model, these observations were later endorsed in a study that confirmed the theory that the bioactivity of implants coated with calcium phosphate can be enhanced by the presence of P-15 and its influence were especially noticeable during the early stages of the healing period [69].

Stem Cells

The primary challenge related to the clinical application of mesenchymal stem cells (MSCs) is the way they are obtained from healthy tissues. The oral cavity in recent years has played a significant role as a vital source of MSCs. The ease of access to the dental surgeons and clinicians in addition to the efficacy of cells being isolated from dental tissues such as freshly extracted teeth render the clinical utilization of oral-derived stem cells such as dental pulp stem cells, periodontal ligament (PDL) stem cells, and dental follicle progenitor cells extremely attractive [1, 81]. Recently, human periapical inflammatory cysts, which are a biological waste intended to be eradicated surgically to avoid disabling pathological conditions in the oral cavity, also exhibit MSC-like properties. MSCs isolated from human periapical cysts have been shown to differentiate into adiopocytes and osteoblasts based on their self-renewal capacity and multi-lineage differentiation potency [82–84]. It has been hypothesized that by

combining autologous stem cells from periapical cysts with a bioactive material such as calcium phosphate could provide a solution that encourages the regenerative healing of oral structures such as alveolar bone [82].

Isolated from extracted teeth, PDL contains stem cells which possess the capability to regenerate cementum and/or PDL-like tissues in vivo based on the observations of an animal study [85]. It has been postulated that an alternative implant therapy could be possible through the combined efforts of dental implants with a cell sheet technique [86]. Transplantation of surface-treated and calcium phosphate-coated commercially pure titanium implants with adhered PDL-derived cells (which contain multipotential stem cells) into bone defects in athymic rat femurs as a xenigeneic model as well as into canine mandibular bone as an autologous model were carried out in a previous study to examine the feasibility of regenerating cementum and PDL in vivo. Observations from the rat model demonstrated that PDL-like and cementum-like tissues was partly noticed on surface-treated and calcium phosphate-coated implants combined with adherent PDL-derived cell sheets. Furthermore, histological observations from the canine model revealed the formation of PDL-like and cementum-like tissues was induced on surface-treated and calcium phosphate-coated implants. It was also noticed that the PDL-like tissue was perpendicularly oriented between the titanium surface with cementum-like tissue and the bone [86].

2.3 Regeneration of Hard Tissues: Scaffold Design and Requirements

Tissue engineering in recent times has adopted a new objective by capturing the benefits of uniting the application of three-dimensional bioceramic scaffolds with living cells to transport essential cells to the damaged sites within the patient. During the past few decades, exceptional manufacturing policies have been introduced to amalgamate biogenic materials into bioceramic implants in the areas of osteogenic cell growth and differentiation.

The advancement of bone tissue engineering substitutes has been met by several clinical arguments such as a necessity for improved filler materials used to reconstruct large bone defects and for implants and scaffolds that are more mechanically suited to their biological surroundings. From a biological perspective, bone defect management typically involves the utilization of autograft and allograft [87–89]. The purpose of a scaffold is to encourage the formation of new bone from the surrounding tissues as well as providing a template or carrier for implanted bone cells and other biological agents. Although the inclusion of prerequisites regarding the types of materials used during the design of tissue engineering scaffolds are common, it is also vital to include any clinical requirements so that medically relevant bone substitutes can be manufactured. In addition to material and design considerations, bone regeneration requires four biologically vital mechanisms:

1. A morphogenetic signal
2. The willingness of the responsive host cells to react to the signal

3. A suitable carrier that will deliver this signal to specific sites; and
4. Scaffold capable of supporting the growth of responsive host cells and providing a well-vascularized host bed.

The process of bone regeneration is common during fracture repair. It is normal for the evolution of bone regeneration to take place during the repair of fractures or bony defects. The steps involved in the remodeling cycle comprises of the introduction of bone grafts, the skeletal homeostasis, and the cascading cycle of biological events [1]. Sustaining the integrity of the skeleton has been accepted as the principle behind the bone remodeling sequence. This is accomplished through the collaborative efforts of osteoblasts and osteoclasts, and this close collaborative during the remodeling process is frequently referred to as the basic multicellular unit. Bone resorption and bone formation are balanced in a homeostatic equilibrium. The synchronized biological and mechanical actions on a cellular level play a governing role in the delicate equilibrium between bone formation, growth, and resorption. Additionally, the combination of osteoblasts and osteoclasts also contributes to the bone remodeling of defects such as micro-fractures [1].

Derived from cells of embryos, fetuses, or adults, stem cells possess the capacity to replicate for extended periods as well as creating specialized cells that provides the structures for organs and tissues of the human body. Moreover, these stem cells have been proven capable of creating highly vascularized bone tissues when it is combined with mineralized three-dimensional scaffolds and implanted into immune-deficient mice. Treatments of defects across bone diaphysis can be carried out using these bioceramic-cell cultured composites with positive clinical outcomes such as excellent integration of the bioceramic scaffold with bone tissue and good functional recovery. Porous materials such as calcium phosphates are being applied as bone grafts at a rapid rate as they allow the ingrowth of natural bone as well as the supply of nutrients and blood, hence providing a strong bond between bone tissues and the graft material.

Stem cells have been incorporated into a number of bioceramics including calcium phosphate. The development of highly vascularized bone tissues is possible once these bioceramics combined with mineralized three-dimensional scaffolds are implanted into the human body. Such cell cultured-bioceramic nanocomposites can be utilized to treat full-thickness gaps in long bone shafts. More importantly, excellent integration between bone tissue and scaffold can be provided by these bioceramic nanocomposites, and ultimately good functional recovery. The reconstruction of bone tissues utilizing nanocomposite bone grafts with compositional, biological, physiochemical, structural and biomechanical characteristics that mimic those of human bone is an objective to be achieved.

2.3.1 Materials Selection: From Synthetic to Natural

Over the past three decades, a considerable amount of attention has been paid to the development of bioactive composite grafts consist of a polymeric matrix and a bioactive ceramic filler. These bioactive composite grafts are designed to achieve interfacial bonding between the scaffolding graft and the host tissues. Furthermore, such a combination would perfectly bring together the advantages of the two materials in which the polymer would enhance the toughness and the bioceramic would improve the bioactivity of the composite [90].

2.3.1.1 Calcium Phosphate

The repair of bone and periodontal defects, maxillofacial reconstruction, bone space fillers, alveolar ridge augmentation, ear implants, and bone cement additives are just a few examples where calcium phosphate bioceramics are being used in the orthopedic and dental arenas [1]. Calcium phosphates that contain interconnecting pores with diameters between 100 and 500 μm are frequently used as bone graft materials, where they are combined with both natural and synthetic polymers such as chitosan and collagen to form bioactive composite grafts for tissue engineering applications [91, 92]. The dissolution rate of calcium phosphate is determined by its chemistry and structure, this in turn governs the *in-situ* strength and long-term stability [11, 12, 93].

Composite grafts consist of collagen and calcium phosphate has been of particular interest and a natural option for bone grafting [94]. This is because skeletal bones are composed primarily of carbonate-substituted hydroxyapatite and collagen, both of which are osteoconductive components. Consequently, a scaffold manufactured from calcium phosphate and collagen is anticipated to perform in a similar fashion. Furthermore, collagen-calcium phosphate composite has been shown to be biocompatible in both humans and animal trials. Their study showed calcium phosphate-collagen composites in comparison to monolithic hydroxyapatite displayed osteoconductive properties once embedded with human-like osteoblast cells and generated calcification of an identical bone matrix [95]. Later, another study was carried out to investigate the effect of osteogenic differentiation using bone marrow-derived MSCs on bone regenerative nanocomposites constructed using nano-amorphous calcium phosphate, nano-hydroxyapatite, and reconstituted collagen [96]. It was observed that the presence of reconstituted collagen within the composite significantly improved the osteogenic differentiation.

A number of approaches have been applied to produce gels and films of collagen-calcium phosphate composites as well as collagen-coated calcium phosphate, calcium phosphate-coated collagen matrices and composite scaffolds for bone tissue repair [97]. Based on the observations of several investigations, it has been hypothesized that the utilization of composites composed of nano-hydroxyapatite and

tricalcium phosphate with a simple incorporation of collagen could offer improvements in bioactivity as well as the physical properties of the composite scaffold [98–100].

First used for bone repair in the early 1900's with great success, it took tricalcium phosphate more than six decades after the first clinical study that a suggestion was made related to the application of porous calcium phosphate scaffolds to treat bone defects [101, 102]. Presently, commercially available synthetic calcium phosphate biomaterials are classified according to their composition and these include α- and β-tricalcium phosphate, hydroxyapatite, and biphasic calcium phosphate (which is a mixture with variable ratio of hydroxyapatite and β-tricalcium phosphate). Other commercially available calcium phosphate biomaterials have been synthesized from biological and marine materials such as marine algae, hydrothermally converted coral, processed human bone, and bovine bone [11, 12, 93].

In addition to collagen, other biodegradable natural polymers have also been postulated and explored as scaffolding materials in combination with calcium phosphate for bone tissue engineering applications [1, 2]. One such polymer is chitosan and the possibilities of combining nano-calcium phosphate with chitosan to create a composite scaffold for bone regeneration have been extensively investigated [103–105]. Synthesized from chitin, a natural polysaccharide that can be isolated from the exoskeletons of crustaceans [106, 107], chitosan contains a structure that is similar to glycosaminoglycan, a vital element of the extracellular matrix and plays a pivotal part in bone regeneration. Observations from a cell culture study have suggested that a calcium phosphate-chitosan scaffold can support the attachment and proliferation of MSCs derived from rat bone marrow and the density of MSC on the scaffold increased by an order of magnitude after 2 weeks [108]. Their study also revealed MSCs attached on the scaffold were able to effectively differentiate down the osteogenic lineage and expressed high levels of ALP. Similarly, findings from different studies also showed MSCs and osteoblast-like cells displayed good proliferation and adhesion onto chitosan-nano-hydroxyapatite composite scaffolds [109–111]. In vivo investigations have also been carried out in an effort to study the bone regeneration capabilities of the nanocomposite and observations from the test results revealed that it might not be as effective as using just nano-hydroxyapatite powder [112] or incorporating MSCs to the nanocomposite scaffold prior to implantation [113].

Considered as one of the most abundant renewable resource and the main component in the rigid cells walls in plants, cellulose has been extensively applied in the pharmaceutical and biomedical industries [2]. Observations from in vitro studies have suggested that a nano-calcium phosphate-cellulose composite scaffold is able to support various cellular activities such as growth, attachment, and proliferation of cells such as human dental follicle cells [114] and osteoblasts [115]. A recent in vivo study using rabbit calvarial defect model demonstrated the potential of a cellulose-nano-hydroxyapatite to form mineralized tissues after loaded into defects [116]. Additionally, bacterial cellulose has also received a considerable amount of attention in tissue engineering and their combination with nano-calcium phosphate

as a possible composite scaffold for bone regeneration have been examined both in vitro and in vivo [117–119].

A well-known fiber used widely in the textile industries, the silk from silkworms has also find applications in tissue engineering due to their excellent biodegradability and biocompatibility. The idea of combining silk fibroin with nano-calcium phosphate was first suggested in 2004 where it was observed that L929 fibroblast cells were able to adhere more abundantly on silk fibroin coated with nano-sintered hydroxyapatite particles [120]. Similar observations were made in another study in which mesenchymal cells adhered and actively proliferated on nano-hydroxyapatite-coated silk fibroin composites [121]. Later, in vitro cell culture study using rat osteoblast cells revealed nonwoven silk fibroin net-nano-hydroxyapatite composite scaffold can enhance the viability of osteoblasts and demonstrated excellent cytocompatibility for cell growth [122]. It has been hypothesized that stem cells could be directed towards osteogenesis using a blended eri-tasar silk fibroin nanofibrous scaffolded with surface precipitated nano-hydroxyapatite. An improved osteogenic differentiation was noticed via ALP assay as well as pattern of gene expression linked to osteogenic differentiation and morphological observations of differentiated cord blood human MSCs under microscopic examination [123]. In addition, in vivo biological performance of silk-nano-calcium phosphate scaffolds was also examined using animal models [124, 125]. Implantation of the scaffold into rabbit knee critical size osteochondral defect models demonstrated a firm integration into the host tissue and de novo bone ingrowths and vessel formation were recorded [125]. Similar bone formation capability was observed when nano-hydroxyapatite mineralized silk fibroin scaffold graft was used to induce greater bone formation and to decrease the height of alveolar bone resorption after tooth extraction in vivo [124].

Apart from natural biodegradable polymers, the manufacture of nanocomposite grafts using synthetic polymers and nano-calcium phosphate have also been postulated and examined [1, 2]. Several advantages are associated with the use of synthetic polymers such as the modification of their physical–chemical properties as well as having the ability to engineer the mechanical and degradation characteristics simply by altering the chemical composition to match specific requirements. Furthermore, their ability to be bioactivated with certain molecules by amalgamation of functional groups and side chains is also another benefit of utilizing synthetic polymers.

The possibility of utilizing high-density polyethylene with calcium phosphate nanoparticles as scaffolds was examine in an in vitro study using human MSCs [126]. The lack of cytotoxic effects of the scaffolds was confirmed by viability assays. After eosin and hematoxylin staining, microscopic images of the cell culture study for six weeks confirmed typical growth and morphology.

The utilization of PLGA or poly(lactic-co-glycolic acid) has sadly been severely limited as a consequence of their poor bioactivity and hydrophobic surface even though it is regarded as one of the most frequently applied biodegradable polymer that can be processed easily. Consequently, a composite has been hypothesized that combines the physiochemical and structural advantages of nano-calcium phosphate in the formation of new bone with the biocompatibility of PLGA. The resultant composite has been believed to be capable of providing a solution in regulating the

adhesion and osteogenic differentiation of human MSCs [127–129]. Observations from an in vivo study using avian vessels from the chick chorioallantoic membrane have suggested that human adipose-derived stem cells are capable of completely penetrating an amorphous calcium phosphate nanoparticle-PLGA composite within one-week post-implantation [127].

Due to its low inflammatory response, sustained biodegradability, and excellent mechanical characteristics [130], polycaprolactone presents an interesting option for tissue engineering applications [131–133]. However, their poor capacity to induce osteogenic cell adhesion, differentiation, and proliferation warrant the creation of a composite that combines polycaprolactone with a bioactive material such as calcium phosphate to overcome these restrictions [133]. It has been shown that the viability and adhesion of human MSCs were enhanced by the presence of nano-hydroxyapatite within the scaffold as revealed by Almar Blue assay as well as higher levels of ALP activity after 14 days of incubation [133]. Moreover, an in vivo study has postulated that the addition of bone marrow-derived MSCs from the patient to a polycaprolactone-nano calcium phosphate scaffold could result in a better environment to promote bone regeneration after implantation into defect site. Observations from a rat critical-sized calvarial defect model revealed noticeably greater bone volume and mineralized regeneration after 2 months post-implantation [131].

2.3.1.2 Bioactive Glass

The work of Hench and his co-workers has led to the discovery of several bioactive glass and glass ceramics, and many clinical Bioglass® and other glass ceramics with similar structures and compositions are being applied in orthopedics as well as in dental and oral and maxillofacial surgery for bone augmentation and restoration. They have also been utilized in the field of tissue engineering in general [134, 135].

Silicon (Si), as one of the important trace elements within the human body, is found at a level of 200–550 ppm attached to extracellular matrix compounds and 100 ppm in the bone [1]. They play a role in the mineralization process of bone growth and they have been discovered in locations of active calcification sites [136]. During the past decade, a new category of bioactive calcium silicate ceramics has been created driven by the bioactive compositions of silicate-based bioglass, the function of silicon within the human body and the behavior of stem cells on silicon mesoporous and nanoporous matrices. Bioactive silicate ceramics with certain compositions has been discovered to promote significantly in vitro osteogenic differentiation of several stem cells and in vivo angiogenesis and osteogenesis. Moreover, studies have been carried out to examine the feasibility of implanting silica-based bioglasses that may also contain small quantities of other crystalline phases [1].

First suggested in 1971, a bioglass known as 45S5 Bioglass® was created (Fig. 2.4) and it was proposed that this glass with a composition of 42% SiO_2, 24.5% CaO, 6% P_2O_5, and 24.5% Na_2O by weight has superior osteoblastic activity that allows for a quicker exchange of alkali ions at the surface with hydronium ions in comparison to hydroxyapatite [137, 138]. Furthermore, the formation of an apatite layer was

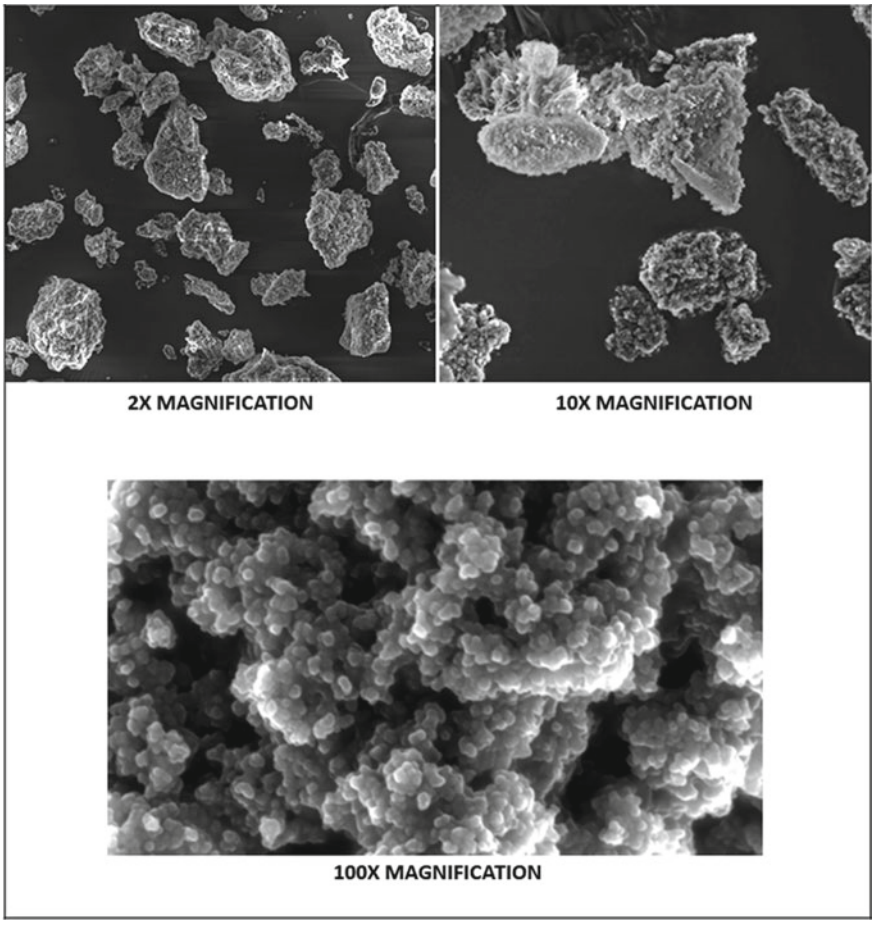

Fig. 2.4 SEM images of sol–gel-derived agglomerated 45S5 Bioglass® nanoparticles taken at different magnifications. Modified and adapted from [145]

also noticed in glass ceramics with a similar composition and different degrees of crystallinity [139]. Bioactive glasses with reduced alkaline oxide content and precipitated crystalline apatite can be synthesized using a specific heat treatment technique. The glass ceramic produced is called Ceravitals, and it possesses greater mechanical strength, but reduced bioactivity compared to Bioglass®.

Proper glass-to-bone bonding has been demonstrated in bioactive glasses with a certain compositional range containing CaO, SiO_2, Na_2O, and P_2O_5 as well as in specific proportions. Results from numerous studies has reached the same conclusion that a firm and unique bonding between the bioactive glass and human bone is achieved as a consequence of the interfacial chemical reactions on the glass surface. This solid and unique bonding was hypothesized to be due to the formation and the even dissolution of a calcium phosphate layer connecting the bioactive glass to the

host bone tissue. This theory can be confirmed by examining the bond strength of implants manufactured from both hydroxyapatite and bioactive glass [140–142].

An important asset of bioactive glass is its capacity to bond firmly to bone via chemical reaction and this eventually allows the glass to be replaced by advancing bone tissues, making it ideal for applications in medical applications. Of vital significance is the elements found within the glass are minerals or physiological chemicals detected in the human body such as silicon, oxygen, magnesium, sodium, potassium, calcium, and phosphorus. It has been demonstrated that the concentration of those elements never increases to a concentration that could lead to a chemical imbalance in the tissues surrounding the glass implant during bonding and bone formation [143, 144].

The brittle nature of glass subsequently means that it cannot be used in scenarios where load-bearing properties are essential. This led to the development of bioactive glass composites. Nanofibers and nanoparticles of bioactive glass have been made available several years ago and they have been used in conjunction with polymers in the form of a nanocomposite. The rationale behind it is to combine and enhance the bioactive phase of glass particles or fibers with the excellent properties of polymers to improve characteristics such as flexibility and being able to withstand deformation under loading. Nano-bioactive glasses have been manufactured using numerous approaches including the sol–gel approach, gas phase or flame spray synthesis, and laser spinning technique [1, 145].

A number of bioglass-based nanocomposites have been manufactured and examined for applications in orthopedics such as bone regeneration matrix and scaffolds [146–152] and in dentistry for periodontal and dental-pulp regeneration [153, 154]. Improvements in degradation kinetics, mechanical properties, bioactivity, and osteoblast responses have been observed due to the presence of bioactive glasses in the nanocomposites when compared to pure polymer or bioglass [151, 155–157].

2.3.1.3 Marine Materials

Highly functional architectural structures with interconnected open pores can be easily found within the marine environment. These structures are ideal for human implantation in its original form or converted to materials more suitable for biomedical applications due to their high mechanical strength and chemical compositions. Furthermore, off-the-shelf organic and inorganic marine skeletons contains an ideal environment for the proliferation of added MSC populations and promoting bone formation that is appropriate from a clinical perspective. The manufacture of highly efficient scaffolds that can perform at the macro-, micro-, and nanoscopic level will play a vital role in making regenerative medicine a clinical success in the future. Cells will be able to be rearranged and reorganized by these scaffolds into tissues and the encapsulated chemical signals will be released in a targeted fashion and conveying them into the body.

Converted coral skeletons and coralline apatites are perfect examples [158–160]. As templates for tissue reconstruction, they have demonstrated substantial clinical

success, and this has encouraged tissue-engineering researchers to explore other marine skeletons with enhanced biological and/or mechanical properties. These unique 3-D marine structures can support the growth and enhancement in differentiation of stem cell progenitors into bone cells. This is different to standard carbonate frameworks as they do not induce stem cell differentiation.

Molecules necessary for the regulation and guiding bone morphogenesis and particularly the actions associated with the mineral metabolism and deposition were also discovered in the earliest marine organisms. This is due to the fact that they signify the first molecular components known for calcification, morphogenesis, and wound healing. Bone morphogenetic protein (BMP), the primary cluster of bone growth factors for human bone morphogenesis, are extensively used in musculoskeletal tissue engineering to promote bone tissue formation and gene expression [161]. It has become apparent that BMP are secreted by endodermal cells into the developing skeleton. The use of biochemical factors to trigger cell proliferation and differentiation is one of the most important factors driving the advancement of tissue regeneration.

The design and availability of marine materials have played a critical role in the establishment of one of the simplest solutions to crucial problems in regenerative medicine and in providing frameworks and opportunities of nanofibers, mineralizing proteins, micro- and macrospheres, and osteopromotive analogues. This is demonstrated by the biological efficiency of marine structures such as corals, sponge skeletons, and shells to accommodate self-sustaining musculoskeletal tissues and to promote bone formation through the application of nacre seashells and sponging extracts [158, 160].

The key idea behind biomimetics is to replicate in a laboratory the structures of selected inorganic biomatrices as they play a distinctive role in the fabrication of calcified tissue replacements [162]. Biomaterials in nature contain advantageous properties such as sophistication and complexity, and we are slowly discovering techniques to mimic nature and establish similar levels of complexity although it is to a limited extent. This can be achieved using techniques found in biomineral-inspired materials chemistry. The plan is to use molecules to manufacture skeletons and turning them into macroscopic structures by applying consecutive developmental pathways of systems that nature employs.

Configuring the material environment at the molecular and macro-molecular levels in an attempt to mimic native extracellular matrix is another method that have been studied and the goal is to further expand and translate this continuing research into the creation of clinically relevant scaffolds for regenerative medicine using a unique set of self-organizing hierarchical structures conceived and manufactured based on biological principles of design. The emphasis on utilizing native biopolymers such as collagen and biocomposites in addition to manufacturing procedures operating at the molecular and nanoscale levels has intensified and this approach permits a more accurate control of chemical and physical properties in the final macrostructure [163, 164]. The resultant structures are designed to be similar to the naturally occurring ones. Electrospun materials are examples that offer fibrous

constructs with dimensions resembling native extracellular matrices and therefore offer the same chemical and physical properties [165].

Naturally occurring biomatrices such as marine shells and sponge skeletons with wide-ranging structural similarities and chemical homologies to human extracellular matrices and whole tissues have thus far been identified as candidates in our search to find scaffolding materials for bone tissue engineering. Certain species of these marine animals has been applied to the regeneration of human bone and the main source of natural skeletons has been natural and converted corals due to its crystallographic, structural, and chemical similarities to native human bone [158–160, 166]. The application of the hydrothermal processing has allowed natural skeletons to be used directly as a scaffold for growing cells into tissues and ultimately in the creation of new bone tissue [166]. Since then, nacre seashells, marine sponges [167], echinoderm spines [168], and the invertebrate marine skeletons of hydrozoans and cuttlefish [169], and others have been examined. Their micro- and macrostructures with suitable pore sizes and its interconnected structural networks are the logic behind the use of these structures as clinical bone-graft materials, which permit easy pathways for sustaining and organizing the growth of bone tissue. Furthermore, diatoms possess natural hierarchical structure making them ideal as functional materials. Despite the lack of comprehensive examination, the regenerative potentials of diatom biogenic silica (such as the transformation of diatom frustule into nanoparticles) have been considered for bone tissue engineering [170].

The development of cost-effective and efficient techniques to synthesize various calcium phosphate phases from biogenic natural materials has received significant amounts of research efforts. Due to their unique compositions which is mainly calcium carbonate as well as their architectures, a number of marine animals such as seashells, nacre, Mediterranean mussels, sea urchins, cuttlefish, and sea corals have been suggested for possible conversions to calcium phosphates bioceramics such as hydroxyapatite and tri-calcium phosphate (α- and β-TCP) for biomedical applications [158–160, 166]. Likewise, the skeletal ossicles from sea stars (*Pisaster giganteus*) have also been studied since they can offer an ideal architecture together with chemical and physical properties conductive to bone restoration [171].

Coral Skeletons in Tissue Engineering

Used extensively in dentistry, orthopedics, craniofacial surgery, and neurosurgery as a bone replacement due to their combination of open porosity, good mechanical properties, and their proficiency to generate chemical bonds with soft tissues and bone in vivo, natural coral exoskeletons have the best mechanical properties of all the porous calcium-based ceramics in general (Fig. 2.5) [158–160]. More importantly, their rates of resorption have been observed to be the same as the formation of new host bone tissues. The excellent biocompatibility and mechanical properties of coral were the result of its organic composition. The composition, abundance, and conformation of the organic matrices are responsible for the successful biological integration of coral with human host [172].

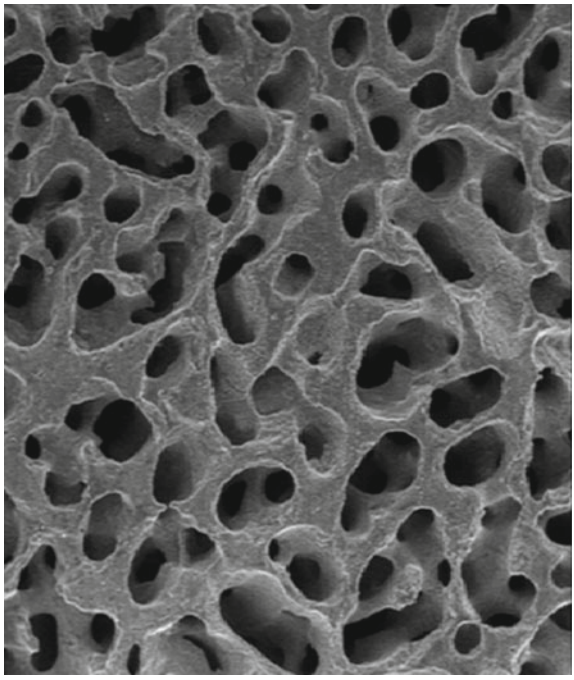

Fig. 2.5 Natural coral structure displaying interconnected pores and its architecture [106]

The exoskeleton of marine madreporic corals is used as a starting material to produce natural coral graft substitutes. The use of coral for dental applications were first attempted by researchers in 1929 and since then corals were recognized and examined in animals during the early 1970s and later in humans in 1979 as a possible candidate as bone graft substitutes. The structure of Porites, a commonly used coral, is comparable to that of human cancellous bone and its initial mechanical properties are also similar. Coral grafts, even though not osteogenic or osteoinductive, are suitable to serve as carriers for growth factors and permit the attachment, growth, differentiation, and spread of cells. Natural coral exoskeletons have been observed to be an excellent bone grafts substitutes if they are utilized in a proper fashion. Consequently, it is also important to select the most appropriate coral so that its resorption rate is identical to the rate of bone formation at the implantation site. In addition, using the composite approach, studies were carried out to combine calcium phosphate converted from corals with polymeric matrix such as polyvinyl acetate and polylactic acid to produce a novel composite bone substitute with improved mechanical properties and functionality [173, 174].

As a consequence of their calcium carbonate structure with high dissolution rates, the application of coral skeletons for tissue engineering and general routine orthopedic surgery has been limited to external fixation devices and not fitting for strictly load-bearing applications. Sol–gel coating techniques on the other hand can be used to improve the strength of corals and as a result enables coral to be applied more frequently at various skeletal locations (Fig. 2.6) [1, 3, 11, 12, 106, 158–160].

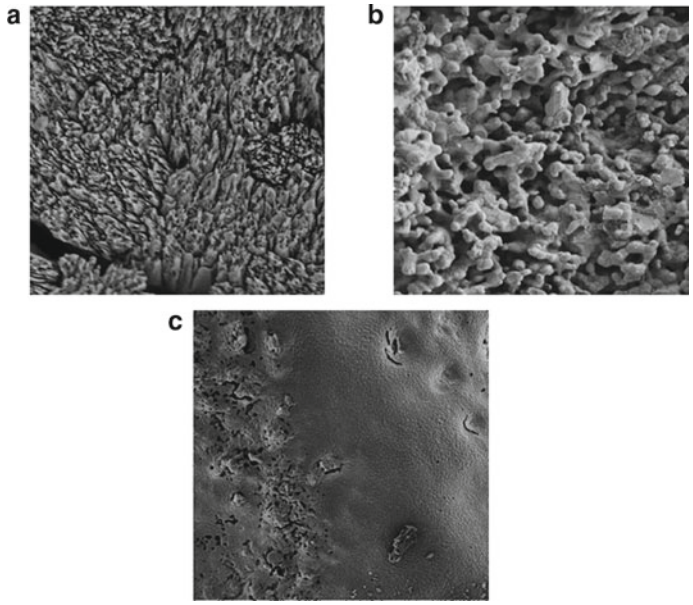

Fig. 2.6 SEM images of the coral structure **a** before and **b** after conversion to hydroxyapatite showing surface morphological changes. **c** Micrograph showing sol–gel coating effectively obliterates the surface meso- and nano-pores, while leaving the macropores intact [180]

Corals, either in their natural or hybridized synthetic forms, offer immense opportunities in bone tissue engineering. Enhancements in osteogenesis is observed when coral skeleton is combined with in vitro expanded human bone marrow stromal cells at levels greater than those recorded with pure scaffold or scaffold including fresh marrow [175]. Clinical results from orthopedic and maxillofacial surgical cases using in vivo large animal segmental defect revealed there is a complete re-corticalization and formation of a medullary canal with mature lamellar cortical bone and onlay graft for contour augmentation of the face, giving rise to clinical union in a lot of cases [176, 177].

Structural and biomineralization studies of coral can be utilized to enhance the development of new advanced functional materials owing to the unique nanoscale organization of organic mineral and tissue. For instance, the characterization of the ultrastructure of deep-sea Bamboo coral (*Anthozoa: Gorgonacea: Isididae*) revealed the internodes display bone-like biochemical and mechanical properties. Furthermore, the organic matrix of the coral, which is comprised of an acidic fibrillar protein framework, shows potential as a model for future applications in tissue engineering. The opportunities arising from the use of this Bamboo coral in tissue engineering are still not fully exploited and understood. The growth of both osteoblast and osteoclast are supported by this organic matrix. It has been suggested that blood vessel implants can be fabricated using the collagen matrix (gorgonin) of this coral due to its exceptional bio-elastomeric properties. Quinones can be utilized to cross-link and

harden collagenous gorgonin proteins and the resultant product resembles closely to human keratin. Lessons could be provided by the mechanisms used in the synthesis of gorgonin and the way it interacts with the mineralization process for the manufacture of synthetic collagen-like materials [178].

As mentioned previously, utilizing marine-derived calcium carbonate exoskeletons for long-term load-bearing applications is not ideal owing to their fast degradation rate. This property, on the other hand, might prove to be potentially useful in drug delivery application where short-term and fast-acting therapy is required. The conversion of the calcium carbonate exoskeleton of coral to the more stable calcium phosphate structures and its derivatives such as hydroxyapatite, TCP, and their mixtures as biphasic apatites in an effort to overcome such limitations [1, 3, 11, 12, 106, 158–160]. To produce calcium phosphates and its derivatives from coral, the abovementioned hydrothermal exchange conversion technique is used in which the carbonate component of the coral is substituted by phosphate at temperatures of around 200–260 °C for a period of 24–48 h (Fig. 2.6) [179, 180]. The adjustment of the molar ratio of calcium to phosphate enables various forms of calcium phosphate to be produced.

Compared to other calcium phosphate compositions, hydroxyapatite or TCP are more suitable for drug delivery applications and for bone grafts under certain conditions. Furthermore, owing primarily to its relatively faster dissolution rate, TCP compared to hydroxyapatite have been extensively investigated and applied as bone grafts [1, 3, 11, 12, 106, 158–160]. This controllable dissolution rate also renders TCP more ideal for drug delivery applications [160]. In order to produce TCP from calcium carbonate exoskeletons, a calcium to phosphate molar ratio of 1.5 is required during the hydrothermal conversion process. Most importantly, the amount of time used for the conversion will determine if carbonated TCP is produced. A complete transformation will occur if the conversion took longer than 48 h, while carbonated TCP is produced when the conversion time is less than 24 h [3, 11, 12]. It should also be mentioned that the conversion time is also dependent on the amount of exoskeleton being converted.

A double-stage conversion method was also developed with the intention to improve the mechanical properties and bioactivity of the converted calcium phosphate. The first stage of the process involved the complete conversion of calcium carbonate exoskeletons until 100% calcium phosphate is attained. During the second stage, a calcium phosphate nanocoating derived from the sol–gel approach is deposited directly to cover the meso- and nanopores within the intra-pore material, while maintaining the large pores [1, 3, 11, 12, 160, 180]. The bioactivity is improved due to the nanograin size and hence large surface area that enhances the reactivity of the nanocoating (Fig. 2.6).

Marine Shells (Nacre)

The assessment of nacre and their capacity to be applied in bone tissue engineering has been conducted using sheep, rabbit, and human models [181, 182]. In human

patients, fresh woven bone bonded itself completely and penetrated the nacre implant, accompanied by the increased activities of osteoclasts and osteoblasts. However, the degradation and resorption of nacre are restricted even though their acceptance in vivo is affirmed, and this could hinder their application within calcified tissue that requires speedy self-regeneration [181, 182].

As an improbable source of biomaterial, the use of the outer nacreous layer of a certain species of mollusc shell for clinical applications and more specifically the engineering of new bone has proven to be valuable. Mollusc shells can provide deeper insights into the complexities of biomineralization such as the interactions between proteins and minerals and how it can be governed and regulated.

First discovered in the early 1990s [183] and later in 2000s [181, 182], the scientific basis concerning the ability of nacre to combine with bone tissue was closely scrutinized and the results demonstrated that skeletal cells were activated by the nacre, and this in turn induced bone formation as well as providing structural support in a human clinical trial [183]. The mechanism behind the methods used by nacre to directly induce human cells towards the creation of new bone could be explained using the idea that a "signaling" biomolecule is accountable for the regulation of cell-mediated biomineralization, and this is common to both nacre and bone tissues of vertebrates (Fig. 2.7).

Different to any other biomaterials, nacre from the pearl oyster (*Pinctada maxima*) is capable of inducing osteogenesis and bone formation from latent osteoprogenitors along an endochondral pathway that consists of a cartilage tissue intermediary phase. Commonly known as the mother of pearl, nacre is the lustrous aragonitic inner layer discovered on molluscan shells in taxa such as abalone and mussels and the powdered form have been used in several studies as composite scaffolds [184, 185]. Nacre contains both inorganic and organic component, is mechanically tough, rapid biodegradable, non-immunogenic, and does not result in detrimental physiological effects. These properties are attributable to the plate-like design and the organic

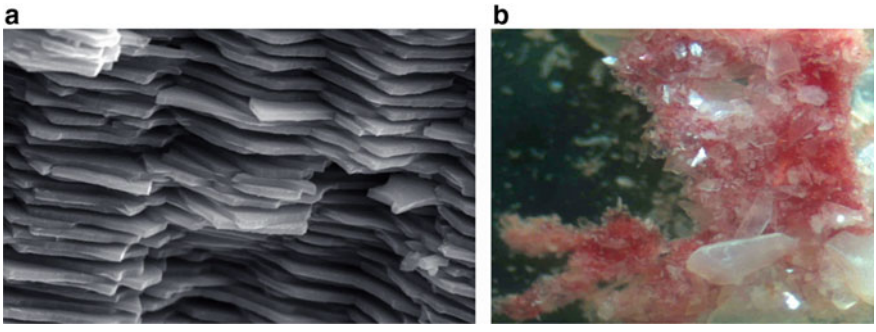

Fig. 2.7 SEM image of plate-like structure of nacre (**a**) and combined in vitro culture of human bone marrow stromal cells (**b**). Nacre chips of various sizes can clearly be seen. The cell mass is stained red for ALP secretion (a primary marker of bone formation) [106]

content of the nacre. In addition, the organic shell matrix consisted of polysaccharides, proteins, and glycoproteins that act as templates for the mineralization of calcium carbonate.

The "water soluble matrix fraction" or WSM of nacre has been recognized to induce the formation of new bone directly and demonstrated to increase bone mineral density in an ovariectomized mouse model of osteoporosis [186–188]. They have also shown to enhance the secretion of cytoplasmic Bcl-2, a key inhibitor of apoptosis. The molecules from nacre matrix displayed a decrease in bone resorption by reducing osteoclast metabolism [187]. Mobile signal transmitters, involved in the biological control of mineralization and serving as an initiator and inhibitor of calcium carbonate crystallization at the growing front of mineralization, has been suggested to disperse into solution based on the evidence available. They have also been displayed to induce differentiation of surrounding latent osteoprogenitor cells [189]. Recently, a study was attempted to improve the release of WSM and calcium ions from natural nacre through intensive crushing into nanometer particles to fully expose the organic bioactive factors of the nacre crystals [185].

The WSM of nacre can be broken down into several fractions containing amino acids of different compositions and sizes. Size exclusion high performance liquid chromatography (HPLC) of the WSM has revealed protein fractions rich in alanine and glycine, with certain biochemical influences on human fibroblasts that controls the differentiation and proliferation of cells [190]. Peptides are widespread in the nacre matrix and certain fractions have been demonstrated to give rise to specific responses from cultured osteoblast cells. For example, protein fractions with molecular weights less than 1 kDa up-regulated ALP secretion, while secretion decreased for high molecular weight fractions. One hundred and ten molecules in the 100 to 70 Da range consisting of glycine-enriched peptides with structural similarities and high affinities for each other have been identified when comprehensive examinations of bioactive low molecular weight molecules were carried out. An increase in human fibroblast cell ALP expression was explicitly displayed by a highly defined matrix protein known as p10 and in the 10 kDa size range [191]. Furthermore, a soluble p60 protein conglomerate extracted from decalcified nacre possesses adequate bioactivity on MSC and 3T3 cells to induce the secretion of mineral nodules [106, 158]. Novel single proteins such as PFMG3 in addition to p10 and p60 have also been discovered and all sourced from the pearl oyster *Pinctada fucata* and these proteins were found to improve crystallization of calcium carbonate in vitro [106, 158].

Moreover, numerous proteins have been recognized within the different species of nacre and a number of them have been suggested to play a role in regulating bone tissue. The oyster *Crassostrea gigas* is an example where four unique proteins were identified from proteomic nacre analysis and believed to aid in shell mineralization, with roles in osteogenesis and with structures comparable to endogenous human proteins. However, there were uncertainties regarding whether nacre proteins were the main cause of osseointegration despite suggestions that nacre was the one responsible. An in vivo study has revealed bone-to-nacre apposition and bonding did occur directly due to the availability of favorable surface chemistry that is rich is phosphorous provided by the nacre which is ideal for the recruitment and attachment

of osteoblast and osteoclast and matrix synthesis. However, it failed to stimulate an in vivo osteogenic response [192]. Another study has hypothesized that the rationale behind the excellent bonding between nacre and bone tissue was the presence of an organic matrix which generates a favorable surface charge for optimal biological association once the nacre is implanted. This creates a new interfacial microenvironment that produces many functional associations with the surrounding bone tissue [193].

2.4 Regeneration of Hard Tissues: Bone Infections and Drug Delivery

Wound contamination as well as post-operative infections during surgical intervention or after implantation in maxillofacial surgery and orthopedics are concerns widely recognized by the medical community that could jeopardize the osseointegration process and can result in serious clinical problems. Antibiotics, as a result, are often provided to the patient as a precaution and they are administrated intravenously or in the oral form.

Moreover, bacterial infections associated with the use of implantable prosthetics and devices in dentistry and orthopedics are complications that happen frequently and by far the most common. Regarded as an opportunistic pathogen, *pseudomonas aeruginosa* causes indwelling device-related infections, particularly in catheters. In cystic fibrosis patients, *pseudomonas aeruginosa* is the main cause of mortality and morbidity. *Staphylococcus aureus* infections on the other hand results in serious infectious complications such as severe deep-seated infections (osteomyelitis, endocarditis, and other metastatic infections), septic-thrombosis, and/or severe sepsis. *Staphylococcus aureus and Staphylococcus epidermidis* strains including methicillin-resistant *staphylococcus aureus* are some of the biofilm infections that are acquired through basic hospital and surgical intervention. In order to defend against biofilm infections, gaining a deeper understanding into the molecular bases of biofilm formation is vital [160].

Numerous mechanisms and interactions are involved during the process in which bacteria adheres to surfaces of materials such as implants and prosthetics, which includes physicochemical, cellular, and molecular. In addition, other factors can influence the complexity of this phenomenon such as the environment where adhesion takes place and the presence of bactericidal substances or serum proteins. Moreover, the characteristics of the bacterial itself and the surface properties of the materials where adhesion will take place also play an important role throughout the process [194].

Given the fact that different adhesives may have been used by bacteria on various surfaces (i.e., different acceptor), limitations have been places on some of the hypothesized models and theories as physical interaction between the bacteria and surface of material is taken into consideration while disregarding the biological attributes

of adhesion. Adhesins are certain bacterial structure responsible for adhesive activities and they regulate the adhesion between different cells as well as cells and abiotic surfaces. From a surface charge, chemistry, and hydrophobicity perspective, the charge of the cell wall and of the substrate are affected by the pH and ionic strength of the medium and this in turn governs their interaction [160].

As discussed above, the development of bone infection is based on the formation of a bacterial biofilm where the bacteria differentiate into sessile forms from planktonic that protect some bacterial cells, which can be released from the biofilm after the termination of antibiotic treatment. Osteomyelitis in orthopedics occurs primarily in tissues surrounding the infected area. The return of bony sequestrum is common and their manifestation is possible given the fact that the existence of damaged bone prevents healing and surgical intervention is needed for their removal.

A widely accepted model of the physiology and pathology associated with osteomyelitis is the devascularization of bone once it becomes infected and bacteria is concealed by the resultant sequestered segments of necrotic cortical bone. The chronicity of osteomyelitis is caused by this sequestered, necrotic, infected bone. The infected sections are encapsulated by pus and granulation tissue and the growth in devascularization of the surrounding bone is driven by bacterial toxins and enzymes through increase in intraosseous pressure. As the infection becomes chronic, relatively avascular fibrous tissue replaces the granulation tissue which envelops the infected area. Motivation to create new reactive bone known as involucrum occurs within the surrounding tissues as well as within the periosteum permeative MSCs that surround the sequestered, necrotic, infected bone [160].

Once the fibrous and bony encapsulation transpires, antibodies and antibiotics must traverse this involucrum and relatively avascular fibrous tissue to reach the microorganisms. The microorganism is also isolated from the defenses of the host as a result of the very effective effort by the human body to quarantine the host from the infection. The infection cannot be eliminated and becomes chronic as soon as this pathological stalemate takes place. This situation is the starting point for surgical intervention and removal of necrotic sequestra. As soon as they are no longer isolated, antibiotic therapy completes the treatment of chronic osteomyelitis by destroying the microorganisms [195]. Thus, models that utilize elimination of infection as a criterion for success along with histological findings of new bone formation, inflammation, sequestration, and intraosseous bacteria, combined with cultures, will provide the most accurate technique for assessing diseases.

Osteomyelitis can be treated with immobilization and antibiotic therapy utilizing a number of medications such as fusidic acid, flucloxacillin, tobermycin, gentamicin, or vancomycin. The main issue related to the application of antibiotics is to make sure its activity and release is maintained for an extended period post operation [196]. Furthermore, high dosage of some antibiotics has been shown to be nephrotoxic and ototoxic as reported by previous studies. The loaded dosages for most controlled release systems are typically high and for that reason, the systemic exposure of antibiotic in urine and blood is a primary safety concern [160].

Thus, a more ideal form of treatment is to deliver antimicrobial agents locally and in a targeted manner. Various approaches have been devised on either controlling and/or preventing bacterial infections. The development and deposition of multi-functional and multi-layered nanocoatings such as nanocomposite coating or nanolaminate on medical implants and devices that have an effect against microbial adhesion or viability will create new opportunities in the prevention of device-related infections. This approach will in turn alter the surfaces of medical devices physically, chemically, or biologically to make the surface free of microbial adhesion.

Several synthetic and natural biomaterials and bioceramics have been suggested as potential candidates to be added to nanocoatings and nanocomposites as biodegradable drug delivery systems [1–3]. On the other hand, manipulating these materials into suitable shape with sufficient microporosity and inserting them into bone defects of various sizes was found to be more difficult. The most ideal material for bone repair and slow drug delivery systems is calcium phosphate [1–3]. Along with their ease of production and drug carrying capacity, they can supply both calcium and phosphate during dissolution. Using a carrier device such as a composite coating on an implant is one of the most effective method of achieving targeted delivery of antibiotics at a specific site and slowly releasing the appropriate dosage. The search for a more efficient method to deliver antibiotics without the toxicity of systemic antibiotics and complications connected to long-term intravenous access has been ongoing. During the last decade or so, numerous studies have been conducted on both commercial and experimental drug delivery vehicles based on calcium phosphate [1–3].

The delivery of antibiotics due to their wide area of applicability has become a major emphasis in the treatment and prevention against infection during surgical interventions and post-operative period. Commercial products based on acrylic polymers or bioceramics such as bioactive glass or calcium sulfate are presently available in pellet form and can be used as slow drug delivery devices. In spite of this, their effectiveness is restricted, and they are either resorbed by the natural physiological process of the body rapidly or being non-resorbable and a second surgery needs to be carried out for their removal due to issues associated to their size and shape, chemical composition, and dissolution rates.

Recently, it has been demonstrated that marine materials such as corals, Foraminifera, and marine shells with specific microspherical design offer desired functions for the delivery of antibiotics [158–160]. The synthesis of a composite consisted of a biodegradable polymer and coralline-derived calcium phosphate loaded with clinically active substance such as gentamicin have been proposed to act as a coating on metallic implants and fracture fixation devices for the prevention of implant-associated infections [158–160]. The use of biodegradable polymer is advantageous due to their ability to degrade over time. It has also been suggested that they could enhance drug stabilization and increase the drug encapsulation efficiency of the composite coating. In addition, it is possible to engineer the rates of drug release to suit the treatment by regulating the interconnectivity and pore sizes of the coralline-derived calcium phosphate particles.

Investigations have been carried to determine the relationship between calcium phosphate particles embedded into the biodegradable polymeric matrix such as

PLA and the release profile of loaded antibiotics such as gentamicin [160]. The release kinetics of gentamicin was found to obey the Power law Krosmeyer Peppas' model with mainly diffusional process via several different drug transport mechanisms. Furthermore, the release profiles were reported to display an early burst stage followed by a continuous rate of release with significant antimicrobial activity against *S. aureus* even at high concentration of bacteria. Even after four weeks of drug release, the growth of bacteria is controlled by the composite coating.

As discussed previously, meso- and nanopores are found within calcium phosphate materials converted from coral. Corals converted to calcium phosphate will contain meso- and nanopores as previously discussed, and throughout the initial loading phase, pharmaceutical drugs such as gentamicin will seep into the pores and the porous network. They will also completely coat the surface of the converted calcium phosphate during the process. Consequently, the term "progressive dissolution process" can be used to describe the three-stage drug dissolution process of composite coating comprised of drug-loaded particles embedded within a biodegradable polymeric matrix.

During the first stage, the immediate dissolution of surface-bound drugs in physiological environment caused by concentration gradient and exposed outer surface area results in an initial burst of antibiotics and presumption can be made that the diffusion of drugs from polymeric matrix surface regulates this release [197]. The rate of dissolution during the second stage is governed by the internal diffusion of drugs infused inside the matrix. It is also conceivable diffusion could occur within the porosities created during the synthesis of the matrix. In comparison to the first stage, the second stage is somewhat slower owing to drug conveying through primarily from the large pores and surface areas of the particles. The diffusion continues with the release of antibiotics from narrow pores of the meso- and nanopores of the particles to the matrix and then to the environment. It is important to note that only dissolution of the drugs takes place in the second stage and there is no degradation of the particles. The use of calcium phosphate could in several ways slow down the release of antibiotics through its internal micropores. The final stage is the terminal release phase, and it involves the degradation and dissolution of the particles together with the gradual deterioration of the polymeric matrix. This results in the slow release of the added drugs or the minerals into the environment. Throughout this stage, there is pore growth due to both mass loss by polymer degradation and micropores joining or amalgamating to create larger pores.

2.5 Concluding Remarks

The birth of nanotechnology has generated novel ideals for the manufacture of synthetic bone-like calcium phosphate nanomaterials and nanocomposites. Due to its ability to imitate the structure and composition of the bone mineral hydroxyapatites, synthetic calcium phosphate is the perfect material when deciding a bone replacement. Furthermore, the accessibility of calcium phosphate nanomaterials has

undoubtedly opened new prospects for the development of superior biocompatible coatings for implants and high-strength nanocomposites. It has been well documented that despite calcium phosphate share similarities in terms of chemistry and composition with human bone, its mechanical properties are far from being ideal. This issue can be addressed through the creation of a nanocomposite that combines the bioactivity of calcium phosphate with other nano- and microscale materials as a secondary phase, and by utilizing this approach, it is feasible to design and produce nanocomposites with mechanical properties much closer to those of natural bone.

Acquiring greater understandings into bioceramics currently used as bone grafts or tissue engineering scaffolds could significantly contribute to the design of new-generation implantable devices. In addition to synthetic calcium phosphate, the application of bioglasses is of vital importance in the restoration of physiological functions by helping the human body to promote tissue regeneration or to heal when used as body-interactive materials. Their application can be further examined in the advancement of next-generation bioactive glasses that can include specific drugs and biogenic materials in an effort to improve their capabilities and functionality. The field of tissue engineering in recent times has been directed to seize the advantage of the combined application of three-dimensional bioglass or ceramic structures and the use of living cells to engineer neotissue to the damaged site of the patient. Currently, practicable and productive strategies have been targeted at merging the acquired knowledge applied to the field of cell growth and differentiation of osteogenic cells with a relatively traditional approach such as bioglass implants.

During the last decade, the marine environment has been extensively explored from biomimetics to soft and hard tissue engineering and controlled drug delivery. The use of biomimetic approach can create promising outcomes for applications in tissue engineering of skeletal tissues. In the future, advanced biomimetic scaffolds must be able to adapt and undergo the ever-changing needs of developing tissues. It is expected that the production of biomaterial scaffolds will interact with surrounding cell population at the macro (bio-functional level), micro (architectural level), and nano/meso (at the contact interface) levels. Nanofabrication using biological principles of assembly and design is still in its early stages and the application of this bio-inspired nanofabrication for tissue engineering is an exceptional approach which has enormous potential to enhance scaffold design that contours to the physicochemical environments with the capacity to micro-evolve. Presently, there is an obvious need for better tissue engineering scaffolds that possess greater natural bio-responsive environments beneficial to guiding the natural processes of regeneration, which can be extremely intricate and dynamic in space and time.

Without doubt, bacterial infections are complications most frequently associated with the use of implantable medical devices such as fracture plates and dental and orthopedic implants. Numerous strategies have been proposed to lessen the problem related to biofilm infections and they are based on either controlling and/or preventing bacterial infections. The development of multi-functional nanocomposite coatings with surface properties that have an effect against microbial viability or adhesion is one promising approach in the prevention of device-related infections. The search is ongoing to discover a more efficient and less costly way to deliver antibiotics

to fight against bacterial infections without the complications associated with long-term intravenous access as well as the toxicity of systemic antibiotics. In the future, research will focus on a process known as gene editing where certain genes of bacteria that are responsible for antibiotic resistance are deactivated and thereby disabling biofilm resistance. This may improve the capability of existing antibiotics to treat infections involving biofilms. Surfaces that would slow-down the formation of biofilm or preventing the colonization of pathogenic bacteria through anti-bacterial or anti-biofilm agents would represent a major improvement in the long-term survival of medical implants and implantable devices.

References

1. Choi AH, Ben-Nissan B (2018) Anatomy, modeling and biomaterial fabrication for dental and maxillofacial applications. Bentham Science Publishers, United Arab Emirates
2. Choi AH, Ben-Nissan B (2017) Calcium phosphate nanocomposites for biomedical and dental applications: recent developments. In: Thakur VK, Thakur MK, Kessler MR (eds) Handbook of composites from renewable materials. Wiley, New Jersey, pp 423–450
3. Choi AH, Ben-Nissan B (2015) Calcium phosphate nanocoatings and nanocomposites, part I: recent developments and advancements in tissue engineering and bioimaging. Nanomedicine 10:2249–2261
4. Choi AH, Ben-Nissan B, Matinlinna JP et al (2013) Current perspective: calcium phosphate nanocoatings and nanocomposite coatings in dentistry. J Dent Res 92:853–859
5. Park EJ, Brasuel M, Behrend C et al (2003) Ratiometric optical PEBBLE nanosensors for real-time magnesium ion concentrations inside viable cells. Anal Chem 75:3784–3791
6. Clark HA, Hoyer M, Philbert MA et al (1999) Optical nanosensors for chemical analysis inside single living cells. 1. Fabrication, characterization, and methods for intracellular delivery of PEBBLE sensors. Anal Chem 71:4831–4836
7. Gavalas VG, Law SA, Christopher Ball J et al (2004) Carbon nanotube aqueous sol-gel composites: enzyme-friendly platforms for the development of stable biosensors. Anal Biochem 329:247–252
8. Vinogradov SV, Batrakova EV, Kabanov AV (2004) Nanogels for oligonucleotide delivery to the brain. Bioconjug Chem 15:50–60
9. Vinogradov SV, Bronich TK, Kabanov AV (2002) Nanosized cationic hydrogels for drug delivery: preparation, properties and interactions with cells. Adv Drug Deliv Rev 54:135–147
10. Eger M, Sterer N, Liron T et al (2017) Scaling of titanium implants entrains inflammation-induced osteolysis. Sci Rep 7:39612
11. Choi AH, Ben-Nissan B (2007) Sol-gel production of bioactive nanocoatings for medical applications: part II: current research and development. Nanomedicine 2:51–61
12. Ben-Nissan B, Choi AH (2006) Sol-gel production of bioactive nanocoatings for medical applications: part I: an introduction. Nanomedicine 1:311–319
13. Surmeneva MA, Surmeneva RA, Nikonova YA et al (2014) Fabrication, ultra-structure characterization and *in vitro* studies of RF magnetron sputter deposited nano-hydroxyapatite thin films for biomedical applications. Appl Surf Sci 317:172–180
14. Roy M, Bandyopadhyay A, Bose S (2011) Induction plasma sprayed nano hydroxyapatite coatings on titanium for orthopaedic and dental implants. Surf Coat Technol 205:2785–2792
15. Jimbo R, Coelho PG, Vandeweghe S et al (2011) Histological and three-dimensional evaluation of osseointegration to nanostructured calcium phosphate-coated implants. Acta Biomater 7:4229–4234
16. Jimbo R, Xue Y, Hayashi M et al (2011) Genetic responses to nanostructured calcium-phosphate-coated implants. J Dent Res 90:1422–1427

17. Orsini G, Piattelli M, Scarano A et al (2007) Randomized, controlled histologic and histomorphometric evaluation of implants with nanometer-scale calcium phosphate added to the dual acid-etched surface in the human posterior maxilla. J Periodontol 78:209–218
18. Sohn SH, Jun HK, Kim CS et al (2006) Biological responses in osteoblast-like cell line according to thin layer hydroxyapatite coatings on anodized titanium. J Oral Rehabil 33:898–911
19. Kim HW, Kim HE, Salih V et al (2005) Sol-gel-modified titanium with hydroxyapatite thin films and effect on osteoblast-like cell responses. J Biomed Mater Res A 74:294–305
20. Oh S, Tobin E, Yang Y et al (2005) *In vivo* evaluation of hydroxyapatite coatings of different crystallinities. Int J Oral Maxillofac Implants 20:726–731
21. Ramires PA, Wennerberg A, Johansson CB et al (2003) Biological behavior of sol-gel coated dental implants. J Mater Sci Mater Med 14:539–545
22. Legeros RZ, Orly L (1991) Substrate surface dissolution and interfacial biological mineralization. In: Davies JE (ed) The bone-biomaterial interface. Toronto Press, Toronto, pp 76–88
23. Ducheyne P, Radin S, Heughebaert M et al (1990) Calcium phosphate ceramic coatings on porous titanium: effect of structure and composition on electropheoretic deposition, vacuum sintering and *in vitro* dissolution. Biomaterials 11:244–254
24. Hench LL, West JK (1990) The sol-gel process. Chem Rev 90:33–72
25. Kokubo T, Kim HM, Kawashita M et al (2000) Novel ceramics for biomedical applications. J Aust Ceram Soc 36:37–46
26. Colling EW (1984) The physical metallurgy of titanium alloys. American Society for Metals, Cleveland
27. Choi G, Choi AH, Evans LA et al (2020) A review: recent advances in sol-gel-derived hydroxyapatite nanocoatings for clinical applications. J Am Ceram Soc 103:5442–5453
28. Negroiu G, Piticescu RM, Chitanu GC et al (2008) Biocompatibility evaluation of a novel hydroxyapatite-polymer coating for medical implants (*in vitro* tests). J Mater Sci Mater Med 19:1537–1544
29. Aguilar A, Zein N, Harmouch E et al (2019) Application of chitosan in bone and dental engineering. Molecules 24:3009
30. Wang J, de Boer J, de Groot K (2004) Preparation and characterization of electrodeposited calcium phosphate/chitosan coating on Ti6Al4V plates. J Dent Res 83:296–301
31. Yamaguchi I, Tokuchi K, Fukuzaki H et al (2001) Preparation and microstructure analysis of chitosan/hydroxyapatite nanocomposites. J Biomed Mater Res 55:20–27
32. Neacsu IA, Arsenie LV, Trusca R et al (2019) Biomimetic collagen/zn^{2+}-substituted calcium phosphate composite coatings on titanium substrates as prospective bioactive layer for implants: a comparative study spin coating vs. MAPLE. Nanomaterials 9:692
33. Ueno FR, Kido HW, Granito RN et al (2016) Calcium phosphate fibers coated with collagen: *in vivo* evaluation of the effects on bone repair. Biomed Mater Eng 27:259–273
34. Zan X, Sitasuwan P, Feng S et al (2016) Effect of roughness on in situ biomineralized CAp-collagen coating on the osteogenesis of mesenchymal stem cells. Langmuir 32:1808–1817
35. Uezono M, Takakuda K, Kikuchi M et al (2013) Hydroxyapatite/collagen nanocomposite-coated titanium rod for achieving rapid osseointegration onto bone surface. J Biomed Mater Res B Appl Biomater 101:1031–1038
36. de Jonge LT, Leeuwenburgh SC, van den Beucken JJ et al (2010) The osteogenic effect of electrosprayed nanoscale collagen/calcium phosphate coatings on titanium. Biomaterials 31:2461–2469
37. Otsuka M, Nakagawa H, Ito A et al (2010) Effect of geometrical structure on drug release rate of a three-dimensionally perforated porous apatite/collagen composite cement. J Pharm Sci 99:286–292
38. Fan Y, Duan K, Wang R (2005) A composite coating by electrolysis-induced collagen self-assembly and calcium phosphate mineralization. Biomaterials 26:1623–1632
39. Rey C, Combes C, Drouet C et al (2007) Physico-chemical properties of nanocrystalline apatites: implications for biominerals and Biomaterials. Mater Sci Eng C BIOS 27:198–205

40. Lee KC, Costandi JJ, Carrao V et al (2020) Autogenous iliac crest versus rhBMP-2 for alveolar cleft grafting: a 14-year single-institution experience. J Oral Maxillofac Surg. https://doi.org/10.1016/j.joms.2020.10.025
41. Min SH, Kang NE, Song SI et al (2020) Regenerative effect of recombinant human bone morphogenetic protein-2/absorbable collagen sponge (rhBMP-2/ACS) after sequestrectomy of medication-related osteonecrosis of the jaw (MRONJ). J Korean Assoc Oral Maxillofac Surg 46:191–196
42. Alraei K, Sharqawi J, Harcher S et al (2020) Efficacy of the combination of rhBMP-2 with bone marrow aspirate concentrate in mandibular defect reconstruction after a pindborg tumor resection. Case Rep Dent 2020:8281741
43. Jahanbin A, Zarch HH, Irani S et al (2019) Recombinant human bone morphogenic protein-2 combined with autogenous bone graft for reconstruction of alveolar cleft. J Craniofac Surg 30:e209–e213
44. Misch CM (2017) Bone augmentation using allogeneic bone blocks with recombinant bone morphogenetic protein-2. Implant Dent 26:826–831
45. Jung J, Yoo HY, Kim GT et al (2017) Short-term teriparatide and recombinant human bone morphogenetic protein-2 for regenerative approach to medication-related osteonecrosis of the jaw: a preliminary study. J Bone Miner Res 32:2445–2452
46. Kim HJ, Chung JH, Shin SY et al (2015) Efficacy of rhBMP-2/hydroxyapatite on sinus floor augmentation: a multicenter, randomized controlled clinical trial. J Dent Res 94:158S-165S
47. Cicciù M, Herford AS, Cicciù D et al (2014) Recombinant human bone morphogenetic protein-2 promote and stabilize hard and soft tissue healing for large mandibular new bone reconstruction defects. J Craniofac Surg 25:860–862
48. Lopes NM, Vajgel A, de Oliveira DM et al (2012) Use of rhBMP-2 to reconstruct a severely atrophic mandible: a modified approach. Int J Oral Maxillofac Surg 41:1566–1570
49. Hart KL, Bowles D (2012) Reconstruction of alveolar defects using titanium-reinforced porous polyethylene as a containment device for recombinant human bone morphogenetic protein 2. J Oral Maxillofac Surg 70:811–820
50. Chen D, Zhao M, Mundy GR (2004) Bone morphogenetic proteins. Growth Factors 22:233–241
51. Croteau S, Rauch F, Silvestri A et al (1999) Bone morphogenetic proteins in orthopedics: from basic science to clinical practice. Orthopedics 22:686–695
52. Urist MR (1965) Bone formation by autoinduction. Science 150:893–899
53. Wozney JM (1992) The bone morphogenetic protein family and osetogenesis. Mol Repord Dev 32:160–167
54. Luyten FP, Cunningham NS, Ma S et al (1989) Purification and partial amino acid sequence of osteogenin, a protein initiating bone differentiation. J Biol Chem 264:13377–13380
55. Wozney JM, Rosen V, Celeste AJ et al (1988) Novel regulators of bone formation: molecular clones and activities. Science 242:1528–1534
56. Urist MR, Nilsson O, Rasmussen J et al (1987) Bone regeneration under the influence of a bone morphogenetic protein (BMP) beta tri-calcium phosphate (TCP) composite in skull trephine defects in dogs. Clin Orthop Relat Res 214:295–304
57. Urist MR, DeLange RJ, Finerman GA (1983) Bone cell differentiation and growth factors. Science 220:680–686
58. Teng F, Zheng Y, Wu G et al (2019) Bone tissue responses to zirconia implants modified by biomimetic coating incorporated with BMP-2. Int J Periodontics Restorative Dent 39:371–379
59. Liu Y, Schouten C, Boerman O et al (2018) The kinetics and mechanism of bone morphogenetic protein 2 release from calcium phosphate-based implant-coatings. J Biomed Mater Res A 106:2363–2371
60. Yoo D, Tovar N, Jimbo R et al (2014) Increased osseointegration effect of bone morphogenetic protein 2 on dental implants: an *in vivo* study. J Biomed Mater Res A 102:1921–1927
61. Liu Y, Enggist L, Kuffer AF et al (2007) The influence of BMP-2 and its mode of delivery on the osteoconductivity of implant surfaces during the early phase of osseointegration. Biomaterials 28:2677–2686

62. Liu Y, de Groot K, Hunziker EB (2005) BMP-2 liberated from biomimetic implant coatings induces and sustains direct ossification in an ectopic rat model. Bone 36:745–757
63. Bae SE, Choi J, Joung YK et al (2012) Controlled release of bone morphogenetic protein (BMP)-2 from nanocomplex incorporated on hydroxyapatite-formed titanium surface. J Control Release 160:676–684
64. Kim TW, Ahn WB, Kim JM et al (2020) Combined delivery of two different bioactive factors incorporated in hydroxyapatite microcarrier for bone regeneration. Tissue Eng Regen Med 17:607–624
65. Amirian J, Linh NT, Min YK et al (2015) Bone formation of a porous gelatin-pectin-biphasic calcium phosphate composite in presence of BMP-2 and VEGF. Int J Biol Macromol 76:10–24
66. Sukul M, Nguyen TB, Min YK et al (2015) Effect of local sustainable release of BMP2-VEGF from nano-cellulose loaded in sponge biphasic calcium phosphate on bone regeneration. Tissue Eng Part A 21:1822–1836
67. Ramazanoglu M, Lutz R, Rusche P et al (2013) Bone response to biomimetic implants delivering BMP-2 and VEGF: an immunohistochemical study. J Craniomaxillofac Surg 41:826–835
68. Ramazanoglu M, Lutz R, Ergun C et al (2011) The effect of combined delivery of recombinant human bone morphogenetic protein-2 and recombinant human vascular endothelial growth factor 165 from biomimetic calcium-phosphate-coated implants on osseointegration. Clin Oral Implants Res 22:1433–1439
69. Coelho PG, Teixeira HS, Marin C et al (2014) The *in vivo* effect of P-15 coating on early osseointegration. J Biomed Mater Res B Appl Biomater 102:430–440
70. Lutz R, Srour S, Nonhoff J et al (2010) Biofunctionalization of titanium implants with a biomimetic active peptide (P-15) promotes early osseointegration. Clin Oral Implants Res 21:726–734
71. Itoh D, Yoneda S, Kuroda S et al (2002) Enhancement of osteogenesis on hydroxyapatite surface coated with synthetic peptide (EEEEEEEPRGDT) *in vitro*. J Biomed Mater Res 62:292–298
72. Roessler S, Born R, Scharnweber D et al (2001) Biomimetic coatings functionalized with adhesion peptides for dental implants. J Mater Sci Mater Med 12:871–877
73. Ruoslahti E (1996) RGD and other recognition sequences for integrins. Ann Rev Cell Dev Biol 12:697–715
74. Ryu JJ, Park K, Kim HS et al (2013) Effects of anodized titanium with Arg-Gly-Asp (RGD) peptide immobilized via chemical grafting or physical adsorption on bone cell adhesion and differentiation. Int J Oral Maxillofac Implants 28:963–972
75. Schliephake H, Scharnweber D, Dard M et al (2002) Effect of RGD peptide coating of titanium implants on periimplant bone formation in the alveolar crest. An experimental pilot study in dogs. Clin Oral Implants Res 13:312–319
76. Elmengaard B, Bechtold JE, Søballe K (2005) *In vivo* study of the effect of RGD treatment on bone ongrowth on press-fit titanium alloy implants. Biomaterials 26:3521–3526
77. Hennessy KM, Clem WC, Phipps MC et al (2008) The effect of RGD peptides on osseointegration of hydroxyapatite biomaterials. Biomaterials 29:3075–3083
78. Petrie TA, Raynor JE, Reyes CD et al (2008) The effect of integrin-specific bioactive coatings on tissue healing and implant osseointegration. Biomaterials 29:2849–2857
79. Dettin M, Conconi MT, Gambaretto R et al (2005) Effect of synthetic peptides on osteoblast adhesion. Biomaterials 26:4507–4515
80. Bhatnagar RS, Qian JJ, Gough CA (1997) The role in cell binding of a beta-bend within the triple helical region in collagen alpha 1 (I) chain: structural and biological evidence for conformational tautomerism on fiber surface. J Biomol Struct Dyn 14:547–560
81. Tatullo M, Marrelli M, Paduano F (2015) The regenerative medicine in oral and maxillofacial surgery: the most important innovations in the clinical application of mesenchymal stem cells. Int J Med Sci 12:72–77
82. Tatullo M, Spagnuolo G, Codispoti B et al (2019) PLA-based mineral-doped scaffolds seeded with human periapical cyst-derived MSCs: a promising tool for regenerative healing in dentistry. Materials 12:597

83. Tatullo M, Codispoti B, Pacifici A et al (2017) Potential use of human periapical cyst-mesenchymal stem cells (hPCy-MSCs) as a novel stem cell source for regenerative medicine applications. Front Cell Dev Biol 5:103
84. Marrelli M, Paduano F, Tatullo M (2013) Cells isolated from human periapical cysts express mesenchymal stem cell-like properties. Int J Biol Sci 9:1070–1078
85. Seo BM, Miura M, Gronthos S et al (2004) Investigation of multipotent postnatal stem cells from human periodontal ligament. Lancet 364:149–155
86. Washio K, Tsutsumi Y, Tsumanuma Y et al (2018) *In vivo* periodontium formation around titanium implants using periodontal ligament cell sheet. Tissue Eng Part A 24:1273–1282
87. Campana V, Milano G, Pagano E et al (2014) Bone substitutes in orthopaedic surgery: from basic science to clinical practice. J Mater Sci Mater Med 25:2445–2461
88. Zhang N, Nichols HL, Tylor S et al (2007) Fabrication of nanocrystalline hydroxyapatite doped degradable composite hollow fiber for guided and biomimetic bone tissue engineering. Mater Sci Eng C 27:599–606
89. Harakas NK (1984) Demineralized bone-matrix-induced osteogenesis. Clin Orthop Relat Res 188:239–251
90. Peroglio M, Gremillard L, Chevalier J et al (2007) Toughening of bioceramics scaffolds by polymer coating. J Eur Ceram Soc 27:2679–2685
91. Oliveira JM, Rodrigues MT, Silva SS et al (2006) Novel hydroxyapatite/chitosan bilayered scaffold for osteochondral tissue-engineering applications: Scaffold design and its performance when seeded with goat bone marrow stromal cells. Biomaterials 27:6123–6137
92. Murugan R, Ramakrishna S (2005) Development of nanocomposites for bone grafting. Compos Sci Technol 65:2385–2406
93. LeGeros RZ (2002) Properties of osteoconductive biomaterials: calcium phosphate. Clin Orthop Relat Res 395:81–98
94. TenHuisen KS, Martin RI, Klimkiewicz M et al (1995) Formation and properties of a synthetic bone composite: hydroxyapatite-collagen. J Biomed Mater Res 29:803–810
95. Scabbia A, Trombelli L (2004) A comparative study on the use of a HA/collagen/chondroitin sulphate biomaterial (Biostite) and a bovine-derived HA xenograft (Bio-Oss) in the treatment of deep intra-osseous defects. J Clin Periodontol 31:348–355
96. Ou KL, Wu J, Lai WF et al (2010) Effects of the nanostructure and nanoporosity on bioactive nanohydroxyapatite/reconstituted collagen by electrodeposition. J Biomed Mater Res A 92:906–912
97. Wahl DA, Czernuszka JT (2006) Collagen-hydroxyapatite composites for hard tissue repair. Eur Cell Mater 11:43–56
98. Ebrahimi M, Pripatnanont P, Monmaturapoj N et al (2012) Fabrication and characterization of novel nano hydroxyapatite/β-tricalcium phosphate scaffolds in three different composition ratios. J Biomed Mater Res A 100:2260–2268
99. LeGeros RZ, Lin S, Rohanizadeh R et al (2003) Biphasic calcium phosphate bioceramics: preparation, properties and applications. J Mater Sci Mater Med 14:201–209
100. Daculsi G, Passuti N, Martin S et al (1990) Macroporous calcium phosphate ceramic for long bone surgery in humans and dogs. Clinical and histological study. J Biomed Mater Res 24:379–396
101. Albee FH, Morrison HF (1920) Studies in bone growth: Triple CaP as a stimulus to osteogenesis. Ann Surg 71:32–39
102. Hulbert SF, Young FA, Mathews RS et al (1970) Potential of ceramic materials as permanently implantable skeletal prostheses. J Biomed Mater Res 4:433–456
103. Venkatesan J, Kim SK (2010) Chitosan composites for bone tissue engineering–an overview. Mar Drugs 8:2252–2266
104. Chesnutt BM, Viano AM, Yuan Y et al (2009) Design and characterization of a novel chitosan/nanocrystalline calcium phosphate composite scaffold for bone regeneration. J Biomed Mater Res A 88:491–502
105. Li Z, Yubao L, Aiping Y et al (2005) Preparation and *in vitro* investigation of chitosan/nano-hydroxyapatite composite used as bone substitute materials. J Mater Sci Mater Med 16:213–219

106. Choi AH, Ben-Nissan B (eds) (2019) Marine-derived biomaterials for tissue engineering applications. Springer series in biomaterials science and engineering, vol 14. Springer Publishing, Singapore
107. Saravanan S, Sameera DK, Moorthi A (2013) Chitosan scaffolds containing chicken feather keratin nanoparticles for bone tissue engineering. Int J Biol Macromol 62:481–486
108. Moreau JL, Xu HH (2009) Mesenchymal stem cell proliferation and differentiation on an injectable calcium phosphate-chitosan composite scaffold. Biomaterials 30:2675–2682
109. Kumar P, Saini M, Dehiya BS et al (2020) Fabrication and *in-vitro* biocompatibility of freeze-dried CTS-nHA and CTS-nBG scaffolds for bone regeneration applications. Int J Biol Macromol 149:1–10
110. Reves BT, Jennings JA, Bumgardner JD et al (2012) Preparation and functional assessment of composite chitosan-nano-hydroxyapatite scaffolds for bone regeneration. J Funct Biomater 3:114–130
111. Palazzo B, Gallo A, Casillo A et al (2011) Fabrication, characterization and cell cultures on a novel composite chitosan-nano-hydroxyapatite scaffold. Int J Immunopathol Pharmacol 24:73–78
112. Tavakol S, Nikpour MR, Amani A et al (2013) Bone regeneration based on nano-hydroxyapatite and hydroxyapatite/chitosan nanocomposites: an *in vitro* and *in vivo* comparative study. J Nanopart Res 15:1373
113. He Y, Dong Y, Cui F et al (2015) Ectopic osteogenesis and scaffold biodegradation of nano-hydroxyapatite-chitosan in a rat model. PLoS One 10:e0135366.
114. Ao C, Niu Y, Zhang X et al (2017) Fabrication and characterization of electrospun cellulose/nano-hydroxyapatite nanofibers for bone tissue engineering. Int J Biol Macromol 97:568–573
115. Gouma P, Xue R, Goldbeck CP et al (2012) Nano-hydroxyapatite-cellulose acetate composites for growing of bone cells. Mater Sci Eng C 32:607–612
116. Daugela P, Pranskunas M, Juodzbalys G et al (2018) Novel cellulose/hydroxyapatite scaffolds for bone tissue regeneration: *in vitro* and *in vivo* study. J Tissue Eng Regen Med 12:1195–1208
117. Kumbhar JV, Jadhav SH, Bodas DS et al (2017) *In vitro* and *in vivo* studies of a novel bacterial cellulose-based acellular bilayer nanocomposite scaffold for the repair of osteochondral defects. Int J Nanomedicine 12:6437–6459
118. Saska S, Barud HS, Gaspar AM et al (2011) Bacterial cellulose-hydroxyapatite nanocomposites for bone regeneration. Int J Biomater 2011:175362
119. Fang B, Wan YZ, Tang TT et al (2009) Proliferation and osteoblastic differentiation of human bone marrow stromal cells on hydroxyapatite/bacterial cellulose nanocomposite scaffolds. Tissue Eng Part A 15:1091–1098
120. Furuzono T, Yasuda S, Kimura T et al (2004) Nano-scaled hydroxyapatite/polymer composite IV. Fabrication and cell adhesion properties of a three-dimensional scaffold made of composite material with a silk fibroin substrate to develop a percutaneous device. J Artif Organs 7:137–144
121. Hirose M, Hamada K, Tanaka T et al (2006) Nano-scaled hydroxyapatite/silk fibroin composites as mesenchymal cell culture scaffolds. Key Eng Mater 309–311:923–926
122. Zhao Y, Chen J, Chou AH et al (2009) Nonwoven silk fibroin net/nano-hydroxyapatite scaffold: preparation and characterization. J Biomed Mater Res A 91:1140–1149
123. Panda N, Bissoyi A, Pramanik K et al (2014) Directing osteogenesis of stem cells with hydroxyapatite precipitated electrospun eri-tasar silk fibroin nanofibrous scaffold. J Biomater Sci Polym Ed 25:1440–1457
124. Nie L, Zhang H, Ren A et al (2019) Nano-hydroxyapatite mineralized silk fibroin porous scaffold for tooth extraction site preservation. Dent Mater 35:1397–1407
125. Yan LP, Silva-Correia J, Oliveira MB et al (2015) Bilayered silk/silk-nanoCaP scaffolds for osteochondral tissue engineering: *In vitro* and *in vivo* assessment of biological performance. Acta Biomater 12:227–241
126. Hild N, Fuhrer R, Mohn D et al (2012) Nanocomposites of high-density polyethylene with amorphous calcium phosphate: *in vitro* biomineralization and cytocompatibility of human mesenchymal stem cells. Biomed Mater 7:054103

127. Buschmann J, Härter L, Gao S et al (2012) Tissue engineered bone grafts based on biomimetic nanocomposite PLGA/amorphous calcium phosphate scaffold and human adipose-derived stem cells. Injury 43:1689–1697
128. Lock J, Nguyen TY, Liu H (2012) Nanophase hydroxyapatite and poly(lactide-co-glycolide) composites promote human mesenchymal stem cell adhesion and osteogenic differentiation *in vitro*. J Mater Sci Mater Med 23:2543–2552
129. Lee JH, Rim NG, Jung HS et al (2010) Control of osteogenic differentiation and mineralization of human mesenchymal stem cells on composite nanofibers containing poly[lactic-co-(glycolic acid)] and hydroxyapatite. Macromol Biosci 10:173–182
130. Ali SA, Zhong SP, Doherty PJ et al (1993) Mechanisms of polymer degradation in implantable devices. I. Poly(caprolactone). Biomaterials 14:648–656
131. Naudot M, Garcia Garcia A, Jankovsky N et al (2020) The combination of a poly-caprolactone/nano-hydroxyapatite honeycomb scaffold and mesenchymal stem cells promotes bone regeneration in rat calvarial defects. J Tissue Eng Regen Med 14:1570–1580
132. Andrade TM, Mello DCR, Elias CMV et al (2019) *In vitro* and *in vivo* evaluation of rotary-jet-spun poly(ε-caprolactone) with high loading of nano-hydroxyapatite. J Mater Sci Mater Med 30:19
133. Domingos M, Gloria A, Coelho J et al (2017) Three-dimensional printed bone scaffolds: the role of nano/micro-hydroxyapatite particles on the adhesion and differentiation of human mesenchymal stem cells. Proc Inst Mech Eng H 231:555–564
134. Hong Z, Reis RL, Mano JF (2009) Preparation and *in vitro* characterization of novel bioactive glass ceramic nanoparticles. J Biomed Mater Res A 88:304–313
135. Hench LL, West JK (1996) Biological applications of bioactive glasses. Life Chem Rep 13:187–241
136. LeGeros RZ (1993) Biodegradation and bioresorption of calcium phosphate ceramics. Clin Mater 14:65–88
137. Huckstep RL, Sherry E (1996) Replacement of the proximal humerus in primary bone tumours. Aust N Z J Surg 66:97–100
138. Vrouwenvelder WCA, Groot CG, de Groot K (1993) Histological and biochemical evaluation of osteoblasts cultured on bioactive glass, hydroxylapatite, titanium alloy, and stainless steel. J Biomed Mater Res 27:465–475
139. Li P, Yang Q, Zhang F et al (1992) The effect of residual glassy phase in a bioactive glass-ceramic on the formation of its surface apatite layer *in vitro*. J Mater Sci Mater Med 3:452–456
140. Niki M, Ito G, Matsuda T et al (1991) Comparative push-out data of bioactive and non-bioactive materials of similar rugosity. In: Davies JE (ed) Bone-material interface. University of Toronto Press, Toronto, pp 350–356
141. Fujiu T, Ogino M (1984) Difference of bone bonding behavior among surface active glasses and sintered apatite. J Biomed Mater Res 18:845–859
142. Wilson J, Pigott GH, Schoen FJ et al (1981) Toxicology and biocompatibility of bioglasses. J Biomed Mater Res 15:805–817
143. Lai W, Ducheyne P, Garino J (1998) Removal pathway of silicon released from bioactive glass granules *in vivo*. In: LeGeros RZ, LeGeros JP (eds) Bioceramics. World Scientific, New York, pp 383–386
144. Andersson ÖH, Karlsson KH, Kangasniemi K (1990) Calcium-phosphate formation at the surface of bioactive glass *in vivo*. J Non-Cryst Solids 119:290–296
145. Ben-Nissan B, Choi AH, Macha I (2017) Advances in bioglass and glass ceramics for biomedical applications. In: Li Q, Mai YW (eds) Biomaterials for implants and scaffolds. Springer series in biomaterials science and engineering, vol 8. Springer, Berlin, pp 133–161
146. Kazemi M, Dehghan MM, Azami M (2019) Biological evaluation of porous nanocomposite scaffolds based on strontium substituted β-TCP and bioactive glass: An *in vitro* and *in vivo* study. Mater Sci Eng C Mater Biol Appl 105:110071
147. Covarrubias C, Cádiz M, Maureira M et al (2018) Bionanocomposite scaffolds based on chitosan-gelatin and nanodimensional bioactive glass particles: *in vitro* properties and *in vivo* bone regeneration. J Biomater Appl 32:1155–1163

148. Hafezi F, Hosseinnejad F, Fooladi AA et al (2012) Transplantation of nano-bioglass/gelatin scaffold in a non-autogenous setting for bone regeneration in a rabbit ulna. J Mater Sci Mater Med 23:2783–2792
149. Valenzuela F, Covarrubias C, Martinez C et al (2012) Preparation and bioactive properties of novel bone-repair bionanocomposites based on hydroxyapatite and bioactive glass nanoparticles. J Biomed Mater Res B Appl Biomater 100:1672–1682
150. Hajiali H, Karbasi S, Hosseinalipour M et al (2010) Preparation of a novel biodegradable nanocomposite scaffold based on poly (3-hydroxybutyrate)/bioglass nanoparticles for bone tissue engineering. J Mater Sci Mater Med 21:2125–2132
151. Chen QZ, Boccaccini AR (2006) Poly(D, L-lactic acid) coated 45S5 Bioglass-based scaffolds: processing and characterization. J Biomed Mater Res A 77:445–457
152. Kim HW, Song JH, Kim HE (2006) Bioactive glass nanofiber-collagen nanocomposite as a novel bone regeneration matrix. J Biomed Mater Res A 79:698–705
153. Mota J, Yu N, Caridade SG et al (2012) Chitosan/bioactive glass nanoparticle composite membranes for periodontal regeneration. Acta Biomater 8:4173–4180
154. Bae WJ, Min KS, Kim JJ et al (2012) Odontogenic responses of human dental pulp cells to collagen/nanobioactive glass nanocomposites. Dent Mater 28:1271–1279
155. Roohani-Esfahani SI, Nouri-Khorasani S, Lu ZF et al (2011) Effects of bioactive glass nanoparticles on the mechanical and biological behavior of composite coated scaffolds. Acta Biomater 7:1307–1318
156. Lee HH, Yu HS, Jang JH et al (2008) Bioactivity improvement of poly(epsilon-caprolactone) membrane with the addition of nanofibrous bioactive glass. Acta Biomater 4:622–629
157. Kim HW, Lee HH, Chun GS (2008) Bioactivity and osteoblast responses of novel biomedical nanocomposites of bioactive glass nanofiber filled poly(lactic acid). J Biomed Mater Res A 85:651–663
158. Choi AH, Cazalbou S, Ben-Nissan B (2016) Biomimetics and marine materials in drug delivery and tissue engineering. In: Antoniac I (ed) Handbook of bioceramics and biocomposites. Springer, Cham, pp 521–544
159. Ben-Nissan B, Macha I, Cazalbou S et al (2016) Calcium phosphate nanocoatings and nanocomposites, part 2: thin films for slow drug delivery and osteomyelitis. Nanomedicine 11:531–544
160. Ben-Nissan B (2003) Natural bioceramic: from coral to bone and beyond. Curr Opin Solid State Mater Sci 7:283–288
161. Bielby RC, Boccaccini AR, Polak JM et al (2004) *In vitro* differentiation and *in vivo* mineralization of osteogenic cells derived from human embryonic stem cells. Tissue Eng 10:1518–1525
162. Mann S (1983) Mineralization in biological systems. Struct Bond 54:125
163. Khademhosseini A, Ling Y, Karp JM et al (2007) Micro- and nanoscale control of cellular environment for tissue engineering. In: Mirkin CA, Niemeyer CM (eds) Nanobiotechnology II: more concepts and applications. Wiley, New York, pp 347–364
164. Chung BG, Kang L, Khademhosseini A (2007) Micro- and nanoscale technologies for tissue engineering and drug discovery applications. Expert Opin Drug Discov 2:1653–1668
165. Chen ZC, Ekaputra AK, Gauthaman K et al (2008) *In vitro* and *in vivo* analysis of co-electrospun scaffolds made of medical grade poly(epsilon-caprolactone) and porcine collagen. J Biomater Sci Polym Ed 19:693–707
166. Hu J, Russell JJ, Ben-Nissan B et al (2001) Production and analysis of hydroxyapatite from Australian corals via hydrothermal process. J Mater Sci Lett 20:85–87
167. Green D, Howard D, Yang X et al (2003) Natural marine sponge fiber skeleton: a biomimetic scaffold for human osteoprogenitor cell attachment, growth, and differentiation. Tissue Eng 9:1159–1166
168. Abramovitch-Gottlib L, Geresh S, Vago R (2006) Biofabricated marine hydrozoan: a bioactive crystalline material promoting ossification of mesenchymal stem cells. Tissue Eng 12:729–739

169. Rocha JHG, Lemos AF, Agathopoulos S et al (2005) Scaffolds for bone restoration from cuttlefish. Bone 37:850–857
170. Lowe B, Guastaldi F, Müller ML et al (2019) Nanobiomaterials for bone tissue engineering. In: Choi AH, Ben-Nissan B (eds) Marine-derived biomaterials for tissue engineering applications. Springer series in biomaterials science and engineering, vol 14. Springer, Singapore, pp 81–97
171. Martina M, Subramanyam G, Weaver JC et al (2005) Developing macroporous bicontinuous materials as scaffolds for tissue engineering. Biomaterials 26:5609–5616
172. Demers C, Hamdy CR, Corsi K et al (2002) Natural coral exoskeleton as a bone graft substitute: a review. Biomed Mater Eng 12:15–35
173. Macha IJ, Ben-Nissan B, Santos J et al (2017) Biocompatibility of a new biodegradable polymer-hydroxyapatite composite for biomedical applications. J Drug Deliv Sci Technol 38:72–77
174. Aragón J, González R, Fuentes G et al (2012) *In vitro* release kinetics and physical, chemical and mechanical characterization of a POVIAC®/$CaCO_3$/HAP-200 composite. J Mater Sci Mater Med 23:259–270
175. Green DW, Ben-Nissan B (2015) Biomimetic applications in regenerative medicine: scaffolds, transplantation modules, tissue homing devices, and stem cells. In: Bawa R, Audette G, Rubinstein I (eds) Handbook of clinical nanomedicine: nanoparticles, imaging, therapy, and clinical applications. Pan Stanford Publishing, Singapore, pp 1109–1140
176. Leupold J, Barfield W, An Y et al (2006) A comparison of ProOsteon, DBX, and collagraft in a rabbit model. J Biomed Mater Res B Appl Biomater 79:292–297
177. Papacharalambous S, Anastasoff K (1993) Natural coral skeleton used as onlay graft for contour augmentation of the face. A preliminary report. Int J Oral Maxillofac Surg 22:260–264
178. Ehrlich H, Etnoyer P, Litvinov SD et al (2006) Biomaterial structure in deep-sea bamboo coral (*Anthozoa: Gorgonacea: Isididae*): perspectives for the development of bone implants and templates for tissue engineering. Mat-wiss u Werkstofftech 37:552–557
179. Roy DM, Linnehan SK (1974) Hydroxyapatite formed from coral skeletal carbonate by hydrothermal exchange. Nature 247:220–222
180. Choi AH, Ben-Nissan B, Conway RC et al (2014) Advances in calcium phosphate nanocoatings and nanocomposites. In: Ben-Nissan B (ed) Advances in calcium phosphate biomaterials. Springer series in biomaterials science and engineering, vol 2. Springer, Berlin, pp 485–509
181. Lamghari M, Berland S, Laurent A et al (2001) Bone reactions to nacre injected percutaneously into the vertebrae of sheep. Biomaterials 22:555–562
182. Lamghari M, Antonietti P, Berland S et al (2001) Arthrodesis of lumbar spine transverse processes using nacre in rabbit. J Bone Miner Res 16:2232–2237
183. Lopez E, Vidal B, Berland S et al (1992) Demonstration of the capacity of nacre to induce bone formation by human osteoblasts maintained *in vitro*. Tissue Cell 24:667–679
184. Huang Q, Liu Y, Ouyang Z et al (2020) Comparing the regeneration potential between PLLA/Aragonite and PLLA/Vaterite pearl composite scaffolds in rabbit radius segmental bone defects. Bioact Mater 5:980–989
185. Xu J, Rao Y, Wu X et al (2019) The osteoinductive effect of nano-nacre particles on MC-3T3 E1 preosteoblast through controlled release of water soluble matrix and calciumions. Dent Mater J 38:981–986
186. Rousseau M, Boulzaguet H, Biagianti J et al (2008) Low molecular weight molecules of oyster nacre induce mineralization of the MC3T3-E1 cells. J Biomed Mater Res A 85(2):487–497
187. Duplat D, Chabadel A, Gallet M et al (2007) The *in vitro* osteoclastic degradation of nacre. Biomaterials 28:2155–2162
188. Rousseau M, Pereira-Mouriès L, Almeida MJ et al (2003) The water-soluble matrix fraction from the nacre of Pinctada maxima produces earlier mineralization of MC3T3-E1 mouse preosteoblasts. Comp Biochem Physiol B: Biochem Mol Biol 135:1–7
189. Westbroek P, Marin F (1988) A marriage of bone and nacre. Nature 392:861–862
190. Almeida MJ, Pereira L, Milet C et al (2001) Comparative effects of nacre water-soluble matrix and dexamethasone on the alkaline phosphatase activity of MRC-5 fibroblasts. J Biomed Mater Res 57:306–312

191. Zhang C, Li S, Ma Z et al (2006) A novel matrix protein p10 from the nacre of pearl oyster (*Pinctada fucata*) and its effects on both $CaCO_3$ crystal formation and mineralogic cells. Marine Biotechnol 8:624–633
192. Liao H, Mutvei H, Hammarström L et al (2002) Tissue responses to nacreous implants in rat femur: an in situ hybridization and histochemical study. Biomaterials 23:2693–2701
193. Kim YW, Kim JJ, Kim YH et al (2002) Effects of organic matrix proteins on the interfacial structure at the bone-biocompatible nacre interface *in vitro*. Biomaterials 23:2089–2096
194. An YH, Friedman RJ (1998) Concise review of mechanisms of bacterial adhesion to biomaterial surfaces. J Biomed Mater Res 43:338–348
195. Evans RP, Nelson CL, Harrison BH (1993) The effect of wound environment on the incidence of acute osteomyelitis. Clin Orthop Relat Res 286:289–297
196. Kargupta R, Bok S, Darr CM et al (2014) Coatings and surface modifications imparting antimicrobial activity to orthopedic implants. Wiley Interdiscip Rev Nanomed Nanobiotechnol 6:475–495
197. Liechty WB, Kryscio DR, Slaughter BV et al (2010) Polymers for drug delivery systems. Annu Rev Chem Biomol Eng 1:149–173

Andy H. Choi is an early career researcher who received his Ph.D. from the University of Technology Sydney (UTS) in Australia in 2004 on the use of computer modelling and simulation known as finite element analysis (FEA) to examine the biomechanical behavior of implants installed into a human mandible. After completing his Ph.D., he expanded his research focus from FEA to sol–gel synthesis of multifunctional calcium phosphate nano coatings and nano composite coatings for dental and biomedical applications.

In late 2010, Dr. Choi was successfully awarded the internationally competitive Endeavour Australia Cheung Kong Research Fellowship Award and undertook post-doctoral training at the Faculty of Dentistry of the University of Hong Kong focusing on the application of FEA in dentistry and the development of calcium phosphate nano-bioceramics.

He is currently serving as an associate editor for the Journal of the Australian Ceramic Society and as an editor for a number of dentistry-related journals. In addition, he is also serving as an editorial board member for several dentistry, nanotechnology, and orthopedics journals. To date, Dr. Choi has authored over 50 publications including 4 books and 30 book chapters on calcium phosphate, nano-biomaterial coatings, sol–gel technology, marine structures, drug delivery, tissue engineering, and finite element analysis in nanomedicine and dentistry.

Chapter 3
Natural and Synthetic Intelligent Self-healing and Adaptive Materials for Medical and Engineering Applications

Besim Ben-Nissan, Gina Choi, Andy H. Choi, Ipek Karacan, and Louise Evans

Abstract During the last two decades, self-healing materials have been attracting increasing interest in both engineering and medical applications. Numerous attempts have been presented focusing on the development of different self-healing systems in both natural and synthetic materials with several new production and synthesis methods and self-repair mechanisms. The current review aims to present some of the most important natural self-healing materials and systems from human hard tissues to marine structures and animal tissue and organ regeneration that can heal or regrow their tissues and parts of their bodies. These are presented in different sections, which include, hard tissue generation and fracture repair, animal tissue generation and organ repair, marine structures, self-repairing coatings for metallic alloys, concrete, hydrogels and polymers just to show the different approaches in this new and fascinating field of self-repair mechanism. Emphasis is given on the areas of tissue engineering, drug delivery, medical materials and devices and implant applications.

Keywords Bone fracture · Bone healing · Drug delivery · Fracture repair · Coatings · Hydrogels · Self-healing polymers

B. Ben-Nissan (✉) · A. H. Choi
Faculty of Science, Biomaterials and Translational Medicine Group, School of Life Sciences, University of Technology Sydney (UTS), Ultimo, Australia
e-mail: Besim.Ben-Nissan@uts.edu.au

G. Choi · L. Evans
Faculty of Science, School of Mathematical and Physical Sciences, University of Technology Sydney (UTS), Ultimo, Australia

I. Karacan
Faculty of Science, Advanced Tissue Engineering and Stem Cell Bilogy Group, School of Life Sciences, University of Technology Sydney (UTS), Ultimo, Australia

A. H. Choi and B. Ben-Nissan (eds.), *Innovative Bioceramics in Translational Medicine I*,
Springer Series in Biomaterials Science and Engineering 17,
https://doi.org/10.1007/978-981-16-7435-8_3

3.1 Introduction

Self-healing smart materials have been the holy grail of regenerative tissue engineering. During the last century, bone fracture and the subsequent healing process have been the two important topics that motivated many tissue engineering investigators and researchers. In the medical field, questions remain: can we produce synthetic bioinspired and/or bio-printed materials and tissues that can repair themselves; or implants that can be coated and if damaged it repairs itself; or if a metallic implant fractures under stress, it still functions under functional movements and repairs itself and its structure. The examples of orthopedic and maxillofacial implants and devices are many, but the solution has always been elusive or not fully satisfactory.

Self-healing engineering materials, with characteristics that allow them to heal themselves when damaged by mechanical, thermal, or other mechanisms and restore their original sets of properties, include a range of metals, polymers, ceramics, and composites [1, 2]. Self-healing can be defined as a natural process or mechanism, which enables the material to recover from the damages caused by any external forces through a specific healing process that returns the material to its original set condition and properties [1–3].

The best example of self-healing in a clinical scenario is the process of bone fracture healing. Fracture repair or healing is a simultaneous biological and biomechanical process to restore the original composition, anatomic structure, and mechanical function of the tissues.

3.2 Bone Fracture Healing and the Healing Cascade

The biomineral medium of bone contains about 30% organic and 70% inorganic segments. Almost, 90% of this organic segment is collagen, whereas the residual 10% is mostly non-collagenous proteins, lipids, proteoglycan molecules, osteopontin (OPN), and other bone matrix proteins [4, 5]. The bone matrix proteins play a vital role in providing the mechanical strength and tissue adhesive characteristics. Principally, the mineral phase of bone is similar to hydroxyapatite crystals [6]. The chemical formula of crystalline hydroxyapatite is $Ca_{10}(PO_4)_6(OH)_2$, where surface binding and electrostatic interactions are related to presence of Ca^{2+} and PO_4^{3-} and other minor elements such as Mg, Sr, Zn and other elements and minerals. The hydroxyapatite crystals are organized parallel to the long axes of collagen fibers by self-assembly of collagen [7].

3.2.1 Bone Cells

Bone is responsible for several roles within the human body including mechanical functions (under functional loadings), synthetic functions (production of blood cells), and metabolic functions (mineral storage and balance, regulation of calcium and phosphate ions, and fat storage). The four most important cells in this bone healing process are: osteoprogenitor bone cells (osteogenic and develop into osteoblast cells), osteoblasts, osteocytes, and osteoclasts, which together are recognized as the basic multicellular unit (BMU) involved in bone regeneration (Fig. 3.1) [8, 9].

The clinical assessment of fracture healing involves a number of steps, and the entire process can be evaluated using a range of testing methods such as radiographic inspections, computerized tomography (CT) scans, mechanical tests and histology [11]. Biological repairs can be assessed through radiographic inspections and through histological analysis if needed. The most common radiographic investigations of fracture healing involve the bridging of fracture site by callus, obliteration of the fracture line, and continuity (Fig. 3.2). In research projects, the volume of callus can at present be calculated using three-dimensional (3D) CT scan reconstructed images or by microtomography [12]. In comparison to CT scans, bone histology is an invasive method used to study the bone structure during fracture healing in the clinical environment. Most healing studies involve animal trials and compare to single longitudinal sections of a healing fracture, which do not capture all of the tissue heterogeneity within callus, transverse sections at the fracture line level can provide the most accurate measurement of cross-sectional area, as well as an estimation of tissue heterogeneity [13]. On the topic of callus cross sections, fibrous cartilage and bone tissues can be measured as the percentage of the total cross-sectional callus area [13]. Bone metabolism can be assessed by staining both osteoblasts and osteoclasts and their activities can then be quantified. In addition, fluorochromes can be used to measure bone formation-related parameters, and these can be used to estimate and assess bone remodeling and stress shielding especially during the middle and final stages of fracture healing [14]. In animal trials, calcein can be injected before the animals such as mice or rats are sacrificed usually at 2, 4, 6, and 16 weeks after femoral osteotomy. Linear calcein labeling indicates lamellar bone formation during callus remodeling.

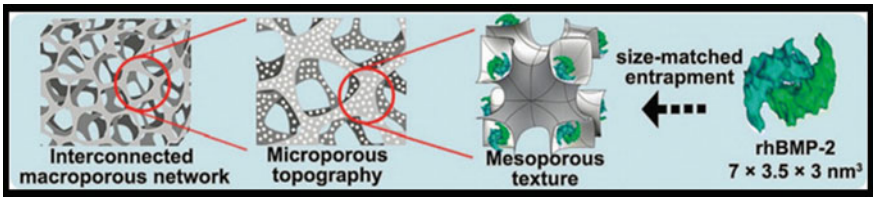

Fig. 3.1 Three common methods in bone attachment and growth for orthopedic and maxillofacial fractures and implants [10] (Modified and adapted with permission from, http://creativecommons.org/licenses/by/4.0/)

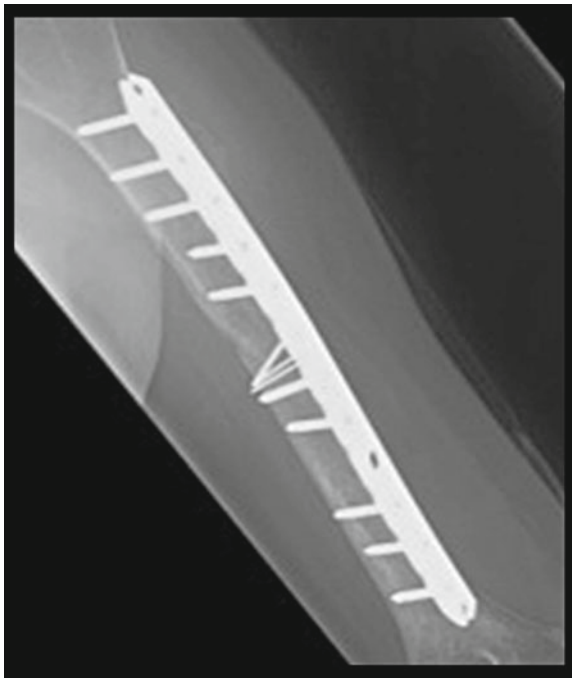

Fig. 3.2 Radiographic inspection of fracture repair in a long bone

Mechanical tests such as flexure, tensile compression, or torsion are frequently used to assess the mechanical properties of bone undergoing the healing process [15]. For long bones, four-point bending and torsion tests are most ideal in assessing the mechanical function of a healing bone. In general, torsion test is a more appropriate as the technique applies the same amount of torque across the entire cross-sectional area of the callus. Furthermore, the test provides a more realistic simulation of orthopedic surgical procedures. In contrast, four-point bending might create a non-uniform bending moment throughout the callus [16]. Care must also be taken when utilizing three-point bending tests to estimate the mechanical properties of a healing bone particularly during early stages of the healing process as the site where the force is applied might be located at the original fracture spot, which at these early stages of healing is primarily new bone composed of cartilage, calcified cartilage, or less mature bone tissue, based on how far the healing has progressed [16].

It must be remembered that these structural properties of a fracture callus depend collectively on the individual tissues, including cartilage, calcified cartilage and woven bone, and the spatial distribution of these tissues, as well as the overall geometry of the callus.

Fracture healing is a regenerative bone healing process in which bone is repaired without any scar tissue formation. The healing cascade begins with a cycle of inflammation, cell migration, proliferation and differentiation of progenitors into mature osteoblasts and osteoclasts under certain biomechanical factors and remodeling

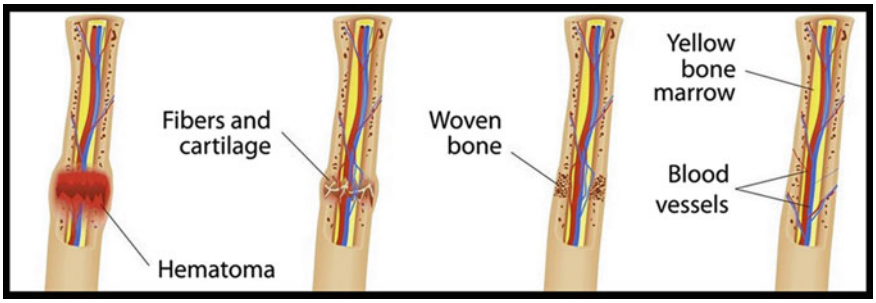

Fig. 3.3 Stages of bone healing process [17] (Modified and adapted with permission from (http://creativecommons.org/licenses/by/4.0/))

(Fig. 3.3) [17]. During the bone healing process, immune cells infiltrate into the hematoma and release cytokines, eliciting inflammation [18]. Since inflammation precedes bone regeneration, it has long been considered that the immune system is crucial in bone fracture healing. Clinicians have reported that bone healing is delayed in patients treated with immunosuppressants and the incidence of non-union is more frequent in certain immune deficient patients.

It has been well established that bone healing commences with an inflammatory reaction which initiates the regenerative healing process leading in the end to reconstitution of bone. An unbalanced immune reaction during this early bone healing phase is hypothesized to disturb the healing cascade in a way that delays bone healing process. The immune cell composition and expression pattern of angiogenic factors can be investigated in a sheep bone osteotomy model and compared to a mechanically-induced impaired/delayed bone healing group. It has been reported that in the delayed healing, significantly higher T cell percentages were present in the bone hematoma and the bone marrow adjacent to the osteotomy gap when compared to the normal healing bone. This was mirrored in the higher cytotoxic T cell percentage detected under delayed bone healing conditions indicating longer pro-inflammatory processes. It has also been reported that the highly activated periosteum adjourning the osteotomy gap showed lower expression of hematopoietic stem cell markers and angiogenic factors such as heme oxygenase and vascular endothelial growth factor. This indicates that a deferred revascularization of the injured area due to ongoing pro-inflammatory processes in the delayed healing in bone fractures. Results from a number of studies suggested that there are unfavorable immune cells and factors participating in the initial healing phase (Fig. 3.4) [19].

Observations made on a study using mice show that immune cells are found only in the endosteal region close to the fractured bone segments and edges during the formation of soft callus. The avascular cartilage filling the fracture callus was devoid of T and B cells [20]. Upon subsequent hypertrophy of the cartilage, the region was revascularized and T and B cells reappear in the callus in areas of newly formed woven bone. The observed large number of T and B cells present during the bone growth and remodeling process correlates with the rising numbers of osteoblasts and osteoclasts

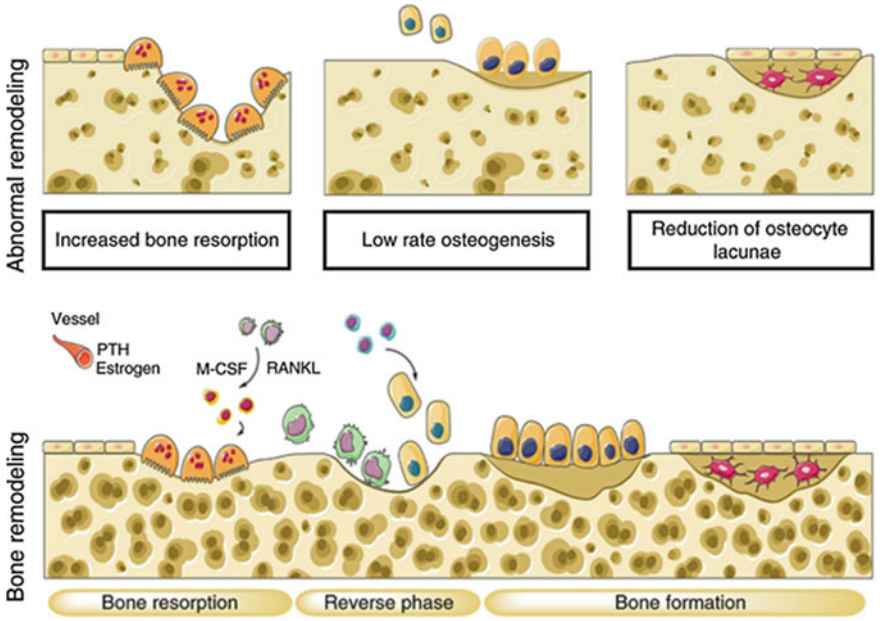

Fig. 3.4 Cascade of new bone generation [19] (Modified and adapted with permission from (http://creativecommons.org/licenses/by/4.0/))

in regions of newly formed bone. Clinical studies carried out showed that strong activation takes place in draining lymph nodes of the patients with fractured bones. Prolonged lymphoid activation correlates with healing and bone union, whereas early termination of nodal reactivity characterizes failure in reparation [21, 22].

In the context of bone fracture healing, B cells are known to increase at the injury site and in the peripheral blood [20, 23]. It has been suggested that a portion of B cells suppress excessive and/or prolonged inflammation. The functions of other B cell subsets in bone regeneration remain largely unknown and further studies are needed.

3.3 Self-healing in Endoskeletons and Exoskeletons

Arthropods are a large group of organisms that include insects and crustacea. A common feature of arthropods is an external skeleton, which is made of cuticle and consists of fibers of chitin, embedded in a matrix of proteins and water [24]. If damage occurs to the exoskeleton, such as the leg or body of an insect, then the immediate effect is leakage of blood followed by a clotting reaction to seal the wound. In this respect, cuticle behaves very much like our skin, but unlike skin, it does not have any living cells near its outer surface. Rather, there is a continuous layer of cells located

on the inner surface of the skeleton. If this layer is breached, the cells will move in an attempt to cover up the gap, and a series of biochemical reactions will be initiated, which results in new cuticle material being produced and deposited in the area over the following days and weeks. An incredible self-healing mechanism [25, 26].

In contrast, a different range of animals including salamanders can regenerate complex structures after injury, including entire body parts and limbs. A pertinent question is whether the generation of progenitor cells during limb regeneration and mammalian tissue repair such as bone occur via a separate or overlapping mechanism. Limb regeneration depends on the formation of a blastema, from which the new appendage develops. Dedifferentiation of stump tissues, such as skeletal muscle, precedes blastema formation, but it was unknown whether dedifferentiation involves stem cell activation [27, 28]. A blastema is a mass of cells capable of growth and regeneration into organs or body parts. Originally, blastemas were thought to be composed of undifferentiated pluripotent cells, but recent research indicates that in some organisms blastemas may retain memory of tissue origin. Blastemas are typically found in the early phases of an organism's development stage such as in embryos, and in the regeneration of soft and hard tissues and organs. Some amphibians and certain species of fish as well as two species of African spiny mice can produce blastemas as adults. However, most animals cannot produce blastemas [29].

It has been reported that a multipotent satellite cell population was observed within the skeletal muscle of the salamander limbs. In addition, that skeletal muscle dedifferentiation was shown to involve satellite cell activation and that these cells can contribute to new limb tissues. Activation of salamander satellite cells occurs in an analogous manner to how the mammalian myofiber mobilizes stem cells during skeletal muscle tissue repair. It was postulated that this limb regeneration and mammalian tissue repair share common cellular and molecular programs. This showed that satellite cells as potential targets in promoting mammalian blastema formation. The amputation or tissue removal can lead to the regeneration of lost structures for example, adult newts can rebuild entire limbs, tails, and jaws through an epimorphic regeneration process that leads to the restoration of complete and functional tissue architecture. Epimorphic limb regeneration proceeds by rapid wound closure and is critically dependent on the formation of a multipotent mesenchymal growth zone, the blastema, which gives rise to the newly formed limb [30].

Research has revealed that mature tissues in the stump (e.g., bone, cartilage, and skeletal muscle) respond to amputation by disorganization, histolysis, and increased cellular proliferation. This process is generally referred to as the dedifferentiation step leading to the formation of blastema progenitors [31]. However, it is unclear to what extent differentiated cells reverse mature phenotypes and to what extent undifferentiated cells, such as stem cells, residing within differentiated tissues become activated, followed by their incorporation into the blastema. The lack of molecular markers has also obstructed the prospective isolation of blastema progenitors [31, 32].

Skeletal muscle is thought to be an important contributor to blastema formation. The skeletal muscle fiber is a syncytial (multinucleate) cell type, whose differentiation during embryonic development is characterized by the cellular fusion of somite-derived precursors. An intriguing aspect of the regenerating salamander appendages

is the reversal of differentiation. Both static analyses and dynamic in vivo tracing showed that skeletal muscle fibers break up, the syncytium becomes fragmented as a response to limb or tail removal, and muscle-derived mononucleate progeny significantly contribute to the blastema. Isolated salamander myotubes can also undergo a cellularization process by which the syncytium turns into mononucleate progeny after reimplantation into the regenerating limb [33, 34].

Although adult mammals do not form blastema after limb amputation, their skeletal muscle tissue does regenerate after injury. Mammalian skeletal muscle regeneration does not involve cellularization of the syncytium. Instead, a stem cell population called satellite cells, which express markers such as Pax7, M-cadherin, and Myf5, enters to the cell cycle, proliferates, and incorporates into nascent or into pre-existing myofibers during mammalian muscle regeneration. Mammalian satellite cells reside between the basal lamina and the sarcolemma of the myofiber [27].

3.3.1 Influence of Macrophages

Researchers analyzed the immune signaling response in axolotl, an aquatic salamander, during limb regeneration and observations revealed a temporally defined requirement for macrophage infiltration in the regenerative process. Although many features of mammalian cytokine/chemokine signaling are retained in the axolotl, they are more dynamically deployed, with simultaneous induction of inflammatory and anti-inflammatory markers within the first 24 h after limb amputation. It was reported that systemic macrophage depletion during this period results in wound closure but permanent failure in limb regeneration, associated with extensive fibrosis and disregulation of extracellular matrix component gene expression. Full limb regenerative capacity of failed stumps was restored by reamputation once endogenous macrophage populations had been replenished. It was suggested that promotion of a regeneration-permissive environment by identification of macrophage-derived therapeutic molecules may therefore can assist in the regeneration of damaged body parts in adult mammals [35].

3.3.2 Schwann Cells

In a recent research, a group of investigators grafted cartilage and Schwann cells from the tip of a limb onto the upper arm of an amputated axolotl [36]. They found that the cartilage cells moved to their old location in the newly formed replacement limb, whereas the Schwann cells were more widely distributed. The researchers first added a section of DNA to an axolotl so that it expressed green fluorescent proteins throughout its body. Then they transplanted cells from this animal into a normal axolotl, whose leg they amputated (Fig. 3.5).

Fig. 3.5 Only Schwann cells (green) wrap around the nerve fibers in the axolotl's regenerated limb [37] (Reprint with permission from)

As the axolotl regrew its limb, the team tracked and reported the fluorescent proteins to comprehend the events taking place to each cell type. Despite going through a blastema stage and dividing, the muscle cells did not turn into any other types of tissue. The same was true of Schwann cells, which form a protective sheath around nerve cells. However, other tissue types were more flexible, with dermis cells also able to differentiate into cartilage tissue, but not muscle [36].

Infiltrating immune cells play a major role in determining the variable outcome of mammalian wound repair, however, little is known about the modulation of immune cell signaling in efficiently regenerating species such as the salamander, which can regrow complete body structures as adults. Although this recent new research is very promising, further research is needed to learn much more about which molecular signals control blastema cells to adapt the salamander's practical approach to new tissue and organ regeneration to new and novel therapies for humans.

3.4 Self-healing Marine Structures

Many marine and freshwater mussels produce a protein-based anchoring holdfast known as a byssus. Most bivalves possess a byssus attachment at the larval stage used for settlement, but only some retain the byssus in adulthood [38, 39]. The

byssus typically consists of numerous individual fibers, which are known as threads that are used to attach itself to substrates within the environment. The byssus fibers of *Mytilus* mussel species have become an important role model in bioinspired materials research due to their impressive high self-healing abilities. However, *Mytilids* only represents a small subset of all byssus-producing bivalves. The process is complicated, and it is species dependent [38, 40]. Recent work has revealed that byssus from other species possess completely different protein composition and hierarchical structures. *Pinna nobilis* byssus in this regard is especially interesting due to its very different morphology, function, and its historical use for weaving lightweight golden fabrics, known as sea silk. *P. nobilis* byssus was reported recently to be comprised of globular proteins organized into a helical protein superstructure [39, 41].

The initial elastic behavior of *P. nobilis* byssus was thought to arise due to stretching and retraction of the helical building blocks comprising the byssus. These findings are important for understanding the convergent evolution of mussel byssus for different species, and also for the field of bio-inspired self-healing materials (Fig. 3.6) [41].

The combination of X-ray scattering, vibrational spectroscopy and tensile testing enabled investigation of the relationship between certain building blocks of *P. nobilis* byssus and its mechanical properties. The stress–strain curves of *P. nobilis* fibers have an unusual shape presenting two distinct yield points, similar to the byssus of the closely related *Atrina rigida*. The first elastic deformation appears to arise from helix stretching, while the post yield plateau appears to originate from breaking of sacrificial bonds, which liberate some hidden length within the tertiary structure of the globular domains. Remarkably, these findings clearly indicate that extremely similar mechanical behaviors to *Mytilus spp.* byssal threads are achieved by an entirely different mechanism - providing further support for the convergent evolution of mussel byssus in multiple instances [41–43].

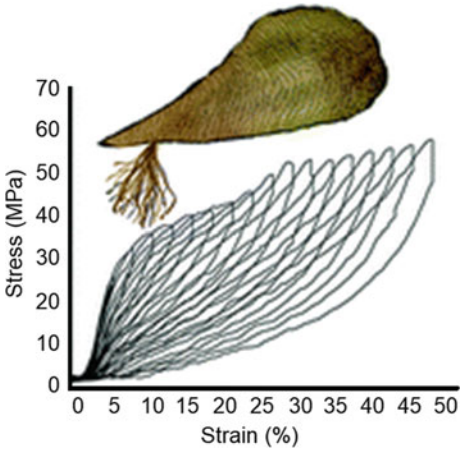

Fig. 3.6 Stretching behavior of *Pinna nobilis* byssus [41] (Modified and reproduced with permission from the Royal Society of Chemistry)

3.4.1 Mechanisms

Mytilus spp. mussels, which inhabit the most wave-exposed regions of the rocky intertidal zones, use a versatile underwater glue to adhere to various surfaces, including rocks, wood pilings and other mussel's shells. The fibers themselves are, self-healing, extremely tough and dissipate energy during cyclic loading from crashing waves arising from a semicrystalline arrangement of collagenous block copolymer-like proteins known as preCols (Fig. 3.7) [41, 44]. Other mussels, including the Mediterranean noble pen shell *P. nobilis*, live in calmer waters, with part of their shell buried beneath the sediment. *P. nobilis* produces a byssus consisting of tens of thousands of long, thin fibers that act as a mooring within the sediment. It has been reported that the byssus fibers of *P. nobilis* possess entirely different protein composition and structural organization in comparison to *Mytilus* [45, 46].

Mytilus byssus threads possess the ability to dissipate up to seventy percent of their mechanical energy and exhibit a capacity to self-heal following pseudoplastic mechanical damage, both of which are of primary importance for their survival on rough seashores [42]. In contrast, *P. nobilis* grows in calm waters and they are not

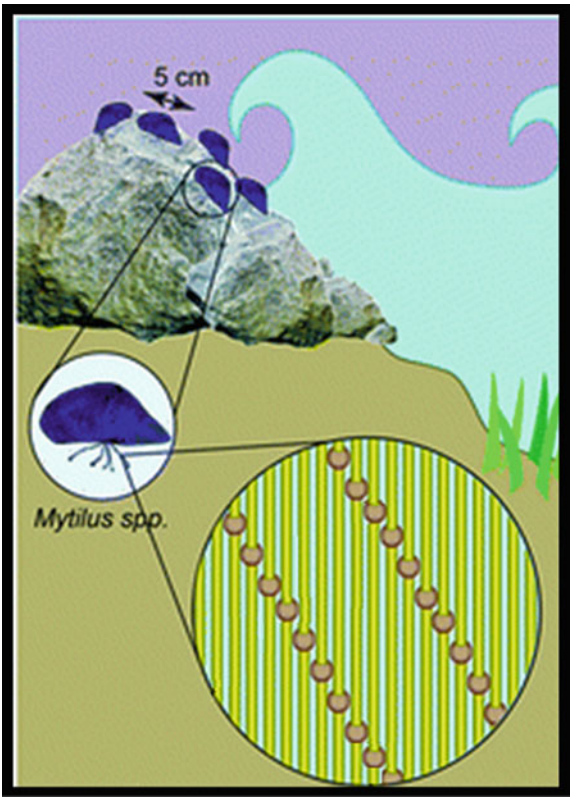

Fig. 3.7 Schematic view of *Mytilus spp.* mussel habitat. *Mytilus* mussels live in the seashore, anchored to hard substrates by 20–70 byssus threads. *Mytilus spp.* threads are comprised of elongated collagenous proteins called preCols arranged in a semicrystalline organization [41] (Modified and reproduced from with permission from the Royal Society of Chemistry)

exposed to high energy crashing waves, and one could therefore postulate that their byssus plays a less important role from a mechanical viewpoint. However, not only is *P. nobilis* a prey for cephalopods (e.g. octopus), who is intended to dislodge them from the sediment, even though they are such large mussels (up to 1 m or more in length). Hence, it can be easily stated that the byssus plays a crucial role in the survival of *P. nobilis* individuals, functioning as a robust subterranean strong anchoring system [46].

Based on X-ray scattering studies, it was postulated that *P. nobilis* byssus is comprised of globular protein helices, resembling bacterial pili, embedded in an amorphous matrix. Recent mechanical studies comparing the tensile properties of *P. nobilis* byssus to other mussel species, including *Mytilus spp*., revealed that while the stress–strain curve appears superficially similar to *Mytilus* threads in their general shape, *P. nobilis* threads exhibited lower extensibility, strength and yield strain than *Mytilus*, which the authors attributed to observed differences in the fiber composition. While these investigations yielded many interesting insights, they did not provide information about the energy dissipating capacity during cyclic loading likely experienced by threads in or whether, like the threads of the *Mytilids*, they are self-healing [39, 41].

3.4.2 Limpets

New research shows that limpets *Patella vulgata* and *Nipponacmea fuscoviridis* can repair their damaged shells with biological material so that they are as strong as the originals. However, they are still vulnerable to multiple impacts and "spalling"—a well-known cause of failure in engineering materials such as concrete [47].

Limpets frequently suffer damage at the apex of their conical shells, but rather than drying out due to dehydration or getting picked off, these creatures quickly patch over small holes with new biological building material from within (Fig. 3.8).

Fig. 3.8 An intact limpet shell (left) and shell of a limpet after an impact test (right) [48] (Modified and adapted with permission from)

However, while the shells have excellent resistance to single impacts, they are not so good at resisting multiple impacts. Electron microscopy studies showed that the layered structure of the shell makes it susceptible to "spalling" [47, 48].

3.5 Self-healing Coatings for Metallic Materials

Metallic biomaterials such as titanium, cobalt chromium alloys and 316L stainless steel used in orthopedics, dentistry, and maxillofacial surgery are selectively applied as bone-fixation devices like intermedullary bone nails, cages and fixation pins are preferably removed after the affected parts have been healed [49]. However, this requires a second surgery for device removal and is a heavy burden, not only to the patient due to the undue pain and suffering but financially to society as well [49].

On the other hand, magnesium and its alloys have been proposed for use as orthopedic implant materials because of their biodegradability and therefore they do not require surgical removal [50]. They also have high specific strength and low modulus of elasticity (41–45 GPa), which is somehow close to that of bone (3–20 GPa) [51]. Biodegradable implants during degradation are expected to maintain enough strength until the surrounding tissues are sufficiently healed to support the functional loads. Various surface modifications such as selective coatings have been developed to maintain the mechanical integrity of magnesium and its alloys for the required period and to improve surface biocompatibility [50].

Self-healing coatings have attracted a considerable amount of attention related to the surface modification of orthopedic magnesium alloys, as it can regain the "protection barrier" capacity from attack by corrosion. Most importantly, implants can be damaged during surgery and reaction and degradation within the body might generate hydrogen gas evolution [50].

A study was carried out to examine the likelihood of accelerated corrosion on the surfaces of AZ31 alloys and pure magnesium coated with hydroxyapatite and octacalcium phosphate coatings that was scratched to expose the surfaces of the metallic substrate. Next, the implants were immersed in a cell-culture medium and in a 9% NaCl solution to assess the behavior and rates of corrosion and degradation. It was reported that the release of magnesium ions was not accelerated by scratching. In both solutions, a corrosion product layer containing magnesium and phosphorus was formed within the scratches, which were identified as self-healing. It was also postulated that these self-healing properties observed with inorganic agents was possibly triggered by changes in pH around coating defects [52]. Based on these facts, hydroxyapatite and octacalcium phosphate coatings were projected to display self-healing capabilities due to the presence of phosphate contained within the coating. Furthermore, a study by Kim et al. noticed that a specific hydroxyapatite coating on pure magnesium led to good corrosion protection, and bone proliferation in the bone-pericranium pouches of rats and in tibial shafts of rabbits [53]. Even though there have been extensive studies within the laboratory environment, there have been only a few reports on the corrosion behaviors of scratched calcium phosphate coatings

on magnesium and its allows in the clinical scenario or within the physiological environments.

A dicalcium phosphate dihydrate (brushite) coating was observed to prolong the in vivo degradation period of an MgZnZr alloy [54]. The thickness of the brushite coating was reduced as the new bone tissue formed around the implanted alloy screws in the mandibles of rabbits. New bone ingrowth around magnesium alloys appeared to be enhanced if a coating composed of degradable calcium phosphate such as tricalcium phosphate was deposited on the surface of the magnesium alloy [55]. An octacalcium phosphate coating was partially degraded in the subcutaneous tissues of mice [56], indicating that it may also enhance new bone tissue ingrowth around implanted octacalcium phosphate-coated magnesium/magnesium alloys. It can be concluded that hydroxyapatite and octacalcium phosphate coatings have good potential as corrosion-protective and bone-conductive coatings for bioabsorbable/biodegradable magnesium/magnesium alloys. On the other hand, it should be mentioned that the self-healing abilities when scratched was not investigated.

To simulate high-speed flow rate of up to 1 m/s for cardiovascular applications, Yamamoto et al. suggested stirring of the test solution with periodic partial replacement [57]. However, in orthopedic applications, the surfaces of the implants are exposed to various mass-transfer conditions with much lower flow speeds than those in arteries. Bone plates are exposed to soft tissue and cortical bone surfaces, and screws are exposed to soft tissue, cancellous and cortical bone, and bone marrow. Sinusoidal capillaries run through bone marrow, which is filled with blood and bone marrow aspirate. The fluid flow speed in the bone marrow is assumed to be like the blood flow in capillaries i.e., 2–15 mm/s [58]. Mass-transfer in soft tissue should be slower than blood flow in capillaries as the mechanism is based on diffusion through concentration differences. The effects of such relatively low-speed mass transfer in bone marrow and soft tissue have not been critically examined. The corrosion morphology of hydroxyapatite- and octacalcium phosphate-coated magnesium alloys in the subcutaneous tissue of mice was not reproduced under static immersion in a cell-culture medium without solution replacement [56]. This difference between in vivo and in vitro corrosion morphologies is presumably to be caused by the adhesion of soft tissue that restrains mass transfer in body fluids on the surface.

Similarly, the self-healing ability of coatings consisting of silk fibroin and potassium phosphate (K_3PO_4) on Mg-Ca alloys were reported by Xiong et al. [59]. The PO_4^{3-} ions was reported to act as corrosion inhibitor, while K^+ ions helped to regulate the secondary structures of silk fibroin (Fig. 3.9). After a number of examinations including scratch tests, scanning vibrating electrode technique (SVET) and electrochemical impedance spectroscopy (EIS) were utilized and it was reported that a pH-sensitive self-healing coating could be successfully produced. Furthermore, multiple responses were observed during cell culture studies including spreading, adhesion, proliferation, and differentiation using MC3T3-E1 cells.

In another study, a phytic acid conversion coating was developed on AZ31 Mg alloy by dipping the alloy into the solution. The effects of heat treatment in the temperature range of 150–400 °C on the chemical composition of the coatings and the self-healing mechanisms were investigated [60]. It was reported that with the increase of

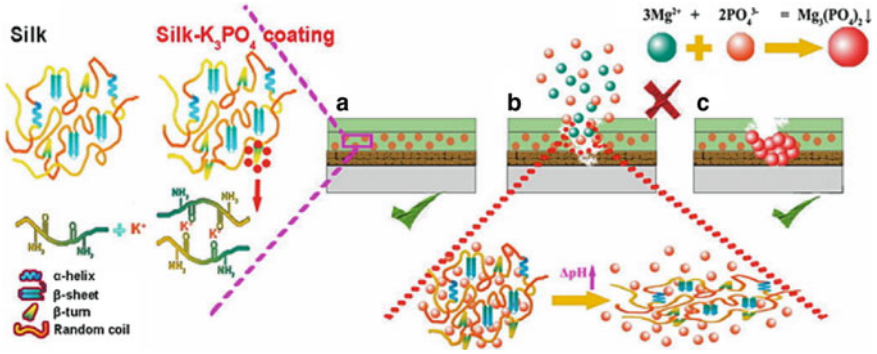

Fig. 3.9 Self-healing ability of coatings consisting of silk fibroin and potassium phosphate (K_3PO_4) on Mg-Ca alloys [59] (Reprint with permission from)

the heat treatment temperature, the cracks on the surface of the conversion coating gradually healed and improved the corrosion resistance of these coated magnesium alloys. During the heat treatment process, the conversion coating composed of amorphous magnesium phytate was transformed to crystalline magnesium pyrophosphate ($Mg_2P_2O_7$). Meanwhile, the macromolecular complex changed into small organic structure, and accompanied the increase of the volume, leading to the self-healing. It was further reported that the coating that was heat-treated at 400 °C exhibited superior surface integrity and corrosion resistance due to the crystallization of $Mg_2P_2O_7$.

Magnesium phosphate coating was applied in two different alloys, the first for ACM522 Mg alloy [61] and the second, cerium/calcium phosphate coating for a Zn alloy showed a self-healing function in NaCl [62]. In the latter case, it was observed that $Zn_3(PO_4)_2{\cdot}4H_2O$ was deposited within scratches, however only a trace amount of calcium was deposited [62].

3.6 Self-healing of Ceramics and Concrete

The specific feature of some of the natural materials is their self-healing ability. Despite considerable research, the exact mechanisms by which this is achieved are still not completely understood, but several useful insights have emerged in recent years.

To repair cracks within concrete in difficult or dangerous conditions such as underground structures, self-healing mechanism is a promising method and the same approach can be applied to engineering ceramics such as those used in tissue engineering. A new idea of self-healing is based on the introduction of sensors that can detect crack initiation prior to the propagation of the crack [63]. Once a crack is formed and detected by these new generation sensors, healing agent can be self-infused into the porous network to fill up voids and seal a crack or cracks in the

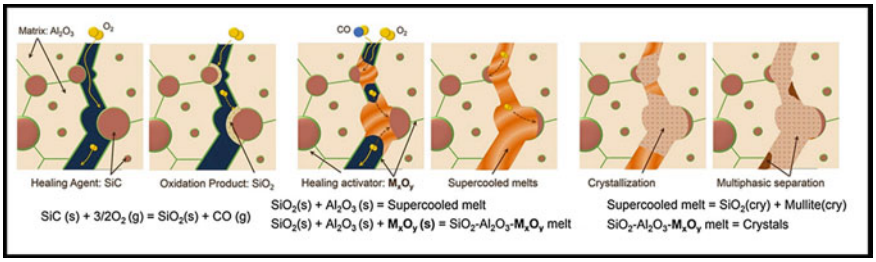

Fig. 3.10 Self-healing in Al_2O_3/SiC composites and effect of healing activator network. Silicon carbide (SiC) is oxidized to SiO_2 upon exposure to oxygen that penetrated from the cracked surface. This is known as the inflammation stage (left). Next, a mechanically weak, low viscosity supercooled melt created through Al_2O_3 and M_xO_y dissolving into SiO_2 completely fills irregularly shaped gaps. This stage is referred to as the repair stage (middle). Lastly, this stage is defined as the remodelling stage where mechanically strong crystals nucleate and grown in the supercooled melt [63] (Modified and adapted with permission from (http://creativecommons.org/licenses/by/4.0/))

concrete or ceramic body (Fig. 3.10). This idea was tested using cylindrical samples. A porous concrete core was placed in the center of the concrete cylinder. Uniaxial direct tensile load was applied to create cracks close to the notch of the sample. A healing action was performed by externally injecting a healing agent manually. The results showed that a macro-crack is sealed and strength of concrete is regained. However, the effect of the sensors as the crack initiated was not covered.

Bacteria-based microspheres with potential self-healing concrete applications were proposed for use in the marine environment [64]. The microspheres consisting of calcium alginate encapsulated bacterial spores and mineral precursor compounds were assessed for oxygen consumption, swelling, and its ability to form a biocomposite in a simulative marine concrete crack solution at 8 °C. After six days of immersion, the microspheres formed a calcite skin on their surface and calcite inclusions in their network, resulting in a calcite-alginate biocomposites. These unique microspheres swelled by 300% to a maximum diameter of three mm after 14 days of immersion, which provided the healing agent required. The alginate-based microspheres shows great potential for the development of bacteria-based self-healing concrete for applications in low temperature marine environments, while the formation of a biocomposite healing material represents an exciting avenue for self-healing in other environments including the tissue engineering.

3.7 Self-healing Polymers and Hydrogels

Polyurethanes and specifically cross-linked polyurethanes have many properties that qualify them as high-performance polymeric materials, but they still suffer from mechanical damage. It has been reported that the development of polyurethane networks that exhibit self-repairing characteristics upon exposure to ultraviolet (UV)

light. The network consists of an oxetane-substituted chitosan precursor incorporated into a two-component polyurethane. Upon mechanical damage of the network, four-member oxetane rings open to create two reactive ends. When exposed to UV light, chitosan chain scission occurs, which forms crosslinks with the reactive oxetane ends, thus repairing the network. These materials are capable of repairing themselves in less than an hour and can be used in many coatings applications, ranging from engineering to dental and biomedical applications.

In polymers and composites, self-healing has been demonstrated by three conceptual approaches: (1) microcapsule-based healing systems; (2) vascular healing systems; and (3) intrinsic healing polymers. A new branch is using hydrogels that might include compositions of organic and inorganic matter. Self-healing can be autonomic without human intervention or may require some external intervention such as energy or pressure. It has been suggested that in all classes of polymers, from thermosets to thermoplastics to elastomers, they might have some degree of potential for self-healing.

Hydrogels are crosslinked polymer networks with high water content and rheological properties that are attractive materials for many engineering applications. Self-healing hydrogels are particularly interesting because of their ability to repair structural damages and recover their original functions, specifically in tissue engineering. In addition, self-healing hydrogels with shear-thinning properties can be potentially used as vehicles for drug delivery or in bio-printing.

3.7.1 Chemistry

Self-healing hydrogels can be synthesized through non-covalent and/or dynamic covalent bonds interactions. The dynamic equilibrium between dissociation and recombination of various interactions leads the hydrogel to repair damages. Normally, dynamic covalent bonds display stable and slow dynamic equilibriums, while non-covalent interactions show fragile and rapid dynamic equilibriums.

Microcapsule-laden hydrogels were developed to release healing agents at damage sites [65, 66]. However, report has shown that the irreversible healing process and potential interference of fillers limited their applications [67, 68]. In addition, dynamic crosslinks in a number of dynamic hydrogels normally rely on external stimuli such as light, low pH, and high temperature [69, 70]. It has been suggested that these external stimuli could have adverse effects on cells and living tissues.

3.7.2 Non-covalent Interactions

Non-covalent interactions such as hydrogen bonding, electrostatic interactions, and hydrophobic interactions can be used to synthesize self-healing hydrogels. In comparison to covalent interactions, non-covalent interactions are less stable and more sensitive to environmental condition such as pH and temperature. However, tough self-healing hydrogels can still be produced based on non-covalent interactions through micro- or nanostructures as well as special manufacturing procedures.

Hydrogen bonding is an attractive interaction between hydrogen atoms and electronegative atoms, in which the hydrogen atom is bound to a highly electronegative atom, such as nitrogen, oxygen, or fluorine. Self-healing hydrogels based on polyvinyl alcohol have been manufactured using a freezing/thawing method via hydrogen bonding [71, 72]. Furthermore, the amalgamation with numerous chemical moieties such as nucleobase moieties [73], gallol moieties [74], deferoxamine moieties [75], and 2-ureido-4-pyrimidone (UPy) moieties [76–82] with self-healing hydrogels based on hydrogen bonding were often reported.

Self-healing hydrogels were created using cytosine- and guanosine-modified hyaluronic acid via Watson–Crick base pairing between the nucleobases through hydrogen bonding [73]. The hydrogel displayed pH-stimulated sol–gel transition in which the hydrogel exhibited sol state in pH <6 or >8 and gel state in pH 6–8. In another similar study, a shear-thinning and self-healing hydrogel synthesized from gallol-conjugated hyaluronic acid combined with a gallol-rich crosslinker (i.e., oligo-epigallocatechin gallate) that is based on extensive hydrogen bonds of gallol-gallol and gallol- hyaluronic acid [74]. The hydrogel displayed resistance to enzymatic degradation by protein such as hyaluronidase immobilization via non-covalent interactions between gallols and proteins.

Self-healing hydrogels can also be produced through reversible electrostatic interactions occurring in charged polymers and ions [83, 84], polyampholytes [85, 86], polyelectrolytes [87–90], and zwitterionic fusions [91]. For instance, a self-healing hydrogel was synthesized through reversible polyelectrolyte complexes of alginate and 2-hydroxypropyltrimethyl ammonium chloride chitosan [88]. The two polymers were mixed to produce a self-healing hydrogel at charge neutrality followed by precipitation for 12 h. The hydrogel demonstrated cytocompatibility, high adhesive behavior, and shear-thinning properties, in addition to a self-healing ability.

Polyampholytes can form self-healing hydrogels between randomly dispersed cationic and anionic repeating groups in polymers that resulted in tunable mechanical properties via electrostatic interactions [86]. Tough polyampholyte hydrogels contained both strong and weak ionic bonds to maintain shapes and enhance the shock absorbance and self-healing abilities, respectively, which is similar to double-network hydrogels.

Hydrophobic interactions occur as a result of aggregative hydrophobes in aqueous media. In a number of scenarios, liposomes [92, 93] or surfactant micelles [94, 95] are utilized as crosslinking points to construct the polymer chains in self-healing hydrogels based on hydrophobic interactions comprising both hydrophilic and hydrophobic

monomers. A study by Sun et al. have demonstrated that less hydrophobic polyampholyte hydrogels displayed soft and adequate self-healing properties, while more hydrophobic polyampholyte hydrogels exhibited the robust and poor self-healing properties [86]. It has also been demonstrated that a self-healing hydrogel could be created via micellar copolymerization of hydrophilic monomer acrylamide and hydrophobic monomer stearyl methacrylate in an aqueous solution of sodium dodecyl sulfate micelles [96–98]. The addition of salt into aqueous sodium dodecyl sulfate solutions was found to cause the growth of micellar and solubilization of hydrophobes within sodium dodecyl sulfate micelles. Good self-healing capability and high elongation ratio were observed in the hydrogel containing sodium dodecyl sulfate micelles with the time-dependent dynamic moduli. On the other hand, no self-healing ability and high mechanical strength were recorded in the hydrogel with time-independent dynamic moduli after the extraction of sodium dodecyl sulfate.

A study by Owusu-Nkwantabisah et al. [99] described the facile preparation and characterization of an autonomous self-healing hydrogel system comprising surfactant-free hydrophobic associations. The hydrogel comprised a copolymer of benzyl methacrylate, octadecyl methacrylate, and methacrylic acid, and were prepared via a controlled dehydration procedure to achieve the formation of strong intermolecular hydrophobic associations of the octadecyl groups above a critical polymer concentration.

3.7.3 Mechanism Based on Dynamic Covalent Bonding

The creation of self-healing hydrogel based on dynamic covalent chemistry including disulfide exchange, boronate ester complexation, imine formation, catechol-iron coordination, and Diels–Alder reaction have been previously reported. In comparison to non-covalent interactions described above, these bonds exhibited stronger but somehow slower dynamic equilibrium.

Disulfide exchange provides dynamic covalent bonds to produce self-healing hydrogels that are sensitive to redox potential or pH [100]. Self-healing hydrogels were produced from 1,2-dithiolane-functionalized polymers with rapid sol–gel transition via the disulfide exchange between the 1,2-dithiolane and dithiols [101–103]. It was demonstrated that under weakly alkaline or neutral conditions, the disulfide exchange of 1,2-dithiolane can reform and this can be further controlled by temperature.

Boronic acid and its derivatives such as phenylboronic acid or phenylboronic acid-incorporated polymers have been extensively developed for the preparation of self-healing hydrogels. The reversible boronate ester bond is created through complexation of a boronic acid and a diol, and its stability is governed by glucose concentration and the pH-value. Self-healing hydrogel were produced by mixing phenylboronic acid with diol-modified poly(ethylene glycol), and the resultant hydrogel displayed glucose-responsive size-dependent release of proteins and a tunable mechanical properties that are responsive to pH [104]. The in vitro study

confirmed the hydrogel was cytocompatible, and it demonstrated a typical foreign body reaction without chronic inflammation in vivo. In another study, self-healing hydrogel with low stability under acidic environments and high stability under alkaline settings were prepared via complexation of a catechol-modified polymer and 1,3-benzenediboronic acid [105]. Later, using a one-pot approach, self-healing hydrogel was fabricated using a mixture of poly(ethylene glycol) diacrylate, dithiothreitol, and borax via permanent thiol-ene Michael addition and dynamic borax diol complexation [106]. Recently, an injectable, glucose-sensitive self-healing hydrogel composed of primarily reversibly crosslinked poly(ethylene glycol) diacrylate and dithiothreitol with borax as the glucose-sensitive motif was utilized as easily removable sacrificial materials to generate branched tubular channels within a construct [107]. After three days, vascular endothelial cells seeded in the lumen of the channels can line the channel wall and migrate into the non-sacrificial hydrogel. Around two weeks, it was observed that the endothelial cells form capillary-like structure (vascular network), while neural stem cells form neurosphere-like structure (neural development) in the construct, revealing the morphology of "a vascularized neural tissue".

A number of self-healing hydrogels have been developed using either aromatic Schiff bases [108, 109] or aliphatic Schiff bases [110–112]. An imine (a Schiff base) is a compound with a carbon–nitrogen double bond formed by nucleophilic attack of amine to an aldehyde or ketone. In comparison to aliphatic Schiff bases, aromatic Schiff bases display higher stability and capable of maintaining their mechanical properties to a larger extent [113]. The use of polysaccharide-based self-healing hydrogels with pH-sensitivity was proposed by Qu et al. [108] as drug delivery vehicles for hepatocellular carcinoma therapy. In their study, the hydrogels were prepared by using N-carboxyethyl chitosan (CEC) synthesized via Michael reaction in aqueous solution and dibenzaldehyde-terminated poly(ethylene glycol) (PEGDA). Doxorubicin was used as a model of water-soluble small molecule anti-cancer drug, and it was encapsulated into the hydrogel in situ. Injectability was confirmed by in vitro injection and in vivo subcutaneous injection in a rat. pH-responsive behavior was validated by in vitro release of doxorubicin from hydrogels in PBS solutions with different pH values. Moreover, the activity of doxorubicin released from hydrogel matrix was evaluated by employing human hepatocellular liver carcinoma. Cytotoxicity test of the hydrogels using L929 cells confirmed their good cytocompatibility. A number of studies also prepared hydrogels for 3D cell culture and cell delivery based on their cytocompatibility and injectability [114–116]. The hydrogels could be degraded by enzymes, acidic pH, vitamin B6 derivatives, and amino acids and they were manufactured rapidly under mild conditions at 20 °C within 60 s. Self-healing hydrogels have also been prepared using acylhydrazone and oxime, which are derivatives of imine with great stability [117–120]. A study by Wei et al. demonstrated the feasibility of synthesizing a self-healing hydrogel through the addition of oxidized sodium alginate into a mixture of N-carboxyethyl chitosan and adipic acid dihydrazide via dynamic imine and acylhydrazone bonds [121]. The resultant hydrogel displayed good cytocompatibility and cell release as exhibited by three-dimensional cell encapsulation.

Self-healing hydrogels can be created through a reversible coordinate bond between catechol and iron. Through the adjustment of the pH condition, the reversibility of the catechol-iron coordinate bond can be regulated [122]. A rapidly self-healing hydrogel with high strength could be produced by adjusting the environmental pH from acidic to basic. Furthermore, a self-healing hydrogel via reversible coordinate bonds at the nanoparticle surface was attempted in which iron oxide nanoparticles were incorporated with catechol-modified polymers. Solid-like mechanics and magnetic properties were observed in self-healing hydrogel based on catechol-iron oxide nanoparticles compared to the fluid-like hydrogel formed by catechol-Fe(III) crosslinking [123].

The biomedical applications of thermally reversible Diels–Alder reaction are limited due to the fact that Diels–Alder bonds need a high temperature and a long duration to cleave and reform for self-healing properties despite their significance in dynamic covalent chemistry and in self-healing hydrogels [124–126]. Self-healing hydrogels based on Diels–Alder chemistry were synthesized through the combination with other reversible interactions such as acylhydrazone bond [127], electrostatic interaction [128, 129], coordination bond [130], and imine bond [131]. The study by Zhao et al. [125] hypothesized the possible applications of polysiloxane elastomer containing Diels–Alder bonds as scaffolds for tissue engineering or as artificial skin based on the results from cytotoxicity evaluation and animal subcutaneous experiments.

3.7.4 Multi-mechanism Interactions

Self-healing hydrogels have been extensively manufactured using supramolecular chemistry through various non-covalent interactions such as protein-ligand recognition and host–guest interaction. Furthermore, self-healing hydrogels with high mechanical properties, long-term stability, multi-responsive behavior, and rapid recovery have been developed using hybrids of non-covalent interactions and/or permanent/dynamic covalent bonds.

Host–guest interactions occur when two or more chemical species assemble via non-covalent interactions such as hydrogen bonding, hydrophobic interaction, van der Waals forces, or electrostatic interactions. In host–guest chemistry, the macrocyclic host moiety is inserted inside the guest moiety to create a unique structure of the inclusion complexation. Self-healing hydrogels have been prepared using the popular host–guest interactions and the healing process is triggered using external stimuli such as redox potentials, pH, temperature, and light in a number of hydrogels. At the moment, there were also attempts to develop host–guest hydrogels that can recover themselves without the intervention of external stimuli. A study by Yamaguchi et al. prepared self-healing hyaluronic acid hydrogel based on the host–guest interactions of β-cyclodextrin-modified hyaluronic acid (host macromer) and adamantane-modified hyaluronic acid (guest macromer), with the hydrogel demonstrating shear-thinning property and rapid recovery at 25 °C [132].

Catechol and gallol are polyphenolic moieties commonly distributed in organisms as important functional groups, which can form various covalent and non-covalent bonds, such as Michael addition or Schiff base reaction with thiol and amine, coordination bonds with metals, hydrogen bonds, and aromatic interactions. An injectable self-healing hydrogel with antimicrobial and antifouling properties was in a study by Li et al. (2017) through self-assembly of an ABA triblock copolymer employing catechol functionalized polyethylene glycol (PEG) as A block and poly([2-(methacryloyloxy)-ethyl] trimethylammonium iodide) (PMETA) as B block [133]. This hydrogel exhibits excellent thermosensitivity and is capable of healing autonomously from repeated damage, through mussel-inspired catechol-mediated hydrogen bonding and aromatic interactions. A study by Krogsgaard et al. [134] demonstrated that it is possible to synthesize self-healing hydrogels using an inexpensive one-pot route with pH-tunable modulus. Hydrogels were formed by reacting tannic acid, trivalent metal ions and polyallylamine. The hydrogels were supramolecular when the pH is below 8, while the hydrogels were strengthened by covalent cross-linking when the pH is above 8.

An injectable polymeric supramolecular hydrogel based on thiols terminated linear poly(ethylene glycol) polymer chain cross-linked by addition of gold(I) ions was prepared by Casuso et al. [135]. A characteristic zig-zag conformation was created via Au-thiolates interactions held by Au–Au metallophilic attractions and it proved to be sufficient to "sew" together polymer chain ends together to produce a 3D network. The metallophilic material was shown to display completely different behavior at acidic and neutral pH due to thiolate/Au–S exchange rate that is closely dependent on the amount of reactive thiolate. At pH 3, the stability of the hydrogel was attributed to the absence of reactive thiolates at pH 3.1, while increasing the number of reactive thiolates at higher pH values resulted in the formation of a free-flowing dynamic hydrogel. Furthermore, rheological studies revealed that the dynamic material behaved like healthy synovial fluid: at low frequency, the hydrogel acted like a viscous liquid was observed at low frequency, this is followed by a liquid-to-hydrogel transition that corresponds to the relaxation time of the dynamic hydrogel; finally, the material exhibited a solid-like behavior at higher frequencies. Later, an injectable, self-healing dynamic hydrogel based on gold(I)-thiolate/disulfide exchange as nucleus pulposus replacement in a spine motion segment model was developed [136]. The dynamic exchange between gold(I)-thiolate species and disulfide bonds resulted in self-healing ability and frequency-dependent stiffness of the hydrogel, which was also confirmed in spine motion segments. Hydrogel nanocomposites with enhanced properties based on the combination of an Au-based 4-arms thiol terminated poly(ethylene glycol) dynamic hydrogel exhibiting self-healing ability with 100 nm bioactive glass nanoparticles agglomerated in 10 μm clusters, produced via a particulate sol–gel method were examined in a study by Gantar et al. [137]. Rheology studies demonstrated that stiffer hydrogels were obtained after the addition of bioactive glass nanoparticles. The presence of the inorganic colloids appeared to affect slightly the dynamic character of the pristine hydrogel by slowing down the exchange reaction between gold-thiolate and disulfides. Compression tests demonstrated the major drawbacks of each individual material were suppressed to

result in a material composite with high resistance to stress and relatively large deformation ability. More importantly, in vitro degradation of bioactive glass nanoparticles embedded in the dynamic hydrogel resulted in the formation of hydroxyapatite.

Dynamic polymer hydrogels were prepared with an environmental adaptive self-healing ability and dual responsive sol–gel transitions by combining acylhydrazone and disulfide bonds together in the same system [138]. Through acylhydrazone exchange or disulfide exchange reactions, the hydrogel can repair damage automatically under both basic (pH 9) and acidic (pH 3 and 6) conditions. At pH 7 on the other hand, the hydrogel was unable to self-heal due to both bonds are kinetically locked. With the aid of catalytic aniline, the hydrogel gains self-healing ability by accelerating acylhydrazone exchange. Furthermore, the hydrogel also demonstrated unique reversible sol–gel transitions in response to both pH (HCl/triethylamine) and redox (DTT/H_2O_2) triggers. Dynamic covalent acylhydrazone linkages were also used to synthesize cellulose-based self-healing hydrogels that displayed pH/redox dual responsive sol–gel transition behaviors [139]. The hydrogels also exhibited excellent self-healing ability with a high healing efficiency and good mechanical properties and were used successfully for the controlled release of doxorubicin. The study also suggested the hydrogel could function as a 3D culture scaffolds for L929 cells, resulting in the encapsulated cells to maintain a high viability and proliferation capacity.

3.8 Self-healing Hydrogels: Applications

3.8.1 Biomedical Applications

Some animal models have been used to verify the biocompatibility and efficacy of self-healing hydrogels. Besides biocompatibility, self-healing hydrogels require injectability and long-term stability for drug delivery, tissue engineering, and for 3D bio-printed hard and soft tissues and organs.

Self-healing hydrogels have received increasing attentions in biomedical applications, such as wound healing, drug delivery, tissue engineering, surface coatings, and 3D printing. In these cases, dibenzaldehyde-based, UPy-based, catechol-based, and host–guest-based self-healing hydrogels are highlighted due to many evaluations of in vivo experiments [140].

3.8.2 Drug Delivery

A self-healing hydrogel based on host–guest interactions between β-cyclodextrin-modified PEI and adamantane-modified PEG was developed for local siRNA release. The modified polymers assembled with siRNA to form polyplexes, which could

improve the transfection efficiency and the viability of cells. When injected into the myocardium, the hydrogel with siRNA encapsulation enhanced the uptake of Cy5.5-siRNA and maintained the silencing of GFP for one week in a GFP-expressing rat [141].

In 2016, an injectable and self-healing collagen-gold hybrid hydrogel with adjustable mechanical properties was reported [142]. This hydrogel was prepared through electrostatic interaction between positively charged collagen chains and negatively charged tetrachloroaurate ($[AuCl_4]^-$) ions, and further non-covalent interactions between subsequent biomineralized gold nanoparticles and collagen. The hydrogel was developed for localized delivery and sustained release of the photosensitive drug. By combinatorial photothermal and photodynamic therapies, the significantly enhanced antitumor efficacy was demonstrated through an in vivo antitumor test using the subcutaneous mouse model.

Self-healing hydrogels based on glycol chitosan and DF-PEG (GC-DP) have been developed for intratumor therapy in vivo. GC-DP hydrogel containing an antitumor drug was injected into the disease position with a steady release in situ. Moreover, the ionic GC-DP hydrogel exhibited microwave susceptibility to produce high-temperature hyperthermia for tumor ablation. A multi-antitumor system was developed based on GC-DP hydrogel containing doxorubicin/docetaxel-loaded poly(lactic-co-glycolic acid) (PLGA) nanoparticles and iron oxide for chemotherapy and magnetic hyperthermia. The system showed the greater in vivo antitumor efficacy under the alternative magnetic field compared to the hydrogel containing doxorubicin/docetaxel-loaded PLGA nanoparticles [143].

3.8.3 Tissue Engineering

Self-healing host-guest hydrogels have been developed to treat myocardial infarction. The self-healing hydrogel, formed through host–guest interactions of adamantine- and β-cyclodextrin-modified hyaluronic acid, was injected into the ischemic myocardium encapsulating endothelial progenitor cells (EPCs). A rodent model of acute myocardial infarction was employed to confirm that a significant increase in vasculogenesis was noted with the hydrogel encapsulating EPCs, compared to the treatment of EPCs alone or hydrogel alone. Moreover, the hydrogel was designed using adamantane/thiol-modified hyaluronic acid and cyclodextrin/methacrylate-modified hyaluronic acid through host–guest interaction and Michael addition. The reversible host–guest interaction and permanent Michael addition provided shear-thinning injection and high retention, respectively. Epicardial injection of the hydrogel in a rat myocardial infarction model showed significant improvement of the outcome compared to the untreated group and the hydrogel without Michael addition [144].

Self-healing hydrogels were designed as injectable carriers for growth factors using PEG end-functionalized with four-fold hydrogen-bonding ureidopyrimidinone (UPy) moieties. UPy-modified PEG hydrogel incorporated with antifibrotic growth

factor was delivered in a pocket introduced under the kidney capsule of rats. The kidney capsule was loosened from the kidney to create a small pocket. After injection of growth factor-containing hydrogels, the number of myofibroblasts stayed the same to the contralateral (healthy) kidney, while significantly increased with the injection of saline or hydrogel alone. In another example, growth factors were delivered by UPy-modified PEG hydrogel to repair the infarcted myocardium. This pH-switchable hydrogel could be injected through the long and narrow lumen of the catheter mapping system, and rapidly formed a hydrogel in contact with tissue. The growth factor-containing hydrogel reduced scar collagen in a chronic myocardial infarction pig model [78].

Self-healing hydrogels based on glycol chitosan-difunctionalized PEG were prepared for tissue repairs [145, 146]. In the application of central nervous system (CNS) repair, neurosphere-like progenitors showed better proliferation and differentiation in glycol chitosan-difunctionalized PEG hydrogel, and injection of glycol chitosan-difunctionalized PEG hydrogel combining neurospheres promoted functional recovery in a zebrafish CNS impaired model. Moreover, the glycol chitosan-difunctionalized PEG hydrogel combining the optogenetic method was developed as a temporal-spatial approach to treat neurodegenerative diseases. The hydrogel containing bacteriorhodopsin plasmid and neural stem cells was injected into CNS impaired zebrafish where the neural repair was observed, particularly under green light exposure. Besides, glycol chitosan-difunctionalized PEG hydrogel was also used to induce blood capillary formation. With the incorporation of fibrin gel, a composite hydrogel could form with an interpenetrating polymer network (i.e., double network) of glycol chitosan-difunctionalized PEG and fibrin. The hydrogel induced vascular endothelial cells to form capillary-like structures, and injection of the hydrogel alone promoted angiogenesis in zebrafish and rescued the blood circulation in ischemic hindlimbs of mice [145, 146].

3.8.4 Other Applications

Self-healing hydrogels, based on the host–guest interaction of β-cyclodextrin- and adamantine-modified hyaluronic acid, were used in 3D printing of high-resolution structures through printing of shearing-thinning ink hydrogel into self-healing support hydrogel [147]. The multicellular structures could be expediently patterned, such as printing of mesenchymal stem cells within an ink hydrogel into a support hydrogel containing 3T3 fibroblasts. The channel-like structure was achieved by writing the ink hydrogel into the methacrylate-modified support hydrogel, followed by UV irradiation for secondary covalent crosslinks of support hydrogel, followed by removal of the physical (i.e., host–guest) ink hydrogel. Meanwhile, the self-supporting structure was obtained by covalently crosslinking the ink hydrogel and removing the non-covalent support hydrogel. This system supported the patterning of multiple inks, cells, and channels in 3D space [147].

A tough self-healing hydrogel was synthesized as cell stimulators and implantable bioelectronics. In the study, graphene oxide was partially converted to conductive graphene through polydopamine reduction, and acrylamide monomers were polymerized in situ to form the hydrogel by interactions between graphene oxide, polydopamine, and polyacrylamide. Meanwhile, the free catechol groups on polydopamine imparted a self-healing property and tissue adhesion to the hydrogel via various non-covalent interactions. The hydrogel could be used not only as an adhesive electrode or motion sensor but also as an in vitro cell stimulator and in vivo implantable intramuscular electrode. For example, the hydrogel electrodes were implanted into the rabbit dorsal muscle and connected to a signal detector using the transcutaneous wires. The electrodes could record the electromyographic signal when the rabbit was interfered with external stimulation [148].

3.9 Future Considerations

By the nature of their structure and stress and external loading related to functional movements, all natural and synthetic materials accumulate micro- and macro-cracks and inevitable fracture. If the damage affected zones exceed the critical limit value, this will bring about partial failure and, subsequently, in loss of the capacity of the product or device. Conversely, self-patching or self-healing materials can switch the damage and improve the reliability.

Improved functionality by self-repair and healing and expected future advancements will have a positive ecological and socioeconomical effect by broadening the working life of products and structures used which will lead to more efficient devices, implants and engineering structures. As the failure of any material customarily starts at the microstructural and nanoscale level, constant monitoring and taking action at that level becomes most pertinent.

Micro-cracks are the signs to auxiliary structural failure and the capacity to recuperate them will empower structures with longer lifetimes and less repair. Self-healing hydrogels are an essential part of these new generation materials. Self-healing hydrogels can be classified as robust and soft hydrogels according to mechanical properties in biomedical applications. Robust self-healing hydrogels are used as soft implantable or wearable biosensors with extended lifetime and mechanical performance due to repairing of the damages or fatigues.

Soft self-healing hydrogels with shear-thinning properties are used in cell/drug delivery and 3D bioprinting due to injection through narrow needles and retention at target sites.

To facilitate wider use of biomedical applications of these new generation self-healing hydrogels we need to address several major concerns including: (1) designing with appropriate mechanical properties; (2) better characterizing the self-healing properties with various assessment methods (3) developing theories on self-healing mechanisms and properties based on chemistry, structure, properties, kinetics, and

thermodynamics and (4) translation to clinic by animal experiments and clinical trials.

Knowing that the tissue-implant interactions take place in harsh environments, and because the self-healing properties of hydrogels are not determined in physiological environments, it would be challenging to verify that the known self-healing properties are well-maintained in physiological conditions such as with electrolytes, under functional loads, mechanical stress, and in the presence of material–cell interactions. In addition, controllable biodegradability and the dissolution kinetics are important in self-healing hydrogels for tissue engineering and drug delivery. Reversible equilibriums of self-healing hydrogels should be controlled according to the various applications.

The use of self-healing materials for skin structure using a UV light reparable BISGMA glass or epoxy are currently employed. If the skin is wounded, the ultraviolet treatable BISGMA glass or epoxy is released and is cured by encompassing UV light. The technology goes back many years to the use of dental resin composites in maxillofacial applications.

Stress-strengthened crosslinking or polymerization reactions that extension the quality of the material at the area of a high-tension is alluded to as mechanochemical establishment. Cross linked PU is a good example of this material.

Research wise by far the most of on-going exploration on self-healing materials currently is directed and without a doubt will be directed on self-healing structures, tissues and implants by 3D bioprinting.

Prior to last decade, the self-repairing microvascular structures have been made from pipettes to a 3D interconnected framework through different fabrication procedures. Changes have been made to redesign the self-healing material chemistry, production methods and to better control the properties and performance of the final products. However, the future will show their adaptability to the clinical environment as efficient soft and hard tissue and organ repair methods and tissue regeneration.

References

1. Dziadek M, Stodolak-Zych E, Cholewa-Kowalska K (2017) Biodegradable ceramic-polymer composites for biomedical applications: a review. Mater Sci Eng C Mater Biol Appl 71:1175–1191
2. Dimitriou R, Tsiridis E, Giannoudis PV (2005) Current concepts of molecular aspects of bone healing. Injury 36:1392–1404
3. Giannoudis PV, Dinopoulos H, Tsiridis E (2005) Bone substitutes: an update. Injury 36:S20–S27
4. Behzadi S, Luther GA, Harris MB et al (2017) Nanomedicine for safe healing of bone trauma: Opportunities and challenges. Biomaterials 146:168–182
5. Fazzalari NL (2011) Bone fracture and bone fracture repair. Osteoporos Int 22:2003–2006
6. Hu C, Ashok D, Nisbet DR et al (2019) Bioinspired surface modification of orthopedic implants for bone tissue engineering. Biomaterials 219:119366
7. LeGeros R (1965) Effect of carbonate ion the lattice parameters of apatite. Nature 24:403–404

8. Florencio-Silva R, Sasso GR, Sasso-Cerri E et al (2015) Biology of bone tissue: structure, function, and factors that influence bone cells. Biomed Res Int 2015:421746. https://doi.org/10.1155/2015/421746
9. Boyle WJ, Simonet WS, Lacey DL (2003) Osteoclast differentiation and activation. Nature 423:337–342
10. Yi H, Ur Rehman F, Zhao C et al (2016) Recent advances in nano scaffolds for bone repair. Bone Res 4:16050
11. Axelrad TW, Einhorn TA (2011) Use of clinical assessment tools in the evaluation of fracture healing. Injury 42:301–315
12. Morgan EF, Mason ZD, Chien KB et al (2009) Micro-computed tomography assessment of fracture healing: relationships among callus structure, composition, and mechanical function. Bone 44:335–344
13. Li J, Kacena MA, Stocum DL (2019) Fracture healing. In: Burr DB, Allen MR (eds) Basic and applied bone biology, 2nd edn. Academic Press, Massachusetts, pp 235–253
14. van Gaalen SM, Kruyt MC, Geuze RE et al (2010) Use of fluorochrome labels in *in vivo* bone tissue engineering research. Tissue Eng Part B Rev 16:209–217
15. Morgan EF, Unnikrisnan GU, Hussein AI (2018) Bone mechanical properties in healthy and diseased states. Annu Rev Biomed Eng 20:119–143
16. Oksztulska-Kolanek E, Znorko B, Michałowska M et al (2016) The biomechanical testing for the assessment of bone quality in an experimental model of chronic kidney disease. Nephron 132:51–58
17. Ansari M (2019) Bone tissue regeneration: biology, strategies and interface studies. Prog Biomater 8:223–237
18. Einhorn TA, Gerstenfeld LC (2015) Fracture healing: mechanisms and interventions. Nat Rev Rheumatol 11:45–54
19. Xie Y, Zhang L, Xiong Q et al (2019) Bench-to-bedside strategies for osteoporotic fracture: from osteoimmunology to mechanosensation. Bone Res 7:25. https://doi.org/10.1038/s41413-019-0066-7
20. Könnecke I, Serra A, El Khassawna T et al (2014) T and B cells participate in bone repair by infiltrating the fracture callus in a two-wave fashion. Bone 64:155–165
21. Szczesny G, Olszewski WL, Gewartowska M et al (2007) The healing of tibial fracture and response of the local lymphatic system. J Trauma 63:849–854
22. Szczesny G, Olszewski WL, Gorecki A (2005) Lymphoscintigraphic monitoring of the lower limb lymphatic system response to bone fracture and healing. Lymphat Res Biol 3:137–145
23. Kolar P, Schmidt-Bleek K, Schell H et al (2010) The early fracture hematoma and its potential role in fracture healing. Tissue Eng Part B Rev 16:427–434
24. Fabritius H, Sachs C, Raabe D et al (2011) Chitin in the exoskeletons of arthropoda: from ancient design to novel materials science. In: Gupta N (ed) Chitin. Topics in geobiology. Springer, Dordrecht, pp 35–60
25. Cremaldi JC, Bhushan B (2018) Bioinspired self-healing materials: lessons from nature. Beilstein J Nanotechnol 9:907–935
26. Tanaka EM (2003) Regeneration: if they can do it, why can't we? Cell 113:559–562
27. Morrison JI, Lööf S, He P et al (2006) Salamander limb regeneration involves the activation of a multipotent skeletal muscle satellite cell population. J Cell Biol 172:433–440
28. Brockes JP, Kumar A (2002) Plasticity and reprogramming of differentiated cells in amphibian regeneration. Nat Rev Mol Cell Biol 3:566–574
29. Brockes JP (1997) Amphibian limb regeneration: rebuilding a complex structure. Science 276:81–87
30. Corcoran JP, Ferretti P (1999) RA regulation of keratin expression and myogenesis suggests different ways of regenerating muscle in adult amphibian limbs. J Cell Sci 112:1385–1394
31. Iten LE, Bryant SV (1973) Forelimb regeneration from different levels of amputation in the newt, Notophthalmus viridescens: length, rate, and stages. Wilhelm Roux Arch Entwickl Mech Org 173:263–282

32. Echeverri K, Clarke JDW, Tanaka EM (2001) *In vivo* imaging indicates muscle fiber dedifferentiation is a major contributor to the regenerating tail blastema. Dev Biol 236:151–164
33. Rosenblatt JD, Lunt AI, Parry DJ et al (1995) Culturing satellite cells from living single muscle fiber explants. In Vitro Cell Dev Biol Anim 31:773–779
34. Lo DC, Allen F, Brockes JP (1993) Reversal of muscle differentiation during urodele limb regeneration. Proc Natl Acad Sci U S A 90:7230–7234
35. Godwin JW, Pinto AR, Rosenthal NA (2013) Macrophages are required for adult salamander limb regeneration. Proc Natl Acad Sci U S A 110:9415–9420
36. Kragl M, Knapp D, Nacu E et al (2009) Cells keep a memory of their tissue origin during axolotl limb regeneration. Nature 460:60–65
37. Laursen L (2009) Salamander cells remember their origins in limb regeneration. Nature. https://doi.org/10.1038/news.2009.614
38. Harrington MJ, Jehle F, Priemel T (2018) Mussel byssus structure-function and fabrication as inspiration for biotechnological production of advanced materials. Biotech J 13:1800133
39. Pasche D, Horbelt N, Marin F et al (2018) A new twist on sea silk: the peculiar protein ultrastructure of fan shell and pearl oyster byssus. Soft Matter 14:5654–5664
40. Carrington E, Gosline JM (2004) Mechanical design of mussel byssus: load cycle and strain rate dependence. Am Malacol Bull 18:135–142
41. Pasche D, Horbelt N, Marin F et al (2019) Self-healing silk from the sea: role of helical hierarchical structure in *Pinna nobilis* byssus mechanics. Soft Matter 15:9654–9664
42. Zechel S, Hager MD, Priemel T et al (2019) Healing through histidine: bioinspired pathways to self-healing polymers via imidazole-metal coordination. Biomimetics 4:20
43. Diana A, Reguzzoni M, Congiu T, Rescigno A, Sollai F, Raspanti M (2017) The byssus threads of *Pinna nobilis*: a histochemical and ultrastructural study. Eur J Histochem 61:2779
44. Krauss S, Metzger TH, Fratzl P et al (2013) Self-repair of a biological fiber guided by an ordered elastic framework. Biomacromol 14:1520–1528
45. Harrington MJ, Gupta HS, Fratzl P et al (2009) Collagen insulated from tensile damage by domains that unfold reversibly: *In situ* X-ray investigation of mechanical yield and damage repair in the mussel byssus. J Struct Biol 167:47–54
46. García-March J, Pérez-Rojas L, García-Carrascosa A (2007) Influence of hydrodynamic forces on population structure of *Pinna nobilis* L., 1758 (*Mollusca: Bivalvia*): the critical combination of drag force, water depth, shell size and orientation. J Exp Mar Biol Ecol 342:202–212
47. Taylor D (2016) Impact damage and repair in shells of the limpet *Patella vulgata*. J Exp Biol 219:3927–3935
48. O'Neill M, Mala R, Cafiso D et al (2018) Repair and remodelling in the shells of the limpet Patella vulgata. J R Soc Interface 15:20180299
49. Park JB, Kim YK (2003) Metallic biomaterials. In: Park JB, Bronzino JD (eds) Biomaterials: principles and applications. CRC Press, Boca Raton, pp 1–20
50. Zeng R, Dietzel W, Witte F et al (2008) Progress and challenge for magnesium alloys as biomaterials. Adv Eng Mater 10:B3–B14
51. Staiger MP, Pietak AM, Huadmai J et al (2006) Magnesium and its alloys as orthopedic biomaterials: a review. Biomaterials 27:1728–1734
52. Hiromoto S (2015) Self-healing property of hydroxyapatite and octacalcium phosphate coatings on pure magnesium and magnesium alloy. Corros Sci 100:284–294
53. Kim SM, Jo JH, Lee SM et al (2014) Hydroxyapatite-coated magnesium implants with improved *in vitro* and *in vivo* biocorrosion, biocompatibility, and bone response. J Biomed Mater Res A 102:429–441
54. Guan X, Xiong M, Zeng F et al (2014) Enhancement of osteogenesis and biodegradation control by brushite coating on mg-nd-zn-zr alloy for mandibular bone repair. ACS Appl Mater Interfaces 6:21525–21533
55. Chai H, Guo L, Wang X et al (2012) *In vitro* and *in vivo* evaluations on osteogenesis and biodegradability of a β-tricalcium phosphate coated magnesium alloy. J Biomed Mater Res A 100:293–304

56. Hiromoto S, Inoue M, Taguchi T et al (2015) *In vitro* and *in vivo* biocompatibility and corrosion behaviour of a bioabsorbable magnesium alloy coated with octacalcium phosphate and hydroxyapatite. Acta Biomater 11:520–530
57. Yamamoto A, Hiromoto S (2009) Effect of inorganic salts, amino acids and proteins on the degradation of pure magnesium *in vitro*. Mater Sci Eng C Mater Biol Appl 29:1559–1568
58. Sugawara M, Maeda N (2010) Blood rheology and blood flow. Corona Publishing, pp 68–81
59. Xiong P, Yan J, Wang P et al (2019) A pH-sensitive self-healing coating for biodegradable magnesium implants. Acta Biomater 98:160–173
60. Zhang R, Cai S, Xu G et al (2014) Crack self-healing of phytic acid conversion coating on AZ31 magnesium alloy by heat treatment and the corrosion resistance. Appl Surf Sci 313:896–904
61. Yagi S, Kuwabara K, Fukuta Y et al (2013) Formation of self-repairing anodized film on ACM522 magnesium alloy by plasma electrolytic oxidation. Corros Sci 73:188–195
62. Aramaki K (2003) Self-healing protective films prepared on zinc electrodes by treatment in a cerium (III) nitrate solution and modification with sodium phosphate and calcium or magnesium nitrate. Corros Sci 45:2361–2376
63. Osada T, Kamoda K, Mitome M et al (2017) A novel design approach for self-crack-healing structural ceramics with 3D networks of healing activator. Sci Rep 7:17853
64. Palin D, Wiktor V, Jonkers HM (2016) A bacteria-based bead for possible self-healing marine concrete applications. Smart Mater Struct 25:084008
65. Toohey KS, Sottos NR, Lewis JA et al (2007) Self-healing materials with microvascular networks. Nat Mater 6:581–585
66. White SR, Sottos NR, Geubelle PH et al (2001) Autonomic healing of polymer composites. Nature 409:794–797
67. Syrett JA, Becer CR, Haddleton DM (2010) Self-healing and self-mendable polymers. Polym Chem 1:978–987
68. Bergman SD, Wudl F (2008) Mendable polymers. J Mater Chem 18:41–62
69. Harada A, Takashima Y, Nakahata M (2014) Supramolecular polymeric materials via cyclodextrin-guest interactions. Acc Chem Res 47:2128–2140
70. Murphy EB, Wudl F (2010) The world of smart healable materials. Prog Polym Sci 35:223–251
71. Zhang Z, Li TT, Chen B et al (2017) Self-healing supramolecular hydrogel of poly(vinyl alcohol)/chitosan carbon dots. J Mater Sci 52:10614–10623
72. Zhang H, Xia H, Zhao Y (2012) Poly(vinyl alcohol) hydrogel can autonomously self-heal. ACS Macro Lett 1:1233–1236
73. Ye X, Li X, Shen YQ et al (2017) Self-healing pH-sensitive cytosine- and guanosine-modified hyaluronic acid hydrogels via hydrogen bonding. Polymer 108:348–360
74. Shin M, Lee H (2017) Gallol-rich hyaluronic acid hydrogels: shear-thinning, protein accumulation against concentration gradients, and degradation-resistant properties. Chem Mater 29:8211–8220
75. Xu GZ, Xiao Y, Cheng L et al (2017) Synthesis and rheological investigation of self-healable deferoxamine grafted alginate hydrogel. J Polym Sci Pol Phys 55:856–865
76. Zhang G, Ngai T, Deng Y et al (2016) An injectable hydrogel with excellent self-healing property based on quadruple hydrogen bonding. Macromol Chem Phys 217:2172–2181
77. Hou S, Wang X, Park S et al (2015) Rapid self-integrating, injectable hydrogel for tissue complex regeneration. Adv Healthc Mater 4(1491–1495):1423
78. Bastings MM, Koudstaal S, Kieltyka RE et al (2014) A fast pH-switchable and self-healing supramolecular hydrogel carrier for guided, local catheter injection in the infarcted myocardium. Adv Healthc Mater 3:70–78
79. Chirila TV, Lee HH, Oddon M et al (2014) Hydrogen-bonded supramolecular polymers as self-healing hydrogels: effect of a bulky adamantyl substituent in the ureido-pyrimidinone monomer. J Appl Polym Sci 131:39932
80. Cui JX, Wang DP, Koynov K et al (2013) 2-Ureido-4-pyrimidone-based hydrogels with multiple responses. ChemPhysChem 14:2932–2938

81. Dankers PY, Hermans TM, Baughman TW et al (2012) Hierarchical formation of supramolecular transient networks in water: a modular injectable delivery system. Adv Mater 24:2703–2709
82. Cui J, del Campo A (2012) Multivalent H-bonds for self-healing hydrogels. Chem Commun 48:9302–9304
83. Wei H, Du S, Liu Y et al (2014) Tunable, luminescent, and self-healing hybrid hydrogels of polyoxometalates and triblock copolymers based on electrostatic assembly. Chem Commun 50:1447–1450
84. Wei Z, He J, Liang T et al (2013) Autonomous self-healing of poly(acrylic acid) hydrogels induced by the migration of ferric ions. Polym Chem 4:4601–4605
85. Ihsan AB, Sun TL, Kuroda S et al (2013) A phase diagram of neutral polyampholyte—from solution to tough hydrogel. J Mater Chem B 1:4555–4562
86. Sun TL, Kurokawa T, Kuroda S et al (2013) Physical hydrogels composed of polyampholytes demonstrate high toughness and viscoelasticity. Nat Mater 12:932–937
87. Li J, Su ZL, Ma XD et al (2017) In situ polymerization induced supramolecular hydrogels of chitosan and poly(acrylic acid-acrylamide) with high toughness. Mater Chem Front 1:310–318
88. Ren Y, Lou R, Liu X et al (2016) A self-healing hydrogel formation strategy via exploiting endothermic interactions between polyelectrolytes. Chem Commun 52:6273–6276
89. Luo F, Sun TL, Nakajima T et al (2015) Oppositely charged polyelectrolytes form tough, self-healing, and rebuildable hydrogels. Adv Mater 27:2722–2727
90. Huang Y, Lawrence PG, Lapitsky Y (2014) Self-assembly of stiff, adhesive and self-healing gels from common polyelectrolytes. Langmuir 30:7771–7777
91. Bai T, Liu S, Sun F et al (2014) Zwitterionic fusion in hydrogels and spontaneous and time-independent self-healing under physiological conditions. Biomaterials 35:3926–3933
92. Hao X, Liu H, Xie YJ et al (2013) Thermal-responsive self-healing hydrogel based on hydrophobically modified chitosan and vesicle. Colloid Polym Sci 291:1749–1758
93. Rao Z, Inoue M, Matsuda M et al (2011) Quick self-healing and thermo-reversible liposome gel. Colloids Surf B Biointerfaces 82:196–202
94. Liu Y, Li Z, Niu N et al (2018) A simple coordination strategy for preparing a complex hydrophobic association hydrogel. J Appl Polym Sci 135:46400
95. Gulyuz U, Okay O (2015) Self-healing poly(acrylic acid) hydrogels: effect of surfactant. Macromol Symp 358:232–238
96. Tuncaboylu DC, Argun A, Sahin M et al (2012) Structure optimization of self-healing hydrogels formed via hydrophobic interactions. Polymer 53:5513–5522
97. Tuncaboylu DC, Sahin M, Argun A et al (2012) Dynamics and large strain behavior of self-healing hydrogels with and without surfactants. Macromolecules 45:1991–2000
98. Tuncaboylu DC, Sari M, Oppermann W et al (2011) Tough and self-healing hydrogels formed via hydrophobic interactions. Macromolecules 44:4997–5005
99. Owusu-Nkwantabisah S, Gillmor JR, Switalski SC et al (2017) An autonomous self-healing hydrogel based on surfactant-free hydrophobic association. J Appl Polym Sci 134:44800
100. Wei Z, Yang JH, Zhou JX et al (2014) Self-healing gels based on constitutional dynamic chemistry and their potential applications. Chem Soc Rev 43:8114–8131
101. Zhang X, Waymouth RM (2017) 1,2-Dithiolane-derived dynamic, covalent materials: cooperative self-assembly and reversible cross-linking. J Am Chem Soc 139:3822–3833
102. Yu H, Wang Y, Yang H et al (2017) Injectable self-healing hydrogels formed via thiol/disulfide exchange of thiol functionalized F127 and dithiolane modified PEG. J Mater Chem B 5:4121–4127
103. Barcan GA, Zhang X, Waymouth RM (2015) Structurally dynamic hydrogels derived from 1,2-dithiolanes. J Am Chem Soc 137:5650–5653
104. Yesilyurt V, Webber MJ, Appel EA et al (2016) Injectable self-healing glucose-responsive hydrogels with pH-regulated mechanical properties. Adv Mater 28:86–91
105. He L, Fullenkamp DE, Rivera JG et al (2011) pH responsive self-healing hydrogels formed by boronate-catechol complexation. Chem Commun 47:7497–7499

106. He L, Szopinski D, Wu Y et al (2015) Toward self-healing hydrogels using one-pot thiolene click and borax-diol chemistry. ACS Macro Lett 4:673–678
107. Tseng TC, Hsieh FY, Theato P et al (2017) Glucose-sensitive self-healing hydrogel as sacrificial materials to fabricate vascularized constructs. Biomaterials 133:20–28
108. Qu J, Zhao X, Ma PX et al (2017) pH-responsive self-healing injectable hydrogel based on N-carboxyethyl chitosan for hepatocellular carcinoma therapy. Acta Biomater 58:168–180
109. Karimi AR, Khodadadi A (2016) Mechanically robust 3D nanostructure chitosan-based hydrogels with autonomic self-healing properties. ACS Appl Mater Interfaces 8:27254–27263
110. Huang J, Deng Y, Ren J et al (2018) Novel *in situ* forming hydrogel based on xanthan and chitosan re-gelifying in liquids for local drug delivery. Carbohydr Polym 186:54–63
111. Zhu D, Wang H, Trinh P et al (2017) Elastin-like protein-hyaluronic acid (ELP-HA) hydrogels with decoupled mechanical and biochemical cues for cartilage regeneration. Biomaterials 127:132–140
112. Lü S, Gao C, Xu X et al (2015) Injectable and self-healing carbohydrate-based hydrogel for cell encapsulation. ACS Appl Mater Interfaces 7:13029–13037
113. Zhang Y, Tao L, Li S et al (2011) Synthesis of multiresponsive and dynamic chitosan-based hydrogels for controlled release of bioactive molecules. Biomacromol 12:2894–2901
114. Zhang YL, Fu CK, Li YS et al (2017) Synthesis of an injectable, self-healable and dual responsive hydrogel for drug delivery and 3D cell cultivation. Polym Chem 8:537–544
115. Li Y, Zhang YL, Wei YN et al (2017) Preparation of chitosan-based injectable hydrogels and its application in 3D cell culture. J Vis Exp 127:e56253
116. Yang B, Zhang YL, Zhang XY et al (2012) Facilely prepared inexpensive and biocompatible self-healing hydrogel: a new injectable cell therapy carrier. Polym Chem 3:3235–3238
117. Mukherjee S, Hill MR, Sumerlin BS (2015) Self-healing hydrogels containing reversible oxime crosslinks. Soft Matter 11:6152–6161
118. Lin F, Yu J, Tang W et al (2013) Peptide-functionalized oxime hydrogels with tunable mechanical properties and gelation behavior. Biomacromol 14:3749–3758
119. Grover GN, Lam J, Nguyen TH et al (2012) Biocompatible hydrogels by oxime click chemistry. Biomacromol 13:3013–3017
120. Deng G, Tang C, Li F et al (2010) Covalent cross-linked polymer gels with reversible sol-gel transition and self-healing properties. Macromolecules 43:1191–1194
121. Wei Z, Yang JH, Liu ZQ et al (2015) Novel biocompatible polysaccharide-based self-healing hydrogel. Adv Funct Mater 25:1352–1359
122. Krogsgaard M, Behrens MA, Pedersen JS et al (2013) Self-healing mussel-inspired multi-pH-responsive hydrogels. Biomacromol 14:297–301
123. Li Q, Barret DG, Messersmith PB et al (2016) Controlling hydrogel mechanics via bio-inspired polymer-nanoparticle bond dynamics. ACS Nano 10:1317–1324
124. Shao CY, Wang M, Chang HL et al (2017) A self-healing cellulose nanocrystal-poly(ethylene glycol) nanocomposite hydrogel via Diels-Alder click reaction. ACS Sustainable Chem Eng 5:6167–6174
125. Zhao J, Xu R, Luo G et al (2016) A self-healing, re-moldable and biocompatible crosslinked polysiloxane elastomer. J Mater Chem B 4:982–989
126. Liu YL, Chuo TW (2013) Self-healing polymers based on thermally reversible Diels-Alder chemistry. Polym Chem 4:2194–2205
127. Yu F, Cao X, Du J et al (2015) Multifunctional hydrogel with good structure integrity, self-healing, and tissue-adhesive property formed by combining Diels-Alder click reaction and acylhydrazone bond. ACS Appl Mater Interfaces 7:24023–24031
128. Ghanian MH, Mirzadeh H, Baharvand H (2018) In situ forming, cytocompatible, and self-recoverable tough hydrogels based on dual ionic and click cross-linked alginate. Biomacromol 19:1646–1662
129. Banerjee SL, Singha NK (2017) A new class of dual responsive self-healable hydrogels based on a core crosslinked ionic block copolymer micelle prepared via RAFT polymerization and Diels-Alder “click” chemistry. Soft Matter 13:9024–9035

130. Li S, Wang L, Yu X et al (2018) Synthesis and characterization of a novel double cross-linked hydrogel based on Diels-Alder click reaction and coordination bonding. Mater Sci Eng C Mater Biol Appl 82:299–309
131. Li S, Yi J, Yu X et al (2018) Preparation and characterization of acid resistant double cross-linked hydrogel for potential biomedical applications. ACS Biomater Sci Eng 4:872–883
132. Yamaguchi H, Kobayashi Y, Kobayashi R et al (2012) Photoswitchable gel assembly based on molecular recognition. Nat Commun 3:603
133. Li L, Yan B, Yang J et al (2017) Injectable self-healing hydrogel with antimicrobial and antifouling properties. ACS Appl Mater Interfaces 9:9221–9225
134. Krogsgaard M, Andersen A, Birkedal H (2014) Gels and threads: mussel-inspired one-pot route to advanced responsive materials. Chem Commun 50:13278–13281
135. Casuso P, Pérez-San Vicente A, Iribar H et al (2014) Aurophilically cross-linked "dynamic" hydrogels mimicking healthy synovial fluid properties. Chem Commun 50:15199–15201
136. Pérez-San Vicente A, Peroglio M, Ernst M et al (2017) Self-healing dynamic hydrogel as injectable shock-absorbing artificial nucleus pulposus. Biomacromol 18:2360–2370
137. Gantar A, Drnovšek N, Casuso P et al (2016) Injectable and self-healing dynamic hydrogel containing bioactive glass nanoparticles as a potential biomaterial for bone regeneration. RSC Adv 6:69156–69166
138. Deng GH, Li FY, Yu HX et al (2012) Dynamic hydrogels with an environmental adaptive self-healing ability and dual responsive sol-gel transitions. ACS Macro Lett 1:275–279
139. Yang XF, Liu GQ, Peng L et al (2017) Highly efficient self-healable and dual responsive cellulose-based hydrogels for controlled release and 3D cell culture. Adv Funct Mater 27:1703174
140. Liu Y, Hsu SH (2018) Synthesis and biomedical applications of self-healing hydrogels. Front Chem 6:449
141. Wang LL, Highley CB, Yeh YC et al (2018) Three-dimensional extrusion bioprinting of single- and double-network hydrogels containing dynamic covalent crosslinks. J Biomed Mater Res A 106:865–875
142. Xing R, Liu K, Jiao T et al (2016) An injectable self-assembling collagen-gold hybrid hydrogel for combinatorial antitumor photothermal/photodynamic therapy. Adv Mater 28:3669–3676
143. Xie W, Gao Q, Guo Z et al (2017) Injectable and self-healing thermosensitive magnetic hydrogel for asynchronous control release of doxorubicin and docetaxel to treat triple-negative breast cancer. ACS Appl Mater Interfaces 9:33660–33673
144. Gaffey AC, Chen MH, Venkataraman CM et al (2015) Injectable shear-thinning hydrogels used to deliver endothelial progenitor cells, enhance cell engraftment, and improve ischemic myocardium. J Thorac Cardiovasc Surg 150:1268–1276
145. Hsieh FY, Han HW, Chen XR et al (2018) Non-viral delivery of an optogenetic tool into cells with self-healing hydrogel. Biomaterials 174:31–40
146. Tseng TC, Tao L, Hsieh FY et al (2015) An injectable, self-healing hydrogel to repair the central nervous system. Adv Mater 27:3518–3524
147. Highley CB, Rodell CB, Burdick JA (2015) Direct 3D printing of shear-thinning hydrogels into self-healing hydrogels. Adv Mater 27:5075–5079
148. Han L, Lu X, Wang M et al (2017) A mussel-inspired conductive, self-adhesive, and self-healable tough hydrogel as cell stimulators and implantable bioelectronics. Small. https://doi.org/10.1002/smll.201601916

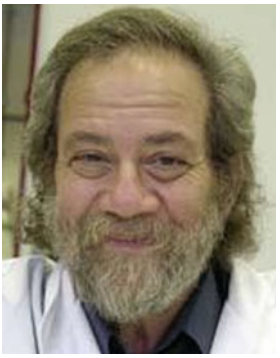

Besim Ben-Nissan Professor Besim Ben-Nissan has higher degrees in Metallurgical Engineering (ITU), Ceranic Engineering (University of New South Wales) and a Ph.D. in Mechanical and Industrial Engineering with Biomedical Engineering (University of New South Wales). Over the last four decades together with a large numbers of PhD students and post-doctoral fellows he has worked on production and analysis of various biomedical materials, implants, calcium phosphate ceramics, advanced ceramics (aluminazirconia, silicon nitrides), sol–gel developed nanocoatings for enhanced bioactivity, corrosion and abrasion protections, optical and electronic ceramics and thermally insulating new generation composites.

He also has contributed in the areas of mechanical properties of sol–gel developed nanocoatings. In the biomedical field, he has involved with the development of materials for slow drug delivery, natural and marine material conversion, implant technology (bioactive materials including conversion of Australian corals to hydroxyapatite bone grafts), biomimetics (learning from nature and its application to regenerative medicine), biocomposites, investigative research on biomechanics and Finite Element Analysis (mandible, knee, hip joints, hip resurfacing), reliability and implant design (modular ceramic knee prosthesis, femoral head stresses). He was part of a research team which initiated the world's first reliable ceramic knee and hydroxyapatite sol gel derived nanocoatings. Since 1990 he has published over 260 papers in journals, five books and over 50 book chapters. He is one of the editors of the Journal of the Australian Ceramic Society and Editorial Board member of three international biomaterials journals. He was awarded "The Australasian Ceramic Society Award" for his contribution to "Ceramic education and research and development in Australia." He also received "Future Materials Award" for his contribution to the "Advanced nanocoated materials field.". He has collaborated with a number of international groups in Japan, USA, Thailand, Finland, Israel, France, UK, Germany and Turkey and held grants from the Australian Academy of Science and the Japan Society for Promotion of Science for collaborative work in the biomedical field in Europe, USA and Japan respectively. After serving as an academic for over 33 years he has retired, however still active and contributes to science by research in the biomedical field and supervising higher degree students.

Gina Choi Ms. Choi is currently a Ph.D. candidate at the University of Technology Sydney (UTS) and her expertise is in calcium phosphate bioceramics and the use of calcified algae for tissue engineering. She has completed her Honours on the conversion of calcified algae to hydroxyapatite for orthopaedic applications. Her most recent publications can be found in the conference proceedings for Bioceramics 29. She is currently working with Prof. Besim Ben-Nissan and Dr Louise Evans to produced nano-sized hydroxyapatite coatings for dental implants using the sol–gel method.

Andy H. Choi Dr. Choi is an early career researcher who received his Ph.D. from the University of Technology Sydney (UTS) in Australia in 2004 on the use of computer modelling and simulation known as finite element analysis (FEA) to examine the biomechanical behavior of implants installed into a human mandible. After completing his Ph.D., he expanded his research focus from FEA to sol–gel synthesis of multifunctional calcium phosphate nano coatings and nano composite coatings for dental and biomedical applications. In late 2010, Dr. Choi was successfully awarded the internationally competitive Endeavour Australia Cheung Kong Research Fellowship Award and undertook post-doctoral training at the Faculty of Dentistry of the University of Hong Kong focusing on the application of FEA in dentistry and the development of calcium phosphate nano-bioceramics. He is currently serving as an associate editor for the Journal of the Australian Ceramic Society and as an editor for a number of dentistry-related journals. In addition, he is also serving as an editorial board member for several dentistry, nanotechnology, and orthopedics journals. To date, Dr. Choi has authored over 50 publications including 4 books and 30 book chapters on calcium phosphate, nano-biomaterial coatings, sol–gel technology, marine structures, drug delivery, tissue engineering, and finite element analysis in nanomedicine and dentistry.

Ipek Karacan Dr. Karacan has a Ph.D. degree in School of Life Sciences at University of Technology Sydney (UTS) in biomedical science. Before her PhD degree, she completed her bachelor's degree in Bioengineering with first honour from Marmara University, Turkey, and currently she is a research assistant at UTS. She is a member of Advanced Tissue Regeneration & Drug Delivery Group and Translational Biomaterials and Medicine Group. Her research focuses on the antibacterial slow drug delivery coating systems for the inhibition of implant and surgery related infections. She has worked on biomaterials, biodegradable polymeric thin film coating on bone implants, marine structures for biomedical applications, and the stem cell development and differentiation in vitro applications, and proteomics. Her recent research focuses on cell engineering and the intracellular delivery techniques for the stem cell therapy applications.

Louise Evans Dr. Evans is a Senior Lecturer in Physical and Inorganic Chemistry at the University of Technology Sydney, specialising in Bioinorganic and Medicinal Chemistry and also Reaction Kinetics. She has authored many publications on biomineralization and bioceramic materials, including chapters in the Encyclopedic Handbook of Biomaterials and in Bioengineering and Marine-Derived Biomaterials for Tissue Engineering Applications. Her current research interests include conversion methods and characterization techniques for marine-derived materials for bone graft substitution applications as well as sol–gel derived calcium phosphate nanocoatings on stainless steel and 3D-printed substrates. She is an editor for the Journal of the Australian Ceramic Society.

Chapter 4
Stem Cells and Proteomics in Biomaterials and Biomedical Applications

Ipek Karacan, Bruce Milthorpe, Besim Ben-Nissan, and Jerran Santos

Abstract The constantly evolving field of regenerative medicine deals with replacing, repairing, or regenerating tissue by using multidisciplinary scientific fields for humans and animals suffering from various injuries to severe diseases. Tissue engineering takes cell biology, materials science, and engineering principles to replace or repair damaged tissues. The scale of stem cell applications in regenerative medicine has increased extensively to develop various clinical-based treatments and potential stem cell-based therapies. This chapter provides an overview of different stem cell sources and their self-renewal, differentiation mechanisms in the regenerative medicine field with the importance of proteomics analyses to understand the stem cell biological processes. Additionally, the importance of biomaterials selection for stem cell-based regenerative medicine and tissue engineering applications is also discussed in this chapter.

Keywords Regenerative medicine · Stem cells · Stem cell differentiation · Biomaterials · Proteomics

4.1 Introduction

Regenerative medicine is dedicated to the process of replacing, repairing or regenerating tissue [1] and has expanded into a multidisciplinary science which has rapidly grown in the past decade [2–11]. The foundation of this evolving branch of medicine and technology is the utilization of a combination of biocompatible materials, stem cells, growth factors and supporting chemical cocktails in effort to repair damaged or failing tissue and organs [1, 12–16]. The scale and breadth of stem cell applications

I. Karacan · B. Milthorpe · J. Santos (✉)
Faculty of Science, Advanced Tissue Engineering and Stem Cell Biology Group, School of Life Sciences, University of Technology Sydney (UTS), Ultimo, Australia
e-mail: Jerran.Santos@uts.edu.au

B. Ben-Nissan
Faculty of Science, Biomaterials and Translational Medicine Group, School of Life Sciences, University of Technology Sydney (UTS), Ultimo, Australia

A. H. Choi and B. Ben-Nissan (eds.), *Innovative Bioceramics in Translational Medicine I*,
Springer Series in Biomaterials Science and Engineering 17,
https://doi.org/10.1007/978-981-16-7435-8_4

in regenerative medicine is continually increasing with various clinical treatments being developed.

The term 'Regenerative Medicine' usually directs people toward thinking about stem cells, particularly embryonic stem cells. While embryonic stem cells are important for the understanding of developmental biology, it has not been a central aspect of regenerative therapies due to long standing public controversy and legislative bans in numerous countries [17]. There are however various other sources of stem cells which have and will continue to play a critical role in the development of therapeutics and regenerative medicine; this will be expanded on in subsequent sections in this chapter.

4.2 Types of Stem Cells

Stem cells are biological and functional living units that play an important role in the regeneration of tissues and organs, and in the development of organisms because of their self-renewal potential and ability to separate into different cell lineages (Table 4.1) [18].

4.2.1 Embryonic Stem Cells (ESCs)

The embryonic stem cells (ESCs) identified were derived from the undifferentiated blastocyst stage of a mouse embryo by Evans and Kaufman [19] in 1981 and ESCs have been well documented for their vast potential for medical applications [20–23]. ESCs are innately pluripotent, with the ability to naturally develop into all cell derivatives of all three germ layers. Their sizeable utility is however overshadowed, due to the nature of their source, there are enormous ethical and political issues associated with their use [24]. Because of these limitations, other sources of stem cells are preferred.

Table 4.1 The types of stem cells and their characteristics

Stem cell types	Source	Characteristics
Embryonic stem cells (ESCs)	Blastocysts	Pluripotent cells
Hematopoietic stem cells (HSCs)	Peripheral, Cord blood	Multipotent cells
Induced pluripotent stem cells (iPSCs)	Fibroblasts, keratinocytes, Peripheral blood mononuclear cells	Pluripotent cells
Mesenchymal stem cells (AMSCs)	Adipose tissue, Bone marrow, Peripheral Blood	Multipotent cells

4.2.2 Induced Pluripotent Stem Cells (iPSCs)

The most similar stem cells to ESCs are induced pluripotent stem cells, which are produced by a reprogramming of adult skin epithelial cells or T-cells to cells with a differentiation potential of embryonic stem cells [25]. These newest stem cells are vastly popular in current regenerative medicine research as developed in 2006 by Shinya Yamanaka's lab. The process introduces four specific genes (named Myc, Oct3/4, Sox2 and Klf4), collectively known as Yamanaka factors, encoding transcription factors that allow for the cellular reprogramming [26]. However, due to their nature of production, there are still limitations and active trials in determining their safety and efficacy in therapeutic use [27].

4.2.3 Hematopoietic Stem Cells (HSCs)

Discovered in 1961, hematopoietic stem cells (HSCs) are stem cells progenitors to blood cells. In a process known as haematopoiesis that occurs within the bone marrow, HSCs give rise to mature blood cell lineages called myeloid and lymphoid. Myeloid linage is made up of cells such as monocytes, macrophages, neutrophils, basophils, eosinophils, erythrocytes, and megakaryocytes. Lymphoid cells include T cells, B cells, natural killer cells, and innate lymphoid cells. HSCs are usually derived from bone marrow, peripheral blood, or umbilical cord blood. Since HSCs are derived from the bone marrow, they are classified from the mesodermal lineage and have similar regenerative capacities akin to other stem cells from the mesodermal layer. Allogenic HSCs are commonly used in the treatment of cancers such as multiple myeloma or leukemia.

4.2.4 Mesenchymal Stem Cells (MSCs)

The mesenchymal stem cells or multipotent stromal cells (MSCs) are originally discovered by Friedenstein et al. [28] in 1970s in the bone marrow as osteoprogenitor cells. The research group initially reported the fibroblast-like cells which were elaborated from bone marrow via attachment to tissue culture plastic were inherently osteogenic. Then researchers from various laboratories found out that these osteogenic cells have differentiation ability into different connective tissue cell types [28, 29]. The primary function of MSCs is in the repair and regeneration of organs and tissues.

Although there are different types of stem cells including foetal, embryonic and pluripotent as explained above, adult stem cells are the most suitable source for clinical applications such as cell therapy and bone regeneration [18, 30]. This is due

to the ease of source acquisition and patient safety with autologous or donor matched allogenic transplants.

Mesenchymal or stromal stem cells (MSCs), which are adult stem cells, are often used in the tissue-engineering field and in stem cell-based therapies such as repairing damaged tissues, because of their multi-potential differentiation ability. MSC reservoirs have been found within different types of tissues including bone marrow, placenta, amniotic fluid, menstrual blood, dental pulp, and adipose tissue [31]. Adipose tissue is a rich source for adult stem cells termed adipose-derived stem cells (ADSC). It is the most abundant and relatively risk-free source of adult stem cells. ADSCs have been expansively used in clinical research, regenerative medicine and tissue regeneration applications [32].

The harvesting process of ADSCs is relatively easier in large quantities with a minimally invasive technique, very low negative impact and discomfort for the patient, whereas the harvesting process of bone marrow-derived MSCs (BMSCs) is highly painful for the patient. ADSCs can be extracted by lipoaspiration from adipose tissue with more than 95% purity, high proliferative ability, and multi differentiation potential. The yield of cells per gram of adipose tissue is higher than that of any other stem cell reservoir tissues [33, 34]. Additionally, BMSCs and adipose-derived MSCs (ADSCs) have been commonly used for bone tissue engineering [18, 35]. Clinical trials conducted with MSCs have a broad range of medical applications. Soft and hard tissue regeneration, immune disorders, cardiovascular diseases, osteoarthritis, liver disorders, respiratory disorders, spinal cord injury, kidney failure, muscular dystrophy, and ischemic injuries are some of the stem cell-based clinical trials as therapeutic targets for MSC applications [36, 37].

4.3 Differentiation of Stem Cells

Differentiation is the process in which stem cells respond to local external stimuli by developing into the cell type caused by the signaling environment. The range of mature cell types a stem cell can differentiate into is known as plasticity, which is the inherent ability of stem cells to cross lineage barriers and adopt the phenotypic, biochemical and functional properties of cells unique to other tissues [38]. This plasticity potential can be sub-categorized depending on the source of the stem cells. Embryonic stem cells (ESCs) are known to be able to differentiate into all cell and tissue types during foetal development and thus are referred to as pluripotent cells. MSCs have the innate potential to differentiate into cells within the mesodermal linage and are said to be multipotent. However, numerous publications have shown that these cells when induced under specific conditions are capable of in vitro transdifferentiation [39–43], effectively developing into cells of ectodermal and endodermal lineages [44–46]. Another commonly used class of cells are the oligopotent cells or progenitor cells that are committed to a tissue type and give rise to a defined set of cell types with a limited number of lineages [47].

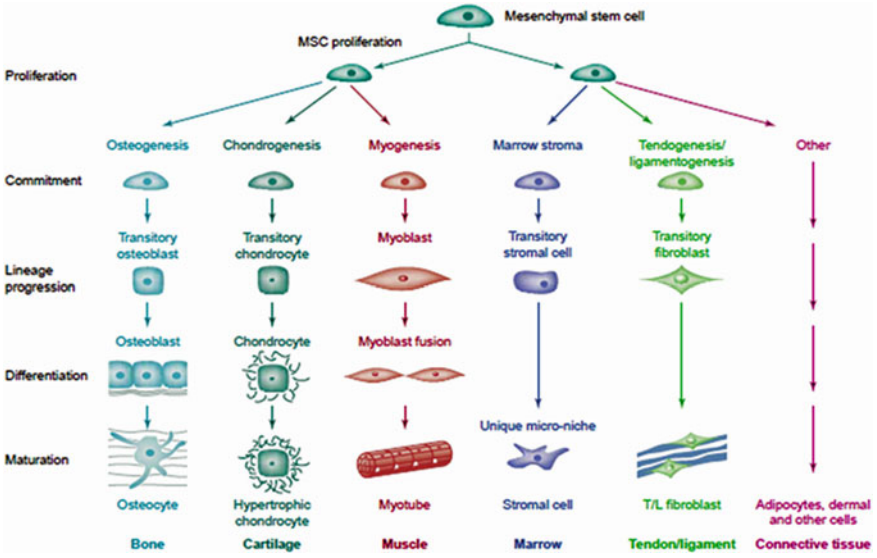

Fig. 4.1 Mesogenic differentiation and maturation of differentiating adult mesenchymal stem cells [52]

The two broad methods of inducing differentiation are chemical stimulation or biological stimulation. The overarching action of chemical stimuli is due to simple small molecule additives acting directly on biochemical pathways promoting the desired differentiation pathway [48]. Biological stimulation uses cocktails of cytokines, growth factors and various bioactive components usually present in the tissue normally containing the desired differentiated cell [49–51]. These constituents not only promote differentiation pathways, but also have an active role in essential mineral and vitamin sequestration, driving the process forward (Fig. 4.1). The subsequent sections detail the current differentiation methods and their clinical significance and potential.

4.3.1 Adipogenic Differentiation

The 'trilineage' differentiation of MSCs to adipogenic, osteogenic and chondrogenic cells has become a benchmark for determining the differentiation potential of tissue derived adult MSCs [45, 50]. Producing adipocytes from the ADSCs is no revelation considering the cell's source tissue, demonstrating an inherent potential for the development of adipocytes in vivo, which can be reproduced in vitro under the correct conditions. Producing adipocytes from MSCs has garnered much attention for their clinical importance in reconstructive surgeries and regenerative therapies. Patients

suffering extensive tissue loss from burns, accidents and tumor removal in mastectomys have a source of autologous soft tissue for reconstructive surgeries. Several studies of in vitro adipose reconstruction have demonstrated the use of MSCs and precursor cells derived from bone and adipose tissue [53–55].

Current methodologies to achieve adipose reconstruction involve ADSCs cultured in serum containing adipogenic media supplemented with a combination of 0.5 mM isobutyl-methylxanthine (IBMX), 1 μM dexamethasone (Dex), 10 μM insulin and 200 μM indomethacin. Following a 21-day differentiation period, the newly formed cells express adipocyte specific marker proteins and present visible accumulation of lipid, confirmed by Oil Red S staining. The adipogenic supplements have demonstrated critical roles in the development of adipocytes. The first component, IBMX, induces an increase in the intracellular concentrations of cAMP [56]. IBMX is non-selective phosphodiesterase inhibitor, which enzymatically convert cAMP to AMP [57]. IBMX also actively stimulates adenylyl cyclize promoting cAMP synthesis [56]. The increased intracellular cAMP is also known to mediate the stimulation of adipocyte differentiation [58]. The second supplement, Dex, is commonly utilized as it is known to regulate the metabolism of glucose and to stimulate the expression of the peroxisome proliferator-activated receptor γ (PPARγ), a transcription factor which is known to play an essential role in adipogenesis [59, 60]. The third component, indomethacin, binds and activates PPARγ which stimulates lipid uptake in adipogenesis [61]. The fourth and final component is the Insulin hormone, which stimulates the uptake and storage of glucose in a variety of cells, especially adipose. The combination of these supplements provides the ideal stimulatory push for adipogenic induction. The expression and detection of markers such as the PPARγ, aP2 and Glut4 have been widely used as confirmation of adipogenesis [62, 63]. In further studies aimed at elucidating the pathway crossover and interactions during differentiation, Enomoto and colleagues [64] noted the inhibition of the RUNX2 gene hinders chondrogenesis while promoting adipogenesis. The study by Dicker et al. concluded that the adipocytes produced in vitro from differentiated BMSCs and ADSCs are phenotypically and functionally identical to the native adipocytes [65].

Both BMSCs and ADSCs have adipogenic capacity in vivo and are usually surgically implanted within scaffolds that possess a degree of biocompatibility [66, 67]. Nonetheless, several areas must be further developed before regenerated adipose tissue could be utilized in a clinical setting. These include the following: (1) proper vascularization of tissue within a 3D scaffold; (2) producing a scaffold that is flexible and robust enough to be manipulated in surgery as well as being bioresorbable; (3) defining the complete proteomic characteristics of the adipogenic cells produced on the various scaffolds while comparing it to the native tissue, and (4) determining the stability of the cells as they do require pre-induction prior to implantation.

4.3.2 Osteogenic Differentiation

Musculoskeletal conditions are the most common cause of severe long-term pain and physical disability affecting hundreds of millions of people around the world [68] while osteoporosis and osteoarthritis are the leading causes of skeletal and joint damage and the fourth leading cause of disability with a worldwide medical cost burden in the billions of dollars. Cellular therapies for such afflictions have become popular in the last decade. Initially, BMSCs were used; however, these cells are limited in number and estimated to be derived at a very dilute 1 per 105 cells using traumatic retrieval methods [69, 70]. Alternatively, primary isolation yields of ADSCs are often a thousand-fold higher than that of BMSCs and the cells demonstrate a high capacity for bone formation in vitro and in vivo [71, 72]. In addition, using autologous cells negates the problem of immunological antigenic rejection [40].

There is now plethora of methods that yield high numbers of differentiated osteogenic cells from a variety of tissue derived MSCs for research and clinical applications. In addition, numerous groups have demonstrated that ADSCs from various species can produce osteoblasts in vitro [42, 63, 73–75]. The most popular method of differentiating cells into osteogeneic lineages utilizes the simple additives dexamethasone (Dex), ascorbic acid (AA), and β-glycerophosphate (βGP) to the basal media of in vitro cells [45]. Alternative induction medias do exist and contain combinations of hormones and growth factor supplements such as vitamin D [73] and Bone Morphological Protein (BMP) 2 and 4 [76–78].

Dex is a synthetic glucocorticoid steroid that is often used interchangeably with naturally occurring 1,25-dihyroxyvitamin D3 (VD3) for in vitro differentiation studies [45]. The endogenous VD3 hormone is involved in a complex signaling cascade and is required for the maintenance of skeletal calcium balance by promoting calcium absorption during normal bone formation in vivo [79, 80]. VD3 deficiency decreases bone density and mineral deposition, usually manifesting as osteoporosis and structurally weak bones. Since Dex is structurally similar to VD3, it has been used in a number of in vitro studies and shown to increase vitamin D receptor (VDR) protein levels in a number of multipotent cell lines [81]. Dex has also been utilized clinically to treat arthritis pain and inflammation. Furthermore, Phillips et al. showed that Dex induces osteogenesis in primary dermal fibroblasts, confirmed by the presence of osteoblast markers, alkaline phosphatase activity, and mineral deposition [80]. When 100uM Dex is added to osteogenic media of MSCs, it appears to initiate the mitogen-activated protein kinase (MAPK) pathway, which activates Runx2/Cbfa1 by phosphorylation [42, 45, 69, 77]. The Runx2/Cbfa1 is an important transcription factor and is the functional partner of several bone morphogenetic proteins vital in osteoblast differentiation and skeletal morphogenesis [82–84].

The second additive, AA or Vitamin C, is an effective antioxidant and essential co-factor in collagen synthesis; however, there is limited research detailing its effect on MSCs. Coelho and Fernandes [85] showed that BMSCs grown in the absence of AA or Dex had a lower percentage of proliferative and differentiating cells in vitro

and failed to form calcium phosphate deposits. Findings by Jun-Beom support this, detailing that AA and β-glycerophosphate (βGP) induced osteodifferentiation with mineralization increasing with Dex treatment in a dose-dependent manner [86]. The treatment of a mouse osteoblastic progenitor cell line with AA increased the hydroxylation of intracellular pro-collagen within one hour of treatment, stimulating the formation of collagenous ECM as well as a time dependent increase in alkaline phosphatase (ALP) and osteocalcin mRNA levels [87]. Franceschi concluded that the addition of AA is sufficient to initiate osteoblast maturation and induce early matrix-associated signals that positively regulate further osteoblast associated genes [87].

β-glycerophosphate (βGP) is a source of inorganic phosphate and is considered a likely mechanism for increasing mineral deposition [88, 89]. The addition of βGP has also been shown to decrease MSC proliferation and increase differentiation toward an osteoblast cell type [85]. Under normal cell culture conditions, MSCs and ADSCs in osteogenic media express morphological and phenotypic similarities to osteoblasts. The broadest changes are observed within 7 days of induction as cells assume a cuboidal and rigid planar morphology. At 14 days, the cells appear structurally similar to primary osteoblasts with very condensed and rigid cell bodies. At this time point, a significant up regulation in the expression of alkaline phosphatase, collagen type 1, osteopontin, osteonectin, osteocalcin, bone sialoprotein, and the receptors BMP-2 and BMP-4 is observed. Furthermore, the osteogenic cells are capable of mineralizing calcium, confirmed by positive staining with alizarin red, in the newly formed collagen matrix [45, 86].

4.3.3 Chondrogenic Differentiation

The development of cartilage regenerative therapies is complementary to bone regenerative therapies. Not surprisingly, the differentiation process of directing MSCs toward a chondrogenic lineage to produce cartilage is somewhat similar to that of osteogenesis. Many osteochondral degenerative diseases and injuries are often related, as are the repair mechanisms. The structural difference between cartilage and other tissues is a main factor for the slower repair process. Cartilage is a unique tissue in that it lacks vascularization and innervations, and as such, the normal healing and tissue repair mechanisms do not apply as stem cells cannot be recruited to sites of damage [90, 91].

Cartilage is classified into three general types, hyaline, elastic and fibrocartilage. The damage to articular hyaline cartilage in joints disrupts the extracellular matrix (ECM) composed primarily of collagen type 2, hyaluranon and proteoglycans. The continuous wear on load bearing joints destroys the dense ECM material and this is most prevalent in osteoarthritis. The ECM is not readily restored and any normal repair by chondroblasts in the load bearing joints often yields structurally fallible fibrocartilage [92].

Cell transplantation [93–95], tissue engineering [7, 96–98] and biomaterial scaffolds [99–102] are in vogue and show much promise in repairing defective cartilage from traumatic injuries and degenerative diseases. The aforementioned approaches have proved that chondrocytes can be produced from MSCs in monolayers and three-dimensional culture systems that are clinically relevant. However, the ability of cells to generate ECM that is as mechanically robust as the native articular cartilage remains elusive. The cell transplant studies have provided minimal evidence of MSCs ability to produce cartilage in vivo compared to the success of in vitro studies [92, 103]. Mapping out the precise differentiation pathways in vivo is a daunting task as there are often hundreds of biochemical interactions and proteomic changes occurring in synchrony. These are initiated not only by differentiation supplements but also by heterogeneous cell populations, as well as physiological and mechanical signals [15, 66, 104–108]. There is also the added difficulty of retrieving sufficient samples from non-experimental animals or human subjects. Defining these events in vitro allows for a controlled system for a clearer understanding of the cells produced.

Current standard in vitro culture techniques for promoting chondrogenesis in vitro consist of chemically defined media using synthetic serum replacements supplemented with recombinant cytokines and growth factors. However, the use of serum-free media is a double-edged sword and a challenging condition to culture cells. Stem cells produced under these conditions generally have a decreased adherence as well as a limited proliferation rate [90, 109]. The positive impact of not using serum is the reduced inter-batch variation introduced by uncharacterized growth factors and differentiation factors, which could potentially induce differentiation into multiple lineages. There are now numerous commercially available serum-free medias with synthetic serum substitutes. The latest research shows that newer serum-free media are proving to be as successful as serum-containing media compatible with chondrogenesis of MSCs [110, 111].

There has been at least a dozen published cytokines and growth factors which induce chondrogenesis [112, 113]. The most efficient and commonly used supplements are transforming growth factor beta (TGF-β), bone-morphogenetic protein-2 (BMP-2), fibroblast growth factor-2 (FGF-2), insulin-like growth factor-1 (IGF-1) and interleukin (IL)-1β [114–117]. The functional overlap of the supplements for differentiation into other lineages is not unexpected, especially within osteochondral differentiation, as many pathways are shared in normal biological processes. Investigating the supplements individually or in a combinatorial mixture allows for a delineated understanding of the chondral differentiation process in the presence of a differentiation induction media. The first component, TGF-β3, is part of a superfamily of highly conserved growth factors that are known to regulate cellular proliferation and differentiation of a variety of cells [118]. The TGF-β3 isoform is the most widely used supplement in chondrogenesis; however, its role in the differentiation process is not implicit. It is hypothesized that TGF-β3 mode of action is directed through the TGF-β type-2 receptor. This activates the R-SMAD cascade and SMAD independent pathways such as the MEK1/2-Erk1/2 cascade [118], which play a prominent role in cartilage development. Interestingly TGF-β3 is also implicated in the inhibition

of adipogenesis, osteogenesis and myogenesis through the functional repression of essential transcription factors that drive these differentiation pathways [118–120].

A group of functionally related cytokines to TGF-β3 are the BMPs which are well known for their role in bone formation. A large focus has been placed on the study of BMP-2, BMP-4 and BMP-7, which has been shown to induce MSCs differentiation toward cartilage formation inclusive of ECM synthesis [121–123]. A number of studies have shown that BMP-4 has the capacity to initiate chondrogenesis in a variety of tissue derived adult MSCs [124, 125]. The study by Nakayama et al. identified that BMP-4 synergistically acts with TGF-β3 in regulating chondrogenesis of MSCs through SMAD pathways [126]. Chondrogenesis in MSCs is activated by several cytokines which often stimulate crosstalk between signaling pathways [90]. TGF-β3 has also been reported to act synergistically in chondrogenesis with other related cytokines such as FGF-2, regulating the MAPK cascade. Interestingly, FGF-2 is known to induce expression of the protein Gremlin1, which antagonises certain BMPs, therefore indirectly acting as an inhibitor in part of the TGFβ signaling pathway which is hypothesized to impede osteogenesis [127].

In monolayer chondrogenic cultures, morphological changes to the MSCs during differentiation are very limited throughout the 21-day incubation period. Cellular structural differences tend to manifest after 7 days as cells become more visibly polygonal in shape and grow in dense clusters resembling nodules. Differentiation is usually confirmed by histological staining and immunoblotting. Histological staining of these cells with alician blue shows a relative increase in the amount of the sulphated glycosaminoglycan, hyaluronan, over the culture period [99]. Hyaluronan is one of the chief components of the ECM of in situ cartilage. Complementing this is characterization by immunoblotting by antibody-marker detection of ECM and collagen proteins. This has been widely conducted to investigate the expression levels for collagen type I and type II [99, 101].

4.3.4 Neurogenic Differentiation

Neurogenic differentiation is one of the most sought-after stem cell differentiation processes for the innumerable potential medical therapies and biotechnological applications it could be applied; however, it has also proven to be very difficult [128]. A number of chemical and biological stimulation techniques were reported and have been shown to promote neural cell induction and differentiation both in vivo and in vitro. The chemical-based differentiation methodologies vary greatly depending on the neuronal cell type required. The Woodbury method [46] to initiate differentiation of bone marrow stem cells into neurons utilizes 1 mM β-mercaptoethanol (BME) for 24 h to serum-containing sub-confluent cultures. The treated cells produced a morphological copy of neuronal cells expressing several neuronal markers, Neuron specific enolase (NSE) and Neurofilament-M (NF-M) expression [46].

Studies have shown that the neuronal like cells produced from such differentiations are capable of producing Schwann cells of which the functionality is still

under investigation [129]. It has been hypothesized by Ishii et al. that the antioxidant properties of BME may play a key role in the neuronal survival and the differentiation process [130]. Santos et al. discovered that shorter treatment times initiated pre-neuronal differentiation pathways [131]. As such, several related chemicals with similar reductive and antioxidant properties have also been investigated such as dimethylsulfoxide (DMSO), butylated hydroxyanisole (BHA) and Valproic acid (VPA) alone or combined [132–134].

In the assessment of a developing nervous system, the process of forming successful stable connections between functional neurons is a long and sensitive biological process. The expectation that stem cells in a monoculture would develop into functional, action potential firing, neurons within 24 h of exposure to a single chemical would be an oversimplification of cell biology. The expression of neuronal-specific tissue markers does not necessarily imply that fully functional signal conducting neurons have been produced, especially since there are dozens of neuronal cell classes, some of which are non-axonal, and the expression of the listed shared markers are not mutually exclusive. As such, the neurogenic differentiation of MSCs could easily produce a wide range of supporting neuronal cells, like astrocytes or glial cells which do not have the electrophysiological potential present in neurons. While the extended exposure to such chemicals may damage the MSCs, a time-limited treatment may be sufficient to initiate the differentiation process to a pre-neuronal stage [74, 135].

These chemical methods of differentiation certainly initiate differentiation toward a pre-neuronal stage; however, the induction media lacks the necessary supporting conditions to complete the differentiation process to a mature neuronal cell. Since the differentiation pathway has yet to be determined, it is highly probable that the current in vitro differentiation methods produce a mixed population of pre-neuronal cells and some differentiated neuronal-like cells. Examining the proteomic profiles will allow a complete comparative measurement of the extent of biological change occurring during the differentiation process. In further studies, the effect of biologically relevant and less harsh chemicals such as Valproic Acid and IBMX should be examined on neural differentiation. It was found that the chemicals sites of action in the molecular pathway affected downstream expression of proteins as well as the ultimate fate of the cell's differentiation destination [136, 137]. Coupling proteomics with systems biology pathway analysis allows for an in-depth investigation of the changes occurring during the development process. Santos et al. explored the expression of subsets of functional proteins and their interactive partners to gain further understanding into the extent of the differentiation process. The phenotypic characterization by proteomic profiling allows for a substantial in-depth analysis of the molecular machinery induced and directing the cellular changes through the process [138].

The notion of transdifferentiation across dermal lineages is relatively recent and is still widely debated. However, the mounting evidence supports that it is possible to direct mesodermal cells to neuroectodermal lineage [139]. In terms of future therapies, the abundance of ADSCs from lipoaspirates promises a wide range of autologous clinical applications for neuronal repair. The caveat that remains is the

confirmation that the biological and functional similarities of the produced cells are the same as their genuine counterparts.

A combined approach of using initiating chemicals, growth factors and importantly biomaterial structures to mimic and modulate a three-dimensional space becomes highly important in tissue engineering. Understanding the cells response at a physical and molecular level expands the knowledgebase and potential applications.

4.4 Stem Cells and Biomaterials

4.4.1 Stem Cells Growth and Interactions

As previously established, stem cells have the potential to differentiate and mature into various progeny cells. However, the initiation of this process is highly dependent on the environment the stem cells are grown in and the interactions they can perceive. Usually, the cellular interactions are firstly in direct physical contact with their environment, for example (1) cells in native tissue are surrounded by other cells, extracellular matrices, blood vessels, various bodily fluids; or (2) cells in a tissue culture flask are in direct contact with the plastic or glass or protein coating on those inorganic surfaces and the full range of contents in growth media. These interactions can affect the growth and state of the cell's life cycle. In a 2D culture dish where cells are grown in a monolayer, the premise that physical space can affect the cells life cycle can be proved in proliferation until the cellular monolayer reaches confluence, where the planar surface growth area is occupied to 100%. If the cells remain at confluence for an extended period, the cells reach a state of senescence where the metabolic and proliferation growth rates irreversibly arrest [140].

4.4.2 Stem Cells Phenotyping

Phenotyping is the collective analytical process for determining a cells phenotype i.e., the observable and measurable properties of a part or whole of an organism. Due to vast complexity of stem cell biology such as phenotyping, the stem cell-based research requires the multidisciplinary studies including genomics, transcriptomics, lipidomics, metabolomics, and proteomics [140].

4.4.2.1 Genomics and Transcriptomics

The phenotype is determined by the genetic make-up, from the inherited genes and dominant characteristic that arises from gene expression. Gene expression is the process were by the genetic information from inherited DNA is translated to a

functional product such as a protein. Gene expression is highly regulated process that allows cells to respond to a changing environment. As a stem cell grows or changes in its environment the cells can be harvested, prepared into reduced fractions of its subsidiary components for further analyses. DNA and genetic information are completed by gene sequencing in a field known as genomics. Furthermore, RNA can be analyzed by transcriptomics, lipids by lipidomics, and metabolites by metabolomics. Each area homing in on the specific classes of molecules, evaluating them quantitatively and qualitatively. The measurements acquired allow for an unprecedented depth of knowledge to be acquired about the changes occurring in stem cells. The generated data can be collected and cross-studied in further analysis as reassembled in silico in the further area of study known as systems biology.

4.4.2.2 Proteomics

Proteins can be invested in a field known as proteomics. The term "Proteome" refers to the entire set of proteins expressed in a cell or organism. The proteome-related important issues such as post-translational modifications (PTM), protein stability, protein amount, and interactions can be defined at the proteome level [141].

Proteins are the main effectors of variations in the transcriptome and genome. Therefore, the global and targeted detection of proteome can provide crucial information about the biological processes. Furthermore, the complex biological processes of stem cells especially stem cell differentiation, cell proliferation, and migration are regulated and shaped by certain complicated patterns of gene expression and protein activity. Therefore, coupling proteomics with genomics is crucial to identify the stem cell-related biological processes and cell behavior precisely [142–144].

Identification and quantification of protein expression, localization, modification, and interactions via advanced mass spectrometric technologies with tailor-made bioinformatics tools improve the understanding of stem cell identity, functions, and cell fate transitions for innovative biochemical and biomedical approaches [141].

One of the most effective tools for both global and targeted proteome analysis is mass spectrometry (MS) due to the determination of protein mass. Tandem mass spectrometry (MS/MS), Liquid chromatography coupled to tandem mass spectrometry (LC–MS/MS), Shotgun proteomics, targeted proteomics, and phosphor proteomics are some of the main mass spectrometric technologies for protein identification. MS/MS is used to determine the mass of peptides. Then the peptides are fragmented to generate fragmentation patterns for identification. On the other hand, LC–MS/MS has a chromatographic separation stage for the large number of complex peptide mixtures that provide more extensive proteome sampling. LC–MS/MS is used for both Shotgun proteomics and targeted proteomics. While shotgun proteomics called 'discovery proteomics' aims to identify all proteins in a sample, targeted proteomics aims to identify and quantify a specific set of pre-defined peptides in a sample [141, 145]. Finally, protein phosphorylation is a major protein regulator and PTM for

signaling transduction that affects most biological processes. The MS-based phosphoproteomics technology provides the quantitative and sensitive measurement of phosphoproteome on a large scale [146].

The ability to quantify protein expression levels in a biological sample is another crucial and beneficial application of proteomics technology in stem cell biology. The isobaric tag for relative and absolute quantitation (iTRAQ), Stable isotope labeling with amino acids (SILAC), and Tandem mass tag (TMT) are some of the important techniques for protein quantification [142, 145]. The iTRAQ method allows a multiplexed stable isotope labeling of all peptides up to 10-plex. The method allows for simultaneous relative quantitative analysis of expressed proteins. iTRAQ has been used successfully in stem cell research for the quantitative analysis of expressed proteins [147, 148]. SILAC, a simple and powerful quantitative proteomics approach, involves supplementing cell culture media with stable isotope versions of amino acids, typically 13C6 or 13C6 15N5 Arginine or Lysine [149]. The TMT process is functionally similar to iTRAQ labeling in that the labels contain heavy and light isotopes that give rise to reporter-ions at different masses after activation in the collision cell of a mass spectrometer [150, 151].

4.4.3 Biomaterial Types and Biomedical Applications

4.4.3.1 Metallic Biomaterials

Metals, especially noble metals such as gold have been used as implantable materials in the medical field for many thousands of years. To design successful metallic implants and devices, the researchers must correctly determine appropriate mechanical and chemical properties such as the fatigue strength and the corrosion resistance. At the same time, the implantable device must have adequate biocompatibility to its surrounding tissue and bone to obtain a successful surgical outcome. Although the metals and metal alloys have wide application areas, especially load-bearing applications, because of the high constraints of the medical areas, only a few metal systems have been used [152–154]. Stainless steel, cobalt-chromium (Co-Cr) alloys, titanium and zirconium alloys are the most common alloys and are utilized in orthopedics, dentistry, and maxillofacial devices.

The undesired biological responses such as chronic inflammatory response or adverse reaction between the bone-metal interfaces after implant insertion are very important problems for metallic implants. For instance, certain stainless-steel alloys support the formation of multilayer fibroblasts between bone and implant which causes loosening of the implants. Many investigators strongly stated biocompatibility, fatigue strength, and corrosion resistance as the required properties for the metallic implants to prevent the implant loosening after surgery and to improve implant integration.

The good mechanical strength, corrosion resistance and high biocompatibility of titanium and titanium alloys, especially for Ti-6Al-4V alloy have been justified

by many researchers [155–157]. Therefore, titanium and titanium alloys have been widely used as a component of the implants especially for hard tissue applications in dental and orthopedic arena. Especially, commercially pure titanium (CP Ti) and Ti-6Al-4V alloy have been accounts for 50% of the total market for the biomedical industry such as implantable devices [158].

However, there is a possible risk with the undesired metal ion release, especially vanadium from the implant surface. In order to reduce the risk, surface modifications on the metallic implants have been investigated recently to improve the properties. The modifications on the metallic implant surfaces with mechanical, chemical and biological means has been reported. Micro and nano coating of the metallic implants with ceramics, polymers or their composites, and combining with biological or pharmaceutical agents is the current research areas of a number of the groups and is very promising [159, 160].

One of the most applicable and attractive methodologies is to combine the metallic implants with the other biomaterials, mostly bioceramics (calcium phosphates, bioglass), biodegradable natural or synthetic polymers or the biocomposite materials that can be designed as a coating material on the implant surface [161–163].

4.4.3.2 Ceramic Biomaterials

Ceramic-based biomaterials are one of the most widely used materials in many different medical applications. In particular, bioceramics have been utilized for repairing, treatment and regeneration of damaged tissue within the human body. Bioceramics in the forms of powders, solid pieces, granules, macro- and nanocoatings have found applications in coating of metallic implants, bone filling and injectable products [164, 165]. Consequently, various components of orthopedic and dental implant devices, bone screws and plates, space-filling materials for damaged bone, coating materials on the metallic surfaces in order to support implant-tissue interactions, drug delivery systems are some of the most important clinical applications of bioceramics [166].

According to their reactivity, bioceramics are categorized into three categories: bioinert, bioactive and bioresorbable. From bio-inert biomaterials to bioresorbable biomaterials, the historical perspective of bioceramics can be observed. The second-generation biomaterials consist of bioactive properties that react with the surrounding tissues [166–168], while the nearly inert bioceramics such as zirconia and alumina are generally used in metallic hip, knee and dental implants. Other second-generation materials are bioglasses and calcium phosphates. Additionally, some calcium phosphates such as β- and α-tri calcium phosphate and coral (which are $CaCO_3$) are some examples of bioresorbable bioceramics [167, 169–171]. The categorization of bioceramics according to their reactivity and application are shown schematically in Fig. 4.2.

Although bioglass and crystalline ceramics have been mostly utilized in clinical and medical applications, crystalline ceramics have generally been used as coating materials for metallic implants and drug delivery systems [160].

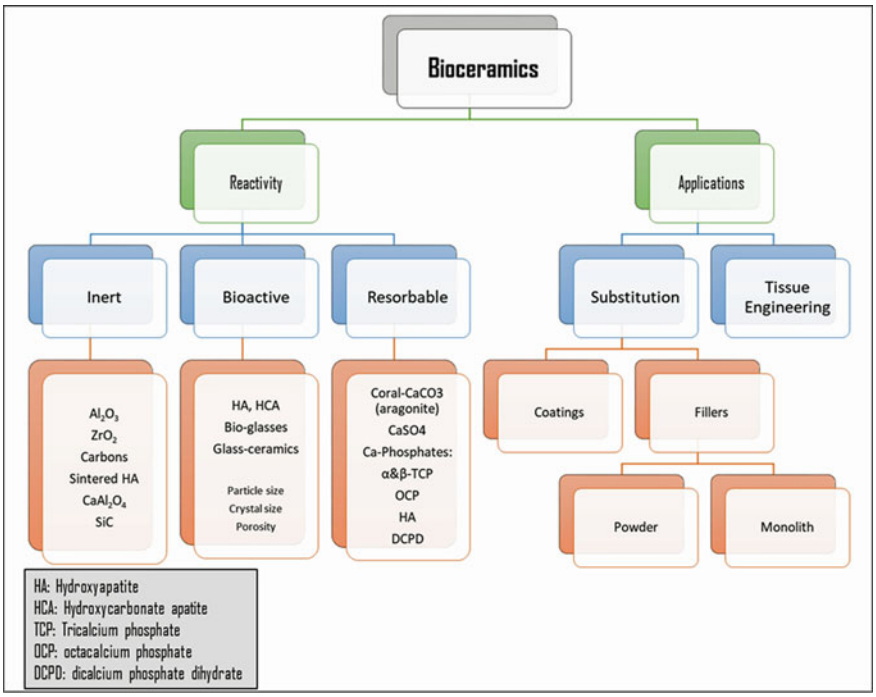

Fig. 4.2 The categorization and application fields of bioceramics. Modified from [165]

Calcium phosphate ceramics (crystalline bioactive or bioresorbable ceramics) have been investigated by researchers since 1920s and were extensively utilized due to their wide clinical application areas. Calcium phosphate bioceramics are used in orthopedic and dentistry areas such as bone augmentation, repair, and substitution. They are also applied to tissue regeneration, maxillofacial and cosmetic surgery [172, 173].

Hydroxyapatite (HAp), brushite (DCPD), monetite (DCPA) and whitlockite (β-TCP), as well as the combination of HAp and (β-TCP), which is referred to as biphasic calcium phosphate (BCP) are some members of the calcium phosphate bioceramic materials [174]. Additionally, the grain sizes of bioceramics have been reported to be around 1–1000 μm, although new generation nanoceramics are between 10 and 100 nm range and are used in many different clinical applications [175].

HAp bioceramic has very similar structure to the inorganic mineral part of natural human bone apatite which includes 70% cancellous bone approximately. It has a hexagonal crystal structure, and its formula is $Ca_{10}(PO_4)_6OH_2$. Therefore, it is commonly used for bone and tissue engineering applications in dentistry and orthopedic arenas, because of its high biocompatibility and osteoconductivity [176].

One of the most important applications for the calcium phosphate bioceramics is to utilize them as a coating material on the metallic implants. Calcium phosphates, especially HAp, were used as coating materials for metallic implants in order to

provide successful bonding with implant-tissue surfaces and improve the osseointegration surrounding tissue surface. Using the sol–gel coating method, Roest et al. reported the deposition of HAp coating on commercially pure titanium and Ti-6Al-4V substrates after anodization were carried out. According to their results, while HAp coated metallic substrates is an effective method in order to improve implant-bone interfacial surface interactions and biological responses, the adhesive bonding of the HAp coated Ti-6Al-4V substrate was better than the commercially pure titanium substrate [177].

According to Rath et al., the anodization of TiAlV alloy substrate followed by the deposition of HAp provides the benefits of both systems. They reported that TiO_2/HAp coated substrate had better corrosion resistance, adhesive strength, and cellular biocompatibility and bioactivity than only HAp coated substrate [159]. Furthermore, Zreiqat et al. also reported that HAp coating on Ti-6Al-4V samples produced enhanced surface bioactivity. As a result, the bioactive bone-like HAp sol–gel coating modulated the extracellular pathway signals of the human bone derived osteoblast cells, and the system was contributing the successful osteoblast growth, function and differentiation on the HAp coating surface [178].

Natural sources have also been used to synthesize calcium phosphate bioceramics, such as animal sources (cow, sheep bone) and marine sources (sea urchin, coral). Marine skeletons have been used to support various functions of human tissues as medical materials due to their unique architecture and interconnected porous structures, mechanical properties, and microstructural composition. Most marine structures such as coral, seashells, cuttlefish, nacre, sea urchins, and marine algae contains calcium carbonate ($CaCO_3$), which is a precursor material of the calcium phosphates such as HAp. During the production of calcium phosphate bioceramics, marine materials are converted to calcium phosphates using various methodologies for applications in pharmaceutical and biomedical arenas. Another important factor is the chemical compositions of marine skeletons, in particular coral skeleton, which contain elements such as Sr and Mg that improves the bioactivity, mechanical properties, and capacity to influence bone growth in osteoporotic patients with additional Ca and Si, which can influence bone growth. In addition, their pore sizes that falls between 20 and 500 μm and pore sizes that falls within this range are extremely appropriate for bone cells and vascularization [179–181].

Marine-based exoskeletons have been of significance for applications in tissue regeneration, drug delivery systems, and drug therapy because of the abovementioned properties as well as their natural unique structures [180, 182, 183]. During the search of calcium phosphates for medical applications, the most important utilization of calcium phosphate particles derived from natural sources are found in drug delivery system with the combination of polymeric biomaterials as a coating system on metallic implant devices. As an example of the combined system of calcium phosphate particles and polymeric biomaterials, Macha et al. reported that drug-loaded calcium phosphate which is HAp microspheres mixed with a biodegradable polymer was utilized as biodegradable PLA film composites. Dissolution studies were carried

out to observe the drug-release rate that was loaded within the calcium phosphate microspheres. The results demonstrated the drug release rate was successfully controlled with calcium phosphate particles [180].

4.4.3.3 Polymeric Biomaterials

Polymers have been used for medical applications especially for implants for approximately 80 years. Polymethacrylate (PMMA) was the first polymer that was applied as biomaterial due to its stiffness, biocompatibility, and optical properties [153]. The evaluation of polymers was carried out from being stable to biodegradable with respect to both enzymatically and hydrolytically. The advantages of using polymer in different implant applications include ease of manufacture and can form complex shapes such as fiber, latex, film sheet at a reasonable cost and they can be applied easily. However, difficulties with sterilization and easy water absorption are some of the disadvantages associated with the use of polymers [160, 184].

The polymers are divided into two main groups, namely natural polymers and synthetic polymers, and both groups have very wide application areas in the biomedical fields. Table 4.2 summarizes the medical applications of the most widely used natural resorbable polymers and synthetic degradable polymers [185]. In addition, the application areas and systems are determined depending on their type and properties [186].

Natural polymers are usually derived from natural sources such as collagen and are generally used in medical and implant applications because of their high flexibility and biocompatibility. The main reason for their biocompatibility is that bone consists of type 1 collagen. In addition to type 1 collagen, the bone contains fundamental substances which are proteoglycans and glycoproteins. The natural polymers support hard and soft human tissues such as muscles, cartilage, and bones; and are biocompatible with the biological environment and cause less inflammatory response. However, they have very poor mechanical properties and a high degradation rate [160, 187].

Synthetic polymers have been utilized in polymeric drug delivery systems, tissue engineering, as well as in dentistry and orthopedics as medical implants and prosthetic devices. A wide range of synthetic polymers have been investigated and developed for biomedical application with emphasis in improving the mechanical properties, promoting osseointegration, and being able to control the rate of degradation. The advantages of biodegradable synthetic polymers are numerous, and these include the capacity of having their shelf-life extended, reduction in inflammatory and toxic effects in implantable devices, improved mechanical properties and processability, reduction in cost, matching the degradation of the polymer with the healing time, and avoiding a second surgical operation to retrieve non-biodegradable implants [160, 165, 187, 188]. The production temperature and strain rate during functional applications are highly important to the mechanical properties of the polymers. On the other hand, the deformation of polymers depends on several parameters such as crystallinity, molecular weight, backbone chemistry and cross-linking [153].

Table 4.2 Various medical applications and devices according to the type of polymers and their performance [185]

Polymer types	Current biomedical applications
Synthetic degradable polyesters	
Poly(glycolic acid)(PGA), Poly(lactic acid)(PLA) and copolymers	Drug delivery, hormone delivery, barrier membranes, guided tissue regeneration, dental, orthopedic applications, stents, stables, sutures, tissue engineering
Poly(hydroxybutyrate)(PHB), Poly(hydroxyvalerate)(PHV), and copolymers	Long-term drug delivery, orthopedic applications stents, artificial skin, surgical patching materials for congenital heart defects
Polycaprolactone (PCL)	Long-term drug delivery, implantable contraceptive drug devices, orthopedic applications, staples, stents
Natural resorbable polymers	
Collagen	Drug delivery, gene delivery, artificial skin, coatings to improve cellular adhesion, tissue regeneration in dental applications, orthopedic applications, tissue engineering, wound closure, scaffold for reconstruction of blood vessels, hemostatic agents
Fibrinogen and Fibrin	Tissue sealant. Cell delivery
Elastin-like peptides (ELP)	Drug delivery, coating of vascular grafts
Gelatin	Capsule coating for oral drug delivery
Hyaluronic acid	Would dressing applications, drug delivery, tissue engineering, synthetic bone graft, synovial fluid substitutes
Polysaccharides: chitosan, alginate	Drug-vaccine delivery, encapsulation of cells, sutures, wound dressing, wound healing
Other synthetic degradable polymers	
Polyanhydrides	Drug delivery
Polycyanoacrylates	Adhesives, drug delivery
Poly(amino acid)s and “pseudo”poly(amino acid)s	Drug delivery, tissue engineering, orthopedic applications, stents, anti-adhesion barriers
Poly(ortho ester)(POE)	Drug delivery and stents
Polyphosphazenes	Blood contacting devices, drug delivery, skeletal construction, vaccine adjuvants
Poly(propylene fumarate)(PPF)	Orthopedic applications

The new application areas for synthetic biodegradable polymers which are currently being investigated in the biomedical areas include drug delivery systems and in the design of new generation implantable devices. The determination of appropriate biodegradable polymers for the desired biomedical applications depends on factors

such as the degree of biodegradability, biocompatibility, surface properties and functionality of the final product. Additionally, the properties of the drug encapsulated, and the drug-releasing profile of the system is also important [188].

Polyglycolide (PGA) is the first biodegradable polymer that has been employed for biomedical applications. The glass transition temperature of PGA is between 35 to 40 °C and the melting temperature is around 225–230 °C. PGA has very acceptable and applicable mechanical properties for biomedical applications due to its high crystallinity (approximately 45–55%). However, its degradation rate is very high, and its solubility in various solvents is very low. PGA loses its strength after 1–2 months while the major mass loss occurs after 6–12 months. In an effort to overcome these disadvantages, copolymers such as PGLA (PLA-PGA copolymer) have been proposed and investigated [169, 184, 186].

In comparison to other copolymers, the degradation rate of Poly(ε-caprolactone) (PCL) is improved through the adjustments of the monomer to final copolymer ratio. It has been reported that its application areas include the drug delivery systems, tissue engineering, and in the design of new generation implants [184]. Some of PCLs most important properties include solvent solubility, great permeability for drugs, and non-toxicity. Additionally, it has low tensile strength (around 23 MPa), a low melting point (between 55 and 60 °C), and a glass transition temperature of −54 °C. As a result of these properties, miscible blends of PCL with various types of polymers can be easily produced. The combination of PCL and human tissues promoted good cell adhesion and mechanical properties even though it has poor wettability [184, 186].

Polylactides (PLA) is the first polyester that is applied in tissue engineering and the most important reasons behind its application are its biodegradability, cost, and ease of manufacturing. The glass transition temperature of PLA is between 60 and 65 °C, while its melting temperature is between 173 and 178 °C. The degradation rate of PLA is less than that of PGA [184, 186, 189]. This allows PLA to be easily mixed with drugs and applied as a slow drug delivery vehicle. It can also be used as a long-term implantable device and as a coating for dental and orthopedic applications. Furthermore, this biodegradable polymer has three stereoisomers that are poly (L-lactic acid) (PLLA), poly (D-lactic acid) (PDLA), and poly (D, L-lactic acid) (PDLLA). The ratio of D and L isomers in PDLLA allows the control of the rate of degradation of the polymer [186, 189]. This adjustable degradation rate is the key feature in biodegradable polymers when used for various biomedical applications such as drug delivery, implant coating systems, and degradable surgery sutures [190].

PLA synthetic biodegradable polymer has been approved by FDA due to its excellent tensile strength, biodegradable characteristics, biocompatibility, and suitable degradation rate. Currently, it has also been used by many biomedical companies as wound dressing and surgical sutures [191]. Additionally, the utilization of PLA for different applications on tissue engineering and local drug delivery systems has been significantly increased with the combination of different types of pharmaceuticals or minerals [190–192].

4.5 Biomedical and Clinical Applications of Stem Cells

Regenerative medicine, cell-based therapy and tissue engineering are the main therapeutic application areas for the stem cells. If the stem cells are transplanted in vivo into a patient or if they are combined with various implantable biomaterials, they maintain the biological functions to generate specific ex vivo tissue [193]. Preclinical studies examining the use of MSCs are numerous, the recent review by Badyra et al. systematically examines the usefulness and application of MSCs through various administration routes for the treatment of neurological disorders [194]. Describing MSCs as the perfect tool cellular therapies for pathological processes in the nervous system driven by excessive inflammation and neurodegeneration. While there are hundreds of stem cell and biomaterial studies being conducted with an ever-growing list of clinical trials testing the application of each in isolation for a host of afflictions. There is still no known approved clinical application available for a stem cell-biomaterial combination for any treatment. An interventional cellular therapy that can limit disease progression by modulating local tissue trauma environment, increase function and repair is needed. Currently, there are only 3 approved uses of allogenic mesenchymal stem cell derived from bone that are approved for use in the case of leukemia, Holoclar (Europe) and Prochymal (Canada). However, the use of the safer autologous MSCs worldwide and in Australia has not been approved for any therapeutic uses or applications.

4.5.1 Current Applications and Clinical Trials

Clinical applications of allogenic stem cells are still few and far between. However, the autologous stem cells have been readily and widely used in skin grafts in conjunction with biomaterials loaded with specific molecules and drugs to assist in the promotion of skin regeneration which is particularly useful in burn patients. While the current numbers of registered stem cell clinical trials are well over 1100 worldwide. This includes research into various biomaterials derived scaffolds with stem cells have been investigated as an alternative therapeutic strategy to improve bone repair and to inhibit implant failures in the treatment of bone fractures and bone-related diseases [195].

The most common implant and prosthesis material are metallic-based materials, particularly titanium and titanium alloys such as Ti-6Al-4V for orthopedic and dentistry implants. The key point of these materials is their bioinert property, meaning no chemical interactions or bonding with bone tissue. Therefore, in order to improve their longevity, the surface of bioinert metallic-based implants has been modified with chemical composition, surface properties and topographical structures.

Implant surface modifications directly improve the stem cell adhesion, proliferation and differentiation. Therefore, bioactivity, osseointegration, and better implant-bone adaptability can be increased by combining stem cells with the implantable biomaterials [196, 197].

4.6 Concluding Remarks

There is a sizeable potential for clinical application of stem cells and biomaterials to be used in conjunction with the next generation of personalized medicine using autologous or allogenic cells and customizable materials for a wide array of applications. The current research and on-going clinical trials have shown promise with negligible side effects or serious adverse reactions. There is however a long road ahead for the above research to become routine clinical application. The promising aspect is the ever-increasing number of trials and growing network of researchers, scientists, medical practitioners, hospitals and larger biotechnology companies linking to drive the development forward gives hope to many.

References

1. Mason C, Dunnill P (2008) A brief definition of regenerative medicine. Regen Med 3:1–5
2. Vallée M, Côté JF, Fradette J (2009) Adipose-tissue engineering: taking advantage of the properties of human adipose-derived stem/stromal cells. Pathol Biol 57:309–317
3. Noël D, Caton D, Roche S et al (2008) Cell specific differences between human adipose-derived and mesenchymal-stromal cells despite similar differentiation potentials. Exp Cell Res 314:1575–1584
4. Pisu M, Concas A, Cao G (2007) A novel simulation model for stem cells differentiation. J Biotechnol 130:171–182
5. Gomillion CT, Burg KJ (2006) Stem cells and adipose tissue engineering. Biomaterials 27:6052–6063
6. Bonilla S, Silva A, Valdés L et al (2005) Functional neural stem cells derived from adult bone marrow. Neuroscience 133:85–95
7. Cancedda R, Dozin B, Giannoni P et al (2003) Tissue engineering and cell therapy of cartilage and bone. Matrix Biol 22:81–91
8. Jiang Y, Jahagirdar BN, Reinhardt RL et al (2002) Pluripotency of mesenchymal stem cells derived from adult marrow. Nature 418:41–49
9. Majumdar MK, Wang E, Morris EA (2001) BMP-2 and BMP-9 promotes chondrogenic differentiation of human multipotential mesenchymal cells and overcomes the inhibitory effect of IL-1. J Cell Physiol 189:275–284
10. Reya T, Morrison SJ, Clarke MF et al (2001) Stem cells, cancer, and cancer stem cells. Nature 414:105–111
11. Devine SM, Hoffman R (2000) Role of mesenchymal stem cells in hematopoietic stem cell transplantation. Curr Opin Hematol 7:358–363
12. Furth ME, Atala A, Van Dyke ME (2007) Smart biomaterials design for tissue engineering and regenerative medicine. Biomaterials 28:5068–5073
13. Casteilla L, Dani C (2006) Adipose tissue-derived cells: from physiology to regenerative medicine. Diabetes Metab 32:393–401

14. Jagur-Grodzinski J (2006) Polymers for tissue engineering, medical devices, and regenerative medicine. Concise general review of recent studies. Polym Adv Technol 17:395–418
15. Thomas V, Dean DR, Vohra YK (2006) Nanostructured biomaterials for regenerative medicine. Curr Nanosci 2:155–177
16. Lutolf MP, Hubbell JA (2005) Synthetic biomaterials as instructive extracellular microenvironments for morphogenesis in tissue engineering. Nat Biotechnol 23:47–55
17. de Wert G, Mummery C (2003) Human embryonic stem cells: research, ethics and policy. Hum Reprod 18:672–682
18. Frontini-López YR, Gojanovich AD, Masone D et al (2018) Adipose-derived mesenchymal stem/stromal cells: from the lab bench to the basic concepts for clinical translation. Biocell 42:67–78
19. Evans MJ, Kaufman MH (1981) Establishment in culture of pluripotential cells from mouse embryos. Nature 292:154–156
20. Spradling A, Drummond-Barbosa D, Kai T (2001) Stem cells find their niche. Nature 414:98–104
21. Pera MF, Reubinoff B, Trounson A (2000) Human embryonic stem cells. J Cell Sci 113:5–10
22. Bodnar AG, Ouellette M, Frolkis M et al (1998) Extension of life-span by introduction of telomerase into normal human cells. Science 279:349–352
23. Thomson JA, Itskovitz-Eldor J, Shapiro SS et al (1998) Embryonic stem cell lines derived from human blastocysts. Science 282:1145–1147
24. Gogarty B, Nicol D, Chalmers D (2002) Regulating biomedical advances: embryonic stem cell research. Macquarie Law J 2:31–59
25. Okita K, Ichisaka T, Yamanaka S (2007) Generation of germline-competent induced pluripotent stem cells. Nature 448:313–317
26. Takahashi K, Yamanaka S (2006) Induction of pluripotent stem cells from mouse embryonic and adult fibroblast cultures by defined factors. Cell 126:663–676
27. Hockemeyer D, Jaenisch R (2016) Induced pluripotent stem cells meet genome editing. Cell Stem Cell 18:573–586
28. Friedenstein AJ, Chailakhjan RK, Lalykina KS (1970) The development of fibroblast colonies in monolayer cultures of guinea-pig bone marrow and spleen cells. Cell Tissue Kinet 3:393–403
29. Phinney DG, Prockop DJ (2007) Concise review: mesenchymal stem/multipotent stromal cells: the state of transdifferentiation and modes of tissue repair—current views. Stem Cells 25:2896–2902
30. Kargozar S, Mozafari M, Hamzehlou S et al (2019) Bone tissue engineering using human cells: a comprehensive review on recent trends, current prospects, and recommendations. Appl Sci 9:174
31. Tsuji W, Rubin JP, Marra KG (2014) Adipose-derived stem cells: Implications in tissue regeneration. World J Stem Cells 6:312–321
32. Feisst V, Meidinger S, Locke MB (2015) From bench to bedside: use of human adipose-derived stem cells. Stem Cells Cloning 8:149–162
33. Argentati C, Morena F, Montanucci P et al (2018) Surface hydrophilicity of poly(l-lactide) acid polymer film changes the human adult adipose stem cell architecture. Polymers 10:140
34. Romagnoli C, Zonefrati R, Galli G et al (2015) *In vitro* behavior of human adipose tissue-derived stem cells on poly(ε-caprolactone) film for bone tissue engineering applications. Biomed Res Int 2015:323571
35. Haimi S, Suuriniemi N, Haaparanta AM et al (2009) Growth and osteogenic differentiation of adipose stem cells on PLA/bioactive glass and PLA/beta-TCP scaffolds. Tissue Eng Part A 15:1473–1480
36. Frese L, Dijkman PE, Hoerstrup SP (2016) Adipose tissue-derived stem cells in regenerative medicine. Transfus Med Hemother 43:268–274
37. Ullah I, Subbarao RB, Rho GJ (2015) Human mesenchymal stem cells—current trends and future prospective. Biosci Rep 35:e00191

38. Bunnell BA, Flaat M, Gagliardi C et al (2008) Adipose-derived stem cells: isolation, expansion and differentiation. Methods 45:115–120
39. Zhang HT, Liu ZL, Yao XQ et al (2012) Neural differentiation ability of mesenchymal stromal cells from bone marrow and adipose tissue: a comparative study. Cytotherapy 14:1203–1214
40. Technau A, Froelich K, Hagen R et al (2011) Adipose tissue-derived stem cells show both immunogenic and immunosuppressive properties after chondrogenic differentiation. Cytotherapy 13:310–317
41. Schilling T, Küffner R, Klein-Hitpass L et al (2008) Microarray analyses of transdifferentiated mesenchymal stem cells. J Cell Biochem 103:413–433
42. Schilling T, Nöth U, Klein-Hitpass L et al (2007) Plasticity in adipogenesis and osteogenesis of human mesenchymal stem cells. Mol Cell Endocrinol 271:1–17
43. Taléns-Visconti R, Bonora A, Jover R et al (2007) Human mesenchymal stem cells from adipose tissue: differentiation into hepatic lineage. Toxicol In Vitro 21:324–329
44. Tatard VM, D'Ippolito G, Diabira S et al (2007) Neurotrophin-directed differentiation of human adult marrow stromal cells to dopaminergic-like neurons. Bone 40:360–373
45. Zuk PA, Zhu M, Ashjian P et al (2002) Human adipose tissue is a source of multipotent stem cells. Mol Biol Cell 13:4279–4295
46. Woodbury D, Schwarz EJ, Prockop DJ et al (2000) Adult rat and human bone marrow stromal cells differentiate into neurons. J Neurosci Res 61:364–370
47. Bryder D, Rossi DJ, Weissman IL (2006) Hematopoietic stem cells: the paradigmatic tissue-specific stem cell. Am J Pathol 169:338–346
48. Hwang KC, Kim JY, Chang W et al (2008) Chemicals that modulate stem cell differentiation. Proc Natl Acad Sci U S A 105:7467–7471
49. Takahashi K, Tanabe K, Ohnuki M et al (2007) Induction of pluripotent stem cells from adult human fibroblasts by defined factors. Cell 131:861–872
50. Pittenger MF, Mackay AM, Beck SC et al (1999) Multilineage potential of adult human mesenchymal stem cells. Science 284:143–147
51. Cattaneo E, McKay R (1990) Proliferation and differentiation of neuronal stem cells regulated by nerve growth factor. Nature 347:762–765
52. Santos J (2013) A proteomic investigation of multi-lineage differentiated adult adipose-derived stem cells. Dissertation, Macquarie University
53. Mauney JR, Nguyen T, Gillen K et al (2007) Engineering adipose-like tissue *in vitro* and *in vivo* utilizing human bone marrow and adipose-derived mesenchymal stem cells with silk fibroin 3D scaffolds. Biomaterials 28:5280–5290
54. Cho SW, Kim I, Kim SH et al (2006) Enhancement of adipose tissue formation by implantation of adipogenic-differentiated preadipocytes. Biochem Biophys Res Commun 345:588–594
55. Hong L, Peptan IA, Colpan A et al (2006) Adipose tissue engineering by human adipose-derived stromal cells. Cells Tissues Organs 183:133–140
56. Parsons WJ, Ramkumar V, Stiles GL et al (1988) Isobutylmethylxanthine stimulates adenylate cyclase by blocking the inhibitory regulatory protein, Gi. Mol Pharmacol 34:37–41
57. van Calker D, Müller M, Hamprecht B (1979) Adenosine regulates via two different types of receptors, the accumulation of cyclic AMP in cultured brain cells. J Neurochem 33:999–1005
58. Petersen RK, Madsen L, Pedersen LM et al (2008) Cyclic AMP (cAMP)-mediated stimulation of adipocyte differentiation requires the synergistic action of Epac- and cAMP-dependent protein kinase-dependent processes. Mol Cell Biol 28:3804–3816
59. Darlington GJ, Ross SE, MacDougald OA (1998) The role of C/EBP genes in adipocyte differentiation. J Biol Chem 273:30057–30060
60. Chawla A, Schwarz EJ, Dimaculangan DD et al (1994) Peroxisome proliferator-activated receptor (PPAR) gamma: adipose-predominant expression and induction early in adipocyte differentiation. Endocrinology 135:798–800
61. Lehmann JM, Lenhard JM, Oliver BB et al (1997) Peroxisome proliferator-activated receptors alpha and gamma are activated by indomethacin and other non-steroidal anti-inflammatory drugs. J Biol Chem 272:3406–3410

62. Prawitt J, Niemeier A, Kassem M et al (2008) Characterization of lipid metabolism in insulin-sensitive adipocytes differentiated from immortalized human mesenchymal stem cells. Exp Cell Res 314:814–824
63. Strem BM, Hicok KC, Zhu M et al (2005) Multipotential differentiation of adipose tissue-derived stem cells. Keio J Med 54:132–141
64. Enomoto H, Furuichi T, Zanma A et al (2004) Runx2 deficiency in chondrocytes causes adipogenic changes *in vitro*. J Cell Sci 117:417–425
65. Dicker A, Le Blanc K, Aström G et al (2005) Functional studies of mesenchymal stem cells derived from adult human adipose tissue. Exp Cell Res 308:283–290
66. Rubin JP, Bennett JM, Doctor JS et al (2007) Collagenous microbeads as a scaffold for tissue engineering with adipose-derived stem cells. Plast Reconstr Surg 120:414–424
67. von Heimburg D, Zachariah S, Heschel I et al (2001) Human preadipocytes seeded on freeze-dried collagen scaffolds investigated *in vitro* and *in vivo*. Biomaterials 22:429–438
68. Woolf AD, Pfleger B (2003) Burden of major musculoskeletal conditions. Bull World Health Organ 81:646–656
69. Wagner W, Wein F, Seckinger A et al (2005) Comparative characteristics of mesenchymal stem cells from human bone marrow, adipose tissue, and umbilical cord blood. Exp Hematol 33:1402–1416
70. Muschler GF, Nitto H, Boehm CA et al (2001) Age- and gender-related changes in the cellularity of human bone marrow and the prevalence of osteoblastic progenitors. J Orthop Res 19:117–125
71. Liu Y, Zhou Y, Feng H et al (2008) Injectable tissue-engineered bone composed of human adipose-derived stromal cells and platelet-rich plasma. Biomaterials 29:3338–3345
72. Flynn L, Prestwich GD, Semple JL et al (2007) Adipose tissue engineering with naturally derived scaffolds and adipose-derived stem cells. Biomaterials 28:3834–3842
73. Jing W, Xiong Z, Cai X et al (2010) Effects of gamma-secretase inhibition on the proliferation and vitamin D(3) induced osteogenesis in adipose derived stem cells. Biochem Biophys Res Commun 392:442–447
74. Liu G, Zhou H, Li Y et al (2008) Evaluation of the viability and osteogenic differentiation of cryopreserved human adipose-derived stem cells. Cryobiology 57:18–24
75. Im GI, Shin YW, Lee KB (2005) Do adipose tissue-derived mesenchymal stem cells have the same osteogenic and chondrogenic potential as bone marrow-derived cells? Osteoarthritis Cartilage 13:845–853
76. Matsubara H, Hogan DE, Morgan EF et al (2012) Vascular tissues are a primary source of BMP2 expression during bone formation induced by distraction osteogenesis. Bone 51:168–180
77. Dragoo JL, Choi JY, Lieberman JR et al (2003) Bone induction by BMP-2 transduced stem cells derived from human fat. J Orthop Res 21:622–629
78. Kramer J, Hegert C, Guan K et al (2000) Embryonic stem cell-derived chondrogenic differentiation *in vitro*: activation by BMP-2 and BMP-4. Mech Dev 92:193–205
79. Bell TD, Demay MB, Burnett-Bowie SA (2010) The biology and pathology of vitamin D control in bone. J Cell Biochem 111:7–13
80. Phillips JE, Gersbach CA, Wojtowicz AM et al (2006) Glucocorticoid-induced osteogenesis is negatively regulated by Runx2/Cbfa1 serine phosphorylation. J Cell Sci 119:581–591
81. Hidalgo AA, Trump DL, Johnson CS (2010) Glucocorticoid regulation of the vitamin D receptor. J Steroid Biochem Mol Biol 121:372–375
82. Suh JH, Lee HW, Lee JW et al (2008) Hes1 stimulates transcriptional activity of Runx2 by increasing protein stabilization during osteoblast differentiation. Biochem Biophys Res Commun 367:97–102
83. Nakashima K, de Crombrugghe B (2003) Transcriptional mechanisms in osteoblast differentiation and bone formation. Trends Genet 19:458–466
84. Ducy P (2000) Cbfa1: a molecular switch in osteoblast biology. Dev Dyn 219:461–471
85. Coelho MJ, Fernandes MH (2000) Human bone cell cultures in biocompatibility testing. Part II: effect of ascorbic acid, beta-glycerophosphate and dexamethasone on osteoblastic differentiation. Biomaterials 21:1095–1102

86. Park JB (2012) The effects of dexamethasone, ascorbic acid, and β-glycerophosphate on osteoblastic differentiation by regulating estrogen receptor and osteopontin expression. J Surg Res 173:99–104
87. Franceschi RT, Iyer BS, Cui Y (1994) Effects of ascorbic acid on collagen matrix formation and osteoblast differentiation in murine MC3T3-E1 cells. J Bone Miner Res 9:843–854
88. Fratzl-Zelman N, Fratzl P, Hörandner H et al (1998) Matrix mineralization in MC3T3-E1 cell cultures initiated by beta-glycerophosphate pulse. Bone 23:511–520
89. Chung CH, Golub EE, Forbes E et al (1992) Mechanism of action of beta-glycerophosphate on bone cell mineralization. Calcif Tissue Int 51:305–311
90. Heng BC, Cao T, Lee EH (2004) Directing stem cell differentiation into the chondrogenic lineage in vitro. Stem Cells 22:1152–1167
91. Hardingham T, Tew S, Murdoch A (2002) Tissue engineering: chondrocytes and cartilage. Arthritis Res 4(Suppl 3):S63–S68
92. Koga H, Engebretsen L, Brinchmann JE et al (2009) Mesenchymal stem cell-based therapy for cartilage repair: a review. Knee Surg Sports Traumatol Arthrosc 17:1289–1297
93. Bartlett W, Skinner JA, Gooding CR et al (2005) Autologous chondrocyte implantation versus matrix-induced autologous chondrocyte implantation for osteochondral defects of the knee: a prospective, randomised study. J Bone Joint Surg Br 87:640–645
94. Peterson L, Brittberg M, Kiviranta I et al (2002) Autologous chondrocyte transplantation. Biomechanics and long-term durability. Am J Sports Med 30:2–12
95. Brittberg M, Lindahl A, Nilsson A et al (1994) Treatment of deep cartilage defects in the knee with autologous chondrocyte transplantation. N Engl J Med 331:889–895
96. Csaki C, Schneider PR, Shakibaei M (2008) Mesenchymal stem cells as a potential pool for cartilage tissue engineering. Ann Anat 190:395–412
97. Lee SH, Shin H (2007) Matrices and scaffolds for delivery of bioactive molecules in bone and cartilage tissue engineering. Adv Drug Deliv Rev 59:339–359
98. Ponticiello MS, Schinagl RM, Kadiyala S et al (2000) Gelatin-based resorbable sponge as a carrier matrix for human mesenchymal stem cells in cartilage regeneration therapy. J Biomed Mater Res 52:246–255
99. Wu SC, Chang JK, Wang CK et al (2010) Enhancement of chondrogenesis of human adipose derived stem cells in a hyaluronan-enriched microenvironment. Biomaterials 31:631–640
100. Hui TY, Cheung KM, Cheung WL et al (2008) *In vitro* chondrogenic differentiation of human mesenchymal stem cells in collagen microspheres: influence of cell seeding density and collagen concentration. Biomaterials 29:3201–3212
101. Betre H, Ong SR, Guilak F et al (2006) Chondrocytic differentiation of human adipose-derived adult stem cells in elastin-like polypeptide. Biomaterials 27:91–99
102. Li WJ, Tuli R, Okafor C et al (2005) A three-dimensional nanofibrous scaffold for cartilage tissue engineering using human mesenchymal stem cells. Biomaterials 26:599–609
103. Liu X, Sun H, Yan D et al (2010) *In vivo* ectopic chondrogenesis of BMSCs directed by mature chondrocytes. Biomaterials 31:9406–9414
104. Her GJ, Wu HC, Chen MH et al (2013) Control of three-dimensional substrate stiffness to manipulate mesenchymal stem cell fate toward neuronal or glial lineages. Acta Biomater 9:5170–5180
105. Nii M, Lai JH, Keeney M et al (2013) The effects of interactive mechanical and biochemical niche signaling on osteogenic differentiation of adipose-derived stem cells using combinatorial hydrogels. Acta Biomater 9:5475–5483
106. Banka S, Mukudai Y, Yoshihama Y et al (2012) A combination of chemical and mechanical stimuli enhances not only osteo- but also chondro-differentiation in adipose-derived stem cells. J Oral Biosci 54:188–195
107. Morgan EF, Hussein AI, Al-Awadhi BA et al (2012) Vascular development during distraction osteogenesis proceeds by sequential intramuscular arteriogenesis followed by intraosteal angiogenesis. Bone 51:535–545
108. Wang L, Wang ZH, Shen CY et al (2010) Differentiation of human bone marrow mesenchymal stem cells grown in terpolyesters of 3-hydroxyalkanoates scaffolds into nerve cells. Biomaterials 31:1691–1698

109. Wong M, Tuan RS (1993) Nuserum, a synthetic serum replacement, supports chondrogenesis of embryonic chick limb bud mesenchymal cells in micromass culture. In Vitro Cell Dev Biol Anim 29A:917–922
110. Shih DT, Chen JC, Chen WY et al (2011) Expansion of adipose tissue mesenchymal stromal progenitors in serum-free medium supplemented with virally inactivated allogeneic human platelet lysate. Transfusion 51:770–778
111. Chin AC, Padmanabhan J, Oh SK et al (2010) Defined and serum-free media support undifferentiated human embryonic stem cell growth. Stem Cells Dev 19:753–761
112. Mendelson A, Frank E, Allred C et al (2011) Chondrogenesis by chemotactic homing of synovium, bone marrow, and adipose stem cells *in vitro*. FASEB J 25:3496–3504
113. Kawamura M, Urist MR (1988) Growth factors, mitogens, cytokines, and bone morphogenetic protein in induced chondrogenesis in tissue culture. Dev Biol 130:435–442
114. Ng F, Boucher S, Koh S et al (2008) PDGF, TGF-beta, and FGF signaling is important for differentiation and growth of mesenchymal stem cells (MSCs): transcriptional profiling can identify markers and signaling pathways important in differentiation of MSCs into adipogenic, chondrogenic, and osteogenic lineages. Blood 112:295–307
115. Sekiya I, Vuoristo JT, Larson BL et al (2002) *In vitro* cartilage formation by human adult stem cells from bone marrow stroma defines the sequence of cellular and molecular events during chondrogenesis. Proc Natl Acad Sci U S A 99:4397–4402
116. De Luca F, Barnes KM, Uyeda JA et al (2001) Regulation of growth plate chondrogenesis by bone morphogenetic protein-2. Endocrinology 142:430–436
117. Hunziker EB, Driesang IM, Morris EA (2001) Chondrogenesis in cartilage repair is induced by members of the transforming growth factor-beta superfamily. Clin Orthop Relat Res. https://doi.org/10.1097/00003086-200110001-00017
118. Derynck R, Zhang YE (2003) Smad-dependent and Smad-independent pathways in TGF-beta family signalling. Nature 425:577–584
119. Grönroos E, Hellman U, Heldin CH et al (2002) Control of Smad7 stability by competition between acetylation and ubiquitination. Mol Cell 10:483–493
120. Liu D, Black BL, Derynck R (2001) TGF-beta inhibits muscle differentiation through functional repression of myogenic transcription factors by Smad3. Genes Dev 15:2950–2966
121. Chubinskaya S, Hurtig M, Rueger DC (2007) OP-1/BMP-7 in cartilage repair. Int Orthop 31:773–781
122. Pang EK, Im SU, Kim CS et al (2004) Effect of recombinant human bone morphogenetic protein-4 dose on bone formation in a rat calvarial defect model. J Periodontol 75:1364–1370
123. Hanada K, Solchaga LA, Caplan AI et al (2001) BMP-2 induction and TGF-beta 1 modulation of rat periosteal cell chondrogenesis. J Cell Biochem 81:284–294
124. Sakaguchi Y, Sekiya I, Yagishita K et al (2005) Comparison of human stem cells derived from various mesenchymal tissues: superiority of synovium as a cell source. Arthritis Rheum 52:2521–2529
125. Huang JI, Zuk PA, Jones NF et al (2004) Chondrogenic potential of multipotential cells from human adipose tissue. Plast Reconstr Surg 113:585–594
126. Nakayama N, Duryea D, Manoukian R et al (2003) Macroscopic cartilage formation with embryonic stem-cell-derived mesodermal progenitor cells. J Cell Sci 116:2015–2028
127. Pereira RC, Economides AN, Canalis E (2000) Bone morphogenetic proteins induce gremlin, a protein that limits their activity in osteoblasts. Endocrinology 141:4558–4563
128. Delcroix GJ, Schiller PC, Benoit JP et al (2010) Adult cell therapy for brain neuronal damages and the role of tissue engineering. Biomaterials 31:2105–2120
129. Kingham PJ, Kalbermatten DF, Mahay D et al (2007) Adipose-derived stem cells differentiate into a Schwann cell phenotype and promote neurite outgrowth *in vitro*. Exp Neurol 207:267–274
130. Ishii K, Katayama M, Hori K et al (1993) Effects of 2-mercaptoethanol on survival and differentiation of fetal mouse brain neurons cultured *in vitro*. Neurosci Lett 163:159–162
131. Santos J, Milthorpe BK, Herbert BR et al (2017) Proteomic analysis of human adipose derived stem cells during small molecule chemical stimulated pre-neuronal differentiation. Int J Stem Cells 10:193–217

132. Choi CB, Cho YK, Prakash KV et al (2006) Analysis of neuron-like differentiation of human bone marrow mesenchymal stem cells. Biochem Biophys Res Commun 350:138–146
133. Romero-Ramos M, Vourc'h P, Young HE et al (2002) Neuronal differentiation of stem cells isolated from adult muscle. J Neurosci Res 69:894–907
134. Safford KM, Hicok KC, Safford SD et al (2002) Neurogenic differentiation of murine and human adipose-derived stromal cells. Biochem Biophys Res Commun 294:371–379
135. Kim BJ, Seo JH, Bubien JK et al (2002) Differentiation of adult bone marrow stem cells into neuroprogenitor cells *in vitro*. NeuroReport 13:1185–1188
136. Fajardo J, Milthorpe BK, Santos J (2020) Molecular mechanisms involved in neural substructure development during phosphodiesterase inhibitor treatment of mesenchymal stem cells. Int J Mol Sci 21:4867
137. Santos J, Hubert T, Milthorpe BK (2020) Valproic acid promotes early neural differentiation in adult mesenchymal stem cells through protein signalling pathways. Cells 9:619
138. Santos J, Dolai S, O'Rourke MB et al (2020) Quantitative proteomic profiling of small molecule treated mesenchymal stem cells using chemical probes. Int J Mol Sci 22:160
139. di Summa PG, Kingham PJ, Raffoul W et al (2010) Adipose-derived stem cells enhance peripheral nerve regeneration. J Plast Reconstr Aesthet Surg 63:1544–1552
140. Ferraro F, Celso CL, Scadden D (2010) Adult stem cels and their niches. Adv Exp Med Biol 695:155–168
141. Abazova N, Krijgsveld J (2017) Advances in stem cell proteomics. Curr Opin Genet Dev 46:149–155
142. Hughes CS, Moggridge S, Müller T et al (2019) Single-pot, solid-phase-enhanced sample preparation for proteomics experiments. Nat Protoc 14:68–85
143. Baharvand H, Fathi A, van Hoof D et al (2007) Concise review: trends in stem cell proteomics. Stem Cells 25:1888–1903
144. Levchenko A (2005) Proteomics takes stem cell analyses to another level. Nat Biotechnol 23:828–830
145. van Hoof D, Krijgsveld J, Mummery C (2012) Proteomic analysis of stem cell differentiation and early development. Cold Spring Harb Perspect Biol 4:a008177
146. Humphrey SJ, Karayel O, James DE et al (2018) High-throughput and high-sensitivity phosphoproteomics with the EasyPhos platform. Nat Protoc 13:1897–1916
147. Unwin RD, Griffiths JR, Whetton AD (2010) Simultaneous analysis of relative protein expression levels across multiple samples using iTRAQ isobaric tags with 2D nano LC-MS/MS. Nat Protoc 5:1574–1582
148. Williamson AJ, Smith DL, Blinco D et al (2008) Quantitative proteomics analysis demonstrates post-transcriptional regulation of embryonic stem cell differentiation to hematopoiesis. Mol Cell Proteomics 7:459–472
149. Ong SE, Blagoev B, Kratchmarova I et al (2002) Stable isotope labeling by amino acids in cell culture, SILAC, as a simple and accurate approach to expression proteomics. Mol Cell Proteomics 1:376–386
150. Dayon L, Pasquarello C, Hoogland C et al (2010) Combining low- and high-energy tandem mass spectra for optimized peptide quantification with isobaric tags. J Proteomics 73:769–777
151. Thompson A, Schäfer J, Kuhn K et al (2003) Tandem mass tags: a novel quantification strategy for comparative analysis of complex protein mixtures by MS/MS. Anal Chem 75:1895–1904
152. Paulo Davim J (ed) (2013) Biomaterials and medical tribology, 1st edn. Woodhead Publishing series in biomaterials. Woodhead Publishing, Cambridge
153. Pruitt LA, Chakravartul AM (eds) (2011) Mechanics of biomaterials: fundamental principles for implant design. Cambridge University Press, Cambridge
154. Merolli A, Joyce T (eds) (2009) Biomaterials in hand surgery. Springer, Milan
155. Shah FA, Trobos M, Thomsen P et al (2016) Commercially pure titanium (cp-Ti) versus titanium alloy (Ti6Al4V) materials as bone anchored implants—is one truly better than the other? Mater Sci Eng C Mater Biol Appl 62:960–966
156. de Viteri VS, Fuentes E (2013) Titanium and titanium alloys as biomaterials. In: Gegner J (ed) Tribology—fundamentals and advancements. IntechOpen, London. https://doi.org/10.5772/55860

157. Bruni S, Martinesi M, Stio M et al (2005) Effects of surface treatment of Ti-6Al-4V titanium alloy on biocompatibility in cultured human umbilical vein endothelial cells. Acta Biomater 1:223–234
158. Singh R, Dahotre NB (2007) Corrosion degradation and prevention by surface modification of biometallic materials. J Mater Sci Mater Med 18:725–751
159. Rath PC, Besra L, Singh BP et al (2012) Titania/hydroxyapatite bi-layer coating on Ti metal by electrophoretic deposition: characterization and corrosion studies. Ceram Int 38:3209–3216
160. Paital SR, Dahotre NB (2009) Calcium phosphate coatings for bio-implant applications: materials, performance factors, and methodologies. Mater Sci Eng R Rep 66:1–70
161. Choi AH, Ben-Nissan B (2017) Calcium phosphate nanocomposites for biomedical and dental applications: recent developments. In: Thakur VK, Thakur MK, Kessler MR (eds) Handbook of composites from renewable materials. Wiley, New Jersey, pp 423–450
162. Choi AH, Ben-Nissan B, Bendavid A (2017) Thin films and nanocoatings of hydroxyapatite on titanium implants: production methods and adhesion testing. Lambert Academic Publishing, Germany
163. Choi AH, Cazalbou S, Ben-Nissan B (2015) Nanobiomaterial coatings in dentistry. In: Deb S (ed) Biomaterials for oral and craniomaxillofacial applications, frontiers of oral biology, vol 17. Karger, Basel, pp 49–61
164. Baino F, Novajra G, Vitale-Brovarone C (2015) Bioceramics and scaffolds: a winning combination for tissue engineering. Front Bioeng Biotechnol 3:202
165. Planell JA (ed) (2009) Bone repair biomaterials. Woodhead Publishing, Cambridge
166. Heness GL, Ben-Nissan B (2004) Innovative bioceramics. Mater Forum 27:104–114
167. Hench LL, Polak JM (2002) Third-generation biomedical materials. Science 295:1014–1017
168. Hench LL (1998) Bioceramics. J Am Ceram Soc 81:1705–1728
169. Mahyudin F, Widhiyanto L, Hermawan H (2016) Biomaterials in orthopaedics. In: Mahyudin F, Hermawan H (eds) Biomaterials and medical devices. Advanced structured materials, vol 58. Springer, Cham, pp 161–181
170. Guillemot F (2005) Recent advances in the design of titanium alloys for orthopedic applications. Expert Rev Med Dev 2:741–748
171. Hench LL (1980) Biomaterials. Science 208:826–831
172. Macha IJ, Charvillat C, Cazalbou S et al (2016) Comparative study of coral conversion, part 3: intermediate products in the first half an hour. J Aust Ceram Soc 52:177–182
173. Gunduz O, Sahin YM, Agathopoulos S et al (2014) A new method for fabrication of nanohydroxyapatite and TCP from the sea snail Cerithium vulgatum. J Nanomaterials. https://doi.org/10.1155/2014/382861
174. Ben-Nissan B, Pezzotti G (2003) Bioceramics processing routes and mechanical evaluation. J Ceram Soc Jpn 110:601–608
175. Hench LL, Jones JR (eds) (2005) Biomaterials, artificial organs and tissue engineering. Woodhead Publishing, Cambridge
176. Franklin-Ford TW, Suarez-Gonzalez D, Lee JS et al (2013) Biomimetic hydroxyapatite materials for therapeutic delivery. In: Zhang S (ed) Hydroxyapatite coatings for biomedical applications. CRC Press, Boca Raton, pp 201–238
177. Roest R, Latella BA, Heness G et al (2011) Adhesion of sol-gel derived hydroxyapatite nanocoatings on anodised pure titanium and titanium (Ti6Al4V) alloy substrates. Surf Coat Technol 205:3520–3529
178. Zreiqat H, Valenzuela SM, Ben-Nissan B et al (2005) The effect of surface chemistry modification of titanium alloy on signalling pathways in human osteoblasts. Biomaterials 26:7579–7586
179. Karacan I, Ben-Nissan B, Sinutok S (2019) Marine-based calcium phosphates from hard coral and calcified algae for biomedical applications. In: Choi AH, Ben-Nissan B (eds) Marine-derived biomaterials for tissue engineering applications. Springer series in biomaterials science and engineering, vol 14. Springer, Singapore, pp 137–153
180. Macha IJ, Ozyegin LS, Oktar FN et al (2015) Conversion of ostrich eggshells (Struthio camelus) to calcium phosphates. J Aust Ceram Soc 51:125–133

181. Andrés-Vergés M, Fernández-González C, Martínez-Gallego M (1998) Hydrothermal synthesis of calcium deficient hydroxyapatites with controlled size and homogeneous morphology. J Eur Ceram Soc 18:1245–1250
182. Chou J, Hao J, Ben-Nissan B et al (2013) Coral exoskeletons as a precursor material for the development of a calcium phosphate drug delivery system for bone tissue engineering. Biol Pharm Bull 36:1662–1665
183. Mann S (1988) Molecular recognition in biomineralization. Nature 332:119–124
184. Wong JY, Bronzino JD, Peterson DR (eds) (2012) Biomaterials: principles and practices. CRC Press, Boca Raton
185. Ratner BD, Hoffman AS, Schoen FJ et al (eds) (2013) Biomaterials science, 3rd edn. Academic Press, Massachusetts
186. Nair LS, Laurencin CT (2007) Biodegradable polymers as biomaterials. Prog Polym Sci 32:762–798
187. Thavornyutikarn B, Chantarapanich N, Sitthiseripratip K et al (2014) Bone tissue engineering scaffolding: computer-aided scaffolding techniques. Prog Biomater 3:61–102
188. Naahidi S, Jafari M, Edalat F et al (2013) Biocompatibility of engineered nanoparticles for drug delivery. J Control Release 166:182–194
189. Rezwan K, Chen QZ, Blaker JJ et al (2006) Biodegradable and bioactive porous polymer/inorganic composite scaffolds for bone tissue engineering. Biomaterials 27:3413–3431
190. Narayanan G, Vernekar VN, Kuyinu EL et al (2016) Poly (lactic acid)-based biomaterials for orthopaedic regenerative engineering. Adv Drug Deliv Rev 107:247–276
191. Ferrández-Montero A, Lieblich M, González-Carrasco JL et al (2019) Development of biocompatible and fully bioabsorbable PLA/Mg films for tissue regeneration applications. Acta Biomater 98:114–124
192. Armentano I, Gigli M, Morena F et al (2018) Recent advances in nanocomposites based on aliphatic polyesters: design, synthesis, and applications in regenerative medicine. Appl Sci 8:1452
193. Argentati C, Morena F, Bazzucchi M et al (2018) Adipose stem cell translational applications: from bench-to-bedside. Int J Mol Sci 19:3475
194. Badyra B, Sułkowski M, Milczarek O et al (2020) Mesenchymal stem cells as a multimodal treatment for nervous system diseases. Stem Cells Transl Med 9:1174–1189
195. Iaquinta MR, Mazzoni E, Bononi I et al (2019) Adult stem cells for bone regeneration and repair. Front Cell Dev Biol 7:268
196. Choi AH, Karacan I, Ben-Nissan B (2020) Surface modifications of titanium alloy using nanobioceramic-based coatings to improve osseointegration: a review. Mater Technol 35:742–751
197. Gao C, Peng S, Feng P et al (2017) Bone biomaterials and interactions with stem cells. Bone Res 5:17059

Ipek Karacan Dr. Karacan has a Ph.D. degree in School of Life Sciences at University of Technology Sydney (UTS) in biomedical science. Before her Ph.D. degree, she completed her bachelor‘s degree in Bioengineering with first honour from Marmara University, Turkey, and currently she is a research assistant at UTS. She is a member of Advanced Tissue Regeneration & Drug Delivery Group and Translational Biomaterials and Medicine Group. Her research focuses on the antibacterial slow drug delivery coating systems for the inhibition of implant and surgery related infections. She has worked on biomaterials, biodegradable polymeric thin film coating on bone implants, marine structures for biomedical applications, and the stem

cell development and differentiation in vitro applications, and proteomics. Her recent research focuses on cell engineering and the intracellular delivery techniques for the stem cell therapy applications.

Bruce Milthorpe Professor Milthorpe was Dean of Science at UTS from November 2008 to August 2016.. Previously he was professor in the Graduate School of Biomedical Engineering, University of New South Wales. From February 2006 to August 2007, he was the Deputy President (Academic) of UNSW Asia. Prior to his time with UNSW Asia, he was Head of School of the Graduate School of Biomedical Engineering, UNSW, from 1998 until March 2006. In 2004 he was elected Fellow Biomaterials Science and Engineering and in 2014 he was elected a Fellow of the Royal Society New South Wales. He is also a Graduate of the Australian Institute of Company Directors.

He has a background as a biochemist and biomaterials scientist with 20 years' experience in biomaterials development and assessment, as well as interests in tissue engineering and cytometry. His research experience is in biomaterials, orthopaedic graft materials for reconstruction, hydroxyapatite ceramic composites, biomaterial interactions with bone, quantitative cytometry, polymer material interactions with proteins, and the use of cell culture and in vivo models for assessment of cellular and tissue interactions with materials. Recently he has been involved in developing an adult stem cell models for neuronal, bone and cartilage tissue engineering. Professor Milthorpe has been an advisor to the Therapeutic Devices Evaluation Committee and the Therapeutic Goods Committee.

He is Chair of Culture at Work and a director of the Sydney Institute for Marine Science. He has been a member of the international editorial board of Biomaterials, and is now on the editorial board of two new journals in the field, as well as having served as an executive member of several research societies. He has published over 100 refereed journal articles and more than 120 conference presentations. Since 2000 he has been a chief investigator on biomedical research projects and grants with total funding in excess of $2.7 million. He has been named on three patents in the area of medical devices.

Besim Ben-Nissan Professor Ben-Nissan has higher degrees in Metallurgical Engineering (ITU), Ceranic Engineering (University of New South Wales) and a Ph.D. in Mechanical and Industrial Engineering with Biomedical Engineering (University of New South Wales). Over the last four decades together with a large numbers of Ph.D. students and post-doctoral fellows he has worked on production and analysis of various biomedical materials, implants, calcium phosphate ceramics, advanced ceramics (aluminazirconia, silicon nitrides), sol–gel developed nanocoatings for enhanced bioactivity, corrosion and abrasion protections, optical and electronic ceramics and thermally insulating new generation composites.

He also has contributed to the areas of mechanical properties of sol–gel developed nanocoatings. In the biomedical field, he has involved with the development of materials for slow drug

delivery, natural and marine material conversion, implant technology (bioactive materials including conversion of Australian corals to hydroxyapatite bone grafts), biomimetics (learning from nature and its application to regenerative medicine), biocomposites, investigative research on biomechanics and Finite Element Analysis (mandible, knee, hip joints, hip resurfacing), reliability and implant design (modular ceramic knee prosthesis, femoral head stresses). He was part of a research team which initiated the world's first reliable ceramic knee and hydroxyapatite sol gel derived nanocoatings. Since 1990 he has published over 260 papers in journals, five books and over 50 book chapters. He is one of the editors of the Journal of the Australian Ceramic Society and Editorial Board member of three international biomaterials journals. He was awarded "The Australasian Ceramic Society Award" for his contribution to "Ceramic education and research and development in Australia." He also received "Future Materials Award" for his contribution to the "Advanced nanocoated materials field.". He has collaborated with a number of international groups in Japan, USA, Thailand, Finland, Israel, France, UK, Germany and Turkey and held grants from the Australian Academy of Science and the Japan Society for Promotion of Science for collaborative work in the biomedical field in Europe, USA and Japan respectively. After serving as an academic for over 33 years he has retired, however still active and contributes to science by research in the biomedical field and supervising higher degree students.

Jerran Santos Dr. Santos is a group leader of the Advanced Tissue Engineering and Stem Cell Biology Group at UTS and holds an Honorary Professorship at the University of Toulouse. He has been awarded the Stem Cell Futures Fellowship and has attracted over $2 million for research programs, has established several international collaborations and is an active consultant for the TGA as well as being a member of the Academy of Science. His research focus is in regenerative and precision medicine, utilizing stem cells and biomaterials in developing translational clinical applications. Focusing on systems biology approach, examining the shift in stem cells phenotype during the differentiation into the targeted cell types. The interactions and changes of various molecules, proteins, nutrients, metabolites, and RNA over time play an important role in the overall functionality and endpoint cell type. Understanding the underlying molecular mechanisms, pathways and their interactions has a significant role in downstream applications. His interests extend to utilizing stem cells and systems biology in developing models for degenerative diseases and biomarker discovery to expand the knowledge database by identifying key pathways in developing diseases. Current research projects involve diseases; Multiple Sclerosis, Allan-Herndon-Dudley Syndrome, Schizophrenia, Alzheimer's, Parkinson's, Motor Neurone Disease, ALS and Osteoarthritis. In the regenerative space projects involving neural, osteochondral, myogenic differentiation, adult mesenchymal stem cells,

induced pluripotent stem cells and biomaterial synthesis for 3D printing technology for materials and cellular components in 3D tissue printing. Dr. Santos has a broad spectrum of expertise in a variety of other areas, which include next generation genome sequencing, bacterial pathogenesis, secreted moonlighting proteins, cytokine and immuno-modulation, 3D molecular modelling and protein interaction network building.

Chapter 5
Antimicrobial Bioceramics for Biomedical Applications

Pietro Riccio, Mohadeseh Zare, Diana Gomes, David Green, and Artemis Stamboulis

Abstract Bioceramics are ideal for hard tissue repair because they are akin to the bone in mechanical and physical properties. The main application of bioceramics is in orthopedics. Orthopedic implants can fail prematurely, mainly due to bacterial colonization and ongoing biofilm formation on implant surfaces. Antimicrobial peptides (AMPs) are small bioactive proteins with unique physicochemical and structural properties, ubiquitous component of the innate immune system, where they play an essential role in modulating both innate and adaptive immune responses. The chapter reviews the fundamental concepts of the design and synthesis of AMPs to functionalize bioceramic coatings, scaffolds, composites and (nano)particles for short- and long-term antibacterial activity.

Keywords Antimicrobial peptides · AMPs · Surface functionalization · Bacterial infection · Coatings · Physical adsorption · Biofilm · Antibacterial · Proteins

5.1 Introduction

Classically used for hard tissue engineering, the first generation of ceramic materials presented acceptable mechanical properties, low cell toxicity, and high tolerance, but displayed limited biocompatibility, because they were biologically inert or commonly referred to as bioinert. Yet, on the surface, such ceramics display high wettability and low surface tension, a characteristic that allows for the rapid adhesion of biological substances, including proteins [1]. So, by selection of adequate compositions, bioceramics—ceramic materials capable of interacting with biological cells and molecules [2]—can be obtained. Today's bioceramics can be classified into three main types, according to their biological behavior, as shown in Table 5.1.

More than just fulfilling a support role, a successful biomaterial should also develop an appropriate initial integration with the host, as fast and complete as

P. Riccio · M. Zare · D. Gomes · D. Green · A. Stamboulis (✉)
Biomaterials Research Group, School of Metallurgy and Materials, College of Physical Science and Engineering, University of Birmingham, Edgbaston, Birmingham B15 2TT, UK
e-mail: A.Stamboulis@bham.ac.uk

A. H. Choi and B. Ben-Nissan (eds.), *Innovative Bioceramics in Translational Medicine I*,
Springer Series in Biomaterials Science and Engineering 17,
https://doi.org/10.1007/978-981-16-7435-8_5

Table 5.1 The three main types of bioceramics and the description of their important characteristics and applications. Mechanical parameters compared to cortical bone [3]

Types of bioceramics	Examples	Applications	Mechanical parameters
Bioinert: No interaction with the surrounding environment [2, 4]	Al_2O_3, ZrO_2	Bone implants and replacements	• High tensile strength • Very high compressive strength • High fracture toughness
Bioresorbable: Actively participate in metabolic processes [2, 5]	Calcium phosphate	Bone graft, Tissue replacement, Drug delivery, Periodontal regeneration	• Very low tensile strength • Very high compressive strength • Very low fracture toughness
Bioactive: Form direct chemical bonds with surrounding tissue (bone, soft tissue) [2, 4–6]	Hydroxyapatite, Bioactive glass	Coating, Bone grafts, Bone defect fillers, Soft tissue regeneration scaffolds	• Very low tensile strength • Very high compressive strength • Very low fracture toughness

possible, and sustain it for the time necessary for native tissues to develop around it [2, 7]. In the evolution of biomaterials, bioceramics have developed from the first generation of inert replacement materials, a second generation of composites and multi-functionality, and to the third generation of dynamic and cell-reactive materials [2]. Bioceramics are ideally suited to hard tissue roles because they are akin to bone and teeth in mechanical and physical properties. However, recent novel bioceramics have demonstrated utility in soft tissue engineering. For example, calcium phosphates and silicates can not only tightly bond with bone tissue, but also stimulate the healing of surrounding soft connective tissues. To illustrate, bioglass is used in scaffolding for cardiac, lung and nervous tissue regeneration [5]. Orthopedics is the main application for bioceramics.

Orthopedic implants are a fairly successful type of medical procedure, but even so around 10% of implants fail prematurely [8]. One of the main causes of premature failure is bacterial colonization and ongoing biofilm formation on implant surfaces. Biofilms evoke inflammatory processes, and the result of infection and inflammation leads frequently to implant failure [8, 9]. Moreover, the act of surgical replacement brings great discomfort to patients, reducing their quality of life, and increasing treatment costs [10]. As the proportion of the aged population increases more patients will require implants, and therefore the overall risk of implant failure is increased, concomitantly [8, 11].

Prior to their application in the body, biomaterials must be always treated to avoid external contamination during surgery or hospitalization prior to wound closure [12], but when in contact with physiological fluids, proteins and other biological molecules are adsorbed, forming a layer onto the medical device, as Fig. 5.1 shows, using the example of a dental implant [13, 14]. This bound layer facilitates the

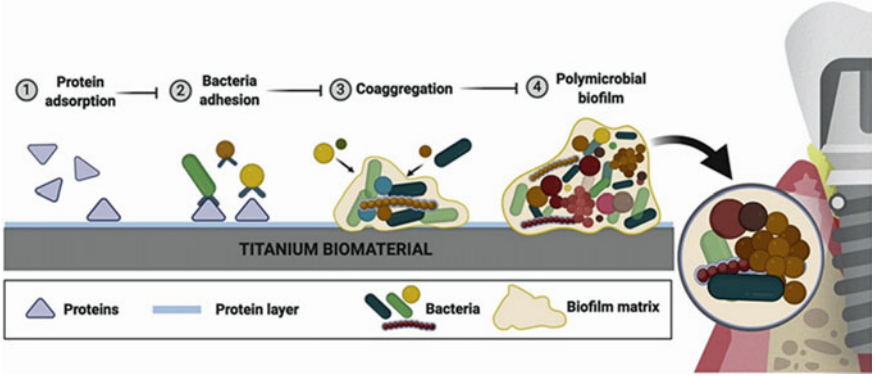

Fig. 5.1 Stages of biofilm formation (Reprint with permission from [14])

attachment of bacteria already in circulation through the body or hematogenous spreading from infections elsewhere in the body [15]. The types of microorganisms that may cause biological material-related infections vary greatly from commensal organisms (mainly on short-term implants or devices that resorb in 4–6 months) to opportunistic pathogens that accumulate in the long-term. Infections on short-term implants are usually caused by *Staphylococcus epidermidis* (*S. epidermidis*), *Staphylococcus aureus* (*S. aureus*), coagulase negative *Staphylococci*, *Streptococcus mutans* (*S. mutans*), *Escherichia coli* (*E. coli*) and *Enterococci*; while infections on long-term implant use are usually caused by species as *Pseudomonas aeruginosa* (*P. aeruginosa*) or *Proteus mirabilis* (*P. mirabilis*) [9]. Most of these bacterial colonies evolve over time to establish biofilms, three-dimensional structures created by the excretion of extracellular matrix substances (ECM) (Fig. 5.1). In this form, bacteria can be up to 1000 times more resistant to antibiotics [8, 16].

To address these challenges, the new generations of orthopedic biomaterials need to integrate anti-bacterial approaches while retaining osteointegration capacities. Bioceramics, already widely used as systems for structural bone replacement [17] can be further improved by integrating therapeutic molecules in their design [18].

5.2 Antimicrobial Peptides for Bioceramics in the Age of Antimicrobial Resistance

Anti-microbial substances are critical tools in medicine, but many are becoming increasingly ineffective. The World Health Organization (WHO) estimates that deaths due to antimicrobial resistance may increase from 700,000 to 10 million by 2050 if no strategies are implemented [19]. While some species of bacteria are intrinsically resistant, others can acquire genetic material that encodes a number of products that allow them to survive antimicrobial agents (e.g. enzymes, efflux pumps,

alterations of intracellular target site or cell wall components). This genetic mechanism can occur between strains or between bacterial species or genera [20], and are linked to the excessive and often inappropriate use of antimicrobial drugs, that has led to the development of the multiple-drug resistant (MDR) bacteria [21]. This phenomenon has accelerated the demand for new antimicrobial discovery. Compared with conventional antibiotics, recent antimicrobial peptides (AMPs) appear to have a great potential.

AMPs are a group of small bioactive proteins with unique physicochemical and structural properties, ubiquitous component of the innate immune system, where they play an important role modulating both innate and adaptive immune responses (Fig. 5.2) [22–24]. Most AMPs are small peptides of 10–50 amino acids, cationic, with net charges between 0 and +7, and have amphiphilic properties, with hydrophobic contents from 31 to 70% [25]. AMPs can form α-helical structures, β-sheets stabilized by disulphide bridges, globular or extended structures, depending on their amino acid sequence [26]. The amphipathic nature, structure and charge are very important for AMP activity: amphipacity allows for the formation of detergent-like structures on the bacterial membrane [27]; the spatial orientation of the different side chains affects amphipathic structure [26]; and the cationic nature of AMPs is thought to be one of the main factors for activity and selectivity against the negatively charged bacterial cell membranes [28].

AMPs exhibit a wide range of activities against a variety of pathogens, including Gram-positive and Gram-negative bacteria, yeast, fungi, enveloped and non-enveloped viruses [23]. The antibacterial activity of AMPs involves both extracellular and intracellular targets. The main targets are bacterial membranes. Due to their amphipathic nature, cationic AMPs bind and destabilize the negatively charged

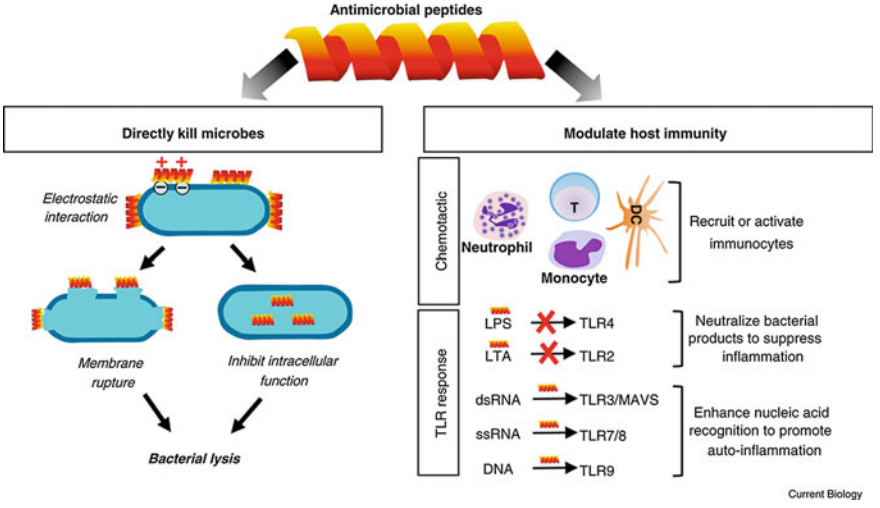

Fig. 5.2 AMPs display antimicrobial activity either by direct interaction with microorganism cells or by having a role in the host immune response (Reprint with permission from [24])

membranes, leading to peptide penetration, and leakage of cytoplasm leading to cell death (Fig. 5.2) [29]. The exact mechanism does not seem to be linked to a particular sequence of amino acids but rather to physicochemical and structural characteristics of the AMP [30]. Three main models of membrane disruption have been proposed (barrel-stave, toroidal pore, carpet models) and a fourth "aggregate" model was also suggested [29, 31]. AMPs can also affect the synthesis of cell wall components and neutralize extracellular virulence factors [32]. Once inside the cell, they can bind with proteins and nucleic acids, interfering with major cellular processes [23, 33]. AMPs also have indirect effects, like inhibiting the formation of biofilms, chemotactically attract host phagocytes and mediate non-opsonic phagocytosis [32]. AMPs are active against viruses, either by destabilizing the viral envelope or binding to the viral capsid, damaging virions, or stripping the virus coating decreasing infectivity [23, 34]. Specific AMPs can bind to cellular receptors used by viruses to gain host cell entry [24, 35] and their mediation of aggregation [23]. Topically, during the COVID-19 pandemic, AMPs and their derivatives have been explored as potential therapies against SARS-CoV-2. So far, these strategies are showing promising results [36]. Fungal and yeast cells have a very different cell wall structure and composition being less negatively charged, so effective AMPs exert different mechanisms [37]. For example, histatins attack fungal intracellular targets, altering mitochondrial functions [38]; cathelicidins and their mimics act against Candida and Aspergillus membranes [37].

AMPs also modulate the host immune response by several mechanisms, including increasing chemokine and cytokines production, enhancing wound healing and angiogenesis, exerting pro- and anti-apoptotic effects on different immune cell types, enhancing leukocyte and monocyte activation and differentiation, as well as having adjuvant activity in promoting adaptive immunity [24, 32, 39–41]. A study has also shown that different AMPs can work additively and synergistically, using different modes of action; that being one of the reasons why these peptides are so effective [42].

Human AMPs encompass three main categories. Defensins are cationic peptides, consisting of 18–45 amino acids, rich in cysteines that form three intramolecular disulphide bonds, stabilizing a β-sheet core. Based on the location of cysteine residues, they can be divided into α-defensins and β-defensins [43, 44]. α-defensins have a broader antibacterial activity compared to β-defensins [45], while the latter chemo-attractive properties, exerting their activity via the immune system [46]. The second category is cathelicidins. Consisting of 23–37 amino acids, these cationic α-helix peptides act mainly by the interaction and disruption of microbial membranes [47]. The only human cathelicidin, LL-37, is a peptide derived from the proteolysis of the C-terminus of human CAP18 protein [43]. Cathelicidins are also immunomodulatory antimicrobials, regulating the inflammatory response [47]. The third category is histatins, small cationic α-helix peptides, consisting of 24–38 amino acids, rich in histidine residues, are mainly found in human saliva [43]. These metal-binding AMPs are less amphipathic than the previous two and may therefore have different modes of action, but display good antifungal properties, making them good candidates for antifungal therapies [48]. Either of human or non-human origin, natural AMPs can

exhibit other functions that are undesirable for drug development. By changing the original sequence, peptides with tailored functions can be synthesized [49]. Various designed peptides based on human cathelicidin LL-37 (e.g., KS-30, KR-20, KR-12) showed promising minimal inhibitory concentration values against *S. aureus* and *P. aeruginosa*, displaying higher antimicrobial activity against Gram-negative bacteria [50]. SAAP-148, also derived from LL-37, is capable of resisting plasma proteases and act against drug-resistant bacterial pathogens [51]. GL13K is based on the modified sequence of the human parotid secretory protein. It showed bactericidal activity against *P. aeruginosa* and *E. coli* and even an affinity for bacterial endotoxins, blocking their action. GL13K has been used to modify the implant surfaces, presenting good physicochemical properties and good biocompatibility [52]. hLF1-11 consists of N-terminal amino acids 1–11 of human lactoferrin and has a broad antimicrobial spectrum, including antimicrobial resistant pathogens [53].

Sometimes, alterations in the peptide sequence can results in molecules with increased levels of cytotoxicity. Applying structure–activity relationship models, computer-aided design of AMPs can provide a predictive biological evaluation of the candidate sequence before synthesis and human use. This de novo design can drive to design of new therapeutic molecules, through the use of statistical analysis tools and machine learning (ML) algorithms [54, 55]. For example, two short AMP candidates, HHC-36 (Tet127) and Tet213, were identified through a large Quantitative-Structure–Activity-Relationship study, where they demonstrated a strong broad-spectrum antimicrobial activity; HHC-36 was comparatively less cytotoxic, so it was considered for the development of antimicrobial surfaces [56, 57]. Inverso-CysHHC10 is a synthetic AMP, mimicking the highly active HHC-10, and is comprised of only D-amino acids. HHC-10 has been shown to be highly effective against common biofilm forming bacteria, with the advantage of a low cytotoxicity and high biocompatibility [58]. KSLW is a synthetic antimicrobial decapeptide, analogue of KSL. It has shown a wide range of antimicrobial activity and cytocompatibility with normal epithelial cells. Based on this peptide, a new molecular bioconjugate was designed, consisting of KSLW and a HAp binding peptide, a common strategy for antimicrobial coating of implants surfaces, in reducing biofilm formation [59, 60].

5.3 Surface Functionalization of Bioceramics

A surface can prevent bacterial colonization either by resisting or repelling the initial attachment of microorganisms (antibiofouling surface) or by causing cell death when microorganisms contact with the surface (biocidal/antimicrobial surface) [15]. To obtain these antimicrobial surfaces, three main strategies can be used: (1) the surface can be coated with an antimicrobial compound/material (surface coating), (2) the surface topography can be altered (physical modifications), and (3) the surface can be modified by adding molecules or agents through chemical modifications (surface chemistry) (Table 5.2) [13, 15]. Surface modification techniques are of particular

Table 5.2 Surface functionalization strategies and their main characteristics

Surface Functionalization Strategy		Examples	Observations
Surface topography [8, 15, 16, 62]		Surface micro or nanostructures (brushes, nanotubes)	Most surfaces display an antibiofouling behavior. However, this kind of alterations might affect the behavior of many biomolecules besides bacterial and mammalian cells, so careful tailoring is needed
Surface coating	To prevent adhesion (antibiofouling) [13, 15, 62]	Pre-adsorbed molecules (hydroxyapatite, chitosan, polymers), superhydrophobic coating	Passive mechanisms to reduce fouling. Coatings might not be uniform and stable over time; in vivo efficiency may vary
	Antimicrobial/biocides [8, 13, 62, 63]	Loaded with biocide molecules, metal ions, antibiotics; doped coatings	Active mechanism against bacteria colonization. Release profile is hard to control, leaching over time reduces efficacy, in vivo efficacy may vary
	Controlled/"Smart" release [62, 64, 65]	Stimuli (pH, temperature, ionic strength) responsive copolymers, hydrolytically degradable films	Bioactive molecules or active conformations occur as responses to changes in cellular environment. Release profile, stability and in vivo efficacy may vary. Need for regenerative mechanisms
	Multifunctional [8, 62, 66]	Complex coatings able to exert antibiofouling and/or antimicrobial activity, while contributing to tissue integration	Extensive optimization needed. Need for regenerative mechanisms
Surface chemistry	Surface polymerization [13, 15, 62]	Covalent bonding, polymeric polycations	Most surfaces display antibacterial behavior. Common drawbacks relate to exhaustion of antimicrobial agents and loss of activity over time

(continued)

Table 5.2 (continued)

Surface Functionalization Strategy		Examples	Observations
Surface topography [8, 15, 16, 62]		Surface micro or nanostructures (brushes, nanotubes)	Most surfaces display an antibiofouling behavior. However, this kind of alterations might affect the behavior of many biomolecules besides bacterial and mammalian cells, so careful tailoring is needed
	Surface derivatization [13, 15, 62]	Cyclic hydrocarbon moieties, PEG, zwitterionic polymers, quaternary ammonium	These methods were developed to enhance the effectiveness of a surface via direct reactions on the surface. Concentration depend; risk of further chemical reactions

interest, since they do not change the properties of the core material and can be used on different kinds of implants [61]. In many cases, a surface can be functionalized using multiple strategies, and the final surface can present a complex behavior.

When using AMPs for creating an antimicrobial surface, some consideration must be taken to guarantee the activity of the peptide once it is immobilized on the surface. AMP proactivity is mostly by direct contact with the cell wall of bacteria [67]. The type of surface material, chemical bonding techniques, the length and strength of the bond, peptide final concentration and orientation on the surface, all should be taken into consideration, as they all contribute to the efficiency of the final product [67].

5.3.1 Surface Topography

The alteration of surface topography usually involves antibiofouling strategies that result in passive structuration [13, 15]. These techniques involve the use of structural units such as polymer brushes or nanotubes layered over the surface, hindering bacterial adhesion and physically tearing apart the membrane as they make contact with the surface structure. These strategies lead to antifouling activity over longer periods of time but may not resolve an infection [8]. Surface modifications can also have broader biological effects. The final topography of glass surfaces with different nanostructures appears to influence not just bacterial adhesion but also the bacteria metabolism [13]. A study of nano-porous bioactive glass monoliths with different nanopore sizes concluded that mammalian cell attachment was influenced not only by how cells interacted chemically with the available surface, but also by how that topography

influenced the absorption of other proteins and their final structure/conformation after attachment [68].

5.3.2 Surface Coatings

Biocidal surfaces can act as a second line of defense, when adhesion of microorganisms has already occurred. Surface coatings are one of the most common strategies used, for their relatively simple procedures and their capacity to create multiple functions in one element. Coatings containing the biomineral, hydroxyapatite are some of the most common constituents, which can be undertaken by several techniques (e.g. plasma spray, electro-chemical deposition, sol–gel-technique); and are able to increase the bioactivity of implants without compromising their mechanical behaviour [8]. AMPs, for instance, can be loaded onto surface biodegradable coatings [61] or simply be attached by electrostatic interactions to a previously coated material surface [67].

Moussa et al. coated hydroxyapatite surfaces with either synthetic GL13K D-enantiomer, synthetic JK2 D-enantiomer or innate defence regulator (IDR) 1018 by a single incubation with AMP solution for 1 min at 37 °C, and final surfaces could significantly reduce biofilm formation when inoculated with dental plaque sample, where bacterial genera *Veillonella* and *Streptococcus* were predominant [69]. Honda et al. produced disks made from hydroxyapatite powder mixed with a protamine solution, able to prevent *E. coli* and *S. aureus* growth in a concentration dependent manner [70]. Kazemzadeh's group coated successfully titanium samples with calcium phosphate containing the AMP Tet213 and those surfaces were able to totally inhibit *S. aureus*, and *P. aeruginosa* in vitro growth after 30 min [71], while not impairing in vivo bone growth [56]. Coating systems have some disadvantages. The coatings tend to be uneven and not very stable over time [15]. In the previous example, titanium coatings still retain antibacterial activity after four 30 min use cycles, but with reduced activity [71]. In some cases, burst release cannot be totally avoided, exhausting the antimicrobial agent in a short period of time. A local spike in concentration could result in toxicity for surrounding tissues [61], like what happened in the previous example, were a high dosage of released protamine exhibited a cytotoxic effect [70]. The unequal release could also compromise the long-term antimicrobial activity of the material and could result in the development of resistance due to sub-optimal concentrations [8, 13, 61]. Multi-layer films, obtained by a layer-by-layer technique (LbL), for example, allowed a better control of release [61]. The gradual degradation of layers permitted a controlled release of AMPs like HHC-36 or LL-37-derived synthetic peptide, reducing the possibility of cytotoxicity or bacterial resistance. However, there is still the issue of decreased bioavailability since AMPs trapped within the layers might not reach bacterial cells and in the correct destructive concentrations [67]. Another possibility is the use of smart biomaterials, designed to respond to external stimuli in order to display antimicrobial activity. These modern smart materials are made mostly using multilayer coatings comprised of polymers

able to change their conformation as response to changes of temperature, pH and enzymatic activity (caused by bacterial presence), surface hydration and basic bacterial contact [64, 66]. When triggered, the conformation change can either activate the antimicrobial capacity of the polymer [66], reveal antimicrobial compounds immobilized within another layer [64] or selectively release an antimicrobial payload [7, 8]. Some of these smart materials are also able to use a stimulus response to clean the surface from cellular debris accumulated after cell death ("kill-and-release"), to maintain the surface available to exert the biocidal activity [65, 66]. The strategies to obtain these smart materials should take into consideration the need for a regenerative process, so that the material maintains activity during different cycles of stimulation [65, 66].

5.3.3 Surface Chemistry

Despite different methodologies available, all surface functionalization strategies by surface chemistry imply the fixation of a bioactive molecule to a surface via a chemical reaction. Compared to coating, an immobilization strategy results in a more stable antimicrobial surface, since the agent will less likely dissociate from the surface, retaining the activity over a longer period of time [61, 67]. Surface immobilization can be done by inducing the formation of functional groups on the surface of the material, that later will react with the antimicrobial agent, forming a covalent bond [15, 61]. One of the most common approaches for coupling peptides, such as AMPs, involves a specific chemical reaction between non-essential cysteine residues with surface-bound thiol groups [72]. In another common technique, salinization, the alkoxy groups of silane molecules are displaced by interacting with the surface material (e.g. hydroxyl groups on metal surfaces such as titanium), forming -Si–O-Si- bonds able to covalently attach functional molecules [73]. AMPs can also be covalently conjugated through functional groups by click chemistry (a peptide bearing an extra azide or alkyne group that binds another surface-bound azide or alkyne group, respectively) [72, 73]. Other techniques include photo cross-linking and oxidation reaction [73]. The concentration and size of surface linkers directly affect the surface's activity. Most importantly, enough linkers must be present to guarantee an adequate concentration of antimicrobial agent and prevent the developing of resistance due to exposure to minimal antibacterial concentrations [61]. The mobility of the agent when connected to the linker also affects the interaction with bacterial cells [61]. Stiff linkers restrict lateral movement of peptides while maintaining the molecule within a specific orientation; flexible spaces allow lateral mobility but also some orientation freedom at the interface [67]. More recently, an alternative to complex chemical methods for surface functionalization with AMPs has appeared in the form of binding peptides. These are small peptide sequences with a natural affinity for a certain material (such as titanium or HAp), due to their characteristic peptide residue sequence. When these sequences are added to an AMP,

successful coating of surfaces can be achieved simply by immersion of the material in a solution containing the AMP-binder construct [59, 74, 75].

5.4 Different Approaches for Immobilization of AMPs on Bioceramics

AMPs immobilized on bioceramics may provide antimicrobial functionality based on either contact killing (AMPs covalently bonded to surfaces) or solution-phase killing (surface degradation or eluting of embedded AMPs). Therefore, the mechanism by which the AMPs are immobilized on the surfaces would affect their activity as well as the duration of their bactericidal performance. There are a variety of strategies for AMPs immobilization on bioceramic surfaces that are different in binding strength and complexity. Poor binding would lead to an inefficient uncontrolled release. Contrarily, strong anchoring provides a controlled release of AMPs but may hinder biological signals and activities. Since a balance between controlled release and stable attachment is demanded for preparing an ideal antimicrobial surface, many studies have examined different strategies of AMP immobilization to provide physiologically effective antimicrobial bioceramics [76].

The simplest and naturally occurring immobilization method is physical adsorption. AMPs can be easily but weakly adsorbed on surfaces through electrostatic and/or hydrophobic interactions (Fig. 5.3a). This method can simply be performed by soaking the ceramics in peptide solutions; thus, the AMPs can be entrapped during processing. In order to provide the AMPs with rather controlled release, some

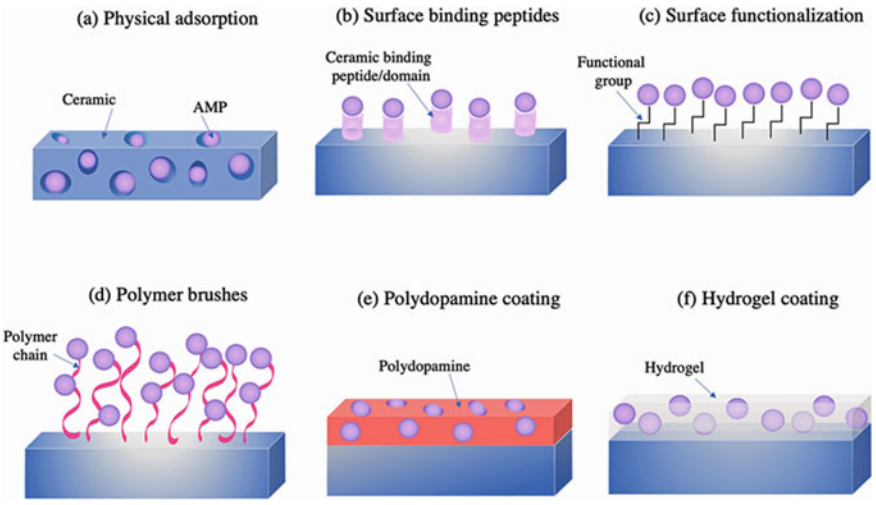

Fig. 5.3 A summary of possible AMP immobilization strategies for bioceramic implants

studies used films formed layer-by-layer from the deposition of cationic and anionic molecules of peptides [77]. Moreover, AMPs can be modified with affinity domains to promote their electrostatic and hydrophobic attractions. Surface binding peptides attach to surfaces based on the mentioned electrostatic interaction strategy where their affinity can be strongly increased by repeating sequences rich in basic amino acids (Fig. 5.3b). Physical adsorption is more applicable for clinical approaches, although it results in poor orientation, low stability, and poor activity compared to covalent interactions [78]. Recently, surface binding peptides composed of histidine and lysine were developed which can directly assemble onto the biomaterials with high affinity. These self-assembly peptides can be utilized to integrate various peptides, principally AMPs, onto biomaterials [79]. Chen et al. integrated a surface binding peptide at the N-terminal of Tet213 AMP and utilized it to prepare antimicrobial implants made of titanium, gold, hydroxyapatite, and polymethyl methacrylate [75].

In order to prepare more stable and durable immobilization compared to the physical adsorption method, covalent binding of AMPs with varied functional groups can be applied, straightforwardly (Fig. 5.3c). So far, the most common functionalization which has been used for AMP immobilization is salinization [80]. Hydroxyl groups on the surface can be modified with alkoxysilane introducing amino groups. Then, the surface is modified directly or by a crosslinker to enable the immobilization of thiol-containing peptides. Depending on the functional groups on the ceramics and reactive groups of AMPs, the peptides can also be covalently attached to the functionalized surfaces using the reactions between amine groups, at the surface or displayed by AMPs, and carboxyl groups or azide-alkyne cycloaddition reactions [81–84].

Another strategy for the covalent conjugation of AMPs is the utilization of polymer brushes as a flexible linker on the surfaces (Fig. 5.3d). At first, the bioceramic surfaces can be functionalized by the surface-initiated polymerization to provide a primary amine functionality. Then, the amine groups may be modified to maleimide groups as a spacer to react with cysteine-containing AMPs [85]. For example, Gao et al. immobilized AMP Tet-20 on a Quartz slide surface using polyacrylamide brushes to inhibit *S. aureus* and *P. aeruginosa* growth and adherence [86].

Moreover, polydopamine (PDA) chains exhibit an ability to form strong adhesive interactions with the surface of diverse materials (Fig. 5.3e). This polymer can be used as a linker for covalent conjugation of AMPs containing amine and thiol groups through Michael addition or Schiff base reaction. In this approach, the PDA can make a thin film on the ceramic surface via self-polymerization, and subsequently, the AMPs functionalized with PDA tag can attach to the PDA coating via catechol groups [87]. Compared to previous techniques, PDA-assisted immobilization is simple, less time-consuming, non-toxic, and applicable for ceramic implants with complex geometry.

As another method for AMP immobilization on ceramic surfaces, hydrogel films can carry AMPs via forming a covalent bond between the polymer chains and AMPs (Fig. 5.3f). This mechanism can be applied by coating the ceramic implant with a hydrogel film. Then, the coated implant can be immersed into an AMP solution. The AMPs are then loaded within the hydrogel normally by covalent conjugation.

For example, polyethylene glycol (PEG) hydrogel can be functionalized with vinyl sulfone groups to react with cysteine residues of peptides owing reactive thiol groups. Similar reactions between maleimide and thiol groups can also be utilized for covalent conjugation between hydrogel and AMPs [88]. Although the hydrogel coating has been introduced as an efficient technique for AMP immobilization on diverse materials [89], this strategy has not been extensively studied for ceramic implants, so far.

Many studies have examined various strategies of AMP immobilizations for different forms of bioceramics such as scaffolds, coatings, composites, and micro/nanoparticles in order to provide them with antimicrobial activities for particular biomedical applications. Different forms of bioceramics, the types of immobilized AMPs, and the immobilization strategies. which has been used in recent studies in the last 10 years have been summarized in Table 5.3. According to the studies reported in Table 5.3, the most common strategy used for AMP immobilization to the ceramic surfaces is the physical adsorption method because of its simplicity and non-toxicity. Additionally, although immobilization methods based on polymer brushes and hydrogel films have been studied widely for the AMP immobilization on polymeric materials [90, 91], these techniques have not been reported yet for the AMP immobilization on bioceramic surfaces.

5.4.1 Bioceramic Scaffolds for Bone and Dental Implants

Bioceramics including bioglasses and calcium phosphate are mainly utilized in orthopedics and dentistry due to their ability to promote osteoblast adhesion and bone tissue formation (principally, hydroxyapatite and tricalcium phosphate (TCP)).

Bone and dental ceramic implants can be functionalized with different bioactivities, particularly peptides involved in bone regeneration or to prevent the colonization of bacteria. Honda et al. developed protamine-loaded hydroxyapatite based on the physical adsorption method [70]. The adsorption of protamine to hydroxyapatite was based on the Langmuir adsorption model as a result of the electrostatic and/or hydrophobic interactions. The protamine released from the hydroxyapatite scaffold could prevent the planktonic bacteria growth in vitro. In another work, Van Staden et al. mixed β-tricalcium phosphate, monocalcium phosphate monohydrate, and nisin AMP, then, molded to prepare a brushite cement [111]. The burst release of the AMP from the cement was because of the physical binding of the AMPs to the cement compositions. The nisin-loaded cement was implanted in the back of a mice with *S. aureus* infection, and it was proved that the brushite cement could successfully prevent the biofilm formation of *S. aureus* (Fig. 5.4a, b).

Townsend et al. applied two binding mechanisms for immobilizing a human defensin-like AMP to a hydroxyapatite scaffold to provide simultaneously a long-term antimicrobial effect and partial release of the AMP into the peri-implant tissue. They used electrostatic binding and covalent attachment methodologies, respectively, to produce a short-term and permanent AMP coating with the aim of both sterilizing

Table 5.3 A summary of recent studies on the immobilization of AMPs on bioceramics for various applications

Bioceramic materials	AMP name	Amino acid sequences	Immobilization strategy	Bacteria tested	Biomedical applications
Hydroxyapatite + collagen [92]	GL13K	GKIIKLKASLKLL-NH_2	Physical adsorption	*E. coli* & *S. gordonii*	Dental scaffold
Hydroxyapatite + silk fibroin [93]	HHC-36	KRWWKWWRR	Polydopamine coating	*E. coli* & *S. aureus*	Orthopedics
Hydroxyapatite + Poly(propylene fumarate)/ poly(caprolactone) [94]	LL-37	LLGDFFRKSKEKIGKE FKRIVQRIKDFLNLVP RTESGGGGSSVSVGM KPSPRP	Ceramic binding peptide	*E. coli* & *S. mutans*	Bone substitutes
Hydroxyapatite [95]	Nisin	ITSISLCTPGCKTGALM GCNMKTATCHCSIHV SK	Polydopamine coating	*S. aureus*	Bone implants and drug delivery
Hydroxyapatite [70]	Protamine	–	Physical adsorption by batch method	*E. coli* & *S. aureus*	Bone substitute
Silica [96]	Melittin	GIGAVLKVLTTGLPAL ISWIKRKRQQ	Physical adsorption	*P. aeruginosa*	Drug delivery system
Calcium phosphate [97]	LL-37	LLGDFFRKSKEKIGKE FKRIVQRIKDFLRNLV PRTES	Physical adsorption	*E. coli* & *S. pneumoniae*	Drug delivery
Glass [98]	Mel4	KNKRKRRRRRRGGRR RR	Surface functionalization - ABA-EDC functionalization	*P. aeruginosa*	Medical devices
Calcium phosphate [99]	Protamine	–	Physical adsorption	*S. mutans*	Dental field

(continued)

Table 5.3 (continued)

Bioceramic materials	AMP name	Amino acid sequences	Immobilization strategy	Bacteria tested	Biomedical applications
Alumina [100]	BP 100 DD K	KKLFKKILKYL-NH_2 GLWSKIKAAGKEAAK AAAKAAGKAALNAVS EAV-NH_2	Surface functionalization—Alkyne-azide reaction	*E. coli & S. typhimurium & S. aureus*	Medicine & orthopedic applications
Hydroxyapatite + TiO_2 nanotubes [74]	Tet127	KRWWKWWRR	Ceramic binding peptides	*E. coli & S. mutans*	Bone implant
Calcium phosphate [101, 102]	HAL-2	GKWMSLLKHILK-NH_2	Physical adsorption	*S. aureus, S. epidermidis & P. aeruginosa*	Bone implant
Alumina [103]	BP100	KKLFKKILKYL-NH_2	Surface functionalization - Silanization	*E. coli & S. typhimurium*	Biological applications
Hydroxyapatite [75]	Tet213	KRWWKWWRRC	Ceramic binding peptide	*E. coli & S. aureus*	Bone implant
Hydroxyapatite [104]	Human defensins	RRRRRRGALAGRRRR RRGALAG	Physical adsorption Surface functionalization - Thiol group	*S. aureus, S. epidermidis & P. aeruginosa*	Orthopedics
Glass [80]	Cysteinylated Lipopeptides	–	Surface functionalization—Silanization	*P. aeruginosa & E. coli*	Medical implants
TiO_2 nanotubes [52]	GL13K	GKIIKLKASLKLL-CONH2	Physical adsorption	*F. nucleatum & P. gingivalis*	Orthopedics
Calcium Aluminium oxide + hydroxyapatite [105]	Inverso-CysHHC10	H-CKRWWKWIRW-NH_2	Surface functionalization—Alkene-thiol reaction	*E. coli*	Bone implant

(continued)

Table 5.3 (continued)

Bioceramic materials	AMP name	Amino acid sequences	Immobilization strategy	Bacteria tested	Biomedical applications
Silica [106]	LL-37	LLGDFFRKSKEKIGKE FKRIVQRIKDFLRNLV PRTES	Physical adsorption	*E. coli*	Drug delivery
Hydroxyapatite [59]	KSLW	KKVVFWVKFK	Ceramic binding peptide	*S. mutans*	Oral infections
Hydroxyapatite [107]	PSI 10	RRWPWWPWRR-NH_2	Physical adsorption	*S. aureus*	Orthopedics
Hydroxyapatite [108]	HHC-36	KRWWKWWRR	Physical adsorption	*S. aureus*	Bone scaffold
Calcium phosphate + TiO_2 nanotubes [109]	HHC-36	KRWWKWWRR-NH_2	Physical adsorption	*S. aureus & P. aeruginosa*	Bone implant
TiO_2 [110]	GL13K	GKIIKLKASLKLL-$CONH_2$	Surface functionalization – Silanization	*P. gingivalis*	Dental applications
Calcium phosphate [56]	HHC-36 Tet213	KRWWKWWRR KRWWKWWRRC	Physical adsorption	*P. aeruginosa & S. aureus*	Orthopedics
TiO_2 nanotubes + calcium phosphate [77]	HHC-36	KRWWKWWRR	Vacuum-assisted physical adsorption	*S. aureus*	Orthopedics
Calcium phosphate [111]	Nisin	ITSISLCTPGCKTGALM GCNMKTATCHCSIHV SK	Physical adsorption	*S. aureus*	Bone cement

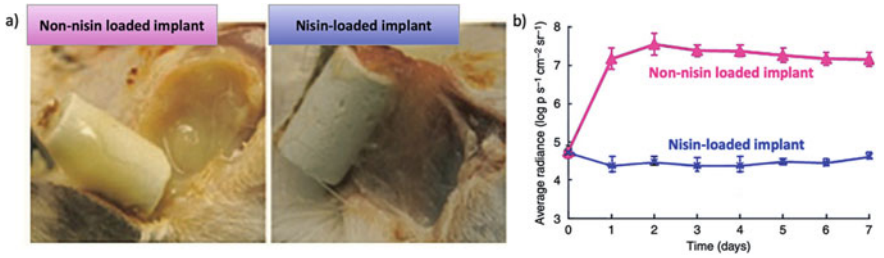

Fig. 5.4 **a** Representative images of implantation sites after 7 days; **b** graphs representing the average radiance of S. aureus for nisin loaded and non-nisin loaded implants (Reprint with permission from [111])

the surgical site and preventing colonization of the implant for an extended time [104]. The long-term stability of the covalently immobilized AMP was the result of the steric hindrance provided by the implant since the peptides were attached directly to the surface without any linker spacer. They applied the thiol-functionalization method using (3-mercaptopropyl) trimethoxysilane (MPTS) to incorporate thiol residues into the hydroxyapatite surface as covalently tethering links [112]. After the immobilization of the AMP on the hydroxyapatite surface, it was assessed against *S. epidermidis*, *S. aureus*, and *P. aeruginosa*. The proposed AMP immobilized implant could destabilize the bacteria membrane due to the pore formation and consequent cell lysis [104].

In another study, Wang et al. developed a PDA and hydroxyapatite composite as a platform for loading nisin as an AMP. At first, they prepared PDA particles via dopamine self-polymerization. Then, these particles could serve as active cores for the in-situ hydroxyapatite mineralization and consequently form PDA-hydroxyapatite composites. Finally, the nisin AMP was loaded on the composite for drug delivery and bio-scaffold applications (Fig. 5.5a) [95]. Ultraviolet visible spectra confirmed that the prepared composite exhibited high loading efficiency of the nisin. The loading efficiency was decreased from 98 to 62% as the initial concentration of nisin was increased from 0.1 to 0.70 mg/mL as shown in Fig. 5.5b. Because of the basic isoelectric points of nisin, it is positively charged and that caused the electrostatic adsorption of nisin to the composite with negative charge. In vitro cumulative release result, as shown in Fig. 5.5c, indicated that the release of nisin reached around 87% and 91% within 32 h and 100 h, respectively.

Bioactive glasses such as Bioglass® contain SiO_2, CaO, P_2O_5, and Na_2O. The higher molar ratio of calcium to phosphorous gives bioactive glasses superior bioactivity and osteoconductivity. Melimine and its derivative (Mel4) are two chimeric cationic AMPs and have been covalently bounded to a glass surface via an azidobenzoic acid linker. In the first step, the glass was functionalized using azidobenzoic acid (ABA) and 1-[(3-dimethylamino)-propyl]-3-ethylcarbodiimide hydrochloride (EDC). Then, the AMPs reacted with the functionalized surfaces. The immobilized AMPs could bind lipopolysaccharides and disrupt the membrane potency of *P. aeruginosa* immediately [98].

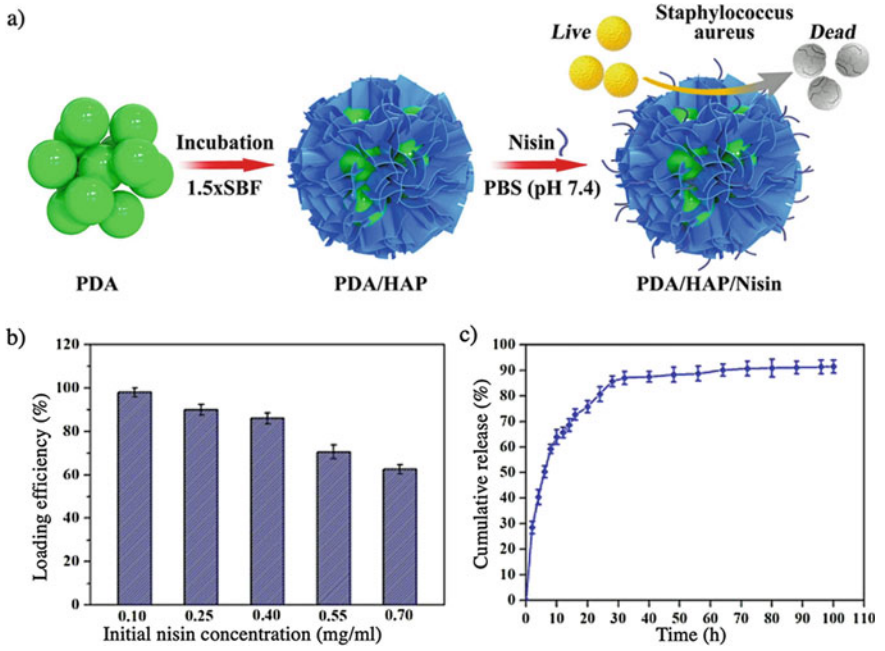

Fig. 5.5 **a** Schematic illustration of the formation of PDA and hydroxyapatite composites and loading of AMP nisin; **b** loading efficiency of the AMP adsorbed by the composites; **c** cumulative release profile of nisin from the composite at pH 7.4 in PBS solution (Reprint with permission from [95])

In another work, De Zoysa et al. immobilized recently discovered lipopeptides (GZ3.163 and GZ3.160) on glass, titanium, and silicon surfaces that were maleimide-functionalized by silanization [80]. The lipopeptides with N-terminal cysteine residues were covalently bounded through a thioether bond by a Michael type addition between maleimide at the bioceramic surface and cysteine sulfhydryl groups. The antimicrobial assay of the lipopeptide-immobilized surfaces showed 98.6–99.9% inhibition of *E. coli* and *P. aeruginosa* adhesion.

Some microorganisms, such as *S. mutans*, *L. acidophilus*, and *A. viscosus* can contribute to oral infectious diseases. Some targeted AMPs are able to selectively eliminate *S. mutans*. However, the application of these AMPs would be limited since the oral cavity continuously secretes saliva making consequently the actual concentration of AMPs lower than the effective concentration [113]. Therefore, one of the approaches to overcome this difficulty is to covalently immobilize the AMPs on the enamel or ceramic implants based on silane-chemistry (silanes as coupling agents) [114]. GL13K AMP, based on parotid secretory protein, was used by Holmberg et al. to modify the surface of dental and orthopedic titanium oxide (TiO_2) implants. They used a silane chemical linker (silanization) to covalently anchor the AMP to the TiO_2 surface [110].

AMP immobilization onto ceramic surfaces via chemical coupling provides a contact active antimicrobial surface. However, silanization as a coupling procedure is usually difficult to control, and it is not practical to salinize the surface of teeth. The outer layer of tooth (enamel) mainly contains hydroxyapatite; thus, Huang et al. designed a hydroxyapatite-binding antimicrobial peptide (HBAMP), consisting of a broad-spectrum AMP (KSLW) and a hydroxyapatite binding heptapeptide (HBP7) to conjugate the KSLW to the tooth enamel [59]. They constructed an antimicrobial coating for tooth enamel to prevent biofilm formation. In vitro studies revealed the cytocompatibility of KSLW and its stability in human saliva. KSLW showed strong antimicrobial activity against various oral bacteria such as *L. acidophilus*, *S. sobrinus*, and *S. mutans* as well as high stability for long-term effectiveness [59].

In another study, Fujiki et al. used protamine to load onto the dicalcium phosphate anhydride (DCPA) as a dental material. The AMP protamine was loaded physically by soaking and stirring the DCPA into the protamine solution based on electrostatic interactions. The antimicrobial behavior of the AMP loaded protamine was evaluated based on its efficacy on biofilm formation of *S. mutans* for dental applications [99].

5.4.2 Bioceramic Coatings for Metallic Implants

Metallic implants such as titanium alloys and stainless steel are mainly used for orthopedic and dental applications because of their high strength and stability [115, 116]. Having different chemical compositions from natural bones, implanting metals in the body inevitably causes unusual cellular responses and serious complications such as, incomplete integration and implant loosening. Contrarily, as bioceramics present excellent osteoconductive behavior and biocompatibility, they can be applied as coatings for metallic implants to promote bone cell attachment and ingrowth into metallic implants. Moreover, bioceramic coatings containing AMPs would endow the implants with antimicrobial activities to prevent biofilm formation at the peri-implant area.

Surface modifications and bioceramic coatings on metallic implants are typically applied to improve osteointegration and surface bioactivity by improving their interaction with the biological environment, inducing bone growth, and biochemical bonding with proteins [117, 118]. A number of techniques used to obtain bioactive coatings include plasma spray [119], micro-arc oxidation [120], electrophoretic deposition [121], sol–gel [122], and biomimetic methods [123]. The method most commonly applied in the orthopaedic and dental industry is plasma spray, but, heterogeneous coatings are usually obtained because of the high temperature process and rapid cooling of the coating [124]. Another popular method for surface coatings is the utilization of NaOH or H_2O_2 to form a surface gel layer which induces ceramic deposition from surrounded fluids [125]. This method uses less energy and is more biomimetic compared with other common coating methods. As an example, applying the etching method using an aqueous solution of H_2O_2 for titanium implants can form a titanium dioxide (TiO_2) or titania gel layer on the surface. The amphoteric behavior

of the titania layer can promote an electrostatic interaction with AMPs at pH 7.5 and other titania peptide binders [126].

In some cases, ceramic coatings are employed as an AMP delivery system to release peptides from the implants in the peri-implant region. For this purpose, calcium phosphate coatings and titania nanotubes have been the most reported for the controlled release of AMPs on metallic implants [127]. Calcium phosphate coatings are mainly porous which support the integration of the metallic implants to the bone tissue. AMPs can be incorporated to the calcium phosphate coated implants through a soaking method and consequently exhibit antimicrobial activity besides osteointegration [71]. One of the common methods for preparing a calcium phosphate coating on metallic implants is biomimetic mineralization [128, 129]. Tian et al. coated a magnesium alloy implant with hydroxyapatite loaded with AMP by immersing the coated implant in an AMP (PSI 10) solution [107]. The release rate of AMP from the hydroxyapatite coating was slow and steady over 7 days. Roughly 57% of the AMP was released during the first 48 h. The AMP molecules could not only deposit on the hydroxyapatite surface but also be incorporated into the hydroxyapatite crystals. The entrapment of the AMP molecules inside the hydroxyapatite crystals could cause this sustained and slow-release rate.

Physical absorption of the AMPs on the ceramic surfaces limits the loaded amounts and release rates. To that end, there is a need to immobilize the AMPs on the ceramics with functional groups to create antimicrobial surfaces. A number of covalent immobilization strategies based on chemical coupling reactions can be applied for AMPs. Self-assembled monolayers of thiol and silane-based molecules are one of the widely used methods for AMP immobilization on ceramic surfaces [130].

Furthermore, biomolecular linkers with high material binding affinity can be applied to induce controlled and selective interactions with the bioceramic surfaces, which enable the precise control of the AMP display. Various material binding peptides have been produced by phage- and cell-based display techniques [131, 132]. As an example, hydroxyapatite binding peptides usually contain aspartic acid and glutamic acid rich domains. The carboxyl groups of these anionic amino acids can interact with the Ca^{2+} ions of the cationic hydroxyapatite crystals. Melo Rodriguez et al. used these mentioned capabilities of hydroxyapatite to develop biomimetic hydroxyapatite coating and immobilization of AMPs [133]. It was reported that peptides with higher negative net charges can be adsorbed by the hydroxyapatite surfaces in higher amounts [134, 135]. Yazici et al. also used this system to apply a self-assembled peptide on the microporous hydroxyapatite coated on a nano-tubular titanium implant. They combined an AMP i.e., Tet127 and a hydroxyapatite-binding peptide (HABP) with a flexible -GGG-linker in a single step. Tet127, used in this work, had high activity against *S. mutans* and *E. coli* while covalently tethered on the surface. This procedure did not involve complex surface modifications and covalent reactions of the interfaces which makes this process simple for clinical approaches [74].

Titania presents excellent corrosion resistance and biocompatibility as well as photocatalytic activity as a candidate for coating metallic implants. TiO_2 nanotube

coating produced by anodization method combines the geometric features and the unique properties of titania for controlled and sustained release of AMPs. It has been reported that TiO_2 nanotubes on titanium surfaces would considerably accelerate the growth and adhesion of osteoblast cells improving the bonding strength. Ma et al. applied TiO_2 nanotubes for the local and continued release of AMPs for 7 days [77]. TiO_2 nanotubes were loaded with an AMP (HHC-36) via a vacuum assisted physical adsorption method. Testing of the antimicrobial activity revealed the reduction of *S. aureus* by about 3 logs. By a similar method, Li et al. also immobilized an AMP (GL13K) into TiO_2 nanotubes as a coating for a titanium implant [52].

One of the common methods for loading the AMPs in the coatings is simple soaking. Ma et al. were one of the groups who used a simple soaking method for entrapping AMP HHC-36 into TiO_2 nanotubes [77]. In both calcium phosphate coating and TiO_2 nanotubes methods for immobilizing the AMPs on the surface of implants, the soaking method is used for loading the AMPs, and consequently, the release rate of AMPs is quite rapid [71, 77]. Therefore, these methods are unreliable for the treatment of long-term infections. In order to provide a sustained release system, some researchers reported the application of layer-by-layer coatings on the metallic implants using calcium phosphate and TiO_2 nanotubes loaded with AMPs [109, 136]. The coatings were topped with a phospholipid film for controlling the peptide release. The phospholipid film is also suitable for cell attachment and osteointegration.

TiO_2 nanotubes and calcium phosphate coatings are the most common platforms for drug delivery from metallic and ceramic implants [137, 138]. Kazemzadeh-Narbat et al. designed a highly effective controlled release of the AMP HHC-36 from a multi-layered coating of calcium phosphate and TiO_2 nanotubes to stop peri-implant infections of orthopedic implants. These thin films were impregnated with the AMP and assembled via a layer-by-layer technique. The films have been topped with a phospholipid film as a barrier for providing an accurately controlled release and the least bacteria growth [109]. Anodization and drop-and-dry method based on evaporation-induced crystallization have been applied in this work to produce, respectively, various thicknesses of calcium phosphate and TiO_2 nanotubes (Fig. 5.6a, b). The AMP was loaded on each layer and the AMP release was expected to occur during degradation and diffusion phenomena after an initial burst release. The modified surface demonstrated sufficient release of AMPs to inhibit *S. aureus* and *P. aeruginosa* growth (Fig. 5.6c) while osteoblast cells could attach to the implant surface and there was no cytotoxicity against the cells after five days.

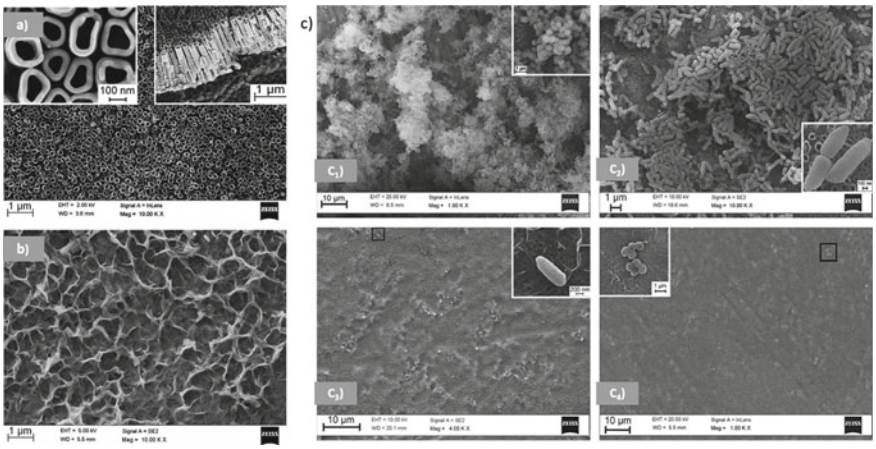

Fig. 5.6 SEM micrographs of **a** TiO_2 nanotubes; **b** calcium phosphate coating on TiO_2 nanotubes; (C_1), (C_2) *S. aureus*, and *P. aeruginosa*, respectively, incubated overnight on the non-AMP loaded coating control, (C_3), (C_4) *S. aureus*, and *P. aeruginosa*, respectively, incubated overnight on the AMP loaded coating (Reprint with permission from [109])

5.4.3 Ceramic-Polymer Composites for Hard Tissue Engineering

Although there have been considerable efforts on developing implants for bone and dental tissue defects, still the success in creating the ideal physicochemical and osteoinductive properties has been unachieved. That is where the composites have attracted recent attention in order to combine the best properties of different materials. This is the same strategy that native biomaterials have evolved. Generally, bone composite implants are a combination of different ceramics or ceramics with polymers. Ceramic-ceramic composites provide a mixture of properties that cannot be found in one kind of ceramic. As an example, ceramic composite implants based on alumina and zirconia have gained growing attention because of their high elastic modulus, hardness, resistance to abrasion, and non-sensitization. In one study, an alumina-zirconia ceramic surface modified by vacuum plasma spraying was used as a bioceramic implant and functionalized with RGD-peptide for osteo-integrative effects [139]. As natural bones are organic–inorganic composites, the combination of polymers (organic materials) and bioceramics (inorganic materials) can mimic respectively the hydroxyapatite and collagen phases of the bone extracellular matrix (ECM). Bioceramics mainly play a role to mechanically reinforce polymer-matrices and improve the bioactivity properties of the blend, based on the local release of active ions for bone regeneration. As an example, scaffolds consisting of chitin-poly(lactic-co-glycolic acid) blend and nano-bioglass were developed by Sowmya et al. to mimic the structure of the periodontium [140].

Natural bones and dentin are typically porous biocomposites consisting of collagen and hydroxyapatite. Various methods have been developed to mimic porous bone scaffolds including freeze casting, electrospinning, and 3D printing of collagen and hydroxyapatite solution. As a new approach, a polymer-induced liquid precursor process can be used to produce the nanostructure of mineralized collagen scaffolds. Ye et al. used this biomimetic process and then coated the mineralized collagen fibrils with GL13K AMP, derived from salivary protein for bone and dental regeneration [92]. GL13K showed strong binding with the mineralized collagen fibril owing to its self-assembly potency that can provide a sustained antimicrobial property to the scaffold. The amphipathic nature of GL13K can help to form a coating with a large loading of the peptide on highly polar and hydrophilic mineralized collagen fibrils [92].

In one study, a combination of silk fibroin and hydroxyapatite was used to electrospin on a titanium plate to mimic the bone structure. Then, the plate coated with fibers was immersed into a dopamine solution and subsequently, HHC-36 AMP was immobilized on the fabricated fibers through dopamine as a linker. The cumulative release profile of the HHC-36 exhibited a burst release within three hours, followed by a steady release over 48 h. The prepared implant could eradicate the *E. coli* and *S. aureus* bacteria within 3 hr and maintain the antimicrobial activity for up to 21 days [93].

Requirements for the high temperature sintering, poor mechanical properties, and brittleness of hydroxyapatite have limited its applicability. Calcium aluminium oxide (CaAlO) has been recently introduced as a bioceramic for bone scaffold applications. Buckholtz et al. prepared a bioceramic composite of CaAlO and hydroxyapatite to combine the strength of CaAlO with the biocompatibility of hydroxyapatite. To improve its antimicrobial properties, its surface was functionalized with Inverso-CysHHC10 antimicrobial peptide using an alkene-thiol reaction [105]. The developed alkene-thiol linker can be applied for the immobilization of peptides which include sacrificial thiol functionality, onto surfaces containing reactive hydroxyl groups. At first, the surface of the implant was modified with an alkene terminated organic film to act as a spacer. Then, the AMP was immobilized through sacrificial cysteine residues. The composite implant with 5% hydroxyapatite showed improved osteoblast activity. The immobilization of Inverso-CysHHC10 had no effect on the osteoblast response of the composite [105].

5.4.4 Bioceramic Micro/Nanoparticles for Drug Delivery and Infection Treatments

Bioceramic microparticles and nanoparticles have broad applications in drug and gene delivery. Ceramic particles made of calcium phosphate play an important role in drug delivery particularly for bone tissues because of excellent biocompatibility, non-immunogenicity, low toxicity, and important osteoconductivity. However, the

mechanism of degradation of ceramic micro/nanoparticles in the biological environment has not been fully understood raising concerns about the biocompatibility of the degradation products. Tsikourkitoudi et al. loaded the AMP LL-37 on calcium phosphate nanoparticles by the physisorption technique [97]. The stability of the loaded AMP on calcium phosphate nanocarriers and its antimicrobial efficiency against *E. coli* and *S. pnuemoniae* was studied and it was reported that loading of LL-37 on calcium phosphate nanoparticles retained the peptide functionality. Moreover, it was also indicated that the antimicrobial mechanism was mainly direct bacterial contact with LL-37 loaded nanoparticles.

Recently, mesoporous silica nanoparticles (MSNs) have attracted great attention as drug nanocarriers because of high loading capacity, large tunable pore volume, and high surface area. The negatively charged silicate ions on the surface of MSNs bring about electrostatic attraction of the cationic drug molecules, particularly cationic antimicrobial peptides. However, MSNs cannot qualify to be a perfect drug carrier, since the porous structure does not provide controlled and sustained release of AMP. To address this critical issue, MSNs are mainly coated with biocompatible polymeric shells to facilitate controlled release as well as amend the biocompatibility of the MSNs. Lu et al. also designed a smart drug delivery system which could be triggered by sensing the motion of swarmer bacteria (*P. mirabilis*). At first, tobramycin was loaded on MSNs. Then, a copolymer based on N-isopropylacrylamide and aminoethyl methacrylate (pNIPAAm-co-pAEMA) was used to cover the AMP-loaded silica nanoparticles through the electrostatic attraction. The pNIPAAm-co-pAEMA chains were also conjugated to the peptide ligands showing the affinity to Gram-negative bacteria. When the *P. mirabilis* came in contact with the MSNs, the AMP immobilized copolymer chains could bind to the lipopolysaccharides on the bacteria membrane. While the bacteria moved away, the AMP-loaded copolymer was stripped off, and consequently, the tobramycin was released from the MSNs into the colony and inhibited the bacteria expansion [141].

A drug carrier composed of colistin-loaded MSN, liposomal shell, and LL-37 was developed as a targeting AMP for lung infections. The liposome layer could degrade after exposure to lipase excreted from *P. aeruginosa* and allow the encapsulated AMP-loaded MSNs to be released. Therefore, there is a considerable increase in the AMP release when the bacteria are present in the biological environment compared to the absence of the bacteria [142].

Some bacteria are able to uptake and reduce gold compounds, and finally, excrete them in the shape of pure gold nanoparticles. To that end, recently, gold and ceramic nanocomposites have been used to design a novel analog to antimicrobial peptides as a stable and effective replacement for silver-based antimicrobials. Vukomanovic et al. developed hydroxyapatite/gold nanoparticles functionalized with arginine using a sonochemical method. The sonification of the arginine solution formed reactive radicals reducing the gold precursor and creating hydroxyapatite/gold nanocomposites with attached arginine remains as shown schematically in Fig. 5.7 [143]. The designed antimicrobial nanocomposite could provide efficient treatment of infections and were vastly applicable in the biomedicine field.

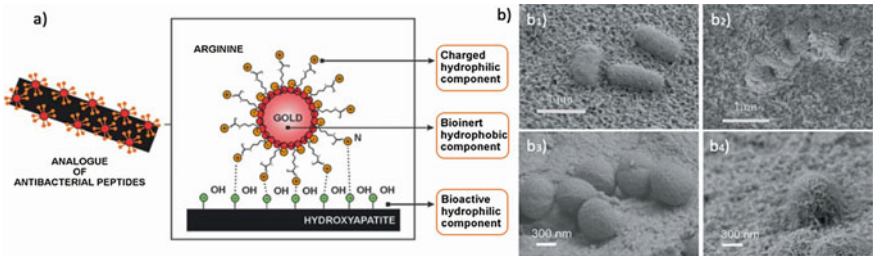

Fig. 5.7 **a** Schematic structure of the hydroxyapatite/gold nanocomposites functionalized with AMP arginine; **b** morphology of intact *E. coli* and *S. aureus* (b_1, b_3) and incubated bacteria with AMP immobilized hydroxyapatite/gold nanocomposites (b_2, b_4) (Reprint with permission from [143])

Despite the remarkable progress and variety of strategies to create antimicrobial bioceramic surfaces, some critical challenges still remain. Long-term stability along with controlled release of AMPs, storage concerns, cytotoxicity, and un-optimized mechanical properties are the most challenging issues which still require to be undertake in order to make them clinically acceptable.

5.5 Conclusions and Future Challenges

The application of ceramics as biomaterials is well established owing to their high hardness, resistance to compression, biocompatibility, as well as their corrosion resistance. Moreover, their surface physiochemical properties facilitate the adhesion of biological moieties for the recapitulation of hard tissues. Bioceramics have come a long way from simple scaffolds for orthopedics and dental applications to organic–inorganic composites and mesoporous silicas for drug delivery technologies. The combination of osteoinductive properties of bioceramics and antimicrobial functionality of peptides immobilized on bioceramics would allow the development of implants that stimulate bone formation while simultaneously providing an antimicrobial mechanism against chronic infections.

This chapter summarized fundamental concepts in designing and synthesizing AMPs used for bioceramics functionalization. AMPs have a broad-spectrum activity, anti-biofilm activity and have the ability to favorably regulate the host's immune response. These functionalization strategies based on covalent and non-covalent conjugation of AMPs to bioceramics can provide sustained release for short- and long-term antimicrobial activities. So far, many studies have examined various strategies of AMP immobilizations for different forms of bioceramics such as scaffolds, coatings, composites, and micro/nanoparticles in order to endow them with antimicrobial activities for particular biomedical applications. However, insufficient verification from clinical trials restricts the application of AMPs. In this regard, some critical areas related to AMP coatings remain for further investigation. Long-term

stability along with the controlled release of AMPs, storage concerns, cytotoxicity, and un-optimized mechanical properties are among the most challenging issues to be tackled.

According to the studies, some amino acids are susceptible to oxidation and/or moisture absorption upon exposure to the air [144]. Difficult storage conditions may limit the utilization of AMP coatings which has to be tackled as a future challenge. In addition, the stability and half-life of the immobilized AMPs in in vivo conditions are still less known and should be explored in clinical trials. Another challenge that restricts the development of AMP coatings is the presence of peptidases (proteolytic enzymes) in vivo which weaken the antimicrobial activity of AMPs. Some studies have encapsulated AMPs into liposomes to protect them from peptidases [145]. However, sustained release of AMPs at an effective dosage needs to be addressed. Smart release of AMPs can be considered as one of the most promising directions for the future. Smart AMP coatings can respond to a variety of internal or external stimuli such as temperature, pH, bacteria presence, peri-implant changes, as well as magnetic field and UV irradiation. Ideally, such smart systems can sense particular changes and independently adjust their properties for AMP releasing.

Computational design and modelling have remarkably evolved over the years to accelerate AMP coatings design and optimize AMP sequences to improve biological activities. The de novo design, linguistic modelling, genetic algorithms, pattern insertion methods, as well as machine learning methods can be employed to design novel and hidden peptides with promising antimicrobial functionalities. The data achieved by computational design can present structure diversity, sequence optimization, accelerated trade-off resolutions, in vivo activity, and therapeutic indices; but these computer-designed AMPs have not been translated into clinical products yet.

In pre-clinical tests, most of the research studies proved remarkable bacterial inhibition or reduction using AMP coatings, but the issue of time duration while bioceramics are implanted in the body, needs to be addressed. Compared to the realistic time for implanted bioceramics, in vitro tests are extremely short and therefore, offer no practical parallel to clinical infections. Moreover, the interactions between implanted bioceramics and body tissues present more realistic challenges than bioceramics alone. These interactions may explain why many products showing high antimicrobial efficacy in vitro fail to have similar behavior in vivo.

Overall, AMP immobilization on bioceramics has shown great potentials for hard tissue engineering. However, their wide-spread clinical applications require extensive, more physiologically realistic pre-clinical investigations intertwined with advances of computational designs and modelling.

References

1. Agrawal S, Srivastava R (2020) Osteoinductive and osteoconductive biomaterials. In: Li B, Moriarty T, Webster T et al (eds) Racing for the surface. Springer, Cham, pp 355–395
2. Shekhawat D, Singh A, Banerjee MK et al (2021) Bioceramic composites for orthopaedic applications: a comprehensive review of mechanical, biological, and microstructural properties. Ceram Int 47:3013–3030
3. Gerhardt LC, Boccaccini AR (2010) Bioactive glass and glass-ceramic scaffolds for bone tissue engineering. Materials 3:3867–3910
4. Thamaraiselvi TV, Rajeswari S (2004) Biological evaluation of bioceramic materials—a review. Trends Biomater Artif Organs 18:9–17
5. Mazzoni E, Iaquinta MR, Lanzillotti C et al (2021) Bioactive materials for soft tissue repair. Front Bioeng Biotechnol 9:613787
6. Dorozhkin SV (2015) Calcium orthophosphate bioceramics. Ceram Int 41:13913–13966
7. Devgan S, Sidhu SS (2019) Evolution of surface modification trends in bone related biomaterials: a review. Mater Chem Phys 233:68–78
8. Raphel J, Holodniy M, Goodman SB et al (2016) Multifunctional coatings to simultaneously promote osseointegration and prevent infection of orthopaedic implants. Biomaterials 84:301–314
9. Sjollema J, Zaat SAJ, Fontaine V et al (2018) *In vitro* methods for the evaluation of antimicrobial surface designs. Acta Biomater 70:12–24
10. Engelsman AF, Saldarriaga-Fernandez IC, Nejadnik MR et al (2010) The risk of biomaterial-associated infection after revision surgery due to an experimental primary implant infection. Biofouling 26:761–767
11. Grainger DW, van der Mei HC, Jutte PC et al (2013) Critical factors in the translation of improved antimicrobial strategies for medical implants and devices. Biomaterials 34:9237–9243
12. Busscher HJ, Ploeg RJ, van der Mei HC (2009) SnapShot: biofilms and biomaterials; mechanisms of medical device related infections. Biomaterials 30:4247–4248
13. Campoccia D, Montanaro L, Arciola CR (2013) A review of the biomaterials technologies for infection-resistant surfaces. Biomaterials 34:8533–8554
14. Souza JGS, Bertolini MM, Costa RC et al (2020) Targeting implant-associated infections: titanium surface loaded with antimicrobial. iScience 24:102008
15. Hasan J, Crawford RJ, Ivanova EP (2013) Antibacterial surfaces: the quest for a new generation of biomaterials. Trends Biotechnol 31:295–304
16. Narayana PSVVS, Srihari PSVV (2020) A review on surface modifications and coatings on implants to prevent biofilm. Regen Eng Transl Med 6:330–346
17. Regi MV, Esbrit P, Salinas AJ (2020) Degradative effects of the biological environment on ceramic biomaterials. In: Wagner WR, Sakiyama-Elbert SE, Zhang G et al (eds) Biomaterials science, 4th edn. Academic Press, Massachusetts, pp 955–971
18. Naidu N, Wadher K, Umekar M (2021) An overview on biomaterials: pharmaceutical and biomedical applications. J Drug Deliv Ther 11:154–161
19. Tangcharoensathien V, Sattayawutthipong W, Kanjanapimai S et al (2017) Antimicrobial resistance: from global agenda to national strategic plan, Thailand. Bull World Health Organ 95:599–603
20. Tenover FC (2006) Mechanisms of antimicrobial resistance in bacteria. Am J Med 119:S3–10; discussion S62–70
21. Gelband H, Miller-Petrie M, Pant S et al (2015) The state of the world's antibiotics. In: The center for disease dynamics, economics and policy. https://cddep.org/wp-content/uploads/2017/06/swa_edits_9.16.pdf. Accessed 18 Apr 2021
22. Magana M, Pushpanathan M, Santos AL et al (2020) The value of antimicrobial peptides in the age of resistance. Lancet Infect Dis 20:e216–e230
23. Mookherjee N, Anderson MA, Haagsman HP et al (2020) Antimicrobial host defence peptides: functions and clinical potential. Nat Rev Drug Discov 19:311–332

24. Zhang LJ, Gallo RL (2016) Antimicrobial peptides. Curr Biol 26:R14–R19
25. Wang G, Mishra B, Lau K et al (2015) Antimicrobial peptides in 2014. Pharmaceuticals 8:123–150
26. Giangaspero A, Sandri L, Tossi A (2001) Amphipathic alpha helical antimicrobial peptides. Eur J Biochem 268:5589–5600
27. Liu X, Cao R, Wang S et al (2016) Amphipathicity determines different cytotoxic mechanisms of lysine- or arginine-rich cationic hydrophobic peptides in cancer cells. J Med Chem 59:5238–5247
28. Mura M, Wang J, Zhou Y et al (2016) The effect of amidation on the behaviour of antimicrobial peptides. Eur Biophys J 45:195–207
29. Jenssen H, Hamill P, Hancock RE (2006) Peptide antimicrobial agents. Clin Microbiol Rev 19:491–511
30. Wimley WC, Hristova K (2011) Antimicrobial peptides: successes, challenges and unanswered questions. J Membr Biol 239:27–34
31. Kumar P, Kizhakkedathu JN, Straus SK (2018) Antimicrobial peptides: diversity, mechanism of action and strategies to improve the activity and biocompatibility *in vivo*. Biomolecules 8:4
32. Fjell CD, Hiss JA, Hancock RE et al (2011) Designing antimicrobial peptides: form follows function. Nat Rev Drug Discov 11:37–51
33. Shah P, Hsiao FS, Ho YH et al (2016) The proteome targets of intracellular targeting antimicrobial peptides. Proteomics 16:1225–1237
34. Zhao H, To KKW, Sze KH et al (2020) A broad-spectrum virus- and host-targeting peptide against respiratory viruses including influenza virus and SARS-CoV-2. Nat Commun 11:4252
35. Wang G (2013) Database-guided discovery of potent peptides to combat HIV-1 or superbugs. Pharmaceuticals 6:728–758
36. Maiti BK (2020) Potential role of peptide-based antiviral therapy against SARS-CoV-2 infection. ACS Pharmacol Transl Sci 3:783–785
37. Ordonez SR, Amarullah IH, Wubbolts RW et al (2014) Fungicidal mechanisms of cathelicidins LL-37 and CATH-2 revealed by live-cell imaging. Antimicrob Agents Chemother 58:2240–2248
38. Puri S, Edgerton M (2014) How does it kill?: understanding the candidacidal mechanism of salivary histatin 5. Eukaryot Cell 13:958–964
39. Hoskin DW, Ramamoorthy A (2008) Studies on anticancer activities of antimicrobial peptides. Biochim Biophys Acta 1778:357–375
40. Hancock RE, Sahl HG (2006) Antimicrobial and host-defense peptides as new anti-infective therapeutic strategies. Nat Biotechnol 24:1551–1557
41. Boman HG (2003) Antibacterial peptides: basic facts and emerging concepts. J Intern Med 254:197–215
42. Hanson MA, Dostálová A, Ceroni C et al (2019) Synergy and remarkable specificity of antimicrobial peptides *in vivo* using a systematic knockout approach. Elife 8:e44341
43. Fazly Bazzaz BS, Seyedi S, Hoseini Goki N et al (2021) Human antimicrobial peptides: spectrum, mode of action and resistance mechanisms. Int J Pept Res Ther 27:801–816
44. Ganz T (2003) Defensins: antimicrobial peptides of innate immunity. Nat Rev Immunol 3:710–720
45. Xu D, Lu W (2020) Defensins: a double-edged sword in host immunity. Front Immunol 11:764
46. Amerikova M, El-Tibi IP, Maslarska V et al (2019) Antimicrobial activity, mechanism of action, and methods for stabilisation of defensins as new therapeutic agents. Biotechnol Biotechnol Equip 33:671–682
47. van Harten RM, van Woudenbergh E, van Dijk A et al (2018) Cathelicidins: immunomodulatory antimicrobials. Vaccines 6:63
48. Melino S, Santone C, Di Nardo P et al (2014) Histatins: salivary peptides with copper(II)- and zinc(II)-binding motifs: perspectives for biomedical applications. FEBS J 281:657–672
49. Cardoso P, Glossop H, Meikle TG et al (2021) Molecular engineering of antimicrobial peptides: microbial targets, peptide motifs and translation opportunities. Biophys Rev 13:1–35

50. Feng X, Sambanthamoorthy K, Palys T et al (2013) The human antimicrobial peptide LL-37 and its fragments possess both antimicrobial and antibiofilm activities against multidrug-resistant *Acinetobacter baumannii*. Peptides 49:131–137
51. de Breij A, Riool M, Cordfunke RA et al (2018) The antimicrobial peptide SAAP-148 combats drug-resistant bacteria and biofilms. Sci Transl Med 10:eaan4044
52. Li T, Wang N, Chen S et al (2017) Antibacterial activity and cytocompatibility of an implant coating consisting of TiO_2 nanotubes combined with a GL13K antimicrobial peptide. Int J Nanomedicine 12:2995–3007
53. Stallmann HP, Faber C, Bronckers AL et al (2004) Osteomyelitis prevention in rabbits using antimicrobial peptide hLF1-11- or gentamicin-containing calcium phosphate cement. J Antimicrob Chemother 54:472–476
54. Cardoso MH, Orozco RQ, Rezende SB et al (2020) Computer-aided design of antimicrobial peptides: are we generating effective drug candidates? Front Microbiol 10:3097
55. Müller AT, Hiss JA, Schneider G (2018) Recurrent neural network model for constructive peptide design. J Chem Inf Model 58:472–479
56. Kazemzadeh-Narbat M, Noordin S, Masri BA et al (2012) Drug release and bone growth studies of antimicrobial peptide-loaded calcium phosphate coating on titanium. J Biomed Mater Res B Appl Biomater 100:1344–1352
57. Fjell CD, Jenssen H, Hilpert K et al (2009) Identification of novel antibacterial peptides by chemoinformatics and machine learning. J Med Chem 52:2006–2015
58. Cleophas RT, Sjollema J, Busscher HJ et al (2014) Characterization and activity of an immobilized antimicrobial peptide containing bactericidal PEG-hydrogel. Biomacromol 15:3390–3395
59. Huang ZB, Shi X, Mao J et al (2016) Design of a hydroxyapatite-binding antimicrobial peptide with improved retention and antibacterial efficacy for oral pathogen control. Sci Rep 6:38410
60. Na DH, Faraj J, Capan Y et al (2007) Stability of antimicrobial decapeptide (KSL) and its analogues for delivery in the oral cavity. Pharm Res 24:1544–1550
61. Wang M, Tang T (2018) Surface treatment strategies to combat implant-related infection from the beginning. J Orthop Translat 17:42–54
62. Wang Y, Jayan G, Patwardhan D et al (2017) Antimicrobial and anti-biofilm medical devices: public health and regulatory science challenges. In: Zhang Z, Wagner V (eds) Antimicrobial coatings and modifications on medical devices. Springer, Cham, pp 37–65
63. Hassert R, Beck-Sickinger AG (2013) Tuning peptide affinity for biofunctionalized surfaces. Eur J Pharm Biopharm 85:69–77
64. Xiao X, Zhao W, Liang J et al (2020) Self-defensive antimicrobial biomaterial surfaces. Colloids Surf B Biointerfaces 192:110989
65. Wei T, Yu Q, Chen H (2019) Responsive and synergistic antibacterial coatings: fighting against bacteria in a smart and effective way. Adv Healthc Mater 8:e1801381
66. Wei T, Tang Z, Yu Q et al (2017) Smart antibacterial surfaces with switchable bacteria-killing and bacteria-releasing capabilities. ACS Appl Mater Interfaces 9:37511–37523
67. Pinto IB, dos Santos Machado L, Meneguetti BT et al (2019) Utilization of antimicrobial peptides, analogues and mimics in creating antimicrobial surfaces and bio-materials. Biochem Eng J 150:107237
68. Thamma U, Kowal TJ, Falk MM et al (2021) Nanostructure of bioactive glass affects bone cell attachment via protein restructuring upon adsorption. Sci Rep 11:5763
69. Moussa DG, Aparicio C (2020) Targeting the oral plaque microbiome with immobilized anti-biofilm peptides at tooth-restoration interfaces. PLoS One 15:e0235283
70. Honda M, Matsumoto M, Aizawa M (2020) Potential application of protamine for antimicrobial biomaterials in bone tissue engineering. Int J Mol Sci 21:4368
71. Kazemzadeh-Narbat M, Kindrachuk J, Duan K et al (2010) Antimicrobial peptides on calcium phosphate-coated titanium for the prevention of implant-associated infections. Biomaterials 31:9519–9526
72. Costa F, Carvalho IF, Montelaro RC et al (2011) Covalent immobilization of antimicrobial peptides (AMPs) onto biomaterial surfaces. Acta Biomater 7:1431–1440

73. Kazemzadeh-Narbat M, Cheng H, Chabok R et al (2021) Strategies for antimicrobial peptide coatings on medical devices: a review and regulatory science perspective. Crit Rev Biotechnol 41:94–120
74. Yazici H, Habib G, Boone K et al (2019) Self-assembling antimicrobial peptides on nanotubular titanium surfaces coated with calcium phosphate for local therapy. Mater Sci Eng C Mater Biol Appl 94:333–343
75. Chen J, Zhu Y, Song Y et al (2017) Preparation of an antimicrobial surface by direct assembly of antimicrobial peptide with its surface binding activity. J Mater Chem B 5:2407–2415
76. Costa F, Gomes P, Martins MCL (2018) Antimicrobial peptides (AMP) biomaterial coatings for tissue repair. In: Barbosa MA, Cristina L. Martins M (eds) Peptides and proteins as biomaterials for tissue regeneration and repair. Woodhead Publishing, Cambridge, pp 329–345
77. Ma M, Kazemzadeh-Narbat M, Hui Y et al (2012) Local delivery of antimicrobial peptides using self-organized TiO_2 nanotube arrays for peri-implant infections. J Biomed Mater Res A 100:278–285
78. Wronska MA, O'Connor IB, Tilbury MA et al (2016) Adding functions to biomaterial surfaces through protein incorporation. Adv Mater 28:5485–5508
79. Micksch T, Herrmann E, Scharnweber D et al (2015) A modular peptide-based immobilization system for ZrO_2, TiZr and TiO_2 surfaces. Acta Biomater 12:290–297
80. De Zoysa GH, Sarojini V (2017) Feasibility study exploring the potential of novel battacin lipopeptides as antimicrobial coatings. ACS Appl Mater Interfaces 9:1373–1383
81. Hou R, Zou Z, Zhang J et al (2018) Novel osteogenic growth peptide C-terminal pentapeptide grafted poly(d, l-lactic acid) improves the proliferation and differentiation of osteoblasts: the potential bone regenerative biomaterial. Int J Biol Macromol 119:874–881
82. Soultan AH, Verheyen T, Smet M et al (2018) Synthesis and peptide functionalization of hyperbranched poly(arylene oxindole) towards versatile biomaterials. Polym Chem 9:2775–2784
83. Li S, Xu Y, Yu J et al (2017) Enhanced osteogenic activity of poly(ester urea) scaffolds using facile post-3D printing peptide functionalization strategies. Biomaterials 141:176–187
84. Maia FR, Barbosa M, Gomes DB et al (2014) Hydrogel depots for local co-delivery of osteoinductive peptides and mesenchymal stem cells. J Control Release 189:158–168
85. Lim K, Chua RR, Saravanan R et al (2013) Immobilization studies of an engineered arginine-tryptophan-rich peptide on a silicone surface with antimicrobial and antibiofilm activity. ACS Appl Mater Interfaces 5:6412–6422
86. Gao G, Lange D, Hilpert K et al (2011) The biocompatibility and biofilm resistance of implant coatings based on hydrophilic polymer brushes conjugated with antimicrobial peptides. Biomaterials 32:3899–3909
87. Pan G, Sun S, Zhang W et al (2016) Biomimetic design of mussel-derived bioactive peptides for dual-functionalization of titanium-based biomaterials. J Am Chem Soc 138:15078–15086
88. Phelps EA, Enemchukwu NO, Fiore VF et al (2012) Maleimide cross-linked bioactive PEG hydrogel exhibits improved reaction kinetics and cross-linking for cell encapsulation and *in situ* delivery. Adv Mater 24:64–70
89. Swartjes JJ, Sharma PK, van Kooten TG et al (2015) Current developments in antimicrobial surface coatings for biomedical applications. Curr Med Chem 22:2116–2129
90. Cleophas TC (2018) Immobilization of stabilized antimicrobial peptides into a bactericidal hydrogel coating. Dissertation, Utrecht University
91. Jiang H, Xu FJ (2013) Biomolecule-functionalized polymer brushes. Chem Soc Rev 42:3394–3426
92. Ye Z, Zhu X, Mutreja I et al (2021) Biomimetic mineralized hybrid scaffolds with antimicrobial peptides. Bioact Mater 6:2250–2260

93. Abbasizadeh N, Rezayan AH, Nourmohammadi J et al (2020) HHC-36 antimicrobial peptide loading on silk fibroin (SF)/hydroxyapatite (HA) nanofibrous-coated titanium for the enhancement of osteoblast and bactericidal functions. Int J Polym Mater Polym BIomat 10:629–639
94. Fateme R, Fatemeh G, Sima S et al (2020) New engineered fusion peptide with dual functionality: antibacterial and strong binding to hydroxyapatite. Int J Pept Res Ther 26:1629–1639
95. Wang N, Yu X, Kong Q et al (2020) Nisin-loaded polydopamine/hydroxyapatite composites: biomimetic synthesis, and *in vitro* bioactivity and antibacterial activity evaluations. Colloids Surf A Physicochem Eng Asp 602:125101
96. Yu Q, Deng T, Lin FC et al (2020) Supramolecular assemblies of heterogeneous mesoporous silica nanoparticles to co-deliver antimicrobial peptides and antibiotics for synergistic eradication of pathogenic biofilms. ACS Nano 14:5926–5937
97. Tsikourkitoudi V, Karlsson J, Merkl P et al (2020) Flame-made calcium phosphate nanoparticles with high drug loading for delivery of biologics. Molecules 25:1747
98. Yasir M, Dutta D, Hossain KR et al (2020) Mechanism of action of surface immobilized antimicrobial peptides against pseudomonas aeruginosa. Front Microbiol 10:3053
99. Fujiki M, Abe K, Hayakawa T et al (2019) Antimicrobial activity of protamine-loaded calcium phosphates against oral bacteria. Materials 12:2816
100. Torres LMFC, Almeida MT, Santos TL et al (2019) Antimicrobial alumina nanobiostructures of disulfide- and triazole-linked peptides: synthesis, characterization, membrane interactions and biological activity. Colloids Surf B Biointerfaces 177:94–104
101. Melicherčík P, Nešuta O, Čeřovský V (2018) Antimicrobial peptides for topical treatment of osteomyelitis and implant-related infections: study in the spongy bone. Pharmaceuticals 11:20
102. Melicherčík P, Čeřovský V, Nešuta O et al (2018) Testing the efficacy of antimicrobial peptides in the topical treatment of induced osteomyelitis in rats. Folia Microbiol 63:97–104
103. Torres LMFC, Braga NA, Gomes IP et al (2018) Nanobiostructure of fibrous-like alumina functionalized with an analog of the BP100 peptide: Synthesis, characterization and biological applications. Colloids Surf B Biointerfaces 163:275–283
104. Townsend L, Williams RL, Anuforom O et al (2017) Antimicrobial peptide coatings for hydroxyapatite: electrostatic and covalent attachment of antimicrobial peptides to surfaces. J R Soc Interface 14(126):20160657
105. Buckholtz GA, Reger NA, Anderton WD et al (2016) Reducing Escherichia coli growth on a composite biomaterial by a surface immobilized antimicrobial peptide. Mater Sci Eng C Mater Biol Appl 65:126–134
106. Braun K, Pochert A, Lindén M et al (2016) Membrane interactions of mesoporous silica nanoparticles as carriers of antimicrobial peptides. J Colloid Interface Sci 475:161–170
107. Tian J, Shen S, Zhou C et al (2015) Investigation of the antimicrobial activity and biocompatibility of magnesium alloy coated with HA and antimicrobial peptide. J Mater Sci Mater Med 26:66
108. Kazemzadeh-Narbat M, Wang Q, Hancock REW (2014) Antimicrobial peptide delivery from trabecular bone grafts. J Biomater Tissue Eng 4:967–972
109. Kazemzadeh-Narbat M, Lai BF, Ding C et al (2013) Multilayered coating on titanium for controlled release of antimicrobial peptides for the prevention of implant-associated infections. Biomaterials 34:5969–5977
110. Holmberg KV, Abdolhosseini M, Li Y et al (2013) Bio-inspired stable antimicrobial peptide coatings for dental applications. Acta Biomater 9:8224–8231
111. van Staden AD, Brand AM, Dicks LM (2012) Nisin F-loaded brushite bone cement prevented the growth of Staphylococcus aureus *in vivo*. J Appl Microbiol 112:831–840
112. Williams RL, Hadley MJ, Jiang PJ et al (2013) Thiol modification of silicon-substituted hydroxyapatite nanocrystals facilitates fluorescent labelling and visualisation of cellular internalisation. J Mater Chem B 1:4370–4378

113. Eckert R, He J, Yarbrough DK et al (2006) Targeted killing of Streptococcus mutans by a pheromone-guided "smart" antimicrobial peptide. Antimicrob Agents Chemother 50:3651–3657
114. Fernandez-Garcia E, Chen X, Gutierrez-Gonzalez CF et al (2015) Peptide-functionalized zirconia and new zirconia/titanium biocermets for dental applications. J Dent 43:1162–1174
115. Geetha M, Singh AK, Asokamani R et al (2009) Ti based biomaterials, the ultimate choice for orthopaedic implants—a review. Prog Mater Sci 54:397–425
116. de Jonge LT, Leeuwenburgh SC, Wolke JG et al (2008) Organic-inorganic surface modifications for titanium implant surfaces. Pharm Res 25:2357–2369
117. Smith AM, Paxton JZ, Hung YP et al (2015) Nanoscale crystallinity modulates cell proliferation on plasma sprayed surfaces. Mater Sci Eng C Mater Biol Appl 48:5–10
118. He FM, Yang GL, Li YN et al (2009) Early bone response to sandblasted, dual acid-etched and H_2O_2/HCl treated titanium implants: an experimental study in the rabbit. Int J Oral Maxillofac Surg 38:677–681
119. Sun L, Berndt CC, Gross KA et al (2001) Material fundamentals and clinical performance of plasma-sprayed hydroxyapatite coatings: a review. J Biomed Mater Res 58:570–592
120. Kim MS, Ryu JJ, Sung YM (2007) One-step approach for nano-crystalline hydroxyapatite coating on titanium via micro-arc oxidation. Electrochem Commun 9:1886–1891
121. Albayrak O, El-Atwani O, Altintas S (2008) Hydroxyapatite coating on titanium substrate by electrophoretic deposition method: effects of titanium dioxide inner layer on adhesion strength and hydroxyapatite decomposition. Surf Coat Technol 202:2482–2487
122. Kim HW, Koh YH, Li LH et al (2004) Hydroxyapatite coating on titanium substrate with titania buffer layer processed by sol-gel method. Biomaterials 25:2533–2538
123. Habibovic P, Barrère F, Van Blitterswijk CA et al (2002) Biomimetic hydroxyapatite coating on metal implants. J Am Ceram Soc 85:517–522
124. Yan L, Leng Y, Weng LT (2003) Characterization of chemical inhomogeneity in plasma-sprayed hydroxyapatite coatings. Biomaterials 24:2585–2592
125. Civantos A, Martínez-Campos E, Ramos V et al (2017) Titanium coatings and surface modifications: toward clinically useful bioactive implants. ACS Biomater Sci Eng 3:1245–1261
126. Sano K, Shiba K (2003) A hexapeptide motif that electrostatically binds to the surface of titanium. J Am Chem Soc 125:14234–14235
127. Andrea A, Molchanova N, Jenssen H (2018) Antibiofilm peptides and peptidomimetics with focus on surface immobilization. Biomolecules 8:27
128. Liu Y, de Groot K, Hunziker EB (2009) Biomimetic mineral coatings in dental and orthopaedic implantology. Front Mater Sci China 3:154–162
129. Kim HM (2003) Ceramic bioactivity and related biomimetic strategy. Curr Opin Solid State Mater Sci 7:289–299
130. Adlhart C, Verran J, Azevedo NF et al (2018) Surface modifications for antimicrobial effects in the healthcare setting: a critical overview. J Hosp Infect 99:239–249
131. Donatan S, Yazici H, Bermek H et al (2009) Physical elution in phage display selection of inorganic-binding peptides. Mater Sci Eng C 29:14–19
132. Sarikaya M, Tamerler C, Jen AK et al (2003) Molecular biomimetics: nanotechnology through biology. Nat Mater 2:577–585
133. Rodriguez GM, Bowen J, Grossin D et al (2017) Functionalisation of Ti6Al4V and hydroxyapatite surfaces with combined peptides based on KKLPDA and EEEEEEEE peptides. Colloids Surf B Biointerfaces 160:154–160
134. Kilpadi KL, Chang PL, Bellis SL (2001) Hydroxylapatite binds more serum proteins, purified integrins, and osteoblast precursor cells than titanium or steel. J Biomed Mater Res 57:258–267
135. Zeng H, Chittur KK, Lacefield WR (1999) Analysis of bovine serum albumin adsorption on calcium phosphate and titanium surfaces. Biomaterials 20:377–384
136. Choi J, Konno T, Takai M et al (2012) Regulation of cell proliferation by multi-layered phospholipid polymer hydrogel coatings through controlled release of paclitaxel. Biomaterials 33:954–961

137. León B, Jansen J (eds) (2009) Thin calcium phosphate coatings for medical implants. Springer, New York
138. Song YY, Schmidt-Stein F, Bauer S et al (2009) Amphiphilic TiO_2 nanotube arrays: an actively controllable drug delivery system. J Am Chem Soc 131:4230–4232
139. Schnabelrauch M, Dubs M, Kautz AR et al (2018) Biofunctionalization of ceramic implant surfaces to improve their bone ingrowth behavior. Mater Sci Forum 941:2483–2488
140. Sowmya S, Mony U, Jayachandran P et al (2017) Tri-layered nanocomposite hydrogel scaffold for the concurrent regeneration of cementum, periodontal ligament, and alveolar bone. Adv Healthc Mater. https://doi.org/10.1002/adhm.201601251
141. Lu S, Bi W, Du Q et al (2018) Lipopolysaccharide-affinity copolymer senses the rapid motility of swarmer bacteria to trigger antimicrobial drug release. Nat Commun 9:4277
142. Rathnayake K, Patel U, Pham C et al (2020) Targeted delivery of antibiotic therapy to inhibit pseudomonas aeruginosa using lipid-coated mesoporous silica core-shell nanoassembly. ACS Appl Bio Mater 3:6708–6721
143. Vukomanović M, Logar M, Škapin SD et al (2014) Hydroxyapatite/gold/arginine: designing the structure to create antibacterial activity. J Mater Chem B 2:1557–1564
144. Turner A, Radburn-Smith K, Mushtaq A et al (2011) Storage and handling guidelines for custom peptides. Curr Protoc Protein Sci. https://doi.org/10.1002/0471140864.ps1812s64
145. Strömstedt AA, Pasupuleti M, Schmidtchen A (2009) Evaluation of strategies for improving proteolytic resistance of antimicrobial peptides by using variants of EFK17, an internal segment of LL-37. Antimicrob Agents Chemother 53:593–602

Pietro Riccio Pietro Riccio received his master's degree in biological sciences from the University of Naples Federico II, Italy, during which he was an intern at the Institute of Biochemistry and Cell Biology of the National Research Council of Naples. Here, he worked in the marine drug discovery field, focusing on the research of antimicrobial molecules from Antarctic bacteria to fight the most common multidrug resistance human pathogens. Pietro followed his interest in drug discovery by moving towards material sciences. Currently, he is an early-stage researcher at the University of Birmingham, England, in the laboratory of Dr. Artemis Stamboulis on a project on the design and synthesis of antimicrobial peptides immobilized on surfaces for orthopedic applications.

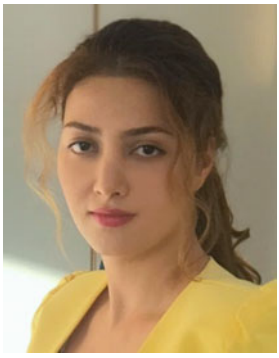

Mohadeseh Zare Mohadeseh Zare is an early-stage researcher within the Marie Sklodowska-Curie Innovative Training Network AIMed and a Ph.D. candidate in the School of Metallurgy and Materials at the University of Birmingham. She has two B.Sc. degrees in materials science and engineering and mechanical engineering. She also received an M.Sc. degree in materials science and engineering from Amirkabir University of Technology (AUT). From 2017 to 2019, she was a visiting researcher at the National University of Singapore (NUS) working on synthesizing and electrospinning of stimuli-responsive polymers utilized for programmed drug delivery systems. Her current research focuses on the synthesis of antimicrobial peptides and the development of new antimicrobial metallic, polymeric, and ceramic implants through

the surface functionalization with antimicrobial peptides for orthopaedic applications.

Diana Gomes Diana S. Gomes obtained her degree in biomedical sciences at the School of Health in the Polytechnic Institute of Porto in Portugal, including a one-year traineeship at major hospitals. Later, she took a degree in biotechnology at the University of Aveiro, with a final year project involving the study of native saltmarsh plants. In 2017, Diana obtained a master's degree in plant biotechnology and bio-entrepreneurship at the University of Minho to use natural plant compounds with recombinant-based natural polymers to create new antibacterial biomaterials. Following her master's thesis, she worked on an international research project developing bio-based antimicrobial materials. Later, she worked on a national project with an industrial partner, using natural compounds on polymeric materials for food packaging applications. From all those works, an interest in material sciences emerged, especially at the frontier of biological functionalization of surfaces. Currently, she is an Early-Stage Researcher at the University of Birmingham, working under the supervision of Dr Artemis Stamboulis on the surface functionalization of titanium surfaces with antimicrobial peptides for orthopedic applications.

David Green Dr. Green is a biomedical materials scientist with substantial expertise in biomimetic materials chemistry (BMC), and developing proto-cellular biomaterials and zoological biomatrices for regenerative ophthalmology, orthopedics, and dentistry. Dr Green has worked across the Asia–Pacific region, leading BMC groups in NZ, Australia, Hong Kong, Korea and Taiwan. He is now co-leading the biomaterials microfabrication facility, developing anti-microbial and proto-cellular bio-inks at the School of Metallurgy and Materials and the Institute of Inflammation and Ageing in the Medical School, University of Birmingham, UK.

Artemis Stamboulis Dr. Stamboulis obtained her first degree in biochemistry from the University of Athens in Greece, and her master's degree in polymer science and technology from UMIST, in the UK. She then obtained her Ph.D. in polymer engineering from the National Technical University of Athens. She completed her postdoctoral research as a Marie Curie Research Fellow and later as a Research Fellow working with biomedical glasses and glass–ceramics in the Department of Materials at Imperial College London. Then she spent one year as a lecturer in nanotechnology at NIBEC in the University of Ulster in Belfast, UK. She then moved to the University of Birmingham in the UK as a Birmingham Fellow in 2005. Since then, she has been working on the microstructural characterization of biomedical glasses, bioceramics and polymers. Recently, she has been developing novel antimicrobial peptides and antimicrobial medical surfaces using 3D printing in two Horizon 2020 research projects. Dr. Artemis is currently an Assoc. Professor and Reader in Biomaterials and has published more than 70 peer-reviewed research papers.

Chapter 6
Surface Functionalization of Titanium for the Control and Treatment of Infections

Masaya Shimabukuro

Abstract Titanium and its alloys are widely used as implant materials owing to their good mechanical properties and tissue compatibilities. Biomaterial-associated infections caused by biofilm formation are a major cause of failure of implant surgeries. Antibacterial biomaterials prevent biofilm formation at its initial stages. Titanium surfaces can be functionalized with various coating technologies to achieve antibacterial or anti-biofouling properties. In this chapter, we will describe titanium, biomaterial-associated infections, and therapeutic strategies using coating technologies and also focus on the use of micro-arc oxidation to prevent infections. Micro-arc oxidation is a conventional wet process involving electrochemical treatment with a specific electrolyte solution under high voltage, enabling the formation of a porous oxide layer on titanium surfaces owing to a micro-arc resulting from the dielectric breakdown of the titanium dioxide layer. This process can potentially help incorporate calcium and phosphorous ions into the surface layer by controlling the composition and concentration of the electrolyte. Micro-arc oxidation has already been used for titanium implants to promote hard-tissue compatibility. Since 2008, titanium surfaces have been modified by micro-arc oxidation treatment using an electrolyte with antibacterial elements such as silver, copper, and zinc to achieve an antibacterial property and biocompatibility on the titanium surface. In particular, the prevention of infectious diseases can be achieved by using micro-arc oxidation to design antibacterial biomaterials and alter the compositional control of the titanium surface.

Keywords Titanium · Infection · Biofilm · Surface treatment · Surface modification · Coating · Antibacterial · Antibiofouling · Micro-arc oxidation · Silver · Copper · Zinc

M. Shimabukuro (✉)
Department of Biomaterials, Faculty of Dental Science, Kyushu University, 3-1-1 Maidashi, Higashi-ku, Fukuoka 812-8582, Japan
e-mail: shimabukuro@dent.kyushu-u.ac.jp

A. H. Choi and B. Ben-Nissan (eds.), *Innovative Bioceramics in Translational Medicine I*,
Springer Series in Biomaterials Science and Engineering 17,
https://doi.org/10.1007/978-981-16-7435-8_6

6.1 Introduction—Titanium for Medical Applications Related to Hard Tissue

Metallic biomaterials are used in many medical devices, which comprise more than 70% of surgical implant devices, and more than 95% of orthopedic implants. Among them, titanium and its alloys are used as the main metallic biomaterials for functional reconstruction surgery, owing to their greater mechanical properties and tissue compatibility, compared with other metals [1]. Commercially pure (CP) titanium (grade 1, 2, 3, and 4) (ASTM F67), Ti–6Al–4V (ASTM F1108 and F1472), Ti–6Al–4V ELI (ASTM F136), Ti–6Al–7Nb (ASTM F1295), Ti–13Nb–13Zr (ASTM F1713), Ti–15Mo (ASTM F2066), and Ti–12Mo–6Zr–2Fe (ASTM F 1813) have been used for medical applications and are typical titanium-based metallic biomaterials.

Compared with other metals, titanium exhibits the specific interfacial reaction for bone tissue, called osteointegration. Osseointegration is defined as the "formation of a direct interface between an implant and bone, without intervening soft tissue. No scar tissue, cartilage, or ligament fibers are present between the bone and implant surface. The direct contact of bone and implant surface can be verified microscopically" [2]. The interfacial reaction between titanium and hard tissue was revealed at the micro- and nanometer scales [3–8] and promotes bone formation and bone bindings. This unique property is advantageous for the use of titanium in implant materials. The titanium surface is covered by an amorphous titanium oxide layer as a passive film. This oxide layer plays a key role in the corrosion resistance in vivo, with low toxicity [9–13].

The XPS survey- and narrow-scan spectra of the titanium surface are shown in Fig. 6.1. An amorphous oxide layer consisting of Ti^{2+}, Ti^{3+}, Ti^{4+}, and oxygen species with a thickness of approximately 6 nm was observed. The compositions of titanium and oxygen were 29 atm.% and 71 atm.% in the surface oxide layer, respectively [14]. The composition and chemical state of this layer gradually changed with the surrounding conditions such as dissolution and precipitation reactions which occur partially and repeatedly on the titanium surface. Among these reactions, the formation

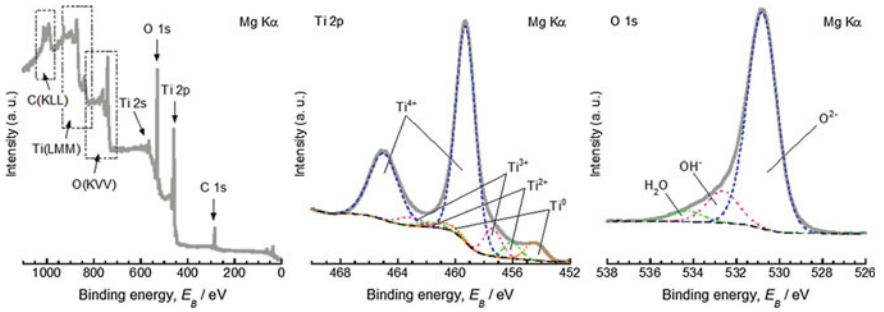

Fig. 6.1 XPS survey and narrow scan spectra obtained from titanium surface

of calcium phosphate is one of the key factors in hard tissue compatibility of titanium. A recent study revealed the details of the initial formation mechanism [15].

Despite greater hard tissue compatibility compared to other metals, there are several clinical issues related to titanium [1]. For example, biomaterial-associated infections caused by the formation of biofilms easily develop on the titanium surface and remain a critical issue. Therefore, therapeutic strategies to prevent biomaterial-associated infections on titanium surfaces are being actively explored. It should be noted that the bacterial and cellular adhesions for zirconium (Zr), niobium (Nb), and tantalum (Ta) substrates have been investigated [14]. These metals are used as β-stabilizer elements for β-type titanium alloys with low Young's modulus, which can prevent stress shielding and bone resorption.

6.2 Biomaterial-Associated Infections

Biomaterial-associated infections can occur on all biomaterial surfaces. Conservative treatments using antibiotics are required to prevent and mitigate biomaterial-associated infections, but often fail to improve the symptoms. These attempts incur additional health care costs, patient morbidities and eventual surgical replacement of the implant.

Titanium and its alloys are commonly used as medical implants and devices, and are beneficial in the reconstruction of lost human body function and diagnosis. Dental implants and prosthetic joints mainly consist of these materials as well. However, the use of these medical devices is hindered by the development of biomaterial-associated infections on their surfaces [16–20]. Peri-implantitis and prosthetic joint infections are serious complications in the dental and orthopedic fields. The current incidence rates of infections in various implant/device applications have been previously well summarized [21]. In addition, revision surgery to replace a total hip arthroplasty triples the cost of the primary implant procedure, amounting to an average of $75,000 [22, 23].

The formation of biofilms on the titanium surface is the main cause of these infections. Biofilms are hallmarks of extracellular polymeric matrix production [24]. Many bacteria such as *Streptococcus mutans*, *Staphylococcus epidermidis*, *Staphylococcus aureus*, *Escherichia coli*, and others, form biofilms and generate a variety of extracellular polymeric substances (EPS). Biofilms are the final state of bacterial infection that may persist despite treatment, exhibiting resistance against various antimicrobial agents, including antibiotics, because of their three-dimensional structure and the change in bacterial physiology [25–29]. Figure 6.2 shows the mechanism of biofilm formation on the titanium surface.

The invading bacteria initiate biofilm formation by adhering to the titanium surface, followed by growth, colony formation, EPS production, quorum sensing signaling, formation of nutrition channels, and finally biofilm formation. Bacterial invasion to the implanted site is caused by biological contamination during implant surgery or hematogenous spread of bacteria. After invasion, bacteria initially adhere

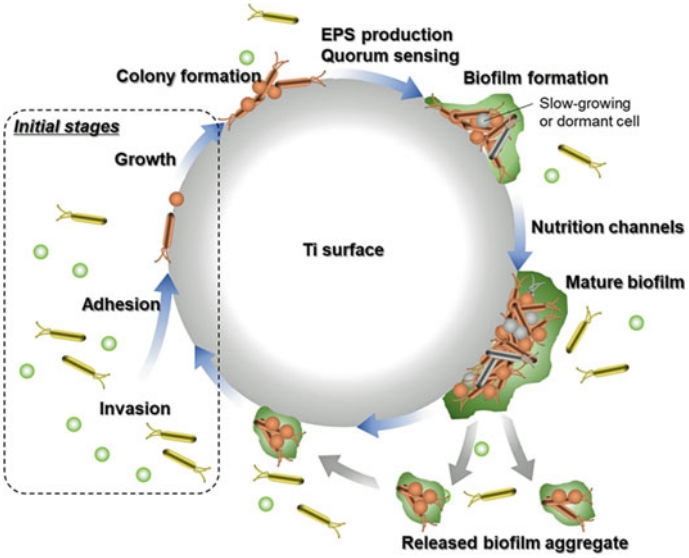

Fig. 6.2 Schematic image of the mechanism of biofilm formation on the titanium surface

to the titanium surface through cell-surface-associated adhesins [25, 30]. These adhesins may be a protein or polysaccharide base and play an important role in hard adhesion to the titanium surface. The attached bacteria then proliferate on the surface. These steps are the initial stages of biofilm formation. When the attached bacteria proliferate, they initiate the colonization and generation of the EPS matrix. The chemical and physical composition of the EPS matrix varies between species and growth conditions [25]. EPS production typically leads to enhanced adhesion of the bacteria embedded in the matrix. In addition to this, the interaction between bacteria and eukaryotic cells is promoted, for example, matrix components produced by some bacteria are required for the adhesion of the bacteria to a variety of protein components of the host cells at the onset of infection [31, 32].

The bacteria are also protected from antibiotics, antimicrobial agents, and host innate immune components owing to the EPS matrix [27, 33–35]. Therefore, the EPS matrix is a multi-functional scaffold that acts as a suitable microenvironment for bacteria, which can improve bacterial adhesion and provides protection from the external environment. Within the biofilm, the bacteria develop a quorum sensing system for communication. Quorum sensing is the regulated gene expression that occurs in response to fluctuations in cell density. The quorum sensing process controls and optimizes a variety of activities and leads to bacterial diversity in biofilms [36]. After the development of quorum sensing on biofilms, antibiotic therapy becomes ineffective due to both the appearance of dormant cells and slow growth. Moreover, mature biofilms release aggregates of EPSs, which can spread the infection. Often, the only way to eradicate the infection and prevent sepsis is to remove the contaminated device from the patient. To avoid this, biofilm formation must be prevented

on titanium surface by inhibiting the initial stage of biofilm formation during device implantation.

6.3 Coating Technologies for Preventing Infection on Titanium Surface

The therapeutic strategies for the prevention of biofilm formation, which are the main cause of biomaterial-associated infections, can be broadly divided into two groups: physical and mechanical approaches, and surface functionalization. Physical and mechanical approaches, such as high-velocity spray and jet irrigators, aim to remove and destroy biofilms. Some researchers have reported that exposure to high-velocity sprays induced instabilities in *S. mutants*, *S. epidermidis*, and *Pseudomonas aeruginosa* biofilms and that the physical interactions were different for the EPS produced by each bacterial species [37, 38]. Details of these strategies have been summarized elsewhere [39].

Surface functionalization based on surface coating technology aims to inhibit the initial stages of biofilm formation, namely bacterial invasion, adhesion, and growth. To date, numerous surface coating techniques have been studied to prevent biofilm formation. Titanium surfaces have been morphemically and compositionally controlled by dry or wet processes considered to be key functional processes in the prevention of the initial stage of biofilm formation, such as anti-biofouling and antibacterial properties. Figure 6.3 shows the anti-biofouling property that relies on the chemical and physical properties of the titanium surface, owing to titanium nitride (TiN) coating, polymer coating, and nanostructured surface. This property can

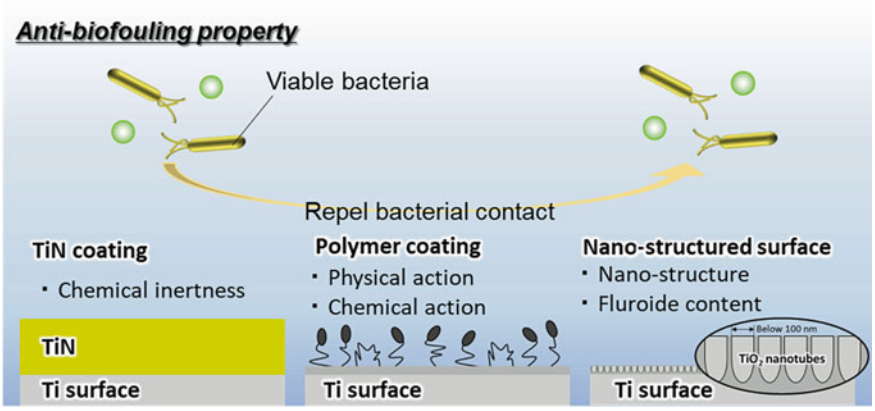

Fig. 6.3 Schematic illustration of anti-biofouling surfaces; TiN coating, polymer coating, and nanostructured surface

control biofilm formation in the absence of antibacterial agents, based on the anti-adhesion of bacteria. TiN coatings exhibit good chemical stability and resistance to high temperatures and corrosion, and its biocompatibility has also been reported [40]. Although not described in detail, it has been reported that the chemical stability of TiN is effective in suppressing bacterial adhesion [41–47].

Polymer coatings have been prepared by the immobilization of polyethylene oxide, polyethylene glycol, 2-methacryloyloxyethyl phosphoryl choline polymer, and other compounds [48–53]. The prevention of biofouling can be achieved with implant surfaces by the physical and chemical actions of polymers. The efficacies of these coatings were confirmed against many bacteria. Nano-structured surfaces are formed by anodic oxidation treatment using fluoride-containing electrolytes. The inhibitory effect on bacterial adhesion by the nanoscale textures formed on the titanium surface has been reported by [54, 55]. These studies concluded that the diameter of the nanotubes and the fluoride content in the surface influenced bacterial adhesion. Moreover, the 60 and 80 nm diameters are suitable for prevention of bacterial adhesion.

The antibacterial strategy has become a very active area of research for the prevention of biofilm formation. Antibacterial agents can kill the bacteria on the titanium surface, and prevent biofilm formation. Numerous antibiotics [56–60], antibacterial peptides [61–63], antibacterial elements [64–67], enzymes [68], organic cationic compounds [68], and organic non-cationic compounds [68] have been used as antibacterial agents. These antibacterial agents are incorporated onto the titanium surface. Bacteria that encounter this surface can be killed, nullifying their adhesion and growth. In addition, antibacterial photocatalytic therapy is demonstrated using TiO_2 based materials as bacteria being killed by reactive oxide species (ROS) [69, 70].

Dry and wet process coatings have been used to incorporate antibacterial elements onto the titanium surface. The dry process is performed at a high temperature, which can be a limitation depending on the target material. The wet process can incorporate antibacterial elements on implant surfaces at lower processing temperatures compared to that required for dry processes. A disadvantage of the wet process is that the strength of adhesion between the modified layer and the substrate is weaker than that fabricated by dry processes. Figure 6.4 shows a schematic illustration of the dry and wet process coatings on the titanium surface and the relationship between the processing temperatures and thickness of the coatings.

Plasma immersion ion implantation (PIII) incorporates and enriches antibacterial elements onto the Ti surface by plasma sheath generation. Jin et al. incorporated Ag and Zn onto the titanium surface by PIII [71]. Hydrothermal, chemical, and electrochemical treatments grow the surface oxide layer and incorporate antibacterial elements. Therefore, the thickness of these coatings is thicker than that of PIII. Hydrothermal treatment is used in combination with other coating technologies [72]. The immersion in alkaline solution is a typical chemical treatment. Kawashita et al. combined this technique with heat treatment, incorporating various metal ions onto the titanium surface [73]. Titania nanotubes and a porous oxide layer are formed by

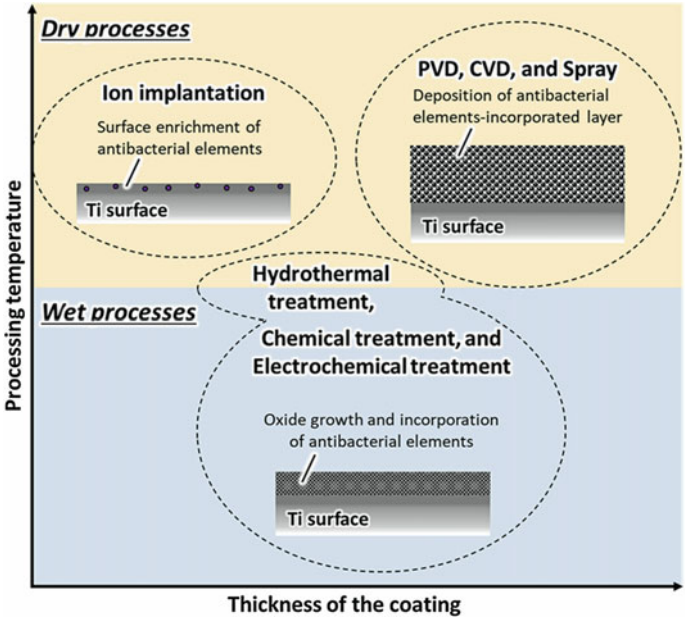

Fig. 6.4 Schematic illustration of dry and wet process coatings on titanium surfaces and their relationship between processing temperatures and thickness of coatings

electrochemical treatment. An example of electrochemical treatment will be introduced in the following section. Chemical vapor deposition (CVD), physical vapor deposition (PVD), and spray deposition can deposit a relatively thicker layers incorporated with antibacterial elements. These coating techniques for the incorporation of antibacterial elements onto the titanium surface have been previously summarized [74, 75].

6.4 Micro-arc Oxidation

Micro-arc oxidation (MAO), also known as anodic spark deposition (ASD) or plasma electrolytic oxidation (PEO), is an electrochemical treatment for valve metals. MAO, which is anodization with arc generation, is performed in a specific electrolyte under high voltage and high current density (Fig. 6.5a). The resultant oxide layer exhibits good adhesive strength between the layer and the substrate because the oxide layer grows in the direction of the titanium substrate at the interface of the titanium surface and the electrolyte. In addition, the typical porous oxide layer is formed by the generation of sparks, and the elements comprising the electrolyte are incorporated into the oxide layer (Fig. 6.5b, c).

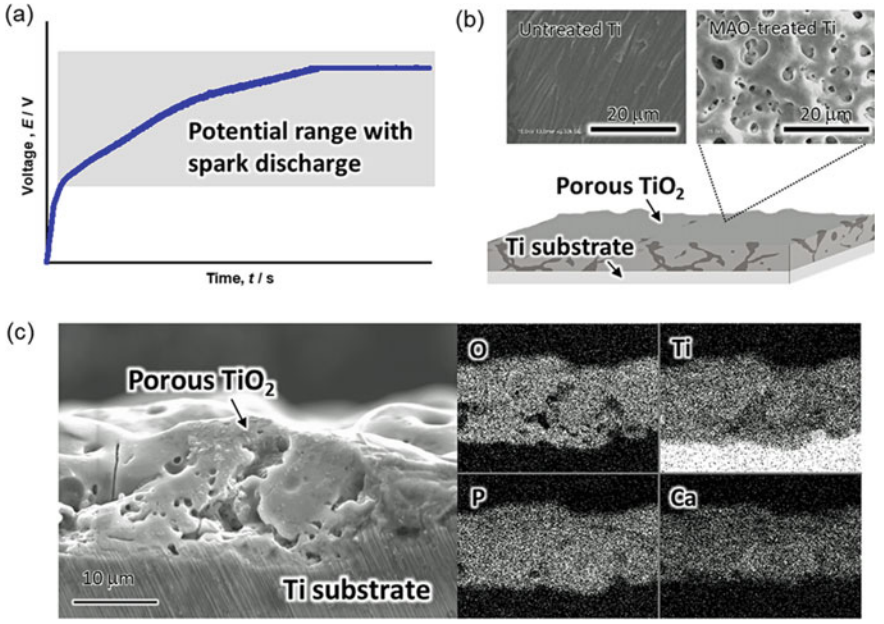

Fig. 6.5 Conceptual diagram of volt-time curve of MAO treatment for titanium (**a**), scanning electron microscopy (SEM) images of titanium surface before and after MAO (**b**), and the energy dispersive X-ray spectroscopy (EDS) mapping of the cross-section of the MAO-treated titanium surface (**c**). Specimens were MAO-treated at 400 V using 150 mM of calcium acetate and 100 mM of calcium glycerophosphate

Many studies have reported the advantages of MAO for titanium and titanium alloys used in medical devices. MAO improves the hard tissue compatibility of titanium when the electrolyte contains calcium and phosphate. The biocompatibility of MAO coatings has been demonstrated in a number of in vitro and in vivo studies [76–88].

Since 2009, MAO has been used to generate antibacterial surfaces on titanium or titanium alloy surfaces because it easily controls both the architecture and composition on the titanium surface [89]. So far, commercially pure titanium, Ti–6Al–4V [89–96], Ni–Ti [97, 98], Ti–29Nb–13Ta–4.6Zr [99], Ti–40Nb [100], and Ti–3Cu [101] were MAO-treated to achieve antibacterial effects on their surfaces. Among them, commercially pure titanium has been the most used for MAO. In addition, MAO has been combined with other dry and wet process coatings such as PIII [102], hydrothermal treatment [103–105], and magnetron sputtering [105–107].

Silver (Ag) [89, 91, 93, 95, 99, 106–116], copper (Cu) [94, 100–102, 104, 110, 111, 117–124], zinc (Zn) [94, 100, 101, 103, 110, 121, 125–127], gallium (Ga) [128], iron (Fe) [129], selenium (Se) [130], bismuth (Bi) [131], boron (B) [132], fluorine (F) [92, 133], and manganese (Mn) [134, 135] have been used as antibacterial elements, incorporated onto the oxide layer of the titanium surface by MAO. MAO has been

extensively used to incorporate these elements onto titanium surfaces, with sufficient data being available, to prove the efficacy of this approach. *S. aureus* and *E. coli*, which are commonly occurring Gram-positive and negative bacteria, are mostly used in antibacterial tests for antibacterial elements-incorporated oxide layers. In addition, the effectiveness of MAO coatings against other bacteria, including *E. coli*, *S. aureus*, *S. mutans* [127], gentamicin-resistant *S. epidermidis* [96], methicillin-resistant *S. aureus* [131], *P. aeruginosa* [132], *Porphyromonas gingivalis* [95], *Acinetobacter baumannii* [128], and *Actinobacillus actinomycetemcomitans* [131] have also been proved.

Since the antibacterial properties and host cell toxicities of antibacterial elements are dose-dependent, it is important to control the concentration of antibacterial elements used to kill the bacteria on implant surfaces with minimal or no harmful effects on the host tissue. Therefore, in the case of implant surfaces, antibacterial properties and biocompatibility are simultaneously required for bone reconstruction and prevention of infections.

Ning et al. [136] reported that suitable concentration ranges of Ag, Cu, and Zn ions that could kill both *S. aureus* and *E. coli* without harmful effects on fibroblasts. Therefore, the use of antibacterial elements in the suitable concentrations on titanium surface can confer antibacterial property and biocompatibility simultaneously (Fig. 6.6).

The half-maximal inhibitory concentration (IC_{50}), which is a quantitative measure of the inhibitory effects of compounds on biological and biochemical functions, is

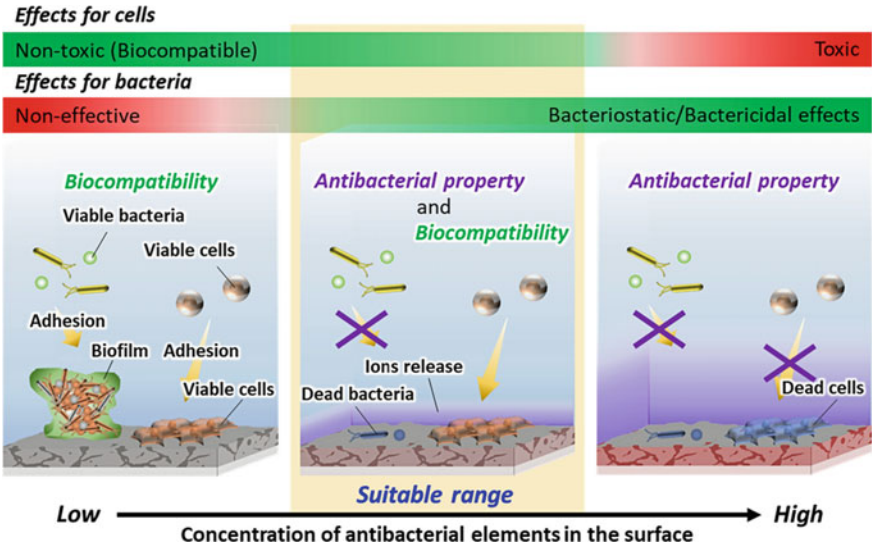

Fig. 6.6 Conceptual diagram of the suitable concentration range of antibacterial metals on the titanium surface for antibacterial property and biocompatibility

used to evaluate toxicity. The IC_{50} values of Ag, Cu, and Zn ions against MC3T3-E1 cells were 2.77 μM, 15.9 μM, and 90.0 μM, respectively [137]. Therefore, Ag was expected to be the most toxic element to osteoblasts. However, a suitable Ag concentration in the oxide layer can generate antibacterial properties on the titanium surface. The suitable Ag concentrations in the oxide layers revealed by previous studies were 0.58 wt.% [108] and 0.5–1.5 atom.% [112]. These concentrations of Ag had no influence on differentiation and accelerated calcification. Moreover, the durability of the antibacterial effect of Ag was also reported, with its effect weakening with time, but maintained for at least 28 days [108, 111].

In a similar manner, Cu and Zn have suitable concentration ranges for concurrent antibacterial properties and biocompatibility. The suitable Cu concentration ranges were reported as follows: 1–2.5 atom.% for antibacterial effect with a good osteoblast response [117], 0.67–1.51 wt.% for a good fibroblast response [122], and 1.3–2.76 atom.% for an endothelial cell response [120]. No change to the antibacterial effect of Cu was observed and can be maintained for at least 28 days [111]. In addition, Huang et al. reported that the Cu-incorporated surface contributed to the improvement of both macrophage-mediated bone formation and bactericidal capacity [119]. Cu develops its antibacterial effect by a specific mechanism called contact killing. According to this mechanism, the bacteria can be killed by the Cu ion released by the contact effects between bacteria and the Cu surface [138–141]. This unique mechanism helps to control the antibacterial effects on the titanium surface. Similarly, suitable Zn concentration ranges were also reported to be around 0.199 and 0.574 atom.% for antibacterial effects with a good osteoblast response [127].

The durability of antibacterial effects is key for long-term inhibition of biofilm formation on the titanium surface. Generally, prosthetic joint infections are categorized into two types: early infections (within 3 months after surgery) and late infections (12 months after surgery). The main cause of late infections is bacterial invasion due to hematogenous spread from another site [142]. Therefore, long-term antibacterial effects should be maintained for the prevention of late infections. Following the implantation of materials, the adsorption of molecules or proteins cell or bacterial adhesion, activation of macrophages, formation of tissues, inflammation, etc. will occur on the material surface. The surface composition and chemical state of the surface layer on materials gradually change with these reactions, which governs their function. Therefore, surface changes are key to the development of antibacterial effects. The surface changes must be precisely characterized to evaluate the antibacterial ability of the materials and the durability of antibacterial effects.

Our previous studies have shown that the biodegradation behavior of Ag-, Cu-, and Zn-incorporated titanium surfaces were simulated by immersion in saline for 28 days, and the changes in surface compositions, chemical states, and antibacterial effects were investigated [111, 125]. As a result, the concentrations of Ag, Cu, and Zn were dramatically decreased through incubation for up to 7 days and remained at slight amounts until 28 days. The antibacterial effect of Ag-incorporated specimens was weakened, the effect of Cu was maintained, and the effect of Zn was improved after 28 days of incubation in saline. In addition, the chemical state of Ag changed from Ag_2O to Ag, that of Cu was maintained as Cu_2O, and that of Zn changed from

Zn^{2+} to ZnO due to immersion in saline. In particular, the Zn-incorporated titanium surface developed a late-onset antibacterial effect owing to the generation of ZnO by biodegradation in simulated body fluid. Therefore, the antibacterial effects of these elements depend on their changes in chemical states. In other words, the biodegradation behavior of antibacterial surfaces must be considered for both understanding their durability and preventing late infections.

These collective findings demonstrate that specific antibacterial effects can be generated on titanium surfaces by the incorporation of antibacterial elements without deleterious actions on osteogenic cells. In other words, the antibacterial property and biocompatibility develop on titanium surfaces by the MAO process, based on the compositional control of antibacterial elements on the titanium surface. These findings are beneficial for both the surface design and bio-function control of implants. We hope that the advanced antibacterial activity is controlled by the use of antibacterial elements. Ag is effective relatively early after implantation because it exhibits its effect by the elution of Ag ions. Moreover, the antibacterial effects of Cu and Zn were weaker than those of Ag. Therefore, Cu and Zn can be effectively used as auxiliary agents for Ag and can be expected to play an active part in the late period of implantation. However, the durability of the antibacterial effect remains unclear and is necessary for preventing late infections. The antibacterial surface on implants should be controlled and designed based on biodegradation behaviors in the body. Finally, we hope that our findings can help to eradicate biomaterial-associated infections.

6.5 Summary and Future Perspective

This chapter provides a general introduction outlining titanium, biomaterial-associated infections, coating technologies for preventing infection on titanium surfaces, and MAO. With regard to the prevention of biomaterial-associated infections on titanium surfaces, the efficacies of various coating technologies have been proven by many researchers. Among them, MAO is a key technology for realizing both antibacterial properties and biocompatibility on titanium surfaces. In particular, the design of antibacterial biomaterials for the prevention of infectious diseases can be provided by the compositional control of antibacterial elements on the titanium surface by MAO.

Antibacterial properties play a key role in preventing infection of the implant material, but surface design according to the external environment and time scale is also necessary to maintain this property for a prolonged time. The importance of transient effects such as surface changes in the body is valuable for the development of novel biomaterials. We hope that the present chapter will enrich the future design of bio-functional materials designed to prevent infection and will contribute to the overall development of antibacterial applications.

Acknowledgements This study was supported in part by JSPS KAKENHI Grant Numbers JP20K23032 and JP21K18057. The author would like to thank Prof. Takao Hanawa (Institute of Biomaterials and Bioengineering, Tokyo Medical and Dental University), Dr. Yusuke Tsutsumi (National Institute for Materials Science), Prof. Kunio Ishikawa, and Assoc. Prof. Koichiro Hayashi (Faculty of Dental Science, Kyushu University) for inspiring the present work.

References

1. Hanawa T (2019) Titanium-tissue interface reaction and its control with surface treatment. Front Bioeng Biotechnol 7:170
2. Brånemark PI, Hansson BO, Adell R et al (1977) Osseointegrated implants in the treatment of the edentulous jaw. Experience from a 10-year period. Scand J Plast Reconstr Surg Suppl 16:1–132
3. Sundell G, Dahlin C, Andersson M et al (2017) The bone-implant interface of dental implants in humans on the atomic scale. Acta Biomater 48:445–450
4. Brånemark R, Ohrnell LO, Skalak R et al (1998) Biomechanical characterization of osseointegration: an experimental *in vivo* investigation in the beagle dog. J Orthop Res 16:61–69
5. Sennerby L, Thomsen P, Ericson LE (1993) Early tissue response to titanium implants inserted in rabbit cortical bone. J Mater Sci Mater Med 4:240–250
6. Listgarten MA, Buser D, Steinemann SG et al (1992) Light and transmission electron microscopy of the intact interfaces between non-submerged titanium-coated epoxy resin implants and bone or gingiva. J Dent Res 71:364–371
7. Davies JE, Lowenberg B, Shiga A (1990) The bone titanium interface *in vitro*. J Biomed Mater Res 24:1289–1306
8. Albrektsson T, Hansson HA (1986) An ultrastructural characterization of the interface between bone and sputtered titanium or stainless steel surfaces. Biomaterials 7:201–205
9. Eliaz N (2019) Corrosion of metallic biomaterials: a review. Materials 12:407
10. Asri RIM, Harun WSW, Samykano M et al (2017) Corrosion and surface modification on biocompatible metals: a review. Mater Sci Eng C Mater Biol Appl 77:1261–1274
11. Manam NS, Harun WSW, Shri DNA et al (2017) Study of corrosion in biocompatible metals for implants: a review. J Alloys Compd 701:698–715
12. Brunette DM, Tenvall P, Textor M et al (eds) (2001) Titanium in medicine. Springer, Berlin
13. Nakayama Y, Yamamuro T, Kotoura Y et al (1989) *In vivo* measurement of anodic polarization of orthopaedic implant alloys: comparative study of *in vivo* and *in vitro* experiments. Biomaterials 10:420–424
14. Shimabukuro M, Ito H, Tsutsumi Y et al (2019) The effects of various metallic surfaces on cellular and bacterial adhesion. Metals 9:1145
15. Hiji A, Hanawa T, Shimabukuro M et al (2021) Initial formation kinetics of calcium phosphate on titanium in Hanks' solution characterized using XPS. Surf Interface Anal 53:185–193
16. Grainger DW, van der Mei HC, Jutte PC et al (2013) Critical factors in the translation of improved antimicrobial strategies for medical implants and devices. Biomaterials 34:9237–9243
17. Tesmer M, Wallet S, Koutouzis T et al (2009) Bacterial colonization of the dental implant fixture-abutment interface: an *in vitro* study. J Periodontol 80:1991–1997
18. MacKintosh EE, Patel JD, Marchant RE et al (2006) Effects of biomaterial surface chemistry on the adhesion and biofilm formation of *Staphylococcus* epidermidis *in vitro*. J Biomed Mater Res A 78:836–842
19. Dibart S, Warbington M, Su MF et al (2005) *In vitro* evaluation of the implant-abutment bacterial seal: the locking taper system. Int J Oral Maxillofac Implant 20:732–737

20. Glauser R, Schüpbach P, Gottlow J et al (2005) Periimplant soft tissue barrier at experimental one-piece mini-implants with different surface topography in humans: a light-microscopic overview and histometric analysis. Clin Implant Dent Relat Res 7:S44–S51
21. Busscher HJ, van der Mei HC, Subbiahdoss G et al (2012) Biomaterial-associated infection: locating the finish line in the race for the surface. Sci Transl Med 4:153rv10. https://doi.org/10.1126/scitranslmed.3004528
22. Lavernia C, Lee DJ, Hernandez VH (2006) The increasing financial burden of knee revision surgery in the United States. Clin Orthop Relat Res 446:221–226
23. Bozic KJ, Ries MD (2005) The impact of infection after total hip arthroplasty on hospital and surgeon resource utilization. J Bone Joint Surg Am 87:1746–1751
24. Costerton JW, Cheng KJ, Geesey GG et al (1987) Bacterial biofilms in nature and disease. Annu Rev Microbiol 41:435–464
25. Koo H, Allan RN, Howlin RP et al (2017) Targeting microbial biofilms: current and prospective therapeutic strategies. Nat Rev Microbiol 15:740–755
26. Høiby N, Bjarnsholt T, Givskov M et al (2010) Antibiotic resistance of bacterial biofilms. Int J Antimicrob Agents 35:322–332
27. Lindsay D, von Holy A (2006) Bacterial biofilms within the clinical setting: what healthcare professionals should know. J Hosp Infect 64:313–325
28. Fux CA, Costerton JW, Stewart PS et al (2005) Survival strategies of infectious biofilms. Trends Microbiol 13:34–40
29. Stewart PS, Costerton JW (2001) Antibiotic resistance of bacteria in biofilms. Lancet 358:135–138
30. Cozens D, Read RC (2012) Anti-adhesion methods as novel therapeutics for bacterial infections. Expert Rev Anti Infect Ther 10:1457–1468
31. Serra DO, Richter AM, Klauck G et al (2013) Microanatomy at cellular resolution and spatial order of physiological differentiation in a bacterial biofilm. mBio 4:e00103–e00113
32. Chapman MR, Robinson LS, Pinkner JS et al (2002) Role of Escherichia coli curli operons in directing amyloid fiber formation. Science 295:851–855
33. Flemming HC, Wingender J, Szewzyk U et al (2016) Biofilms: an emergent form of bacterial life. Nat Rev Microbiol 14:563–575
34. Van Acker H, Van Dijck P, Coenye T (2014) Molecular mechanisms of antimicrobial tolerance and resistance in bacterial and fungal biofilms. Trends Microbiol 22:326–333
35. Lebeaux D, Ghigo JM, Beloin C (2014) Biofilm-related infections: Bridging the gap between clinical management and fundamental aspects of recalcitrance toward antibiotics. Microbiol Mol Biol Rev 78:510–543
36. Miller MB, Bassler BL (2001) Quorum sensing in bacteria. Annu Rev Microbiol 55:165–199
37. Fabbri S, Li J, Howlin RP et al (2017) Fluid-driven interfacial instabilities and turbulence in bacterial biofilms. Environ Microbiol 19:4417–4431
38. Fabbri S, Johnston DA, Rmaile A et al (2016) Streptococcus mutans biofilm transient viscoelastic fluid behaviour during high-velocity microsprays. J Mech Behav Biomed Mater 59:197–206
39. Gloag ES, Fabbri S, Wozniak DJ et al (2020) Biofilm mechanics: implications in infection and survival. Biofilm 2:100017
40. Cui W, Qin G, Duan J et al (2017) A graded nano-TiN coating on biomedical Ti alloy: low friction coefficient, good bonding and biocompatibility. Mater Sci Eng C 71:520–528
41. Lin N, Huang X, Zou J et al (2012) Effects of plasma nitriding and multiple arc ion plating TiN coating on bacterial adhesion of commercial pure titanium via *in vitro* investigations. Surf Coat Technol 209:212–215
42. Lin N, Huang X, Zhang X et al (2012) *In vitro* assessments on bacterial adhesion and corrosion performance of TiN coating on Ti6Al4V titanium alloy synthesized by multi-arc ion plating. Appl Surf Sci 258:7047–7051
43. Annunziata M, Oliva A, Basile MA et al (2011) The effects of titanium nitride-coating on the topographic and biological features of TPS implant surfaces. J Dent 39:720–728

44. Grössner-Schreiber B, Teichmann J, Hannig M et al (2009) Modified implant surfaces show different biofilm compositions under *in vivo* conditions. Clin Oral Implants Res 20:817–826
45. Groessner-Schreiber B, Hannig M, Dück A et al (2004) Do different implant surfaces exposed in the oral cavity of humans show different biofilm compositions and activities? Eur J Oral Sci 112:516–522
46. Scarano A, Piattelli M, Vrespa G et al (2003) Bacterial adhesion on titanium nitride-coated and uncoated implants: an *in vivo* human study. J Oral Implantol 29:80–85
47. Grössner-Schreiber B, Griepentrog M, Haustein I et al (2001) Plaque formation on surface modified dental implants. An *in vitro* study. Clin Oral Implants Res 12:543–551
48. Campoccia D, Montanaro L, Arciola CR (2013) A review of the biomaterials technologies for infection-resistant surfaces. Biomaterials 34:8533–8554
49. Tanaka Y, Matin K, Gyo M et al (2010) Effects of electrodeposited poly(ethylene glycol) on biofilm adherence to titanium. J Biomed Mater Res A 95:1105–1113
50. Fujii K, Matsumoto HN, Koyama Y et al (2008) Prevention of biofilm formation with a coating of 2-methacryloyloxyethyl phosphorylcholine polymer. J Vet Med Sci 70:167–173
51. Roosjen A, Kaper HJ, van der Mei HC et al (2003) Inhibition of adhesion of yeasts and bacteria by poly(ethylene oxide)-brushes on glass in a parallel plate flow chamber. Microbiology 149:3239–3246
52. Leckband D, Sheth S, Halperin A (1999) Grafted poly(ethylene oxide) brushes as nonfouling surface coatings. J Biomater Sci Polym Ed 10:1125–1147
53. Park KD, Kim YS, Han DK et al (1998) Bacterial adhesion on PEG modified polyurethane surfaces. Biomaterials 19:851–859
54. Narendrakumar K, Kulkarni M, Addison O et al (2015) Adherence of oral streptococci to nanostructured titanium surfaces. Dent Mater 31:1460–1468
55. Ercan B, Taylor E, Alpaslan E et al (2011) Diameter of titanium nanotubes influences antibacterial efficacy. Nanotechnology 22:295102
56. Davidson H, Poon M, Saunders R et al (2015) Tetracycline tethered to titanium inhibits colonization by Gram-negative bacteria. J Biomed Mater Res B Appl Biomater 103:1381–1389
57. Park SW, Lee D, Choi YS et al (2014) Mesoporous TiO_2 implants for loading high dosage of antibacterial agent. Appl Surf Sci 303:140–146
58. Rams TE, Degener JE, van Winkelhoff AJ (2014) Antibiotic resistance in human peri-implantitis microbiota. Clin Oral Implants Res 25:82–90
59. Popat KC, Leoni L, Grimes CA et al (2007) Influence of engineered titania nanotubular surfaces on bone cells. Biomaterials 28:3188–3197
60. Darouiche RO (2004) Treatment of infections associated with surgical implants. N Engl J Med 350:1422–1429
61. Bronk JK, Russell BH, Rivera JJ et al (2014) A multifunctional streptococcal collagen-mimetic protein coating prevents bacterial adhesion and promotes osteoid formation on titanium. Acta Biomater 10:3354–3362
62. Holmberg KV, Abdolhosseini M, Li Y et al (2013) Bio-inspired stable antimicrobial peptide coatings for dental applications. Acta Biomater 9:8224–8231
63. Kazemzadeh-Narbat M, Kindrachuk J, Duan K et al (2010) Antimicrobial peptides on calcium phosphate-coated titanium for the prevention of implant-associated infections. Biomaterials 31:9519–9526
64. Unosson E, Rodriguez D, Welch K et al (2015) Reactive combinatorial synthesis and characterization of a gradient Ag-Ti oxide thin film with antibacterial properties. Acta Biomater 11:503–510
65. Mei S, Wang H, Wang W et al (2014) Antibacterial effects and biocompatibility of titanium surfaces with graded silver incorporation in titania nanotubes. Biomaterials 35:4255–4265
66. Xu J, Ding G, Li J et al (2010) Zinc-ion implanted and deposited titanium surfaces reduce adhesion of *Streptococccus mutans*. Appl Surf Sci 256:7540–7544
67. Chen W, Liu Y, Courtney HS et al (2006) *In vitro* anti-bacterial and biological properties of magnetron co-sputtered silver-containing hydroxyapatite coating. Biomaterials 27:5512–5517

68. Cloutier M, Mantovani D, Rosei F (2015) Antibacterial coatings: challenges, perspectives, and opportunities. Trends Biotechnol 33:637–652
69. Ueda T, Sato N, Koizumi R et al (2020) Formation of carbon-added anatase-rich TiO_2 layers on titanium and their antibacterial properties in visible light. Dent Mater 37:e37–e46
70. Hayashi K, Nozaki K, Tan Z et al (2019) Enhanced antibacterial property of facet-engineered TiO_2 nanosheet in presence and absence of ultraviolet irradiation. Materials 13:78
71. Jin G, Qin H, Cao H et al (2014) Synergistic effects of dual Zn/Ag ion implantation in osteogenic activity and antibacterial ability of titanium. Biomaterials 35:7699–7713
72. Huo K, Zhang X, Wang H et al (2013) Osteogenic activity and antibacterial effects on titanium surfaces modified with Zn-incorporated nanotube arrays. Biomaterials 34:3467–3478
73. Ferraris S, Spriano S (2016) Antibacterial titanium surfaces for medical implants. Mater Sci Eng C Mater Biol Appl 61:965–978
74. Chouirfa H, Bouloussa H, Migonney V et al (2019) Review of titanium surface modification techniques and coatings for antibacterial applications. Acta Biomater 83:37–54
75. Ha JY, Tsutsumi Y, Doi H et al (2011) Enhancement of calcium phosphate formation on zirconium by micro-arc oxidation and chemical treatments. Surf Coat Technol 205:4948–4955
76. Correa DRN, Rocha LA, Ribeiro AR et al (2018) Growth mechanisms of Ca- and P-rich MAO films in Ti-15Zr-xMo alloys for osseointegrative implants. Surf Coat Technol 344:373–382
77. Liu W, Cheng M, Wahafu T et al (2015) The *in vitro* and *in vivo* performance of a strontium-containing coating on the low-modulus Ti35Nb2Ta3Zr alloy formed by micro-arc oxidation. J Mater Sci Mater Med 26:203
78. Wang Y, Yu HJ, Chen CZ et al (2015) Review of the biocompatibility of micro-arc oxidation coated titanium alloys. Mater Des 85:640–652
79. Zhang RF, Qiao LP, Qu B et al (2015) Biocompatibility of micro-arc oxidation coatings developed on Ti6Al4V alloy in a solution containing organic phosphate. Mater Lett 153:77–80
80. Wang L, Shi L, Chen JJ et al (2014) Biocompatibility of Si-incorporated TiO_2 film prepared by micro-arc oxidation. Mater Lett 116:35–38
81. Cimenoglu H, Gunyuz M, Kose GT et al (2011) Micro-arc oxidation of Ti6Al4V and Ti6Al7Nb alloys for biomedical applications. Mater Charact 62:304–311
82. Chen HT, Chung CJ, Yang TC et al (2010) Osteoblast growth behavior on micro-arc oxidized β-titanium alloy. Surf Coat Technol 205:1624–1629
83. Wang G, Zreiqat H (2010) Functional coatings or films for hard-tissue applications. Materials 3:3994–4050
84. Kim DY, Kim M, Kim HE et al (2009) Formation of hydroxyapatite within porous TiO_2 layer by micro-arc oxidation coupled with electrophoretic deposition. Acta Biomater 5:2196–2205
85. Li Y, Lee IS, Cui FZ et al (2008) The biocompatibility of nanostructured calcium phosphate coated on micro-arc oxidized titanium. Biomaterials 29:2025–2032
86. Li LH, Kong YM, Kim HW et al (2004) Improved biological performance of Ti implants due to surface modification by micro-arc oxidation. Biomaterials 25:2867–2875
87. Son WW, Zhu X, Shin HI et al (2003) In vivo histological response to anodized and anodized/hydrothermally treated titanium implants. J Biomed Mater Res B Appl Biomater 66:520–525
88. Suh JY, Jang BC, Zhu X et al (2003) Effect of hydrothermally treated anodic oxide films on osteoblast attachment and proliferation. Biomaterials 24:347–355
89. Song WH, Ryu HS, Hong SH (2008) Antibacterial properties of Ag (or Pt)-containing calcium phosphate coatings formed by micro-arc oxidation. J Biomed Mater Res A 88:246–254
90. Li GQ, Wang YP, Qiao LP et al (2019) Preparation and formation mechanism of copper incorporated micro-arc oxidation coatings developed on Ti-6Al-4V alloys. Surf Coat Technol 375:74–85
91. Aydogan DT, Muhaffel F, Acar OK et al (2018) Surface modification of Ti6Al4V by micro-arc oxidation in $AgC_2H_3O_2$-containing electrolyte. Surf Innov 6:277–285. https://doi.org/10.1680/jsuin.18.00007
92. Santos-Coquillat A, Gonzalez Tenorio R, Mohedano M et al (2018) Tailoring of antibacterial and osteogenic properties of Ti6Al4V by plasma electrolytic oxidation. Appl Surf Sci 454:157–172

93. Muhaffel F, Cempura G, Menekse M et al (2016) Characteristics of multi-layer coatings synthesized on Ti6Al4V alloy by micro-arc oxidation in silver nitrate added electrolytes. Surf Coat Technol 307A:308–315
94. Zhao D, Lu Y, Wang Z et al (2016) Antifouling properties of micro arc oxidation coatings containing Cu_2O/ZnO nanoparticles on Ti6Al4V. Int J Refract Met Hard Mate 54:417–421
95. Lan Z, Guo-Hua L, Fei-Fei M et al (2014) Preparation of biomedical Ag incorporated hydroxyapatite/titania coatings on Ti6Al4V alloy by plasma electrolytic oxidation. Chin Phys B 23:035205. https://doi.org/10.1088/1674-1056/23/3/035205
96. Gasquères C, Schneider G, Nusko R et al (2012) Innovative antibacterial coating by anodic spark deposition. Surf Coat Technol 206:3410–3414
97. Liu Z, Xiao K, Hou Z et al (2020) Multifunctional coating with both thermal insulation and antibacterial properties applied to nickel-titanium alloy. Int J Nanomedicine 15:7215–7234
98. Karabudak F, Yeşildal R, Şüküroğlu EE et al (2017) An investigation of corrosion resistance and antibacterial sensitivity properties of nano-Ag-doped coating and coating grown on NiTi alloy with the micro-arc oxidation process. Arab J Sci Eng 42:2329–2339
99. Tsutsumi Y, Niinomi M, Nakai M et al (2016) Electrochemical surface treatment of a β-titanium alloy to realize an antibacterial property and bioactivity. Metals 6:76
100. Sedelnikova MB, Komarova EG, Sharkeev YP et al (2019) Zn-, Cu- or Ag-incorporated micro-arc coatings on titanium alloys: properties and behavior in synthetic biological media. Surf Coat Technol 369:52–68
101. Hu J, Li H, Wang X et al (2020) Effect of ultrasonic micro-arc oxidation on the antibacterial properties and cell biocompatibility of Ti-Cu alloy for biomedical application. Mater Sci Eng C Mater Biol Appl 115:110921
102. Zheng L, Qian S, Liu X (2019) Enhanced osteogenic activity and bacteriostatic effect of TiO_2 coatings via hydrogen ion implantation. Mater Lett 253:95–98
103. Zhang L, Zhang J, Dai F et al (2017) Cytocompatibility and antibacterial activity of nanostructured $H_2Ti_5O_{11}{\cdot}H_2O$ outlayered Zn-doped TiO_2 coatings on Ti for percutaneous implants. Sci Rep 7:13951
104. Wu Q, Li J, Zhang W et al (2014) Antibacterial property, angiogenic and osteogenic activity of Cu-incorporated TiO_2 coating. J Mater Chem B 2:6738–6748
105. Zhang XG, Wang HZ, Li JF et al (2017) The fabrication of Ag-containing hierarchical micro/nano-structure on titanium and its antibacterial activity. Mater Lett 193:97–100
106. He XJ, Zhang XY, Bai L et al (2016) Antibacterial ability and osteogenic activity of porous Sr/Ag-containing TiO_2 coatings. Biomed Mater 11:045008
107. Zhang XY, Hang RQ, Wu HB et al (2013) Synthesis and antibacterial property of Ag-containing TiO_2 coatings by combining magnetron sputtering with micro-arc oxidation. Surf Coat Technol 235:748–754
108. Zhang YY, Zhu Y, Lu DZ et al (2021) Evaluation of osteogenic and antibacterial properties of strontium/silver-containing porous TiO_2 coatings prepared by micro-arc oxidation. J Biomed Mater Res B Appl Biomater 109:505–516
109. Zhang L, Zhang XL, Wang DH et al (2020) Biological and antibacterial properties of TiO_2 coatings containing Ca/P/Ag by one-step and two-step methods. Biomed Microdevices 22:24
110. Shimabukuro M (2020) Antibacterial property and biocompatibility of silver, copper, and zinc in titanium dioxide layers incorporated by one-step micro-arc oxidation: a review. Antibiotics 9:716
111. Shimabukuro M, Hiji A, Manaka T et al (2020) Time-transient effects of silver and copper in the porous titanium dioxide layer on antibacterial properties. J Funct Biomater 11:44
112. Shimabukuro M, Tsutsumi Y, Yamada R et al (2019) Investigation of realizing both antibacterial property and osteogenic cell compatibility on titanium surface by simple electrochemical treatment. ACS Biomater Sci Eng 5:5623–5630
113. Aydogan DK, Muhaffel F, Kilic MM et al (2018) Optimisation of micro-arc oxidation electrolyte for fabrication of antibacterial coating on titanium. Mater Technol 33:119–126
114. Jia Z, Xiu P, Li M et al (2016) Bioinspired anchoring AgNPs onto micro-nanoporous TiO_2 orthopedic coatings: trap-killing of bacteria, surface-regulated osteoblast functions and host responses. Biomaterials 75:203–222

115. Teker D, Muhaffel F, Menekse M et al (2015) Characteristics of multi-layer coating formed on commercially pure titanium for biomedical applications. Mater Sci Eng C Mater Biol Appl 48:579–585
116. Zhang XY, Wu HB, Geng ZH et al (2014) Microstructure and cytotoxicity evaluation of duplex-treated silver-containing antibacterial TiO_2 coatings. Mater Sci Eng C Mater Biol Appl 45:402–410
117. Shimabukuro M, Tsutsumi Y, Nozaki K et al (2020) Investigation of antibacterial effect of copper introduced titanium surface by electrochemical treatment against facultative anaerobic bacteria. Dent Mater J 39:639–647
118. Zhao Q, Yi L, Hu A et al (2019) Antibacterial and osteogenic activity of a multifunctional microporous coating codoped with Mg, Cu and F on titanium. J Mater Chem B 7:2284–2299
119. Huang Q, Li X, Elkhooly TA et al (2018) The Cu-containing TiO_2 coatings with modulatory effects on macrophage polarization and bactericidal capacity prepared by micro-arc oxidation on titanium substrates. Colloids Surf B Biointerfaces 170:242–250
120. Zhang X, Li J, Wang X et al (2018) Effects of copper nanoparticles in porous TiO_2 coatings on bacterial resistance and cytocompatibility of osteoblasts and endothelial cells. Mater Sci Eng C Mater Biol Appl 82:110–120
121. Zhang L, Gao Q, Han Y (2016) Zn and Ag co-doped anti-microbial TiO_2 coatings on Ti by micro-arc oxidation. J Mater Sci Technol 32:919–924
122. Zhang L, Guo J, Huang X et al (2016) The dual function of Cu-doped TiO_2 coatings on titanium for application in percutaneous implants. J Mater Chem B 4:3788–3800
123. Yao X, Zhang X, Wu H et al (2014) Microstructure and antibacterial properties of Cu-doped TiO_2 coating on titanium by micro-arc oxidation. Appl Surf Sci 292:944–947
124. Zhu W, Zhang Z, Gu B et al (2013) Biological activity and antibacterial property of nano-structured TiO_2 coating incorporated with cu prepared by micro-arc oxidation. J Mater Sci Technol 29:237–244
125. Shimabukuro M, Tsutsumi Y, Nozaki K et al (2019) Chemical and biological roles of zinc in a porous titanium dioxide layer formed by micro-arc oxidation. Coatings 9:705
126. Zhao QM, Li GZ, Zhu HM et al (2017) Study on effects of titanium surface microporous coatings containing zinc on osteoblast adhesion and its antibacterial activity. Appl Bionics Biomech 2017:2906575
127. Zhao BH, Zhang W, Wang DN et al (2013) Effect of Zn content on cytoactivity and bacteriostasis of micro-arc oxidation coatings on pure titanium. Surf Coat Technol 228:S428–S432
128. Cochis A, Azzimonti B, Della Valle C et al (2016) The effect of silver or gallium doped titanium against the multidrug resistant *Acinetobacter baumannii*. Biomaterials 80:80–95
129. Li K, Liu S, Xue Y et al (2019) A superparamagnetic Fe_3O_4-TiO_2 composite coating on titanium by micro-arc oxidation for percutaneous implants. J Mater Chem B 7:5265–5276
130. Zhou JH, Wang XL (2020) The osteogenic, anti-oncogenic and antibacterial activities of selenium-doped titanium dioxide coatings on titanium. Surf Coatings Technol 403:126408
131. Lin DJ, Tsai MT, Shieh TM et al (2013) *In vitro* antibacterial activity and cytocompatibility of bismuth doped micro-arc oxidized titanium. J Biomater Appl 27:553–563
132. Sopchenski L, Cogo S, Dias-Ntipanyj MF et al (2018) Bioactive and antibacterial boron doped TiO_2 coating obtained by PEO. Appl Surf Sci 458:49–58
133. Zhou J, Li B, Han Y (2018) F-doped TiO_2 microporous coating on titanium with enhanced antibacterial and osteogenic activities. Sci Rep 8:17858
134. Zhang X, Lv Y, Fu S et al (2020) Synthesis, microstructure, anti-corrosion property and biological performances of Mn-incorporated Ca-P/TiO_2 composite coating fabricated via micro-arc oxidation. Mater Sci Eng C Mater Biol Appl 117:111321
135. Zhang X, Lv Y, Shan F et al (2020) Microstructure, corrosion resistance, osteogenic activity and antibacterial capability of Mn-incorporated TiO_2 coating. Appl Surf Sci 531:147399
136. Ning C, Wang X, Li L et al (2015) Concentration ranges of antibacterial cations for showing the highest antibacterial efficacy but the least cytotoxicity against mammalian cells: implications for a new antibacterial mechanism. Chem Res Toxicol 28:1815–1822

137. Yamamoto A, Honma R, Sumita M (1998) Cytotoxicity evaluation of 43 metal salts using murine fibroblasts and osteoblastic cells. J Biomed Mater Res 39:331–340
138. Shimabukuro M, Manaka T, Tsutsumi Y et al (2020) Corrosion behavior and bacterial viability on different surface states of copper. Mater Trans 61:1143–1148
139. Hans M, Erbe A, Mathews S et al (2013) Role of copper oxides in contact killing of bacteria. Langmuir 29:16160–16166
140. Hong R, Kang TY, Michels CA et al (2012) Membrane lipid peroxidation in copper alloy-mediated contact killing of Escherichia coli. Appl Environ Microbiol 78:1776–1784
141. Grass G, Rensing C, Solioz M (2011) Metallic copper as an antimicrobial surface. Appl Environ Microbiol 77:1541–1547
142. Kapadia BH, Berg RA, Daley JA et al (2016) Periprosthetic joint infection. Lancet 387:386–394

Masaya Shimabukuro Dr. Shimabukuro is Research Assistant Professor at Kyushu University, Faculty of Dental Science, Department of Biomaterials, Japan. He received his Ph.D. under the guidance of Professor Takao Hanawa and Associate Professor Yusuke Tsutsumi at Tokyo Medical and Dental University, Institute of Biomaterial and Engineering, Department of Metallic Biomaterials. His research focuses on the development of antibacterial carbonate apatites for bone regeneration without causing any bacterial infections with Professor Kunio Ishikawa and Associate Professor Koichiro Hayashi. His research interests include biomaterials, surface treatment, surface modification, and antibacterial materials.

Chapter 7
Synthesis of Hydroxyapatite: Crystal Growth Mechanism and Its Relevance in Drug Delivery Applications

Yuta Otsuka

Abstract In this chapter, we planned to outline the infrared spectrum of hydroxyapatite and the non-destructive analysis method by multivariate analysis, as well as the introduction of the mechanism behind crystal growth inhibition through monitoring and adsorption of hydroxyapatite crystal growth. We anticipate this can be applied to alternative medicine materials and pharmaceutical preparations using bioceramics such as apatite cement as a base material. We hope that a more detailed understanding of the basic research on crystal growth in calcium phosphate and investigation of interactions between hydroxyapatite and drugs will advance our understanding, and that the field of drug delivery system will be further developed and put into practical use.

Keywords Drug delivery system · Self-setting apatite cement · Amino acid · Chloroapatite · Tetracalcium phosphate · Dicalcium phosphate · ATR-IR spectroscopy · Principal component analysis · Crystal structure

7.1 Introduction

Japan has entered an aging era and it is a nation with many elderly people. The number of patients with osteoporosis is on the rise and is currently estimated to be around 13 million. Bone strength in patients with osteoporosis is low, and even a slight fall can result in bone fracture or breakage. Osteoporosis is also socially important issues, and the demand for the development of alternative medicine bioceramics used as bone fillers is expected to increase further. Zirconia [1], alumina [2], silica [3], apatite [4] and the likes have been reported and classified as bioceramics.

Zirconia and alumina are one of the materials widely used in orthopedic materials for a long time; however, they are known to have poor bone conductivity [5]. Biomaterials that combine apatite and silica have also been reported [6]. In general, apatites are represented by the chemical formulae $M_{10}(ZO_4)_6X_2$, where various elements can

Y. Otsuka (✉)
Faculty of Pharmaceutical Sciences, Tokyo University of Science, 2641 Yamazaki, Noda, Chiba 278-8510, Japan

A. H. Choi and B. Ben-Nissan (eds.), *Innovative Bioceramics in Translational Medicine I*, Springer Series in Biomaterials Science and Engineering 17,
https://doi.org/10.1007/978-981-16-7435-8_7

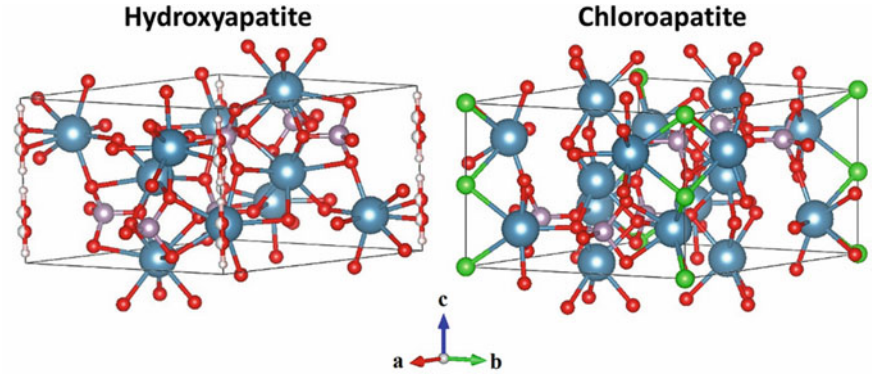

Fig. 7.1 Crystal structures of hydroxyapatite and chloroapatite

be used as M, Z, and X. However, these substitutions are dependent on the synthesis method and materials used. Among them, Hydroxyapatite (HAp) with a chemical formula of $Ca_{10}(PO_4)_6(OH)_2$, which is composed of phosphoric acid and calcium, is known as a bioceramic with high biocompatibility. Hydroxyapatite accounts for 70% of the skeletal components in mammals including humans. It also serves as a storage for many elements. Hydroxyapatite is among the biomaterials that are currently used extensively in clinical applications as bone fillers due to their excellent biocompatibility and osteoconductivity. The M^{+2} site can be replaced with divalent cations such as calcium, magnesium and lead ions. In addition, monovalent sodium ions and trivalent ions can also be utilized. At the Z site, ions of aluminium, silica, or carbonate can be used, while halogen anions and hydroxyl groups can be used as candidates at the X site.

Figure 7.1 shows the crystal structures of hydroxyapatite [7] and chloroapatite with the chemical formula of $Ca_{10}(PO_4)_6Cl_2$ [8]. Figure 7.2 demonstrates the simulated diffraction patterns of these two crystals. In the diffraction pattern of hydroxyapatite and chloroapatite, the difference between the peak intensity of (100) at $2\theta = 10.8$ and the peak intensity of (101) at $2\theta = 16.8$, which is remarkable. The in vivo degradability and mechanical strength of apatite are determined by the composition ratio and crystallinity. It is important during the development of inorganic materials to control these according to the intended application. Powder X-ray diffraction is effective in evaluating the composition of apatite, in addition to revealing its crystallinity and peaks according to composition. A powder diffraction study by Tonegawa et al. demonstrated the complete carbonate substitution at A-sites (OH) of low-crystallinity hydroxyapatite with near stoichiometric composition (i.e. Ca/P ratio of 1.65) can be accomplished through heating in a dry carbon dioxide flow at 1173 K for 64 h [9].

Construction of a drug delivery system using calcium phosphate such as hydroxyapatite has been a hot topic. Takechi et al. investigated the feasibility of using a fast-setting calcium phosphate cement with antibiotics skeleton type drug delivery system [10]. Chevalier et al. examined the influence of the location of a drug substance

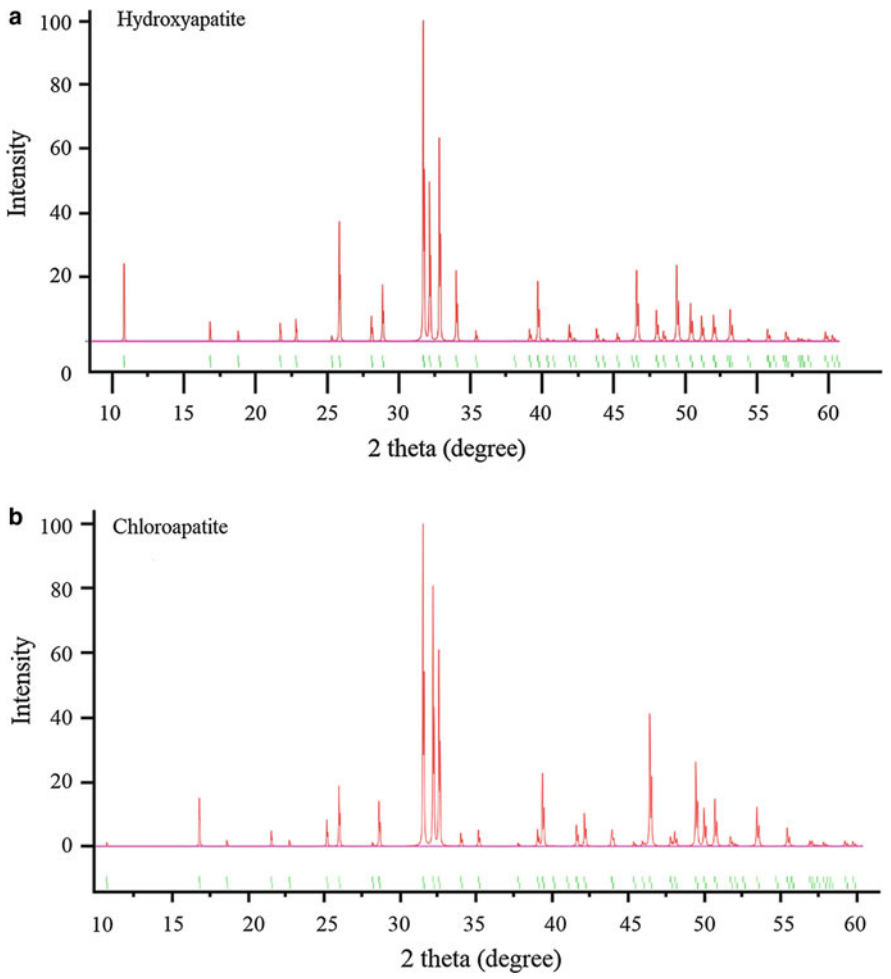

Fig. 7.2 Simulated diffraction patterns of hydroxyapatite and chloroapatite

on the physicochemical and mechanical properties of calcium phosphate granules loaded with different contents of ibuprofen [11]. Previously, we have reported the synthesis of chloroapatite and zinc-incorporated chloroapatite in which zinc ions are introduced into calcium sites and confirmed through IR and powder X-ray diffraction evaluation. In this chapter, we will explain the monitoring of crystal growth with phase transition of apatite and the interactions in crystal growth.

7.2 Self-setting Apatite Cement

A self-setting cement consisting of only calcium phosphate compounds was developed Brown and Chow in 1986 [12]. The mixing of dicalcium phosphate (DCPD, $CaHPO_4$) and tetracalcium phosphate (TTCP, $Ca_4(PO_4)_2O$) enables the phase transformation into pure hydroxyapatite. The synthesis is dependent on the calcium and phosphate phase diagrams. Based on the solubility phase diagram, it has been discovered that hydroxyapatite is the most stable phase of calcium phosphate, and the chemical equation is described as (7.1):

$$2Ca_4(PO_4)_2O + 2CaHPO_4 \cdot 2H_2O \rightarrow Ca_{10}(PO_4)_6(OH)_2 + 4H_2O \tag{7.1}$$

However, it is known that carbonate ions are incorporated into crystals during the formation of apatite. The bulk powders of TTCP and DCPD are mixed and kneaded. The mixed sample then transformed into hydroxyapatite in the presence of CO_2 as described in Eq. (7.2):

$$\begin{aligned} 2Ca_4(PO_4)_2O + 2CaHPO_4 \cdot 2H_2O + xH^+ + xCO_3^{2-} \rightarrow Ca_{10-x}(PO_4)_{6-x}(CO_3)_x(OH)_{2-x} \\ + xCa^{2+} + xPO_4^{3-} + (4+x)H_2O \end{aligned} \tag{7.2}$$

The pH of the sample is considered to increase during the hydroxyapatite crystal growth. It is well known that the pH of the suspension changed from acidic to natural if TTCP and DCPD are dissolved in 20 mM phosphoric acid and a powder/liquid ratio of 5 mL/g is used [13].

Hydroxyapatite can be easily manufacture without heating or laser irradiation of apatite using this approach. The advantage is that the basic material of the drug delivery system can be synthesized with relative ease through kneading together with the intended drug. Many drug delivery studies using self-setting apatite cement have been reported. Hamanishi et al. reported the delivery of vancomycin using self-setting apatite cement [14]. 5% vancomycin was added to the self-setting apatite cement. The study concluded that slow delivery of vancomycin from a self-setting apatite cement could be used to treat osteomyelitis. Otsuka et al. reported a novel skeletal drug delivery system using self-setting apatite cement for the delivery of indomethacin [15]. In the study, sustained-release formulations were synthesized by combining 1–5% indomethacin with self-setting apatite cement. In the in vivo test, a deeper insight into the formulation characteristics was attempted by evaluating the area under the curve, and gaining a greater understanding is important for the application of self-setting apatite cement as drug delivery system.

In this section, we have reported on the phase transformation mechanism in self-setting apatite cement. The next section discusses the relationship between carbon dioxide and hydroxyapatite crystal growth in the self-setting apatite cement transition mechanism.

7.3 Hydroxyapatite Crystal Growth Monitoring Using ATR-IR Spectroscopy with Principal Component Analysis

As described earlier, Chow et al. reported a self-setting apatite cement that contains a mixture of TTCP and DCPD with a calcium/phosphate ratio of 1.67 would transformed into hydroxyapatite [12]. This method is a very easy way of producing hydroxyapatite without heating or quenching. More importantly, this technique enables the encapsulation of active pharmaceutical ingredients [16], protein [17], and DNA [18] due to the fact that the heating of hydroxyapatite can be avoided. This synthesis approach is anticipated to produce base materials for drug delivery systems.

In our previous study, we investigated the phase transformation of TTCP and DCPD mixture kneaded with water. The mixture transformation was evaluated by ATR-IR spectra. ATR-IR spectra were obtained by an FTIR spectrometer (FT/IR-6500, JASCO Co., Tokyo, Japan) with an ATR accessory. The paste sample was put on a germanium point of ATR accessory. The sample was covered with a Parafilm®. ATR-IR spectra of the samples were obtained in the range from 600 to 3800 cm^{-1} with resolution of 8 cm^{-1}. Figure 7.3 shows ATR-IR spectra temporal changes of time of the self-setting apatite cement. The spectra of the calcium phosphates mixture shown phosphate ion infrared band in the range of 900–1200 cm^{-1}, carbonated ion

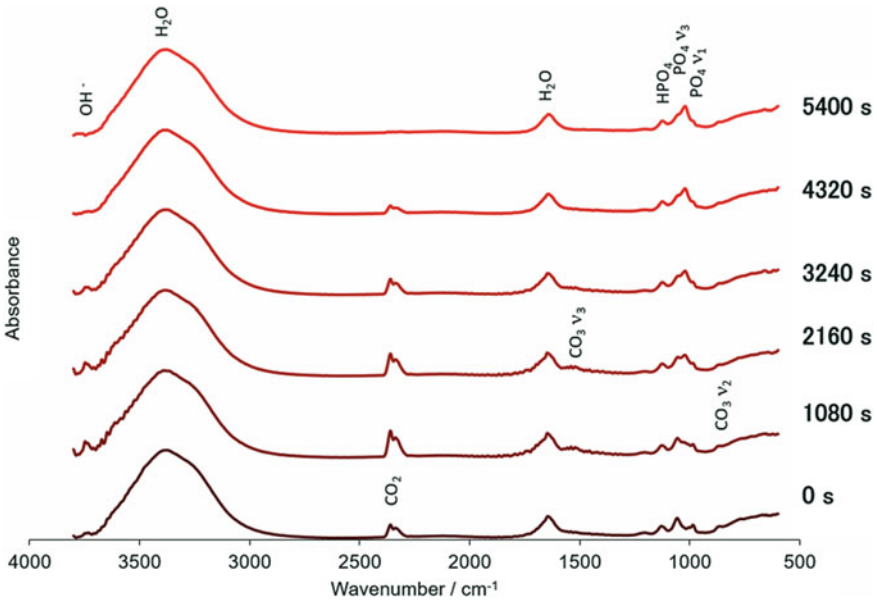

Fig. 7.3 Temporal profiles of FT-ATR-IR spectra of apatite cement during the course of the setting. Reprint with permission [13]

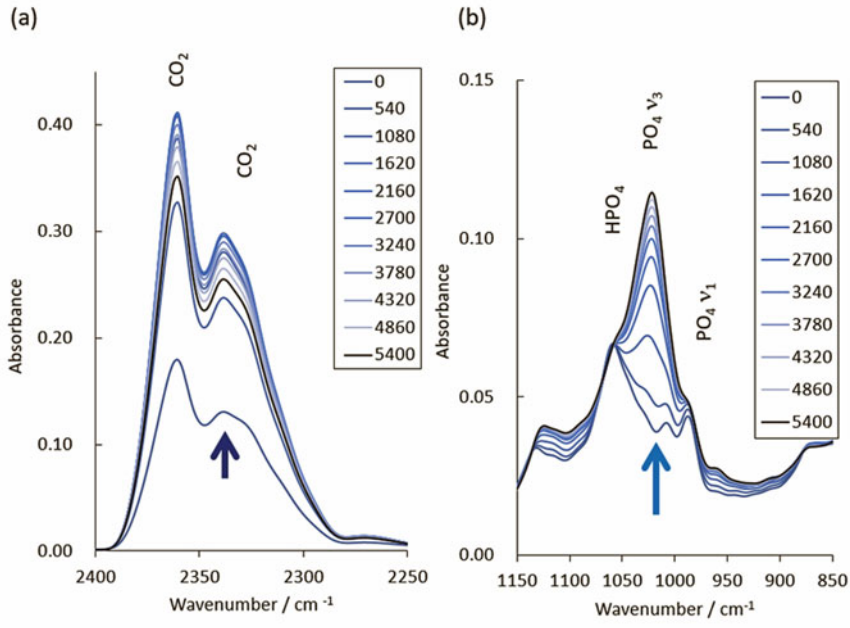

Fig. 7.4 The normalized ATR-IR spectra in the ranges of 850–1150 and 2250–2500 cm^{-1}. Reprint with permission [13]

band on 850–1500 cm^{-1}, carbon dioxide in the range of 2200–2300 cm^{-1} and OH band from 3000 to 3700 cm^{-1}.

Figure 7.4 shows cutout of spectra in the ranges of carbon dioxide and phosphate ion vibrations. It was discovered that ATR-IR spectra could detect carbon dioxide concentration within the apatite cement. The twin peaks at 2360 and 2337 cm^{-1} correspond to the carbon dioxide gas in the sample. At 0 s, the infrared absorption bands at 983, 1058, and 1135 cm^{-1} correspond to the phosphate ions, which were a mixture of TTCP and DCPD. The 1024 cm^{-1} of hydroxyapatite phosphate ion peak was found to increase from 0 to 5400 s. Pleshko et al. reported that poorly crystalline hydroxyapatite has six peaks in the range from 900 to 1200 cm^{-1} [19]. The results agreed with the study by Peshko et al. as reported. These changes in phosphate band suggested that there was a phase transformation into hydroxyapatite. By estimating the concentration of hydroxyapatite, we can apply principal component analysis (PCA) to the infrared spectra within the ranges for carbon dioxide and phosphate ion.

The chemometrics were performed using UNSCRAMBLER version 10.2. Figure 7.5 shows loadings of PCA calculation. The spectra dataset was the decomposition of principal component 1 (PC1) and principal component 2 (PC2). The results suggested that PC1 was due to carbon dioxide and PC2 was due to hydroxyapatite PO_4 ν_3 peaks as hypothesized. Analyzing the score values of PC1 and PC2 enable the

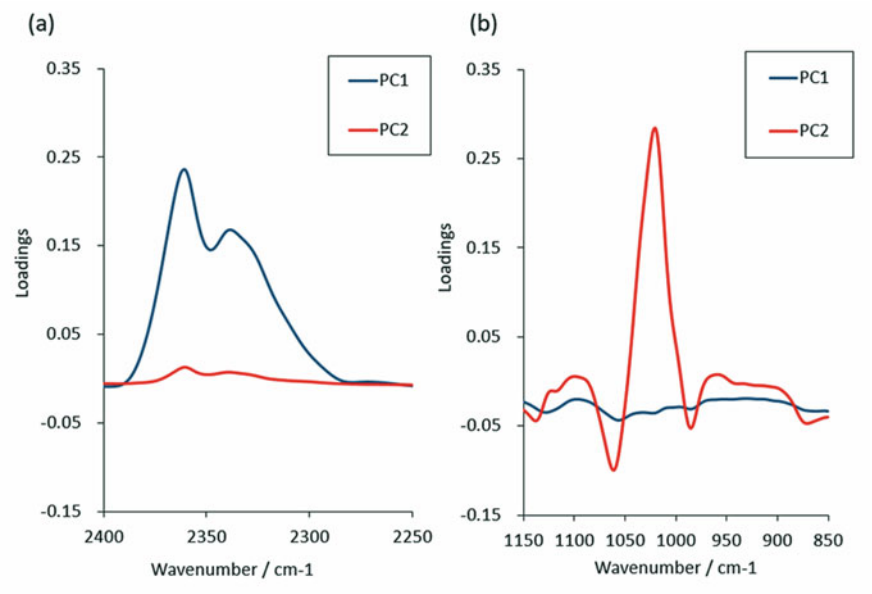

Fig. 7.5 Loading vectors **a** PC1 and **b** PC2 for principal component analysis. Reprint with permission [13]

detection in changes in concentration of carbon dioxide and hydroxyapatite crystal growth. It was found that the carbon dioxide spectrum appeared in both PCs. This indicates that the fluctuation of carbon dioxide is collinear. On the other hand, it can be seen that the vibration of phosphate ions does not have collinearity.

Figure 7.6 shows the graphs of score verses time as well as the differential scores verses time of PC1 and PC2. It should be mentioned that the experiments were conducted four times ($n = 4$). The carbon dioxide concentrations were found to increase from 0 to 900 s and the concentration decreases over time after this increase. The score for hydroxyapatite increased sharply from 0 to 900 s and the speed of increase remained constant afterwards. It was suggested that crystal growth in the non-normal state occurred during the early stages and crystal growth in the normal state occurred in the late stage. During the non-normal time stage, an increase in the carbon dioxide concentration was observed. It can be suggested that the carbon dioxide concentration and the crystal growth rate of hydroxyapatite are closely related. It has been reported that carbonate apatite can be synthesized using water and a mixture of TTCP and DCPD. Furthermore, it has also been suggested that carbonic acid apatite can be produced by incorporating carbon dioxide into the solution. The presence of carbon dioxide changes its concentration in conjunction with the pH in the sample, and such behavior was shown in previous studies.

The relationship between differentiated scores of PC1 and PC2 are shown in Fig. 7.7. During the early stages, the crystal growth rate of hydroxyapatite in the sample increases while absorbing carbon dioxide. Once it reaches a certain saturation,

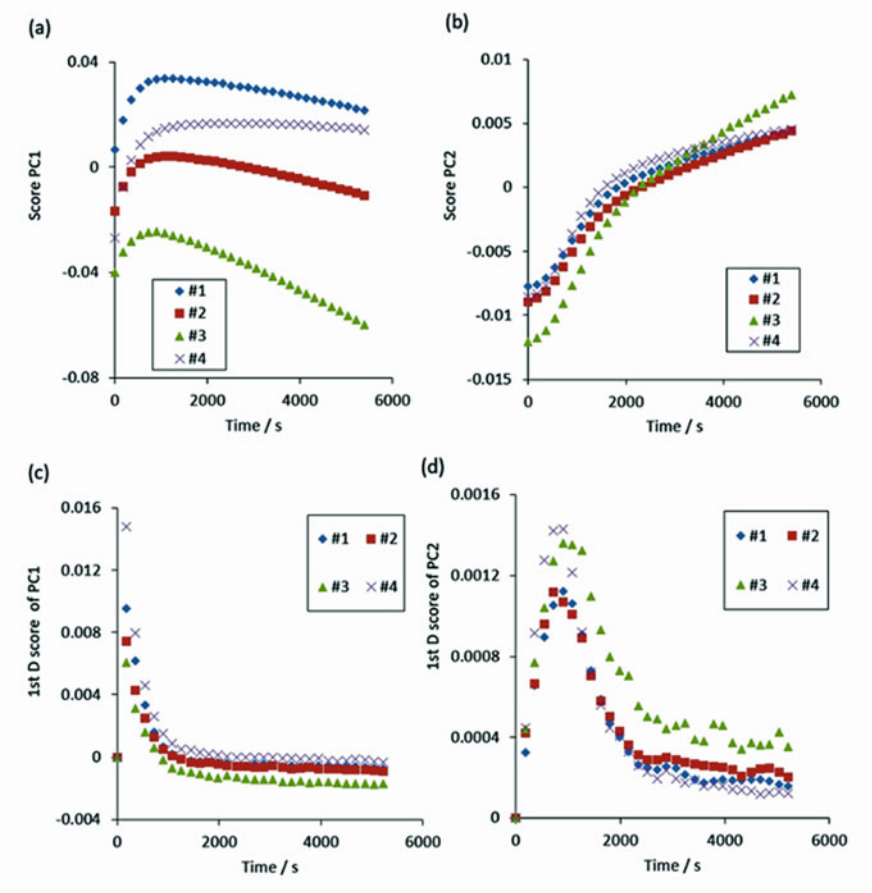

Fig. 7.6 Score profiles of **a** PC1 and **b** PC2 for the ATR-IR spectral data matrix of each self-setting apatite cement setting process. Differentiated score profiles for **c** PC1 and **d** PC2 for each self-setting apatite cement phase transformation process. Reprint with permission [13]

the growth of hydroxyapatite became stable at around 3000 s, suggesting that the crystal growth of hydroxyapatite is taking place under normal conditions.

The hydroxyapatite crystal growth process from TTCP and DCPD mixture was evaluated using ATR-IR and PCA. The derivative score plots were useful in our understanding of the complicated concept of HAp crystal growth. This approach has found usefulness in evaluating rapid reaction such as self-setting apatite cement. The phase transformation and hydroxyapatite crystal growth had three process, and CO_2 played an important role in the phase transformation.

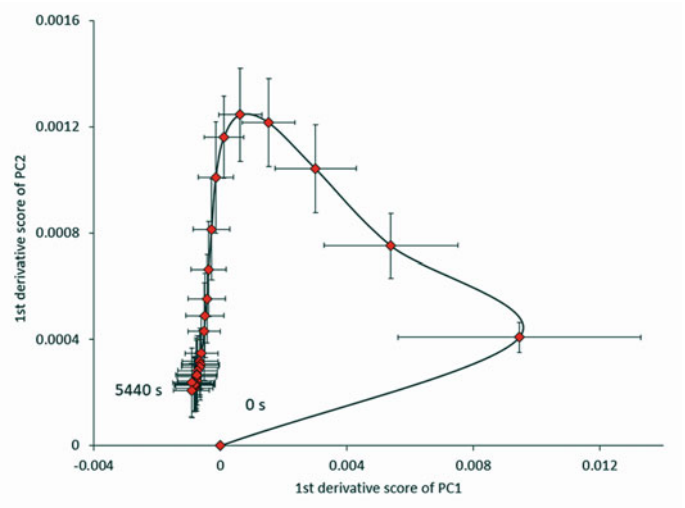

Fig. 7.7 Relationship between differentiated PC1 and PC2 scores for the setting process of the self-setting apatite cement. *Note* The horizontal and vertical bars indicate respective standard deviation (n = 4). Reprint with permission [13]

7.4 Effects of Amino Acid on Hydroxyapatite Crystal Growth—ATR-IR Spectroscopy Monitoring with MCR-ALS

The proteins involved in mineralization are also involved in the calcification of hard tissues in the human body [20]. The adsorptions of amino acids and peptide on the hydroxyapatite surface are reported to have a specific effect on the crystalline growth rate of hydroxyapatite [21]. The molecular interaction between amino acids and calcium phosphate is an important factor concerning the biophysics of the human body.

To investigate effect of amino acids on hydroxyapatite crystal growth, TTCP and DCPD mixture with amino acid solutions were kneaded. A 0.2 M phosphate buffer with a pH of 6.8 or aqueous solutions of 0.1 w/v% amino acids (alanine, asparagine, serine, and o-phospho-L-serine) were used as the kneading solutions. The IR spectra of kneaded sample were obtained by ATR-IR spectroscopy [22]. Figure 7.8 shows ATR-IR spectra of kneaded samples with amino acid solutions. Samples kneaded with phosphate buffer, asparagine and alanine solutions displayed increase hydroxyapatite specific phosphate ion vibration peaks from 0 to 54 min. The peak detected at 850 cm^{-1} was due to the presence of carbonate apatite. The hydroxyapatite peak for kneaded samples using serine solution showed a smaller increase compared to those recorded at hydroxyapatite specific phosphate ion bands. The hydroxyapatite peak was not recorded for the kneaded sample using the o-phospho-L-serine solution until after 54 min. Multivariate Curve Resolution with

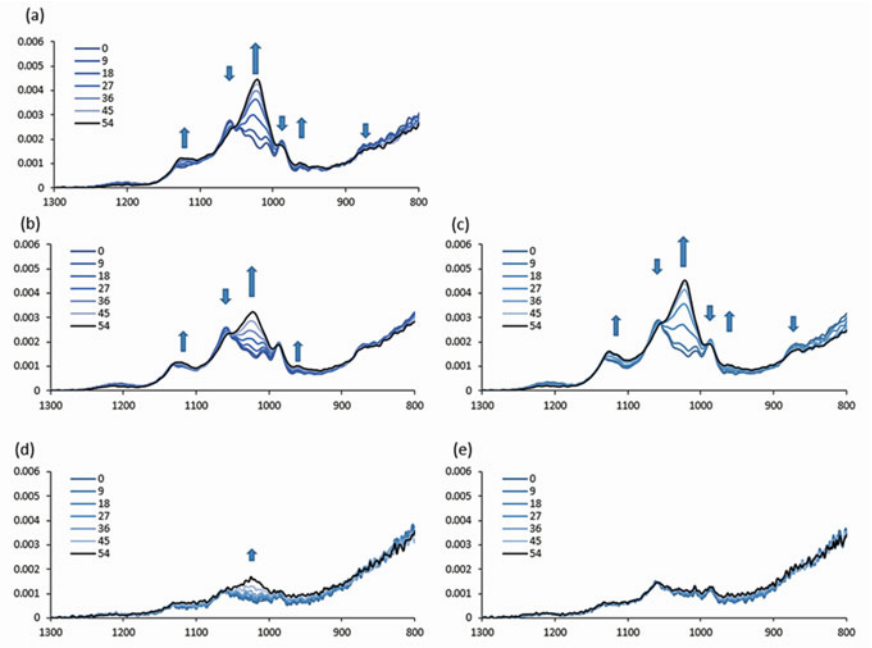

Fig. 7.8 Infrared spectra of the supersaturated samples with several solutions. **a** pH 6.8 phosphate buffer, **b** asparagine solution, **c** alanine solution, **d** serine solution, and **e** o-phospho-l-serine solution. Color line legends show time (min). Reprint with permission [22]

Alternating Least Squares (MCR-ALS) is a chemometric method and it is a useful tool in estimating the concentration based on specific peak absorbance. MCR-ALS was applied to IR spectra dataset to determine the amount of hydroxyapatite crystal growth from 1024 cm^{-1} peak absorbance.

Figure 7.9 shows the decomposed sources based on previous spectra dataset and materials spectra. Source 1 was quite similar to DCPD spectra. Combes et al. reported the IR spectra of DCPD nucleation on titanium surfaces [23]. The spectra shape in Fig. 7.9 is in agreement with the IR spectra reported in their study. Source 2 was similar to the hydroxyapatite phosphate ion peak at 1024 cm^{-1}. Gadaleta et al. reported the hydroxyapatite phosphate ion peaks occurred at around 1030 cm^{-1} [24]. Another study by Xie et al. also reported the phosphate band of hydroxyapatite occurring at the same band position [25]. They investigated hydroxyapatite phase transformation from DCPD into hydroxyapatite using bovine serum albumin. Source 3 suggested base line contribution from 1000 to 800 cm^{-1}. A decrease in concentration of DCPD and TTCP material was hypothesized based on the concentration of Source 2. The concentration of Source 2 was further analyzed to investigate hydroxyapatite crystal growth.

Figure 7.10 shows time profile of hydroxyapatite concentration in supersaturated samples based on Source 2 values. Kneaded sample with phosphate buffer and

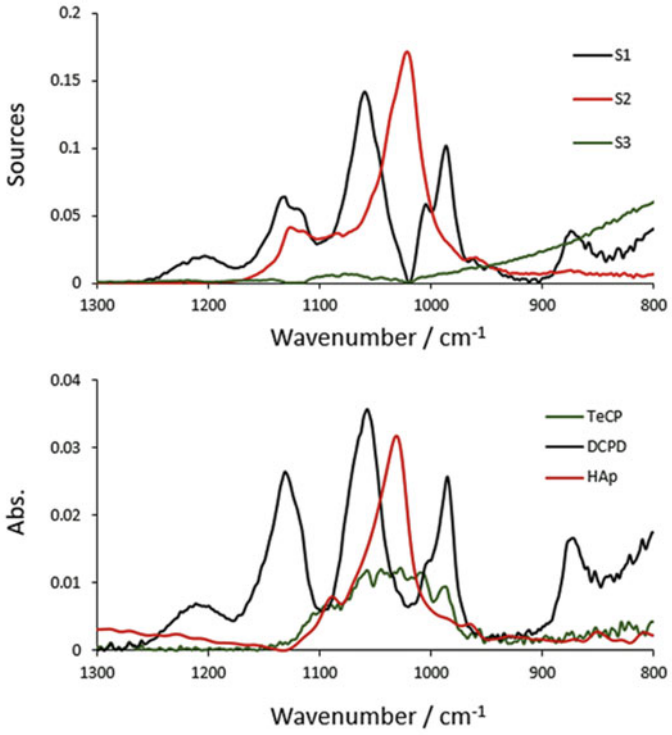

Fig. 7.9 Decomposed sources based on (top) IR spectra with MCR-ALS calculation, and (bottom) IR spectra of reference bulk materials. Reprint with permission [22]

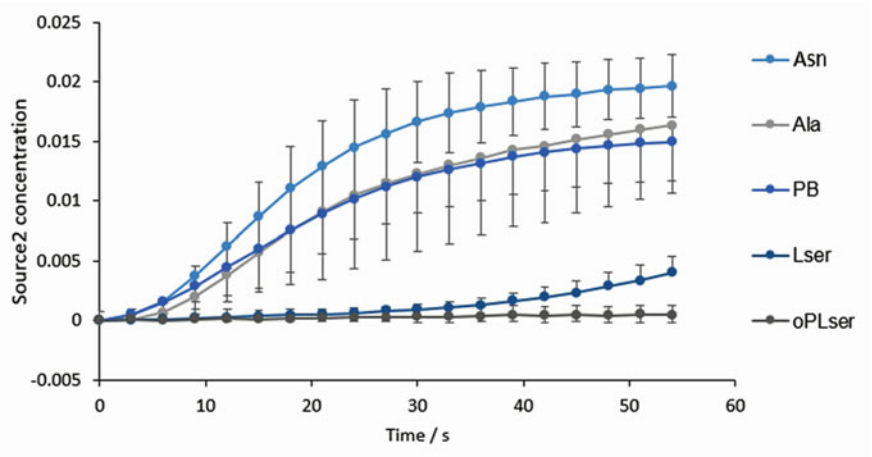

Fig. 7.10 Time profiles of HAp concentration in supersaturated samples based on source 2 values (Asn: asparagine solution; Ala: alanine solution; PB: phosphate buffer; Lser: serine solution; oPLser: o-phospho-l-serine solution). Reprint with permission [22]

asparagine and alanine solutions displayed sigmoidal increase when plotted against time. The increase was similar to previous discussions concerning changes in hydroxyapatite concentration. The growth of hydroxyapatite crystals has been suggested to occur within the samples. Very little increase was detected for the sample kneaded with the serine solution from 40 to 54 min. It was postulated that the serine solution has an effect on inhibiting the growth of hydroxyapatite crystal. No hydroxyapatite crystal growth was found in samples kneaded with the o-phospho-l-serine solution across changes in concentration and time. It was suggested that a more powerful inhibition existed between hydroxyapatite seed crystals and the o-phospho-l-serine solution.

There are many studies examining the interactions between hydroxyapatite and Phosphorylation amino acid or proteins. Shimabayashi and Tanizawa et al. reported the effects of o-phospho-l-serine solution on supersaturated calcium phosphate solution [26]. They concluded the crystal growth of hydroxyapatite were retarded in the presence of phosphorylated polyvinylalcohol and phosphoserine and the retardation were caused by the competitive adsorption between inorganic phosphate ion and the phosphate group of the organic compounds for the active growth sites on the hydroxyapatite crystal or nucleus. The study by Tavafoghi and Cerruti reported that negative charged amino acids such as glutamic acid and phosphoserine controlled the nucleation of hydroxyapatite [27]. Dissolved amino acids can inhibit hydroxyapatite crystal growth by chelating calcium ion and phosphate ions or binding to nuclei of calcium phosphate and preventing their further growth, amino acids bound to surfaces can promote hydroxyapatite precipitation by attracting calcium ion or phosphate ions and increasing the local supersaturation. As mentioned earlier, Xie et al. reported DCPD phase transformation into hydroxyapatite in the presence of bovine serum albumin with ATR-IR spectroscopy [25]. Protein adsorption on hydroxyapatite crystal surface was indicated by their spectra investigation. Their study indicated hydroxyapatite crystal is dependent on the surface properties. Villarreal-Ramirez et al. examined the adsorption of phosphoproteins on hydroxyapatite surface using molecular dynamic analysis [28]. Phosphorylated peptides are rapidly absorbed on the hydroxyapatite surface as reported. According to these reports, it can be considered that the phosphoserine was adsorbed on the hydroxyapatite seed crystals and inhibit the growth of hydroxyapatite crystals.

The effect of asparagine, alanine, serine, and o-phospho-l-serine adsorption on seed crystal of hydroxyapatite was investigated using IR spectra. The rate of transformation for TTCP and DCPD mixture were found to be dependent on the amino acids. It was also discovered that samples kneaded with asparagine and alanine solutions transformed to hydroxyapatite, while serine and o-phospho-l-serine solutions inhibited the phase transformation to hydroxyapatite. Kinetic analysis suggested that serine and o-phospho-l-serine were adsorbed on the hydroxyapatite surface with electrostatic force. The findings suggested that the adsorption of solution decreases the surface free energy of hydroxyapatite seed crystals.

7.5 Hydroxyapatite and Interactions with Biological Materials and Biomaterials

The interactions between hydroxyapatite and amino acids and proteins have been extensively investigated. Bovine serum albumin is frequently used as a model protein. This is because albumin has a high protein content in the body. The interaction between hydroxyapatite and bovine serum albumin was investigated by Swain and Sharker [29]. In their study, hydroxyapatite nanoparticles were prepared using $(CH_3COO)_2Ca$ and KH_2PO_4 as starting materials. Both solutions were mixed thoroughly with continuous stirring and pH was controlled by the addition of NH_4OH and tris-buffer. 0.1 mg hydroxyapatite nanoparticle was mixed with 5 mg/mL of bovine serum albumin solution. The sample was incubated for 240 h at 37 °C. The supernatant solution was collected and lyophilized. The adsorption behavior to hydroxyapatite followed the Langmuir adsorption isotherm. This indicates that bovine serum albumin is adsorbed on the hydroxyapatite surface as a single film. They conclude that the electrostatic interaction between bovine serum albumin and hydroxyapatite dominates the adsorption. Hydroxyapatite nanoparticles have demonstrated the usefulness of the substrate as a protein carrier.

The problem of recent infections in orthopedic implants is very important. It is often known to be a Gram-positive bacterial infection. Therefore, attempts to prevent bacterial infection by adsorbing a preparation against Gram-positive bacteria on hydroxyapatite have been reported. Bacteria colonize the implant material and appear as a biofilm. Problems often occur one year after implants. Townsend et al. reported antimicrobial peptide (AMP) coating for hydroxyapatite system [30]. 1 M calcium nitrate and 0.6 M diammonium hydrogen phosphate dibasic were prepared at pH 10 using ammonium hydroxide. The phosphate salt solution was added dropwise to the calcium salt solution and the pH is adjusted using ammonium hydroxide to maintain a pH level of 10. The prepared samples were washed by five cycles of centrifugation and resuspension with pure water before filtering. The sample was resuspended with deionized water prior to filtering and the typical yield of solid product was approximately 30 g, with 1 g resuspended at 1 mg ml^{-1} in deionized water adjusted to pH 7 and dried overnight in an oven at 60 °C to give hydroxyapatite as a powder. In the production of coating consists of AMPs covalently bonded to the hydroxyapatite, the prepared hydroxyapatite pellets were incubated in 10 ml N,N-dimethylformamide, 0.2 M succinimidyl trans-4-(maleimidylmethyl)cyclohexane-1-carboxylate, and AMP for 12 h with shaking. The stability of the AMP to incubation suggested that the peptide has formed a covalent bond with the surface that will not permit peptides to be desorbed from the surface. The electrostatically released AMP inhibits bacterial growth in solution while the covalently bonded peptide inhibits adherence and biofilm construction. It was concluded that both mechanisms together inhibit the colonization of bacteria at the interface of an engineered surface with tissue.

Hydroxyapatite is known to coexist with collagen in in vivo bone and exist as an extracellular matrix. Electrostatic interactions work between collagen and hydroxyapatite to promote bone formation. Glutaraldehyde (GA) forms a crosslink between the two, providing further improvement in mechanical strength. GA has two functional groups that can bind to the free amine groups of collagen lysine and hydroxylysine amino acid residues. The free amine group of collagen reacts with the aldehyde group of GA to form a Schiff base. Chang et al. reported the FR-IR analysis of hydroxyapatite/collagen cross-linked by GA [31]. IR spectra for hydroxyapatite/collagen nanocomposite samples cross-linked by GA shows N–H stretching at 3310 cm^{-1} for amide A and C=O stretching at 1600–1700 cm^{-1} for the amide I. They concluded that the IR spectra for the cross-linked hydroxyapatite/collagen samples include the effect of the characteristic microstructure development of hydroxyapatite/collagen fibrils induced by the cross-linking.

The high stiffness of bone results from the combination of the triple helix structure of hydroxyapatite and collagen fibrils. Biomaterials made from a combination of hydroxyapatite and collagen mean imitating living bones. It is useful as a hybrid material for clinical applications. Amyloid fibrils are β-sheet-based fibril aggregates. It is effective for bottom-up synthesis because it is easier to control fibrogenic ability than collagen. It also has an advantage in terms of material cost. Li et al. reported a composite material of amyloid fibrils and hydroxyapatite [32]. In β-lactoglobulin amyloid fibrils, it can be seen that amyloid fibrils and hydroxyapatite are organized into intercalations in a layered structure. The elastic moduli and densities of rigid composite materials correspond to the elastic moduli and densities of cancellous bone in vivo.

Zhang et al. reported that the interaction between amelogenin protein and hydroxyapatite was used to form hydroxyapatite on a molecular assembly [33]. They found that the pH control of the sample solution could manipulate the precipitated calcium phosphate phase. Phospho solid-state NMR analysis showed a sharp peak at 3.54 ppm, the same as human enamel. They are also investigating the protein conformation formed in detail.

Drug delivery from the scaffolding system consists of the application of a combination of drug interactions with the base matrix and subsequent release. The combination of chitosan and hydroxyapatite allows the synthesis of biodegradable hybrid materials. A sustained-release formulation can be constructed by mixing the drug with the material. Ardakani et al. described the sustained release of naproxen from scaffold materials based on chitosan-hydroxyapatite-poly(acrylic acid) matrix [34]. Naproxen sodium was loaded into the prepared nanocomposite scaffolds by ionic interactions. The prepared scaffold with the highest amount of nano hydroxyapatite was able to maintain 58% of the active pharmaceutical ingredient after 14 days. It was revealed that the drug release behavior is controlled by the Fick diffusion process. It shows that the proposed scaffold may be a promising drug carrier for bone tissue engineering.

Titanium oxide has high biocompatibility and is known to be a useful biomaterial. In addition, hydroxyapatite has a high affinity for titanium oxide and is often used as a hybrid material due to its high opportunity strength. Wang et al. incubated

the thermally oxidized titanium in the simulated body fluid solution and coated the surface with apatite [35]. It was concluded that crystal growth of hydroxyapatite in simulated body fluid solution was dependent on the heating temperature of titanium. They also reported interaction between titanium surface and hydroxyapatite with hydrogen peroxide and NaOH in another study [36]. The heating with hydrogen peroxide and incubating with NaOH solution induce anatase titania gel layer. The pretreatment method of gel layer indicated a function to support the growth of HAp on the titanium surface.

7.6 Concluding Remarks

In this chapter, we reviewed the usefulness of apatite as a material for drug delivery system and examined the interaction concerning hydroxyapatite crystal growth. Apatite has the potential for further development of medical materials and bioceramics in the field of orthopedic treatment and dentistry. The formation of apatite in vivo is dominated by the degree of supersaturation of calcium and phosphoric acid. There have been many reports that adsorption on the surface of hydroxyapatite crystal growth affects the crystal growth surface. Amino acids, peptides and proteins regulate the growth of hydroxyapatite through electrostatic interactions. We believed that this is ideal for the loading of next generation protein medicines. Practicality is expanded through the combination of a pharmacological approach with hydroxyapatite. The combination of protein nanofibers and hydroxyapatite is also constructed through electrostatic interaction. We anticipated that these biomaterials and bioceramics will continue to develop in the future.

References

1. Gillani R, Ercan B, Qiao A (2010) Nanofunctionalized zirconia and barium sulfate particles as bone cement additives. Int J Nanomed 5:1–11
2. Kurtz SM, Kocagöz S, Arnholt C et al (2014) Advances in zirconia toughened alumina biomaterials for total joint replacement. J Mech Behav Biomed Mater 31:107–116
3. Honda M, Kikushima K, Kawanobe Y et al (2012) Enhanced early osteogenic differentiation by silicon-substituted hydroxyapatite ceramics fabricated via ultrasonic spray pyrolysis route. J Mater Sci Mater Med 23:2923–2932
4. Ben-Nissan B (ed) (2014) Advances in calcium phosphate biomaterials. Springer series in biomaterials science and engineering, vol 2. Springer, Berlin
5. Chevalier J (2006) What future for zirconia as a biomaterial? Biomaterials 27:535–543
6. Nakata K, Kubo T, Numako C et al (2009) Synthesis and characterization of silicon-doped hydroxyapatite. Mater Trans 50:1046–1049
7. Yilmaz B, Alshemary AZ, Evis Z (2019) Co-doped hydroxyapatites as potential materials for biomedical applications. Microchem J 144:443–453
8. Hughes JM, Cameron M, Crowley KD (1989) Structural variations in natural F, OH, and Cl apatites. Am Mineral 74:870–876

9. Tonegawa T, Ikoma T, Yoshioka T et al (2010) Crystal structure refinement of A-type carbonate apatite by X-ray powder diffraction. J Mater Sci 45:2419–2426
10. Takechi M, Miyamoto Y, Ishikawa K et al (1998) Effects of added antibiotics on the basic properties of anti-washout-type fast-setting calcium phosphate cement. J Biomed Mater Res 39:308–316
11. Chevalier E, Viana M, Cazalbou S et al (2010) Ibuprofen-loaded calcium phosphate granules: combination of innovative characterization methods to relate mechanical strength to drug location. Acta Biomater 6:266–274
12. Chow LC (1991) Development of self-setting calcium phosphate cements. J Ceram Soc Jpn 99:954–964
13. Otsuka Y, Takeuchi M, Otsuka M et al (2015) Effect of carbon dioxide on self-setting apatite cement formation from tetracalcium phosphate and dicalcium phosphate dihydrate; ATR-IR and chemoinformatics analysis. Colloid Polym Sci 293:2781–2788
14. Hamanishi C, Kitamoto K, Tanaka S et al (1996) A self-setting TTCP-DCPD apatite cement for release of vancomycin. J Biomed Mater Res 33:139–143
15. Otsuka M, Nakahigashi Y, Matsuda Y et al (1997) A novel skeletal drug delivery system using self-setting calcium phosphate cement VIII: the relationship between *in vitro* and *in vivo* drug release from indomethacin-containing cement. J Control Release 43:115–122
16. Terukina T, Saito H, Tomita Y et al (2017) Development and effect of a sustainable and controllable simvastatin-releasing device based on PLGA microspheres/carbonate apatite cement composite: *In vitro* evaluation for use as a drug delivery system from bone-like biomaterial. J Drug Deliv Sci Technol 37:74–80
17. Kamegai A, Shimamura N, Naitou K et al (1994) Bone formation under the influence of bone morphogenetic protein/self-setting apatite cement composite as a delivery system. Biomed Mater Eng 4:291–307
18. Ito T, Koyama Y, Otsuka M (2012) DNA complex-releasing system by injectable self-setting apatite cement. J Gene Med 14:251–261
19. Pleshko N, Boskey A, Mendelsohn R (1991) Novel infrared spectroscopic method for the determination of crystallinity of hydroxyapatite minerals. Biophys J 60:786–793
20. Sukhodub LF, Moseke C, Sukhodub LB et al (2004) Collagen-hydroxyapatite-water interactions investigated by XRD, piezogravimetry, infrared and Raman spectroscopy. J Mol Struct 704:53–58
21. Jungbauer A, Hahn R, Deinhofer K et al (2004) Performance and characterization of a nanophased porous hydroxyapatite for protein chromatography. Biotechnol Bioeng 87:364–375
22. Otsuka Y, Ito A, Takeuchi M et al (2019) Effect of amino acid on calcium phosphate phase transformation: attenuated total reflectance-infrared spectroscopy and chemometrics. Colloid Polym Sci 297:155–163
23. Combes C, Rey C, Freche M (1998) XPS and IR study of dicalcium phosphate dihydrate nucleation on titanium surfaces. Colloids Surf B 11:15–27
24. Gadaleta SJ, Paschalis EP, Betts F et al (1996) Fourier transform infrared spectroscopy of the solution-mediated conversion of amorphous calcium phosphate to hydroxyapatite: new correlations between X-ray diffraction and infrared data. Calcif Tissue Int 58:9–16
25. Xie J, Riley C, Kumar M et al (2002) FTIR/ATR study of protein adsorption and brushite transformation to hydroxyapatite. Biomaterials 23:3609–3616
26. Shimabayashi S, Tanizawa Y (1990) Formation of hydroxyapatite in the presence of phosphorylated polyvinylalcohol as a simplified model compound for mineralization regulator phosphoproteins. Chem Pharm Bull 38:1810–1814
27. Tavafoghi M, Cerruti M (2016) The role of amino acids in hydroxyapatite mineralization. J R Soc Interfac 13:20160462
28. Villarreal-Ramirez E, Garduño-Juarez R, Gericke A et al (2014) The role of phosphorylation in dentin phosphoprotein peptide absorption to hydroxyapatite surfaces: a molecular dynamics study. Connect Tissue Res 55:134–137

29. Swain SK, Sarkar D (2013) Study of BSA protein adsorption/release on hydroxyapatite nanoparticles. Appl Surf Sci 286:99–103
30. Townsend L, Williams RL, Anuforom O et al (2017) Antimicrobial peptide coatings for hydroxyapatite: electrostatic and covalent attachment of antimicrobial peptides to surfaces. J R Soc Interface 14:20160657
31. Chang MC, Tanaka J (2002) FT-IR study for hydroxyapatite/collagen nanocomposite cross-linked by glutaraldehyde. Biomaterials 23:4811–4818
32. Li C, Born AK, Schweizer T et al (2014) Amyloid-hydroxyapatite bone biomimetic composites. Adv Mater 26:3207–3212
33. Zhang J, Wang J, Ma C et al (2020) Hydroxyapatite formation coexists with amyloid-like self-assembly of human amelogenin. Int J Mol Sci 21:2946
34. Asadian-Ardakani V, Saber-Samandari S, Saber-Samandari S (2016) The effect of hydroxyapatite in biopolymer-based scaffolds on release of naproxen sodium. J Biomed Mater Res A 104:2992–3003
35. Wang XX, Yan W, Hayakawa S et al (2003) Apatite deposition on thermally and anodically oxidized titanium surfaces in a simulated body fluid. Biomaterials 24:4631–4637
36. Wang XX, Hayakawa S, Tsuru K et al (2001) A comparative study of in vitro apatite deposition on heat-, H_2O_2-, and NaOH-treated titanium surfaces. J Biomed Mater Res 54:172–178

Yuta Otsuka Dr. Otsuka received his Ph.D. in 2018, after which he was appointed as a research associate (2018–Current) at the Faculty of Pharmaceutical Sciences, Tokyo University Sciences. His research attempts to investigate co-crystallization and phase transformation using Raman, Near-infrared, Mid-infrared spectroscopy with multi-variate analysis.

Chapter 8
Intelligent Drug Delivery System for Artificial Bone Cement Based on Hydroxyapatite-Related Organic/Inorganic Composite Materials

Makoto Otsuka

Abstract The self-setting apatite-based bone cement, prepared using the solubility phase diagram of calcium phosphates, consists of metastable calcium phosphates and can be transformed to the low-crystallinity apatite with bio-affinity to natural bones. Various drugs were kneaded into the cement to create an artificial bone cement with sustained drug release capability and the drug release from the cement matrices can be controlled based on the parameters of the Higuchi equation, such as drug concentration, porosity, granular diameter, and diffusion coefficient. Results from in vitro and in vivo drug release experiments suggested that in vivo drug release from the apatite cement was dependent on calcium concentration in the body fluids. The results indicated that anti-osteoporosis drug release from apatite bone cement could be controlled based on the severity of the disease in osteoporotic rats. In addition, the amount of diseased bone in the rat increased with the apatite bone cement. Furthermore, anti-osteoporotic drugs were added to the apatite-collagen composite cement for the manufacture of three-dimensional perforated macro-porous bone cell scaffold. The collagen-HAp cement containing DNA complex was administered, and the growth of cancer cells was effectively suppressed by the continuous DNA release of the injected collagen-HAp cement containing DNA complex. This highly functional artificial bone was shown to be suitable for bone regeneration.

Keywords Apatite bone cement · Bioaffinity · Higuchi equation · Osteoporosis responsive drug release · Apatite-collagen composite cement · Three-dimensionally perforated macro-porous bone cell scaffold

M. Otsuka (✉)
Faculty of Pharmacy, Research Institute of Pharmaceutical Sciences, Musashino University, Nishi-tokyo, Japan
e-mail: motsuka@ep.musashino-u.ac.jp

Research Institute of Electronics, Shizuoka University, Hamamatsu, Japan

A. H. Choi and B. Ben-Nissan (eds.), *Innovative Bioceramics in Translational Medicine I*,
Springer Series in Biomaterials Science and Engineering 17,
https://doi.org/10.1007/978-981-16-7435-8_8

8.1 Introduction

Bone-related diseases, such as osteoporosis, often involve bone fracture accidents and result in a bedridden state, which greatly reduces the patient's quality of life. Artificial bones and hip joints have been used as medical devices to restore the functionality of osteoporosis patients and improve their quality of life [1]. Artificial bones are made of metal (titanium and stainless steel), ceramics (zirconia, alumina, and calcium phosphate), or polymers (poly-ether-ether-keton and polyethylene terephthalate) [2, 3].

Hydroxyapatite (HAp), which has good compatibility with hard tissues in the body, has been used for artificial bones, artificial joints, and dental implants [4, 5]. However, time is required for the stabilization of HAp implants after surgical implantation. Clinically, it is desirable to develop an artificial bone system that allows a faster bone cell proliferation and has high cohesiveness with natural bones.

An implantable drug delivery system using a biodegradable polymer material such as gelatin has been developed as a novel drug delivery system to deliver loaded pharmaceuticals to natural hard tissue and promote bone formation [6–8]. However, when using these implants in patients with bone defects, it is difficult to obtain good clinical scores. Therefore, artificial bone systems have been developed in which antibiotics and anticancer agents are embedded in synthetic porous HAp beads and are composed of biocompatible inorganic materials that fill bone defects and control drug release [9, 10]. However, it is not easy to control the amount of drug being loaded and sintering at high temperatures eliminates the possibility of using the artificial bone cement for sustained drug release applications as the drug is only physical adsorbed on surface of the micro-pores.

On the other hand, when using self-setting HAp bone cement [11] that is transformed to stable crystalline HAp after kneading, as the bone cement material, the drug can be easily sustained released for long-term effects by embedding the drug powder in the cement. Intelligent drug delivery systems (DDS) have been developed that release various drugs in response to the degree of pathological condition by making use of the drug release control technology and biomimetic technology based on apatite-related bone cement. In this study, the development process of these DDS has been described.

8.2 Self-hardening Mechanism of the Setting HAp-Related Bone Cement

Brown and Chou [11] prepared a self-setting HAp-related bone cement based on the solubility phase diagram of calcium phosphates. The metastable calcium phosphates in the cement rapidly underwent crystal transition to form stable HAp by kneading with a phosphoric acid solution. The cement rapidly self-set to HAp with low crystallinity as observed by powder X-ray diffraction analysis. Self-setting HAp

bone cement was developed using this technique, and it has been used clinically and has been confirmed as an excellent biocompatible artificial bone material. The artificial bone cement was used as a base material to control drug delivery function by incorporating various drug powder into the self-setting HAp cement. Since the drug-containing cement was self-hardened and transformed to low-crystalline carbonate HAp with high biocompatibility, the drug powder was distributed in the interconnected pores that exists within the cement. Therefore, after the cement is set within the human body, drug powder is dissolved and slowly released from the artificial bone cement throughout micro-pores of the HAp cement matrices.

8.3 Diffusion Theory of Controlled Drug Release from Self-setting HAp-Related Bone Cement, and Therapeutical Applications of These Cement Systems

The first application of self-setting HAp-related bone cement was to treat infections caused by methicillin-resistant *Staphylococcus aureus*, often occurring after surgery to attach an artificial bone. Traditionally, antibacterial agents either in the form of an injection or in the tablet form is administered after the surgical implantation of artificial bone in an effort to prevent bacterial infections after surgery. However, the disadvantage of this approach is the fast dissolution of normal drug powder, rapid drug diffusion from the implanted site, the body metabolizes the medication, and eventually gets broken down absorbed by the body. Therefore, a biocompatible HAp cement was used as the base cement to prevent postoperative infections for an extended period, and consequently, a HAp bone cement containing the antibiotic cephalexin (CEX) was synthesized [12].

Figure 8.1 shows the in vitro drug release profile of the HAp bone cement in a phosphate buffer at 37 °C. It indicated that the HAp cement had CEX sustained-release characteristics for an extended period of 1 week or more, and the rate of drug release increased depending on the drug content. The drug filled in the hardened cement matrix was released by diffusion through the micro-pores. Higuchi reported that the drug release rate from the cement matrices with micro-pores at time t is dependent on the porosity of the cement, drug content, drug solubility, surface area of the cement, and tortuosity of the pores, and was expressed by the following equation [13]:

$$M_t = AM_0\sqrt{C_s\frac{D_i\varepsilon}{\tau}(2C_d - \varepsilon C_s)t} \tag{8.1}$$

where M_t is the drug release amount at time t; A is the surface area of the cement; t is time; D_i is the drug diffusion constant; τ is the tortuosity; ε is the porosity; C_d is the drug concentration; M_0 is the total amount of drug; and C_s is the drug solubility.

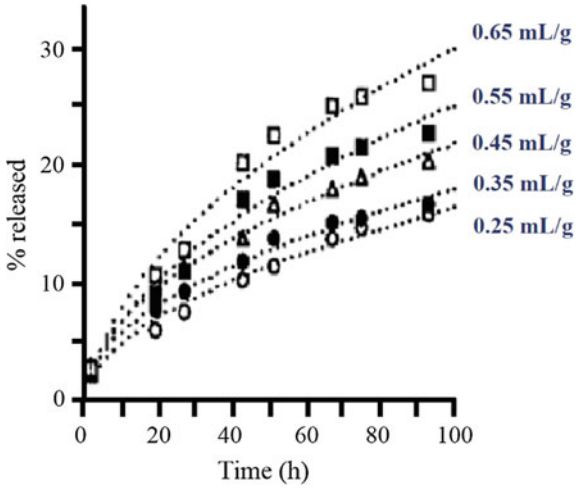

Fig. 8.1 Drug release profiles of HAp cement containing various concentrations of cephalexin. ▲: 4.8% drug cement; ■: 2.6% drug cement; •: 0.9% drug cement

The CEX release profiles of the HAp bone cements were applied to the Higuchi equation, as shown in Fig. 8.2 [12]. Since good linear relationships were observed, the drug diffusion rate in the micro-pores in the cements was the rate-determining step of the drug release rate, and it indicated that the drug content affected the release of the drug from the cement [14]. Based on this result, when considering the Higuchi equation (8.1), it was possible to control the drug release rate without restraints from artificial bone cement by controlling the geometrical elements of the cement and the elements related to the drug diffusion characteristics.

Second, based on the Higuchi equation (8.1), the drug release from the HAp bone cement should be controlled by changing the cement surface area based on the

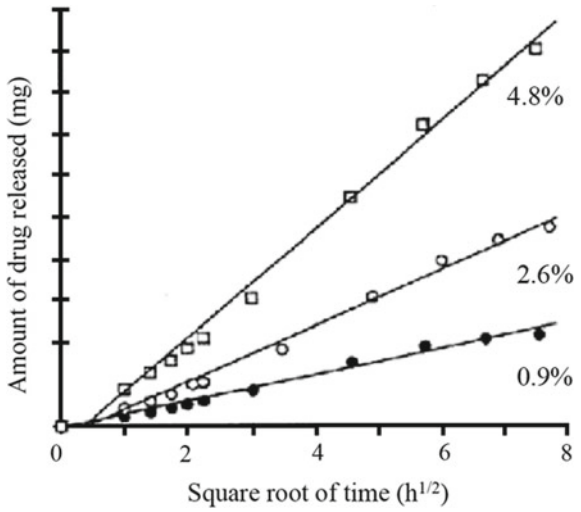

Fig. 8.2 Effect of drug concentration on drug release profiles of the HAP cement containing cephalexin, based on the Higuchi plots. □: 4.8% drug cement; o: 2.6% drug cement; •: 0.9% drug cement

particle size. As application to treat rheumatic bone deformity, the anti-inflammatory drug release from the cements containing indomethacin (IMC) with various granular size and drug concentration of the bone cement granules were tested [15]. The HAp cement granules with diameters of 2, 4, and 15 mm were prepared and their drug release rate tested, as shown in Fig. 8.3. The drug release rate of the granules increased with decrease in granular size of the cement, implying that their release rates were dependent on the size and drug concentrations. However, when the amounts of drugs released were corrected to release amount per surface area, the initial drug release profiles from the granular cements of all sizes overlapped to produce nearly identical drug release profiles, as shown in Fig. 8.4. This was an evidence that the drug release from the HAp cement with various size granules followed the Higuchi equation. The

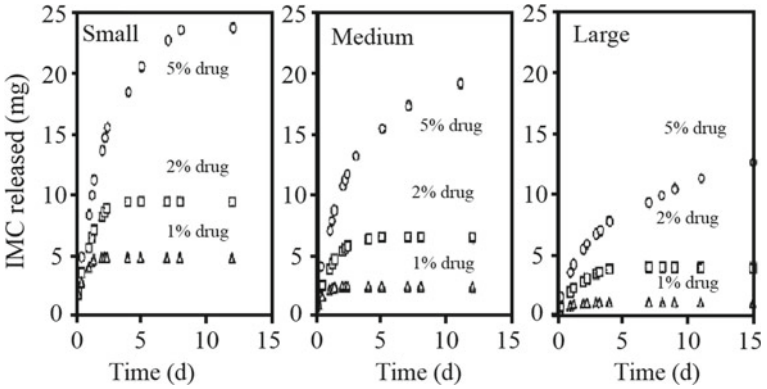

Fig. 8.3 Effect of granule size and drug concentration on drug release profiles of the HAp bone cement granules containing anti-inflammatory agent, indomethacin (IMC)

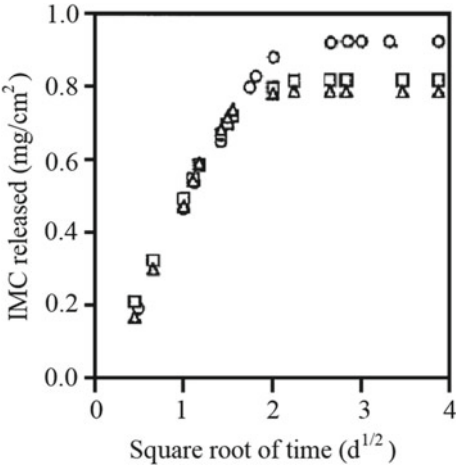

Fig. 8.4 The HAp bone cement granules containing 5% IMC. △: small size, 2 mm in diameter; □: medium size, 4 mm in diameter; o: large size, 15 mm in diameter

result also suggested that it was possible to control drug release by changing the granular size of the cements.

In addition, as an application to correct bone defects after bone cancer resection surgery, controlling the release rate of an anticancer drug, 6 mercaptopurine (6-MP), from the sustained-release bone cement was examined by changing the cement powder and kneading liquid ratio [16]. Based on the Higuchi equation (8.1), the geometric structural factors of the micro-pores, such as the porosity (ε) and the tortuosity (τ), in the self-setting HAp cement can control drug release, and hence, the pore parameters of the cements were varied by changing the powder-liquid ratio of the cement. Figure 8.5 shows the effect of change in the powder-liquid ratio of the HAp cement containing 6-MP on the release rate. The symbols and dotted lines represent the measured values and simulated values, respectively, based on the Higuchi equation (8.1). The 6-MP release from the HAp cement increased with increasing in the powder-liquid ratio, and the measured values were fitted with Higuchi equation (8.1). The result indicated that the drug release parameters, the porosity (ε) and the porosity (τ), in the Higuchi equation were dependent on the powder-liquid ratio. Thus, it was concluded that the anticancer drug release rate from the HAp bone cement could be freely controlled by varying the powder/liquid ratio.

HAp is known to have high adsorption on proteins and peptides and has been utilized as a material in separation column for liquid chromatography owing to this property [17]. Therefore, the physicochemical properties, including the adsorption property of the applied drug to HAp, significantly affects the drug release property from HAp bone cement. Thus, the interaction between HAp and highly therapeutic polypeptide-based drugs, such as calcitonin (a therapeutic agent for osteoporosis), bone growth factors, and anticancer agents were investigated.

In this study, insulin, bovine serum albumin (BSA), and the tripeptide drug cephalexin were applied to self-setting HAp cement as model peptide drugs with different molecular weights [18], and the drug release rates from the pores of HAp

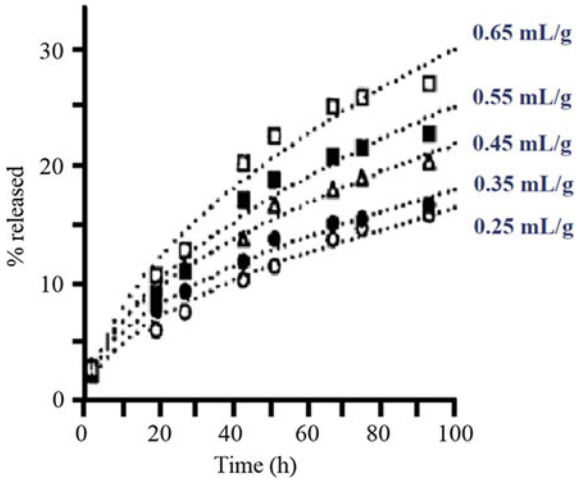

Fig. 8.5 Effect of amount of kneading liquid on drug release of HAp bone cement containing anti-cancer drug

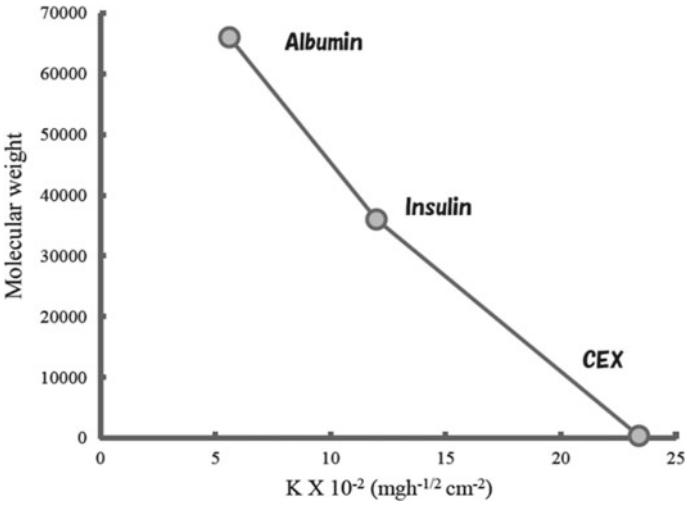

Fig. 8.6 Relationship between drug diffusion rate constant and molecular weight of polypeptide of the HAp bone cement

bone cement were compared. The in vitro BSA release from the HAp bone cement was very slow, since BSA has a greater molecular weight and a high affinity for apatite crystals. In contrast, the drug release of short peptide, cephalexin, was much faster than that of BSA or Insulin.

Figure 8.6 shows the relationship between the drug release rate and the molecular weight of various polypeptide drugs from the HAp bone cement matrices. The relationship revealed a decrease in the drug release rate as the molecular weight increases, and the result supports the theoretical relationship between diffusion rate constant and molecular weight. Therefore, it is considered that the drug release rate from the HAp bone cement decreases as the molecular weight increases. Based on this finding, it was shown that the polypeptide-based drug can be released in a sustained manner from the apatite cement DDS for an extended period of several months.

8.4 Effect of Drug Loading Geometrical Structure on Controlled Drug Release from Self-setting HAp-Related Bone Cement

Figure 8.7 shows application models of the homogeneous drug loaded-HAp bone cement and heterogeneous drug loaded-HAp bone cement. As described in the previous sections, the drug powder was distributed homogeneously within the bone cement base, and the drug release followed the Higuchi equation. The homogeneous drug loaded system was a clinically feasible application method, and had an

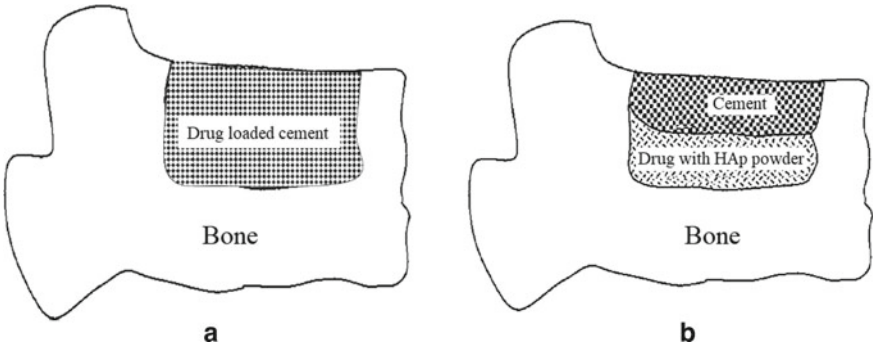

Fig. 8.7 Homogeneous (**a**) and heterogeneous (**b**) bone cement application models of HAp bone cement

advantage that safety at the time is ensured during surgery. In contrast, heterogeneous drug-loaded cement was prepared by designing a drug storage compartment inside the cement and the outer surface of the compartment encapsulated by the cement to maintain porosity and tortuosity of the cement pores by increasing or decreasing the cement kneading solution [19]. The device could control drug release from bone cement by a release mechanism according to the Fick's equation. The heterogeneous drug filling system allowed for much longer drug release than the homogenous system.

Figure 8.8 shows the drug release profile from HAp bone cement filled with aspirin, which is an anti-inflammatory drug, in a heterogeneous drug loading system. Since the HAp bone cement of the release control layer was prepared by changing the amount of seed crystal and kneading liquid, the porosity and tortuosity of micro-pores in the molded cement were changed in the formulation. The drug release rate of the

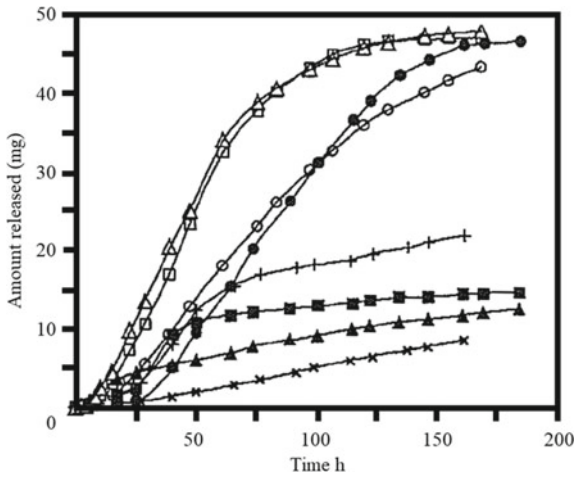

Fig. 8.8 Effect of micro pore structure on drug release from heterogeneous aspirin-loaded HAp bone cement

prepared HAp bone cement system varied significantly depending on the formulation (amount of seed crystal and kneading liquid) of the release control cement layer. Accurate drug release behavior could be controlled over a long period by filling the bone defect with aspirin-containing cement and encapsulating the outside with apatite cement.

8.5 Osteoporosis-Responsive Drug Delivery System Based on Self-setting HAp Bone Cement

By applying the basic concept of drug release kinetics, the relationship between the physicochemical properties and drug release properties of the artificial bones made from self-setting HAp bone cement were theoretically elucidated in the above section. However, in the process of developing HAp bone cement containing anti-inflammatory drug indomethacin [20], in order to clarify interaction between HAp cement matrices and bone cells, the in vitro and the in vivo drug release profiles were directly compared, but those were not matched well in long-term drug release period. The ionic concentrations of calcium and phosphoric acid in the serum of healthy humans are high and supersaturated with respect to HAp contained in bone. Therefore, it has been reported that low crystalline HAp, similar to natural bone, precipitates in simulated body fluid (SBF) containing calcium, phosphoric acid, etc. in the same concentrations as in healthy human body fluid [21]. In contrast, the phosphate buffer solution used the in vitro experiments in above section was an unsaturated solution because it did not contain calcium ion and was similar to those observed in osteoporotic condition, so the HAp cement matrices were dissolved and disintegrated from the cement surface. To explain quantitatively the gap phenomenon of drug release of HAp bone cement containing the anti-inflammatory drug indomethacin between in vitro and in vivo experiments, drug kinetics method was applied to the plasma drug concentration profiles [20]. The in vivo drug release rate from the HAp bone cement implanted in normal rats was determined based on the plasma drug concentration profiles using the deconvolution method. After implanting the bone cement into the living body, rapid in vivo drug release in the deconvoluted drug release profiles was confirmed during the initial stages; however, it slowed down significantly after 1 week when compared to the in vitro drug release in phosphate buffer after 1 week [20]. Figure 8.9 shows the relationship between the in vitro (in phosphate buffer) and in vivo drug release profiles [20]. In initial drug release stage within a week, the drug released amount of the in vitro drug release was almost the same as that of the in vivo release. However, the drug release profile for a prolonged period, i.e. 1 week or longer, revealed that the in vitro release tend to be significantly higher than that of the in vivo release [20].

Based on the findings of the in vitro and in vivo drug release from various HAp bone cements, the authors attempted to design an intelligent HAp bone cement that

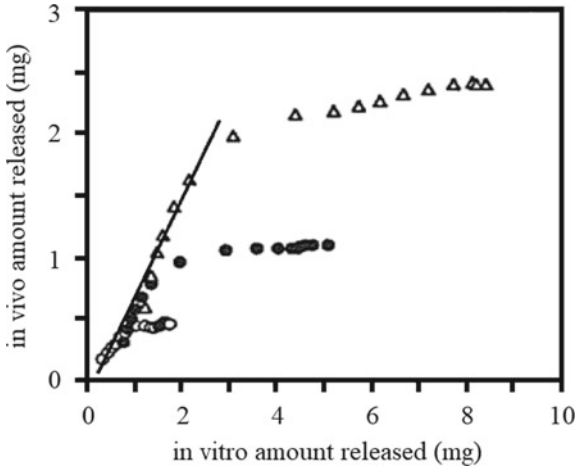

Fig. 8.9 Relationship between in vitro and in vivo drug release from the HAp bone cement containing indomethacin. In vitro test was performed in 0.1 M phosphate buffer at pH 6.8, while the in vivo test was performed in healthy rats. o: 1% drug-loaded cement; •: 2% drug-loaded cement; △: 5% drug-loaded cement

had drug release responsive to osteoporosis pathology. In vitro release test of anti-osteoporosis drug estrogen from the HAp bone cement DDS in SBF with various calcium concentrations showed that the drug release in SBF containing a high concentration of calcium (10 mg/100 mL Ca^{+}) was suppressed by precipitated HAp-like crystals on the surface of the cement (Fig. 8.10) [21]. In contrast, in the SBF solution containing no calcium (0 mg/100 mL Ca^{+}), it was observed that the HAp dissolved and disintegrated on the cement surface, and the volume of pores present within the increased, which accelerated drug release. From these findings, it was confirmed that the plasma calcium concentration-dependent drug release control mechanism

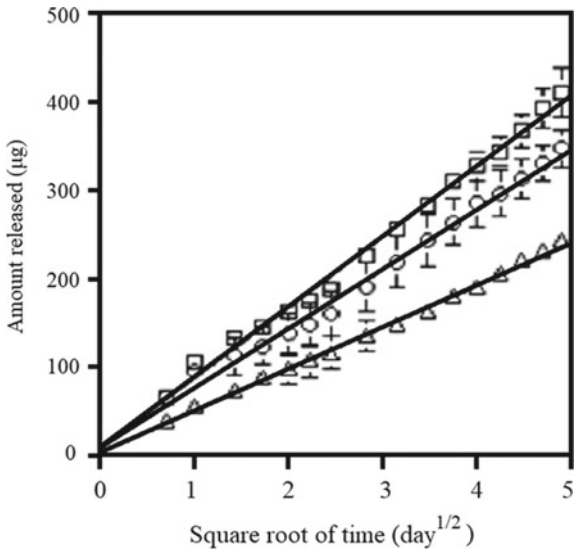

Fig. 8.10 Effect of calcium concentration on the estradiol release rate on the Higuchi plots of the HAp bone cements. △: 10 mg/100 mL Ca^{+}; o: 5 mg/100 mL $Ca^{\pm}$; □: 0 mg/100 mL Ca^{-}

of HAp bone cement in rats with osteoporosis was consistent with the results of the in vitro physicochemical experiments.

To assess the therapeutic application for the treatment of osteoporosis, an in vivo anti-osteoporosis drug release test of HAp bone cement DDS was conducted using three groups of rats: rats with osteoporosis pathology, rats recovering from pathology, and healthy rats. As shown in Fig. 8.11, the plasma concentration of calcium in osteoporotic pathological rats was 5 mg/100 mL, and that of healthy rats was 10 mg/100 mL. The plasma concentration of calcium in the recovery model rats changed from 5 mg/100 mL at initial stage to 10 mg/100 mL after 14 days.

Figure 8.12 shows the graph of plasma drug concentration after implanting the HAp bone cements containing anti-osteoporosis drug estradiol in these three groups of rats, including rats with osteoporosis [22]. In vivo estradiol release in osteoporotic rats was significantly accelerated, whereas normal rats were significantly suppressed. In addition, the plasma drug concentration in the recovery rat model was equivalent to

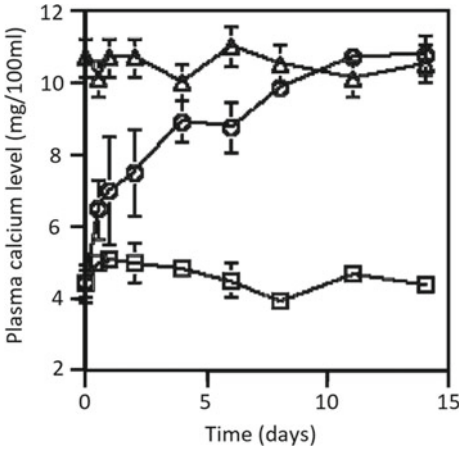

Fig. 8.11 Plasma levels of calcium in osteoporosis model rats and recovery model rats. △: healthy rats; o: rats recovering from pathology; □: rats with osteoporosis pathology

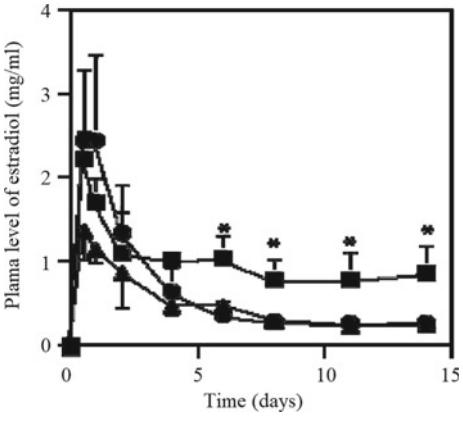

Fig. 8.12 Plasma drug concentration profiles after implanting HAP bone cements containing anti-osteoporosis drug estradiol in the osteoporotic rats. ▲: healthy rats; •: rats recovering from pathology; ■: rats with osteoporosis pathology

that in osteoporotic rats at the initial stage. However, the plasma drug concentration was suppressed to the same level as that in normal rats after 2 weeks. Based on these findings, it was confirmed that the drug release from HAp bone cement DDS was dependent on the plasma concentration of calcium [22].

Results of an in vivo study showed that HAp bone cement was dissolved or disintegrated by the acid secreted by the activated osteoclasts cells under the condition of progressive osteoporosis and decrease in the plasma concentration of calcium, and the drug release was accolated from the cement. Subsequently, it was shown that when the pathological condition improved and plasma concentration of calcium increased, osteoblasts were activated on the surface of bone cement to form new bone and drug release was suppressed. To verify the therapeutic effect of the HAp bone cement DDS containing estradiol, the bone mineral density of the lumbar vertebrae of the osteoporotic rats was examined 22 days after implanting DDS cement. Figure 8.13 shows the radiograms of osteoporotic rats treated with the DDS cement and/or fed a calcium diet, and the result of the bone mineral density evaluated from the radiogram. The bone mineral density of the rat groups treated with both the DDS cement and the calcium diet was significantly higher than that of the other groups, and the implantation of the DDS cement to the osteoporotic rats resulted in higher therapeutic effect to improve the bone mineral density.

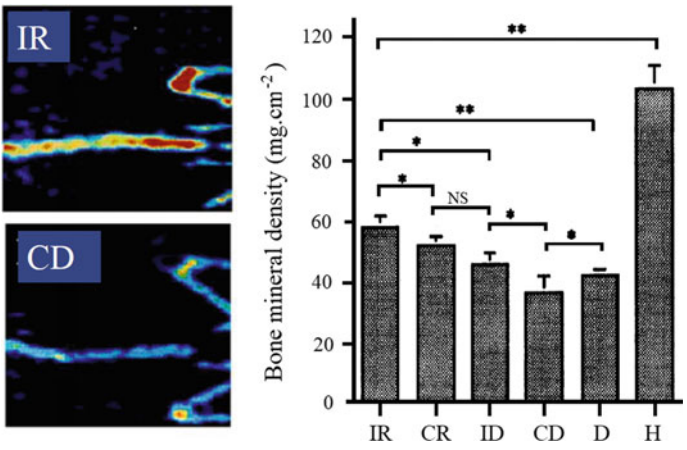

Fig. 8.13 Radiography and cement density after implanting the HAp bone cements containing anti-osteoporosis drug estradiol in osteoporotic rats. IR: DDS implant + calcium diet; CR: calcium diet; ID: DDS implant; CD: control; D, prior to implementing control conditions; H: healthy

8.6 Drug Delivery System for Hard Tissues Based on Self-setting Collagen-HAp Composite Cement

In the biological hard tissue, dense bones and shells of marine creatures are functionally arranged by a complex of HAp and collagen to form a light, strong and supple geometric structure. In addition, the space between bones includes osteoblasts, osteoclasts, and hematopoietic cells, and has various physiological functions. To obtain a bio-absorbable and high-strength bone material that mimics biological hard tissue, an attempt was made to synthesize an organic–inorganic composite material using HAp and collagen. The HAp cement and insoluble type I collagen were mechanochemically treated in a centrifugal ball mill to obtain self-setting collagen HAp bone cement.

As shown in Fig. 8.14, the main part of the HAp bone cement was transformed into HAp; however, its X-ray diffraction profile showed some small diffraction peaks attributable to original tetra-calcium phosphate, suggesting that the transformation was not perfect [23]. In contrast, X-ray diffraction profile of the collagen HAp bone cement indicated that the cement was almost 100% transformed into HAp. These results suggest the following: the collagen-HAp bone cement, as an organic–inorganic composite, was a functional material that had the ability to self-set and harden when kneaded with phosphoric acid and undergoes biodegradation after implantation in a living body [23]. The collagen-HAp bone cement was transformed on the collagen fiber to HAp with low crystallinity and was similar to natural bone (Fig. 8.14). In addition, the biodegradation rate of the hardened cement matrices could

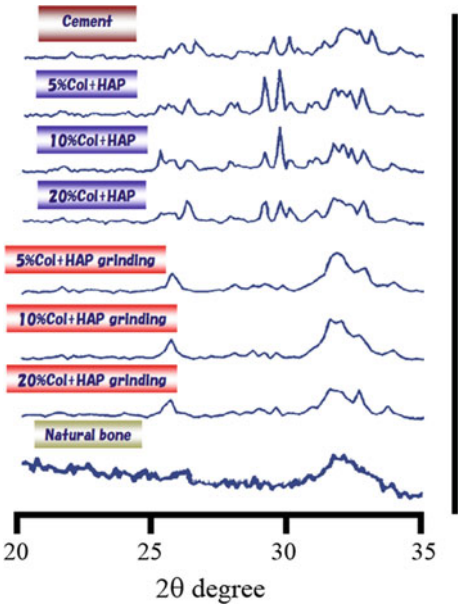

Fig. 8.14 Mechanochemical effect on the X-ray diffraction profiles of HAp-collagen bone cements

be controlled by changing the amount of collagen to 5–20%. These results showed that the collagen-HAp composite bone cement, which was capable of controlling biodegradation rate and drug delivery rate, could be prepared by mechanochemical treatment [23, 24].

The artificial bone implant for osteoporosis treatment that had a bone proliferative effect was designed based on the collagen-HAp composite bone cement containing phytonadione (VK2) [23], which acted on osteoblasts and had a bone growth effect. After implantation of the bone cement DDS containing VK2 in the back of osteoporotic rats, the mineral mass of the cement devices was measured by radiography. It was observed that the mass of the cement with VK2 was significantly higher than that without (Figs. 8.15 and 8.16). After 22 days of implantation, the bone cements were removed from the osteoporotic rats and stained. Figure 8.17 shows the microphotographs of the tissue cross sections of the implanted bone cement DDS after 22 days. Collagen and new bone were observed inside the collagen-HAp bone cements, with and without VK2. This indicated that bone remodeling had occurred within the implant. However, the implanted cement with VK2 showed a tendency to increase mineral mass, whereas the cement without VK2 showed a tendency to decrease mineral mass. In the former, the bone grew in the cement, but in the latter, the cement was phagocytosed from outside by bone cells.

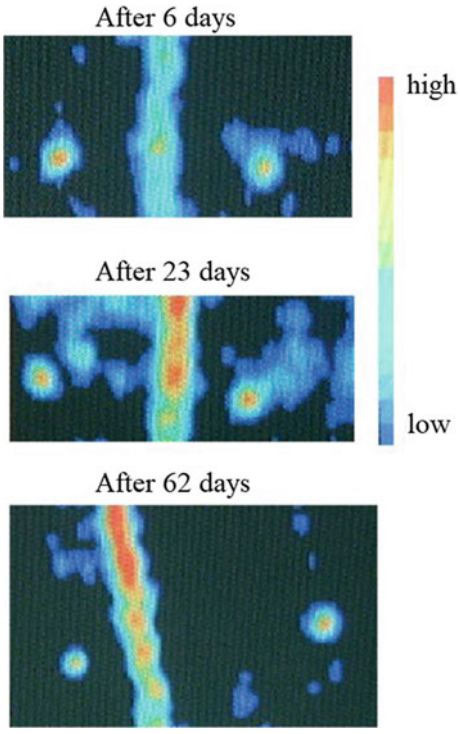

Fig. 8.15 Change in the radiography of collagen/HAp bone cement containing VK2 after implantation into the back of osteoporotic rats

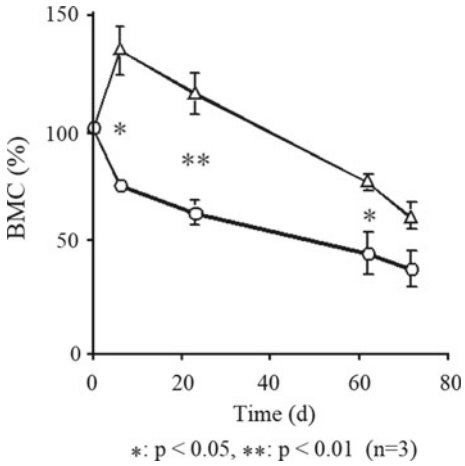

Fig. 8.16 Mineral density profiles of collagen-HAp bone cement with and without VK2 after implantation in the back of osteoporotic rats. o: Collagen-HAp bone cement; △: Collagen-HAp bone cement containing VK2

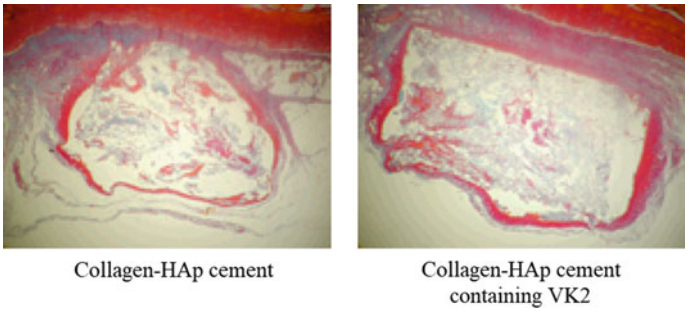

Fig. 8.17 Micrographs of collagen-HAp bone cements containing VK2 after implantation in the back of osteoporotic rats for 62 days

8.7 Bone Cell Scaffold with Biodegradable Collagen-HAp Composite Cement with Inter-connective-Macro-pores

Conventional bone implant without micro-pore structure, made from sintered HAp, is commonly used as a filler for bone defects in patients. However, the binding of the HAp implants to bone is not sufficient. Therefore, the HAp implant with macro-pores similar to spongy bone was developed as shown in Fig. 8.18. However, their therapeutic score was limited since the pore shape of the implant was similar to an inkbottle, and it was not easy for bone cells and blood vessels to penetrate the implant. In contrast, the biodegradable biomaterial developed and described in the previous section could freely regulate drug release, was an intelligent material to control

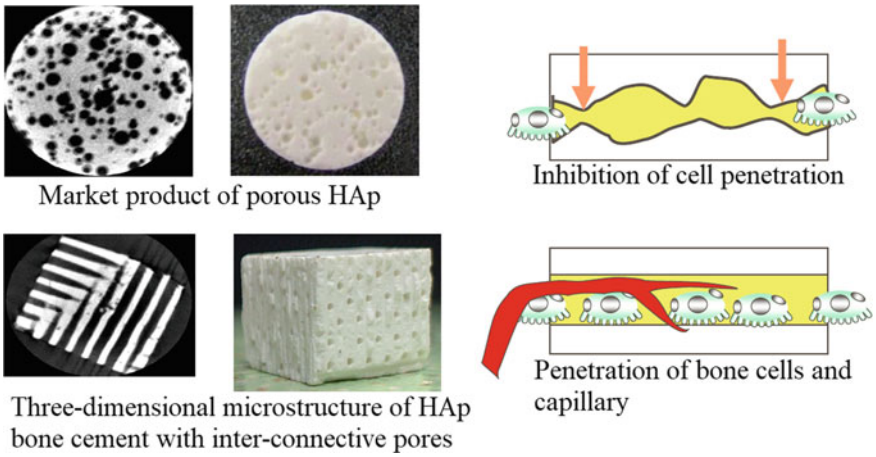

Fig. 8.18 Cross-sectional images of X-ray computed tomography of the collagen-HAp bone cement with inter-connective macro-pores and the commercial porous HAp block

bone growth. Therefore, it was possible to prepare the material having a function closer to that of living bone using collagen-HAp composite material. Additionally, the preparation of a novel functional material (including living bone cells) having a bone formation function closer to living bone was attempted.

To develop a new artificial bone that solves these problems, biomaterials containing three-dimensional nano-pore-structures with inter-connective-macro-pores were designed, as shown in Fig. 8.18. These biomaterials allow the penetration of bone cells, supporting their activities, and enabling the formation of capillaries that promote nutritional supply to the cells. Three-dimensional cement with macro-pores was prepared using self-setting collagen/HAp cement, and their cross-sections imaged using X-ray CT, as shown in Fig. 8.18 [25]. The collagen-HAp cement having inter-connective-macro-pores and HAp cement without macro-pores were implanted in healthy rats and the in vivo absorption rates were measured and compared using X-ray CT (Fig. 8.19). The collagen-HAp cement with inter-connective-macro-pores was rapidly invaded by osteoclast cells and biodegraded and absorbed by remodeling, as shown in Fig. 8.19 [23, 25]. However, in other cases, bone cells invaded the macro-pores and showed biocompatibility, but their implants were not absorbed. The collagen-HAp cement with macro-pores was shown to be remodeled rapidly by bone cells. The result indicated that if bone growth factors could be released in a sustained manner from the collagen-HAp cement with inter-connective macro-pores bone structure, the cell invasion into the artificial bone could be accelerated and osteoblasts could be activated, thereby enhancing the function of bone formation, and thus it could be used as an ideal cell scaffold. Therefore, to design a biomimetic artificial bone close to the biological hard tissue, it is necessary to equip a drug release control capability from the collagen-HAp cement structure. To control drug release

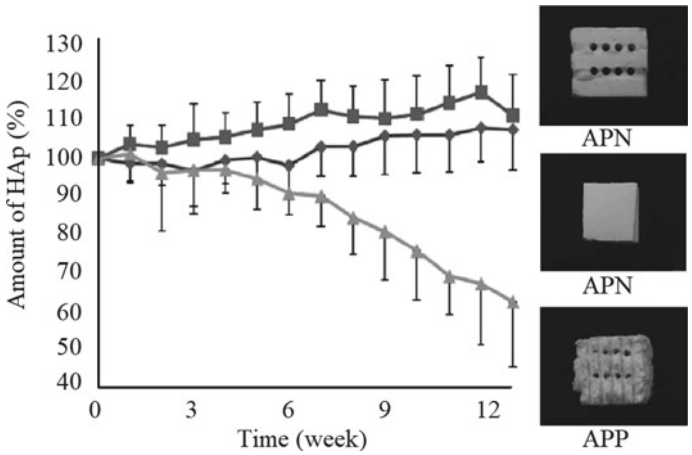

Fig. 8.19 Effect of macro-pores on the mineral density profiles of the HAp-collagen bone cement with and without inter-connective macro pores. ▲: Collagen-HAp bone cement with inter-connected-macro-pores; ■: HAp bone cement with inter-connected-macro-pores; ◆: HAp-bone cement block

from the collagen- HAp cement with inter-connective macro-pores, the cement with various number of the macro-pores was designed and prepared.

Figure 8.20 shows the effect of the number of macro-pores on the drug release from the collagen-HAp device containing indomethacin [26]. All drug release profiles showed straight lines, with a lag time on the Higuchi plot, and the drug release rates increased as the number of macro-pores increased. It was thus confirmed that the drug release accelerated because the cement surface area increased as the number

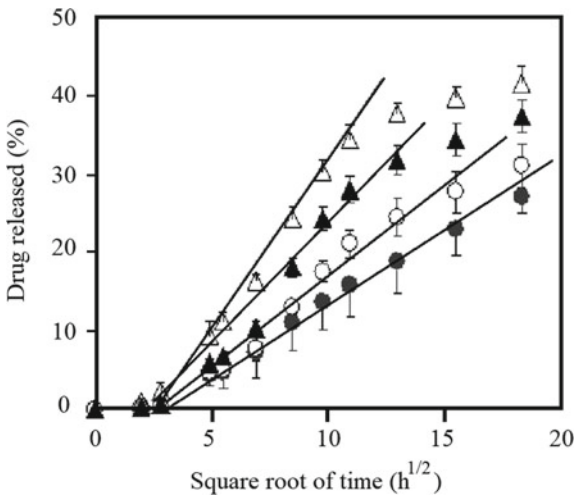

Fig. 8.20 Effect of macro-pores on the drug release rate of the Higuchi plots of the HAp-collagen bone cement with inter-connective macro pores. •: PN0; o: PN20; ▲: PN40; △: PN60

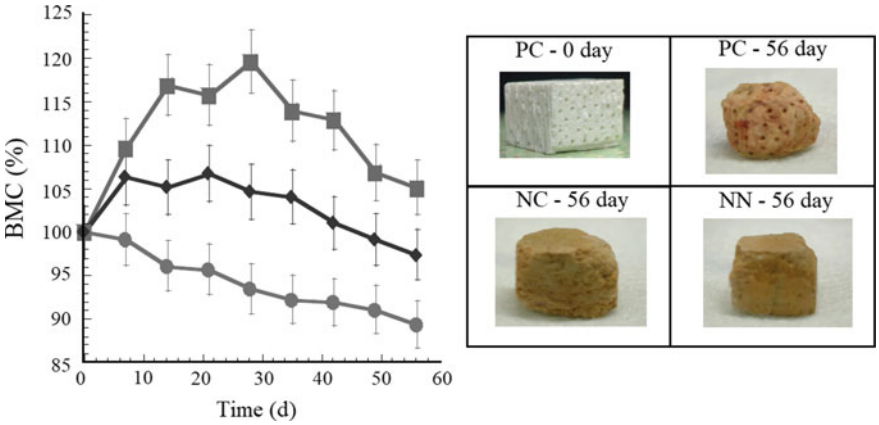

Fig. 8.21 Effect of macro-pores on the mineral density profiles of the HAp-collagen bone cement containing VK2. ■: collagen-HAp bone cement with inter-connected-macro-pores; ◆: collagen-HAp bone cement; •: HAp bone cement

of macro-pores increased. Therefore, it was shown that by controlling the geometric structure of the HAp cement device, the drug release rate could be appropriately controlled, and cell activity could be activated. Artificial bone implants with inter-connected macro-pores made by the collagen-HAp composite cement containing VK2 (PC) [24] were designed similar to natural hard tissues and were implanted in osteoporotic rats. Figure 8.21 shows the implant mass profiles of the PC, collagen-HAp cement implant (NC) and HAp cement implant (NN), which were evaluated based on their respective radiograms. In the initial 30 days, the implant mass of the PC increased due to the invasion of bone cells into the macro pores, and then the total implant mass decreased after 30 days due to the phagocytosis from the outside of the device. In the NC, after the slight increase in mass due to bone cell invasion, the implant mass decreased. In NN, no increase in mass was observed, and the implant mass gradually decreased due to external phagocytosis.

After the animal experiments, the X-ray diffraction profiles, thermal analytical curves, and infrared absorption spectra of the removed implanted artificial bone were measured. The mass of the implants increased and/or decreased due to new bone-like substance formation by osteoblast-like cells and/or absorption by the osteoclast-like-cells during bone remodeling [27]. As shown here, an artificial bone with inter-connective-macro-pore structure that mimicked the geometric structure of the natural bone was prepared with collagen HAp cement that mimicked the molecular level structure of the bone, and their biocompatibility and bone formation were demonstrated in actual osteoporotic rats. These results indicate that the development of a biomimic artificial bone is possible using such bone cement.

8.8 Gene Delivery System Consisting of Collagen-HAp Based Cement with a Cell-Activity-Dependent Drug Release Mechanism

Various viral vectors have been investigated in gene therapy with high gene expression efficiency. However, problems with safety, such as immunogenicity, have been encountered [28]. Therefore, liposomes and micelles have been widely studied as safe non-viral vectors, instead of viral vectors. Among these, DNA/polycation complexes, using a cationic component that electrostatically adheres to DNA, have been developed with high efficacy and safety [29]. The DNA/polycation complexes have already achieved extremely high gene expression efficiency in some experiments using cultured cells [30]. It was found that by adding hyaluronic acid to the DNA/polycation complex, a ternary complex with excellent dispersibility could be obtained. Furthermore, by concentrating the ternary DNA complex prepared at a low concentration by freeze-drying, a DNA complex nanoparticle concentrated having a diameter of about 70 nm could be obtained [30].

Injectable collagen HAp cement with good biocompatibility has been developed for controlled drug release rate by adjusting the crystallinity and additives [31]. To develop a gene delivery system that could control gene release over a long period of time, stable hyaluronic acid-coated DNA-cation polymer complex nanoparticles [30] were encapsulated in self-setting collagen-HAp cement. The collagen-HAp composite cement, containing the ternary DNA complexes, was cultured with osteoclast-like model cells (MCL-6 cells) and osteoblast-like model cells (B16 melanoma) of the osteoclast model, followed by the measurement of the device weight change and DNA release amount.

Figure 8.22 shows the effect of the type of bone cells on the DNA release pattern from the collagen-HAp composite cement containing the ternary DNA complexes [31]. When the collagen-HAp device containing DNA was cultured with osteoclast-like model cells, it showed significantly higher DNA concentrations than when cultured with osteoblasts model cells. At this stage, based on the result regarding the behavior of osteocyte-like-cells under a microscope, it was observed that the model cells aggregated and adhered on the cement surface and dissolved the surface.

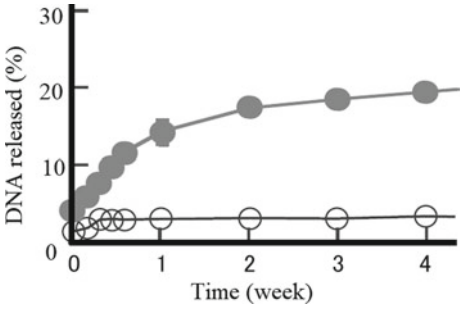

Fig. 8.22 Effect of bone cells on the DNA release profiles from the collagen-HAp bone cement containing DNA after implantation in cancer-bearing rat. •: osteoclast-like cells; o: osteoblast-like cells

In addition, the HAp cement containing DNA and the collagen-HAp composite cement containing DNA were injected into mice transplanted with solid cancer cells to examine the growth of cancer cells. The mass change profiles of the injected cement device in the mice were measured with an X-ray CT device [31]. Figure 8.23 shows the mass change profile of the cement devices implanted in mice [31]. The biodegradation rate of the HAp cement containing DNA was extremely slow, and even after 12 weeks, the cement mass was 95% or more, resulting in almost no biodegradation. In contrast, the collagen-HAp cement containing DNA showed a cement mass of 60% at 4 weeks and 30% or less at 12 weeks, indicating that it was gradually biodegraded.

Figure 8.24 shows the therapeutic effect after injecting the HAp cement containing DNA complex and the collagen-HAp cement containing DNA complex into mice transplanted with solid cancer cells in the abdomen [31]. When the DNA complex was injected alone, cancer cells proliferated 1 week later. After injecting the HAp cement containing DNA complex, cancer cells proliferated after 3 weeks. In contrast, when the collagen-HAp cement containing DNA complex was injected, the cancer

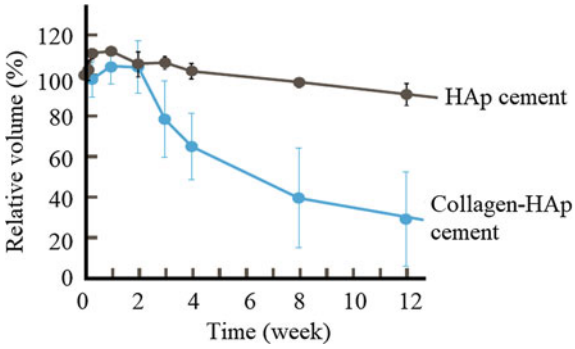

Fig. 8.23 Effect of bone cells on the mineral amount profiles of the collagen-HAp bone cement containing DNA after implantation in cancer-bearing rat

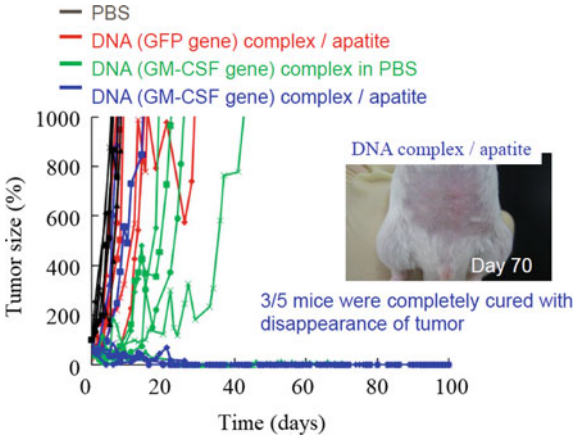

Fig. 8.24 Therapeutic effect of collagen-HAp bone cement containing DNA after implantation in cancer-bearing rat. Reprint with permission [31]

cells hardly proliferated during the 100-day test period. Therefore, it was considered that the growth of cancer cells was effectively suppressed by the continuous release of the injected collagen-HAp cement containing DNA complex at an appropriate DNA concentration.

8.9 Concluding Remarks

Various bone metabolism-stimulating compounds can be applied to HAp-based artificial bone to control drug release from the device. By activating biological bone metabolism, these devices could contribute to the regeneration of hard tissue that is difficult to regenerate using other means. It was confirmed that the drug released from the HAp cement matrix was dependent on the concentration of calcium in the biological fluid, and it was possible to construct an osteoporotic responsive drug release control system. By controlling the release of various anti-osteoporotic drugs from these devices, it is possible to maintain the homeostasis in the living hard tissue. An artificial bone with inter-connected macro-pores was prepared from collagen HAp composite cement, with high functionality, such as biodegradable character and three-dimensional geometric structure that could retain bone cells. Addition of the controlled release of bone growth factor VK2 to the three-dimensional geometrically designed artificial bones allowed controlled bone formation and bone remodeling, and thereby contribute to hard tissue regenerative medicine. The release of DNA from functional artificial bones could effectively suppress solid cancers in cancer-bearing rats and develop into new biomaterials that could contribute to bone regenerative medicine.

Acknowledgements The author would like to thank Professor William I. Higuchi of the University of Utah for his scientific advice and encouragement. This research received partial financial support from the Creating Happiness Incubation Musashino University, Research Center for Biomedical Engineering (No. 2042) and from the Japan Agency for Medical Research and Development (No. JP19mk0101105h0102).

References

1. Pharmaceuticals and Medical Device Agency (2017) Surgical simplex® Radiopaque bone cement. http://www.info.pmda.go.jp/downfiles/md/PDF/730093/730093_15700BZY01342000_A_C3_04.pdf. Accessed 14 Apr 2017
2. Webster TJ, Patel AA, Rahaman MN et al (2012) Anti-infective and osteointegration properties of silicon nitride, poly(ether ether ketone), and titanium implants. Acta Biomater 8:4447–4454
3. Niwa S (2004) Current status and future prospects of biomaterials for artificial bones. Mater Jpn 43:186–192
4. The Ceramic Society of Japan (2008) Hydroxyapatite artificial bone replacement material. http://www.ceramic.or.jp/museum/contents/pdf/seitai01.pdf. Accessed 24 Apr 2017

5. Aizawa M, Furuzono T (2012) Recent advance, artificial materials (inorganic materials). Jinkou Zouki 43:207–211
6. Elzoghby AO (2013) Gelatin-based nanoparticles as drug and gene delivery systems: reviewing three decades of research. J Control Release 172:1075–1091
7. Kumari A, Yadav SK, Yadav SC (2010) Biodegradable polymeric nanoparticles based drug delivery systems. Colloids Surf B Biointerfaces 75:1–18
8. Tabata Y (2007) Development of functional drug carriers to realize advanced medical therapy. Yakugaku Zasshi 127:825–837
9. Chou J, Valenzuela S, Green DW et al (2014) Antibiotic delivery potential of nano- and microporous marine structure-derived β-tricalcium phosphate spheres for medical applications. Nanomedicine 9:1131–1139
10. Yamamura K, Chou G, Iwata H (1991) The development of antibiotics loaded hydroxyapatite beads. Drug Deliv Syst 6:103–108
11. Brown WE, Chou LC (1986) Combinations of sparingly soluble calcium phosphates in slurries and pastes as mineralizers and cements. US Patent 4,612,053A, 16 Sept 1986
12. Yu D, Wong J, Matsuda Y et al (1992) Self-setting hydroxyapatite cement: a novel skeletal drug-delivery system for antibiotics. J Pharm Sci 81:529–531
13. Higuchi T (1963) Mechanism of sustained-action medication. Theoretical analysis of rate of release of solid drugs dispersed in solid matrices. J Pharm Sci 52:1145–1149
14. Otsuka M, Matsuda Y, Suwa Y et al (1994) A novel skeletal drug delivery system using self-setting calcium phosphate cement. 2. Physicochemical properties and drug release rate of the cement-containing indomethacin. J Pharm Sci 83:611–615
15. Otsuka M, Nakahigashi Y, Matsuda Y et al (1998) Effect of geometrical cement size on in vitro and in vivo indomethacin release from self-setting apatite cement. J Control Release 52:281–289
16. Otsuka M, Matsuda Y, Fox JL et al (1995) A novel skeletal drug delivery system using self-setting calcium phosphate cement. 9: effects of the mixing solution volume on anticancer drug release from homogeneous drug-loaded cement. J Pharm Sci 84:733–736
17. Kawasaki T, Takahashi S, Ikeda K (1985) Hydroxyapatite high-performance liquid chromatography: column performance for proteins. Eur J Biochem 152:361–371
18. Otsuka M, Matsuda Y, Suwa Y et al (1994) A novel skeletal drug-delivery system using self-setting calcium phosphate cement. 3. Physicochemical properties and drug-release rate of bovine insulin and bovine albumin. J Pharm Sci 83:255–258
19. Otsuka M, Matsuda Y, Suwa Y et al (1994) A novel skeletal drug-delivery system using self-setting calcium phosphate cement. 4. Effects of the mixing solution volume on the drug-release rate of heterogeneous aspirin-loaded cement. J Pharm Sci 83:259–263
20. Otsuka M, Nakahigashi Y, Matsuda Y et al (1997) A novel skeletal drug delivery system using self-setting calcium phosphate cement VIII: the relationship between in vitro and in vivo drug release from indomethacin-containing cement. J Control Release 43:115–122
21. Kim HM, Himeno T, Kokubo T et al (2005) Process and kinetics of bonelike apatite formation on sintered hydroxyapatite in a simulated body fluid. Biomaterials 26:4366–4373
22. Otsuka M, Yoneoka K, Matsuda Y et al (1999) Effect of plasma-calcium-level-responsive oestradiol release from apatitic bone cement on bone mineral density in ovariectomized rats. J Pharm Pharmacol 51:475–481
23. Otsuka M, Kuninaga T, Otsuka K et al (2006) Effect of nanostructure on biodegradation behaviors of self-setting apatite/collagen composite cements containing vitamin K_2 in rats. J Biomed Mater Res B Appl Biomater 79:176–184
24. Otsuka M, Nakagawa H, Otsuka K et al (2013) Effect of geometrical structure on the in vivo quality change of a three-dimensionally perforated porous bone cell scaffold made of apatite/collagen composite. J Biomed Mater Res B Appl Biomater 101:338–345
25. Hamada H, Ohshima H, Ito A et al (2010) Effect of geometrical structure on the biodegradation of a three-dimensionally perforated porous apatite/collagen composite bone cell scaffold. Biol Pharm Bull 33:1228–1232

26. Otsuka M, Nakagawa H, Ito A et al (2010) Effect of geometrical structure on drug release rate of a three-dimensionally perforated porous apatite/collagen composite cement. J Pharm Sci 99:286–292
27. Ohshima H, Otsuka M (2016) Stimulus-responsive intelligent drug delivery system based on hydroxyapatite-related materials. In: Ohshima H (ed) Encyclopedia of biocolloid and biointerface science. Wiley, New York, pp 403–411
28. Taira K, Kataoka K, Niidome T (eds) (2005) Non-viral gene therapy: gene design and delivery. Springer, Tokyo
29. Morille M, Passirani C, Vonarbourg A et al (2008) Progress in developing cationic vectors for non-viral systemic gene therapy against cancer. Biomaterials 29:3477–3496
30. Ito T, Otsuka M, Koyama Y (2008) Preparation of fine DNA particles and high-level tumor-targeted in vivo gene expression after intravenous injection. Mol Ther 16:S366. https://doi.org/10.1016/S1525-0016(16)40381-3
31. Ito T, Koyama Y, Otsuka M (2012) DNA complex-releasing system by injectable self-setting apatite cement. J Gene Med 14:251–261

Makoto Otsuka Prof. Ostuka is a registered pharmacist and received his Ph.D. from Showa University in pharmaceutical science and he is currently working in Research Institute of Electronics, Shizuoka University, Japan. His area of research includes drug delivery, composite materials, calcium phosphate bioceramics, and bone cement. He has over 9,000 citations and has received numerous awards.

Chapter 9
Chitosan-Hydroxyapatite Composite Scaffolds for the Controlled Release of Therapeutic Metals Ions

Lukas Gritsch

Abstract Therapeutic ions such as calcium, magnesium or copper, play an essential role in maintaining the correct physiology of our organism. They act as cofactors of enzymes, modulating cell signaling and homeostasis through various pathways. Developing biomaterials for tissue engineering that control the concentration of these ions in vivo has been proven a successful strategy to tailor cell response and, ultimately, improve tissue regeneration. Among others, chitosan, a naturally sourced polysaccharide, and hydroxyapatite, the major component of the mineral phase of bone, showed encouraging results as ion carriers. This chapter offers an overview of the use of these two materials for the purpose. Initially, the main ions used in tissue engineering and their modes of action are listed. Then, the opportunities and challenges of chitosan and hydroxyapatite in the field are discussed: their key properties, their processing into composites and the methods to fabricate tissue engineering scaffolds.

Keywords Therapeutic metal ions · TMI · Transition metals · Antibacterial activity · Tissue engineering · Biomaterials · Composite

9.1 Introduction

Materials used for tissue repair or regeneration must satisfy a long list of design requirements. Adequate mechanical properties, tailored degradation, optimized three-dimensional structure and healthy biological response are just a few of the many criteria that biomaterials research has to take into account when envisioning new technologies for biomedical applications.

One emerging challenge is the improvement of the control over cell and tissue response. In the past decades, great progress has been made in the development of strategies that can actively influence cell behavior, direct new tissue growth and

L. Gritsch (✉)
Laboratoire de Physique de Clermont, UMR CNRS 6533, Université Clermont Auvergne, 4 avenue Blaise Pascal, 63178 Aubière, France
e-mail: lukas.gritsch@clermont.in2p3.fr

A. H. Choi and B. Ben-Nissan (eds.), *Innovative Bioceramics in Translational Medicine I*, Springer Series in Biomaterials Science and Engineering 17,
https://doi.org/10.1007/978-981-16-7435-8_9

elicit a specific physiological response in cells (e.g. differentiation towards a desired phenotype). Among promising candidates to expand current technologies, a special focus is often given to controlled delivery of growth factors (GFs) [1] and cell-based tissue engineering therapies [2]. They are promising candidate approaches with already a robust record of successful results, able to provide highly specific and tailored solutions for regenerative medicine. Nevertheless, these therapies tend to be complex and very expensive. They are often hard to scale-up to reach a broader pool of patients and, especially in the case of GF delivery, they pose serious safety and regulation concerns. For instance, vascular endothelial growth factors (VEGFs) is a family of biomolecules with a broad diagnostic and therapeutic potential for the treatment of cardiac diseases [3]. However, the same researchers that advocate for the clinical potential of VEGFs warn against the possible risk of cardiotoxicity, nephropathy and neurodegeneration [3]. Growth factors are also very expensive and highly perishable. The general opinion is that the need to further corroborate the safety of GF-based therapies will ultimately determine a delay in the industrialization of such technologies. For this reason, several alternative approaches have been proposed. Among these, therapeutic metal ions (TMIs) could offer a valid alternative to growth factors without the same safety concerns and at a fraction of the cost [4, 5]. TMIs are a family of metal ions, often transition elements, known for their ability to elicit a specific therapeutic effect on eukaryotic cells (e.g. osteostimulation, angiogenesis) (Fig. 9.1) [6] and/or for their antibacterial activity (Fig. 9.2). Some examples of TMIs are strontium, zinc, magnesium or copper. They have specific interactions with physiological pathways that ultimately result in beneficial changes in cell metabolism.

Gold standard approaches to use TMIs in biomaterials science usually aim to embed TMIs within a suitable material carrier that can later deliver the ions in a controlled fashion. It is important to achieve precise tailoring of the ion release since these ions could develop cytotoxic effects at excessive concentration. Glass–ceramics are the most studied family of materials to reach this goal, especially bioactive glasses [7] and hydroxyapatite [8]. Zeolites and carbon fibers are also possible candidates [5]. Generally speaking, bioactive glass-based technologies tend to have higher degradation rates and reactivity compared to hydroxyapatite-based ones [9]. The reason behind this choice lies in the structure of these materials and the possibility to successfully insert TMIs within their glass network (for bioactive glasses) or the crystalline lattice (for hydroxyapatite). Since TMIs are effectively part of the structure of the material, their release is sustained and coupled with the degradation of the whole bulk of the carrier, reducing possibly harmful burst release phenomena and offering the therapeutic effect of ions over a long period of time. In light of its high biomimicry (i.e. it highly resembles the physiological bone mineral phase), in this work the focus will be on hydroxyapatite: why it is a relevant biomaterial, how TMIs, both cationic and anionic, can be substituted into its crystalline structure and how this affects its biological performance.

Traditionally, therapeutically active hydroxyapatite is often used as a filler in combination with a polymeric matrix for the fabrication of composites. This approach

increases the processability of hydroxyapatite and optimizes its mechanical properties, resulting in a suitable composite material for implants or tissue engineering scaffolds. Polymer/hydroxyapatite composites have been extensively investigated in the past decades using a wide variety of fabrication techniques and polymers, including for example bioresorbable polyesters [10], polyurethanes [11] or polyhydroxyalkanoates [12] (chosen for their availability and processability); or chitosan [13] and collagen [14] (for more biomimetic approaches). Recently, however, the concept of using the polymeric matrix as a second carrier for TMIs started to emerge. The idea is to move beyond the "processable organic - therapeutic inorganic" dualism and design new composite materials that exploit the capability of both the organic and inorganic component to carry desired ions. Due to the different chemical nature and degradation profiles of the two phases, a more complex and decoupled ion release behavior could be engineered, highly expanding the therapeutic effects that an implantable and resorbable biomaterial can have over time. The use of chitosan as matrix material, in particular, seems the most promising approach due to its ability to coordinate with metal ions, a process that goes under the name of chelation [15]. Chelation is a fascinating, versatile and promising property of chitosan, already under investigation using several TMIs for various applications in the medical field, including orthopedics, antibacterials and dentistry [16, 17].

In this chapter, an overview of the most important TMIs identified to date, their therapeutic properties and the mechanisms behind them will be presented. Recent technologies will be discussed with particular emphasis on chitosan/hydroxyapatite composites, a combination that could be a real game-changer in the future of TMI controlled delivery. The key properties, benefits and limitations of chitosan and hydroxyapatite will be discussed, together with the techniques used to include TMIs into their structure and the fabrication methods used to process these composites into implants and scaffolds. Finally, possible avenues for future development will be proposed.

9.2 Overview of the Most Relevant Therapeutic Ions

Metallic ions are a fundamental component of our organism. Their role is mainly to act as cofactors of enzymes, controlling cell signaling and maintaining the correct physiology of cells and tissues. As observed by Mouriño et al. [5], the biological importance of metallic ions is directly reflected in the wide range of pathologies associated with metallic ion imbalance: these include gastrointestinal, nervous and endocrine disorders, infectious diseases and several types of cancer. Due to their key role, research extensively focused on expanding the use of trace elements in medicine, as drugs and diagnostic tools, in a wide variety of treatments [18]. Biomaterial-based ion delivery is generally praised for its fine time/space control compared to traditional approaches [7]. For instance, it was widely demonstrated in animal models that the ionic dissolution products of bioactive glasses (e.g. silicates, calcium, sodium, phosphates) could promote cell osteogenic differentiation [19], overexpress genes related

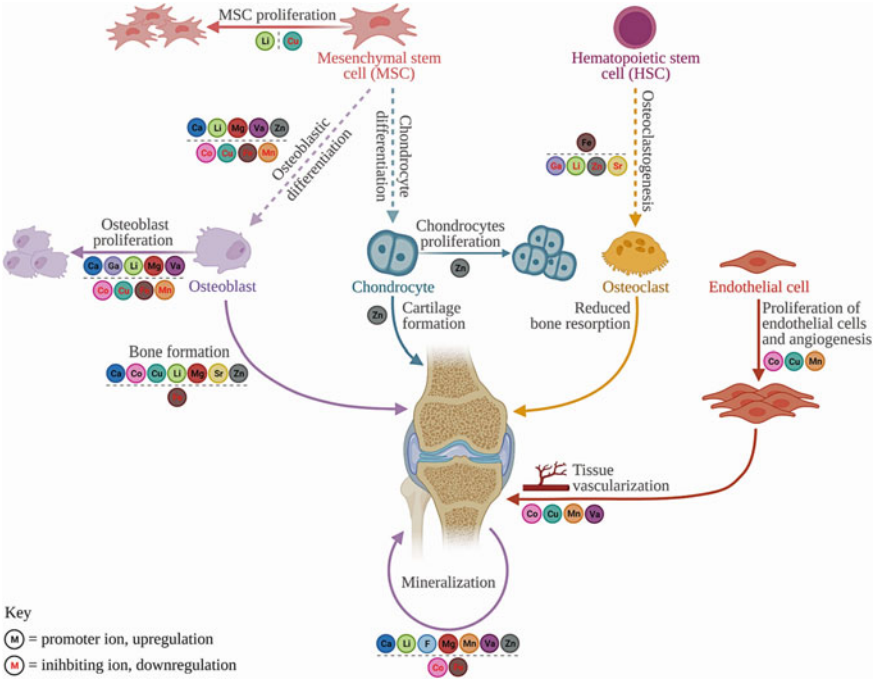

Fig. 9.1 A schematic representation of the major regulatory effects of therapeutic ions on bone and cartilage stimulation, angiogenesis and osteoclastogenesis

to bone regeneration [20] and enhance angiogenesis [21]. In view of the significant number of relevant ions that can be delivered according to the targeted application, the possibilities for new effective technologies are practically endless. However, in-depth understanding of the mechanisms at the origin of the therapeutic effect of each ion is key. In this section, an overview of the most relevant therapeutic metal ions used in tissue engineering and their mechanism of action will be proposed. For further information on the subject, recent reviews are available [4, 5, 7, 22].

9.2.1 Boron

Boron is known for its anti-inflammatory, anti-oxidant and oxidative stress protective properties: it can help raise the level of antioxidant enzymes while lowering inflammatory biomarkers. Boron can also stimulate bone growth and remodeling by influencing the metabolism of calcium [23]. It improves wound healing, increases magnesium absorption, regulates the metabolization of estrogen, testosterone and vitamin D, increases cognitive performance and short-term memory in the elders and has preventive and therapeutic effects in the treatment of tumors. The beneficial

properties of boron are currently commercially applied in products for the treatment of myeloma, several forms of dermatitis and onychomycosis [24]. In materials science, boron is mainly exploited for its osteogenic and angiogenic properties. Boron-releasing materials are primarily used for the fabrication of bone tissue engineering scaffolds, although soft tissue engineering [25] and wound healing [26] applications were also successfully explored. The osteogenic effect of boron appears to be linked to the activity of the enzyme SETD7, a histone methylase directly implicated in osteoblastic differentiation. The results of a recent study on the topic suggest that boron induces the activation of the Wnt/β-catenin signaling pathway through the phosphorylation of the GSK-3 kinase [27]. This ultimately results in osteostimulation, as demonstrated both in vitro [28] and in vivo [29].

9.2.2 Calcium

Accounting to approximately 1–2% of total adult human body weight (99% of which is found in bone and teeth) [30], calcium has several key roles in the body: its movements across the cytoplasm of cells serve as signal for many cellular mechanisms that lead to correct muscle contraction, heartbeat regulation, blood clotting and synapsis activity. Most interestingly, calcium is a well-known enhancer of biomineralization [31]. In addition, it can also stimulate the proliferation and differentiation of osteoblasts [32]. The underlying mechanisms mediating this property are complex. Some investigated cell pathways include (i) the modulation of the activity of seven transmembrane extracellular calcium-sensing receptors influencing intracellular signaling [33]; (ii) the increase in the expression of insulin-like growth factors (IGF-1 and 2), important in the regulation of osteoblast proliferation; (iii) the overexpression of angiopoietin 1 and 2, which in turn increase the expression of connexin43 (major marker of cell–cell interaction) and integrin β1 (marker for cell–matrix interaction), respectively [34]; and (iv) the enhancement of bone mechanosensitivity through increased release of glutamate by osteoblasts [35].

9.2.3 Cerium

Evidence shows that the use of cerium as a therapeutic agent can have beneficial effects on osteoblasts growth, promoting bone formation and ultimately improving bone strength [36]. Mainly, however, the biomedical applications of cerium focus on its antibacterial properties. The mechanism of antibacterial action of cerium is based on the formation of reactive oxygen species as a consequence of the conversion of the ion between its two oxidation states Ce^{3+} and Ce^{4+}. The increase in oxidative stress that follows oxidation changes in the proximity of the bacterial membrane disturbs the physiological permeability and causes membrane damage. Inside the cell, ions can engage in similar reactions, damaging nucleic acids, proteins and other

bacterial structural components. In particular, cerium was associated with significant hydrolysis of extracellular DNA oligomers, thus making this ion a promising agent to disrupt biofilms [37].

9.2.4 Cobalt

Traces of cobalt can be normally found in the human body, notably as a necessary component of vitamin B12. It contributes to the formation of the myelin sheath in nerve cells, to the synthesis of several neurotransmitters and to mitosis [38]. In addition, cobalt is known to be able to promote the expression of several signaling proteins, notably erythropoietin (EPO), p21 and VEGF, through the activation of the hypoxia inducible factor-1 (HIF-1) [5]. This pathway can lead to a beneficial increase of erythrocytes in blood and improving aerobic performance probably as a consequence of interactions of cobalt with oxygen in tissue. This in turn leads to mild hypoxia, a known physiological trigger of erythropoietin production. Although the specific mechanism of action is still under investigation to date, this beneficial property has long been exploited for the development of several treatments, mainly targeting anemia [39]. In parallel, the properties of cobalt have been investigated in the context of bone and cartilage tissue engineering scaffolds to fabricate devices that lead to improved vascularization and osteostimulation [40]. The use of cobalt as an antibacterial and antiviral agent was also successfully explored [41].

9.2.5 Copper

Copper is a well-known antibacterial ion. It is a highly water soluble and reactive element against which bacteria have little buffer capacity. An increase in copper concentration is very dangerous for prokaryotes and quickly leads to the degradation of several vital structures. The main target is the cell membrane, disrupted via peroxidation of lipids. Consequently, cytosol leaks out, nutrients are lost, ultimately leading to cell starvation. Since copper is not required to be internalized for these reactions to occur, this process is largely independent from the homeostasis ability of attacked cells. Inside cells, copper can (i) compete against zinc and iron, impeding correct enzymatic functions [42]; (ii) interact with proteins altering their structure, depleting active sites or breaking them down (especially thiol-containing domains) [43]; (iii) generate reactive oxygen species and cause multiple hit damage [44]; (iv) corrupt vital genetic information [42]. This multifaceted action leaves little chance for bacteria to respond and evolve mechanisms of defense. If its medical use is engineered properly, copper resistance is considered unlikely [45]. In parallel, trace amounts of copper (~1–10 ppm) can influence the proliferation of endothelial cells through the ATOX1 pathway, the main intracellular mechanism for copper mobilization in mammals. Evidence shows that copper-ATOX1 complexes are promoters of

the transcription of cyclin D1, a protein facilitating the onset of mitosis (S phase) [46]. The pro-angiogenic action of copper is also well-documented and applied to biomaterials to promote vascularization via the secretion of pro-angiogenic growth factors such as VEGF, interleukin 1α (IL-1α), basic fibroblast growth factor (bFGF) and angiogenin. The copper-mediated overexpression of these factors is primarily due to a protective effect of copper on the fate of HIF-1 (the same pathway influenced by cobalt): the ion can bind the HIF-1α subunit, making it less susceptible to degradation by ubiquitination.

9.2.6 Fluorine

Traditionally associated with applications in dentistry and orthodontics, the beneficial effect of fluorine on remineralization and its antibacterial properties have been recently explored for orthopedic applications, especially in the context of hydroxyapatite-based coatings for metallic [47] and composite [48] implants. Although not a metal ion, it made the list owing to its key therapeutic properties. Fluoride ions can substitute hydroxyls within the hydroxyapatite lattice. This property is either used to produce synthetic fluorapatites [49] or directly in situ to modulate the mineralization of enamel. For decades now, fluoride-based technologies (e.g. toothpastes, orthodontic adhesives, dental implants) have been used in the treatment of dental caries thanks to their ability to restore correct enamel mineralization while simultaneously reducing oral infections in cariogenic subjects [50–52]. The metabolism of oral bacteria tends to lower salivary pH (~5), which in turn reduces the deposition rate of hydroxyapatite, more soluble at acidic conditions. Since fluorapatite is intrinsically less soluble than hydroxyapatite, it precipitates even at cariogenic pH, restoring remineralization and reducing the risk of caries [50, 53]. In addition, fluorine has antibacterial properties. It enters bacteria as hydrogen fluoride, acidifying the cytosol, disrupting enzymatic activity and impairing cell adhesion and bacterial metabolism [54].

9.2.7 Gallium

Similarly to copper, gallium has biologically relevant effects on both prokaryotes and eukaryotes. Studies investigating cell-gallium interactions report a dose-dependent reduction in bone resorption and osteoclast differentiation both in vitro and in vivo, without significant effects on osteoblasts [55]. Results suggest that gallium downregulates the expression of NFATC1, a major transcription factor for osteoclastogenesis [56, 57]. In particular, it binds and interacts with several molecular targets at various stages of NFTAC1 expression, from its initial induction to self-amplification [57]. The same authors also report that gallium seems to inhibit a number of calcium

channels, altering cell permeability and opening up to its use in the treatment of hypercalcaemia [55]. In parallel, gallium was proposed as a doping agent for biomaterials due to its antibacterial properties against both Gram-positive and Gram-negative strains [58–60]. Its efficacy relies on chemical mimicry: Ga(III) can replace Fe(III) in target molecules of the bacterial metabolism, thereby perturbing the physiology of the cell [61].

9.2.8 Iron

In medicine, iron compounds, especially Fe_2O_3 and Fe_3O_4 nanoparticles, are usually considered for their magnetic properties. From cancer treatment and drug delivery to tissue engineering, the concept of magnetic guidance is a highly attractive goal. Iron-containing scaffolds can for instance provide magneto-mechanical cell stimulation and cell growth following desired patterns [62]. As a TMI, iron has an essential role for the metabolism of cells. It is a structural component of important proteins, the most notable example being hemoglobin, and has a key role in ensuring the physiological expression of several cyclins regulating the cell cycle progression. Iron depletion using iron chelators is commonly used as therapy against thalassemia (to avoid excessive free iron in the blood) and it was recently proposed as a promising treatment to reduce the proliferation for aggressive cancers [63]. On the other hand, iron delivery of therapeutic amounts can upregulate cell proliferation and differentiation when desired, as it was shown on a muscle precursor cell line using phosphate glass fibers as iron carrier [64].

9.2.9 Lithium

Lithium is normally known for its use as an antidepressant psychiatric medication. However, anti-viral, anti-cancer, immunomodulatory, neuroprotective and osteoprotective side effects have been highlighted by research [65]. Particularly on bone, it was observed that lithium has a dual influence: it promotes osteoblasts, through the activation of the Wnt/β-catenin, Akt/ PI3K and bone morphogenetic protein-2 (BMP-2) transduction pathways, while suppressing osteoclastogenesis by indirectly down-regulating NFTAC1 through the inhibition of the RANK/RANKL/OPG system. These mechanisms were confirmed in animal models with defective bone tissue, but not in healthy ones. Clinically, evidence of an effect of the metal on bone metabolism was often observed in bipolar patients under lithium treatment [66]. However, results tend to be heterogeneous in humans and authors agree that a clinical use of this TMI to treat bone conditions awaits further validation [65]. Nevertheless, lithium was proposed as candidate TMI to modulate bone regeneration [67], stimulate chondrogenic differentiation [68] and promote of angiogenesis [69].

9.2.10 Magnesium

Magnesium is a known cofactor of more than three hundred enzymes with various roles inside the cells. Oxidoreductases, transferases, hydrolases, lyases, isomerases, ligases, lectins, integrins and glutamine synthetase, all use magnesium to function correctly. It is also contained in whitlockite, the second most abundant mineral in human bone [70]. As biomaterial, magnesium is exploited for its optimal resorbability and can be found in various forms, including as metal [71], salt [72], oxide [73] or embedded in inorganic networks [74–76]. Research on the topic collected a significant body of evidence showing that Mg^{2+} release can promote both osteogenesis and angiogenesis [76, 77]. The effect of magnesium on osteoblasts is still under investigation, but a recent publication on the topic highlights the formation of alkaline microenvironments following magnesium release [78]. The higher pH seems to promote the MAPK/ERK signaling pathway, a major regulatory pathway for osteoblastic proliferation and differentiation. In addition, tailoring the level of free magnesium in the environment was confirmed to be effective in modulating the differentiation of bone-marrow-derived mesenchymal stem cells between the osteoblastic (at high Mg^{2+}) and osteoclastic (at low Mg^{2+}) phenotypes [79].

9.2.11 Manganese

Although relatively niche compared to other therapeutic elements, doping with manganese was also explored as a possible strategy to increase the biological performance of orthopedic coatings [80] and of bone tissue engineering scaffolds [81]. It can be found in the body in six out of its eleven different oxidation states, and it has important beneficial effects on bone tissue [82]. It is in fact an important co-factor in maintaining the correct balance between osteoblastic and osteoclastic activity by regulating the synthesis of IGF-1 [83]. Tailored manganese release can help the physiological formation of bone cartilage, secretion of bone collagen and bone mineralization [84]. Manganese has also a crucial part in controlling the scavenging of reactive oxygen species, subsequently reducing oxidation within the cell lumen. This protective role is mostly exerted by manganese superoxide dismutase (Mn-SOD), a primary controller of mitochondrial oxidative stress.

9.2.12 Selenium

Bone reinforcement, anticancer, antibacterial activity and oxidative stress protection are the four major therapeutic properties of selenium [85, 86]. Selenium-containing materials can reduce bone turnover and increase bone mineral density through the enhancement of the activity of selenoproteins, antioxidant enzymes that help maintain

cell redox balance, thus regulating inflammation and bone cell proliferation [87]. At the same time, selenium produces reactive oxygen species in bacteria, causing membrane damage and nutrient leakage [88]. Selenium was successfully added to hydroxyapatite as an antibacterial component of coatings for orthopedic prostheses used in the treatment of comorbid impairments due to bone cancer [85]. Another successful application of selenium, in combination with chitosan this time, is the development of electrically conductive cardiac patches to treat cardiomyopathies [89]. Interestingly, a recent study also shows that a synergy between the antibacterial activity of selenium and chitosan may occur [90].

9.2.13 Silicon

The beneficial effect of silicon has been described in association with, among others, the regulation of collagen synthesis, bone mineralization and immune system response [91]. It is also known that the major bioavailable form of silicon is orthosilicic acid [92]. These promising results fostered the development of silica-based bioactive glasses, zeolites and nanomaterials that were confirmed to have stimulatory effects on bone tissue [93]. However, the underlying mechanism of action of silicon is not yet fully characterized [91]. Current in vitro evidence confirms a positive effect on bone health via an overexpression of connexin-43, which enhances gap junction communication, and of osteocalcin and endoglin, important markers of osteogenic differentiation [94, 95]. Remarkably, the overexpression was detected even without the supplementation of osteogenic induction medium [95].

9.2.14 Silver

Among TMIs, silver is probably the most well-known. Its use as an antibacterial agent is massively widespread, with countless commercial applications not only as medical devices, but also as diverse consumer products in personal hygiene, domestic care and agriculture [96]. Antimicrobial silver technologies exploit this element in all forms, including the native nanocrystalline form, the monoatomic ionic state (Ag^+, such as the one occurring in silver sulfadiazine, a very common ointment for wound treatment) and silver oxide. From a microbiological standpoint, the antibacterial activity of silver comes mainly from the biological action of its ion form, a highly disruptive agent to bacterial integrity and to their biochemical functions form [97]. There are several known mechanisms of silver action: outside the cell, ions can react with peptidoglycans in the cell wall, leading to impaired osmoregulation and leakage of cellular content. Inside the cell, it generates reactive oxygen species, causing protein denaturation and disruption of metabolic pathways. Finally, ions can bind to microbial DNA, preventing replication. As discussed for copper, the ability to disturb and disrupt several bacterial structures simultaneously is a common characteristic to

most antimicrobial TMIs. Compared to more specific drugs, antibacterial TMIs can attack bacteria from multiple fronts, killing them rapidly and reducing the risk of resistance development. Nevertheless, lower tendency to develop resistance does not mean being immune to it: the possibility of bacteria developing resistance to silver is a well-known phenomenon [98]. The current extreme commercial diffusion of silver-containing products poses a significant risk. Healthcare experts and researchers will probably have to tackle this issue in upcoming years. More information regarding the antimicrobial effect of silver can be found in recently published in-depth reviews [99, 100].

9.2.15 Strontium

The effect of strontium on bone repair is a key focus of medical research, investigating diverse strategies to deliver the ion to target tissues, including oral drug delivery, composite scaffolds, bone cements and coatings [101–103]. Osteoprotegerin, alkaline phosphatase, osteopontin, osteocalcin and VEGF are all overexpressed in cells cultured in contact with strontium-releasing biomaterials [104]. In addition, evidence shows that the presence of strontium has also an effect on osteoclasts, decreasing both osteoclastogenesis and bone resorption [101]. The simultaneous increase in bone formation and reduction in bone resorption ultimately results in improved bone mass with stronger mechanical properties [105]. Although the mechanism of action of strontium is still under investigation [106], several studies confirmed a key interaction with calcium-sensing receptors (CaSR) due to the agonism occurring between calcium and strontium [107]. In the context of biomaterials science, the similarity between the two ions has another relevant consequence: calcium is very effectively substituted with strontium within the hydroxyapatite structure both synthetically and in newly formed bone in vivo, preferably in trabecular areas [105].

9.2.15.1 Vanadium

Vanadium compounds have been primarily investigated as potential therapeutic agents mainly for diabetes, but also as possible treatments for cancer and atherosclerosis. Positive effects on bone mineralization and osteoblastic response were also reported [5]. Research so far seems to have identified in the redox properties of the element one of the major reasons for its pharmacological effects. Vanadium inhibits/stimulates enzymes thanks to vanadate–phosphate antagonism. The phenomenon is particularly evident on phosphatases and in particular on protein-tyrosine phosphatase 1B (PTP1B), a critical phosphatase involved in insulin signaling. Vanadium acts as a competitive inhibitor on this pathway, possibly explaining the therapeutic effect of this metal against diabetes [108].

9.2.15.2 Zinc

Zinc is studied primarily for its osteostimulative [109] and antibacterial [110] actions. An anti-inflammatory pro-neural growth effect was also reported [5]. Zinc ions have an essential role in bone metabolism, in particular high zinc concentrations are associated with increased extracellular matrix mineralization via alkaline phosphatase [111]. In presence of zinc, osteoblast proliferation increases, SMAD signaling is activated and Runx2 overexpressed [112]. Chondrocytes are also stimulated to proliferate (Akt/PI3K pathway) and to increase proteoglycan synthesis, collagen type 2 production and mineral deposition [113, 114]. In parallel, osteoclastogenesis decreases, probably through the inhibition of the receptor activator NF-κB of the RANK/RANKL pathway [115]. Similar to other TMIs, zinc also has antibacterial properties. These are thought to occur mainly by two proposed mechanisms of action: (i) membrane permeabilization and damage through electrostatic interactions [116] and (ii) formation of reactive oxygen species causing increased oxidative stress [117].

9.3 Chitosan

Chitosan is a glucose-based unbranched polysaccharide (similar to cellulose) widely exploited in biomaterials science for its remarkable set of beneficial properties: cytocompatibility, antibacterial and antifungal activity, mucoadhesion, hemostasis regulation and, most importantly in the context of TMIs, the ability to chelate metal ions [118]. Owing to its numerous advantages, the use of chitosan in a multitude of applications has been reported, including as food preservative, biocatalyst in wastewater treatment, anticancer drug and as biomaterial for tissue engineering [118]. In addition, it is also selected for its availability at low cost as a by-product of fish industry and its versatility in terms of chemical functionalization thanks to the numerous reactive side groups (–OH and $–NH_2$). Typically, the main drawbacks associated with this polysaccharide are an intrinsic variability in properties typical of natural polymers, the potential allergenicity and its relatively poor mechanical properties.

Chitosan is obtained from the partial deacetylation of chitin, a semi-crystalline homopolymer of β-(1 → 4)-linked N-acetyl-D-glucosamine extracted primarily from the exoskeleton of crustaceans, but also found in many species of insects and fungi [119] (Fig. 9.3). Deacetylation is typically performed by alkaline treatment at high temperature, resulting in the exposure of protonable side primary amino groups ($–NH_2$). These residues are generally considered responsible for many of the beneficial properties of chitosan, including the ability to complex with metal ions [13, 15]. Two models describing metal chelation by chitosan have been proposed: on one hand, the amine and hydroxyl groups of chitosan interact with ions one-to-one in a pendant-like fashion [120]. Secondly, coordination can occur between a TMI and several residues from one or more chitosan molecules, creating a bridge between adjacent chains [121]. Bridging TMIs are effectively crosslinking chitosan, which in

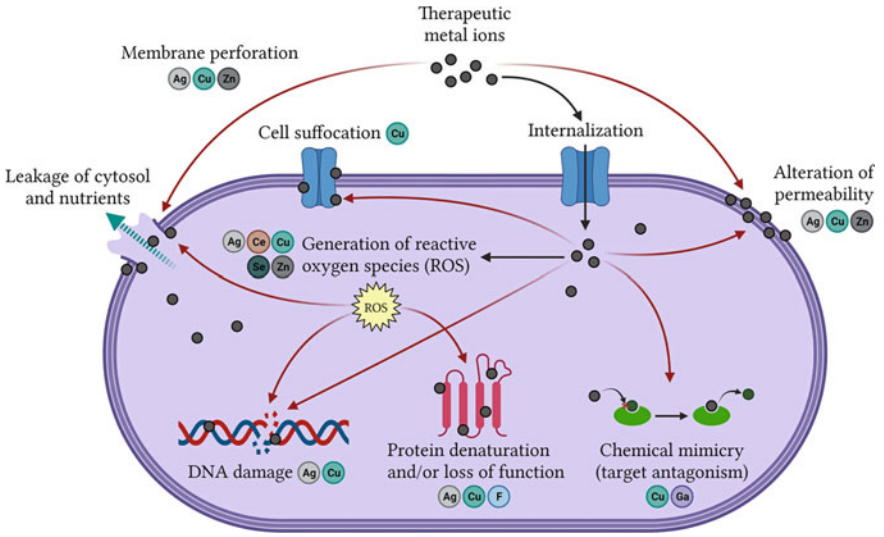

Fig. 9.2 Proposed mechanisms of antibacterial action of therapeutic ions

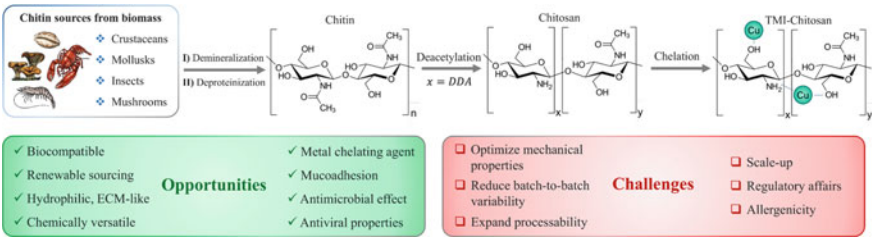

Fig. 9.3 Summary of chitosan showing sourcing, chemical structure, processing and main opportunities and challenges of this material in bone tissue engineering applications

turn can determine significant changes in its physicochemical properties, especially degradation and swelling rates, as well as mechanical properties [17, 122]. The two models are probably coexisting and many factors, including the considered ion, play a role in determining the prevalence of one over the other and, as a consequence, the overall properties of the final material [122]. In particular, it is known that chitosan has particular affinity with transition elements due to the presence of d and f unsaturated orbitals and, conversely, lower affinity with alkaline-earth metals (e.g., calcium). The variations in chelation affinity were directly linked to significant structural changes in the molecular packing and macrostructure of the final chitosan derivative [123].

To date, chitosan has been combined with several metal ions, including calcium [123], copper [122–124], silver [125], zinc [126], magnesium [72] and iron [17]. The complexation with antibacterial TMIs (i.e. silver and copper) is the subject of most investigations due to the synergic effect between the intrinsic antibacterial effect

of chitosan and the further action introduced by the ions. This results in materials inhibiting and/or killing bacteria quickly, by means of several simultaneous mechanisms of action, thus reducing problems related to resistance development. Most remarkably, different concentrations of copper release can be tailored and used to produce either antibacterial or pro-angiogenic materials. For instance, the incorporation of copper(II)-chitosan in PCL-based electrospun scaffolds was recently associated with an increase in expression of VEGF by stromal cells [124], indicating that the material can increase the stimulation of new vascularization. Biomaterials based on iron(III)-chitosan complexes were also proposed. Iron chelation could be a possible solution for applications in either cardiovascular medicine or orthopedics. For instance, the introduction of Fe^{3+} in the structure of chitosan significantly increases its mechanical properties [17]. The coordination of ferric ions with chitosan results in denser chain packing and increased bending strength. The authors suggest that iron(III)-chitosan could be used for the development of resorbable bone fixation devices.

9.4 Hydroxyapatite

Since the 1950s, hydroxyapatite has been used as a biomaterial. It is the most abundant mineral in human bone (circa 69% wt.) and, as such, it was a natural choice for the development of bone fillers. Over the following decades the biological activity of hydroxyapatite was described, and the range of applications increased exponentially, especially in biomimetic approaches for bone and enamel tissue engineering [127]. Chemically, hydroxyapatite is a crystalline calcium phosphate organized in a hexagonal lattice ($Ca_{10}(PO_4)_6(OH)_2$, Ca/P = 1.67). It can be either naturally harvested from bovine bone or corals, or synthesized by various routes, including wet precipitation and sol–gel chemistry (Fig. 9.4). Most interestingly, the crystalline structure

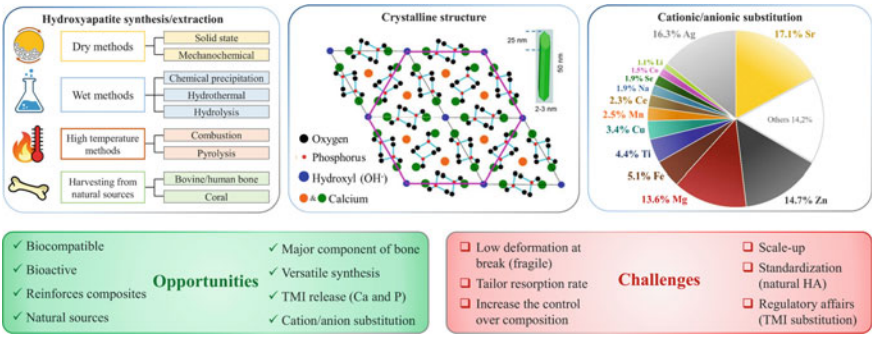

Fig. 9.4 Summary of hydroxyapatite showing sourcing/synthesis, crystalline structure, ionic substitutions and main opportunities and challenges of this material in bone tissue engineering applications

of hydroxyapatite is prone to the inclusion of several vicarious ions, both cations and anions, many of which are known TMIs with remarkable beneficial properties. The substitution of ions or atomic clusters within the hydroxyapatite lattice is in fact a major strategy used to enhance the biological performance of biomaterials. On one hand, multi-substituted hydroxyapatite more closely resembles the structure of natural hydroxyapatite, which is characterized by trace amounts of many elements. Simultaneously, cleverly tailored substitution can lead to the preparation of synthetic hydroxyapatite with superior properties. A typical example is the substitution of calcium with silicon ions. Even in trace amounts, the release of silicon from hydroxyapatite was associated with increased bioactivity, upregulated osteogenesis markers and improved osteoid calcification already at the early stages of bone mineralization [128]. Strontium can also be effectively included in the hydroxyapatite lattice for osteostimulation. For instance, Sr-hydroxyapatite implanted in rats resulted in higher bone formation and increased biomechanical strength of the novel tissue compared to a non-doped hydroxyapatite control [129]. Strontium doping is also linked to reduced osteoclast proliferation and, in parallel, upregulation of ALP, osteocalcin, type I collagen and increased ratio between osteoprotegerin and TNF-related activation-induced cytokine-receptor [130].

Furthermore, antibacterial ions have also been considered for substitution. Copper [131], selenium [132], silver [133] and zinc [134] among others have been investigated for the development of intrinsically antibacterial hydroxyapatite. Results confirm that substitution is an effective strategy to impart the therapeutic properties of TMIs to hydroxyapatite. The efficacy of antibacterial hydroxyapatites was confirmed with several strains of bacteria, including *Staphylococcus aureus*, the bacterial strain most commonly associated with bone infections [135]. At the same time, many of these ions are also able to positively influence mammalian cells. For instance, it was demonstrated that Zn-hydroxyapatite can guide osteoblast differentiation [134], while Cu-hydroxyapatite had a positive effect on angiogenesis markers [131]. Considering that co-substitutions and multi-substitutions of hydroxyapatite are also possible, hydroxyapatite is an all-round ideal carrier for the controlled delivery of TMIs for a wide range of therapeutic purposes. By cleverly choosing the array of TMIs to introduce in the calcium phosphate lattice it is possible to tailor materials with specific beneficial effects depending on the targeted application. Since there are virtually endless possibilities to exchange ions within the lattice, it is impossible to describe them exhaustively within the limits of the present work. In this context, the aim was to provide some relevant examples to highlight the potential of hydroxyapatite substitution. For further information, the effects of different vicarious ions on the structural, physicochemical and mechanical properties of hydroxyapatite are discussed in detail elsewhere [8].

9.5 Chitosan/Hydroxyapatite Scaffolds

Composites produced by combining chitosan and hydroxyapatite are a popular strategy in the development of materials for tissue engineering, especially targeting bone, cartilage and the musculoskeletal system. They can be considered as a biomimetic approach, where chitosan mimics the extracellular matrix (ECM) and hydroxyapatite the mineral phase of bone. Furthermore, the addition of an inorganic particulate filler (i.e., hydroxyapatite) is an effective strategy to enhance the native mechanical properties of chitosan, otherwise relatively low compared to bone tissue [13]. Chitosan/hydroxyapatite composites can be fabricated into 3D scaffolds that support the migration of cells and the in-growth of new tissue within the whole bulk of the material. A significant body of evidence proves that the two materials have good affinity and result in composites that are generally characterized by easy handling during surgery. The major goal of scaffold fabrication techniques is introducing high porosity and surface area into the material while simultaneously maintaining sufficient mechanical properties. Chitosan/hydroxyapatite composites have been used to prepare scaffolds using a wide variety of fabrication techniques (Fig. 9.5), including solvent casting [136], electrospinning [137] and additive manufacturing [138]. However, the most diffused method is freeze-drying [139, 140]. It is a relatively simple, reliable and scalable technique that results in homogeneous and

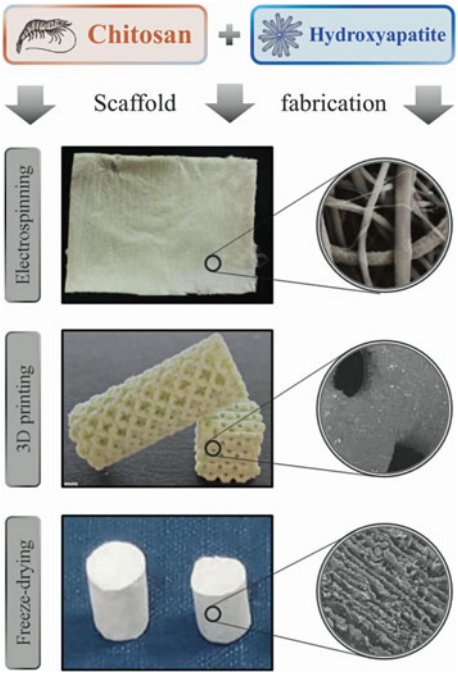

Fig. 9.5 Main fabrication techniques used to prepare chitosan/hydroxyapatite scaffolds. Typical macroscopic (left) and microscopic (right) features of each technique are shown. Images of electrospinning and 3D printing are reproduced with permission from [137] and [138]

highly porous 3D structures with a well-developed hierarchical network of interconnected pores ideal for cell infiltration (Ø = 30–100 μm), vascularization and tissue in-growth (Ø = 100–400 μm).

Bioactivity, biocompatibility, good handling and versatile processability are all definitely strong assets when it comes to chitosan/hydroxyapatite, even before 3D processing. Appropriately tailored macro-, microporosity and surface topography, however, can go a long way in enhancing the biological performance of these composites. High porosity was correlated with significantly increased apatite formation rate, most probably as a consequence of higher surface areas and, therefore, of increased ion release (important for TMI delivery). In parallel, porosity can also promote better fixation between the material and surrounding tissues by providing a template for bone ingrowth. In a recent study, for instance, the biological performance of 3D electrospun hydroxyapatite/chitosan scaffolds was compared with that of two controls: electrospun pure chitosan and 2D hydroxyapatite/chitosan membranes. The nanofibrous composites were confirmed to exert beneficial effects on the adhesion, shape and proliferation of bone marrow mesenchymal stem cells (BMSCs). Thanks to a higher number of available topographical cues, the response of 3D nanofibrous scaffolds was significantly improved compared to 2D membranes prepared using analogous chitosan/hydroxyapatite composites. The addition of hydroxyapatite as inorganic bioactive filler determined the activation of several pathways leading to osteogenic differentiation thanks to calcium and phosphate release. Upregulation in the expression of Smad1, BMP-2/4, Runx2, ALP, collagen I, integrin subunits and myosins was observed in the 3D scaffolds and was absent in the controls, suggesting the occurrence of a synergy between the chemical/biological stimulation of hydroxyapatite and the physical effect of 3D morphology. In vivo results confirmed the superior bone regeneration potential of 3D nanofibrous composites in a cranial defect rat model.

So far, most research studies focused on the optimization of the properties of undoped chitosan and hydroxyapatite. However, a smaller but promising body of work started to emerge introducing TMIs into composite scaffolds to increase the biological functionalities of these constructs. Chitosan and hydroxyapatite are in fact very versatile materials when it comes to TMI delivery. They can accommodate numerous ions within their structure and release them over time with significant effects on cells in the surrounding environment, being them prokaryotes (inhibited/killed) or eukaryotes (stimulated in various ways). Generally, a particulate phase of hydroxyapatite with various formulations is dispersed within a chitosan matrix. For example, strontium-substituted nanocrystals were dispersed in chitosan and freeze-dried to obtain 3D scaffolds developed to stimulate osteoblasts thanks to the release of Sr^{2+} ions. Data confirmed the effectiveness of this strategy in significantly promoting the proliferation of BMSCs and their differentiation towards an osteoblastic phenotype. Chitosan/hydroxyapatite scaffolds are per se cytocompatible. They support cell adhesion, migration and proliferation. However, the addition of strontium as TMI gave a remarkable boost to ALP activity, mineralization and production of

type 1 collagen [141]. In a similar study, composites were prepared using dual-substituted hydroxyapatite co-doped with magnesium and silver [142]. Initial investigation showed promising results for the use of these TMI-doped composites in the development of bone tissue engineering scaffolds: the substitution with Mg^{2+} played a crucial role in increasing the mechanical properties of the composites, while Ag^{+} successfully inhibited bacterial growth (~70% growth reduction). Cytocompatibility assays, however, showed a detrimental effect of silver on fibroblast viability, highlighting the need for further optimization before the clinical application of this technology. In particular, tailoring the ion release seems to be one key challenge for the successful therapeutic ion controlled delivery from chitosan/hydroxyapatite scaffolds. Current TMI release technologies tend to be characterized by slow ion release kinetics as a consequence of the low degradation rate of hydroxyapatite in body fluids. For this reason, the idea to use both phases to deliver TMIs was recently proposed. Since chitosan and hydroxyapatite are characterized by different degradations, both in terms of rate and mechanism, the ion release will also follow different profiles depending on the carrier. In this way, it is possible to obtain materials with decoupled releases of several ions over time depending on whether a specific TMI is chelated by chitosan or substituted in hydroxyapatite. Decoupling is particularly effective when considering both an antibacterial and a stimulatory effect at the same time. In fact, while it is preferable to have a relatively faster release for a higher antibacterial effect (i.e. to inhibit bacteria before they start growing), therapeutic effects on eukaryotic cells are better when supplied at lower dosage over longer periods of time. This concept was recently demonstrated on freeze-dried scaffolds using strontium-substituted hydroxyapatite with a copper(II)-chitosan matrix [140]. The release of ions from the two phases of the composite follows completely different profiles: copper is quickly released upon contact, resulting in outstanding antibacterial effect [122]; strontium, on the other hand, is tightly substituted within the hydroxyapatite lattice and has a slower release rate with potential effects on osteoblasts [140]. The mechanical properties of the composites are also affected by the hydroxyapatite composition.

9.6 Concluding Remarks

Therapeutic metal ions (TMIs) are a family of elements, transition metals especially, known for their numerous beneficial biological properties. They can enter metabolic pathways, interact with enzymes and engage in competitive antagonism with other essential ions both in prokaryotes and in eukaryotes. These interactions determine a wide range of ion-specific effects, including osteostimulation, promotion of angiogenesis, protection against oxidative stress, anti-inflammatory action and antibacterial activity, as discussed in the first sections of this chapter. Fostered by the plethora of beneficial properties associated with TMIs, research started investigating strategies to harvest their potential and use it in biomedical applications, especially in the context of tissue engineering and regenerative medicine. Controlled release of

therapeutic metal ions (TMIs) is an emerging approach to improve the biological performance of biomaterials used to fabricate tissue engineering scaffolds. In particular, chitosan and hydroxyapatite are ideal carriers for TMIs thanks to their structures, both able to accommodate them and release them over time. Current results show that these two materials can be successfully combined into composites, fabricated into 3D porous scaffolds using various techniques and, most importantly, that they can be simultaneously doped with multiple TMIs. Although multiple doping is still at an early stage of development, the evidence gathered so far using copper, strontium, magnesium and silver is encouraging. Future investigation will probably look into expanding the array of ions to get more complex and tissue-specific therapeutic effects.

Acknowledgements The author would like to thank Dr. Cédric Bossard, Prof. Jonathan Lao and Dr. Isabel Orlando for their scientific support in shaping this chapter. Many thanks also to Mr. Ludovico Angelini for proof reading.

References

1. Kowalczewski CJ, Saul JM (2018) Biomaterials for the delivery of growth factors and other therapeutic agents in tissue engineering approaches to bone regeneration. Front Pharmacol 9:513
2. Muschler GF, Nakamoto C, Griffith LG (2004) Engineering principles of clinical cell-based tissue engineering. J Bone Joint Surg Am 86:1541–1558
3. Giacca M, Zacchigna S (2012) VEGF gene therapy: therapeutic angiogenesis in the clinic and beyond. Gene Ther 19:622–629
4. Safiaghdam H, Nokhbatolfoghahaei H, Khojasteh A (2019) Therapeutic metallic ions in bone tissue engineering: a systematic review of the literature. Iran J Pharm Res 18:101–118
5. Mouriño V, Cattalini JP, Boccaccini AR (2012) Metallic ions as therapeutic agents in tissue engineering scaffolds: an overview of their biological applications and strategies for new developments. J R Soc Interface 9:401–419
6. Bose S, Fielding G, Tarafder S et al (2013) Understanding of dopant-induced osteogenesis and angiogenesis in calcium phosphate ceramics. Trends Biotechnol 31:594–605
7. Mouriño V, Vidotto R, Cattalini JP et al (2019) Enhancing biological activity of bioactive glass scaffolds by inorganic ion delivery for bone tissue engineering. Curr Opin Biomed Eng 10:23–34
8. Šupová M (2015) Substituted hydroxyapatites for biomedical applications: a review. Ceram Int 41:9203–9231
9. Bellucci D, Braccini S, Chiellini F et al (2019) Bioactive glasses and glass-ceramics versus hydroxyapatite: comparison of angiogenic potential and biological responsiveness. J Biomed Mater Res A 107:2601–2609
10. Fu Z, Cui J, Zhao B et al (2021) An overview of polyester/hydroxyapatite composites for bone tissue repairing. J Orthop Translat 28:118–130
11. Sultan M (2018) Hydroxyapatite/polyurethane composites as promising biomaterials. Chem Pap 72:2375–2395
12. Marcello E, Maqbool M, Nigmatullin R et al (2021) Antibacterial composite materials based on the combination of polyhydroxyalkanoates with selenium and strontium co-substituted hydroxyapatite for bone regeneration. Front Bioeng Biotechnol 9:647007

13. Pighinelli L, Kucharska M (2013) Chitosan-hydroxyapatite composites. Carbohydr Polym 93:256–262
14. Wahl DA, Czernuszka JT (2006) Collagen-hydroxyapatite composites for hard tissue repair. Eur Cell Mater 11:43–56
15. Guibal E (2004) Interactions of metal ions with chitosan-based sorbents: a review. Sep Purif Technol 38:43–74
16. Guibal E, Vincent T, Navarro R (2014) Metal ion biosorption on chitosan for the synthesis of advanced materials. J Mater Sci 49:5505–5518
17. Qu J, Hu Q, Shen K et al (2011) The preparation and characterization of chitosan rods modified with Fe^{3+} by a chelation mechanism. Carbohydr Res 346:822–827
18. Taylor A (1985) Therapeutic uses of trace elements. Clin Endocrinol Metab 14:703–724
19. Day RM, Boccaccini AR, Shurey S et al (2004) Assessment of polyglycolic acid mesh and bioactive glass for soft-tissue engineering scaffolds. Biomaterials 25:5857–5866
20. Hench LL, Polak JM (2002) Third-generation biomedical materials. Science 295:1014–1017
21. Gorustovich AA, Roether JA, Boccaccini AR (2010) Effect of bioactive glasses on angiogenesis: a review of *in vitro* and *in vivo* evidences. Tissue Eng Part B Rev 16:199–207
22. Glenske K, Donkiewicz P, Köwitsch A et al (2018) Applications of metals for bone regeneration. Int J Mol Sci 19:826
23. Cossey AJ, Paterson RS (2005) Loose intra-articular body following anterior cruciate ligament reconstruction. Arthroscopy 21:348–350
24. Fernandes GFS, Denny WA, Dos Santos JL (2019) Boron in drug design: recent advances in the development of new therapeutic agents. Eur J Med Chem 179:791–804
25. Balasubramanian P, Büttner T, Pacheco VM et al (2018) Boron-containing bioactive glasses in bone and soft tissue engineering. J Eur Ceram Soc 38:855–869
26. Naseri S, Lepry WC, Nazhat SN (2017) Bioactive glasses in wound healing: hope or hype? J Mater Chem B 5:6167–6174
27. Yin C, Jia X, Miron RJ et al (2018) SETD7 and its contribution to boron-induced bone regeneration in boron-mesoporous bioactive glass scaffolds. Acta Biomater 73:522–530
28. Ying X, Cheng S, Wang W et al (2011) Effect of boron on osteogenic differentiation of human bone marrow stromal cells. Biol Trace Elem Res 144:306–315
29. Chen X, Zhao Y, Geng S et al (2015) *In vivo* experimental study on bone regeneration in critical bone defects using PIB nanogels/boron-containing mesoporous bioactive glass composite scaffold. Int J Nanomedicine 10:839–846
30. Institute of Medicine (US) Standing Committee on the Scientific Evaluation of Dietary Reference Intakes (1997) Dietary reference intakes for calcium, phosphorus, magnesium, vitamin D, and fluoride. https://doi.org/10.17226/5776
31. Wu X, Walsh K, Hoff BL et al (2020) Mineralization of biomaterials for bone tissue engineering. Bioengineering 7:132. https://doi.org/10.3390/bioengineering7040132
32. Viti F, Landini M, Mezzelani A et al (2016) Osteogenic differentiation of msc through calcium signaling activation: transcriptomics and functional analysis. PLoS One 11:e0148173
33. Marie PJ (2010) The calcium-sensing receptor in bone cells: a potential therapeutic target in osteoporosis. Bone 46:571–576
34. Nakamura S, Matsumoto T, Sasaki J et al (2010) Effect of calcium ion concentrations on osteogenic differentiation and hematopoietic stem cell niche-related protein expression in osteoblasts. Tissue Eng Part A 16:2467–2473
35. Valerio P, Pereira MM, Goes AM et al (2009) Effects of extracellular calcium concentration on the glutamate release by bioactive glass (BG60S) preincubated osteoblasts. Biomed Mater 4:045011
36. Kurtuldu F, Mutlu N, Michálek M et al (2021) Cerium and gallium containing mesoporous bioactive glass nanoparticles for bone regeneration: bioactivity, biocompatibility and antibacterial activity. Mater Sci Eng C Mater Biol Appl 124:112050
37. Qi M, Li W, Zheng X et al (2020) Cerium and its oxidant-based nanomaterials for antibacterial applications: a state-of-the-art review. Front Mater 7:213. https://doi.org/10.3389/fmats.2020.00213

38. Battaglia V, Compagnone A, Bandino A et al (2009) Cobalt induces oxidative stress in isolated liver mitochondria responsible for permeability transition and intrinsic apoptosis in hepatocyte primary cultures. Int J Biochem Cell Biol 41:586–594
39. Czarnek K, Terpiłowska S, Siwicki AK (2015) Selected aspects of the action of cobalt ions in the human body. Cent Eur J Immunol 40:236–242
40. de Laia AGS, Barrioni BR, Valverde TM et al (2020) Therapeutic cobalt ion incorporated in poly(vinyl alcohol)/bioactive glass scaffolds for tissue engineering. J Mater Sci 55:8710–8727
41. Chang EL, Simmers C, Knight DA (2010) Cobalt complexes as antiviral and antibacterial agents. Pharmaceuticals 3:1711–1728
42. Hong R, Kang TY, Michels CA et al (2012) Membrane lipid peroxidation in copper alloy-mediated contact killing of Escherichia coli. Appl Environ Microbiol 78:1776–1784
43. Thurman RB, Gerba CP, Bitton G (1989) The molecular mechanisms of copper and silver ion disinfection of bacteria and viruses. Crit Rev Environ Control 18:295–315
44. Samuni A, Aronovitch J, Godinger D et al (1983) On the cytotoxicity of vitamin C and metal ions. A site-specific Fenton mechanism. Eur J Biochem 137:119–124
45. Hans M, Mathews S, Mücklich F et al (2015) Physicochemical properties of copper important for its antibacterial activity and development of a unified model. Biointerphases 11:018902
46. dos Santos NV, Matias AC, Higa GS et al (2015) Copper uptake in mammary epithelial cells activates cyclins and triggers antioxidant response. Oxid Med Cell Longev 2015:162876. https://doi.org/10.1155/2015/162876
47. Mansoorianfar M, Mansourianfar M, Fathi M et al (2020) Surface modification of orthopedic implants by optimized fluorine-substituted hydroxyapatite coating: enhancing corrosion behavior and cell function. Ceram Int 46:2139–2146
48. Ali W, Mehboob A, Han M.G. et al (2019) Effect of fluoride coating on degradation behaviour of unidirectional Mg/PLA biodegradable composite for load-bearing bone implant application. Compos Part A Appl Sci Manuf 124:105464
49. Borkowski L, Przekora A, Belcarz A et al (2020) Fluorapatite ceramics for bone tissue regeneration: synthesis, characterization and assessment of biomedical potential. Mater Sci Eng C Mater Biol Appl 116:111211
50. Amaechi BT, AbdulAzees PA, Alshareif DO et al (2019) Comparative efficacy of a hydroxyapatite and a fluoride toothpaste for prevention and remineralization of dental caries in children. BDJ Open 5:18
51. Al-Eesa NA, Johal A, Hill RG et al (2018) Fluoride containing bioactive glass composite for orthodontic adhesives—apatite formation properties. Dent Mater 34:1127–1133
52. Berglundh T, Abrahamsson I, Albouy JP et al (2007) Bone healing at implants with a fluoride-modified surface: an experimental study in dogs. Clin Oral Implants Res 18:147–152
53. Kanduti D, Sterbenk P, Artnik B (2016) Fluoride: a review of use and effects on health. Mater Sociomed 28:133–137
54. Liao Y, Brandt BW, Li J et al (2017) Fluoride resistance in Streptococcus mutans: a mini review. J Oral Microbiol 9:1344509
55. Bernstein LR (1998) Mechanisms of therapeutic activity for gallium. Pharmacol Rev 50:665–682
56. Verron E, Masson M, Khoshniat S et al (2010) Gallium modulates osteoclastic bone resorption in vitro without affecting osteoblasts. Br J Pharmacol 159:1681–1692
57. Verron E, Loubat A, Carle GF et al (2012) Molecular effects of gallium on osteoclastic differentiation of mouse and human monocytes. Biochem Pharmacol 83:671–679
58. Łapa A, Cresswell M, Campbell I et al (2020) Gallium- and cerium-doped phosphate glasses with antibacterial properties for medical applications. Adv Eng Mater 22:1901577
59. Valappil SP, Ready D, Abou Neel EA et al (2009) Controlled delivery of antimicrobial gallium ions from phosphate-based glasses. Acta Biomater 5:1198–1210
60. Mouriño V, Newby P, Boccaccini AR (2010) Preparation and characterization of gallium releasing 3-D alginate coated 45S5 Bioglass® based scaffolds for bone tissue engineering. Adv Eng Mater 12:B283–B291

61. Minandri F, Bonchi C, Frangipani E et al (2014) Promises and failures of gallium as an antibacterial agent. Future Microbiol 9:379–397
62. Gloria A, Russo T, D'Amora U et al (2013) Magnetic poly(ε-caprolactone)/iron-doped hydroxyapatite nanocomposite substrates for advanced bone tissue engineering. J R Soc Interface 10:20120833
63. Le NT, Richardson DR (2002) The role of iron in cell cycle progression and the proliferation of neoplastic cells. Biochim Biophys Acta 1603:31–46
64. Ahmed I, Collins CA, Lewis MP et al (2004) Processing, characterisation and biocompatibility of iron-phosphate glass fibres for tissue engineering. Biomaterials 25:3223–3232
65. Wong SK, Chin KY, Ima-Nirwana S (2020) The skeletal-protecting action and mechanisms of action for mood-stabilizing drug lithium chloride: current evidence and future potential research areas. Front Pharmacol 11:430
66. Eren I, Yildiz M, Çivi I (2006) The effects of lithium treatment on bone mineral density in bipolar patients. Neurol Psychiatry Brain Res 13:174–179
67. Yuan Y, Yuan Q, Wu C et al (2019) Enhanced osteoconductivity and osseointegration in calcium polyphosphate bioceramic scaffold via lithium doping for bone regeneration. ACS Biomater Sci Eng 5:5872–5880
68. Hu Y, Chen L, Gao Y et al (2020) A lithium-containing biomaterial promotes chondrogenic differentiation of induced pluripotent stem cells with reducing hypertrophy. Stem Cell Res Ther 11:77
69. Liu L, Liu Y, Feng C et al (2019) Lithium-containing biomaterials stimulate bone marrow stromal cell-derived exosomal miR-130a secretion to promote angiogenesis. Biomaterials 192:523–536
70. Zhou D, Qi C, Chen YX et al (2017) Comparative study of porous hydroxyapatite/chitosan and whitlockite/chitosan scaffolds for bone regeneration in calvarial defects. Int J Nanomedicine 12:2673–2687
71. Malladi L, Mahapatro A, Gomes AS (2018) Fabrication of magnesium-based metallic scaffolds for bone tissue engineering. Mater Technol 33:173–182
72. Adhikari U, Rijal NP, Khanal S et al (2016) Magnesium incorporated chitosan based scaffolds for tissue engineering applications. Bioact Mater 1:132–139
73. Suryavanshi A, Khanna K, Sindhu KR et al (2017) Magnesium oxide nanoparticle-loaded polycaprolactone composite electrospun fiber scaffolds for bone-soft tissue engineering applications: in-vitro and in-vivo evaluation. Biomed Mater 12:055011
74. Ran J, Jiang P, Sun G et al (2017) Comparisons among Mg, Zn, Sr, and Si doped nano-hydroxyapatite/chitosan composites for load-bearing bone tissue engineering applications. Mater Chem Front 1:900–910
75. Diba M, Tapia F, Boccaccini AR et al (2012) Magnesium-containing bioactive glasses for biomedical applications. Int J Appl Glass Sci 3:221–253
76. Gu Y, Zhang J, Zhang X et al (2019) Three-dimensional printed Mg-doped β-TCP bone tissue engineering scaffolds: effects of magnesium ion concentration on osteogenesis and angiogenesis *in vitro*. Tissue Eng Regen Med 16:415–429
77. Venkatraman SK, Swamiappan S (2020) Review on calcium- and magnesium-based silicates for bone tissue engineering applications. J Biomed Mater Res A 108:1546–1562
78. Wang Y, Geng Z, Huang Y et al (2018) Unraveling the osteogenesis of magnesium by the activity of osteoblasts in vitro. J Mater Chem B 6:6615–6621
79. Mammoli F, Castiglioni S, Parenti S et al (2019) Magnesium is a key regulator of the balance between osteoclast and osteoblast differentiation in the presence of vitamin D3. Int J Mol Sci 20:385
80. Kang JI, Son MK, Choe HC et al (2016) Bone-like apatite formation on manganese-hydroxyapatite coating formed on Ti-6Al-4V alloy by plasma electrolytic oxidation. Thin Solid Films 620:126–131
81. Azizi F, Heidari F, Fahimipour F et al (2020) Evaluation of mechanical and biocompatibility properties of hydroxyapatite/manganese dioxide nanocomposite scaffolds for bone tissue engineering application. Int J Appl Ceram Technol 17:2439–2449

82. Avila DS, Puntel RL, Aschner M (2013) Manganese in health and disease. Met Ions Life Sci 13:199–227
83. Clegg MS, Donovan SM, Monaco MH et al (1998) The influence of manganese deficiency on serum IGF-1 and IGF binding proteins in the male rat. Proc Soc Exp Biol Med 219:41–47
84. Pepa GD, Brandi ML (2016) Microelements for bone boost: the last but not the least. Clin Cases Miner Bone Metab 13:181–185
85. Laskus A, Zgadzaj A, Kolmas J (2018) Selenium-enriched brushite: a novel biomaterial for potential use in bone tissue engineering. Int J Mol Sci 19:4042
86. Guan B, Yan R, Li R et al (2018) Selenium as a pleiotropic agent for medical discovery and drug delivery. Int J Nanomedicine 13:7473–7490
87. Zeng H, Cao JJ, Combs GF Jr (2013) Selenium in bone health: roles in antioxidant protection and cell proliferation. Nutrients 5:97–110
88. Zhang H, Li Z, Dai C et al (2021) Antibacterial properties and mechanism of selenium nanoparticles synthesized by Providencia sp. DCX. Environ Res 194:110630
89. Kalishwaralal K, Jeyabharathi S, Sundar K et al (2018) A novel biocompatible chitosan-selenium nanoparticles (SeNPs) film with electrical conductivity for cardiac tissue engineering application. Mater Sci Eng C Mater Biol Appl 92:151–160
90. Dorazilová J, Muchová J, Šmerková K et al (2020) Synergistic effect of chitosan and selenium nanoparticles on biodegradation and antibacterial properties of collagenous scaffolds designed for infected burn wounds. Nanomaterials 10:1971
91. Jurkić LM, Cepanec I, Pavelić SK et al (2013) Biological and therapeutic effects of ortho-silicic acid and some ortho-silicic acid-releasing compounds: new perspectives for therapy. Nutr Metab 10:2
92. Martin KR (2007) The chemistry of silica and its potential health benefits. J Nutr Health Aging 11:94–97
93. Al-Harbi N, Mohammed H, Al-Hadeethi Y et al (2021) Silica-based bioactive glasses and their applications in hard tissue regeneration: a review. Pharmaceuticals 14:75
94. Yang X, Li Y, Liu X et al (2016) The stimulatory effect of silica nanoparticles on osteogenic differentiation of human mesenchymal stem cells. Biomed Mater 12:015001
95. Uribe P, Johansson A, Jugdaohsingh R et al (2020) Soluble silica stimulates osteogenic differentiation and gap junction communication in human dental follicle cells. Sci Rep 10:9923
96. Sim W, Barnard RT, Blaskovich MAT et al (2018) Antimicrobial silver in medicinal and consumer applications: a patent review of the past decade (2007–2017). Antibiotics 7:93
97. Le Ouay B, Stellacci F (2015) Antibacterial activity of silver nanoparticles: a surface science insight. Nano Today 10:339–354
98. Panáček A, Kvítek L, Smékalová M et al (2018) Bacterial resistance to silver nanoparticles and how to overcome it. Nat Nanotechnol 13:65–71
99. Möhler JS, Sim W, Blaskovich MAT et al (2018) Silver bullets: a new lustre on an old antimicrobial agent. Biotechnol Adv 36:1391–1411
100. Dakal TC, Kumar A, Majumdar RS et al (2016) Mechanistic basis of antimicrobial actions of silver nanoparticles. Front Microbiol 7:1831
101. Jiménez M, Abradelo C, San Román J et al (2019) Bibliographic review on the state of the art of strontium and zinc based regenerative therapies. Recent developments and clinical applications. J Mater Chem B 7:1974–1985
102. Neves N, Linhares D, Costa G et al (2017) *In vivo* and clinical application of strontium-enriched biomaterials for bone regeneration: a systematic review. Bone Joint Res 6:366–375
103. Kuang GM, Yau WP, Wu J et al (2015) Strontium exerts dual effects on calcium phosphate cement: accelerating the degradation and enhancing the osteoconductivity both *in vitro* and *in vivo*. J Biomed Mater Res A 103:1613–1621
104. Zarins J, Pilmane M, Sidhom E et al (2016) Does local application of strontium increase osteogenesis and biomaterial osteointegration in osteoporotic and other bone tissue conditions: review of literature. Acta Chir Latv 16:17–23
105. Dahl SG, Allain P, Marie PJ et al (2001) Incorporation and distribution of strontium in bone. Bone 28:446–453

106. Fonseca JE, Brandi ML (2010) Mechanism of action of strontium ranelate: what are the facts? Clin Cases Miner Bone Metab 7:17–18
107. Thomsen AR, Worm J, Jacobsen SE et al (2012) Strontium is a biased agonist of the calcium-sensing receptor in rat medullary thyroid carcinoma 6–23 cells. J Pharmacol Exp Ther 343:638–649
108. Treviño S, Díaz A, Sánchez-Lara E et al (2019) Vanadium in biological action: chemical, pharmacological aspects, and metabolic implications in diabetes mellitus. Biol Trace Elem Res 188:68–98
109. O'Connor JP, Kanjilal D, Teitelbaum M et al (2020) Zinc as a therapeutic agent in bone regeneration. Materials 13:2211
110. Singh A, Singh NB, Afzal S et al (2018) Zinc oxide nanoparticles: a review of their biological synthesis, antimicrobial activity, uptake, translocation and biotransformation in plants. J Mater Sci 53:185–201
111. Ciancaglini P, Pizauro JM, Curti C et al (1990) Effect of membrane moiety and magnesium ions on the inhibition of matrix-induced alkaline phosphatase by zinc ions. Int J Biochem 22:747–751
112. Cho YE, Kwun IS (2018) Zinc upregulates bone-specific transcription factor Runx2 expression via BMP-2 signaling and Smad-1 phosphorylation in osteoblasts. J Nutr Health 51:23–30
113. Rodríguez JP, Rosselot G (2001) Effects of zinc on cell proliferation and proteoglycan characteristics of epiphyseal chondrocytes. J Cell Biochem 82:501–511
114. Burgess D, Iversen T, Cottrell J (2018) Zinc chloride treatment in ATDC5 cells induces chondrocyte maturation. Int J Regen Med. https://doi.org/10.31487/j.RGM.2018.02.008
115. Hie M, Tsukamoto I (2011) Administration of zinc inhibits osteoclastogenesis through the suppression of RANK expression in bone. Eur J Pharmacol 668:140–146
116. Xie Y, He Y, Irwin PL et al (2011) Antibacterial activity and mechanism of action of zinc oxide nanoparticles against Campylobacter jejuni. Appl Environ Microbiol 77:2325–2331
117. Sirelkhatim A, Mahmud S, Seeni A et al (2015) Review on zinc oxide nanoparticles: antibacterial activity and toxicity mechanism. Nanomicro Lett 7:219–242
118. Bakshi PS, Selvakumar D, Kadirvelu K et al (2020) Chitosan as an environment friendly biomaterial—a review on recent modifications and applications. Int J Biol Macromol 150:1072–1083
119. No HK, Meyers SP (1995) Preparation and characterization of chitin and chitosan-a review. J Aquat Food Prod Technol 4:27–52
120. Ogawa K, Oka K, Yui T (1993) X-ray study of chitosan-transition metal complexes. Chem Mater 5:726–728
121. Schlick S (1986) Binding sites of copper^{2+} in chitin and chitosan. An electron spin resonance study. Macromolecules 19:192–195
122. Gritsch L, Lovell C, Goldmann WH et al (2018) Fabrication and characterization of copper(II)-chitosan complexes as antibiotic-free antibacterial biomaterial. Carbohydr Polym 179:370–378
123. Nie J, Wang Z, Hu Q (2016) Chitosan hydrogel structure modulated by metal ions. Sci Rep 6:36005
124. Gritsch L, Liverani L, Lovell C et al (2020) Polycaprolactone electrospun fiber mats prepared using benign solvents: blending with copper(II)-chitosan increases the secretion of vascular endothelial growth factor in a bone marrow stromal cell line. Macromol Biosci 20:e1900355
125. Lin S, Chen L, Huang L et al (2015) Novel antimicrobial chitosan-cellulose composite films bioconjugated with silver nanoparticles. Ind Crops Prod 70:395–403
126. Rogina A, Vidović D, Antunović M et al (2020) Metal ion-assisted formation of porous chitosan-based microspheres for biomedical applications. Int J Polym Mater Polym Biomater. https://doi.org/10.1080/00914037.2020.1776283
127. Palmer LC, Newcomb CJ, Kaltz SR et al (2008) Biomimetic systems for hydroxyapatite mineralization inspired by bone and enamel. Chem Rev 108:4754–4783

128. Sprio S, Tampieri A, Landi E et al (2008) Physico-chemical properties and solubility behaviour of multi-substituted hydroxyapatite powders containing silicon. Mater Sci Eng C 28:179–187
129. Tao ZS, Bai BL, He XW et al (2016) A comparative study of strontium-substituted hydroxyapatite coating on implant's osseointegration for osteopenic rats. Med Biol Eng Comput 54:1959–1968
130. Capuccini C, Torricelli P, Sima F et al (2008) Strontium-substituted hydroxyapatite coatings synthesized by pulsed-laser deposition: in vitro osteoblast and osteoclast response. Acta Biomater 4:1885–1893
131. Elrayah A, Zhi W, Feng S et al (2018) Preparation of micro/nano-structure copper-substituted hydroxyapatite scaffolds with improved angiogenesis capacity for bone regeneration. Materials 11:1516
132. Maqbool M, Nawaz Q, Atiq Ur Rehman M et al (2021) Synthesis, characterization, antibacterial properties, and in vitro studies of selenium and strontium co-substituted hydroxyapatite. Int J Mol Sci 22:4246
133. Khurshid Z, Safar MS, Hussain S et al (2020) Silver-substituted hydroxyapatite. In: Khan AS, Chaudhry AA (eds) Handbook of ionic substituted hydroxyapatite. Woodhead Publishing, England, pp 237–257
134. Thian ES, Konishi T, Kawanobe Y et al (2013) Zinc-substituted hydroxyapatite: a biomaterial with enhanced bioactivity and antibacterial properties. J Mater Sci Mater Med 24:437–445
135. Dudareva M, Hotchen AJ, Ferguson J et al (2019) The microbiology of chronic osteomyelitis: changes over ten years. J Infect 79:189–198
136. Li X, Nan K, Shi S et al (2012) Preparation and characterization of nano-hydroxyapatite/chitosan cross-linking composite membrane intended for tissue engineering. Int J Biol Macromol 50:43–49
137. Frohbergh ME, Katsman A, Botta GP et al (2012) Electrospun hydroxyapatite-containing chitosan nanofibers crosslinked with genipin for bone tissue engineering. Biomaterials 33:9167–9178
138. Chavanne P, Stevanovic S, Wüthrich A et al (2013) 3D printed chitosan/hydroxyapatite scaffolds for potential use in regenerative medicine. Biomed Tech. https://doi.org/10.1515/bmt-2013-4069
139. Nezafati N, Faridi-Majidi R, Pazouki M et al (2019) Synthesis and characterization of a novel freeze-dried silanated chitosan bone tissue engineering scaffold reinforced with electrospun hydroxyapatite nanofiber. Polym Int 68:1420–1429
140. Gritsch L, Maqbool M, Mouriño V et al (2019) Chitosan/hydroxyapatite composite bone tissue engineering scaffolds with dual and decoupled therapeutic ion delivery: copper and strontium. J Mater Chem B 7:6109–6124
141. Lei Y, Xu Z, Ke Q et al (2017) Strontium hydroxyapatite/chitosan nanohybrid scaffolds with enhanced osteoinductivity for bone tissue engineering. Mater Sci Eng C Mater Biol Appl 72:134–142
142. Mansour SF, El-dek SI, Dorozhkin SV et al (2017) Physico-mechanical properties of Mg and Ag doped hydroxyapatite/chitosan biocomposites. New J Chem 41:13773–13783

Lukas Gritsch Dr. Gritsch is a biomaterials scientist specialized in antimicrobial technologies and 3D manufacturing for tissue engineering. Working at the crossroad between biology and engineering, his investigations explored, among others, the electrospinning of chitosan for therapeutic ion delivery and the fused deposition modeling of hybrid materials for bone grafting. As a Marie Curie fellow, his research was focused on tackling the problem of antibiotic resistance using metallic ions as antimicrobial agents. His achievements granted him the Julia Polak European doctoral award by the European Society of Biomaterials (ESB).

He holds an M.Sc. and a B.Sc. hon in Biomedical Engineering obtained at Politecnico di Milano. He gained an industrial PhD in Materials Science pursued under the supervision of Prof. Aldo Boccaccini at the Institute of Biomaterials of Erlangen. His career also includes a two-year post-doc at Université Clermont Auvergne and visiting research positions at Lucideon Ltd. in Stoke-on-Trent, UK and at Polytechnique de Montréal. To date, he is the author of 9 scientific papers and 3 book chapters with more than 300 citations. He also presented at >10 international conferences.

Chapter 10
Alumina: Implantable Bionics and Tissue Scaffolds

Andrew J. Ruys, David J. Cowdery, and Edwin K. L. Soh

Abstract This chapter has a two-fold focus: the first section focuses on the bionic application, and the second section focuses on the tissue scaffold application. **Bionics**: Alumina is an essential component of the hermetic encapsulation and electrical feedthrough system used in implantable bionics. This has been the case since 1970 when the transition was made from the rudimentary epoxy encapsulation systems used in the developmental era of implantable bionics, to the alumina/titanium hermetic electrical feedthrough system used for all implantable bionics since then. Implantable bionics is a global industry currently worth $25 billion per annum and growing rapidly. Thus, implantable bionics is one of the most important commercial applications for alumina advanced ceramics in the world today. The alumina/titanium hermetic feedthrough system for implantable bionics was invented in 1970 by Author Cowdery and has now become the standard hermetic encapsulation for all bionic implants in the global $25 Billion market. This chapter outlines the science and engineering underlying this feedthrough technology and explores its application in 3 key bionic implants (of the 14 or so types of bionic implants on the market): the pacemaker (Cowdery), bionic ear (Cowdery), and bionic eye (Ruys). **Tissue Scaffolds**: Alumina is a very strong ceramic, far superior to calcium phosphates, and has a high strength even at porosities of over 90%. It can be rendered bioactive by surface-doping with bioactivity-enhancing ions, such as calcium, phosphorous, magnesium and silicon. Authors Soh and Ruys pioneered a novel doped-porous-alumina tissue scaffold technology with an extremely high porosity of 94.4%, a high compressive strength of 384 MPa, with an average pore size of 300 microns, more than large enough for bone ingrowth. This chapter outlines the science and engineering underlying these developments.

Keywords Pacemaker · Alumina · Bone tissue scaffold · Implantable bionics · Bionic ear · Bionic eye · Brain-computer interface

A. J. Ruys (✉) · D. J. Cowdery · E. K. L. Soh
Biomedical Engineering, School of Aerospace, Mechanical and Mechatronic Engineering, Faculty of Engineering, University of Sydney, Sydney, NSW 2006, Australia
e-mail: andrew.ruys@sydney.edu.au

A. H. Choi and B. Ben-Nissan (eds.), *Innovative Bioceramics in Translational Medicine I*, Springer Series in Biomaterials Science and Engineering 17,
https://doi.org/10.1007/978-981-16-7435-8_10

10.1 Alumina in Implantable Bionics

One of the most important commercial applications of alumina ceramics in the world today is for electrical feedthrough seals in bionic implants. The biocompatible, impervious, electrically resistive, alumina seal uniquely enables electrical signal transmission across a hermetic alumina barrier between the sensitive internal electronics of the bionic implant and the corrosive fluids of the body cavity. Bionic implants are a global $25 billion industry. Alumina feedthroughs are an essential platform technology in all of these bionic implants.

The field of implantable bionics began with the development of the cardiac pacemaker. Development outside of the pacemaker field was relatively slow throughout the 1960s and 1970s. However, the widespread availability of microprocessors from the 1980s onward, and highly evolved alumina feedthrough technology thanks to the innovations of medical device pioneers Telectronics and Cochlear over the period 1970 to 1982, led to a global explosion of sophisticated bionic innovation in the late twentieth century, and early twenty-first century. This continues to the present day, and from this, the numerous bionic implantable systems listed below arose.

Heart

1. Cardiac pacemaker (Heart Rhythm)
2. Cardioverter Defibrillator (Heart Defibrillation)
3. Cardiac pacemaker/defibrillator (Heart Rhythm, Heart Defibrillation).

Sensory Organs

4. Cochlear Implant (Hearing)
5. Bionic Eye (Vision).

Brain and Central Nervous System

6. Deep-Brain Stimulator (Parkinsons Disease, Essential Tremor, Dystonia, OCD)
7. Spinal cord stimulator (Back Pain, Angina Pain, Peripheral Artery Disease Pain).

Peripheral Nerve Stimulators

8. Vagal nerve stimulator (Epilepsy, Depression)
9. Occipital Nerve Stimulator (Migraine, Brain Trauma)
10. Sacral-Nerve Stimulator (Incontinence, Pelvic Pain, ED)
11. Gastric stimulator (Obesity, Gastroparesis, IBS)
12. Pulmonary Stimulator (Respiratory Support)
13. Functional electrical stimulation/Peripheral Nerve Stimulation (Foot drop, mobility for spinal cord injured patients).

Functional Implants

14. Implantable drug delivery pumps.

In essence, the three drivers for this bionic innovation were as follows:

(1) The invention of the transistor in 1947 kick-started the field of implantable bionics in the 1950s and enabled the development of the world's first wearable pacemaker in 1957 by Aquilina [1]. This was an external device with percutaneous electrodes.
(2) The invention of the titanium/alumina hermetic feedthrough concept in 1970 by author David Cowdery [2–4] made implantable bionic medical devices a viable technology thereafter.
(3) The invention of the microprocessor in 1949 by Jacobi [5], and its subsequent wide availability and usage that arose in the 1970s. This spawned the microcomputer industry, and also had the effect of accelerating development in the field of implantable bionics from the 1980s onwards.

Thus, a clear lesson emerges from the history of bionics. Each leap forward was made possible by the invention of a key platform technology: the transistor, the titanium/alumina hermetic feedthrough, and the microprocessor. As a consequence, the bionics explosion since the late twentieth century has brought us now the 14 different types of commercial hermetic-bionic-implants listed above. Moreover, there are more under development for the future.

Three key platform technologies enabled the development of the field of implantable bionics: the transistor, the microprocessor, and the alumina/titanium hermetic feedthrough system. The focus in this chapter is on the third innovation: the invention, development, and evolution of the alumina/titanium hermetic feedthrough system.

We will begin this section with a brief background in feedthrough technology.

10.1.1 The Electrical Feedthrough: Definition and Historical Background

10.1.1.1 Hermeticity

Hermeticity is defined by the Oxford English Dictionary as "the state of being airtight or sealed against water, ion, and gas diffusion". Proving absolute hermeticity is impossible because even with the most sensitive leak detection equipment available (the helium mass spectrometer), infinitely small leaks cannot be found. In practice, all that can be achieved is to ensure that the implant internal environment remains adequately dry for a period significantly greater than the maximum possible implant lifetime. Measurement sensitivity can be optimized by incorporating a percentage of helium into the internal implant environment during seal welding. By assuming that that a leak exists at the threshold of sensitivity of testing, it is simple to calculate the weight of water vapor that could diffuse through this leak during the implant lifetime. Vacuum baked electronic assemblies inside the implant have the ability to absorb a certain weight of water in a bound or immobile state up to a desired maximum end of life relative humidity. The use of 4-Angstrom molecular sieve desiccant can also

be used to adsorb a selected weight of water up to this relative humidity limit. In some implants such as defibrillators, the energy storage capacitors can also release water vapor inside the implant and this must also be taken into account.

It has been shown that water vapor forms monolayers on the surface of internal components and that a relative humidity of 35% minimum is required for the first monolayer to form with up to five monolayers at 70% RH. The presence of monolayers of water molecules permit the existence of electrical surface currents, which can result in the formation of conductive dendrites leading to electronic failure. Hence, the absolute worst-case relative humidity of 30% at 37 °C is often chosen as the acceptable limit for worst-case end of life of the implant. It should be noted that the dendrites referred to are thin surface phenomena. These have nothing to do with the so-called dendrites occurring in lithium batteries, which are in fact metal whiskers, which form by totally different mechanisms.

In October 1958, in Sweden, Rune Elmqvist produced the first implantable pacemaker, which Ake Senning successfully implanted in a human patient making it the world's first implanted pacemaker [6]. It was encapsulated in (recently invented) epoxy resin to temporarily seal the battery and circuitry from the body. While the epoxy resin was biocompatible, and an innovative solution to encapsulation, it was not hermetic. This meant that it was not stable in the body in the medium-term to long-term, gradually swelling due to moisture ingress, and ultimately dissolving [7]. It has also been observed that the bonding of epoxy to the electronic components fails after extended exposure to body fluids, allowing monolayers of water to accumulate in the interface between the components and the epoxy resin. Implantable epoxy-encapsulated pacemakers were first developed in the USA by pioneer Wilson Greatbatch in 1958 and first implanted in 1960. Paul Zoll, one of the pioneers of the external pacemaker in 1951, became a significant pioneer in implantable pacemakers in 1961.

Thus, while epoxy-encapsulated pacemakers were an important step along the pathway to the development of implantable bionics, they were only a stepping stone, since epoxy encapsulation was not hermetic. These epoxy-clad pacemakers were durable in the body cavity for only a matter of months. Durability for tens of years is what is required.

10.1.1.2 The Electrical Feedthrough Concept

A crucial characteristic of a bionic implant is the electrical feedthrough. This is a system that enables the transmission of electrical signals through the wall of the implant casing, while simultaneously preventing the transmission of fluids and gases through the wall of the implant casing.

The concept of the electrical feedthrough dates back to the nineteenth century, as it was the key platform technology for the electric light globe. Bright light requires electrical heating of a filament to an incandescent temperature, around 3000 °C, at which temperature, a carbon or metal filament will rapidly burn out in air. The filament therefore needs to be electrically heated either in a vacuum chamber, or in a chamber

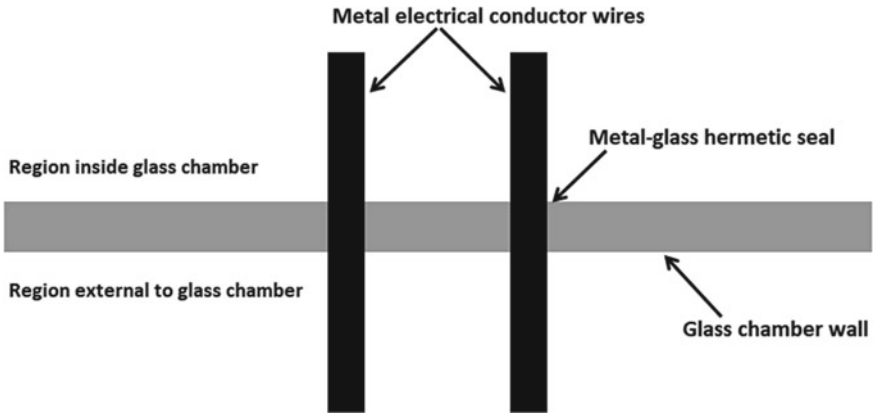

Fig. 10.1 Glass-metal hermetic feedthrough seal of the type used in the light globe and other spin-off technologies such as triode valves and x-ray tubes, to protect an incandescent filament (commonly tungsten or carbon) from oxidation. The metal conductor wires are usually Kovar, which has a perfect thermal expansion match to borosilicate glass, the usual glass used. The kovar is fused into the wall of the glass chamber, while the chamber is either under vacuum or filled with inert gas

filled with inert gas: the evacuated or inert gas filled glass globe. This requires a means of getting electrical current through the wall of a sealed chamber and forming a hermetic seal that would be unaffected by the differential thermal expansion, during the heating and cooling cycles, as the heat-generating incandescent light is switched on and off. This differential thermal expansion occurs between:

- The glass chamber wall, and;
- The electrical conductors passing through that wall.

This technical challenge consumed the best efforts of some of the greatest engineering minds over the period 1760–1880. It began with the first documented demonstration of heating a wire to incandescence by Ebenezer Kinnersley in 1761, to the invention of the electrical feedthrough around 1840,[1] to the first optimally engineered, carbon-filament in a vacuum, commercially viable light globe of Thomas Edison in 1880 [8]. The electrical-industry feedthrough is a very old and simple technology, essentially metal wires passing through the wall of a glass globe, sealed with a fused-glass seal. It is quite flexible from a materials point of view. It is cheap mass-produced technology, and the kovar/borosilicate wire/glass system has remained the standard for incandescent and fluorescent light globes for a century and remains so today. This is shown conceptually in Fig. 10.1.

[1] There is some controversy as to who actually invented the electrical feedthrough concept for the electric light globe, whether it was James Bowman Lindsay in 1835, Marcellin Jobard in 1838, Warren de la Rue in 1840, or Fredrick de Moleyns who patented the first hermetic light globe in 1841.

10.1.1.3 The Origin of Alumina/Metal Hermetic Seals

Today, not all feedthroughs are electrical. Feedthroughs come in two main forms:

Electrical feedthrough: Hermetic seal through which electrical conductor wires pass.

- Bionic feedthrough (alumina)
- Electrical-industry feedthrough (glass or alumina).

Window feedthrough: Radiation-transparent hermetic feedthrough.

- Microwave window (alumina, in rare cases BeO)
- Vacuum-furnace-viewing window (fused silica or synthetic sapphire)
- Sealed reactor-vessel viewing window (Glass).

In the early twentieth century glass/metal hermetic seals evolved to the next technology evolution: the patenting of the "audion" by Lee De Forest in 1906 [9, 10], the precursor to the triode vacuum valve, a key enabling technology for radio transmitters/receivers. The filing of the original Kovar patent, by Howard Scott in 1929 (granted in 1936 [11]), was an important step forward, because Kovar was a metal alloy deliberately engineered, by inventor Howard Scott [11], to have perfect thermal expansion matching to borosilicate glass [12]. Kovar remains a dominant metal alloy for metal–glass hermetic feedthroughs today, although alumina is now commonly used in advanced and high-temperature feedthroughs.

Alumina/metal seals have their origins dating back to the mid-twentieth century. They are commonly used for vacuum electronic devices for which the hermeticity is generally measured by the helium leak test in accordance with MIL-STD-883 [13]. There are many examples of alumina/metal hermetic seals in the electrical industry, for example:

- Thermionic converters.
- Vacuum equipment requiring transfer of electrical signals, energy, or fluids, through a chamber wall.
- Sealed equipment (liquid or controlled-gas content) requiring transfer of electrical signals, energy, or fluids, through a chamber wall.
- Microwave tube seals.
- High-temperature microwave windows.

These applications are beyond the scope of this chapter, which is focused on alumina/metal hermetic seals for bionic implants.

Bonding metals to glass hermetically is a simple fusion process, requiring thermal expansion matching. The big challenge in the mid-twentieth century was finding a way to bond metals hermetically to ceramics. For this, there are three main criteria:

(1) Thermal expansion matching of ceramic and metal.
(2) Selection of a suitable brazing alloy that is compatible with metal and ceramic and has a melting temperature neither too high for impracticality, nor too low for the end-use application.

(3) Metallizing, or in some other way, treating the ceramic surface so as to enable the braze to wet it and bond to it.

Research into ceramic–metal seals began in the 1930s, driven by the need for higher power, higher temperatures, and higher frequencies, conditions for which a metal/glass feedthrough is inadequate. A quantum leap forward in feedthrough technology was required: from glass-sealed systems to the next evolution—ceramic–metal bonding systems. In this evolution, the ceramic evolved to be alumina and the metal evolved to be Kovar. Copper is also relatively common in this role. Ceramics, especially alumina, have many advantages over glass. These include:

- Much higher temperature capability (glass is limited to a few hundred degrees Celsius).
- Alumina and ceramics in general are much mechanically stronger than glass.
- Alumina and ceramics in general are more thermal shock resistant than glass.
- Alumina and ceramics in general are less sensitive to flaws and stress concentrators than glass.
- Alumina specifically has much better electrical insulation than glass.
- Alumina specifically has a much better dielectric loss tangent than glass.

Some of the main demands placed on an alumina-metal joint include:

- Hermetic sealing as per the helium leak test.
- Ductile strain relief at the metal-ceramic interface.
- High-temperature strength.
- Corrosion resistance.

Three leading German electrical companies and one US company were the drivers of the early ceramic–metal feedthrough development: Siemens, AEG, and Telefunken from Germany, and General Electric in the USA. Notable early developments were the 1935 S patent of Vatter [14] and the 1939 General Electric patent of Pulfrich [15]. The first reference to the possibility of using alumina in a ceramic–metal hermetic seal came in the mid-1950s, with the patents of Nolte [16], originally filed in 1947, but not granted until 1954. In 1954, a key study laid the foundation for metal-ceramic bonding, defining seven methodologies that could be used [17]:

(1) Metal-ceramic bonding by sintering a metal oxide onto the surface of a ceramic and then reducing the oxide to a metal.
(2) Metal-ceramic bonding by sintering laminates comprising metal and ceramic powders in differing ratios (the functionally graded material approach).
(3) Metal-ceramic bonding by hot-pressing in a vacuum or inert atmosphere.
(4) Metal-ceramic bonding by utilizing active metals or metal alloys, or active metal hydrides.
(5) Metal-ceramic bonding by using glazes in an oxidizing atmosphere
(6) Metal-ceramic bonding by using a combination of glazes and metal powders in a reducing atmosphere.

(7) Metal-ceramic bonding utilizing refractory metal powders (such as molybdenum) with or without manganese (for continuity), nickel or copper (for build-up), and utilizing solder for the final bond.

Of this list, four remain niche applications, and three methods have risen to dominate alumina-metal bonding technology today:

- Method 4 (active brazing): The lynch-pin of bionic implants and commercialized much later.
- Method 5 (solder glass bonding): has continued to be important for regular applications, as it was in the pre-ceramic era. This method is sometimes referred to as brazing with glass.
- Method 7 (the Nolte molybdenum-manganese method): The first and the dominant commercialized process.

Of these three, active brazing has become the industry standard for the electrical feedthroughs of bionic implants, utilizing an alumina seal, and a titanium casing, actively brazed together.

10.1.2 The Bionic Feedthrough Defined

The Bionic feedthrough is one specific case of the very much older parent concept: the electrical feedthrough. The great leap forward of the bionic feedthrough is driven by the fact that biocompatibility and the warm, moist and corrosive, human body environment are not requirements for electrical-industry feedthroughs. Bionic feedthrough technology has grown rapidly in recent decades to be an industry of comparable magnitude in dollar value to its parent industry, electrical-industry feedthroughs. Biomedical alumina-based electrical feedthrough systems can be distinguished from non-biomedical systems by the following definitions:

Electrical-Industry Feedthroughs (Non-Biomedical)

- Ceramic feedthrough insulator: predominantly alumina or glass (amorphous glass commonly, sometimes glass ceramic): other ceramics have been used in the early days.
- Metal casing: various metals.
- Ceramic-casing bond: various metal brazes, or solder glass.
- Conductor wires: various metals, commonly Kovar or copper.

Bionic Feedthroughs (Biomedical)

- Ceramic feedthrough insulator: exclusively alumina.
- Metal casing: exclusively titanium.
- Ceramic–metal bond: titanium-based braze or gold-based braze.
- Conductor wires: titanium in the early days. In the twenty-first century, exclusively platinum or other noble metal alloys.

The alumina-feedthrough/titanium-canister concept is a biocompatible material combination that combines hermetic sealing with electrical signal feedthrough from the internal electronics to the exterior of the implant. This enables the connection of external leads, which terminate in neural tissue stimulating electrodes. The titanium/alumina implant itself (also known as the generator or the implantable pulse generator—IPG) enables isolation of the internal battery and microcircuitry from the corrosive fluids, ions, and gases of the body cavity.

The assumption is that a hermetic-bionic-implant, that utilizes the alumina/titanium feedthrough system, is hermetic for the lifetime of the device. Hermeticity is generally measured by the helium leak test according to the military standard MIL-STD-883.1014 (A1-A4) [13] or MIL-STD-750.1071 (H1 and H2) [18], which is based on the Howl-Mann equation [19]. Hermeticity requires a seal with a helium leakage rate of less than 10^{-9} cm^3 s^{-1}. Helium is the smallest molecule known and therefore its diffusion rate for permeating through a hermetic seal will exceed any in vitro moisture, gas, or ion.

10.1.3 Invention of the Hermetic Alumina/Titanium Bionic Feedthrough: Pacemaker (1970)

The invention of the alumina/titanium feedthrough in 1970 was the key enabling technology of the world's first modern (hermetic and durable for years in vivo) implantable bionic medical device: the Telectronics P10 cardiac pacemaker. All subsequent bionic implants globally, have used adaptations of the alumina/titanium feedthrough concept, which has evolved substantially in terms of the electrode density per square millimeter of alumina, and the associated device miniaturization. However, the basic platform technology of the alumina/titanium feedthrough of the 1970 P10 pacemaker, still dominates the bionic implant industry today, which has now grown to $25 billion per annum.

Author David Cowdery was the inventor of the alumina/titanium bionic feedthrough. In 1970 Cowdery, an electrical engineer with a background of five years of advanced welding research [20, 21], was recruited by pacemaker company Telectronics and tasked with developing a durable hermetic encapsulation system for pacemakers. He achieved this objective with a unique and innovative combination of alumina seal, titanium casing, and a titanium-based active braze. It was a paradigm shifting technology, from the old epoxy-clad pacemakers pre-1970. It was first used in the Telectronics P10 cardiac pacemaker, developed in 1970 and commercialized in 1971. This development is outlined in the following case study.

The fundamental principles underlying the 1970 alumina feedthrough invention are essentially the "ship in a bottle" concept, where the "ship" was the electronics and battery, the "bottle" was the titanium canister, and the "cork" was the alumina feedthrough. Key issues were:

- Biocompatibility of "bottle", "cork", and electrical terminal.

- Appropriate thermal expansion matching for "cork" and "bottle".
- Appropriate sealing (brazing) technology for the cork-bottle sealing interface,
- A system for passing an electrical conductor through the "cork" hermetically, to electrically stimulate the cardiac tissues, thereby enabling the electronics encapsulated inside the implant to electrically stimulate the tissues while remaining hermetically sealed from the fluids and gases of the body cavity.

10.1.3.1 The Alumina/Titanium Feedthrough Innovation

The schematic of the original alumina/titanium feedthrough system of the world's first hermetic pacemaker, the Telectronics P10, is shown in Fig. 10.2.

10.1.3.2 Alumina Ceramic

The first key innovation was the use of high-purity biocompatible alumina. The specific alumina used in the 1970 innovation was 95% pure high alumina. The first prototype alumina ceramics for the 1970 feedthrough prototype were made by Mr. Kay of the Ceramics Corporation, a company that specialized in porcelain.

The early alumina ceramics for the feedthrough were made by die pressing, which was problematic in that die wear life was poor, and the process produced unwanted die flashing. Telectronics then approached a company called Gallard and Robinson who made extruded ceramics, and production thereafter was by extrusion. The extruded alumina was also a high alumina 95% formulation. It contained a glassy phase, along with some TiO_2 to promote bonding with the titanium brazing alloy.

The alumina ceramic composition (known as A14 grade) was as follows:

- Al_2O_3: 95%
- Mg_2CO_3: 0.5%
- TiO_2: 1.66%
- MnO_2: 2.84%
- Grinding size: 3 microns.

This formula contained sufficient glassy phase and other components to lower the sintering temperature into the practical range for the available production equipment, without materially reducing its strength. With the closure of Gallard and Robinson some years later, Telectronics switched to in-house production.

As can be seen in the schematic of Fig. 10.2, the alumina ceramic was not brazed to the titanium terminal in the central hole in the alumina ceramic through which the terminal passed through the centre of the ceramic. Rather, the hole in the ceramic was slightly oversize, providing clearance between the alumina and the titanium terminal. All brazing was on the perimeter of the alumina ceramic, thereby enabling thermal expansion to do its work and shrink-fit the titanium around the alumina ceramic disk, to which it was brazed using the low-temperature TiCuNi brazing alloy. Thus, all the brazed bonding was on the outside of the ceramic and was designed to be a

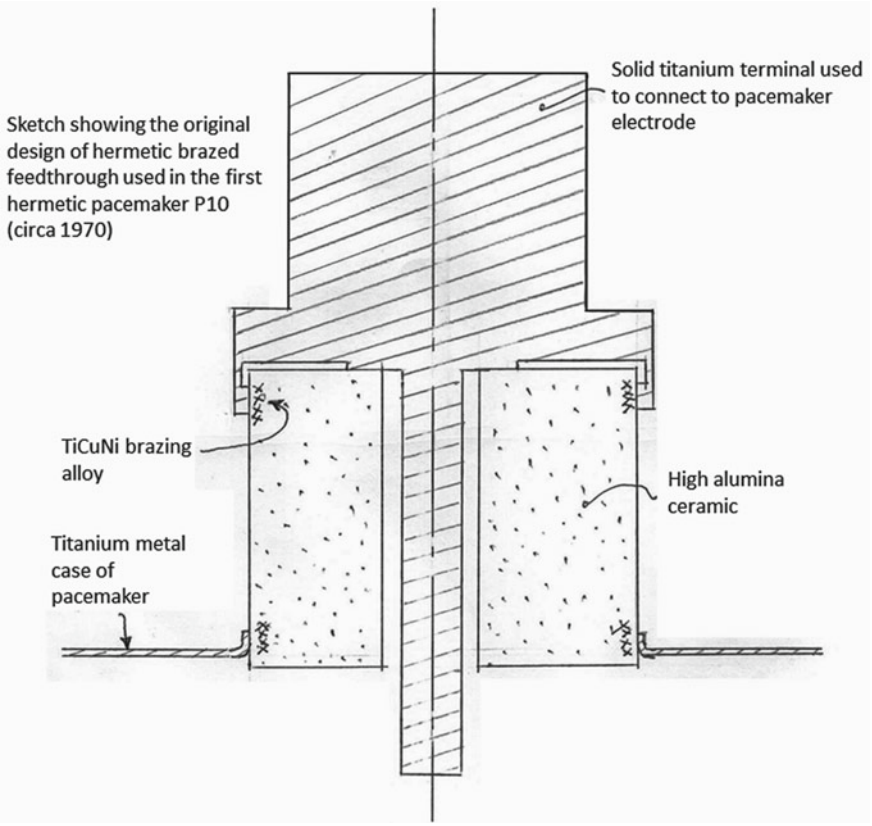

Fig. 10.2 Schematic of the original alumina/titanium feedthrough system of the world's first hermetic pacemaker, the Telectronics P10. The alumina cylinder is 9.6 mm in diameter, with a 2.3 mm hole, through which is passed a 1.5 mm titanium terminal. This electrical conductor feedthrough system can be seen on the top of the P10 pacemaker shown in Figs. 10.3 and 10.4. *Note 1* Flanged hole in the titanium metal case of the pacemaker where it mates with the bottom of the alumina cylinder, and the flange where the electrical conductor terminal mates with the top of the alumina cylinder. *Note 2* The brazing at each flange. All brazing is on the periphery of the alumina cylinder so as to utilize the residual thermal contraction of the titanium flange onto the alumina cylinder due to the slightly higher thermal expansion coefficient of the titanium

compression bond due to the appropriately matched thermal expansion coefficients of alumina and titanium.

High-purity alumina as the seal in the bionic feedthrough, brazed to a titanium casing, remains the industry standard for hermetic-bionic-implants today.

10.1.3.3 Titanium Casing

The second key innovation was the use of titanium as the casing, as it is highly biocompatible, corrosion resistant, and hermetic in the body for a lifetime. It is also a perfect thermal expansion match for alumina. In 1970, Telectronics was the first company in Australia to have titanium cases deep-drawn from titanium sheeting. This specialist titanium fabrication work, now routine in the manufacture of bionic implants today, was a significant breakthrough at the time, enabled by the services of GA and L Harrington at Padstow, New South Wales (NSW) in Australia, who produced two identical deep drawn half cases from titanium sheeting. The deep drawing process radically changes the shape of the sheet metal whilst maintaining approximately the original wall thickness of the case over its entire surface. Titanium casings remain the standard for hermetic-bionic-implants today.

10.1.3.4 The Titanium Electrical-Terminal Feedthrough System

The third key innovation was the use of a titanium terminal (this first hermetic pacemaker had a single feedthrough electrical terminal) that was fed through the center of the ceramic. The titanium terminal was brazed to the perimeter of the ceramic disk, thereby providing a hermetic seal for the cylindrical terminal segment that passed through the hole in the alumina ceramic, as shown in the sketch in Fig. 10.2. All the Telectronics pacemakers until 1996 used titanium conductors for the feedthrough electrodes. Niobium and noble metal conductors for the feedthrough electrodes gradually appeared in hermetic pacemaker feedthroughs globally from the late 1970s and platinum was introduced in the 1980s by Cochlear in its development of the world's first bionic ear [4]. Platinum, and its alloys has today become the standard for the conductor wires fed through the alumina in bionic implants, because platinum has slightly higher electrical conductivity than titanium, and platinum can be hermetically bonded directly to an alumina ceramic, by a process known as co-firing, opening up a range of possibilities [4].

However, in 1970, in the leap from epoxy encapsulation to alumina/titanium feedthrough technology, the use of platinum was not necessary for the pacemaker as only one feedthrough terminal of large cross-section was used for the pacemaker (the titanium canister itself was the reference electrode), unlike the 22 electrodes required for the next evolution, the Cochlear bionic ear. Since it was necessary for only a single terminal to be fed through in the pacemaker feedthrough, and it could be quite large in diameter, the metal used for the terminal therefore did not require such a high electrical conductivity as platinum, given its high cross-sectional area.

In fact, neither platinum (9.4×10^6 S/m) nor titanium (2.5×10^6 S/m) have particularly high electrical conductivity values compared to copper (59×10^6 S/m) or silver (62×10^6 S/m) [22]. Platinum is 3.75 times more conductive than titanium, but 6.6 times less conductive than silver. So, while platinum is an improvement over titanium in conductivity, it is by no means one of the best electrical conductors, but

rather the best combination of biocompatibility, corrosion resistance, and electrical conductivity of the proven biomaterials.

In respect of this combination of important criteria, titanium is certainly comparable to platinum. The electrical conductivity of platinum and titanium could be described as moderately high, while their biocompatibility and bioinertness is outstanding. However, when it comes to the ultra-fine platinum conductor microwire conductors, used in the twenty-first century leap forward in bionic implant feedthrough technology for the bionic eye retinal implant [4], the somewhat higher electrical conductivity of platinum does become important.

10.1.3.5 Biocompatible Brazing Technology

The fourth key innovation of the alumina/titanium hermetic feedthrough was the use of active brazing to seal the alumina to the titanium, i.e., to braze the alumina "cork" to the titanium "bottle". This was a very challenging task. The "ship" inside the bottle is sensitive electrical circuitry and battery, and the alumina "cork" needs to be brazed to the titanium "bottle", a process involving heat, which must not damage the sensitive electrical circuitry or battery inside. Author Cowdery's unique background as an electrical engineer with specialist welding research experience was an important factor in solving this challenging problem.

TiCuNi braze was used because it is a high titanium alloy with the lowest practical melting point of suitable titanium alloys. Both TiNi and TiCuNi were tested but the flow properties of TiCuNi were superior and the melting point of the TiCuNi alloy was slightly lower. Brazing temperature and time need to be minimized when brazing alumina to titanium so as to prevent recrystallization of the titanium canister and prevent titanium penetration of the alumina ceramic which can compromise the strength of the alumina. It was also necessary for the brazing alloy to be high in titanium for maximum corrosion resistance and biocompatibility. This is an "active braze", which is a braze capable of brazing (wetting and bonding) directly and simultaneously onto the metal and native ceramic surfaces, it does not require pre-metallization of the ceramic. An active braze contains metal components that chemically react with the ceramic. This generally means titanium, sometimes zirconium.

Gold brazing could have been used in this role, but Author Cowdery specifically avoided gold brazing due to the concern that prevailed at that time about the risk of gold sensitivity in patients. Today, gold brazing is commonly used with platinum and other noble metal feedthrough wires in alumina bionic feedthroughs. The alumina ceramic is pre-sputtered with gold, and then gold brazed to the electrical feedthrough wire. Gold sensitivity can be prevented through designs which prevent gold exposure to the body fluids. Gold brazing is commonly done with platinum feedthrough wires, but it would have been equally viable for the original Telectronics titanium terminal with its 1.5 mm terminal "wire" feedthrough. In many cases these days, platinum feedthrough conductor wires are directly sintered into the alumina ceramic feedthrough [4].

The titanium and alumina ceramic components (titanium casing, alumina disk, and titanium external terminal) were manufactured to tight tolerances. Brazing powder covered the outside diameter surface of the ceramic. The very small clearance between the titanium components and alumina disk was filled with molten braze and allowed to cool. During cooling, the small thermal expansion mismatch of titanium and alumina meant that the titanium components would shrink more than the alumina on cooling and compress onto the alumina, thereby enhancing the seal. The system was designed so that the compression was sufficient for a hermetic seal, and not so much as to risk failure of the ceramic.

The final stage, after cooling, was the removal by sandblasting of excess brazing on the ceramic, to eliminate a potential short-circuit between the exterior titanium terminal, and the titanium casing which was the reference electrode. This geometry can be seen in Fig. 10.2. In later evolutions of the technology, the surface of the exposed alumina disk was coated in silicone.

10.1.3.6 The World's First Hermetic Bionic Implant: Telectronics P10 Pacemaker

In the first commercial manifestation of this innovation, the Telectronics P10, the following dimensions applied (refer also to Fig. 10.2):

- Diameter of the hole in the alumina: 2.3 mm
- Diameter of the titanium terminal shaft passing through the alumina hole: 1.5 mm
- Peripheral clearance of the titanium terminal in the alumina hole: 0.4 mm
- Outside diameter of the alumina cylinder: 9.6 mm
- Length of the alumina cylinder: 7 mm.

The first prototype brazed alumina pacemaker feedthroughs were tested by the same thermal shock testing systems used for standard electrical components: boiling water and liquid nitrogen.

Subsequent to this prototyping work at the Amalgamated Wireless Valve company, Author Cowdery developed for Telectronics a novel alumina-ceramic/titanium-casing brazing system, and a controlled atmosphere welding machine that could produce clean welds in titanium without transmitting any damaging heat to the enclosed electronic circuits. This was one of the major challenges in the development of the alumina bionic feedthrough, and this developmental work has formed the platform technology for subsequent bionic implants to this day (Figs. 10.3, 10.4, 10.5 and 10.6).

10.1.3.7 Impact of the Telectronics P10 Pacemaker Quantum Leap

Author Cowdery's invention of the alumina/titanium hermetic bionic feedthrough triggered a global boom in the bionics industry. For the following three reasons:

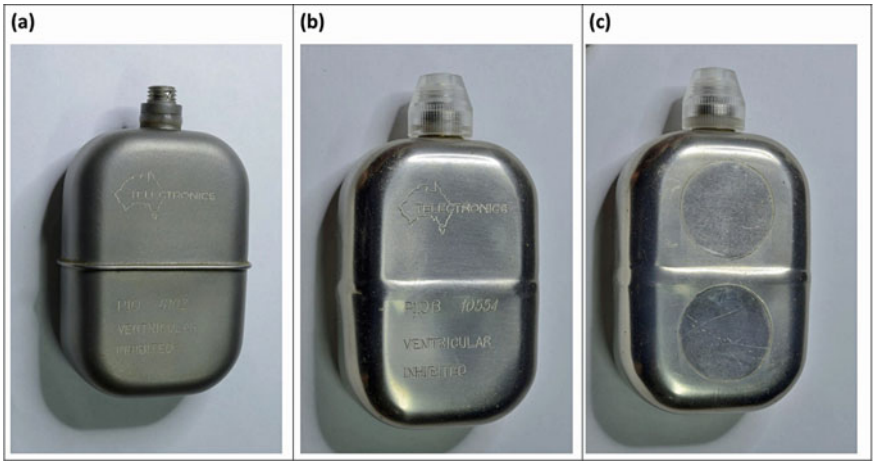

Fig. 10.3 **a** The Telectronics P10, the world's first hermetic pacemaker (1971). This is a single terminal unit; the case is the reference electrode. The terminal with alumina ceramic feedthrough is on the top of the titanium canister and is fitted with a silicon elastomer electrical sealing ring; **b** Later model of Telectronics P10 (circa 1975) with flush weld and silicone elastomer coating. Plastic sealing cap is fitted over the terminal; **c** 1975 version of P10 showing silicone elastomer coating (Images copyright David Cowdery, supplied courtesy of David Cowdery)

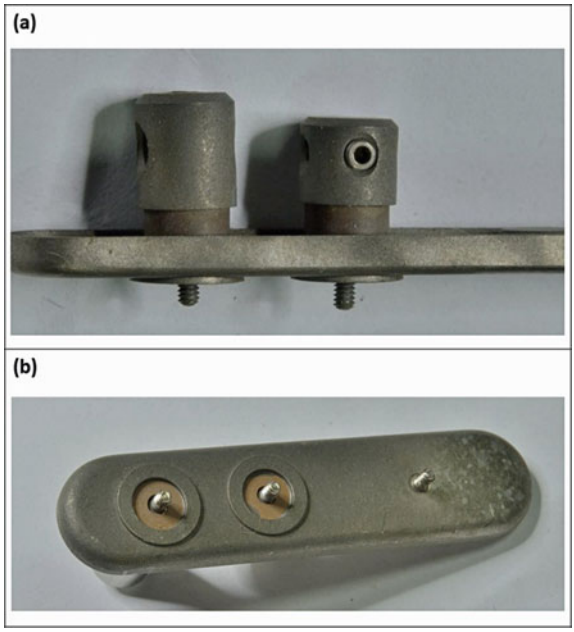

Fig. 10.4 **a** Later model of the Telectronics pacemaker terminal feedthrough assembly as brazed. This is for a smaller thinner pacemaker than the P10. It is about 9 mm thick; **b** The underside of the same terminal feedthrough assembly. The two titanium electrical terminals can clearly be seen exiting through the alumina ceramic on the left-hand end (Images copyright David Cowdery, supplied courtesy of David Cowdery)

Fig. 10.5 A later model Telectronics pacemaker (circa 1976) with a bare terminal assembly identical to that used on the first P10 (Image copyright David Cowdery, supplied courtesy of David Cowdery)

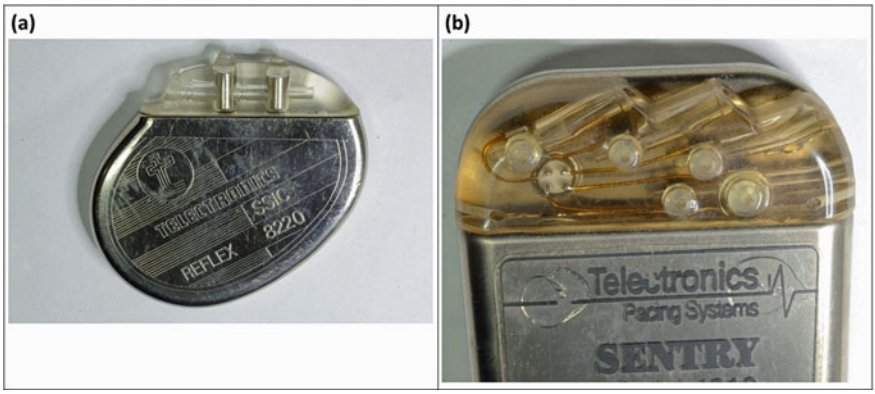

Fig. 10.6 **a** A more modern Telectronics pacemaker prototype (circa 1995) that is only 6 mm thick and similar to pacemakers available today; **b** The multiple terminal assembly for an advanced Telectronics defibrillator (circa 1996) that never went into manufacture (Images copyright David Cowdery, supplied courtesy of David Cowdery)

(1) **It was paradigm-shifting technology**: implantable pacemakers could now have a service life measured in years rather than months.
(2) **Huge global demand for pacemakers**: an abundance of desperate cardiac arrhythmia patients globally.
(3) **The invention was not patented**: this enabled rapid global dissemination of the technology by a global biotechnology community eager to commercialize pacemakers.

The result was that millions of arrhythmia patients globally have received a pacemaker in the last few decades. In 2021, about 2 million pacemakers are implanted a

year, a global market of around $12 billion [23]. Moreover, there are now 14 bionic implant technologies on the market today treating 25 disease states, encompassing a global $25 billion market in implantable bionics, all using the alumina/titanium feedthrough technology invented by author Cowdery.

Telectronics continued to use titanium conductors in their alumina right up to 1996 when the company was shut down and its technology sold to St Jude Medical. However, elsewhere, conductors of platinum and other noble metals, gradually became an industry norm for the more than 14 bionic implants in the world today.

10.1.3.8 Alternatives to Titanium

A titanium or niobium alloy provides the best thermal expansion match with alumina (Fig. 10.7). A process for bonding tantalum and niobium to alumina was developed by Elssner et al. [24] from within the electrical industry. This ultimately saw no significant commercial application in the electrical industry. However, the alumina/niobium bonding technology of Elssner et al. [24] was adapted by the newly established US pacemaker industry in the late 1970s, from which the world's second bionic pacemaker technology was launched in the late 1970s: alumina/niobium. A competitor for the alumina/titanium pacemaker feedthrough technology developed by Telectronics Australia in 1970.

While niobium is biocompatible, its mechanical property limitations are its Achilles heel. This was a problem in the 1970s when it was first trialed in bionic implants, and it remains a problem today [26]. Moreover, the thermal expansion of niobium (Fig. 10.7), is so close to alumina that niobium is incapable of placing the alumina in significant stable residual compression on cooling. This makes the seal more susceptible to leakage. In the 1970s, US pacemaker manufacturers experimented with gold-brazing of niobium to alumina. The softness and ductility of the gold, combined with the very close thermal expansion characteristics of alumina and niobium, resulted in minimal interfacial stresses. However, the design needs to be

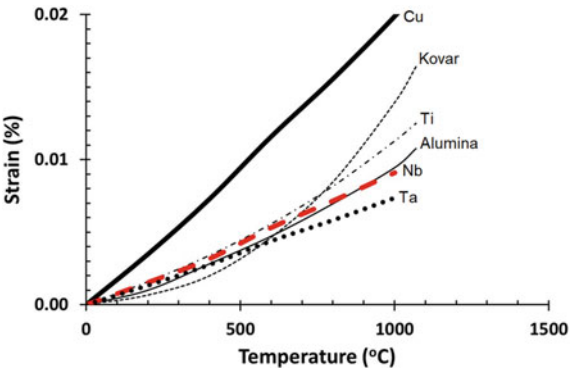

Fig. 10.7 Comparative dilatometry data for the two metals commonly bonded to alumina in electrical feedthroughs (Kovar and Copper), as well as the three native metals with the closest thermal expansion match with alumina: titanium, tantalum, and niobium [25]

made in such a way that body fluids are not exposed to gold due to the hazard of gold sensitivity.

Thus, while niobium can be made to work, it is not well suited to the role and never proved to be as successful as titanium in alumina-metal seals. Ultimately the alumina/niobium technology was supplanted globally by the alumina/titanium technology. Titanium on the other hand has an outstanding combination of excellent mechanical properties, and excellent biocompatibility, with over half a century track record of proven performance in orthopedics, bionics, dentistry, and other implantable medical devices.

Alumina/stainless steel, alumina/platinum, and alumina/niobium bonding systems have all been explored. However, the only lasting materials innovation since 1980 has been the introduction of platinum conductors, originally by Cochlear Ltd for the bionic ear in the early 1980s. Platinum is now dominant in this role, as discussed in the next section.

10.1.4 Co-fired Titanium/Alumina-Platinum Feedthrough: The Bionic Ear (1985)

In the early 1980s, Telectronics became the parent company to bionic ear innovator Graeme Clark and his team, during the formative stages of Cochlear Ltd. Cochlear has been the world leader since the 1980s in bionic ear technology and remains so today. In the early 1980s, Telectronics was a large and thriving pacemaker company possessing advanced in-house hermetic encapsulation technology for bionic implants (pacemakers), and therefore were the world leaders in the manufacturing infrastructure and engineering expertise required for developing a hermetic encapsulation system for a bionic ear implant. Thus, Telectronics gave the Cochlear Ltd. team a significant head start over the global competition in bionic ear hermetic encapsulation development. All that was required was to adapt the Telectronics pacemaker feedthrough technology to the bionic ear requirements, rather than the much more challenging task faced by their global bionic ear competitors, of developing this from scratch.

The bionic ear required 22 electrodes (the P10 pacemaker had one electrode) and so a quantum leap in alumina feedthrough technology was required, which came in the year 1982 with the adaptation of the Telectronics alumina/titanium bionic feedthrough technology to the 22-electrode bionic ear feedthrough, by Janusz Kuzma, with the support of author Cowdery and other Telectronics personnel. This involved a co-fired titanium/alumina-platinum feedthrough. Fortuitously, alumina offers the capacity to be co-sintered with platinum forming a solid-state diffusion bond, which was essential for the evolution of high electrode-number feedthroughs of the 1982 Cochlear feedthrough. Essentially the Cochlear feedthrough innovation involved the following developments:

Fig. 10.8 First Cochlear feedthrough with titanium flange before welding to the titanium case that housed the electronic circuitry (Image copyright David Cowdery, supplied courtesy of David Cowdery)

- Small platinum tubes were placed in the green alumina in closely fitting holes. Tubes were used rather than solid wires to prevent tensile cracking of the alumina during firing. This is shown in Fig. 10.8.
- Holes were created in the unfired green ceramic and the platinum tubes were placed into these 22 holes.
- The tubes were polished, so they became flush with the alumina surface after firing.
- When the alumina was fired, the large diametral firing shrinkage of the alumina caused the soft platinum tubes to form a tight seal without the need for any brazing material. The finished diameter of the platinum tubes was about 1.2 mm OD × 0.6 mm ID.
- This process is known as alumina-platinum co-firing, i.e., placing the platinum into the green alumina and sintering it in, using the heat, the glass formation, and the diametral shrinkage to create a hermetic seal by two physical mechanisms: (1) platinum-alumina solid-state diffusion bonding, and (2) platinum-glass-alumina bonding.
- The alumina disc containing the platinum tubes was very different in dimensions to the Telectronics feedthrough. It was 14.5 mm in diameter and 1.5 mm thick. This was necessary because the Cochlear implant needed to be as slim as possible.
- The slim ceramic disk with the 22 platinum tubes co-fired into it was then brazed around its circumference to a round titanium casing. This is shown in Fig. 10.8.
- Final hermetic closure was achieved using similar welding procedures as used on the Telectronics pacemakers.
- The platinum tubes were finally sealed by soldering wires into the hollow tubes at one end.
- The 25-micron platinum micro-electrodes were attached to the platinum tube terminals at the “electrode side” of the feedthrough (the external implantable-electrode connection side), and the internal electronics attached at the “micro-electronics side” of the feedthrough (the internal microelectronics side).

Fig. 10.9 The electrode side of the first Cochlear feedthrough with polyimide insulator and parylene-coated platinum electrode wires soldered into the platinum tubes (Image copyright David Cowdery, supplied courtesy of David Cowdery)

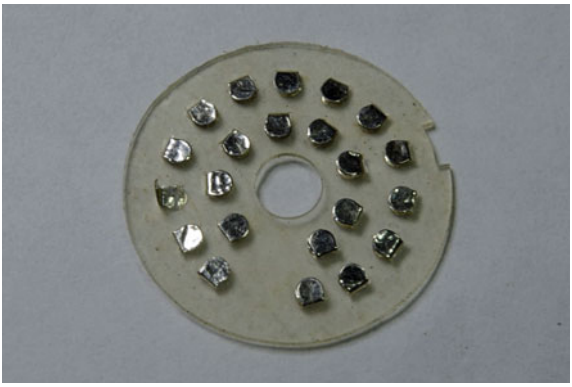

Fig. 10.10 Silicone-mounted platinum strips for contacting the 22 platinum tubes on the first Cochlear feedthrough (Image copyright David Cowdery, supplied courtesy of David Cowdery)

The other end was connected electrically by an array of spring-loaded platinum contacts set in a sheet of silicone elastomer (Figs. 10.9 and 10.10).

10.1.4.1 Alumina-Platinum Co-firing

The feedthrough developed for the first bionic ear was the world's first co-fired titanium/alumina-platinum hermetic feedthrough system. This is the concept on which all subsequent bionic implants are based, to this day. Conceptually it is shown in Fig. 10.11. It was the next evolution from the original titanium/alumina feedthrough developed by author Cowdery in 1970. It uses the same original concept of the titanium casing brazed to an alumina seal. The evolutionary step is the use of platinum conductor tubes that are sealed to the alumina seal by direct sintering, i.e., by co-firing. So the key enhancement depends on the concept of platinum-alumina cofiring, and the diffusion bond developed. Platinum is a biocompatible, chemically inert, and highly oxidation resistant metal, and alumina a highly biocompatible, chemically inert, impervious ceramic. They make a perfect combination, provided that

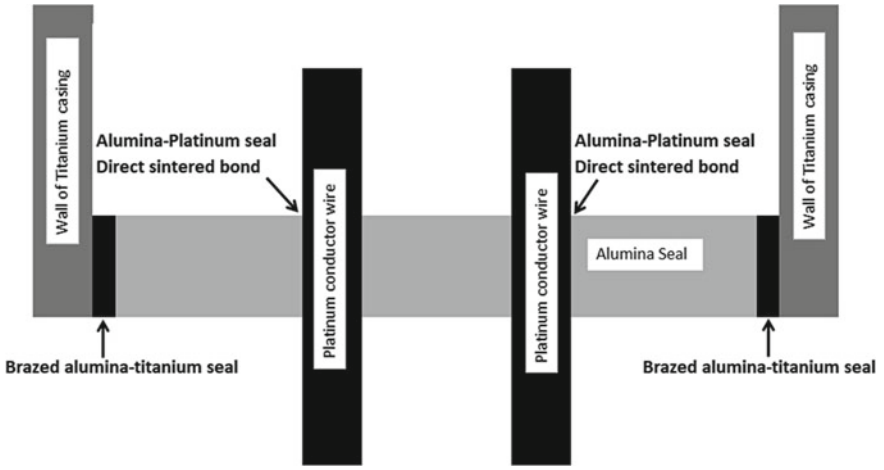

Fig. 10.11 The concept of the co-fired titanium/alumina-platinum hermetic feedthrough system of the bionic ear implant, and the concept on which all subsequent bionic implants were based, to this day. Its evolution from its original ancestral concept, the glass/Kovar lightbulb feedthrough, can be seen by comparison to Fig. 10.1

a hermetic seal can be formed between alumina and titanium by diffusion bonding during sintering. At the time of the Cochlear innovation, this was highly experimental science, with very little documentary guidance to be found in the literature.

The first report of alumina-platinum bonding was in 1977, which documented pressure-assisted alumina-platinum bonding experiments using 25 micron platinum foil pressed at 100 kPa between 12.5 mm thick pre-sintered (1500 °C) alumina disks up to a temperature of 1055 °C, and suggested that theoretically this could be viable up to 100 °C below the metal melting point (platinum melts at 1769 °C) [27]. This is significantly different from what Janusz Kuzma of Cochlear did. Kuzma used green alumina, pressureless sintering, and a temperature more than 500 °C higher than the reported 1055 °C, and his alumina was in the form of thick-walled tubes, not foil. Nonetheless, the 1977 pressure-assisted platinum-alumina bonding experiments suggested that a solid-state alumina-platinum bond could form, and the fact that there were probably no unexpected Al–Pt–O binary or ternary phases or Al–Pt–O volatilization products produced that could have made such an approach impossible [27]. Therefore, though the de Bruin's work [27] was of little relevance to Kuzma's co-firing methodology, its chief value was in the phase equilibria deductions one could make from it, deductions that might have given Kuzma reassurance, from a phase equilibrium point of view, that he was on safe ground with his co-firing strategy.

Kuzma was otherwise flying blind in that there were no published binary or ternary phase diagrams in the Al–Pt–O system in 1982. The literature contains no published Al–Pt–O ternary phase diagram to date. The Al-Pt binary phase diagram was published in 1985 [28] and the Al–O binary phase diagram was also published

in 1985, by different authors [29]. These two binary phase diagrams came too late for Kuzma. Moreover, there is nothing further in the literature on platinum-alumina bonding after 1977 until 1983, when more pressure-assisted presintered-alumina/platinum-foil experiments were published [30]. These went into much more detail than the 1977 work [27], exploring bonding temperature, bonding pressure, and their effects on bonding strength, and reporting that an optimal bond was achieved at 1700 °C for 10 h at 2 MPa pressure. Again, this was pressure-assisted bonding of pre-sintered alumina, not co-firing, and therefore of only peripheral relevance to Kuzma's co-firing methodology, other than the phase equilibria deductions one could make from it.

Finally, the 1977 study involved high-purity alumina [27]. Kuzma was using 96% alumina with a significant glassy component. Glass-platinum interactions could have proven problematic indeed. Fortuitously, as it turned out, the glass helped rather than hindered.

The second important question to explore is the thermal expansion issue. A thermal expansion appraisal shows that Kuzma was very fortunate that his platinum-tube/alumina co-fired feedthrough was hermetic. The thermal expansion coefficients of the respective materials are [31]:

- Alumina: 8.1 μ/mK
- Titanium: 8.5 μ/mK
- Platinum 9.0 μ/mK.

Of course, dilatometry curves show that thermal expansion coefficients are not necessarily linear with temperature and therefore the thermal expansion coefficients quoted here are indicative of probable mismatch only, not a quantitative indication over the entire co-fired temperature range of 20–1500 °C. Nonetheless, the following analysis based on these thermal expansion coefficients demonstrates the potential problem.

In the case of linear thermal expansion coefficients over the entire sintering range, an internal platinum tube would theoretically shrink away from alumina on cooling, as calculated below:

- 14.5 mm alumina disk
- 1200 micron OD 600 micron ID platinum tube
- 25 micron platinum electrode soldered in.

Cooling from 1500 °C, across a 1200 micron span, alumina will contract:

- $8.1\ \mu/\text{mK} \times 1500\ \text{K} \times 1.2 \times 10^{-3}\ \text{m} = \underline{14.6\ \mu\text{m}}$.

Cooling from 1500 °C, across a 1200 micron span, platinum will contract:

- $9.0\ \mu/\text{mK}$ x $1500\ \text{K} \times 1.2 \times 10^{-3}\ \text{m} = \underline{16.2\ \mu\text{m}}$.

From the calculations above, we can see that the differential diametral contraction is 1.6 μm (16.2–14.6 μm), corresponding to a 800 nm (0.8 μm) radial clearance between the 1.2 mm platinum tube outer wall and the inner wall of the hole in the alumina.

Given that the grain size of the alumina is in the order of a micron (1000 nm), 800 nm is a significant amount in the context of the alumina-platinum interface and could potentially be sufficient to break the hermetic seal sufficient for helium permeation in the helium leak test, and for water/gas/ion diffusion in vivo. However, history shows that it did work. Kuzma delivered a functional feedthrough. This thermal expansion problem arose again to a more serious extent with the development of alumina retinal implants containing hundreds of co-fired embedded platinum electrode "microwires". An innovative hot-pressing solution was developed by bionic eye feedthrough innovator Gregg Suaning, in collaboration with Thomas Guenther, author Ruys, and others [32], as discussed in the next section.

In retrospect, the 1981/1982 development of the bionic ear commercial implant was an extraordinary achievement, producing, in just 18 months, a titanium-encapsulated hermetic 22-electrode bionic ear with alumina feedthrough, and complex computing power for a portable external speech processor for 22 electrodes of auditory output in real time. All in all, an incredible challenge for the early 1980s. Moreover, this device needed to be miniaturized more than had been achieved for the contemporary pacemaker, since the bionic ear IPG implant needed to be located beneath the scalp near the ear, and there was a strong imperative, for obvious cosmetic reasons, for it to be as slim as possible, so as not to have an unsightly bulge under the scalp.

This rapid development was made possible by a number of reasons. Firstly, the bionic ear initiative was managed by Telectronics/Nucleus. Thus, the now prosperous global pacemaker company Telectronics, as it had become a decade after the launch of the world's first hermetic pacemaker the P10, became the big brother to the fledgling bionic ear company Cochlear. This provided financial resources, technological/intellectual resources, and Telectronics "know-how" in bionics manufacture and design.

Secondly, the alumina feedthrough headstart. One of the most challenging aspects of developing the Cochlear implant was developing an alumina feedthrough with 22 electrodes, i.e., 22 independent platinum conductor "wires" passing through the alumina. Moreover, the alumina feedthrough disk needed to be as slim as possible. The importance of the headstart the bionic ear team received in having the viable, proven, and optimized Telectronics feedthrough technology as a starting point was a factor that proved very important in solving the Cochlear feedthrough challenge in such a short time. Furthermore, Janusz Kuzma was an engineer with a strong background in hermetically-sealed packaging from working in the semiconductor industry in Europe. He was the right man for the job.

Thirdly, the recent invention of the microprocessor made complex speech processing possible, for the first time, in a miniaturized speech processor device that was worn externally. Nonetheless, it was a major challenge to develop and perfect this in the time, and it is a testament to the strength of the electrical and computing expertise in the Cochlear team, led by Jim Patrick since 1975, that they succeeded in the time available, and with the microprocessor technology then available.

Finally, the problem of batteries was a major potential roadblock. With such device miniaturization required, and limited battery miniaturization technology available in

that era, a novel solution was called for. This novel solution was inductive powering. The microprocessor/microphone/battery external device mounted on the ear was inductively coupled to the Cochlear implant, which resided beneath the scalp near the ear. This solved the battery problem and the implant miniaturization problem in one elegant solution.

10.1.4.2 Impact of the Bionic Ear Alumina Feedthrough

The obvious impact of the Cochlear Implant feedthrough innovation is that it was an enabling technology that has brought hearing to hundreds of thousands of profoundly deaf patients over the last four decades.

However, its impact was more wide-reaching. Today, the 14 bionic implants on the market, as summarized at the start of this chapter, generally utilize many platinum electrodes in their alumina feedthroughs and utilize the exact same platform technology as developed for the Cochlear bionic ear: co-fired titanium/alumina-platinum feedthroughs brazed into a titanium casing.

10.1.5 Thick-Film Alumina/Titanium-Platinum Feedthroughs: Bionic Eye (2012)

In the last decade, the third quantum leap in alumina bionic feedthrough technology was achieved. Pioneered by Gregg Suaning [32], this involved the adaptation of thick-film technology to producing co-fired titanium/alumina-platinum mini-feedthroughs for the bionic eye, containing hundreds of platinum electrodes in an alumina feedthrough, which was in the order of a centimeter in diameter, small enough to be able to be implanted directly behind the retina.

In this advanced version of co-fired alumina-platinum bionic feedthrough technology, hundreds of exposed platinum electrode pads, embedded within the thin alumina disk of a miniature alumina feedthrough, directly stimulate the retinal tissue of the eye in an array (Fig. 10.12). The stimulation is achieved from input via an external camera, commonly affixed to a pair of glasses. In this way, the resolution limit of the bionic eye directly correlates to the electrode-density of the platinum microwire electrodes embedded in the alumina feedthrough.

This innovation culminated in a record-breaking electrode density: 1145 electrodes in a 7 mm diameter alumina-platinum co-fired bionic eye feedthrough of 2012, a development in which Author Ruys was involved, in collaboration with Gregg Suaning, Thomas Guenther, and a number of other participants [32]. This quantum leap was necessary because, while tens of electrodes are sufficient for a bionic ear and most of the other bionic implants on the market today, a bionic eye needs hundreds, preferably thousands of electrodes, as is demonstrated in Fig. 10.13.

Fig. 10.12 Co-fired alumina-platinum feedthrough with the record-breaking 1145 electrodes [32]. This was achieved in a diameter of just 7 mm, as shown by the millimeter scale (Image copyright Andrew Ruys, supplied courtesy of Andrew Ruys)

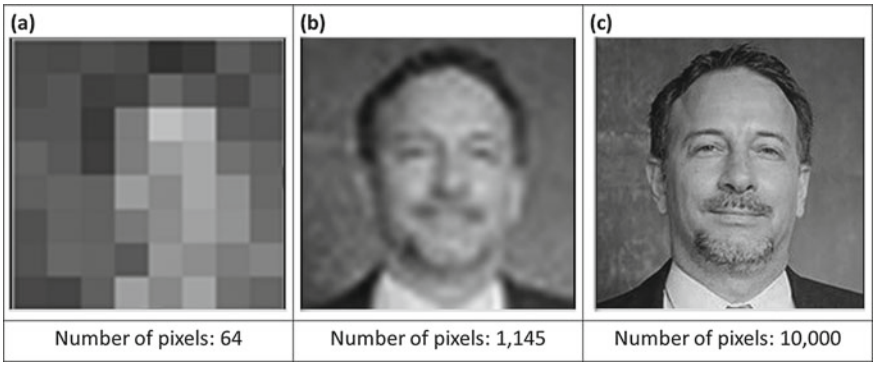

Fig. 10.13 Electrode number (pixel number) and resolution for a bionic eye feedthrough, demonstrated with three images of author Ruys. **a** Shown at the resolution of the electrode density of the feedthrough of the world's first commercial bionic eye (Argus II FDA approved 2012) with 60 pixels, which is only useful for discerning light from dark, and movement of large objects. **b** Shown at the resolution of the highest electrode-density co-fired alumina-platinum feedthrough yet achieved for a retinal implant (1,145 electrodes), by the Suaning group in 2012 [32]. Prototyped, but not yet commercialized, a bionic eye with this electrode-density is sufficient to recognize a human face. **c** A resolution of 10,000 of pixels, as seen by a healthy human eye

Essentially there are five aspects to this quantum leap of Suaning, which work in combination [32, 33]:

(1) The **concept of the stepped feedthrough pathway** taken by the printed platinum "microwires", through the alumina feedthrough from the front face (retinal side) to the rear face (microchip side). This overcomes the problem of platinum/alumina thermal expansion mismatch, and its potentially negative impact on hermeticity.
(2) The **use of hot-pressing** to ensure 100% hermeticity of the stepped feedthrough pathways of the printed platinum "microwires".
(3) **Thick-film manufacturing process** involving printing the platinum electrodes into the alumina via tape-casting, laser micromachining, screen printing, and hot-pressing.
(4) **Mounting of the alumina-platinum co-fired feedthrough disk in a titanium casing**, by brazing, to produce a hermetic implant, with sensitive internal microelectronics, as a single miniaturised implant that can be implanted directly behind the retinal tissue of the eye.
(5) **External camera and battery which transmits electrical power and live image feed** via an inductive coupling through the tissue of the scalp, using the same principle developed by Cochlear for the bionic ear in the early 1980s. The camera and battery are typically mounted on a pair of externally-worn glasses.

In addition to enabling vast numbers of electrodes in a small alumina feedthrough, this thick film approach has other advantages. Chief among them is enhanced hermeticity through hot pressing. Also, it is possible to align the electrodes to the microprocessor chip, on the internal "microchip side" of the feedthrough.

The thick-film manufacturing process for the alumina-platinum mini-feedthroughs is described in detail in publications by the Suaning team, and is briefly summarized below [32, 33]:

(1) **Alumina composition**: A powdered 96% pure alumina was used containing 2 wt% SiO_2, 0.5 wt% MgO, 0.25 wt% CaO, and other trace additives.
(2) **Tape-casting the powdered alumina**: A tape casting slurry was prepared by mixing the alumina powder with a proprietary wax binder. Tape thickness was 200 microns.
(3) **Designing the electrode array**: AutoCAD was used to design the stepped platinum pathway, and surface platinum electrode pads, for the electrode array, such that retinal-stimulating electrode positions on the external surface of the alumina feedthrough (retinal side) corresponded appropriately to the microchip terminals on the "microchip-side" of the alumina feedthrough. The design was saved as a dxf file, which could be read by the laser-patterning machine.
(4) **Laser machining**: The alumina tapes were cut into 20 × 20 mm pieces, attached to a microscope slide using adhesive cellotape, so as to enable precise alignment in the laser machining unit. Each tape had precision holes laser ablated in the 200 micron thick alumina tape, which were subsequently filled with platinum paste by screen printing.

(5) **Preparing the platinum screen-printing paste**: A platinum paste was prepared using the same proprietary wax binder that was used to prepare tape casting slurries of the powdered alumina.

(6) **Preparing the platinum paste-printing stencil**: A screen-printing stencil was prepared from 50 micron thick stainless steel foil with a hole cut into it of a diameter matching the desired feedthrough and thickness matching the desired microwire and electrode pad dimensions.

(7) **Paste printing the powdered platinum**: A stainless steel stencil was placed on top of the laser-machined alumina tape, and the platinum paste was screen printed onto it using a rubber squeegee. The result was platinum-filled holes in the alumina tape, and a thin surface layer of platinum paste on the surface of the alumina tape. The platinum paste was then dried for 15 min at 130 °C. The surface paste, and the paste in the hole, corresponded to the lateral and vertical pathways, respectively, of a microwire through that alumina laminate, and were laser machined accordingly.

The result was a 200 micron thick alumina tape, with embedded platinum, that aligned with exposed platinum on its top surface, patterned in accordance with the AutoCAD feedthrough design file. A feedthrough needed a minimum of two layers, and in most cases more than two layers, typically around five layers.

Steps 4 to 7 were therefore repeated to create duplicate layers.

(8) **Aligning the layers**: The laminates were stacked on top of each other in the correct sequence, and precision-aligned, using a proprietary micron-precision alignment system.

(9) **Lamination by warm-pressing**: The stack of aligned layers was warm-pressed at 80 °C and 50 MPa, in a hot press which melted the proprietary wax binder and fused the assembly into a coherent laminate.

(10) **Co-firing**: The laminate was sintered at 1500 °C.

Using this advanced thick-film forming process, it was possible to manufacture platinum electrode "wires" with a minimum width of 20 microns, and a minimum centre to centre distance of 40 microns [33], giving a maximum theoretical electrode density of 2500/cm^2 [32]. Figure 10.13 shows an alumina-platinum feedthrough disk for a bionic eye implant produced by this method, with the highest yet reported number of electrodes: 1145 in a diameter of just 7 mm [32]. This was not just a quantum leap forward from Kuzma of 1982 (13 electrodes/cm^2), but also three times higher than the nearest competitor, Schuettler et al. [34], who in 2010 reported a feedthrough with 360 electrodes.

Cell culture testing using neural cells has validated that the feedthrough itself, and all the materials used to produce the feedthrough (as listed above) did not impact on the cell growth and survival properties [33]. It is important to note here that while alumina implants have been used in dentistry, orthopedics, and bionics for half a century, this retinal implant in which the alumina/platinum feedthrough surface is in direct contact with the neural tissue (rather than silicone-platinum as for the bionic ear

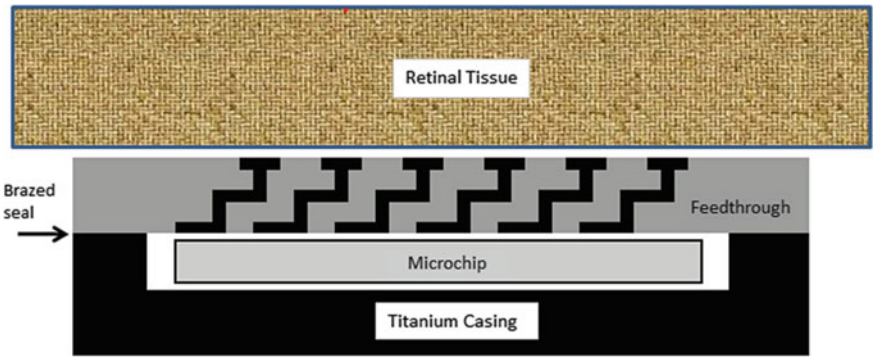

Fig. 10.14 Schematic of the bionic eye implant. The alumina-platinum co-fired feedthrough, is shown in this schematic as a two-layer laminate with two steps, with its exposed platinum electrode pads directly stimulating the retinal tissue. The feedthrough is brazed to a titanium casing. The exposed platinum electrode pads of the feedthrough on the "microchip-side" are directly stimulated by the microchip terminals. In practice, the feedthroughs typically contained about five laminates with five steps, so as to maximize hermeticity

and other bionic implants) is a relatively unique case of an alumina-platinum/neural-tissue direct-neurostimulation system. However, given alumina's outstanding reputation as the most bioinert and biocompatible material in established clinical usage, and the long-proven biocompatibility of platinum with 35 years clinical use in direct platinum/neural-tissue contact for the bionic ear, this biocompatibility is unsurprising (Fig. 10.14).

10.1.6 The Future for Alumina in Bionics

It seems probable that the 14 bionic implant types on the market today, with their hermetic titanium/alumina-platinum packaging systems, and their high-electrode-number capabilities, all have a long and successful future for many decades ahead, and that many more disease-states may become treatable by the existing bionic implants. Moreover, it is likely that more bionic implants for new commercial neural tissue applications that may currently be a research topic, or not yet imagined, will come onto the market in due course using the same trusted, safe and proven titanium/alumina-platinum hermetic feedthrough systems. The most obvious new application on the horizon is the brain computer interface (BCI).

10.1.6.1 The Implantable BCI (Brain-Computer-Interface)

The most futuristic bionic implant technologies today are the brain-computer interface (BCI) multi-pin implants, which currently are purely for experimental use by

direct implantation into the cerebral cortex (top surface of the brain) by an open craniotomy. The small sharp pins penetrate brain tissue, and there is some associated risk of inflammatory response, a risk that could potentially outweigh the benefits in some cases. They do not have a titanium/alumina hermetic long-term stable encapsulation system at this stage, as the BCI is highly experimental technology. For long-term implantation, a hermetic durable and biocompatible encapsulation system would be needed, and the tried and proven gold standard of the last half century:

(a) Titanium/alumina-platinum hermetic-implantable bionic system, perhaps with the gentler electrode system of the retinal implant (platinum electrode pads flush with the surface of an alumina feedthrough).
(b) Information and power transfer via inductive coupling across the scalp.

This would be a wise, low-risk approach to take for commercial clinical applications of BCI implants. Whether this is how the future develops is beyond our current event horizon, but it seems a sensible strategy to explore.

Connecting the brain to the computer is not a new idea; the earliest BCI (brain computer interface) study was in 1929 when Hans Berger discovered Electroencephalography (EEG) a recording of the electrical activity along the scalp [35]. This was done using cutaneous scalp electrodes (adhesive to skin), still a common procedure, which suffers from a high signal to noise ratio due to the electrical impedance of the skull and scalp. However, with the development of the advanced computer and its wide availability since the late twentieth century, the number of BCI studies began to increase in the early 1990s, and increased dramatically from about 2003 as shown by a PubMed analysis of the field shown in Fig. 10.15.

This 2003 date coincides surprisingly closely with the filing by Brown University in 2002 of a paradigm-shifting patent on a BCI cerebral cortex implant, which was granted in 2007 [36]. In 2012, a ground-breaking paper was published in the

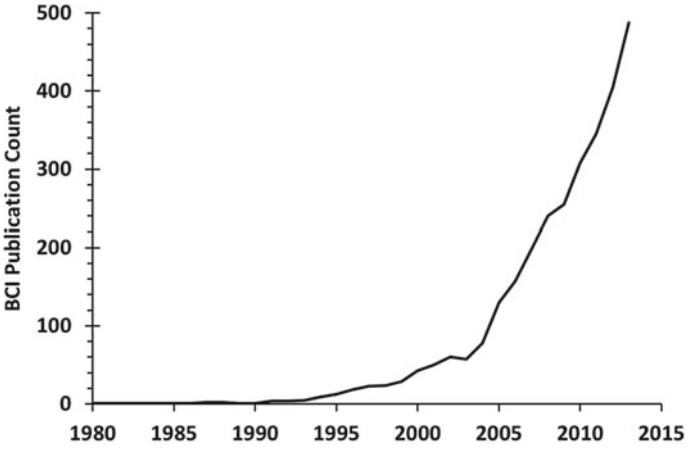

Fig. 10.15 A PubMed analysis of brain computer interface (BCI) studies published since 1980

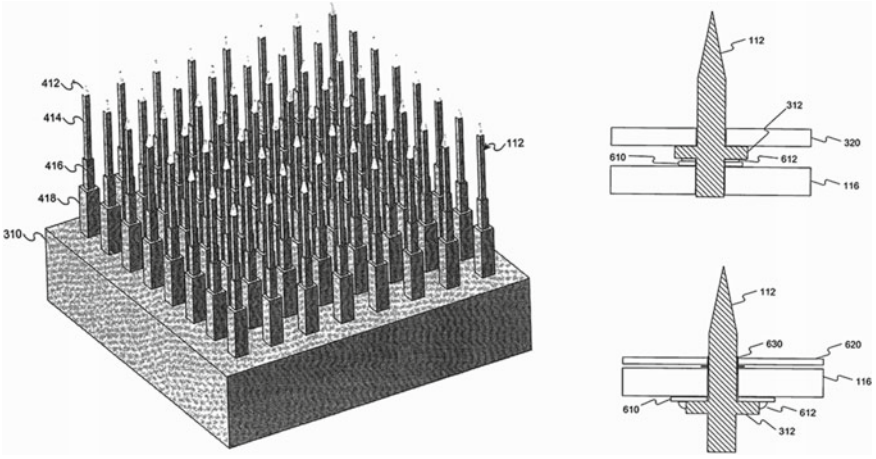

Fig. 10.16 The BrainGate™ cortical implant, from the original patent by the BrainGate™ pioneers at Brown University USA, filed in 2002 and granted in 2007 [36]

journal Nature [37] by the same Brown University team, on success with BCI-driven thought-controlled robotics for paralyzed patients using the patented BCI implant device (called BrainGate™) [36]. Two paralyzed patients fitted with a brain-computer-interface implant successfully used thought-control to move a robotic arm in a meaningful way. One of them famously, and on camera,[2] picked up a bottle with the robotic arm to drink from it [37].

Figure 10.16 shows the schematic of the BCI implant, much like the one implanted, which was a 4 mm × 4 mm 96-electrode microelectrode array, with the pin electrode system. The figure also shows an illustration of one of the actual implant pins. Figure 10.17 shows the implantation site of the cerebral cortex. Figure 10.18 shows a dummy with the BCI driver coupled to the BCI, which can then be connected to the robotic arm.

There are of course many other potential applications for the BCI, Theoretically, such technology could be used to drive an exoskeleton, for example by a tetraplegic patient. Sufferers of advanced motor neurone disease such as the late Stephen Hawking, and sufferers of other such degenerative conditions, would benefit greatly from such technology. Such a multi-tasking activity might require multiple BCI implants for the different motor regions of the cerebral cortex, and extensive brain/machine training. There are also other non-motor applications potentially possible with a BCI, such as synthetic telepathy (transmitting thoughts via a BCI implant), using a BCI for implantation of memories directly into the brain of a recipient, and BCI implants for the visual cortex as a futuristic solution to visual impairment. The future possibilities for the BCI are potentially revolutionary.

[2] Paralysed woman moves robot with her mind—by Nature Video. https://www.youtube.com/watch?v=ogBX18maUiM&t=0s.

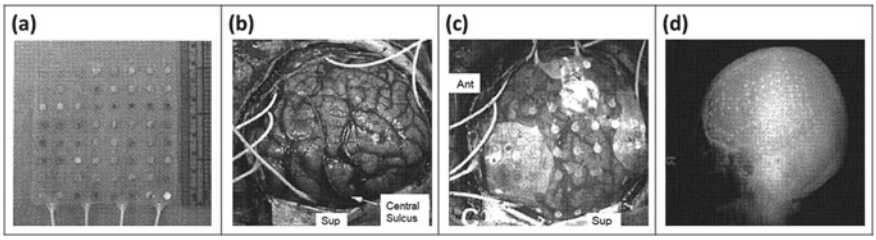

Fig. 10.17 Electrocorticography, recording the electrical activity of the cerebral cortex by means of electrodes placed directly on it, beneath the skull: **a** is the electrode grid to be implanted; **b** shows the exposed cortical surface of the brain of a human patient with epilepsy, before placement of the electrode grid; **c** shows the placement of the electrode grid on the exposed cortical surface of the brain of the patient. For orientation purposes, the reference "Ant" refers to the anterior (front) of the subject's brain. **d** Is an X-ray of the patient's skull from one side, showing the electrode grid in place after surgery. From the Washington University BCI patent of Leuthardt [38]

Fig. 10.18 Dummy unit illustrating the design of the BrainGate™ interface. The BrainGate™ implant in the cerebral cortex (top surface of the brain) interfaces with the robotic arm via the external device shown here (*Image Author* Paul Wicks). Reproduced from Wikipedia (Public Domain Image Library)

BCI visual cortex research is very new and highly experimental technology, and it is difficult to forecast at this stage whether such bionic implants would restore sight at all, and if so whether they would be an improvement over the current and proven technology of retinal implants. Again, how the future develops is beyond our current event horizon, but it appears that interesting times lie ahead.

While experimental short-term BCI prototypes have not necessarily involved alumina feedthrough systems (as indeed experimental prototypes of the bionic ear and bionic eye did not), long-term BCI implants will depend on alumina feedthroughs, and probably also inductive coupling systems for transcutaneous power and information transfer, such as those used in the bionic ear and bionic eye. Moreover, rather

than the invasive pin-electrode technology (penetrating neural tissue) of the experimental BCI implants, long-term BCI implants are likely to use the non-invasive high-electrode-density "electrode pad" technology (surface contact with neural tissue) outlined in the previous section.

In the coming decades, it is likely that we will see long-term BCI implants becoming as commonplace as the bionic ear is today, almost certainly utilizing alumina feedthroughs and inductive transcutaneous power and information transfer, much the same as the bionic ear and bionic eye. Their immediate and most obvious application is for spinal-cord-injured patients, such as quadriplegics, tetraplegics, as well as sufferers of degenerative diseases such as motor neurone disease.

However, there is a significant competitor technology to the implantable BCI, invented in 2016, which is much less invasive, and may prove to be the future for BCI technology: the Stentrode.

10.1.6.2 The Stentrode

A much less invasive option than the BCE is the Stentrode, i.e., the Stent-Electrode. Unveiled in Nature Biotechnology in 2016 [39], the Stentrode was invented at the University of Melbourne two decades after the Brown University implantable multi-electrode-pin BCI. The Stentrode is a stent that embodies electrodes, connected to a lead, thence a hermetic connector, and thence a transcutaneous wire link. This was just a temporary solution for the sheep trials. Ultimately, a hermetic bionic feedthrough with inductive coupling could be the ideal system to use with a Stentrode.

The Stentrode, being a stent, can be percutaneously implanted in the brain vasculature via a safe day-surgery procedure. It is a very new development, one of the most advanced developments in bionics at the time of writing. Being a stent, the Stentrode is a much safer and more convenient way to implant electrodes directly in the brain, no open brain surgery, no pins penetrating brain tissue. Moreover, it has less limitations in terms of the brain locations that are accessible by this means. Surgically implanted multi-pin brain implants such as BrainGate™ can only be safely implanted on the outer surface of the brain, whereas the Stentrode can be implanted in many locations both deep within the brain or near the surface, anywhere where the brain vasculature is large enough in diameter to accommodate it. Given the scale of the vascularization in the brain, this gives substantial scope. The intracranial stent is already a well-established treatment for blockages in brain vasculature. The coronary stent has been in use for 3 decades now and is a very safe and proven technology.

The electrodes on the Stentrode clinically tested in sheep [39] were 750 micron diamond-cut platinum electrodes. An electrode lead was run from the Stentrode at the implant site, through the brain vasculature to the Jugular vein, where it was passed through a perforation in the vein, tunneled subcutaneously to a custom-made hermetic connector secured to the muscle, and exited the skin via a flexible transcutaneous lead, which terminated in a plug. The specifics of the hermetic connector are not yet publicly disclosed, but the possibility exists that alumina may be involved, if not at the animal testing stage, possibly in the commercial stage with an inductive

coupling rather than a transcutaneous lead. This would be an obvious fit for the standard titanium/alumina-platinum mini-implant package used in a contemporary bionic ear. One could envisage Stentrode systems as being much like the bionic ear, with remote electrodes deep in the brain vasculature (Stentrode) connected to a lead running through the vasculature, connected at the other end to the feedthrough of a hermetic titanium/alumina-platinum implant beneath the skin that communicates transcutaneously, by induction, with an external processor.

At this point we have gone as far into the future as it is reasonable to go, without stepping into the realms of science fiction and speculation. Clearly, the rest of the twenty-first century is going to be an exciting time for implantable bionics, and alumina remains at the forefront of bionic hermetic packaging technology at the end of the second decade of the twenty-first century.

10.2 Alumina in Implantable Tissue Scaffolds

Bone tissue scaffolds have four key requirements:

(1) Bioactivity,
(2) Very high porosity (preferably >80%, ideally >90%),
(3) Large pore size of at least 100 microns to allow bone ingrowth, and
(4) High strength at a high porosity.

Currently, the bone tissue scaffolds field is dominated by calcium phosphate ceramics (hydroxyapatite, tricalcium phosphate, bioglass), biodegradable polymers (polylactic acid (PLA), poly(glycolic acid) (PGA), poly(glycolide-co-lactide) (PGLA), and polycaprolactone (PCL)), and calcium phosphate-doped biodegradable polymers. However, these suffer some limitations:

(a) Biodegradable polymers are not bioactive and are very low in strength.
(b) The in vivo dissolution of biodegradable polymers releases acidic monomers in the tissues which can cause inflammation.
(c) Calcium phosphate doping can impart bioactivity to biodegradable polymers, but strength and acidic-monomer-inflammation are two fundamental flaws in the biodegradable polymer tissue scaffold application.
(d) Calcium phosphates are highly bioactive, and do not cause inflammation.
(e) The strength of calcium phosphates is low, especially at high porosity.
(f) It is not possible to produce calcium phosphate ceramics of viable mechanical strength with porosities anywhere near 90%.

Alumina is a very strong ceramic, far superior to calcium phosphates, and has a high strength even at porosities of over 90%, as shown by a series of papers published between 2005 and 2015 on foamed alumina tissue scaffolds published by authors

Ruys and Soh[3] [40–43]. This research ultimately achieved the following: at the extremely high porosity of 94.4%:

- A high compressive strength of 384 MPa, at 94.4% porosity
- Average pore size of 300 microns, more than large enough for bone ingrowth [41].

Of course, it is well known that alumina is bioinert, and therefore while bone ingrowth into an alumina tissue scaffold is possible, it is going to be a slow process because, just like biodegradable polymers, alumina has no inherent bioactivity. While biodegradable polymers can be calcium phosphate-doped to impart bioactivity, mixing calcium phosphate into an alumina ceramic will turn it into an alumina-calcia-phosphate compound, and thereby take away its main advantage of strength.

In 2004, a paper was published by Pabbruwe et al. [44] demonstrating that surface-doping of alumina tubes (1.3 mm outer diameter, 0.6 mm inner diameter, 15 mm length) with calcium, magnesium, or chromium ions, could impart bioactivity to alumina and stimulate bone ingrowth to an alumina pore.

Combining the innovation of Pabbruwe et al. [44] with the Parakala innovation of the high-strength foamed alumina scaffold [43], Soh and the author developed a high-strength (380 MPa) high porosity (94.4%) large-pore (300 micron) bioactive alumina tissue scaffold by surface-doping the foamed alumina scaffolds with calcium, phosphorous, magnesium, or silicon. The in vitro response of bone cells (MG63 osteosarcoma cells) to this scaffold was then studied [41]. Bioactivity was demonstrated, with the silicon and phosphorus doping proving the most effective at stimulating bone cell response [41].

The manufacturing process was as follows:

(1) $(NH_4)_2{\cdot}Al_2(SO_4)_3{\cdot}24H_2O$ salt solution is placed in an alumina crucible and foamed at 100–200 °C
(2) $(NH_4)_2{\cdot}Al_2(SO_4)_3$ dehydroxylation at 300–500 °C
(3) $Al_2(SO_4)_3 + NH_3$ ammonia volatilizes at 300–500 °C
(4) $Al_2O_3 + SO_3$ sulphate volatilizes at 500–1000 °C
(5) β-Al_2O_3 foamed porous β-alumina intermediate stage
(6) α-Al_2O_3 foamed porous α-alumina after calcining at 1000–1600 °C
(7) Scaffold cooled and soaked for 24 h in bioactive dopant-ion solution
(8) Soaked scaffold calcined to 900 °C to bond bioactive dopant ions to pore surface.

This innovation has significant potential in the bone tissue engineering field. Never before has a bioactive bone scaffold been seen with such a favorable high-porosity/high-strength/large-pore combination. It is early days yet, and it remains to be seen how this 2015 innovation fares in the bone tissue engineering realm (Fig. 10.19).

[3] The concept and technology of foamed alumina was originally conceived of by Dr Padmaja Parakala, and successfully executed by author Edwin Soh.

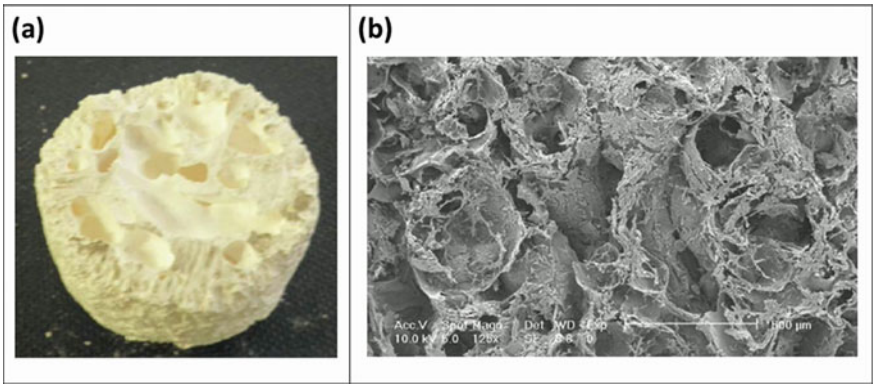

Fig. 10.19 **a** Foamed scaffold as removed from the crucible, ready for trimming. **b** Scanning electron microscopy image of a 94% porous foamed scaffold (note the 1 mm scale bar) with average pore size of 300 microns (Image copyright Edwin Soh, supplied courtesy of Edwin Soh)

References

1. Aquilina O (2006) A brief history of cardiac pacing. Images Paediatr Cardiol 8:17–81
2. Wickham GG, Cowdery DJ (1971) An hermetically sealed implantable cardiac pacemaker. In: Proceedings of the 9th international conference on medical and biological engineering, Melbourne
3. Bondarew V, Seligman P (2012) The Cochlear story (bright ideas series). CSIRO Publishing, Australia
4. Ruys AJ (2019) Alumina ceramics. Biomedical and industrial applications. Elsevier, Oxford
5. Jacobi W (1952) Halblieterverstarker. German Patent DE 833366, Filed 1949
6. Fiandra O (1988) The first pacemaker implant in America. Pacing Clin Electrophysiol 11:1234–1238
7. Davies JG, Siddons H (1965) Experience with implanted pacemakers: technical considerations. Thorax 20:128–134
8. Edison TA (1880) Electric lamp. US Patent 223898, Filed 1879
9. De Forest L (1906) Oscillation-responsive device. US Patent 824637, Filed 1906
10. De Forest L (1906) Oscillation-responsive device. US Patent 836070, Filed 1906
11. Scott H (1936) Glass Metal Seal. US Patent 2062335, Filed 1929
12. Elan Technology (2017) Glass recommendations for Kovar. https://www.elantechnology.com/support/glass-recommendations/kovar-alloy/. Accessed 08 Apr 2021
13. US Department of Defense (2006) Test method standard—microcircuits, MIL-STD-883G
14. Vatter H (1937) A method for producing vacuum-tight electric vessels after soldering. German Patent 645871, Filed 1935
15. Pulfrich H (1939) Ceramic to metal seals. US Patent 2163407, Priority 1936
16. Nolte HJ (1954) Method of metallizing a ceramic member. US Patent 2,667,427
17. Burnside DG (1954) Ceramic seals of the tungsten-iron type. RCA Rev 15:46–61
18. US Department of Defense (2006) Test method standard—test methods for semiconductor devices. MIL-STD-750E
19. Howl DA, Mann CA (1965) The back-pressurising technique of leak-testing. Vacuum 15:347–352
20. Cowdery DJ (1969) The pulsed TIG welding process Part 1. Equipment design. Welding Inst Res Bull 10:201–203

21. Cowdery DJ (1969) Pulsed arc MIG welding with variable pulse width, Report No.672. British Oxygen Company Research Laboratory, Welding Products Division
22. Mathematica (2017) Electrical conductivity of the elements, Mathematica Element Data, Wolfram Research. https://reference.wolfram.com/language/ref/ElementData.html. Accessed 08 Apr 2021
23. Zion Market Research (2016) Cardiac pacemaker market by product (implantable cardiac pacemaker and external cardiac pacemaker) by technology (biventricular, single chambered, and dual chambered): global industry perspective, comprehensive analysis and forecast, 2015–2021. https://www.zionmarketresearch.com/report/cardiac-pacemaker-market. Accessed 08 Apr 2021
24. Elssner G, Pabst R, Puhr-Westerheide J (1974) Schichtverbundkombinationen aus hochschmelzenden metallen und oxiden. Zeitschrift fuer Werkstofft 5:61–69
25. Sirota NN, Zhabko TE (1981) X-ray study of the anisotropy of thermal properties in titanium. Phys Stat Sol 63:K211–K215
26. O'Brien B (2015) Niobium biomaterials. In: Niinomi M, Narushima T, Nakai M (eds) Advances in metallic biomaterials. Springer series in biomaterials science and engineering, vol 3. Springer, Heidelberg, pp 245–272
27. De Bruin HJ, Warble CE (1977) Chemical bonding of metals to ceramic materials. US Patent 4050956, Filed 1975
28. McAlister AJ, Kahan DJ (1986) The Al−Pt (Aluminum-Platinum) system. Bull All Phase Diagram 7:47–51
29. Wriedt HA (1985) The Al-O (Aluminum-Oxygen) system. Bull All Phase Diagrams 6:548–553
30. Allen RV, Borbidge WE (1983) Solid state metal-ceramic bonding of platinum to alumina. J Mater Sci 18:2835–2843
31. The Engineering Toolbox (2017) Coefficients of linear thermal expansion. http://www.engineeringtoolbox.com/linear-expansion-coefficients-d_95.html. Accessed 08 Apr 2021
32. Guenther T, Kong C, Lu H et al (2014) Pt-Al_2O_3 interfaces in cofired ceramics for use in miniaturized neuroprosthetic implants. J Biomed Mater Res B Appl Biomater 102:500–507
33. Green RA, Guenther T, Jeschke C et al (2013) Integrated electrode and high density feedthrough system for chip-scale implantable devices. Biomaterials 34:6109–6118
34. Schuettler M, Ordonez JS, Silva Santisteban T et al (2010) Fabrication and test of a hermetic miniature implant package with 360 electrical feedthroughs. Annu Int Conf IEEE Eng Med Biol Soc 2010:1585–1588
35. Haas LF (2003) Hans Berger (1873–1941), Richard Caton (1842–1926), and electroencephalography. J Neurol Neurosurg Psychiatry 74:9. https://doi.org/10.1136/jnnp.74.1.9
36. Donoghue J, Hatsopoulos N, Martel S et al (2007) Microstructured arrays for cortex interaction and related methods of manufacture and use. US Patent 7212851
37. Hochberg LR, Bacher D, Jarosiewicz B et al (2012) Reach and grasp by people with tetraplegia using a neurally controlled robotic arm. Nature 485:372–375
38. Leuthardt EC, Schalk G, Moran DW et al (2006) Brain computer interface. US Patent US7120486B2, Filed 2003
39. Oxley TJ, Opie NL, John SE et al (2016) Minimally invasive endovascular stent-electrode array for high-fidelity, chronic recordings of cortical neural activity. Nat Biotechnol 34:320–327
40. Soh E, Kolos E, Ruys AJ (2015) Cellular response to doping of high porosity foamed alumina with Ca, P, Mg, and Si. Materials 8:1074–1088
41. Soh E, Kolos E, Ruys AJ (2015) Foamed high porosity alumina for use as a bone tissue scaffold. Ceram Int 41:1031–1047
42. Soh E, Ruys AJ (2009) Characterisation of foamed porous alumina tissue scaffolds. J Biomim Biomater Tissue Eng 4:21–26

43. Soh KH, Ruys AJ, Parakala P (2005) Foamed alumina bioceramics for use as tissue scaffolds. In: International Federation for Medical and Biological Engineering (IFMBE) proceedings ICBMEC 2005. The 12th international conference on biomedical engineering, vol 12. Singapore
44. Pabbruwe MB, Standard OC, Sorrell CC et al (2004) Bone formation within alumina tubes: effect of calcium, manganese, and chromium dopants. Biomaterials 25:4901–4910

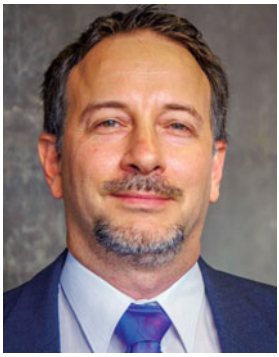

Andrew J. Ruys Professor Ruys was a founding Director of Biomedical Engineering at the University of Sydney, Australia, between 2003 and 2018. He has worked in bioceramics and advanced ceramics research for over 30 years, as researcher, educator and industrial consultant. He is not only an experienced researcher in bioceramics (ceramics for biomedical applications) but has also been an industrial consultant in the world-changing applications of armour ceramics, advanced ceramics in wear-resistance linings in mineral processing, and numerous other important industrial applications of ceramics. He has 230 publications, including 8 books and 5 patents, with over 3000 citations of his work. He has also published two leading monographs with Elsevier: Alumina Ceramics—Biomedical and Industrial Applications (2019) and Metal-Reinforced Ceramics (2021). He serves on three editorial boards and is a reviewer for 24 scientific journals. In addition to bioceramicsbiomaterials, and medical device technology for three decades, he has also taught on dental materials, industrial ceramics, chemistry, physics, and general engineering.

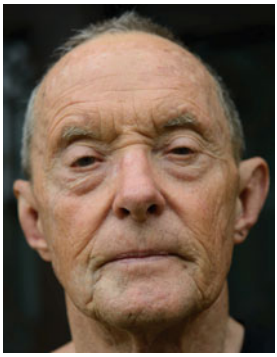

David J. Cowdery Mr. Cowdery graduated from Sydney University in 1965 with a B.Sc. and a B.E. (Hons 1) in Electrical Engineering. He began work in welding research in Australia and at the Welding Institute in Cambridge UK. David began his Biomedical career in 1970 joining a small company making epoxy encapsulated implantable pacemakers. These had severe reliability problems which David addressed by inventing the world's first hermetically sealed reliable pacemaker, using a titanium case and brazed alumina ceramic feedthrough. This invention was later copied worldwide by all other pacemaker manufacturers and has now become the global industry standard for implantable bionics.

Edwin Soh Dr. Soh is a Senior Business Development Manager at the Advanced Remanufacturing and Technology Centre (ARTC), an institute of the Agency for Science, Technology and Research (A*STAR), Singapore. He graduated with a B.E. in Mechanical Engineering in 2004 and Ph.D. in Biomedical Engineering in 2013 from the University of Sydney, Australia. His Ph.D. research focused on alumina tissue scaffolds. He works closely with industry, academic and government organizations to identify new developments and transformation opportunities, aligning with the national research and innovation roadmap. He manages strategic accounts in a Private–Public-partnership environment, involving multimillion funding, supported by the government. He has worked as a scientist in surface finishing and remanufacturing processes for implementing in the aerospace industry. He is a product owner for a platform technology developed for Robotics Applications.

Chapter 11
Biocomposites and Bioceramics in Tissue Engineering: Beyond the Next Decade

Sandra Pina, Il Keun Kwon, Rui L. Reis, and J. Miguel Oliveira

Abstract Current strategies in the field of tissue engineering are bringing functional biomaterials with required structural, mechanical, and biological performance able to endorse the repair and regeneration of injured or diseased tissues. Biocomposites formed by biodegradable polymers matrix and bioceramics have proved their effectiveness in clinics, namely in orthopedics and dental medicine. They are being used as suture anchors and interference screws, while bioceramics are indicated as cements, blocks, granules, or as coatings for metal implants. The biocompatibility and osteoconductivity of the bioceramics together with the high mechanical properties provided by the polymers make them ideal candidates towards the designing of advanced scaffolds and implants. A comprehensive overview of recent research on bioceramics and bioceramics-related biocomposites for several tissue engineering purposes are herein presented. Bioceramics and biocomposites comprising bioinert, bioactive and bioresorbable ceramics, and natural and synthetic biodegradable polymers for scaffolds processing, and respective properties are demonstrated. Interest is given to advanced manufacturing as an emergent technology for complex personalized structures fabrication. Commercial bioceramics and biocomposites available for biomedical use are also summarized.

Keywords Bioceramics · Natural-derived bioceramics · Alumina · Zirconia · Bioglasses · Glass–ceramics · Calcium phosphates · Biocomposites · Biofabrication · Biocompatibility · Osteogenesis · Vascularization · Bone regeneration · Tissue engineering · Scaffolds

S. Pina (✉) · R. L. Reis · J. M. Oliveira
3B's Research Group, I3Bs - Research Institute on Biomaterials, Biodegradables and Biomimetics, University of Minho, Headquarters of the European Institute of Excellence on Tissue Engineering and Regenerative Medicine, AvePark, Parque de Ciência e Tecnologia, Zona Industrial da Gandra, 4805-017 Barco, Guimarães, Portugal
e-mail: sandra.pina@i3bs.uminho.pt

ICVS/3B's-PT Government Associate Laboratory, Braga/Guimarães, Portugal

I. K. Kwon
Department of Dental Materials, School of Dentistry, Kyung Hee University, 26, Kyungheedae-ro, Dongdaemun-gu, Seoul 02477, Republic of Korea

A. H. Choi and B. Ben-Nissan (eds.), *Innovative Bioceramics in Translational Medicine I*,
Springer Series in Biomaterials Science and Engineering 17,
https://doi.org/10.1007/978-981-16-7435-8_11

11.1 Introduction

Advanced biomedical implants have nowadays drastically altered millions of patients' lives. They are used to replace and/or regenerate damaged tissues, or to fill defects, in several tissue engineering and regenerative medicine applications [1]. Bioceramics and bioceramics-derived composites are the most commonly type of biomaterials used as bone and dental implants [2]. These biomaterials have been applied in numerous medical fields, namely as artificial total hip, knee, and shoulder, plates and screws, vertebrae spacers and extensors, alveolar bone replacements, mandibular reconstruction, spinal fusion, end osseous tooth replacement implant and orthodontic anchors.

Bioceramics are inorganic non-metallic biomaterials ranging from bioinert (e.g., zirconia and alumina), bioactive (e.g., bioglass) to bioresorbable ceramics (e.g., calcium phosphates, calcium phosphates-based cements (CPCs), calcium carbonates, calcium silicates, and natural coral-derived apatites), according to their bonding ability with the surrounding tissues upon implantation [3]. These materials are well known by their excellent biocompatibility, osteoconductivity, hard brittle, and corrosion resistance. Nevertheless, bioresorbable ceramics possess limited fracture toughness, brittleness, elasticity and very high stiffness, which can be turned by combining them with different polymers resulting in composites [4]. Biocomposites containing bioceramics and biodegradable polymers are the most successful strategy for bone tissue engineering and regeneration, holding tailored structural stability, mechanical and biological performance to be used as implants and dental healing materials [5–13]. These biomaterials are able to replace the typically used metallic implants, with no need of a second surgical intervention for implant removal, neither corrosion nor accumulation of metal in tissues, and reduced stress-shielding [14–20]. Synthetic biodegradable polymers, such as poly α-hydroxy acids (e.g. polylactic acid (PLA), polyglycolic acid (PGA), and their copolymers polylactic-co-glycolic acid (PLGA) and poly-L-lactide PLLA), polycaprolactone (PCL), as well as natural-derived polymers as the case of collagen, are mainly used in biocomposites manufacturing [21–23]. Those materials provide appropriate strength whilst degrading in a predictable fashion with no adverse clinical reactions during the healing and regenerative processes [24].

The development of biofunctional tissue-engineered scaffolds/constructs as temporary matrices, with satisfactory mechanical support and architecture able to promote cell growth and new tissue formation, is the most challenging in the field of tissue engineering [25]. Furthermore, the scaffolds fabrication comprising bioceramics and bioceramics-derived biocomposites brings significant advantage owing their capacity on mimicking the bone tissue. A number of conventional fabrication technologies including particulate-leaching, freeze drying, gas foaming, and phase separation, generate optimized properties and low costs scaffolds [26–29]. Advanced manufacturing, as 3D bioprinting, is appearing as an innovative frontline technology to obtain complex micro- and nano-scale structures and spatial heterogeneity, by combining design and imaging techniques [30–33].

Herein, it is provided an up-to-date of bioceramics and bioceramics-based biocomposites used in different tissue engineering approaches, including their structure, mechanical performance, and biological response. Advanced design strategies, such as biofabrication technology, are covered. A compilation of marketed bioceramics and biocomposites used in the biomedical field is also provided.

11.2 Bioceramics in Tissue Engineering

A myriad of bioceramics for different biomedical applications is available in the market (Table 11.1). Zirconia and alumina are typically used for hip/knee arthroplasty, femoral head, and dental replacement, owing their chemical inertness and high hardness. Calcium phosphates and bioglass are applied in the regeneration/replacement of bone defects, degenerative joints, vertebroplasty/kyphoplasty, and oral/maxillofacial surgery [34]. Regarding their limited biomechanical function, some bioceramics (e.g., calcium phosphates and bioglass) implants are restrictedly applied in non-load-bearing or compressive load conditions, namely as bone fillers, cements or as coatings on metallic implants.

Bioceramics obtained from natural sources, as for example the commercial product Endobon (Biomet), hold single microstructure and mechanical properties for bone tissue applications [35–37]. These natural biomaterials (e.g., corals, nacres, algae, sponges, and animal bones) provide an abundant source of calcium compounds (e.g., calcium carbonate) as raw materials that can be further used to prepare calcium phosphate biomaterials for different biomedical purposes.

Bioceramics are currently gaining ground for the development of tissue-engineered scaffolding strategies for soft and hard tissue regeneration, bone tumor therapy, and delivery of drugs [38–41]. Furthermore, doping with bioactive ions (e.g., Mg^{2+}, Sr^{2+}, Zn^{2+}, Mn^{2+}, Co^{2+}, Cu^{2+}, Fe^{3+}, and Ag^{+}), which are highly promising in directing cell fate, is a key to develop fine-tuned therapeutics [42–46]. Examples are calcium phosphates-based cements and bioglass functionalized with several ions that confer osteogenic, angiogenic and antibacterial properties for new bone formation and regeneration [47–52].

Nowadays, several studies have been carried out using 3D-printed bioceramic scaffolds, some of them incorporating ionic dopants, antibiotics/drugs, and/or growth factors, with successful results in stimulating bone regeneration [38, 44, 53, 54]. For instance, ion-doped bioglass scaffolds fabricated through 3D printing exhibited excellent osteogenic differentiation capacity and photothermal anti-tumor function [38, 54]. Bioglass (BGC)-based printed scaffolds, with composition of $(M_{0.0x})(Ca_{0.25-0.0x})P_{0.05}Si_{0.75}$, where (M = Cu, Fe, Mn, Co; x = 0, 2, 5), showed different microstructures and colors depending on the dopant ion, while BGC alone were white (Fig. 11.1) [54]. In vivo tests performed on scaffolds implanted in the center of tumor tissues of nude mice displayed a trend of photothermal performance as 5Cu-BGC > 5Fe-BGC > 5Mn-BGC > 5Co-BGC > BGC (Fig. 11.2).

Table 11.1 Commercially available bioceramics-based implants used in the biomedical field (CaP: calcium phosphate; DCPD: dicalcium phosphate dehydrate; MCPM: monocalcium phosphate monohydrate; TCP: tri-calcium phosphate; TTCP: tetracalcium phosphate; ZTA: zirconia-toughened alumina)

Company (Country)	Product	Material	Properties	Applications
Bicon Dental Implants (USA)	SynthoGraft™ (Granulated ceramic)	β-TCP	• Biocompatible and resorbable granulate ceramic • micro- and nano-porosity to allow vascularization and resorption	• Oral and maxillofacial bone regeneration or augmentation
Biomet (USA)	Calcibon® (Cement paste and granules)	TCP/$CaCO_3$/$CaHPO_4$	• Osteoconductive and biodegradable • Stable osseous integration • Cement final strength of up to 45 MPa after 3 days	• Large bone defects • Kyphoplasty
	Endobon (Blocks, cylinders and granules)	Natural origin HAp	• Osteoconductive • Macro and micro pores with pore sizes of 100–1500 μm • Porosity: 45–85 vol.%	• Distal radius fractures • Calcaneus fractures • Tibia plateau fractures
CeramTec (Germany)	BIOLOX® (femoral head)	Al_2O_3	• Excellent biocompatibility and chemically stable in the physiological environment	• Joint arthroplasty
	BIOLOX® delta (femoral head)	Al_2O_3/ZrO_2/SrO (80/17/3)	• Tough and strong • Able to prevent the initiation and propagation of cracks	• Joint arthroplasty

(continued)

Table 11.1 (continued)

Company (Country)	Product	Material	Properties	Applications
	DENSILOX® (screw)	ZTA	• High hardness • High fracture strength • High toughness Low bacteria adhesion	• Tooth replacement
	VERILOX® (femoral head)	Al_2O_3	• Hypoallergenic; • Display rapid bone ingrowth • Less bacteria adhesion	• Hip replacement in veterinary medicine
CeraRoot (Spain)	CeraRoot implants	ZrO_2	• Hypoallergenic • Optimal osseointegration without any signs of inflammation or foreign body rejection	• Tooth root replacements
DePuy (USA)	α-BSM® (injectable cement)	Amorphous CaP/DCPD	• Setting time: 5 min • Compressive strength: 30–50 MPa • New bone formation, remodeling and resorption characteristics up to 52 weeks observed in rabbit critically sized femoral defects	• Bone void filler
DePuy Synthes (USA)	Norian SRS® (injectable cement)	α-TCP/ $CaCO_3$/ MCPM	• Setting time: 10 min • Injectable cement • Compressive strength: 50 MPa	• Skeletal repair system (bone void filler)

(continued)

Table 11.1 (continued)

Company (Country)	Product	Material	Properties	Applications
	Norian CRS® (injectable cement)	α-TCP/ $CaCO_3$/ MCPM	• Moldable bone cement • Setting time: 3–6 min • Compressive strength: 60 MPa after 24 h • Gradual resorption and replacement with bone during the healing process	• Cranial repair system (bone void filler)
	ChronOS Inject® (injectable cement)	β-TCP/ MCPM	• Injectable cement • Resorbable • Osteoconductive	• Treatment primarily of metaphyseal bone defects (non-load-bearing)
HOYA Technosurgical Corporation (Japan)	Biopex®-R (injectable cement)	α-TCP/ TTCP/ DCPD	• Injectable • Compressive strength: 80 MPa after 24 h post-implantation	• Bone void filler
	APACERAM (blocks and granules)	HAp	• Triple pore structure up to 60% • Interconnecting pore structure and porous inner wall structure • Early bone formation	• Bone graft substitute

(continued)

Table 11.1 (continued)

Company (Country)	Product	Material	Properties	Applications
	SUPERPORE (blocks and granules)	β-TCP	• Three types of porosity: 57–75% • Compressive strength: 5–48 MPa • Fast bone regeneration and balanced absorption	• Bone graft substitute
Straumann (Switzerland)	Straumann® BoneCeramic® (implant)	HAp/β-TCP (60/40)	• 90% porosity	• Bone regeneration
	Straumann® PURE (implant)	ZrO_2	• Excellent osseointegration	• Dental implant
Stryker (USA)	Vitoss, Vitoss BA, Vitoss BA2X (graft)	Bioglass	• Highly porous • Resorbable • Bone regeneration	• Bone void filler
	Vitoss BiModal (graft)	Bioglass*	• Increased CaP deposition compared to other forms of Vitoss • Resorbable • Bone regeneration	• Bone void filler
	VENADO (granules)	β-TCP/HAp (40/60)	• Biodegradable • Resorbable • Radiopaque for radiographic visualization	• Bone void filler
	HydroSet™ (injectable cement)	DCPD/ TTCP/	• Self-setting cement • Injectable	• Cranial repair (neurosurgical burr holes, contiguous craniotomy cuts and other cranial defects)

(continued)

Table 11.1 (continued)

Company (Country)	Product	Material	Properties	Applications
	DirectInject (injectable cement)	CaP	• Self-setting cement • Injectable • Setting time: 7.5 min • Repair of cranial defects with a surface area of 4 cm^2	• Cranial repair (neurosurgical burr holes, contiguous craniotomy cuts and other cranial defects)
Teknimed (France)	TRIHA+® (granules, sticks, shapes)	β-TCP	• Absorbable • Biocompatible • Osteoconductive	• Filling small bone defects
	CERAFORM® (granules)	HAp/β-TCP (65/35)	• Absorbable • Biocompatible • Osteoconductive	• Filling small bone defects
	NANOGEL® (nanoparticle gel)	HAp	• Particle size: 200–200 nm • Injectable • Absorbable • Osteoconductive • Percutaneous use	• Dental or maxillofacial surgery
	Cementek LV® (injectable cement)	TTCP/α-TCP (49/38)	• Malleable for about 15 min and hardens in situ	• Bone void filler
	Bonefuse® Putty (injectable cement)	TCP	• Fast bioabsorption	• Bone void filler

(continued)

Table 11.1 (continued)

Company (Country)	Product	Material	Properties	Applications
Zimmer Biomet (USA)	β-bsm® (injectable cement)	Nanocrystalline CaP	• Injectable • Setting time: 3–5 min • Compressive strength: 30 MPa • New bone growth while undergoing cell-mediated remodeling as the bone heals	• Bone (minimally invasive procedures)
	Pro Osteon 200R and 500R (granules)	HAp/$CaCO_3$	• Interconnected porosity: ~200 μm • Small granules: 0.5–1 mm • Resorbs in 6 to 18 months	• Bone void filler (small defects)
	Mimix® and Mimix QS (injectable cement)	α-TCP/ TTCP	• Easily moldable • Radiopaque • Mimix allows for better contouring of large defects (25 cm^2 in size) while the shorter setting time of Mimix QS allows for quicker closure	• Cranial defects repair

* Broader range of bioactive glass particle size distribution than other forms of Vitoss

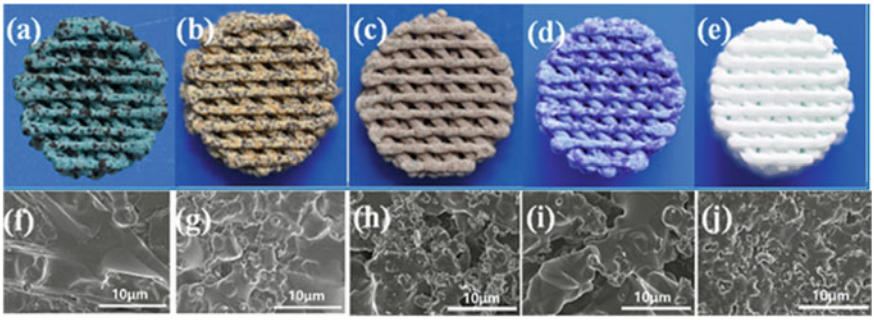

Fig. 11.1 3D-printed scaffolds images and respective scanning electron micrographs (SEM) of 5Cu-BGC (**a**, **f**); 5Fe-BGC (**b**, **g**); 5Mn-BGC (**c**, **h**); 5Co-BGC (**d**, **i**); and BGC (**e**, **j**). Adapted with permission from [54]

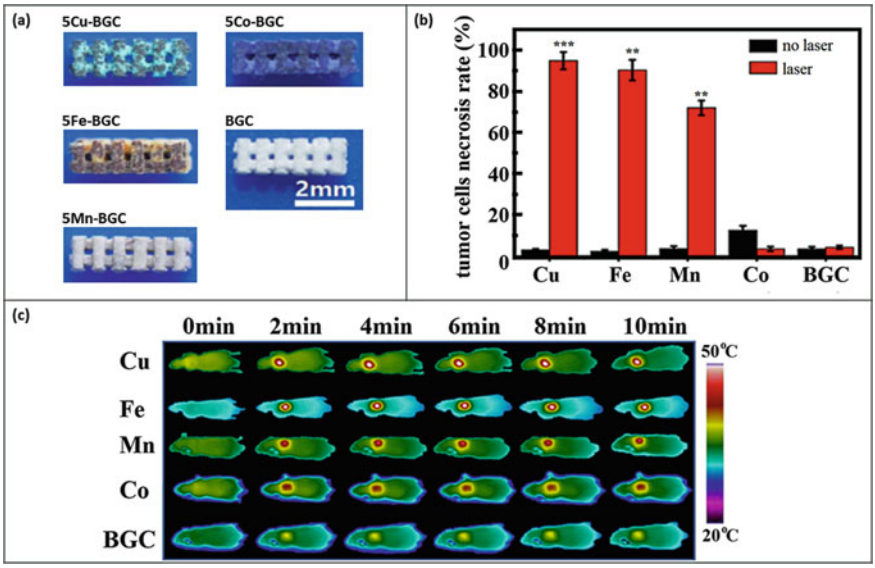

Fig. 11.2 **a** Scaffolds (5Cu-BGC, 5Fe-BGC, 5Mn-BGC, 5Co-BGC and BGC) after implantation in mice tumor site; **b** Tumor cell necrosis rate; **c** Infra-red thermal images of tumor bearing mice post-implanted with scaffolds. Adapted with permission from [54]

After treatment laser irradiation (0.75 W/cm^2), the 5Cu-BGC and 5Fe-BGC scaffolds presented the best photothermal anti-tumor behavior. Biocompatibility and osteogenic differentiation of rabbit bone mesenchymal stem cells (rBMSCs) cultured on the scaffolds, up to 7 days, indicated that 5Fe-BGC and 5Mn-BGC better supported cell attachment and proliferation (Fig. 11.3). In another study, Mg-doped β-tricalcium phosphate (β-TCP) printed scaffolds unveiled favorable vascularization

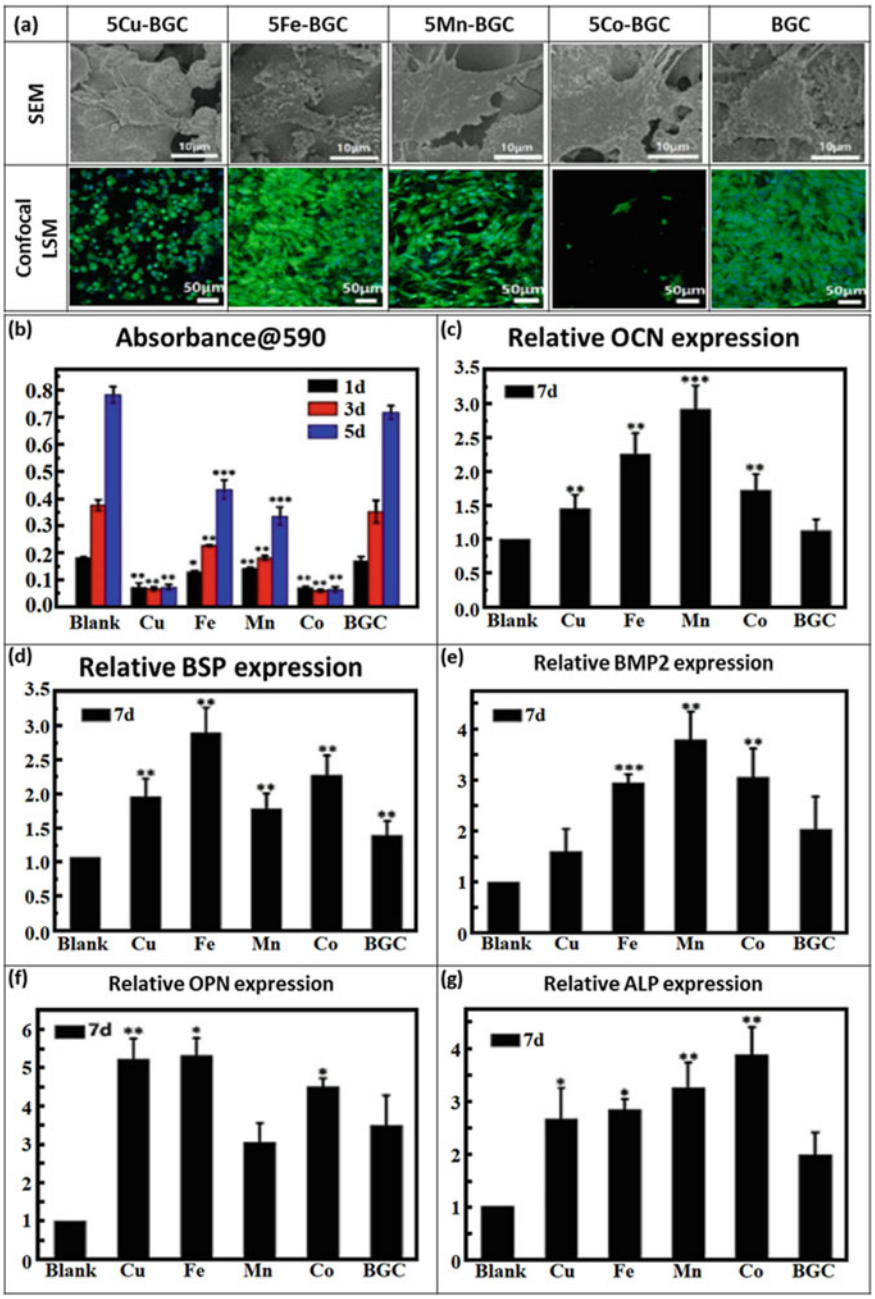

Fig. 11.3 **a** SEM and confocal LSM images of rBMSCs cultured in the scaffolds for 1 day. **b** Proliferation of rBMSCs in scaffolds at day 1, day 3, and day 7. **c–g** Osteogenic gene expression (OCN, BSP, BMP2, OPN, ALP) at day 7. Adapted with permission from [54]

and osteogenic potential after culturing with human bone marrow mesenchymal stem cells (hBMSCs) and human umbilical vein endothelial cells (HUVECs) [44].

Interestingly, bioceramics have been also explored as a strategy to activate the specific immune responses, with significant impact on osteogenesis and osteoclastogenesis [55–61]. It was observed that highly porous nanoscale calcium deficient HAp scaffolds modulate its inflammatory capability after cultured with murine RAW 264.7 cells and promote osteogenesis [61]. Also, by means of culturing macrophages with β-TCP showed decreased pro-inflammatory cytokines in comparison to calcium deficient HAp, while the osteogenic differentiation of osteoblasts for the macrophages-calcium deficient HAp interaction [58]. In a different approach, dicalcium phosphate bioceramic scaffolds coated with bone-ECM extracts could enhanced their surface proteomic interactions and modulate the host immune reactions [57]. Significant lower levels of cytokines in Sprague–Dawley rats were observed when filled with bioceramics coated with bone extract rich in calcium-binding proteins (E-extract) compared to the ones filled with uncoated bioceramics and bone extract rich in collagen (G-extract) coating (Fig. 11.4a). It was also observed reduced inflammatory response on the scaffolds with enhanced new bone formation, particularly on the scaffolds coated with E-extract (Fig. 11.4b). According to the authors, the high regenerative effect of E-extract coating-based scaffolds can be attributed to the integrin signaling pathway expression leading to the activation of mitogen-activated protein kinase signaling, and to the immune response modulation capacity of E-extract, thus contributing to the scaffold's integration and function.

11.3 Biocomposites in Tissue Engineering

Bioceramics-based composites commercially available are mainly being used in interference screws and suture anchors manufacturing for bone fixation and grafts, fractures stabilization, and soft tissues attachment (Table 11.2). They are manufactured with biodegradable polymers such as PLA and respective copolymers (PLLA and PLGA), and collagen combining resorbable bioceramics as β-TCP and HAp.

A huge amount of progress has been made in the development of functionally nanostructured bioceramics-based composites fabricated with constituents based on natural biopolymers as the case of silk fibroin, collagen, gelatin, and others, for a number of tissue engineering and regeneration applications [62–64]. Silk fibroin is a fibrous protein holding a semi-crystalline structure that provides mechanical strength, elasticity and slow degradability to the biomaterials, and through enzymatic crosslinking, it can yield advanced stiff and improved stable structures [65]. An example is the use of silk fibroin crosslinked by horseradish peroxidase and an oxidizer (e.g., hydrogen peroxide, H_2O_2) to fabricate hierarchical scaffolds for osteochondral tissue engineering and regeneration [7]. The scaffolds containing distinct cartilage-like and subchondral bone-like layers, respectively made of horseradish peroxidase-crosslinked silk fibroin and horseradish peroxidase-crosslinked silk fibroin with undoped and ion-doped β-TCP (Fig. 11.5a), and a well-

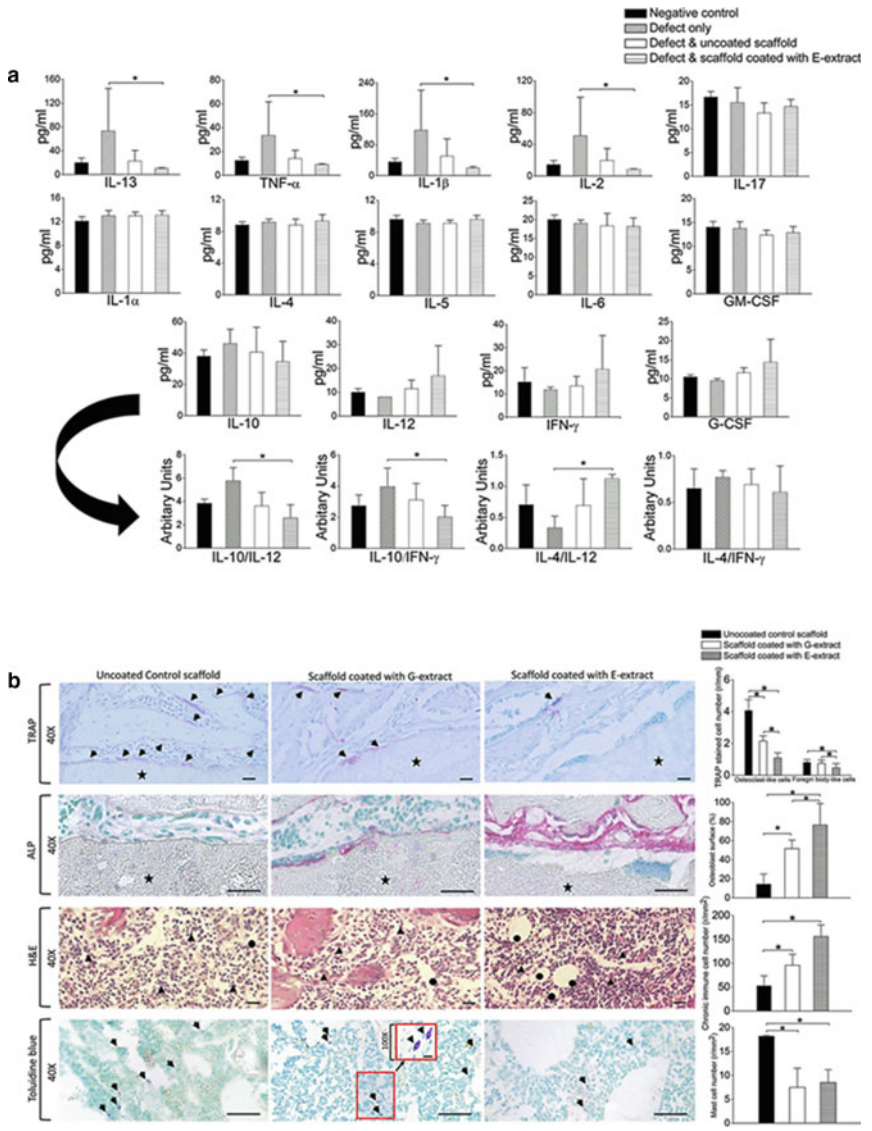

Fig. 11.4 **a** Blood cytokines analysis obtained by Luminex xMAP 200 system of the scaffolds after 3 days post-operatively from 14 weeks, in tibial defects of rats. **b** Histological analysis of the scaffolds. TRAP-stained sections, 40X magnification, scale bar 20 = μm. ALP-stained sections, 40X magnification, scale bar = 50 μm. Immune cells (i.e., lymphocytes and macrophages [arrows]), and new blood vessel formation (circles) (hematoxylin and eosin-stained sections, 40X magnification, scale bar = 20 μm). Acidified toluidine blue stained sections, 40X magnification, scale bar = 50 μm. Higher magnification to show mast cell morphology was carried out at 100X magnification, scale bar = 20 μm. E-extract: bioceramics coated with bone extract rich in calcium-binding proteins; and G-extract: bioceramics coated with bone extract rich in collagen. Reprinted with permission from [57]

Table 11.2 Commercially available bioceramics-based composites for biomedical applications (ACL: anterior cruciate ligament; BCP: biphasic calcium phosphate; CaP: calcium phosphate; HAp: hydroxyapatite; PCL: posterior cruciate ligament; PLA: poly lactic acid; PLDLA: poly (L-co-D,L lactic acid); PLGA: poly lactide glycolic acid; PLLA: poly-L-lactide; TCP: tricalcium phosphate)

Company (Country)	Product	Material	Properties	Applications
Arthrex (USA)	TraansFix Biocomposite®	BCP/PLDLA (30/70)	• Osteoconductive and controlled degradation	• Knee
	FastThread™ Biocomposite Interference Screws	BCP and PLDLA	• New bone within the screw site and is well-integrated into the surrounding bone • Bone ingrowth is observed at 4 months	• ACL reconstruction
	GraftBold®	PLA/β-TCP	• Not reported	• ACL tibial fixation
	SutureTak® Suture Anchor	PLDLA/ β-TCP (85/15)	• The strength is kept throughout the degradation cycle and eliminates suture abrasion during knot tying	• Shoulder
	Corkscrew® FT Anchor	PLLA/β-TCP (85/15)	• Excellent contact between tendon-bone and stability in rotation • Protection of broad healing zone from synovial fluid infiltration	• Rotator cuff repair

(continued)

Table 11.2 (continued)

Company (Country)	Product	Material	Properties	Applications
	PushLock® Anchor	PLLA/β-TCP (85/15)	• The amount of tension can be adjusted on the tissue intraoperatively, allowing precise suture and tissue reduction	• Rotator cuff repair
	SwiveLock® Anchor	Not reported	• Available for instability repair and provides very high pullout and insertion strength while saving time	• Rotator cuff repair
Biocomposites Ltd. (UK)	Bilok® Interference screw	PLLA/β-TCP (70/30)	• High strength with no tunnel expansion, no screw failure for 1 cm incision	• Rotator cuff repair
ConMed (USA)	Doubleplay™ Suture Anchor	PLLA/β-TCP (70/30)	• The unique "eyeless" design provides increased strength to the implant	• Soft tissue

(continued)

Table 11.2 (continued)

Company (Country)	Product	Material	Properties	Applications
	GENESYS™ Matryx® Interference Screw	PLDLA(96L/4D)/β-TCP (75/25)	• Deliver strong initial fixation during the critical healing period and provide a scaffold to enable bone ingrowth during the subsequent resorption period	• ACL reconstruction
	GENESYS Cross™ Suture Anchor	PLDLA(96L/4D)/β-TCP (75/25)	• Bone ingrowth and exceptional pullout strength	• ACL reconstruction
	GENESYS Press™ Suture Anchor	PLDLA(96L/4D)/β-TCP (75/25)	• Combine small size with exceptional strength	• Hip and shoulder labral repair
DePuy Synthes/Mitek Sports Medicine (USA)	Intrafix® Advance Screw	PLA/β-TCP	• High fixation strength and low displacement • Provides 360° of graft to bone compression	• ACL reconstruction
	MILAGRO® ADVANCE Interference Screw	PLGA/β-TCP (70/30)	• Exceptional bone engagement and rapid insertion	• ACL reconstruction

(continued)

Table 11.2 (continued)

Company (Country)	Product	Material	Properties	Applications
	Biocryl Rapide™ Interference Screw	PLGA/β-TCP (70/30)	• Osteoconductive and radiopaque • It absorbs and allows for ossification of the implant site in 3 years	• ACL reconstruction
	HEALIX ADVANCE™ Anchor	PLGA/β-TCP (70/30)	• High anchor torque strength for harder bone applications and ensures better anchor performance upon insertion	• Bone fixation
	CRANIOS REINFORCED®	CaP/PLGA fibers and sodium hyaluronate	• Moldable and self-setting cement • Setting time: 3–6 min • Compressive strength of 25 MPa after 24 h	• Bone void filler
	Lupine™ BR Anchor	PLGA/β-TCP (70/30)	• Faster resorption and bone ingrowth with optimal pullout strength	• Soft tissue repair/ arthroscopy
	BioKnotless™ BR Anchor	PLGA/β-TCP (70/30)	• Fast resorption and bone ingrowth • Pull-out strength while maintaining its proven design characteristics	• Soft tissue repair/ arthroscopy

(continued)

Table 11.2 (continued)

Company (Country)	Product	Material	Properties	Applications
	GRYPHON® Suture Anchor	PLGA/β-TCP (70/30)	• Provides audible feedback and confidence of fixation	• Glenoid labrum to bone reattachment
HOYA Technosurgical Corporation (Japan)	ReFit (Blocks)	HAp/Collagen (80/20)	• Becomes elastic when hydrated • Porosity: 95% • Pore diameter: 100–500 μm • Bone regeneration and absorption in vivo	• Bone graft substitute
SBM (France)	Duosorb®	PLDLA/β-TCP (40/60) and (70/30)	• Increased torsional and bending strength and greater elasticity with 30% β-TCP, suitable for implants subjected to high stresses • High compressive strength and rigidity with 60% β-TCP, suitable for compressive stresses in indications where consolidation is the dominant factor	• ACL reconstruction

(continued)

Table 11.2 (continued)

Company (Country)	Product	Material	Properties	Applications
Smith & Nephew (UK)	BIOSURE™ REGENESORB Interference Screw	PLGA/β-TCP/ $CaSO_4$ (65/15/20)	• Osteoconductive • Bone ingrowth within 24 months in preclinical studies • Associated with increased levels of local growth factors	• ACL repair
	BIORCI-HA® Screw System	PLLA/HAp (75/25)	• Excellent pullout strength and resistance to breakage	• ACL and PCL reconstruction
	OSTEORAPTOR Suture Anchor	PLLA/HAp (75/25)	• 2.3 mm anchors allow for precise positioning, with a reliable track record	• Shoulder and hip labral repair
Stryker (USA)	Biosteon® Interference screw	PLLA/HAp (75/25)	• Improve strength retention • Improve implant/bone integration and reduced tunnel widening and risk of graft slippage post-operatively	• ACL reconstruction

(continued)

Table 11.2 (continued)

Company (Country)	Product	Material	Properties	Applications
	Inion OTPS™	PLLA/PLDA/ Trimethylene carbonate	• Strength loss after 18–36 weeks in vivo with complete strength loss and resorption within two to four years	• Hand
	Venado Carbonate Block/Strip	Collagen type I/ carbonated Cap (20/80)	• Resorbable	• Bone graft system
	Venado Carbonate Sponge	Collagen type I/ carbonated Cap (45/55)	• Resorbable	• Bone graft system
Teijin, Ltd. (Japan)	OSTOTRANS-OT and OSTOTRANS-MX	PLLA/ Unsintered HAp (60/40)	• Strength higher than that of the human cortical bone • High bioresorbability and bioactivity	• Fracture bone fixation
Teknimed (France)	EUROSCREW® TCP NG	PLA/β-TCP (70/30)	• Radiopaque • Resorbable • Controlled degradation • Mechanically stable for respectively 8–10 months and 6 months post-operative	• ACL and ankle lateral ligament reconstruction
Zimmer Biomet (USA)	ComposiTCP™ (30 Interference Screw)	PLDLA/β-TCP (70/30)	• The materials showed faster degradation kinetics and less inflammatory reaction and promoted osteogenesis in an in vivo animal study	• ACL fixation

(continued)

Table 11.2 (continued)

Company (Country)	Product	Material	Properties	Applications
	ComposiTCP™ (60 Interference Screw)	PLDLA/β-TCP (40/60)	• The materials showed faster degradation kinetics and less inflammatory reaction and promoted osteogenesis in an in vivo animal study	• Soft tissue fixation

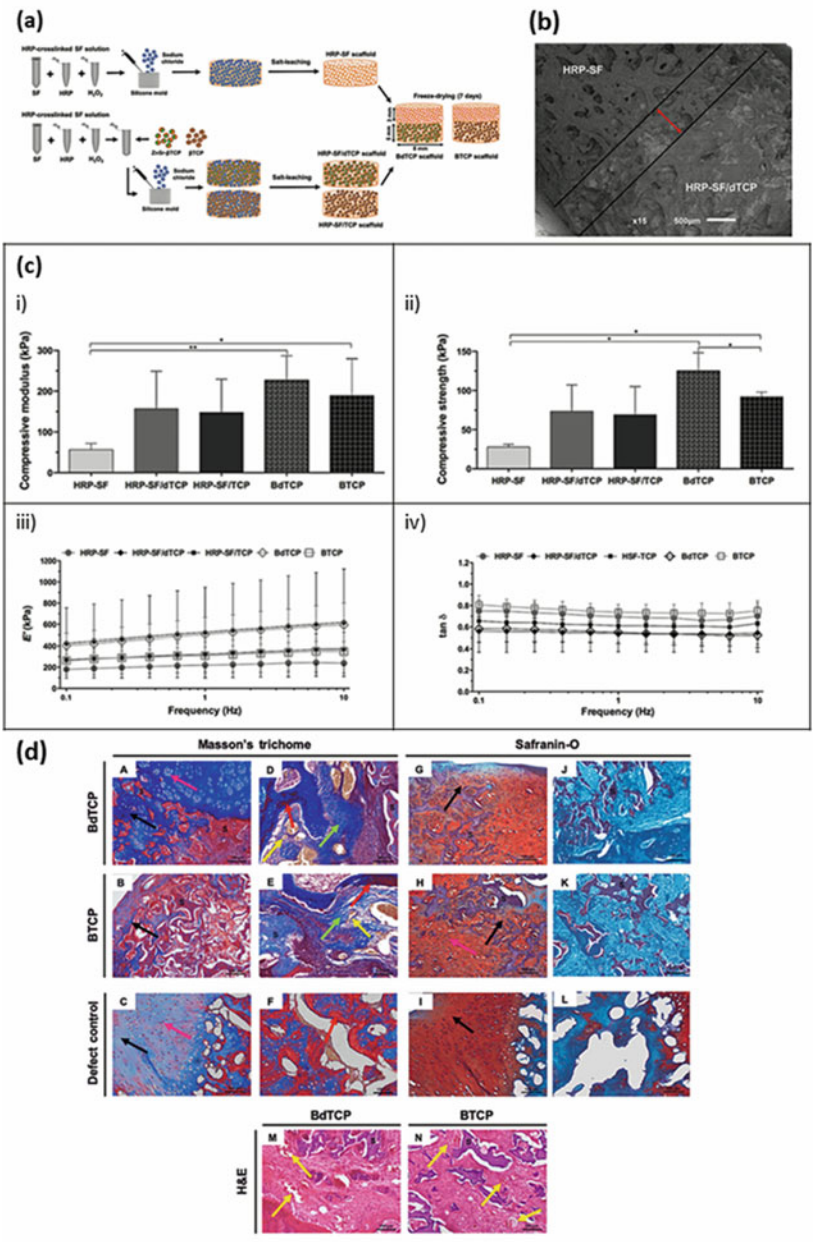
(a)
(b)
HRP-SF
HRP-SF/dTCP
(c)
i)
Compressive modulus (kPa)
HRP-SF
HRP-SF/dTCP
HRP-SF/TCP
BdTCP
BTCP
ii)
Compressive strength (kPa)
iii)
E' (kPa)
Frequency (Hz)
iv)
tan δ
Frequency (Hz)
(d)
Masson's trichome
Safranin-O
BdTCP
BTCP
Defect control
H&E

◀**Fig. 11.5** **a** Schematic of the experimental setup used for mono- and bilayered scaffolds fabrication through salt-leaching and freeze-drying processing techniques. **b** Scanning electron micrographs of the bilayered scaffolds. **c** Compressive modulus (i) and compressive strength of the scaffolds evaluated in wet conditions (ii); storage modulus (E') (iii) and loss factor (tan δ) of the scaffolds obtained by Dynamic Mechanical Analysis at pH 7.4 and 37 ºC (iv). Reprinted with permission from [7]. **d** Histological analysis of the implanted scaffolds after 8 weeks: (A–F) Masson's trichrome and (G–L) Safranin-O staining of the longitudinal sections of the explants. (A–C) cartilage region and (D–F) subchondral bone region Masson's trichrome staining; (G–I) cartilage region and (J–L) subchondral bone region Safranin-O staining; (M and N) Subchondral bone region of the bilayered scaffolds containing ion-doped β-TCP (BdTCP) and bilayered scaffolds containing pure β-TCP (BTCP) scaffolds haematoxylin and eosin (H&E) staining. Black arrows indicate collagen (blue) and glycosaminoglycans (red) deposition in neocartilage tissue formation and infiltration within the horseradish peroxidase-silk fibroin layers of the BdTCP and BTCP scaffolds. The pink arrows indicate chondrocytes. The red arrows indicate new bone tissue (red) formation surrounded by immature fibrous connective tissue (blue; green arrows). The yellow arrows indicate blood vessels (orange). "S" indicates stained scaffolds (HRP-SF/dTCP, HRP-SF/TCP and HRP-SF monolayered scaffolds). Reprinted with permission from [66]

interconnected interface region (Fig. 11.5b), showed suitable structural integrity, and adequate mechanical and viscoelastic properties (Fig. 11.5c). The compressive modulus and compressive strength of the bilayered scaffolds were higher than the respective monolayered ones, which was mainly attributed to the dopant ions presence (Table 11.3). In vivo performance of the scaffolds assessed by filling them in New Zealand white rabbits knee defects for 8 weeks demonstrated good integration and new bone formation (Fig. 11.5d) [66]. Collagen type-II and glycosaminoglycans formation was observed in the cartilage-like layer, especially on the bilayered scaffolds containing ion-doped β-TCP (BdTCP) scaffolds (Fig. 11.5d (A and B)). New bone formation and blood vessels infiltration were observed in the subchondral bone like-layer (Fig. 11.5d (D and E)). An interesting approach is also the fabrication of biocomposite nanospheres aiming bone tissue engineering, comprising silk fibroin and HAp doped with Sr, obtained by ultrasonic coprecipitation method [67]. The nanospheres (500–700 nm in size) were able to promote mice BMSCs adhesion, growth, and proliferation, and osteogenic differentiation, partially encouraged by the Sr release. In another study, Bochicchio et al. [5] reported the use of gelatin, bioactive RKKP glass–ceramics and PLDLA to produce electrospun scaffolds able

Table 11.3 Comparison between the compressive modulus and compressive strength between monolayered scaffolds and bilayered scaffolds [7]

	Compressive Modulus (kPa)	Compressive Strength (kPa)
Horseradish peroxidase-crosslinked silk fibroin/ZnSr-doped β-TCP (HRP-SF/dTCP) [Monolayered]	156.88 ± 92.36	73.41 ± 33.71
Hierarchical HRP-SF|HRP-SF/dTCP scaffold (BdTCP) [Bilayered]	226.56 ± 60.34	124.84 ± 23.42

to support and promote osteogenic differentiation in bone tissue engineering. The bioactive RKKP glass–ceramics contain La^{3+} and Ta^{5+}, which can regulate some proteins adherence as the case of albumin.

The use of biomaterials derived from decellularized extracellular matrix (ECM) to fabricate biocomposite scaffolds has recently gained high interest in bone tissue engineering [68–71]. Decellularized ECM maintains the native matrix structure, growth factors and cytokines, hence improving cell growth and viability [72]. For instance, multilayered scaffolds obtained with decellularized bovine small intestinal submucosa, PCL and HAp showed mechanical stability and differentiation into the osteoblastic lineage, after 21 days in rat BMSCs culture [70].

As aforementioned, 3D bioprinting technology has gaining noteworthy interest to develop biomaterials with precise architecture and accuracy, and thus it has also been applied for functional biocomposites manufacturing [73–78]. Kim et al. [77] reported on the printing of gelatin/HAp biocomposites with help of glycerol as a processing agent. The scaffolds showed well-attained interconnected pores and hyperelastic properties, while the obtained compressive modulus was lower than that of the human bone because no sintering process was applied to the ceramic material. However, the scaffolds may have potential for non-load-bearing applications, compensated by the osteogenic properties of the employed materials. Zhao et al. [78] prepared printed scaffolds from calcium phosphate (mixture of α-TCP, $CaHPO_4 \cdot 2H_2O$, $CaCO_3$ and HAp) pastes with well-dispersed PLGA fibers and observed good injectability and formability for compositions with up to 3 wt.% of fibers.

An alternative to overcome possible printing limitations when using thermally unstable materials (e.g., ceramics, natural polymers, and composites), is the application of indirect printing [79, 80]. In this process, a negative mold is produced based on the scaffold design, followed by biomaterial cast, and the final scaffold is obtained by sacrificing the mold. A study by Costa et al. [30] reported the fabrication of hierarchical biocomposite scaffolds through indirect printing for patient-specific meniscus tissue engineering. The scaffolds were fabricated with two different regions, one of which made of enzymatically crosslinked silk fibroin and the other containing the horseradish peroxidase-silk fibroin/ion-doped β-TCP aiming to improve the anchorage of the scaffolds to the bone (Fig. 11.6a, b). The scaffolds demonstrated high porosity degree with mean pore size in the range 113.3–137.5 μm. In vivo tests performed by subcutaneous implantation of the scaffolds in CD-1 mice for 8 weeks, showed good biocompatibility with the surrounding connective tissues, and a minimal inflammatory response (Fig. 11.6c). The formation of collagenous surround tissue is visible from Masson's trichrome staining images (Fig. 11.6d).

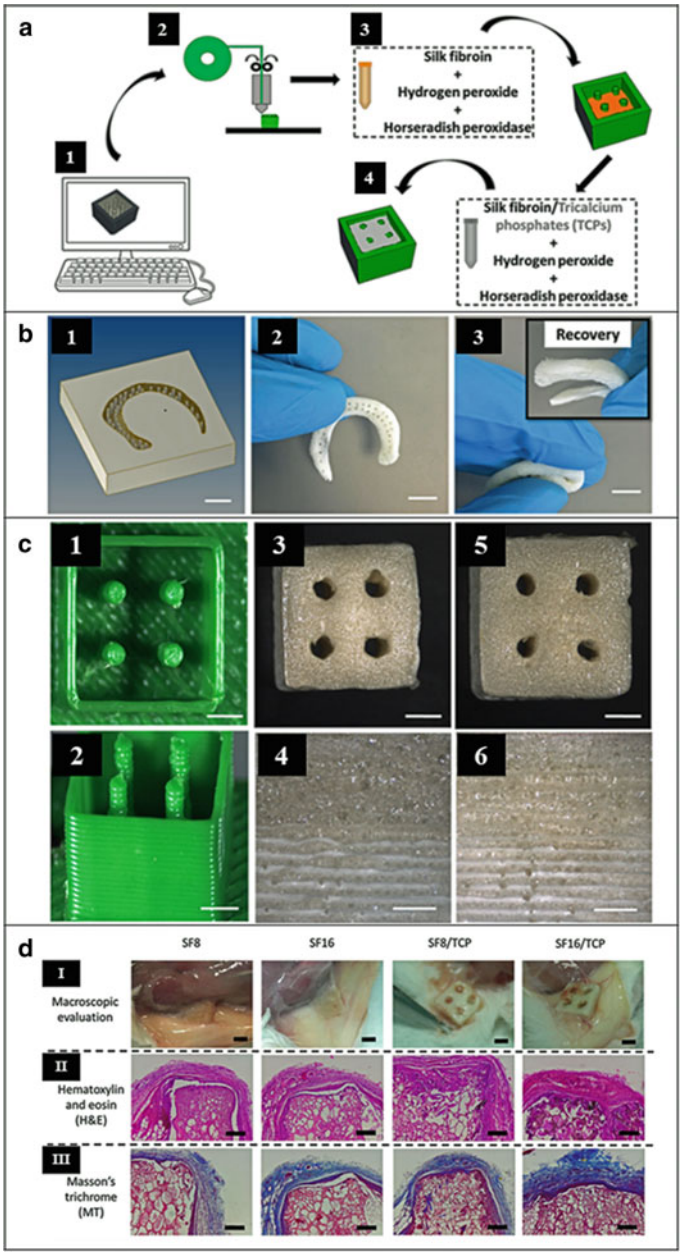
a
1
2
3
Silk fibroin
+
Hydrogen peroxide
+
Horseradish peroxidase
4
Silk fibroin/Tricalcium phosphates (TCPs)
+
Hydrogen peroxide
+
Horseradish peroxidase
b
1
2
3
Recovery
c
1
3
5
2
4
6
d
SF8
SF16
SF8/TCP
SF16/TCP
I
Macroscopic evaluation
II
Hematoxylin and eosin (H&E)
III
Masson's trichrome (MT)

◀**Fig. 11.6** Hierarchical biocomposite scaffolds obtained through indirect printing: **a** production steps: (1) negative mold design, (2) printing, and (3, 4) mold casting. **b** negative mold model (1), meniscus scaffold (2), and meniscus scaffold compressed showing shape recovery (3) (scale bar = 1 cm). **c** Macroscopic images of cube-shaped scaffolds: negative molds (1, 2) and final printed scaffolds (3–6). Two different silk fibroin concentrations were analyzed, namely 8% (3, 4) and 16% (5, 6) (scale bar = 2 mm for (1–3) and (5); scale bar = 1 mm for (4) and (6)). **d** Subcutaneous implantation in CD-1 mice: (I) Macroscopic images of the explants after 8 weeks of implantation (scale bar = 4 mm); (II) Hematoxylin and eosin (H&E) staining (scale bar = 200 μm); (III) Masson's trichrome (MT) staining (scale bar = 200 μm). Reprinted with permission from [30]

11.4 Conclusions and Future Trends

Remarkable advances have been made on using bioceramics and bioceramics-based biocomposites as scaffolding materials for the healing and reconstruction of diseased tissues. These biomaterials can easily be processed with outstanding osteoconductive/osteoinductive, angiogenic and immunomodulatory properties, antibacterial activity, and to act as carriers for drug delivery.

The development of functionalized bioceramics is a crucial strategy to modulate positively the tissue response-biomaterial interactions and to trigger desired immune responses. In this regard, the incorporation of ionic elements into bioceramics structure not only accelerates bone ingrowth and in vivo resorption by increasing the osteogenic and angiogenic levels, but also lead to physicochemical modifications (e.g., lattice structure, crystallinity, and dissolution rate), thus yielding mechanically stable implants.

The design of hierarchically structured bioceramics/biocomposites tissue engineering scaffolding is of paramount importance to address the mimetic requirements of the tissue aimed to be regenerated and to meet the personalized needs of the patients. In this sense, advanced manufacturing, as 3D bioprinting, has presented fundamental advantages of complex geometries, precision, and capability of dispensing cell-laden structures. The micro- and nanostructure, porosity and interconnected network of the structures tune their mechanical integrity upon implantation.

Significant development and advances with bioceramics/biocomposites research bring great opportunity to achieve more sophisticated and functional systems to broaden their use in the clinics. Improvements on biomaterials functionalization, design, mechanobiological stimulation, long-term performance, and fully understanding of cell-material interplay can possibly contribute towards overcome the current clinical challenges and limits.

Acknowledgements The authors thank the financial support from the Portuguese Foundation for Science and Technology for the funds provided under the distinctions attributed to JMO (IF/01285/2015) and SP (CEECIND/03673/2017).

References

1. Bijukumar DR, McGeehan C, Mathew MT (2018) Regenerative medicine strategies in biomedical implants. Curr Osteoporos Rep 16:236–245
2. Mohamad Yunos D, Bretcanu O, Boccaccini AR (2008) Polymer-bioceramic composites for tissue engineering scaffolds. J Mater Sci 43:4433–4442
3. Raquel Maia F, Correlo VM, Oliveira JM et al (2019) Natural origin materials for bone tissue engineering: properties, processing, and performance. In: Atala A, Lanza R, Mikos AG et al (eds) Principles of regenerative medicine, 3rd edn. Academic Press, Boston, pp 535–558
4. Hasan MS, Ahmed I, Parsons AJ et al (2013) Investigating the use of coupling agents to improve the interfacial properties between a resorbable phosphate glass and polylactic acid matrix. J Biomater Appl 28:354–366
5. Bochicchio B, Barbaro K, De Bonis A et al (2020) Electrospun poly(d, l-lactide)/gelatin/glass-ceramics tricomponent nanofibrous scaffold for bone tissue engineering. J Biomed Mater Res A 108:1064–1076
6. Nie L, Wu Q, Long H et al (2019) Development of chitosan/gelatin hydrogels incorporation of biphasic calcium phosphate nanoparticles for bone tissue engineering. J Biomater Sci Polym Ed 30:1636–1657
7. Ribeiro VP, Pina S, Costa JB et al (2019) Enzymatically cross-linked silk fibroin-based hierarchical scaffolds for osteochondral regeneration. ACS Appl Mater Interfaces 11:3781–3799
8. Pina S, Oliveira JM, Reis RL (2015) Natural-based nanocomposites for bone tissue engineering and regenerative medicine: a review. Adv Mater 27:1143–1169
9. Yan LP, Silva-Correia J, Oliveira MB et al (2015) Bilayered silk/silk-nanoCaP scaffolds for osteochondral tissue engineering: *in vitro* and *in vivo* assessment of biological performance. Acta Biomater 12:227–241
10. Yun PY, Kim YK, Jeong KI et al (2014) Influence of bone morphogenetic protein and proportion of hydroxyapatite on new bone formation in biphasic calcium phosphate graft: two pilot studies in animal bony defect model. J Craniomaxillofac Surg 42:1909–1917
11. Yan LP, Silva-Correia J, Correia C et al (2013) Bioactive macro/micro porous silk fibroin/nano-sized calcium phosphate scaffolds with potential for bone-tissue-engineering applications. Nanomedicine 8:359–378
12. Canadas R, Pereira D, Silva-Correia J et al (2012) Novel bilayered Gellan gum/Gellan gum hydroxyapatite scaffolds for osteochondral tissue engineering applications. J Tissue Eng Regen Med 6:8–39
13. Oliveira JM, Rodrigues MT, Silva SS et al (2006) Novel hydroxyapatite/chitosan bilayered scaffold for osteochondral tissue-engineering applications: scaffold design and its performance when seeded with goat bone marrow stromal cells. Biomaterials 27:6123–6137
14. Stockmann P, Böhm H, Driemel O et al (2010) Resorbable versus titanium osteosynthesis devices in bilateral sagittal split ramus osteotomy of the mandible—the results of a two centre randomised clinical study with an eight-year follow-up. J Craniomaxillofac Surg 38:522–528
15. Kukk A, Nurmi JT (2009) A retrospective follow-up of ankle fracture patients treated with a biodegradable plate and screws. Foot Ankle Surg 15:192–197
16. Mittal R, Morley J, Dinopoulos H et al (2005) Use of bio-resorbable implants for stabilisation of distal radius fractures: the United Kingdom patients' perspective. Injury 36:333–338
17. Pietrzak WS (2000) Principles of development and use of absorbable internal fixation. Tissue Eng 6:425–433
18. Kim YK, Yeo HH, Lim SC (1997) Tissue response to titanium plates: a transmitted electron microscopic study. J Oral Maxillofac Surg 55:322–326

19. Alpert B, Seligson D (1996) Removal of asymptomatic bone plates used for orthognathic surgery and facial fractures. J Oral Maxillofac Surg 54:618–621
20. Agins HJ, Alcock NW, Bansal M et al (1988) Metallic wear in failed titanium-alloy total hip replacements. A histological and quantitative analysis. J Bone Joint Surg Am 70:347–356
21. Causa F, Netti PA, Ambrosio L et al (2006) Poly-epsilon-caprolactone/hydroxyapatite composites for bone regeneration: *in vitro* characterization and human osteoblast response. J Biomed Mater Res A 76:151–162
22. Blasier RD, Bucholz R, Cole W et al (1997) Bioresorbable implants: applications in orthopaedic surgery. Instr Course Lect 46:531–546
23. Bucholz RW, Henry S, Henley MB (1994) Fixation with bioabsorbable screws for the treatment of fractures of the ankle. J Bone Joint Surg Am 76:319–324
24. Peltoniemi H (2000) Biocompatibility and fixation properties of absorbable miniplates and screws in growing calvarium. Dissertation, University of Helsinki
25. Hubbell JA (1995) Biomaterials in tissue engineering. Biotechnology 13:565–576
26. Sola A, Bertacchini J, D'Avella D et al (2019) Development of solvent-casting particulate leaching (SCPL) polymer scaffolds as improved three-dimensional supports to mimic the bone marrow niche. Mater Sci Eng C Mater Biol Appl 96:153–165
27. Gay S, Lefebvre G, Bonnin M et al (2018) PLA scaffolds production from thermally induced phase separation: effect of process parameters and development of an environmentally improved route assisted by supercritical carbon dioxide. J Supercrit Fluids 136:123–135
28. Song P, Zhou C, Fan H et al (2018) Novel 3D porous biocomposite scaffolds fabricated by fused deposition modeling and gas foaming combined technology. Compos B Eng 152:151–159
29. Brougham CM, Levingstone TJ, Shen N et al (2017) Freeze-drying as a novel biofabrication method for achieving a controlled microarchitecture within large, complex natural biomaterial scaffolds. Adv Healthc Mater. https://doi.org/10.1002/adhm.201700598
30. Costa JB, Silva-Correia J, Pina S et al (2019) Indirect printing of hierarchical patient-specific scaffolds for meniscus tissue engineering. Bio-des Manuf 2:225–241
31. Kim WJ, Yun HS, Kim GH (2017) An innovative cell-laden α-TCP/collagen scaffold fabricated using a two-step printing process for potential application in regenerating hard tissues. Sci Rep 7:3181
32. Gu BK, Choi DJ, Park SJ et al (2016) 3-dimensional bioprinting for tissue engineering applications. Biomater Res 20:12
33. Meininger S, Mandal S, Kumar A et al (2016) Strength reliability and *in vitro* degradation of three-dimensional powder printed strontium-substituted magnesium phosphate scaffolds. Acta Biomater 31:401–411
34. Ben-Nissan B, Cazalbou S, Choi AH (2019) Bioceramics. In: Narayan R (ed) Encyclopedia of biomedical engineering. Elsevier, Amsterdam, pp 16–33
35. Silva TH, Alves A, Ferreira BM et al (2012) Materials of marine origin: a review on polymers and ceramics of biomedical interest. Int Mater Rev 57:276–306
36. Correlo VM, Oliveira JM, Mano JF et al (2011) Natural origin materials for bone tissue engineering—properties, processing, and performance. In: Atalas A, Lanza R, Thomson JA et al (eds) Principles of regenerative medicine, 2nd edn. Academic Press, San Diego, pp 557–586
37. Oliveira JM, Grech JMR, Leonor IB et al (2007) Calcium-phosphate derived from mineralized algae for bone tissue engineering applications. Mater Lett 61:3495–3499
38. Zhuang H, Lin R, Liu Y et al (2019) Three-dimensional-printed bioceramic scaffolds with osteogenic activity for simultaneous photo/magnetothermal therapy of bone tumors. ACS Biomater Sci Eng 5:6725–6734
39. Adel-Khattab D, Giacomini F, Gildenhaar R et al (2018) Development of a synthetic tissue engineered three-dimensional printed bioceramic-based bone graft with homogenously distributed osteoblasts and mineralizing bone matrix *in vitro*. J Tissue Eng Regen Med 12:44–58
40. Kim H, Mondal S, Bharathiraja S et al (2018) Optimized Zn-doped hydroxyapatite/doxorubicin bioceramics system for efficient drug delivery and tissue engineering application. Ceram Int 44:6062–6071

41. Wang X, Li T, Ma H et al (2017) A 3D-printed scaffold with MoS2 nanosheets for tumor therapy and tissue regeneration. NPG Asia Mater 9:e376. https://doi.org/10.1038/am.2017.47
42. Ma L, Cheng S, Ji X et al (2020) Immobilizing magnesium ions on 3D printed porous tantalum scaffolds with polydopamine for improved vascularization and osteogenesis. Mater Sci Eng C Mater Biol Appl 117:111303
43. Xu Z, Xu Y, Basuthakur P et al (2020) Fibro-porous PLLA/gelatin composite membrane doped with cerium oxide nanoparticles as bioactive scaffolds for future angiogenesis. J Mater Chem B. https://doi.org/10.1039/d0tb01715a
44. Gu Y, Zhang J, Zhang X et al (2019) Three-dimensional printed Mg-doped β-TCP bone tissue engineering scaffolds: effects of magnesium ion concentration on osteogenesis and angiogenesis *in vitro*. Tissue Eng Regen Med 16:415–429
45. Stähli C, James-Bhasin M, Hoppe A et al (2015) Effect of ion release from Cu-doped 45S5 Bioglass® on 3D endothelial cell morphogenesis. Acta Biomater 19:15–22
46. Rath SN, Brandl A, Hiller D et al (2014) Bioactive copper-doped glass scaffolds can stimulate endothelial cells in co-culture in combination with mesenchymal stem cells. PLoS One 9:e113319
47. Amudha S, Ramana Ramya J, Thanigai Arul K et al (2020) Enhanced mechanical and biocompatible properties of strontium ions doped mesoporous bioactive glass. Compos B Eng 196:108099
48. Köse N, Asfuroğlu ZM, Köse A et al (2020) Silver ion-doped calcium phosphate-based bone-graft substitute eliminates chronic osteomyelitis: an experimental study in animals. J Orthop Res. https://doi.org/10.1002/jor.24946
49. Lin Z, Cao Y, Zou J et al (2020) Improved osteogenesis and angiogenesis of a novel copper ions doped calcium phosphate cement. Mater Sci Eng C Mater Biol Appl 114:111032
50. Motameni A, Alshemary AZ, Dalgic AD et al (2020) Lanthanum doped dicalcium phosphate bone cements for potential use as filler for bone defects. Mater Today Commun. https://doi.org/10.1016/j.mtcomm.2020.101774
51. Sayahi M, Santos J, El-Feki H et al (2020) Brushite (Ca,M)HPO_4, $2H_2O$ doping with bioactive ions (M = Mg^{2+}, Sr^{2+}, Zn^{2+}, Cu^{2+}, and Ag^{+}): a new path to functional biomaterials? Mater Today Chem 16:100230
52. Sikder P, Coomar PP, Mewborn JM et al (2020) Antibacterial calcium phosphate composite cements reinforced with silver-doped magnesium phosphate (newberyite) micro-platelets. J Mech Behav Biomed Mater 110:103934
53. Bolaños RV, Castilho M, de Grauw J et al (2020) Long-Term *in vivo* performance of low-temperature 3d-printed bioceramics in an equine model. ACS Biomater Sci Eng 6:1681–1689
54. Liu Y, Li T, Ma H et al (2018) 3D-printed scaffolds with bioactive elements-induced photothermal effect for bone tumor therapy. Acta Biomater 73:531–546
55. Zhai D, Chen L, Chen Y et al (2020) Lithium silicate-based bioceramics promoting chondrocyte maturation by immunomodulating M2 macrophage polarization. Biomater Sci 8:4521–4534
56. Humbert P, Brennan MÁ, Davison N et al (2019) Immune modulation by transplanted calcium phosphate biomaterials and human mesenchymal stromal cells in bone regeneration. Front Immunol 10:663
57. Mansour A, Abu-Nada L, Al-Waeli H et al (2019) Bone extracts immunomodulate and enhance the regenerative performance of dicalcium phosphates bioceramics. Acta Biomater 89:343–358
58. Sadowska JM, Wei F, Guo J et al (2019) The effect of biomimetic calcium deficient hydroxyapatite and sintered β-tricalcium phosphate on osteoimmune reaction and osteogenesis. Acta Biomater 96:605–618
59. Kurzina I, Churina Y, Shapovalova Y et al (2018) Immunomodulatory properties of composite materials basedon polylactide and hydroxyapatite. Bioceram Dev Appl 8:109
60. Li T, Peng M, Yang Z et al (2018) 3D-printed IFN-γ-loading calcium silicate-β-tricalcium phosphate scaffold sequentially activates M1 and M2 polarization of macrophages to promote vascularization of tissue engineering bone. Acta Biomater 71:96–107
61. Sadowska JM, Wei F, Guo J et al (2018) Effect of nano-structural properties of biomimetic hydroxyapatite on osteoimmunomodulation. Biomaterials 181:318–332

62. Moonesi Rad R, Alshemary AZ, Evis Z et al (2020) Cellulose acetate-gelatin-coated boron-bioactive glass biocomposite scaffolds for bone tissue engineering. Biomed Mater 15:065009
63. Wu S, Ma S, Zhang C et al (2020) Cryogel biocomposite containing chitosan-gelatin/cerium-zinc doped hydroxyapatite for bone tissue engineering. Saudi J Biol Sci 27:2638–2644
64. Pina S, Canadas RF, Jiménez G et al (2017) Biofunctional ionic-doped calcium phosphates: silk fibroin composites for bone tissue engineering scaffolding. Cells Tissues Organs 204:150–163
65. Ribeiro VP, da Silva MA, Maia FR et al (2018) Combinatory approach for developing silk fibroin scaffolds for cartilage regeneration. Acta Biomater 72:167–181
66. Ribeiro VP, Pina S, Canadas RF et al (2019) *In vivo* performance of hierarchical HRP-crosslinked silk fibroin/β-TCP scaffolds for osteochondral tissue regeneration. Regen Med Front 1:e190007. https://doi.org/10.20900/rmf20190007
67. Wang L, Pathak JL, Liang D et al (2020) Fabrication and characterization of strontium-hydroxyapatite/silk fibroin biocomposite nanospheres for bone-tissue engineering applications. Int J Biol Macromol 142:366–375
68. Elomaa L, Keshi E, Sauer IM et al (2020) Development of GelMA/PCL and dECM/PCL resins for 3D printing of acellular *in vitro* tissue scaffolds by stereolithography. Mater Sci Eng C Mater Biol Appl 112:110958
69. Nokhbatolfoghahaei H, Paknejad Z, Bohlouli M et al (2020) Fabrication of decellularized engineered extracellular matrix through bioreactor-based environment for bone tissue engineering. ACS Omega 5:31943–31956
70. Parmaksiz M, Elçin AE, Elçin YM (2019) Decellularized bovine small intestinal submucosa-PCL/hydroxyapatite-based multilayer composite scaffold for hard tissue repair. Mater Sci Eng C Mater Biol Appl 94:788–797
71. Kim YS, Majid M, Melchiorri AJ et al (2018) Applications of decellularized extracellular matrix in bone and cartilage tissue engineering. Bioeng Transl Med 4:83–95
72. Taylor DA, Sampaio LC, Ferdous Z et al (2018) Decellularized matrices in regenerative medicine. Acta Biomater 74:74–89
73. Custodio CL, Broñola PJM, Cayabyab SR et al (2021) Powder loading effects on the physicochemical and mechanical properties of 3D printed poly lactic acid/hydroxyapatite biocomposites. Int J Bioprint 7:326
74. Oladapo BI, Zahedi SA, Ismail SO et al (2021) 3D printing of PEEK-cHAp scaffold for medical bone implant. Bio-des Manuf 4:44–59
75. Wang Q, Ma Z, Wang Y et al (2021) Fabrication and characterization of 3D printed biocomposite scaffolds based on PCL and zirconia nanoparticles. Bio-des Manuf 4:60–71
76. Backes EH, de Nóbile Pires L, Selistre-de-Araujo HS et al (2020) Development and characterization of printable PLA/β-TCP bioactive composites for bone tissue applications. J Appl Polym Sci 138:e49759
77. Kim D, Lee J, Kim G (2020) Biomimetic gelatin/HA biocomposites with effective elastic properties and 3D-structural flexibility using a 3D-printing process. Addit Manuf 36:101616
78. Zhao G, Cui R, Chen Y et al (2020) 3D Printing of well dispersed electrospun PLGA fiber toughened calcium phosphate scaffolds for osteoanagenesis. J Bionic Eng 17:652–668
79. Wang JQ, Jiang BJ, Guo WJ (2019) Indirect 3D printing technology for the fabrication of customised β-TCP/chitosan scaffold with the shape of rabbit radial head-an *in vitro* study. J Orthop Surg Res 14:102
80. Houben A, Van Hoorick J, Van Erps J et al (2017) Indirect rapid prototyping: opening up unprecedented opportunities in scaffold design and applications. Ann Biomed Eng 45:58–83

Dr. Sandra Pina is an Assistant Researcher at the 3B's Research Group on Biomaterials, Biodegradables and Biomimetics (member of the ICVS/3B's Associate Laboratory), University of Minho. Her research has been focusing on the field of bioresorbable bioceramics for tissue engineering and regenerative medicine with main applications in bone and osteochondral defects and diseases. In addition, she has been developing different ion-doped materials with great potential for being used in MRI (cell tracking and biodistribution studies) and immunomodulation. Sandra Pina has been participating in the preparation/implementation/co-coordination of national and international projects. She produced so far 37 publications in SCI journals, 2 books, 18 book chapters, with over than 1588 citations and an h-index of 19. She has also 2 granted patents, related with ionic-doped bioceramics. She presented more than 50 communications in major conferences in the field.

Professor Il Keun Kwon is a Vice-Dean at Dental School and Head of Medical Device Institute at Medical Center, Kyung Hee University, and a special committee member of the Ministry of Health and Welfare (Regenerative Medicine Bio-tissue & organ in Future Advanced Medicine field) in Republic of Korea. His recent research is focused on bone tissue engineering: (1) biocompatible hydrophilic materials from natural-based polymers; (2) 3D bioprinting using above natural-based hydrogels (bioinks); (3) drug delivery system using nano-biotechnologies; and (4) in vitro/in vivo biological studies for angiogenesis/osteogenesis using peptides, O_2, Ca^+ ion, and nitric oxide delivery. He has been working on many projects related to implantable medical devices and biomaterials for Tissue Engineering. He produced more than 200 publications, with citations and an h-index of 51, 11 book chapters, 20 patents and 3 technology transfer to company.

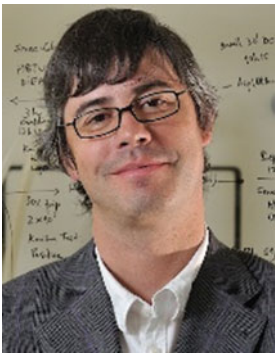

Professor Rui L. Reis is the Vice-President for R&D of University of Minho, Portugal, Director of the 3B's Research Group and of the ICVS/3B's Associate Laboratory of UMinho. He is the CEO of the European Institute of Excellence on Tissue Engineering and Regenerative Medicine. His main area of research is the development of biomaterials from natural origin polymers proposed for bone replacement and fixation, drug delivery carriers, partially degradable bone cements and tissue engineering scaffolding for different tissues. He is an FBSE, FTERM and NAE member. He has been the co-coordinator of four major EU research project, funded under FP6 and FP7 european commission. He is also the main responsible for several other projects funded by Portuguese, European and American biomaterials and polymeric industries and for a range of bilateral concerted actions. He was awarded a European Research Council Advanced Grant. He also coordinates a large international Ph.D. programme funded by FCT on TERM and stem cells, as well as two Structural Programmes He has been

awarded several prizes, such as ESAFORM 2001 Scientific Prize, Jean LeRay Award 2002, Stimulus to Excellence Award 2004, Pfizer Award for Clinical Research, START Innovation Award. He has produced, so far 1360 publications, around 100 filled/awarded patents, 18 books, 6 special issues in scientific journals, around 280 book chapters, and more than 2050 communications in conferences. His work has been cited around 41,000 times, and he has an ISI h-index of 94.

Dr. J. Miguel Oliveira is a Principal Investigator that has focused his work on the field of biomaterials for tissue engineering, nanomedicine, stem cells and cell/drug delivery. He has been involved in the development of biomaterials from natural origin polymers (chitin, chitosan, carboxymethylchitosan, algae-based materials such as ulvan, silk-fibroin, and gellan gum and its derivatives) and bioceramics for a wide range of regenerative medicine applications including, bone, cartilage, osteochondral tissue, peripheral nerve, spinal cord injury, meniscus and intervertebral disc (IVD) regeneration. It is truly remarkable the range of processing routes proposed including 3D printing, in developing a whole range of structures spanning from micro/nanoparticles, micro/nanofibres, membranes, conduits or hydrogels. He is Vice-President of I3Bs, University of Minho. He is also Director of Pre-Clinical Research at the FIFA MEDICAL CENTER, PT. He has published more than 400 scientific contributions, 7 books, 6 special issues, and 106 book chapters, and 20 patents. He has participated in more than 200 communications and invited/keynote speaker in more than 30 plenary sessions. He has an h-index of 53 and received more than 10300 citations. He has been awarded several prizes including Jean Leray Award 2015.

Index

A. H. Choi and B. Ben-Nissan (eds.), *Innovative Bioceramics in Translational Medicine I*, Springer Series in Biomaterials Science and Engineering 17,
https://doi.org/10.1007/978-981-16-7435-8

C

I

L

M

N

O